F

# KERNFORSCHUNGSANLAGE JÜLICH GmbH

## Institut für Kernphysik

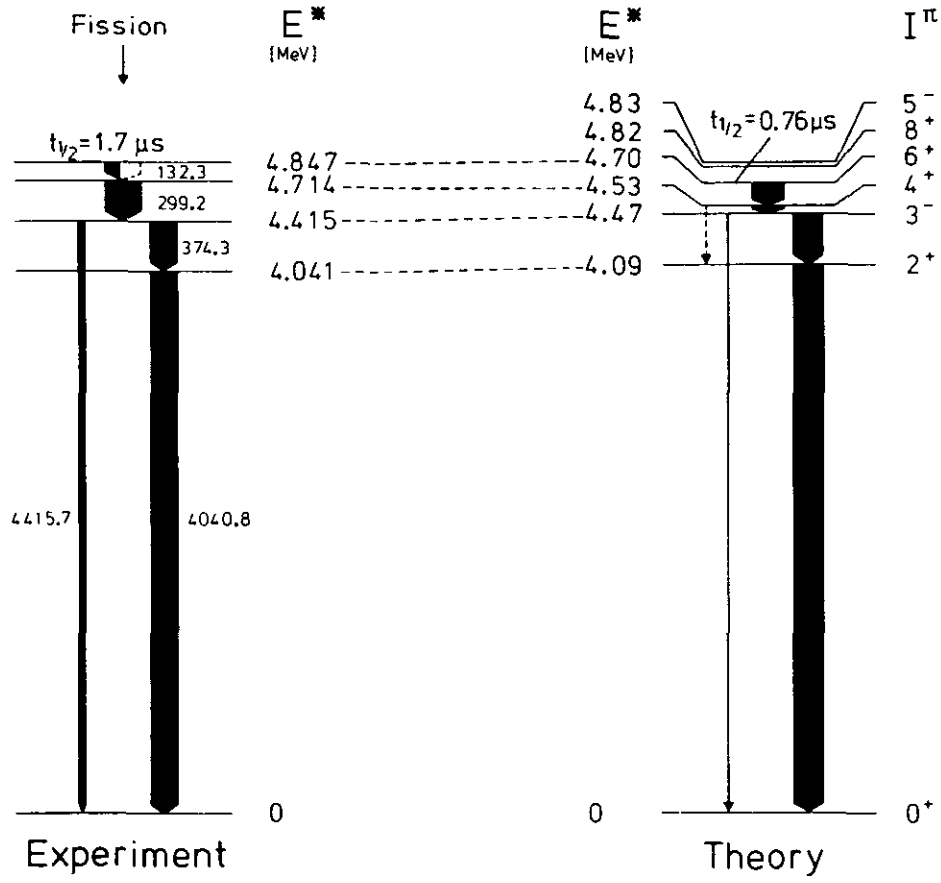


$^{132}_{50}Sn_{82}$


**Jül - Spez - 15**
Juni 1978
ISSN 0343-7639


# Annual Report 1977

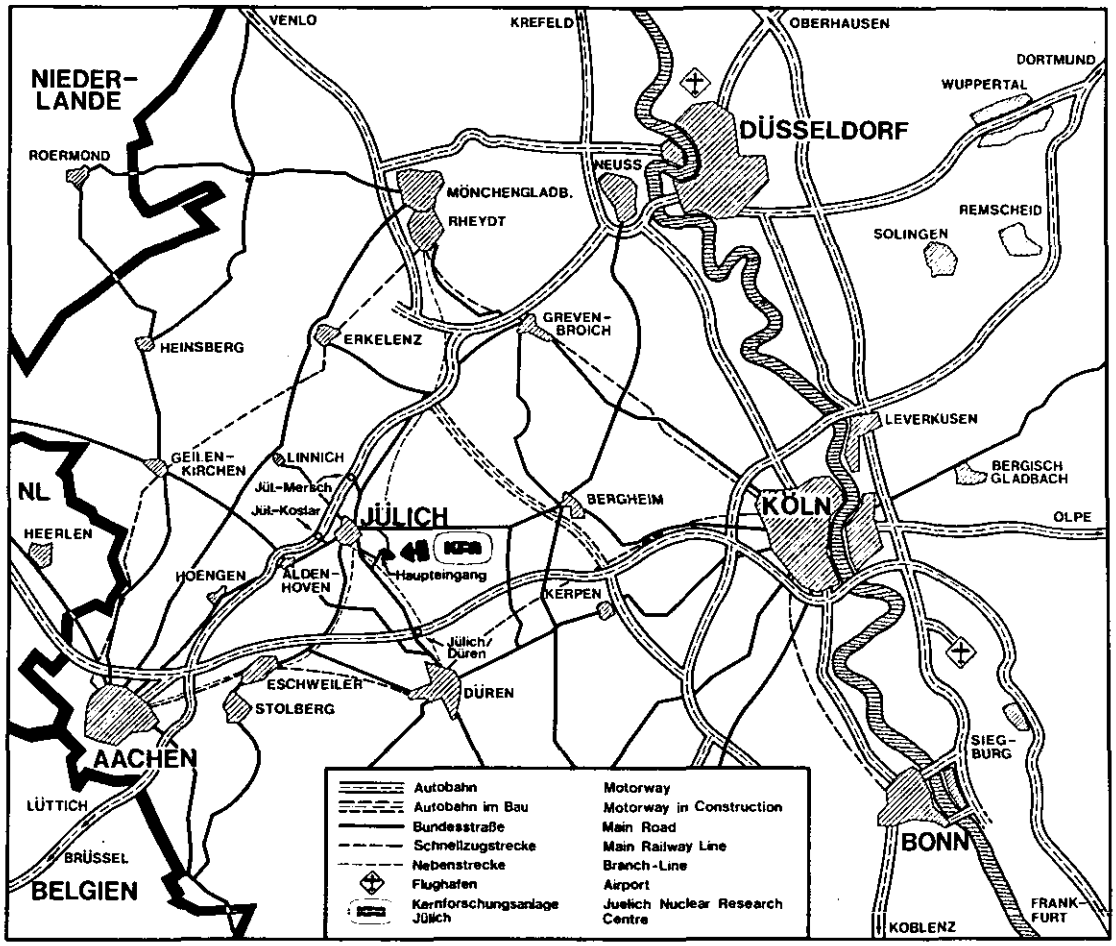


Als Manuskript gedruckt

**Spezielle Berichte der Kernforschungsanlage Jülich - Nr. 15**

Institut für Kernphysik Jül - Spez - 15

Zu beziehen durch: ZENTRALBIBLIOTHEK der Kernforschungsanlage Jülich GmbH,
Jülich, Bundesrepublik Deutschland

# Annual Report 1977



*Front cover: Comparison between the experimental and a theoretical (RPA) level scheme of the double magic nucleus* $^{132}_{50}Sn_{82}$. *For details see contributions 2.27 and 4.2.2.*

# Preface

*This annual report of the Department of Nuclear Physics of the Kernforschungsanlage Jülich is a brief display of the research activities of the Institute of Experimental Nuclear Physics I, the Institute of Experimental Nuclear Physics II, and the Institute of Theoretical Nuclear Physics and it contains short descriptions of the technological and instrumental developments achieved by our infrastructure groups. It covers the period from January to December 1977. The report is intended to inform all of our colleagues working in related fields in other laboratories. It is, therefore, more detailed than a series of abstracts, but the contributions are, on the other hand, short so that they constitute condensed packages of the essential information.*

*The scientific problems which have been dealt with, have naturally developed out of our previous work. The main subjects have been studies of giant resonances, of high spin states in Ba, Ce, and Nd isotopes with $N \leq 80$ and in Hf, W and Au isotopes, studies of the structures of nuclei around $^{146}Gd$ and of $^{100}Zr$ and $^{132}Sn$, of K-X ray energy shifts, of very high spin states. of backbending in odd A nuclei, of reaction processes, of the nuclear many-body problem and of mesonic degrees of freedom in nuclei. Technological work is undertaken in connection with the IEA solarcollector test program and for the development of an instrument package for solar-meteorologic data.*

*The scheduled time of operation of the cyclotron JULIC was 7425 h in 1977. A total of 85 % of this time could be used for experiments. About 20 % of the beam time was made available for external groups. In addition about 14 % of the beam time was used by other institutes of the Kernforschungsanlage Jülich. The first three magnets of our QQDDQ magnetic spectrograph have been assembled in their final positions on the support. Measurements of their magnetic quality indicate a reasonably good performance of the system.*

*Most of the experiments have been performed with the beams from our cyclotron. In addition, extensive use has been made of the research reactor DIDO. Furthermore a number of studies have been carried out at the high flux reactor of the ILL, at the CERN and at other laboratories, in general in close cooperation with scientists from these institutions. The scientific exchange is very intense due to the guest groups which use our cyclotron beams, our scientists carrying out research abroad and many guest scientists working together with the groups in our nuclear physics department.*

*Also in the past year the work of our scientists has been very well supported by other groups of our research center, and, in particular, by all of the infrastructure groups in our institute. It is a special pleasure for me to express my sincerest thanks to all of them for this support and help.*

*March, 1978*

Otto Schult

**Institute for Nuclear Physics**
Managing director: Prof. Dr. O. Schult
Experimental Nuclear Physics I,
director: Prof. Dr. C. Mayer-Böricke
Experimental Nuclear Physics II,
director: Prof. Dr. O. Schult
Theoretical Physics, director: Prof. Dr. A. Fäßler
Kernforschungsanlage Jülich GmbH
Postfach 1913, 5170 Jülich, W.-Germany

# Contents
## Institute for Nuclear Physics

# I. Experimental Nuclear Physics

## 1. Nuclear Reactions and Scattering Processes

### 1.1. Elastic Scattering of 172.5 MeV Alpha Particles on Ni Isotopes

A. Budzanowski, C. Alderliesten, J. Bojowald, C. Mayer-Böricke, W. Oelert, P. Turek and S. Wiktor

The elastic scattering of alpha particles on $^{58}$Ni, $^{60}$Ni, $^{62}$Ni and $^{64}$Ni isotopes was measured at $E_\alpha$ = 172.5 MeV using the α-particle beam from the Jülich isochronous cyclotron. The purpose of this work was to investigate the shape of the optical model potential, the isotopic dependence of its imaginary part and the applicability of the global optical model potential developed recently[1]. It has been shown in terms of the microscopic double folding model[2] that the real part of the α-nucleus potential has a shape, which can be better described by the Saxon-Woods squared formfactor. The $(SW)^2$ formfactor has already been used by several authors[3,4,1].

Angular distributions of elastically scattered alpha particles were measured in the angular range from 4.5° – 70° (lab), using the 1 m scattering chamber equiped with 2 semiconductor ΔE-E telescopes. Special care has been taken to minimize the error in the absolute value of the cross-section. The data were analyzed in terms of a six-parameter optical model potential with volume absorption only. This form of absorption at high energy α-scattering, as has been shown in our previous investigation[5], is superior to that of surface absorption. Similarly as in the case of light nuclei[5] only one, discrete set of parameters has been found. Angular distributions of elastically scattered α-particles on all four Ni-isotopes and corresponding fits with $(SW)^2$ (full line) and (SW) (dashed line) potentials are shown in fig. 1. The corresponding parameters are listed in table 1. The quality of fits differs at angles larger than 50° in favour of the $(SW)^2$ formfactor. This fact is also consistent with the $\chi^2$ values for $^{58}$Ni, $^{60}$Ni and $^{62}$Ni with exception of $^{64}$Ni as can be seen from table 1. Further investigations are in progress.

*Table 1:*

| | $^{58}$Ni | (SW) $^{60}$Ni | $^{62}$Ni | $^{64}$Ni |
|---|---|---|---|---|
| V (NeV) | 111.47 | 111.29 | 108.84 | 112.54 |
| $r_v$ (fm) | 1.248 | 1.245 | 1.256 | 1.240 |
| $a_v$ (fm) | 0.972 | 0.804 | 0.797 | 0.818 |
| W (MeV) | 22.73 | 21.68 | 22.20 | 21.22 |
| $r_w$ (fm) | 1.564 | 1.577 | 1.572 | 1.586 |
| $a_w$ (fm) | 0.580 | 0.603 | 0.623 | 0.608 |
| $\chi^2$/N | 3.78 | 2.13 | 2.89 | 2.21 |
| | | $(SW)^2$ | | |
| V (MeV) | 149,76 | 142.79 | 140.84 | 154.02 |
| $r_v$ (fm) | 1.340 | 1.354 | 1.361 | 1.316 |
| $a_v$ (fm) | 1.336 | 1.319 | 1.316 | 1.423 |
| W (MeV) | 25.55 | 24.35 | 26.42 | 2014 |
| $r_w$ (fm) | 1.671 | 1.696 | 1.672 | 1.756 |
| $a_w$ (fm) | 1.123 | 1.143 | 1.197 | 1.024 |
| $\chi^2$/N | 2.60 | 1.38 | 2.20 | 2.92 |

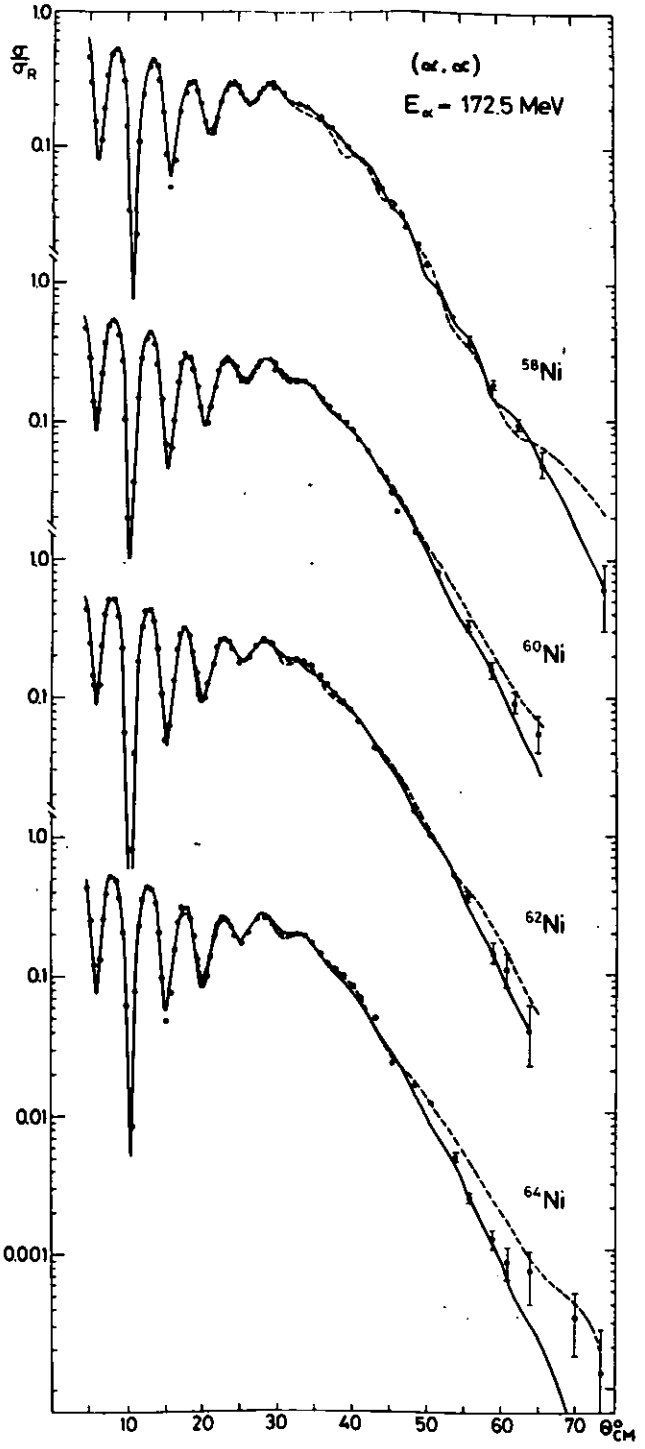


*Figure 1:*
*Angular distributions of elastically scattered alpha-particles on Ni-isotopes fitted with $(SW)^2$ (full line) and (SW) (dashed line).*

## References

[1] A. Budzanowski, H. Dabrowski, L. Freindl, K. Grotowski, S. Micek, R. Planeta, A. Strzalkowski, M. Bosmann, P. Leleux, P. Macq, J.P. Meulders and C. Pirart, IFJ Rep. 962/PL, 1977 (accepted for publication in Phys. Rev. C)
[2] Z. Majka, A. Budzanowski, K. Grotowski, A. Strzalkowski, IFJ Rep. 940/PL, 1977 (accepted for publication in Phys. Rev. C)
[3] A. Budzanowski, K. Grotowski, M. Grzywacz, A. Strzalkowski, Institute of Nuclear Physics Cracow, Progress Rep. 1 (1971) 2
[4] D.A. Goldberg, Phys. Lett. 55B (1975) 59
[5] S. Wiktor, C. Mayer-Böricke, A. Kiss, M. Rogge and P. Turek, Annual Report KFA (1976) 1 (and to be published)


## 1.2. Elastic Scattering of 130 MeV $^3$He


A. Djaloeis, J.P. Didelez, A. Galonsky, W. Oelert


The measurement of the elastic scattering angular distribution of 130 MeV $^3$He incident on $^{24}$Mg, $^{90}$Zr, $^{120}$Sn and $^{208}$Pb has been extended toward larger angles.

Figs. 1–4 show the angular distributions of the measured ratio of the elastic to the Rutherford cross section. As the target mass increases the angular distance between two diffraction maxima decreases and at the same time the diffraction region extends towards larger angles. The onset of the region where the cross section exhibits an approximately exponential fall-off (refraction region) thereby moves from about 35° in $^{24}$Mg to an angle larger than 50° in $^{208}$Pb. It can be seen also that for $^{24}$Mg, $^{90}$Zr and $^{120}$Sn the experimental data extend considerably into the refraction region.

The results of the optical model analysis are shown in figs. 1–4. The best-fit parameters are listed in table 1. From the analysis of the present experimental data the following points can be made:

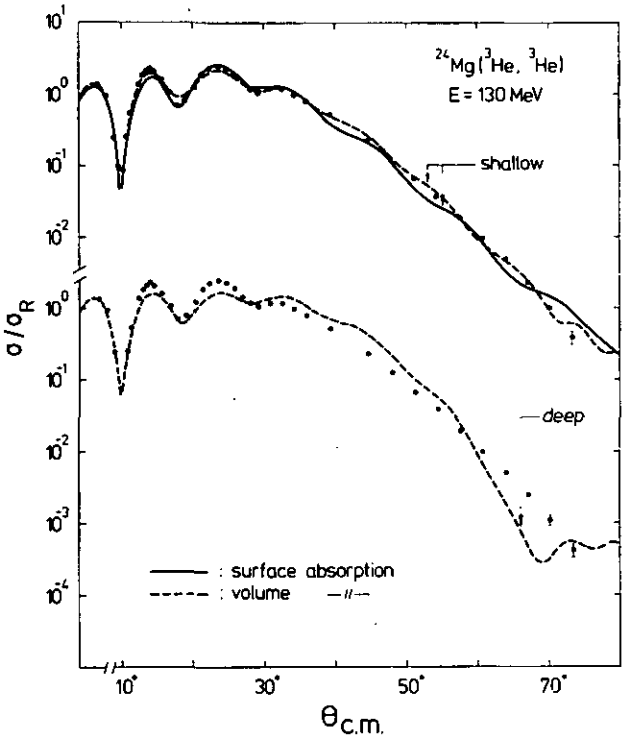


*Figure 1:*
*Comparison between the experimental data and the optical model predictions for the 130 MeV $^3$He scattered on $^{24}$Mg.*

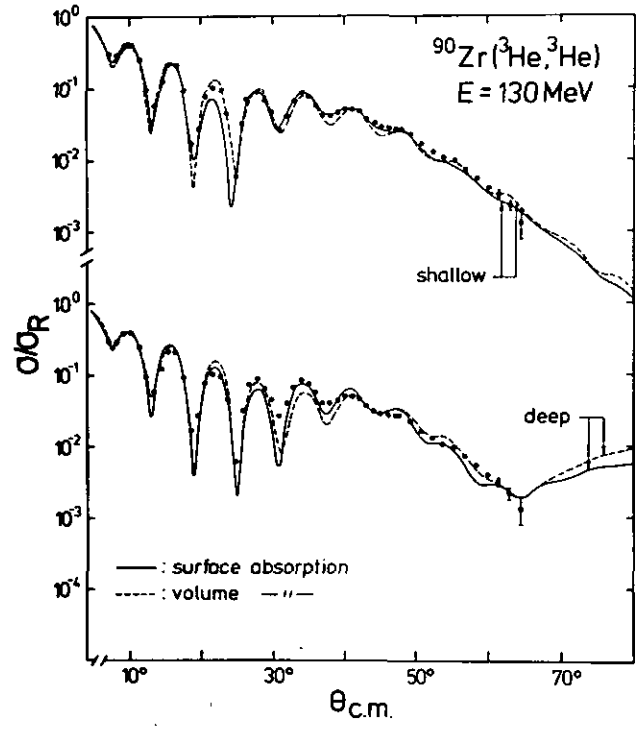


*Figure 2:*
*As for fig. 1 but for $^{90}$Zr.*

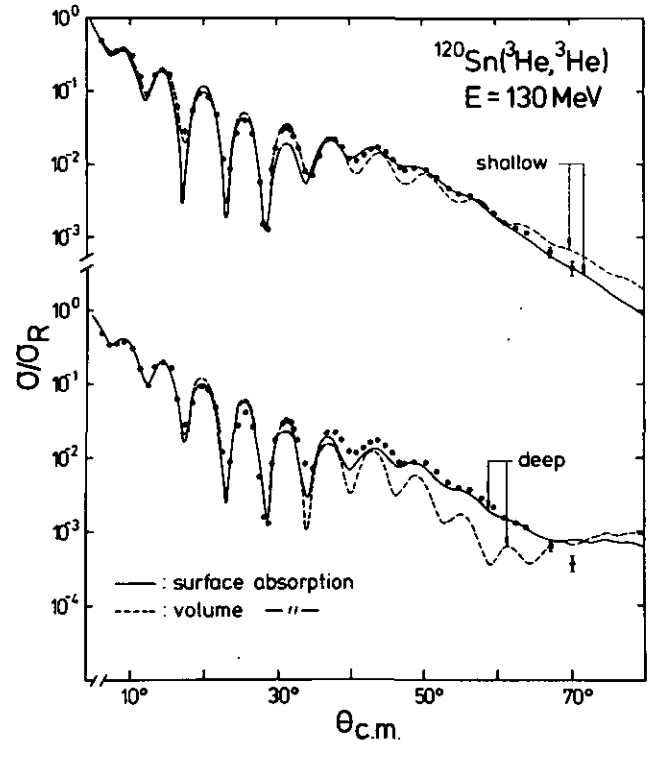


*Figure 3:*
*As for fig. 1 but for $^{120}$Sn.*

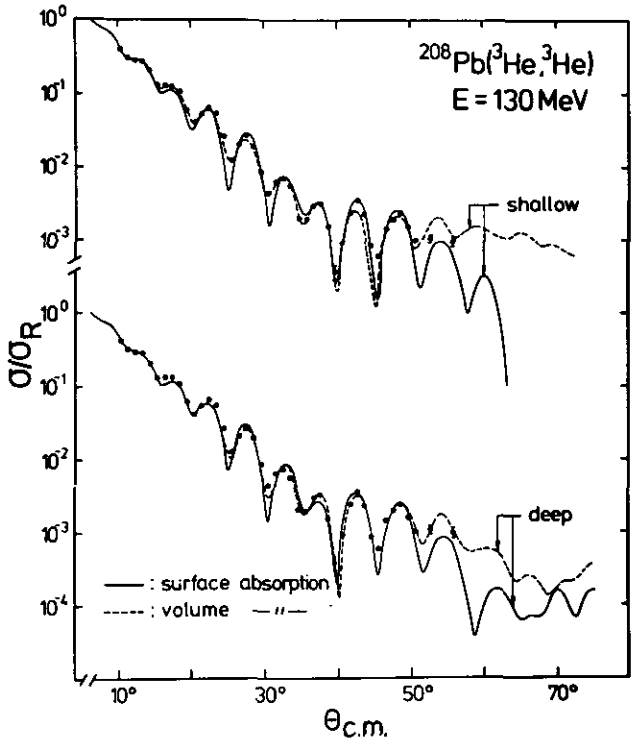


*Figure 4:*
*As for fig. 1 but for $^{208}$Pb.*

*Table 1:*
*Optical model parameters for the 130 MeV $^3$He scattering on $^{24}$Mg, $^{90}$Zr, $^{120}$Sn and $^{208}$Pb*

| Absorption | Target Nucleus | V (MeV) | $r_V$ (fm) | $a_V$ (fm) | W (MeV) | $r_W$ (fm) | $a_W$ (fm) | $J_R$ (MeV·fm$^3$) |
|---|---|---|---|---|---|---|---|---|
| SURFACE | $^{24}$Mg | 85.0 | 1.264 | 0.752 | 14.3 | 1.356 | 0.776 | 340 |
| | $^{90}$Zr | 100.0 | 1.243 | 0.770 | 20.5 | 1.222 | 0.835 | 319 |
| | | 155.0 | 1.257 | 0.613 | 28.1 | 1.101 | 0.894 | 480 |
| | $^{120}$Sn | 120.0 | 1.194 | 0.875 | 27.3 | 1.173 | 0.847 | 347 |
| | | 181.5 | 1.159 | 0.788 | 35.6 | 1.066 | 0.951 | 469 |
| | $^{208}$Pb | 130.0 | 1.149 | 0.919 | 31.6 | 1.242 | 0.732 | 325 |
| | | 179.7 | 1.115 | 0.875 | 34.5 | 1.204 | 0.795 | 408 |
| VOLUME | $^{24}$Mg | 95.4 | 1.197 | 0.907 | 24.2 | 1.587 | 0.645 | 384 |
| | | 140.0 | 1.022 | 0.952 | 25.9 | 1.587 | 0.638 | 423 |
| | $^{90}$Zr | 105.0 | 1.211 | 0.832 | 22.7 | 1.515 | 0.655 | 321 |
| | | 179.6 | 1.168 | 0.715 | 26.8 | 1.450 | 0.752 | 473 |
| | $^{120}$Sn | 105.0 | 1.191 | 0.869 | 19.4 | 1.553 | 0.724 | 301 |
| | | 180.0 | 1.141 | 0.810 | 28.2 | 1.488 | 0.726 | 450 |
| | $^{208}$Pb | 115.0 | 1.182 | 0.857 | 17.2 | 1.551 | 0.769 | 304 |
| | | 180.0 | 1.092 | 0.902 | 17.8 | 1.538 | 0.757 | 419 |

1) For all four target nuclei studied here the shallow family ($J_R \approx$ 330 MeV fm$^3$) of the real part of the $^3$He optical potential was found to give consistently good fits to the data. This is in agreement with the results obtained by other authors[1,2].

2) For the shallow family it was found that the surface and the volume types of absorption give essentially equivalent fits. Comparison between the two types of fit can be seen in figs. 1–4. This result disagrees with that reported in refs.[2,3,4]. For the surface absorption, table 1 shows that the geometrical parameters $r_W$ and $a_W$ do not exhibit any systematic difference from $r_V$ and $a_V$ (e.g. $r_W < r_V$ and $a_W < a_V$) as found in ref.[5]. In particular for $^{208}$Pb, which was studied in ref.[5] at 71 MeV, $r_W$ and $a_W$ are found to be larger and smaller than $r_v$ and $a_v$, respectively, a feature oppositve to that found previously. For the volume absorption, the imaginary potential was found to have consistently larger radius and smaller diffuseness than those of the real part.

3) As a result of an extensive search, it was generally found possible to obtain deep potentials ($J_R \approx 450$ MeV fm$^3$) although the present experimental data (except those for $^{208}$Pb) extend considerably into the refractive region. For $^{120}$Sn the best-fit using the volume absorption is very poor for $\Theta > 40^\circ$, whereas for $^{24}$Mg it was not possible to obtain any fit with the surface absorption. Compared to those of the shallow family, the „deep" theoretical curves exhibit a stronger oscillation in the refraction region and at large enough angles cease to follow the downward exponential trend. The same behaviour was also observed for $^{58}$Ni at 83.5 MeV[6]. It may be interesting physically to extend the measurement at this high energy to angles in the backward hemisphere to see whether the elastic cross section continues to decrease exponentially (as the shallow potential predicts) or behaves differently. However, in the region where the elastic cross sections are very small, the contribution from other processes, as has been shown in ref.[6], may be significant. This casts doubt to the validity of the application of the standard optical model analysis to this region and thereby puts the procedure to eliminate the discrete ambiguity on the basis of large angle data in question.

### References


[1] C.B. Fulmer, J.C. Hafele, Phys. Rev. C8 (1973) 172
[2] D.A. Goldberg, S.M. Smith, Annual Report, University of Maryland, 1973, p. 22
[3] P.P. Urone, L.W. Put, B.W. Ridley, G.D. Jones, Nucl. Phys. A167 (1971) 383
[4] C.B. Fulmer, J.C. Hafele, Phys. Rev. C5 (1972) 1969
[5] C.B. Fulmer, J.C. Hafele, N.M. Clarke, Phys. Rev. C12 (1975) 87
[6] J.R. Shepard, P.D. Kunz, J.J. Kraushaar, Phys. Lett. 56 (1975) 135 and references therein


## 1.3. Elastic Deuteron Scattering


J. Bojowald, C. Mayer-Böricke, M. Rogge, and P. Turek


Measurements and data analyses to investigate the elastic deuteron scattering in the energy range of the JULIC isochronous cyclotron were continued. The analysed beam was used but with partly more opened slits than in the standard analysing mode. In this way the energy resolution of the beam is decreased, but it was possible to measure with more beam intensity and stable geometrical conditions of the beam. The semiconductor telescopes developed in this institute[1] were used. The usual ΔE-E technique was performed with preamplifiers modified for higher energies.

The data at 85 MeV incident energy were completed and some other measurements were carried out at 59 MeV. Dead time, loss of efficiency due to radiation damage and due to nuclear reactions in the Ge(Li)-detector, and deviations of the beam from the optical axis were taken into account in the data evaluation. The correction for losses due to nuclear reactions in the Ge(Li)-detector is about 8 % at 85 MeV and 4 % at 59 MeV incident energy.

The data were analysed in the framework of the optical model using the program „MAGALI"[2] with Woods-Saxon-type form factors. The imaginary potential W was of surface type as is usual in deuteron scattering analyses. The radial dependence of the spin-orbit potential was of the Thomas type. The analyses showed, that also in elastic deuteron scattering, the influence of the rainbow scattering is important. This effect was described by Goldberg et al.[3] firstly for $^4$He-scattering: If data with an angular range up to the rainbow angle are analysed, different discrete parameter families give equally good fits to the experimental data. But by taking into account also data beyond the rainbow angle only one potential family is strongly preferred. The rainbow angle in deuteron scattering at 85 MeV is in the region of 75° for middle weighted target nuclei.

In table 1 the parameters are listed for the nuclei $^{27}$Al, $^{89}$Y, $^{120}$Sn, $^{208}$Pb investigated at 85 MeV incident energy. They are the result of analyses which used the same geometrical parameters for the spin-orbit-potential as for the real potential.

*Table 1:*
*List of optical parametewrs (best fit) at 85 MeV incident energy*

| | $^{27}$Al | $^{89}$Y | $^{120}$Sn | $^{208}$Pb |
|---|---|---|---|---|
| V (MeV) | 74.6 | 79.9 | 81.1 | 83.1 |
| $r_v$ (fm) | 1.05 | 1.10 | 1.10 | 1.15 |
| $a_v$ (fm) | 0.86 | 0.91 | 0.95 | 0.89 |
| W (MeV) | 10.1 | 13.1 | 14.3 | 14.9 |
| $r_w$ (fm) | 1.20 | 1.24 | 1.19 | 1.19 |
| $a_w$ (fm) | 0.87 | 0.83 | 0.91 | 0.91 |
| $V_{LS}$ (MeV) | 9.5 | 12.2 | 12.2 | 9.4 |
| $r_{LS}$ (fm) | 1.05 | 1.10 | 1.10 | 1.15 |
| $a_{LS}$ (fm) | 0.86 | 0.91 | 0.95 | 0.89 |
| $\chi^2/N$ | 1.1 | 0.9 | 0.9 | 1.1 |
| $I/2A_T$ (MeV fm$^3$) | 314 | 298 | 294 | 309 |

### References


[1] G. Riepe and D. Protic, Nucl. Instr. 101 (1972) 77
[2] Optical Model Program 'MAGALI'; J. Raynal, CEN-Saclay, France
[3] D.A. Goldberg and S.M. Smith, Phys. Rev. Lett. 29 (1972) 500


## 1.4. Concentration of Octupole-Strength in Alpha-Scattering on $^{27}$Al


C. Mayer-Böricke, W. Oelert, A. Kiss M. Rogge, P. Turek, S. Wiktor


In the last Annual Report[1] investigations on inelastic scattering of α-particles on $^{27}$Al were reported. Special attention was paid to the excitation energy range of 4 to 14 MeV. Here a strong compact group of levels with maximum intensity around 7.2 MeV excitation energy having a bell shape like envelope with a FWHM of about 4 MeV was observed. The main property of the compact group turns out to be that the entire group as well as all observed peaks with excitation energies ≥ 6.0 MeV can be rather well repreduced by a linear superposition of L = 2 and L = 3 DWBA curves in a cross section ratio of 1 : 2, respectively.

To test the notion that the peak like regions of the compact level group (see fig. 1 of Ref.[1]) are really due to a superposition of at least two levels, a single high resoltion spectrum (90 keV FWHM) was measured[2]. The figure shows this energy spectrum of 172.5 MeV α-particles scattered from $^{27}$Al. The compact group of levels is still clearly observed. However, a striking doublet structure of several former unresolved peaks is observable. This supports the use of incoherent superpositon of two DWBA curves with different L in describing the experimental angular distributions.

For the total level group an upper limit for the depletion of the corresponding energy weighted sum rule limit was found to be $9^{+8}_{-4}$% of the E3 isoscalar strength.

The analysis of the angular distribution of the entire compact level group in $^{27}$Al gives a L = 3 cross section of ≤ 50 mb/sr at 8° c.m.[1]. In (α,α') experiments on $^{28}$Si[3] a strong peak shows up at 6.88 MeV excitation energy (known 3$^-$, 4$^+$ doublet). The angular distribution for the yield of this peak can well be described by L = 3 DWBA calculations. For this state 8 % of the total E3-EWSR limit is observed with a cross section of 43 mb/sr at 8° c.m. This rather good agreement supports the conjecture that the E3 strength in $^{28}$Si is split up in $^{27}$Al, possibly due to a weak coupling situation involving the $d_{5/2}$ proton hole state of $^{27}$Al.

### References


[1] C. Mayer-Böricke, W. Oelert, A. Kiss, M. Rogge, P. Turek, S. Wiktor, Annual Report 1976, KFA-IKP 1O/77 p. 10, and to be published in Nucl. Phys. A 293 (1977) 189
[2] *The help of Dr. G. Riepe and D. Protic is appreciated*
[3] K.T. Knöpfle, G.J. Wagner, A. Kiss, M. Rogge, C. Mayer-Böricke, Th. Bauer, Phys. Lett. 64B (1976) 263 and private communication

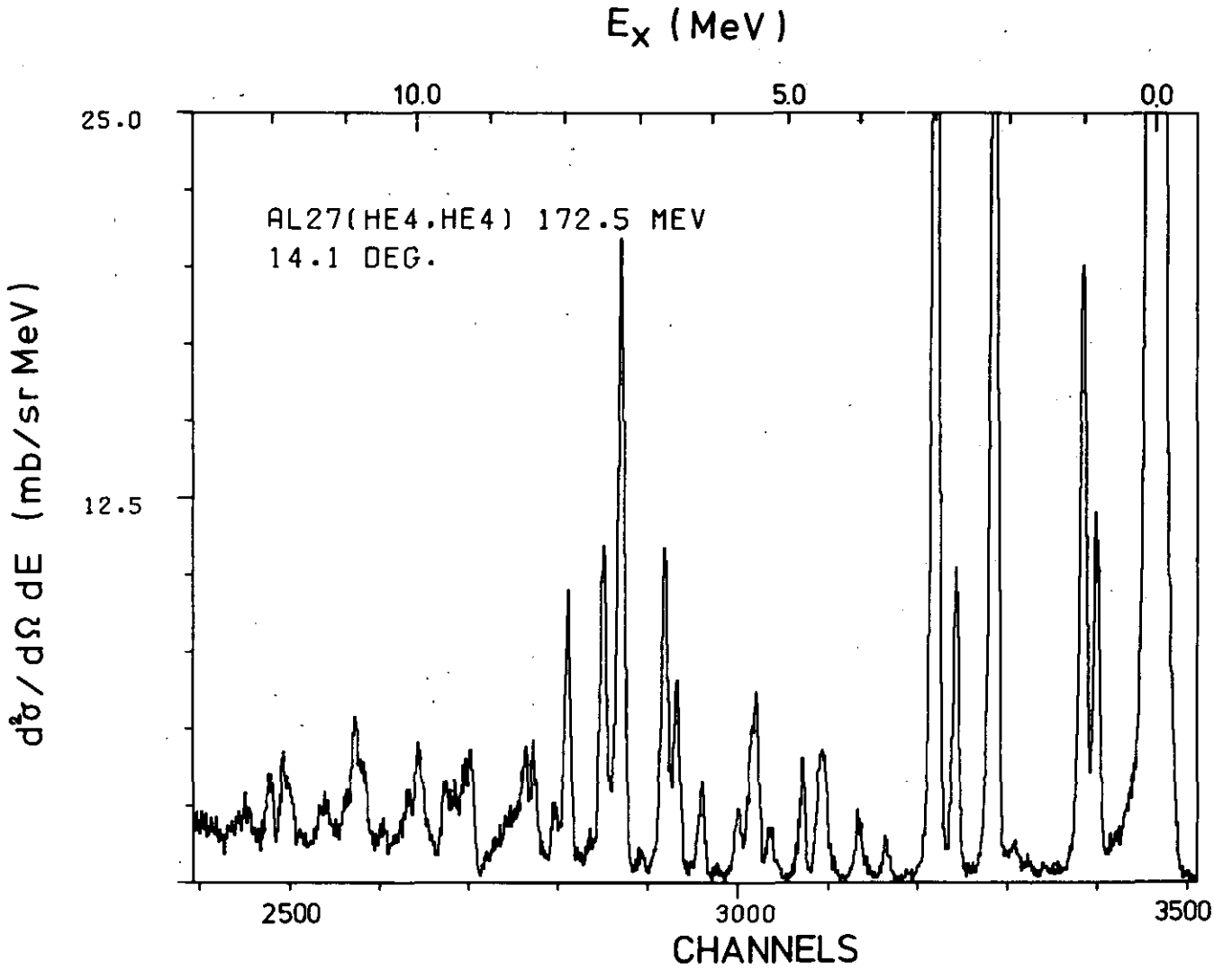


*Figure 1:*
*Energy spectrum of the reaction $^{27}Al$ ($\alpha,\alpha'$)*

## 1.5. Fine Structure of the Giant Quadrupole Resonance in $^{27}$Al

C. Mayer-Böricke, A. Kiss, M. Rogge, P. Turek, and S. Wiktor

The fine structure of the isoscalar giant quadrupole resonance (GQR) in $^{27}$Al was studied by inelastic $\alpha$-scattering at different incident energies. Fig. 1 shows an expanded view of the GQR region in the inelastic $\alpha'$ spectrum for incident $\alpha$ energies of 145 and 172.5 MeV. The fine structure of the GQR, excited selectively in ($\alpha,\alpha'$) is consistently seen in these spectra.

In addition (p,p'), (d,d') and ($^3$He,$^3$He') spectra were measured. As can be seen in Fig. 1 these data show again the GQR fine structure as observed in the ($\alpha,\alpha'$)-spectra. For (d,d) scattering this is to be expected since also in this case the isoscalar E2 resonance is excited selectively. Inelastic $^3$He and p scattering, however, could excite the GQR as well as the isovector giant dipole resonance (GDR) which is also located in this region of excitation energies. The surprising fact that in these two cases only the fine structure of the GQR is seen leads to the conclusion that the GDR contribution to the measured cross section must be small.

This result allows interesting conclusions with respect to models used for the interpretation of the GDR. Actually, the analysis of the

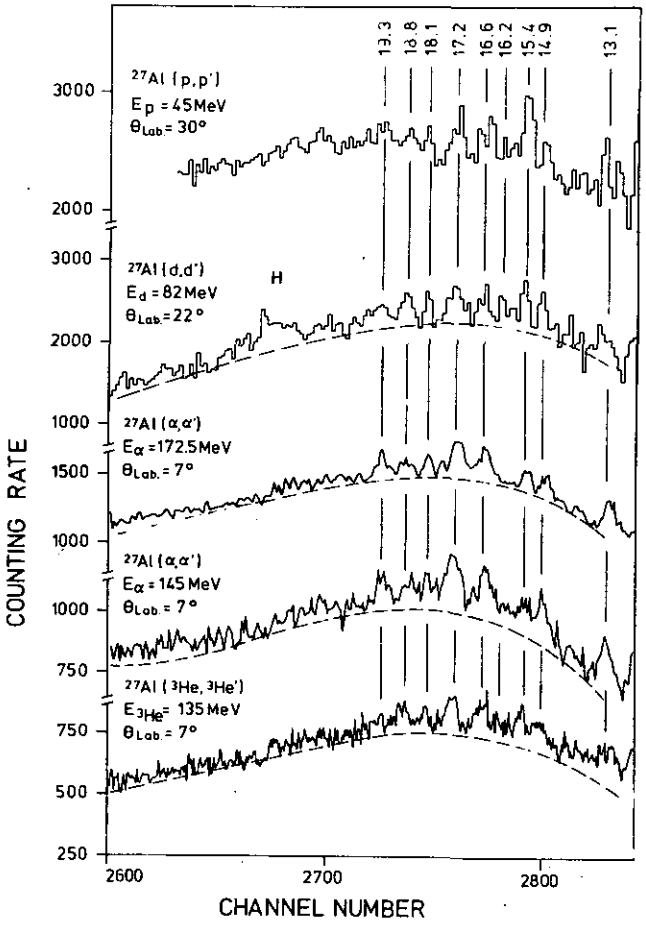


(p,p') giant resonance data shows that the Goldhaber-Teller (GT) model is strongly favoured[1] over the Steinwedel-Jensen (SJ) model for the description of the GDR in $^{27}$Al. It is only the GT model[2] which in accordance with our experimental results provides a small GDR contribution to the cross section so that the remaining part of the experimental cross section can be attributed to the GQR. The SJ model[2], on the other hand, would misinterpret the whole experimental GR cross section as being due to the excitation of the GDR.

### References


[1] C. Mayer-Böricke, Report of KFA Jülich; Jül-1436, July 1977
[2] F.E. Bertrand, Ann. Rev. Nucl. Sci. 26 (1976) 458


*Figure 1:*
*Comparison of fine structure in the GR region of $^{27}$Al obtained in inelastic scattering of protons, deuterons, $^{3}$He and alphas.*

## 1.6. Study of the Giant Quadrupole Resonance in $^{40}$Ar


J.P. Didelez, C. Mayer-Böricke, W. Oelert, M. Rogge, P. Turek, S. Wiktor


The Giant Quadrupole Resonance (GQR) in $^{40}$Ar has been studied by 172.5 MeV α particle inelastic scattering. The main goal was to record data as clean as possible both by using a very pure target and taking advantage of the larger peak to underlying continuum ratio generated by high energy projectiles[1].

The experiment was carried out using the unanalysed 172.5 MeV α beam from the Jülich isochronous cyclotron. Argon gas was contained in a gas cell with 2 mg/cm$^2$ Havar windows at a pressure of about 350 Torr. We used the highest purity of the Ar gas easily available on the industrial market (99.9997 Vol%). Reaction products were detected and identified with 2 ΔE-E telescopes (3 degrees apart) consisting of a 2000 μ Si surface barrier followed by a 2.4 cm thick home made Germanium detector. Due to the particular geometry of a gas target the total angular acceptance of the detectors was fairly large and equal to 1.3° and 1.55°. The beam energy spread, straggling in the target and reaction kinematics limited the overall energy resolution to 350–650 keV depending on the scattering angle. Spectra were taken at lab angles from 7.2° to 42° mostly in steps of 1°. It was checked with empty target runs that even at the smallest angles the window contribution to the background was smooth.

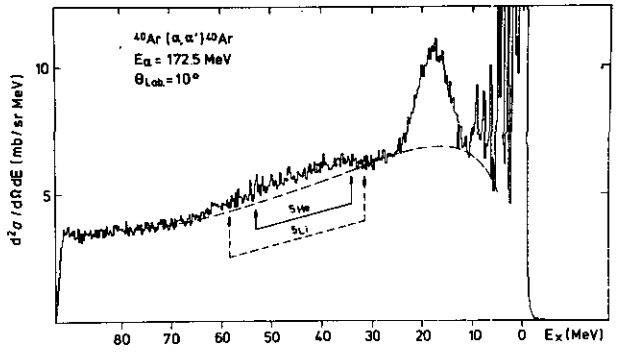


*Figure 1:*
*Spectrum of α particles recorded at $\Theta_{Lab} = 10°$ The arrows indicate the kinematic limits for α-decay of the intermediate formations of $^{5}$He and $^{5}$Li; the dashed line the empirical background.*

All spectra are characterized by a well defined broad peak at the expected position of the GQR (Ex = 63 A$^{-1/3}$), fairly easy to distinguish from the underlying α continuum. Fig. 1 shows a typical spectrum recorded at 10°; it can be noted that the peak to background ratio is considerably larger than in inelastic studies at smaller energies (100 MeV)[2]. The GR peak showed a fairly symmetrical shape throughout the angular range spanned by the data. It appeared at an excitation energy of 17.65 ± 0.8 MeV with a FWHM of 6.94 ± 0.56 MeV.

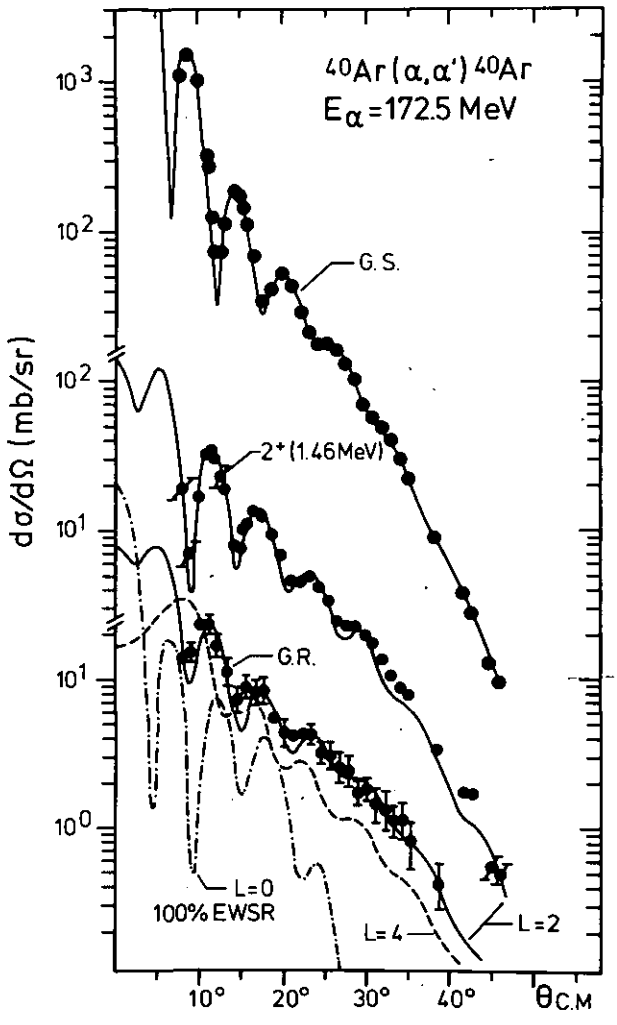


In fig. 2 are displayed the angular distributions for the ground state, the first excited state and the GR peak. It is immediately apparent that the diffraction pattern of the GR is very close to the one of the known 2⁺. The continuum underlying the GR was considered as a background and subtracted empirically. Various independent evaluations using different forms of the background (linear, quadratic) and different procedures (fit, graphic analysis) gave rather consistent results.

Given the selectivity of α scattering, the experimental results were compared with calculations (DWUCK)[3] for isoscalar transitions only and the results are displayed in fig. 2. The calculation with L=2 provides excellent fits to the experimental data except for a small angle shift (1°) towards larger angles in the case of the GR. A similar small shift was already noted by Youngblood[2] in his survey of GR studies by 90 MeV α scattering. The respective deformation parameters are $\beta_2^2(1.46) = 0.035$ and $\beta_{2GR}^2 = 0.029$ which correspond to 4.2 ± 0.5 % and 61 ± 15 % of the E2 EWSR. It is clear from fig. 2 that the angular distribution corresponding to a monopole transition falls off to fast with increasing angle to fit the data. In addition the cross sections are too small, even if the L=O EWSR is supposed to be completely exhausted. Finally, given the experimental points at small angles, a possible L=4 contribution would be very small.

### References


[1] A. Kiss, C. Mayer-Böricke, M. Rogge, P. Turek, S. Wiktor, Phys. Rev. Lett, Vol. 37, 1188 (1976)
[2] D.H. Youngblood, T.M. Moss, C.M. Rozsa, J.D. Bronson, A.D. Bacher, D.R. Brown, Phys. Rev. C13, 994 (1976)
[3] P.D. Kunz, University of Colorado, Boulder, unpublished


◀ *Figure 2:*
*Angular distributions corresponding to the G.S., the first 2⁺ and the G.R. All curves are calculated. The GS fit provided OM parameters to generate the inelastic angular distributions.*

## 1.7. Dominance of α-Decay from the Isoscalar Giant Qudrupole Resonance in $^{16}O$


H. Breuer*), K.T. Knöpfle*), C. Mayer-Böricke, P. Paul*), M. Rogge, P. Turek and G.J. Wagner*)


The $^{16}O(\alpha,\alpha'c)$ experiment at 155 MeV which was briefly described in the last annual report[1] is now fully analyzed. In this experiment the emission of charged particles c from the isoscalar giant quadrupole resonance (GQR) in $^{16}O$ (ref.[2]) has been studied by angular correlation measurements. As a result of the coincidence requirement the background (see fig. 1a) is strongly reduced and the GQR becomes clearly visible (fig. 1b). A most interesting observation is the strong decay by α-emission notably leading to the ground state (fig. 1c) and first excited state of $^{12}C$ (fig. 1d).

As fig. 2 shows, angular correlations may be fitted reasonably well assuming PW (or DW, fig. 2a) substate populations. Interestingly, the striking forward-backward asymmetry of the $\alpha_o$ and $\alpha_1$ (not $p_o$!) angular correlations is easily explainable by assuming interference of $2^+$ and $3^-$ resonances in $^{16}O$ with $\sigma_3/\sigma_2 \sim 0.01$ only. By this angular correlation measurement the spin 2 of the isoscalar resonance at $<E_x> = 21$ MeV in $^{16}O$ was thus unambiguously determined.

By integrating the experimental angular correlations, branching ratios into the various decay channels were obtained. Between 17.9 and 27.3 MeV of excitation energy in $^{16}O$ 13, 36 and 9 % of the E2 energy weighted sum rule were found in the $\alpha_o$, $\alpha_1$ and $p_o$ channels, respectively. We conclude that the dominant decay mode of the isoscalar GQR in $^{16}O$ proceeds by α-emission.

Prompted by the success of this coincidence experimented we have started a $^{28}Si(\alpha,\alpha'c)$ experiment with improved techniques.


*) Max-Planck-Institut für Kernphysik, Heidelberg


### References


[1] K.T. Knöpfle et al., Annual Report Jülich 1976, KFA-IKP 1O/77, p. 14
[2] K.T. Knöpfle et al., Phys. Rev. Lett. 35 (1975) 779

*Figure 1:*
*Spectrum of inelastically scattered α' -particles at $\vartheta_{LAB} = 14^{\circ}$ (a) without coincidence requirement, (b) in coincidence with all singly and doubly charged reaction products emitted at -65° (top) or with protons of more than 4 MeV (black area); (c) in coincidence with α-particles leading to the ground state or (d) the first exited state of $^{12}C$.*

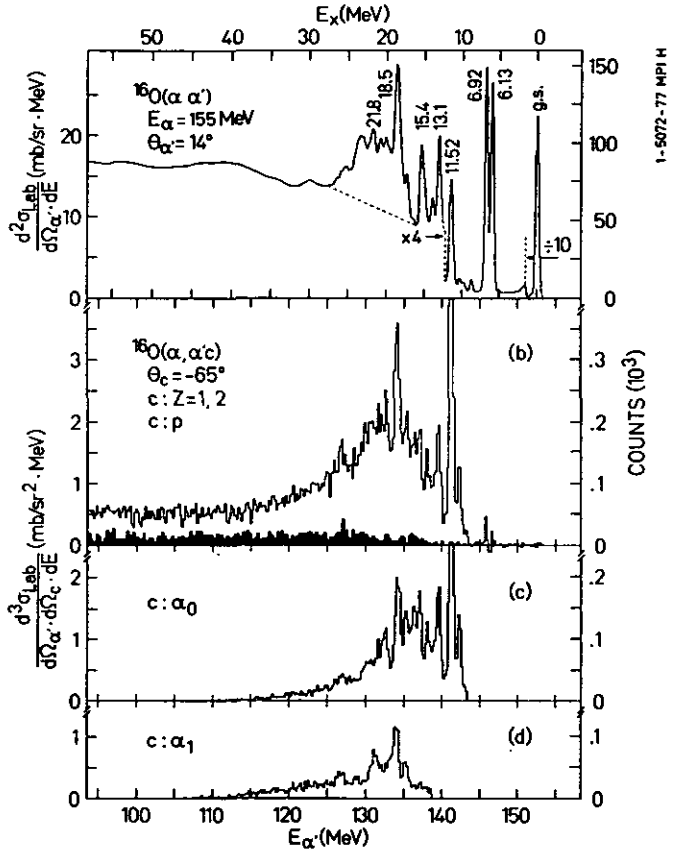


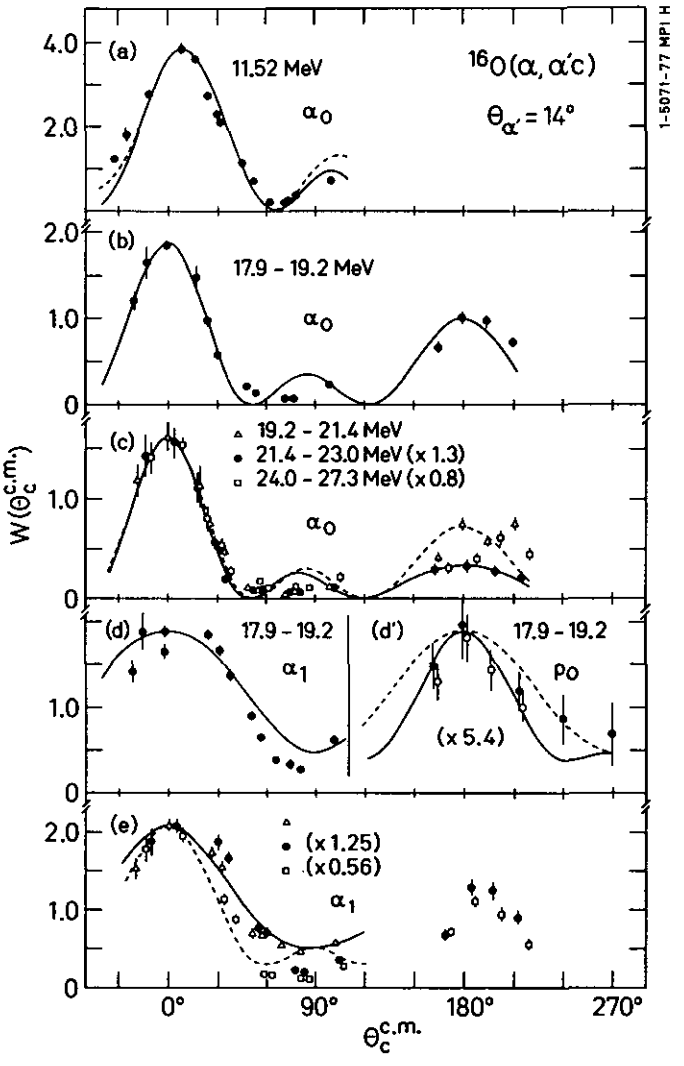


*Figure 2:*
*Measured angular correlations of $p_o$, $\alpha_o$ and $\alpha_1$-decay from various regions of excitation energy in $^{16}O$. The angle $\Theta^{cm}$ is measured with respect to the $^{16}O$ recoil direction. In (d') open points represent data taken at $\Theta^{cm} - \pi$. The curves represent angular correlations calculated under various assumptions on substate populations and contributing partial waves..*

## 1.8. Charged Particle Decay of the Giant Resonance in $^{27}Al$

A. Djaloeis, H. Machner, M. Manko, C. Mayer-Böricke, M. Rogge and P. Turek

The existence of giant resonances (GR) centered at $E_x \simeq 63\ A^{-1/3}$ MeV in nuclei has been experimentally established[1]. Although deviations are observed in very light nuclei[2] such as $^{24}Mg$ and $^{27}Al$, the GR generally appears, in inelastic hadron spectra for example, as a broad structure with a width of several MeV.

The excitation of the GR has been interpreted to be predominantly due to the isoscalar collective quadrupole oscillation of the nucleus (ΔL = 2, ΔT = O). This interpretation, so far, has been mainly based on the comparison between the experimental angular distribution of hadrons inelastically scattered to this resonance and the DWBA prediction. However, it is well known that the information extracted from such an analysis may suffer from uncertainties, such as the background subtraction. Since the nucleus excited to the GR region is unstable against particle decay, coincidence measurements, of the type A(x,x'c)B for example, will provide more direct information on the GR character.

Investigations of the decay properties of the GR in $^{27}Al$ has been started at the end of this year by measuring the $^{27}Al(\alpha,\alpha'p)^{26}Mg$ and $^{27}Al(\alpha,\alpha'\bar{\alpha})^{23}Na$ reations. The α'-telescope, which consisted of a 2 mm thick silicon surface barrier ΔE and a 28 mm thick Ge(Li)[3] E detector, subtended a solid angle $\Delta\Omega_{\alpha'}$ of O.192 msr. Two ΔE-E telescopes (each having $\Delta\Omega_{\bar{\alpha}} = 7.42$ msr), located 3O° apart and with thicknesses of 12 μm (ΔE) – 372 μm (E) and 5O μm (ΔE) – 2OOO μm (E), were used to detect the low energy alphas

($\bar{\alpha}$) and protons ($\bar{p}$), respectively. Charged particles that penetrated both the $\Delta E$ and E detectors were rejected by means of a veto detector. An electronic module[4] operating on the basis of the Bethe-Bloch formula was used for particle identification.

An $\alpha$-beam of 172.5 MeV from JULIC was focussed on the 1.3 mg/cm$^2$ $^{27}$Al target. The $\alpha'$-telescope was located at $\Theta_L$ = 14°, where an L = 2 angular distribution has a maximum. The $\bar{\alpha}$-telescope was placed at $\Theta_L$ = -67.5°, which is the recoil angle of $^{27}$Al at $E_x$ = 20 MeV. The $\bar{p}$-telescope was positioned at $\Theta_L$ = -97.5°. The three energies $E_{\alpha'}$, $E_{\bar{\alpha}}$, and $E_{\bar{p}}$ and the flight time difference between $\alpha'$ and a decay particle $\bar{\alpha}$ or $\bar{p}$ were recorded as 4-parameter list-mode data.

Figure 1 shows the partial level scheme of $^{27}$Al, $^{26}$Mg and $^{23}$Na relevant for the $^{27}$Al($\alpha,\alpha'\bar{\alpha}$) and $^{27}$Al($\alpha,\alpha'\bar{p}$) reactions. The upper part of fig. 2 shows an $\alpha'$-spectrum at 14° as obtained from the usual single telescope measurement[2]. The GR appears as a predominant broad structure at $12.5 \lesssim E_x \lesssim 27$ MeV. An $\alpha'$-spectrum coincident with $\alpha$-particles is shown in the lower part of fig. 2. In spite of low statistics the following features are observed:

a) There appears to be a broad structure in the excitation energy region $12.5 \lesssim E_x \lesssim 36$ MeV. In the region $12.5 \leq E_x \leq 27$ MeV the enhancement can be related to the $\alpha$-decay of the GR. A statement on the physical significane of the structure in the region $27 \lesssim E_x \lesssim 36$ MeV will have to wait until data with better statistics are obtained.
b) Compared to the single telescope measurement it can be seen that the background under the GR peak is reduced by a factor of about 6.

In an $\alpha'$-spectrum taken in coincidence with p, no clear indication of an enhancement in the GR region was observed. However, the data in this case suffered still from insufficient statistics.

We thank Dr. C. Alderliesten for his help in preparing the experiment.

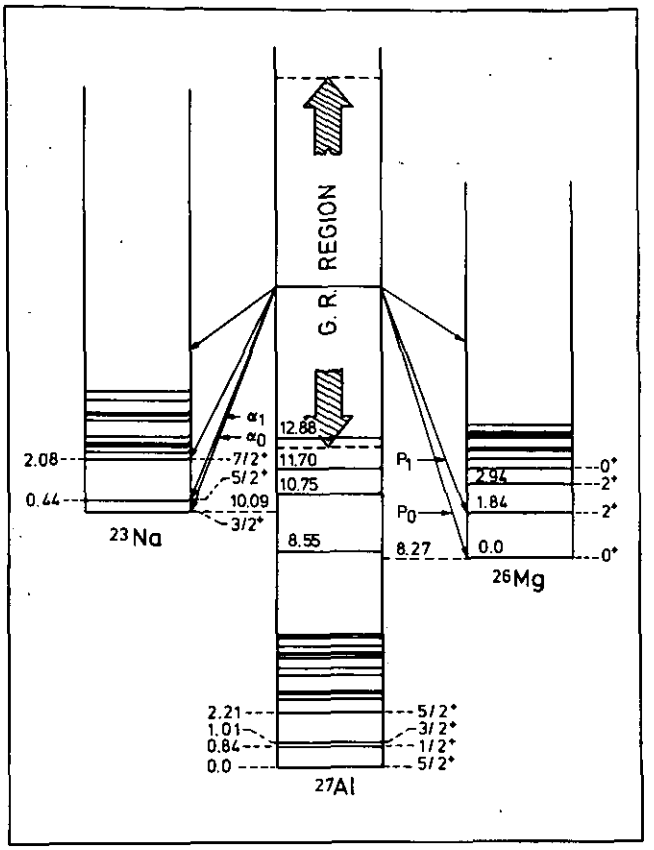


*Figure 1:*
*Partial level scheme of $^{23}$Na, $^{26}$Mg and $^{27}$Al.*


**References**

[1] F.E. Bertrand, Ann. Rev. Nucl. Sci. 26 (1976) 457
[2] A. Kiss, C. Mayer-Böricke, M. Rogge, P. Turek, S. Wiktor, Phys. Rev. Lett. 37 (1976), 1188
[3] G. Riepe and D. Protic, Nucl. Instr. & Meth. 101 (1972) 77
[4] J.B.A. England, Nucl. Instr. & Meth. 106 (1973) 45


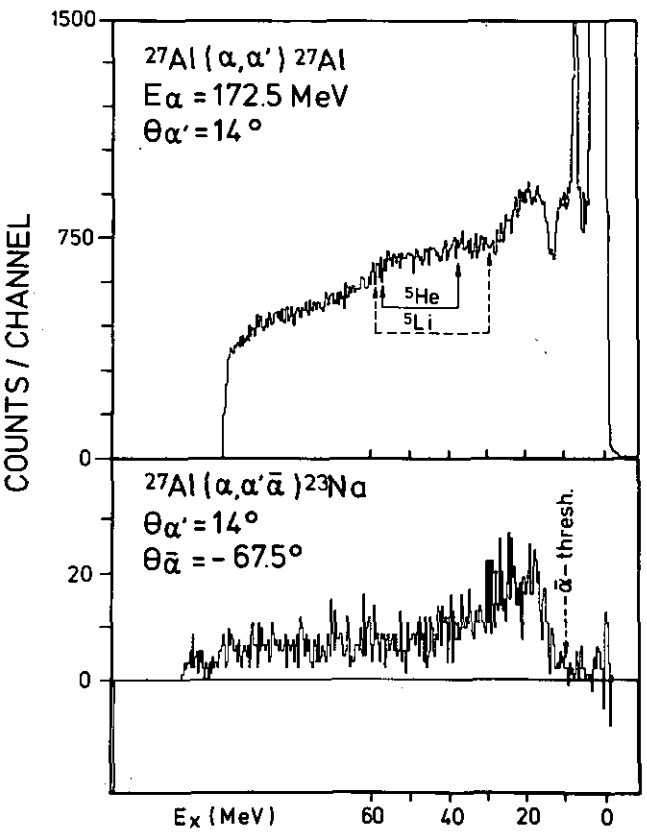


*Figure 2:*
*Singles and coincidence ($\alpha,\alpha'\bar{\alpha}$) reaction taken at $\Theta_{\alpha'}$ = 14° and $\Theta_{\bar{\alpha}}$ = -67.5°.*

## 1.9. Observation of the α-Particle Break-up Process at $E_\alpha^{lab}$ = 172.5 MeV

A. Budzanowski, G. Baur, C. Alderliesten, J. Bojowald, C. Mayer-Böricke, W. Oelert and P. Turek

Spectra of $^3$He emitted in the reactions induced by 172.5 MeV alpha particles on $^{58,60,62,64}$Ni isotopes have been studied in the broad energy range from 50–160 MeV. The experiment has been performed in the 100 cm scattering chamber using two ΔE-E semiconductor telescopes. Each telescope consisted of a 1000 μ commercial silicone surface barrier ΔE transmission detector and a Ge(Li) drifted E detector of the side entry type developed in the detector laboratory of the institute[1].

At forward angles the $^3$He spectra show beside the peaks corresponding to stripping to bound states (neutron transfer) a broad peak of the half width ≃ 40 MeV which is centred around $E_{^3He}$ = 122 MeV in CM system. This broad peak falls off in intensity by several orders of magnitude with increasing angle of reaction. The energy of this peak is much higher than the expected position of the evaporation maximum (≃ 20 MeV). It is natural to assume that this broad peak is connected with some fast one step process namely the break-up of the alpha particle into neutron and helion on the edge of the nuclear potential.

Figure 1 shows the $^3$He spectrum obtained from $^{60}$Ni target. The three distinct sharp lines on the high energy side of the spectrum correspond to 0.068 MeV $1f_{5/2}$, 2.13 MeV $1g_{9/2}$ and 3.5 MeV $1g_{9/2}$ single neutron states in $^{61}$Ni. The strong intensity of these peaks can easily be explained by the angular momentum matching at the nuclear surface which favours $l_n$ = 4 transfer:

$$\ell_n = L_\alpha - L_{^3He} \simeq (k_\alpha - k_{^3He})\, R \simeq 4$$

where $l_n$, $L_\alpha$ and $L_{^3He}$ indicate the angular momenta of the transferred neutron, incoming alpha particle and outgoing helion at the nuclear surface respectively, R denotes the radius of the target nucleus, $k_\alpha$ and $k_{^3He}$ the corresponding wave numbers. The arrow indicates on the energy limit of the stripping into continuum. Below this limit the spectrum exhibits one characteristic broad maximum which we are trying to ascribe to the break-up process. Similar spectra have been obtained for other Ni isotopes.

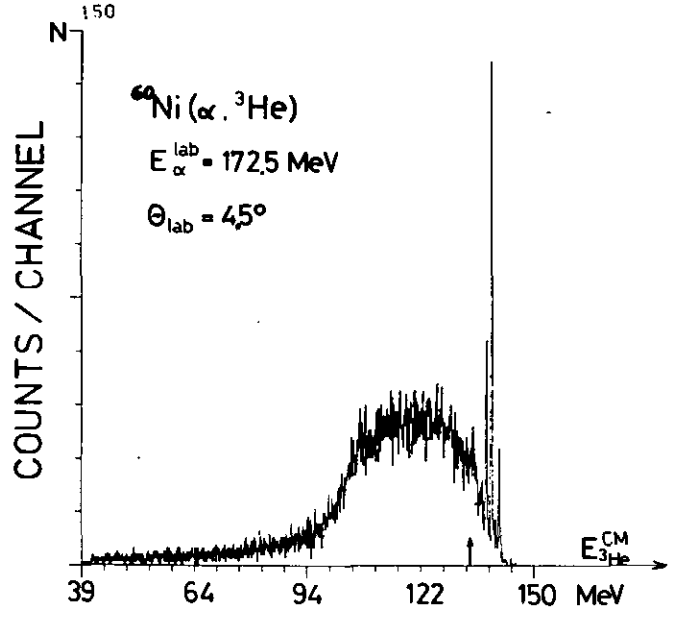


*Figure 1:*
*$^3$He spectrum for the $^{60}$Ni (α, $^3$He) reaction at $\Theta_{lab}$ = 4.5°.*

In Fig. 2 the double differential cross-section $d^2\sigma/d\Omega_{CM}\, dE_{CM}^{^3He}$ for $^{62}$Ni(α,$^3$He) reaction is shown. The cross-sections were calculated by integrating the $^3$He spectra in 6 MeV bins so that the discrete structures are smeared out. The arrows indicate the energies of the ground state stripping and the free break-up process respectively. As can be seen the break-up peak merges with the low energy background around 20°. We notice also that the cross-sections corresponding to large energy transfer fall down with increasing reaction angle less rapidly what may indicate on the importance of multistep processes for helions emerging with lower energies.

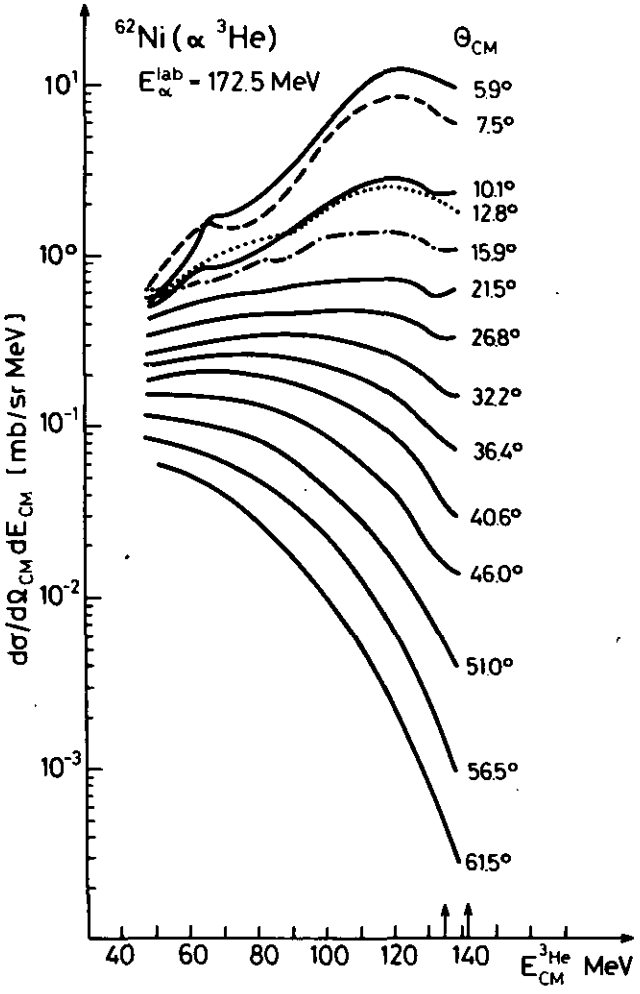


*Figure 2:*
*$d^2\sigma/d\Omega_{CM}\, d\, E_{CM}$ for the $^{62}$Ni(α,$^3$He) reaction at $E_\alpha$ = 172.5 MeV.*

It should be pointed out that the simple spectator particle model[2] predicts the energy of the $^3$He break-up peak at

$$E_{^3He}^{CM} = 104 \text{ MeV}$$

where $E_{^3He}^{CM}$ indicates the CM energy of helion, The width of the peak predicted by the spectator model reflects the momentum distribution of neutron bound in the alpha particle and comes out at the right value Γ ≃ 40 MeV when using harmonic oscillator wave functions for the alpha particle internal state. The 20 MeV shift of the peak position observed experimentally can be partly explained by the influence of the Coulomb barrier which increases the $^3$He energy by about 13 MeV.

Due to the strong binding energy of the neutron in the alpha particle (Q = –20.6 MeV) the break-up can occur only in the nuclear surface of the target nucleus where the gradient of the potential is large at least of the order of 20.6 MeV/$R_a$ ($R_a$ = 1.6 fm denotes the radius of the alpha particle). This means that the distortion effects should be rather strong. Calculation with full DWBA in the continuum are in progress.


**References**

[1] G. Riepe and D. Protic, Nucl. Instr. Meth. 101 (1972) 77; G. Riepe, D. Protic and J. Reich, Nucl. Instr. Meth. 124 (1975) 527; G. Riepe and D. Protic, IEEE Transactions Nucl. Science, NS-22 (1975) 1

[2] G. Baur, Z. Physik A277 (1976) 147


## 1.10. Analysis of the $^{62,64}$Ni(α,τ) Reaction at 172.5 MeV


C. Alderliesten, J. Bojowald, A. Budzanowski, H.V. von Geramb*), M. Kröger*), C. Mayer-Böricke, W. Oelert and P. Turek


To further confirm the superiority of other phenomenological optical model potential form factors[1] than standard Saxon Woods and folding potentials, we have investigated the $^{62,64}$Ni(α,τ) reaction. Thereby we populated the well defined $J^\pi = 5/2^-$ and $9/2^+$ states in $^{63,65}$Ni. Namely in the DWBA T-matrix element, the distorted waves enter in radial integrals which have a finite integrand, practically only in the surface region of the nucleus due to the highly localized form factors. More precisely, in a zero range (ZR) DWBA, the form factors are proportional to the $1f_{5/2}$ and $1g_{9/2}$ radial bound state wave function.

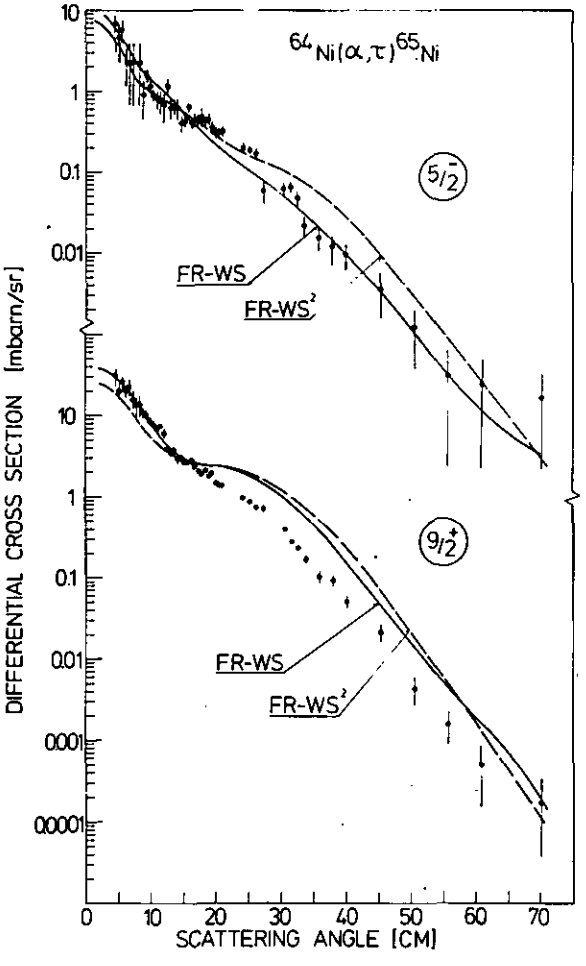


*Figure 1:*
*Angular distributions for $^{64}$Ni (α, τ)$^{65}$ Ni reactions leading to 5/2⁻ ground and 9/2⁺ 1.013 MeV states in $^{65}$Ni.*

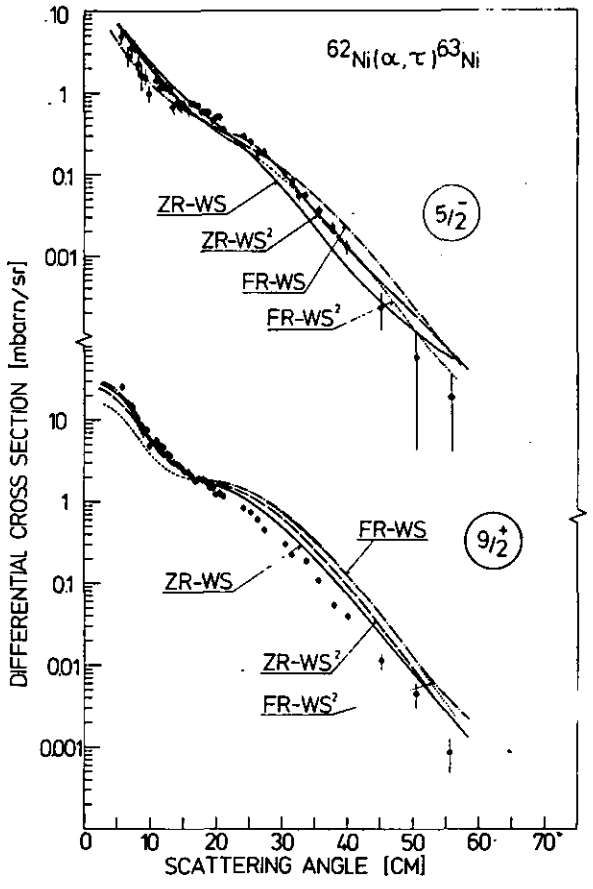


*Figure 2:*
*Angular distributions for $^{62}$Ni (α, τ)$^{63}$ Ni reactions leading to 5/2⁻ 0.087 MeV and 9/2⁺ 1.294 MeV states in $^{63}$Ni.*

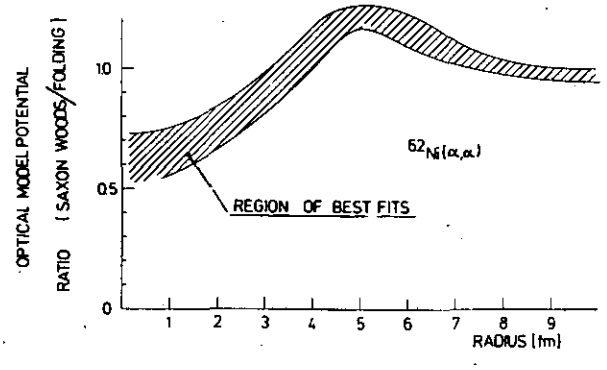


*Figure 3:*
*Ratio of the real part of the phenomenological optical model potential to the folded potential. Upper and lower curves correspond to (SW)² and (SW) potentials respectively.*

Elastic α-scattering data[2] at 172 MeV have been analyzed for $^{58,60,62,64}$Ni isotopes, for scattering angles between 5 and 60°. The $^3$He angular distributions were measured with the same detection system. In the optical model were applied standard Saxon Woods (SW), Saxon Woods Square $(SW)^2$ form factors for the real and imaginary parts, or double folding form factors for the real part respectively. In the transfer analysis we used the final parameters listed in table 1. It is noticeable that the folded potential gives the worst fits in the transfer calculations (as well as for the elastic channel itself). We take this as an indication that the distorted waves are sensitively tested in this reaction and that α-particles penetrate deeply into the nucleus at such high projectile energies. For the folding model we suggest to use a more sophisticated density dependent (and energy dependent) nucleon-α interaction as originally proposed by Bernstein[4]. The quotients of (SW)/Folding and $(SW)^2$/Folding, shown in Fig. 3, show that the density dependence of the interaction should reduce the strength by approximately 50 % with respect to the low density region. A more fundamental approach to further investigate this density dependence in the framework of nuclear matter theory is under way[5].

*Table 1:*
*Optical model parameters*

| Isotope | | V | $r_o$ | $a_o$ | w | $r_i$ | $a_i$ |
|---|---|---|---|---|---|---|---|
| | | MeV | fm | fm | MeV | fm | fm |
| $^{62}$Ni | $^4$He(SW) | 108.84 | 1.256 | 0.797 | 22.20 | 1.572 | 0.623 |
| | $^4$He$(SW)^2$ | 140.84 | 1.361 | 1.316 | 26.42 | 1.672 | 1.197 |
| | $^3$He(SW) | 74.10 | 1.240 | 0.860 | 25.30 | 1.410 | 0.790 |
| $^{64}$Ni | $^4$He(SW) | 112.54 | 1.240 | 0.818 | 21.22 | 1.586 | 0.608 |
| | $^4$He$(SW)^2$ | 154.02 | 1.361 | 1.432 | 20.14 | 1.756 | 1.024 |
| | $^3$He(SW) | 74.10 | 1.240 | 0.860 | 25.30 | 1.410 | 0.790 |

*) Permanent address: I. Institut für Experimentalphysik, Universität Hamburg

### References


[1] A. Budzanowski et al., Phys. Rev. (in print) and IJF-Report 962/PL-1977; Z. Majka et al., Phys. Rev. (in print) and IJF-Report 940/PL-1977
[2] see further contribution in this Ann. Report
[3] N. Willis et al., Nucl. Phys. A204 (1973) 454 Y.R. Shephard, W.R. Zimmermann and J.J. Kraushaar, Nucl. Phys. A275 (1977) 189
[4] A.M. Bernstein, Adv. in Nucl. Phys. Vol. 3 ed. M. Baranger and E. Vogt, Plenum Press (1969) 325
[5] H.V. von Geramb, Hamburg – Internal Theory Report (1977)


## 1.11. $^3$He-induced Reactions on $^{58}$Ni at 130 MeV


A. Djaloeis, C. Alderliesten, J. Bojowald, C. Mayer-Böricke, W. Oelert, P. Turek


Criteria for the elimination of discrete ambiguities in nuclear optical potentials have been proposed by Goldberg and Smith[1]. It was argued that, for that purpose, the elastic scattering data must be measured:

a) at incident energy where the rainbow angle $\Theta_r$ is less than 180° and
b) in an angle range extending beyond $\Theta_r$.

The proposed criteria[1] have been applied to determine the unique $^3$He potential[2]. Some success in resolving the discrete ambiguity has been reported[2,3]. For high energy $^3$He scatterings (e.g. 101 MeV), it was reported that such a procedure was still possible although the measurement did not extend beyond the rainbow angle[3].

The unique real potential was found to be „shallow" characterized by the volume integral $J_R \approx 330$ MeV · fm$^3$. The depth V turned out to be significantly smaller than $n \cdot V_N$[4], where n is the number of nucleons in the projectile and $V_N$ is the depth of the nucleon potential. It is worth noting that the shallow potential is claimed to give a distinctly inferior DWBA description of the transfer reactions compared to the „deep" one[5].

Considering the facts that:

a) the determination of the „unique" optical potential critically depends on the large angle data (namely $\Theta > \Theta_r$) where contributions from processes other than the shape-elastic may be significant and that
b) the deeper potentials are generally required to describe transfer reactions[5],

a natural question poses itself whether it is at all meaningful to describe the large angle elastic scattering data solely in terms of a potential scattering. Indeed, an attempt to answer this question has been pioneered by Shepard, Kunz and Kraushaar[5]. In their analysis of 83.5 MeV $^3$He elastic scattering data on $^{58}$Ni, where the angular range extended to about 40° beyond $\Theta_r$, it was found that the coupling of pickupstripping channels had a large effect on the elastic cross section at back angels. They concluded that, in the framework of their analysis, the deep family gave a fit superior to the shallow. This result solves the discrepancy mentioned above.

In this work the measurement of ($^3$He,d), ($^3$He, $^3$He) and ($^3$He,α) on $^{58}$Ni has been performed at 130 MeV incident energy, which is considerably higher than that in the previous work[5]. The elastic scattering data have been taken in the region $6° \leq \Theta_L > 70°$ ($\Theta_r$ at about 45°), the single nucleon transfer data up to 40° (lab.). With the available data it will be possible to extract the $^3$He optical model parameters in the usual way and test how well these parameters describe the one-nucleon transfer data. Analysis of the data is in progress.

### References


[1] D.A. Goldberg, S.M. Smith, Phys. Rev. Lett. 29 (1972) 500
[2] C.B. Fulmer, J.C. Hafele, Phys. Rev. C8 (1973) 172
[3] D.A. Goldberg, S.M. Smith, Annual Report, University of Maryland, 1973, p. 22
[4] P.E. Hodgson, Nuclear Reactions and Nuclear Structure, Clarendon Press, Oxford, 1971, p. 253
[5] J.R. Shepard, P.D. Kunz, J.J. Kraushaar, Phys. Lett. 56 (1975) 135 and references therein

## 1.12. Investigation of Few-Nucleon Transfer Reactions on Light Nuclei

W. Oelert, A. Djaloeis, C. Mayer-Böricke, P. Turek, S. Wiktor, M. Betigeri

a) Op-Shell Targets

Alpha-like pickup reactions of the type (d,$^6$Li) have been studied in our laboratory throughout the last years. $^{14}$N, $^{16}$O and $^{20}$Ne were employed as target nuclei. The outgoing particles $^6$Li and as a byproduct $^7$Li and $^7$Be were detected in a conventional ΔE–E telescope arrangement in a 1 m diameter scattering chamber.

Extensive Zero-Range and Finite-Range DWBA analyses have been performed in the case of the $^{16}$O(d,$^6$Li)$^{12}$C reaction. In general, rather good fits between theoretical predictions and experimental angular distributions could be achieved. Acceptable agreement with respect to relative spectroscopic factors between both kinds

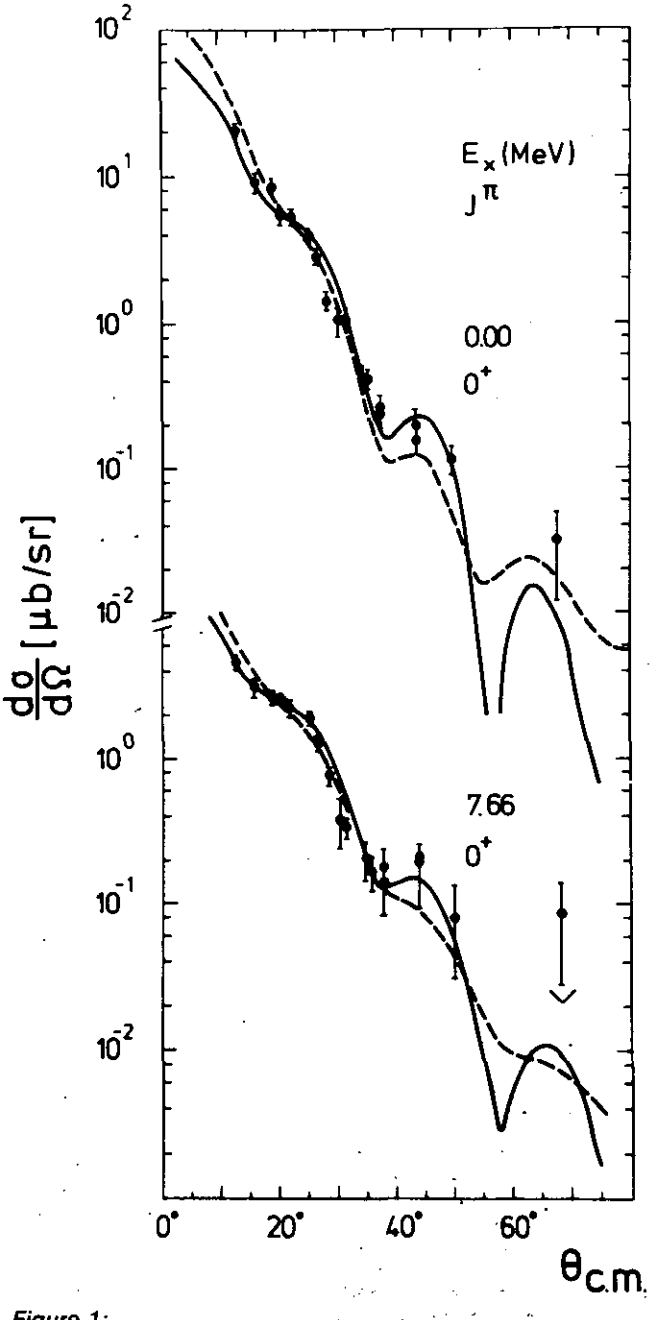


*Figure 1:*
*Angular distributions from $O^+$ states in $^{12}$C populated by the (d,$^6$Li) reaction at $E_d$ = 80 MeV. The solid (dashed) line represents FR (ZR) DWBA calculations.*

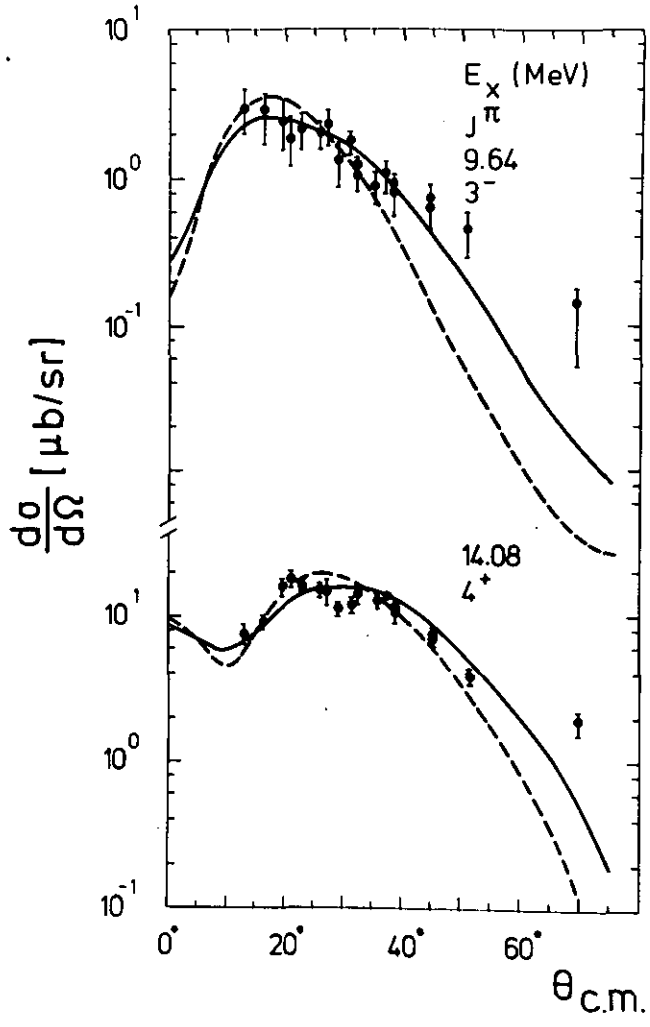


*Figure 2:*
*Angular distributions from known 3$^-$ and 4$^+$ states in $^{12}$C populated by the (d,$^6$Li) reaction at $E_d$ = 80 MeV, curves as in fig. 1.*

of analysis (ZR- and FR-DWBA) is obtained. However, it turns out that the choice of the $^6$Li optical model parameters is essentially critical. Even the relative spectroscopic factors for the members of the g.s. band in $^{12}$C are influenced by the parametersets employed. This may result from the fact that $^6$Li optical model parameters are not available for the exact energy of our investigation and, in addition, that perhaps an energy-dependent set should be used. Furthermore the radius parameter used for determining the bound state wave function is very critical with respect to the consideration of absolute spectroscopic strength. Using this radius as a free parameter by searching for best fits it turnes out that for different combinations of d- and $^6$Li optical potential sets different values of this radius parameter are requiered. For our analysis a radius of R = 1.65 $A^{1/3}$fm has been chosen along with optical model parameters which have been taken from ref.[1]: d and from ref.[2]: $^6$Li. Fits between experimental data and theoretical curves in the framework of the ZR- (dashed line) and FR- (solid line) approximation are shown in fig. 1 (observed $O^+$ states in $^{12}$C) and in fig. 2 (known 9.64 MeV 3$^-$ and 14.08 MeV 4$^+$ states in $^{12}$C).

The analysis for the case of $^{14}$N and $^{20}$Ne as target nuclei is in progress.

b) sd-Shell Targets

Further investigations on the α-like (d,$^6$Li) transfer reaction have been done or are planned for the near future on targets of the sd-shell. The analysis of these experiments is in progress, experi-

mental results in the form of cross sections for the cases of the targets $^{24,25,26}$Mg and $^{40}$Ca are available.

For some nuclei of the sd-shell we try to observe several outgoing channels simultaneously, which have reasonable cross sections and can be observed with one detector setup, using deuterons as projectiles. The aim is to get at least good relative spectroscopic fac tors for nuclei of the sd-shell and to compare those to calculations of Chung and Wildenthal[3].

## References


[1] J.D. Childs, W.W. Daehnick, M.J. Spisak, Phys. Rev. C1O (1974) 217 and „Report of current Research", University of Pittsburgh (1975-1976) 55
[2] L.T. Chua, F.D. Becchetti, J. Jänecke, F.L. Milder, Nucl. Phys. A273 (1976) 243
[3] see contribution in this Annual Report


## 1.13. Alpha Spectroscopic Factors Calculated in the Full sd-Shell Model Space


W. Chung


In conjunction with the investigation of A(d,$^6$Li)B reactions on light nuclei here at Jülich, theoretical alpha spectroscopic factors are being calculated using wave functions generated in large shell-model spaces. In particular, we have used the method described by Bennett[1], with wave functions generated in the full $d_{5/2}$-$s_{1/2}$-$d_{3/2}$ shell-model space using the Chung and Wildenthal interactions[2], to calculate alpha spectroscopic factors for sd-shell nuclei. The alpha particle transition operator is described by wave functions labeled |[f],(λ,μ),L,S,J,> expanded in the j-j basis. Here [f] labels the space symmetry of the wave function, and (λ,μ) are the SU(3) quantum numbers[3]. The wave functions were obtained by diagonalizing the Hamiltonian H = a Q·Q + bM. Here M = $\Sigma_{i<j}$ $P_{ij}$ is the Majorana operator which orders states according to their orbital symmetry [f], and the Q Q interaction is diagonal in the SU(3) representation.

*Table 1:*
*Relative spectrocopic strengths for $^{20}$Ne($^6$Li,d)$^{24}$Mg*

| $E_x$(MeV) | $J^\pi$ | S($^6$Li,d) | S[SU(3)] | S(PW) | S(CW) |
|---|---|---|---|---|---|
| 0.0 | $0^+$ | 1.00 | 1.00 | 1.00 | 1.00 |
| 1.37 | $2^+$ | 0.42 | 0.37 | 0.43 | 0.32 |
| 4.12 | $4^+$ | 0.03 | 0.00 | 0.03 | <0.01 |
| 4.24 | $2^+$ | 0.13 | 0.05 | 0.04 | 0.09 |
| 6.01 | $4^+$ | 0.28 | 0.46 | 0.34 | 0.46 |
| 6.43 | $0^+$ | 3.87 | 0.86 | 0.86 | 0.83 |
| 7.35 | $2^+$ | 0.37 | 0.22 | 0.05 | 0.17 |
| 8.12 | $6^+$ | 0.09±0.04 | 0.15 | 0.00 | 0.03 |
| 8.65 | $2^+$ | 0.22 | | | 0.06 |

Table 1 compares the relative spectroscopic strength (normalized to unity for the ground-state transition) obtained from the present calculation with experimental results and other theoretical predictions for $^{20}$Ne($^6$Li,d)$^{24}$Mg. The experimental strengths are those of Anantaraman et al.[4]. The numbers in the column headed S[SU(3)] were calculated assuming a $(OS)^4$ α-particle transfer between states of pure SU(3)-SU(4) symmetry[4,5]. The numbers in the column headed S(PW) were also calculated assuming a $(OS)^4$ α-particle transfer, with the wave functions for initial and final states generated in an expanded SU(3) basis[6]. However, only the $O^+$ states in both $^{20}$Ne and $^{24}$Mg were generated in the full sd-shell model space, the $J^\pi > O^+$ states were calculated in a truncated space. The numbers in the column headed S(CW) are the results of the present calculation. The initial and final state wave functions were all generated in the full sd-shell model space. The transition operator for the α-particle assumed to be in a $(OS)^4$ state is described by wave functions labeled |[4],(8,O),L,S=O,J,T=O>[7]. Except for the strength of the second $O^+$ level, the theoretical results are in very good agreement with experimental spectroscopic strengths. The present results are very similar to the results of pure-symmetry calculation and the expanded SU(3) basis calculation[6].

Table 2 shows similar comparisons for the relative spectroscopic strength (normalized relative to unity for the L = 2 transition to the $5/2^+$ ground state) for $^{21}$Ne($^6$Li,d)$^{25}$Mg. The experimental strengths are those of Anantaraman et al.[4,8]. For the numbers in the column headed by S(PW), the ground state of $^{21}$Ne was taken to be that determined by Strottman and Arima[9] and the wave functions for $^{25}$Mg were generated in a truncated sd-basis[10]. For the ground

*Table 2:*
*Relative spectrocopic strengths for $^{21}$Ne($^6$Li,d)$^{25}$Mg*

| $E_x$(MeV) | $K^\pi$ | J | ℓ | S($^6$Li,d) | S[SU(3)] | S(PW) | S(CW) |
|---|---|---|---|---|---|---|---|
| 0.00 | $5/2^+$ | 5/2 | 2 | 1.00 | 1.00 | 1.00 | 1.00 |
| | | | 4 | | 0.00 | 0.03 | 0.04 |
| 1.61 | | 7/2 | 2 | 1.90 | 2.20 | 2.32 | 1.69 |
| | | | 4 | | 0.04 | 0.02 | 0.07 |
| 0.58 | $1/2^+$ | 1/2 | 2 | 0.24 | 0.51 | 0.73 | 0.02 |
| 0.98 | | 3/2 | 0 | | 0.49 | 1.01 | 0.43 |
| | | | 2 | 1.94 | 2.92 | 5.19 | 1.77 |
| 1.97 | | 5/2 | 2 | 1.45 | 1.28 | 1.42 | 0.71 |
| | | | 4 | | 0.01 | 0.02 | 0.31 |
| 2.74 | | 7/2 | 2 | 0.98 | 0.01 | 0.23 | 0.59 |
| | | | 4 | 1.17 | 1.32 | 4.66 | 2.04 |
| 2.56 | $1/2^+$ | 1/2 | 2 | 0.37 | 1.27 | 0.90 | 0.99 |
| 2.80 | | 3/2 | 0 | 2.12 | 0.01 | 0.15 | 0.89 |
| | | | 2 | 0.88 | 0.54 | 0.01 | 1.01 |
| 3.90 | | 5/2 | 2 | 0.42 | 0.14 | 0.49 | 0.22 |
| | | | 4 | 0.26 | 2.53 | 0.13 | 0.39 |

state band, the present results are in good agreement with experimental spectroscopic strengths and is very similar to previous theoretical predictions. For the excited bands, comparisons of S(CW) with S[SU(3)] and S(PW) show that the spectroscopic factors are quite sensitive to the configuration space and the effective interaction used. The present result is in general better compared with the experimental strengths.

Calculations for all possible ground-state to ground-state transitons in sd-shell nuclei are presently in progress. Pick-up α-spectroscopic factors for $^{24,25,26}$Mg are also being calculated and compared with experimental results from this laboratory.

## References


[1] C.L. Bennett, Nucl. Phys. A284 (1977) 301
[2] W. Chung and B.H. Wildenthal (to be published)
[3] M. Harvey, Advances in Nuclear Physics, Vol. 6 (1968), eds. M. Baranger and E. Vogt (Plenum Press, New York)
[4] N. Anantaraman, et al. Nucl. Phys. A279 (1977) 474
[5] J.P. Draayer, Nucl. Phys. A237 (1975) 157
[6] M. Conze, Ph.D. Dissertation, Technische Hochschule Darmstadt, Darmstadt, 1976
[7] M. Ichimura, et al. Nucl. Phys. A204 (1973) 225
[8] N. Anantaraman, et al. Phys. Lett. 60B (1976) 149
[9] D. Strottman and A. Arima, Nuclear Physics Theoretical Group Report no. 46, Nuclear Physics Laboratory, Oxford University, 1973
[10] J.P. Draayer, Nucl. Phys. A216 (1973) 457


## 1.14. The Reaction Mechanism of the (p,α) Reactions on $^{11}$B, $^{15}$N and $^{19}$F


W. Buck*), F. Hoyler*), M. Reuther*), T. Rohwer*), G. Staudt*), and P. Turek


We have continued the systematic study of (p,α) reactions on light nuclei. For the reactions $^{11}$B(p,α)$^{8}$Be, $^{15}$N(p,α)$^{12}$C and $^{19}$F(p,α)$^{16}$O experimental data are now available for proton energies $E_p$ = 5.0 −45.0 MeV. In fig. 1 a summary of the measured angular distributions is given together with the results of other authors. The figure illustrates a distinct variation in the shape of the angular distributions for lower energies and a diffraction pattern at higher energies indicating a pure direct reaction behaviour of these reactions in this energy range. An analysis of the excitation functions and of the energy dependence of the Legendre coefficients shows that for these reactions the direct reaction mechanism becomes dominant at excitation energies of about 20 MeV above the α-threshold. This behaviour is caused by a number of decay channels with thresholds near this excitation energy. These decay channels are correlated with a break-up of an α-cluster in the α-like compound systems. A similar result has been found in the reaction $^{6}$Li(p,α)$^{4}$He[1]; a similar behaviour can be expected for the reaction $^{23}$Na(p,α)$^{20}$Ne and $^{27}$Al(p,α)$^{24}$Mg. A study of these reactions is underway.

*Figure 1:*
*Summary of the angular distributions of the reaction $^{11}B(p,\alpha)^{8}Be$, $^{15}N(p,\alpha)^{12}C$ and $^{19}F(p,\alpha)^{16}O$.*

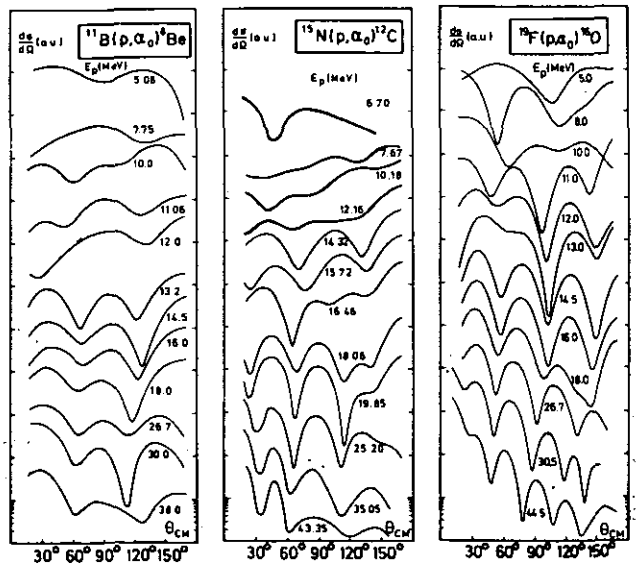


In the high energy range, the angular distributions can be reproduced by a simple zero-range DWBA calculation using a triton pick-up process (s. fig. 2). The potential parameters we used are quite similar for the three reactions under investigation. Figure 3 shows the integrated cross section compared with the DWBA calculation in the case of the reaction $^{11}$B(p,α)$^{8}$Be.

*Figure 2:*
*DWBA calculation for $^{15}N(p,\alpha)^{12}C$ at $E_p$ = 25.2 MeV.*

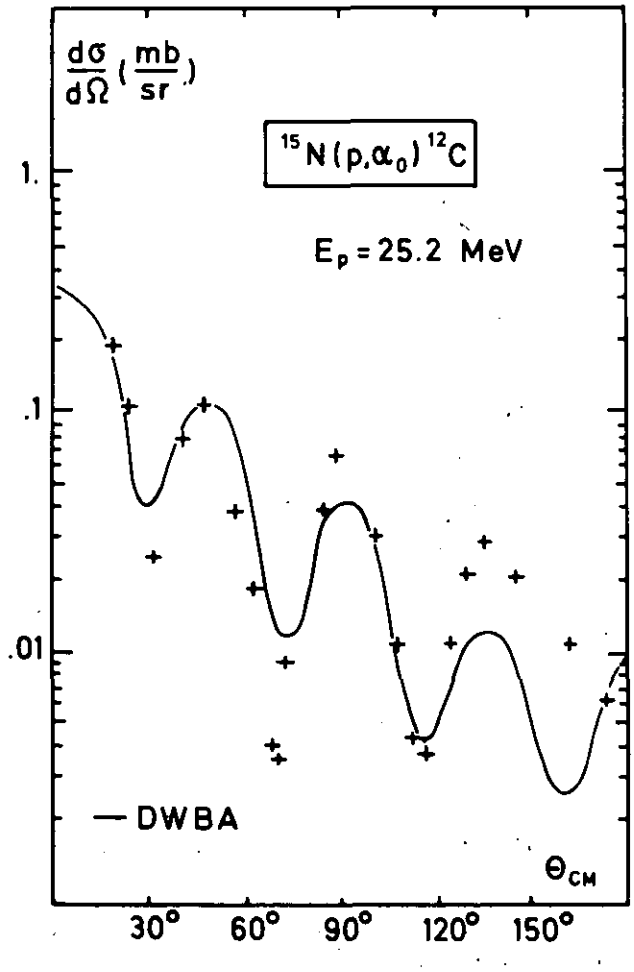


In recent years the excitation of giant electric quadrupole resonances in nuclei has been studied intensively. Experimentally it has been found that the GQR in $^{12}$C is centred at an excitation energy of about 27 MeV. Most of the experimental results concern-

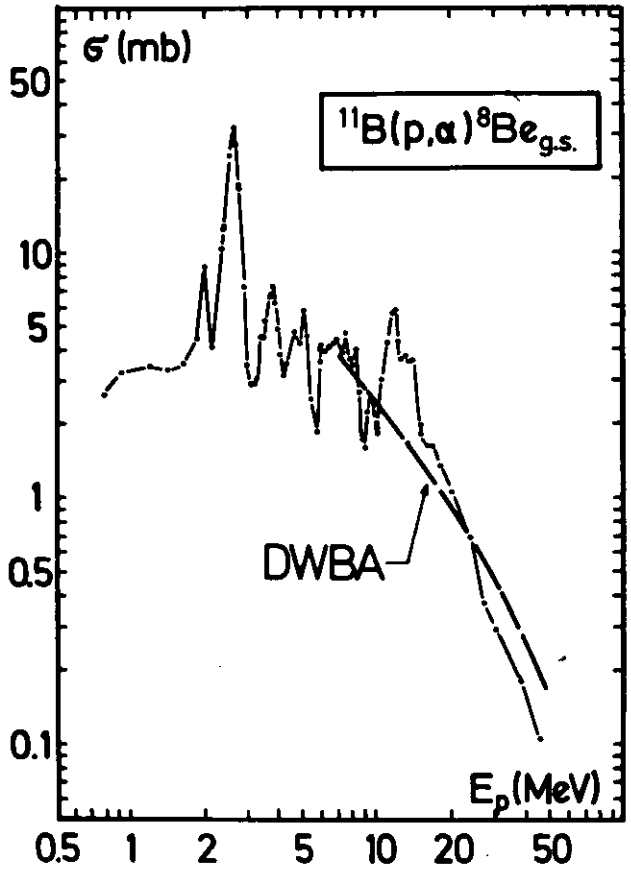


*Figure 3:*
*Integrated cross section of $^{11}B(p,\alpha)^{8}Be$.*

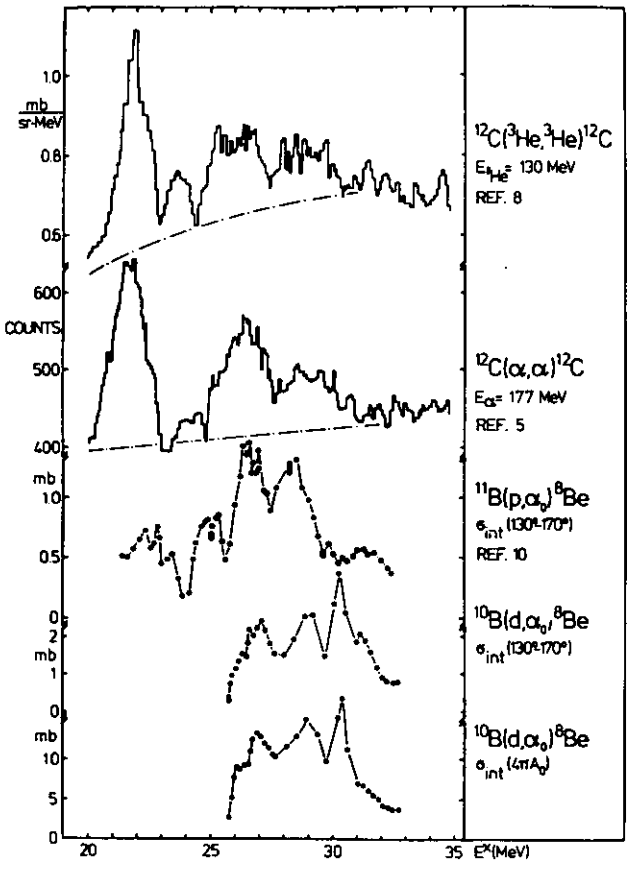


*Figure 4:*
*Comparision of excitation functions of the reaction $^{10}B(d,\alpha)^{8}Be(g.s.)$ with spectra from $^{3}He$- and $\alpha$-scattering at 2C and the backward-angle excitation function of the reaction $^{11}B(p,\alpha)^{8}Be(g.s.)$.*

ing the excitation of the GQR in $^{12}C$ have been achieved by inelastic $\alpha$-scattering[2]. In a preceding paper[3] we have shown that the GQR in $^{12}C$ also can be observed in the reactions $^{11}B(p,\alpha)^{8}Be(g.s.)$. In a further experiment, performed with the deuteron beam of the Tübingen University Van de Graaff accelerator and the Erlangen University EN tandem, we have investigated the reaction $^{10}B(d,\alpha)^{8}Be(g.s.)$. As can be seen in fig. 4, the resonance structures of the (d,α)-reaction coincide well in position, width and form with the GQR obtained from inelastic α- and $^{3}He$-scattering[2,4] and the excitation functions of $^{11}B(p;\alpha)^{8}Be$. At higher energies in the reaction $^{10}B(d,\alpha)^{8}Be$ a strong and rather small (O.5 MeV) compound resonance can be seen at $E_x$ = 3O.5 MeV. Although this resonance can be observed in elastic scattering, there is on the contrary no indication for it in the reaction $^{11}B(p,\alpha)^{8}Be$. Thus, because of the negligible proton width, this resonance has to be related to a $^{10}B \otimes d$ cluster structure in $^{12}C$.

*) Physikalisches Institut der Universität Tübingen

**References**


[1] K. Schenk et al., Phys. Lett. 52B (1974) 36
[2] P. Turek et al., Verhandl. DPG (VI) 12 (1977) 1OO8
[3] W. Buck et al., Nucl. Phys. A281 (1977) 469
[4] M. Buenerd et al., J. Physique 37 (1977) L53


## 1.15. Study of Two-Body Final States in the d + d Interaction in the 50-85 MeV Incident Energy Range


C. Alderliesten, J. Bojowald, A. Djaloeis, C. Mayer-Böricke, G. Paic*) and T. Sawada**)


Experimental $^{2}H(d,p)^{3}H$ angular distributions measured[1] at six incident energies in the $E_d^{lab}$ = 5O-85 MeV range have been analyzed in terms of a direct reaction model. Both the basic formalism and its physical input (interaction potentials, wave functions) are from a previous paper[2]. Distortion effects, however, have now been simulated by a cut-off in the lower orbital angular momenta3)ı instead of by a radial cut-off[2].

The post form matrix elements of the reaction were calculated in the PWBA, taking into account full anti-symmetrization in identical nucleons. The N-N interactions of the outgoing proton with the nucleons of the $^{3}H$ residual nucleus are taken of the Serber type. This choice simplifies the differential cross section to an incoherent sum over the values S = O and S = 1 of the channel spin S.

Each of the two-terms was then symmetrized in projectile and target, because these are identical Bosons. The calculation of the matrix elements can be reduced to that of two radial integrals. These contain (i) the radial parts of the interaction potentials and of the intrinsic wave functions (taken as, or approximated by, linear combinations of Gaussians[2]), and (ii) the plane waves representing the relative motion of the centers-of-mass of the fragments in the channels. By partial wave expansion of these plane waves, as required for $\ell$-cut-off[3], it can be proved that a given cut-off value $\ell_{c.o.}$ in the entrance channel, in the exit channel or in both leads to identical results.

This nice feature implies an advantage of the $\ell$-cut-off procedure over the more familiar r-cut-off prescription. The $\ell$-cut-off was applied „smoothly" using the function $f(\ell) = 1 - \{1+\exp(\ell-\ell_{c.o.})/\Delta\}^{-1}$.

Comparison with experiment has clearly shown that any agreement within the present framework requires the suppression of the lower partial waves in the calculations. As a tentative „best fit" for all incident energies, the values $\ell_{c.o.} = 3$, $\Delta = 0.1$ have been obtained; they provide reasonable agreement with the experimental data, both in shape and in magnitude (see fig. 1).

This result indicates that the description of the $^2H(d,p)^3H$ reaction as predominantly a simple process only holds for $\ell \gtrsim 3$, in other words: for large impact parameters.

Such a peripheral character was observed earlier[4] for the $^2H(d,dp)n$ reaction measured under quasi-free d-p scattering conditions. The $^2H(d,dp)n$ data were analyzed[4] in the framework of the Modified Simple-Impulse Approximation model[5], where a radial cut-off $R_{c.o.}$ is introduced in the target wave function. A semi-classical conversion of the $R_{c.o.}$-values thus obtained, also leads to $\ell_{c.o.} \simeq 3$, which indicates a comparable peripherality for both „simple" d+d reactions.

It should be noted that similar conclusions can be derived[3] from $^3He(p,d)pp$ (and similar) experiments, and from Faddeev calculations[6] on the $^2H(p,pp)n$ quasi-free scattering process.

*) Institute Rudjer Boscovic, Zagreb, Yugoslavia
**) Faculty of Engineering Science, Toyonaka, Osaka, Japan

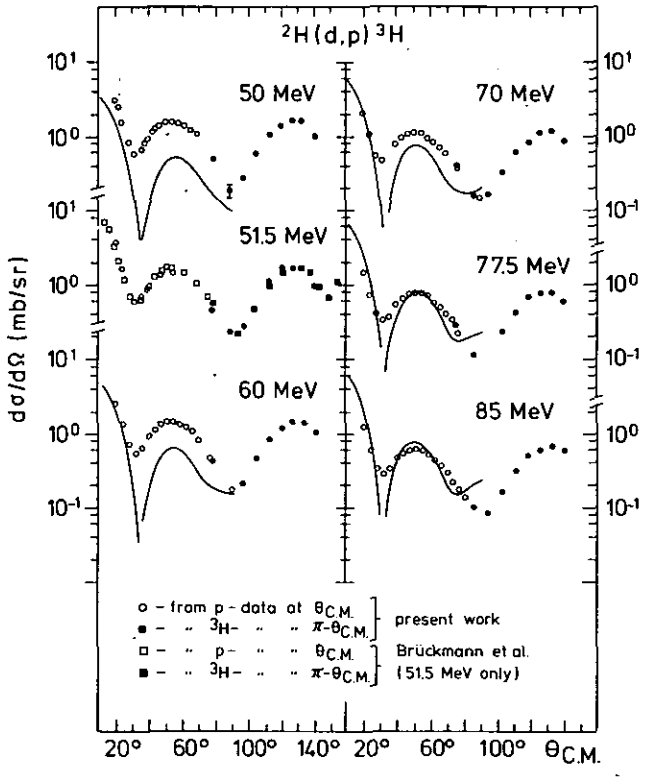


*Figure 1:*
*Angular distribution for the $^2H(d,p)^3H$ reaction at six incident energies[1]. The open and solid squares at 51.5 MeV represent the measurements of ref.[7]. The solid curves are the PWBA predictions as described in the text.*

## References


[1] C. Alderliesten, J. Bojowald, A. Djaloeis, G. Paic and C. Mayer-Böricke, Annual Report 1976 of IKP, KFA-IKP 10/77, p. 22
[2] T. Sawada, G. Paic, M.B. Epstein and J.G. Rogers, Nucl. Phys. A141 (1970) 169
[3] G. Paic and T. Sawada, Research program of the Nuclear Consortium at the UCLA Cyclotron Laboratory, 1970, p. 83, and Conference on the Nuclear Three-Body Problems, Budapest, 1971
[4] A. Djaloeis et al., Nucl. Phys. A273 (1976) 29
[5] G. Paic, J.C. Young and D.J. Margaziotis, Phys. Lett. 32B (1970) 437
[6] M.I. Haftel, E.L. Petersen and J.M. Wallace, Phys. Rev. C14 (1976) 419
[7] H. Brückmann, E.L. Haase, W. Kluge and L. Schänzler, Z. Physik 230 (1970) 383 and W. Kluge, Karlsruhe, private communication, 1976


## 1.16. Investigation of Two-Body Exit-Channels in the $\alpha+\alpha$ Interaction


C. Alderliesten, J. Bojowald, A. Djaloeis, C. Mayer-Böricke and G. Paic


The quasi-free d-p scattering data[1] from the $^2H(d,dp)n$ reaction measured at this laboratory at energies between 50 and 85 MeV had been analyzed in terms of the Modified Simple Impulse Approximation[2] (MSIA). The analysis results showed that the energy variation of the contribution of the target deuteron to the quasi-free process was similar to that found previously[3] in the $^2H(p,2p)n$ quasi-free case. This is surprising in view of the large size of the projectile deuteron.

Considering the above results it would be of interest to extend the measurement to the $\alpha+\alpha$ system. Although here the entrance-channel symmetry is preserved, because of its compactness the $\alpha$-particle (as the result of its high binding energy and small size) appears to be a very unlikely target for quasi-free scattering. It would then be useful to obtain information on the magnitude of the quasi-free (e.g. $\alpha$-p, $\alpha$-d) cross section and on the distortion of the quasi-free spectrum caused by short-range correlations in the $\alpha$-particle.

As a first step, charged particle (p, d, t, $^3He$ and $\alpha$) spectra from the $\alpha+\alpha$ interaction at 130 MeV incident energy have been obtained at several angles in the $9^\circ \leq \Theta_L \leq 40^\circ$ range. The experiment was performed with the unanalyzed beam of the Jülich cyclotron. The

$^4$He-gas was contained in a ∅ = 6 mm gas cell with Havar windows at a pressure of about 300 Torr. The gas cell and the detector assembly were placed in a ∅ = 100 cm scattering chamber. The charged particles were detected by means of a ΔE-E telescope. Commercial silicon surface-barrier (1-2 mm thick) and Ge(Li) detectors (produced by the detector group[4] of the laboratory) were used as ΔE and E counters, respectively. The telescope was coupled to standard electronics, including a particle identifier of the Goulding-Landis type and an 8x2K analyzer. The collected p,d,t, $^3$He, $^4$He as well as the particle identifier spectra were written onto magnetic tape for off-line analysis. Data reduction is in progress.

### References


[1] A. Djaloeis, J. Bojowald, C. Alderliesten, C. Mayer-Böricke, G. Paic and Z. Bajzer, Nucl. Phys. A273 (1976) 29
[2] G. Paic, J.C. Young and D.J. Margaziotis, Phys. Lett. 32B (1970) 437
[3] D.J. Margaziotis, G. Paic, J.C. Young, J.W. Verba, W.J. Braithwaite, J.M. Cameron, D.W. Storm and T.A. Cahill, Phys. Rev. C2 (1970 2050
[4] G. Riepe and D. Protic, Nucl. Instr. 101 (1972) 77


## 1.17. Experimental Yields of Proton Induced Reactions on Ti, V, Fe, Co, Ni and Comparison with Theory


R. Michel*), G. Brinkmann*), H. Weigel*), W. Herr*)


Thin target production cross sections can be regarded as a basis for the interpretation of cosmic ray produced radionuclides in extraterrestrial matter. With regard to the radiation history of meteoritic and lunar material the bombardement with solar protons of energies below 100 MeV is an important factor. However, there exists a considerable lack of experimental excitation functions for the light and medium weight elements, which are the main target elements in such matter.

For this reason a systematic study of p-induced reactions with cosmochemically relevant elements was started. Up to now 40 individual excitation functions were measured in the energy region from 10 to 45 MeV on Ti, V, Fe, Co, and Ni by way of the stacked foil technique. These excitation functions describe reactions of the types (p,Xn) to (p,4pXn).

In order to compare the experimental data with actual theories of nuclear reactions the established excitation functions were calculated by means of the computer code OVERLAID ALICE[1] combining the Weisskopf-Ewin evaporation theory[2] with the pre-equilibrium hybrid model of Blann[3].

A comparison between experimental and theoretical excitation functions for the (p,2pXn) reactions on Ni is presented in fig. 1. For the product nuclides $^{56}$Co, $^{57}$Co, and -valid with minor restrictions – for $^{60m+g}$Co the agreement is surprisingly good. The production of $^{58m+g}$Co at energies below 22 MeV via the $^{61}$Ni(p,α)- and $^{62}$Ni(p,αn)-reactions is underestimated by theory. Similar discrepancies were observed with respect to the evaporation of α-particles in p-induced reactions on Ti[4]. In the case of the $^{55}$Co-production from Ni the theory comes out to be too low by an order of magnitude at 30 MeV. We guess, that this deviation should be due to a pre-equilibrium emission of α-particles not considered in the hybrid model.

By further calculations the influence of changes in the nuclear parameters will be studied in order to come to a consistent description of all the excitation functions measured.

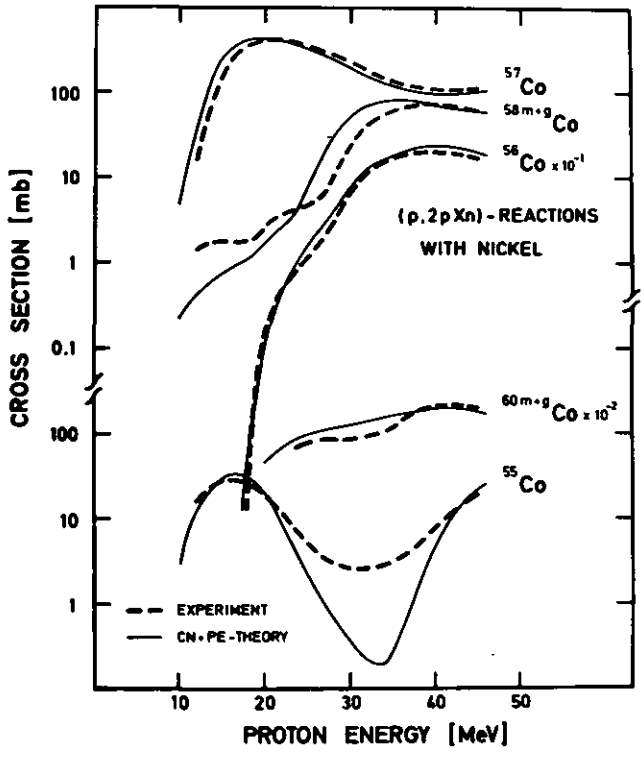


*Figure 1:*
*Experimental excitation functions for (p,2pXn) reactions on Ni and predictions based on the theory of the compound nucleus (CN) in statistical equilibrium and of pre-equilibrium (PE) reactions.*


*) Institute for Nuclear Chemistry, University of Cologne


### References


[1] M. Blann, Rep. COO-3494-32 (1977)
[2] V.F. Weisskopf, D.H. Ewing, Phys. Rev. 57, (1940) 472
[3] M. Blann, Phys. Rev. Letters 27 (1971) 337
[4] R. Michel, G. Brinkmann, H. Weigel, W. Herr, submitted to J. Inorg. Nucl. Chem.

## 1.18. Hybrid-Model Analysis of $^{197}$Au(τ,ypxn) Excitation Functions

C. Alderliesten, O. Bousshid, P. Jahn, H.J. Probst, C. Mayer-Böricke

The hybrid-model has been shown to reproduce reasonably well the excitation functions of deuteron[1] and α-particle[2] induced (particle,ypxn) reactions on gold. The same was found for proton induced reactions of this type in a somewhat limited range of $E_p$ and x[3]. These investigations were extended by including the measurement[4] and the hybrid-model analysis of $^{197}$Au(τ,ypxn) excitation functions. The main results of the comparison between experiment and calculations are given below.

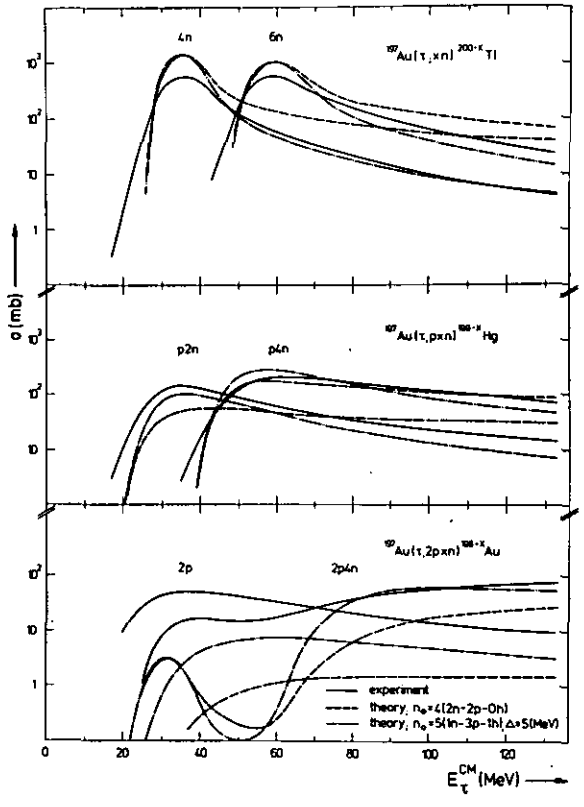


*Figure 1:*
*Hybrid-model calculations of $^{197}$Au(τ,ypxn) excitation functions using inititial exciton configurations $n_o$ = 4 (2n-2p-oh) and $n_o$ = 5 (1n-3p-1h) and comparison with experiment.*

The most important parameter of the hybrid-model is the initial exciton configuration. In the first calculation of (τ,ypxn) excitation functions a $n_o$ = 4 (2n-2p-oh) configuration was assumed in analogy to the finding for (α,ypxn) reactions[2]. It can be interpreted as the excitation of a neutron from the Fermi surface. The results for some selected cases are shown in fig. 1. The main features of this calculation are the overestimation of the evaporation peaks of the (τ,xn) excitation functions and the generally too flat high-energy tails.

The assumption of a $n_o$ = 5 (2n-2p-1h) configuration improves the shape of the calculated excitation functions, but overestimates the (τ,xn) and underestimates the (τ,pxn) cross sections. The best fit could be obtained using a $n_o$ = 5 (1n-3p-1h) initial exciton configuration in combination with a Rosenzweig effect[1] correction of Δ = 5 MeV. This correction takes into account in a simple way the fact that level densities increase in going further away from the closed proton shell at Z = 82 by proton emission. The result of the calculation is again shown in fig. 1. The agreement with experiment is rather good. It should be mentioned for completeness, that the parameter „nucleon mean free path multiplier" was kept fixed at k = 1 in all calculations.

Although a reasonably good reproduction of the experimental data could be obtained from the hybrid-Model, one should consider following fact: τ-particle induced reactions may have noticeable direct or other components which cannot be described by the model. There is some danger, that unphysical parameter values are used to compensate deficiencies of the model. For a further investigation of these problems, the measurement and analysis of continuous charged-particle spectra for instance $^{197}$Au(τ,p) in our case may prove to be important[5].

### References

[1] P. Jahn, H.J. Probst, A. Djaloeis, W.F. Davidson and C. Mayer-Böricke, Nucl. Phys. A209 (1973) 333
[2] A. Djaloeis, P. Jahn, H.J. Probst and C. Mayer-Böricke, Nucl. Phys. A250 (1975) 149
[3] Ann. Report 1975, p. 38
[4] Ann. Report 1976, p. 26-27
[5] Ann. Report 1977 ($^{197}$Au(τ,p)-spectra, p. 23

## 1.19. α-Decaying Evaporation Residues Following α-Induced Reactions on Thorium

R. Ibowski*), W. Scholz*), J. Bisplinghoff*), H. Ernst*), J. Rama Rao*) and T. Mayer-Kuckuk*)

Little is known on the yields of neutron-deficient isotopes in charged particle bombardments of thorium or heavier elements except that the cross section for particle evaporation is rather small due to fission competition. Most of the evaporation residues produced are α-emitters in the trans-lead region having half-lives of the range from some tens of nano-seconds up to many years.

As described previously[1] the on-line apparatus BANDIT[2] was modified for the spectroscopy of short lived α-emitters (20 ms ≤ $T_{1/2}$ ≤ 8 min) using the „Slow pulsing" of JULIC for background reduction. The calculated life-time selectivity of the α-BANDIT system is shown in fig. 1. This facilitates the identification of many different decay-chains with overlapping α-lines as demonstrated in fig. 2. E.g. the peak at 9.06 MeV is due to the decay of $^{213}$Po being fed by $^{221}$Ac and the longer lived $^{225}$Pa. The results for the most short-lived isotopes of each element observed are condensed in table 1.

*Table 1:*
*Short lived mother nuclides produced in $^{232}Th$ + α-reactions ($T_\alpha$ = 130 MeV)*

| mother nuclide | $T_{1/2}$ (exp.) | $T_{1/2}$(theor.) (ref. 3) | rel. production cross section |
|---|---|---|---|
| $^{225}Pa$ | ( 1.7 ± 0.1 ) s | 1.8 s | 17 ± 2 |
| $^{223}Th$ | ( 0.63 ± 0.04) s | 0.66 s | 40 ± 3 |
| $^{224}Th$ | ( 1.05 ± 0.02) s | 1.03 s | 102 ± 3 |
| $^{221}Ac$ | ( 51.6 ± 2.2 ) ms | 52 ms | 45 ± 3 |
| $^{223}Ac$ | (135 ± 8 ) s | 132 s | 175 ± 12 |
| $^{220}Ha$ | ( 31 ± 8 ) ms | 23 ms | 56 ± 3 |

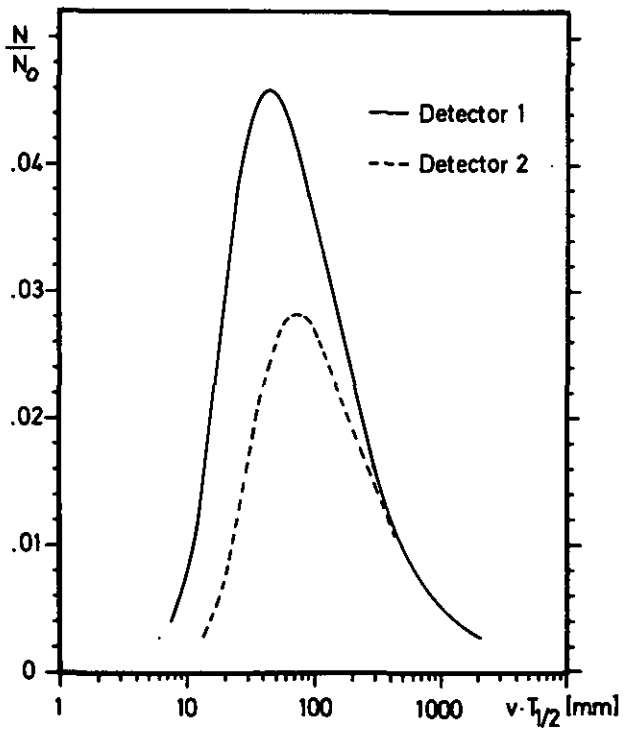


*Figure 1:*
*Relative yield curves for detector 1 and 2 of the α-BANDIT system as a function of tape velocity times half-life. The geometry depen-det parameters are the distance target – detector 60 mm (det. 1) resp. 100 mm (det. 2) and the length of the detectors 8 mm each.*

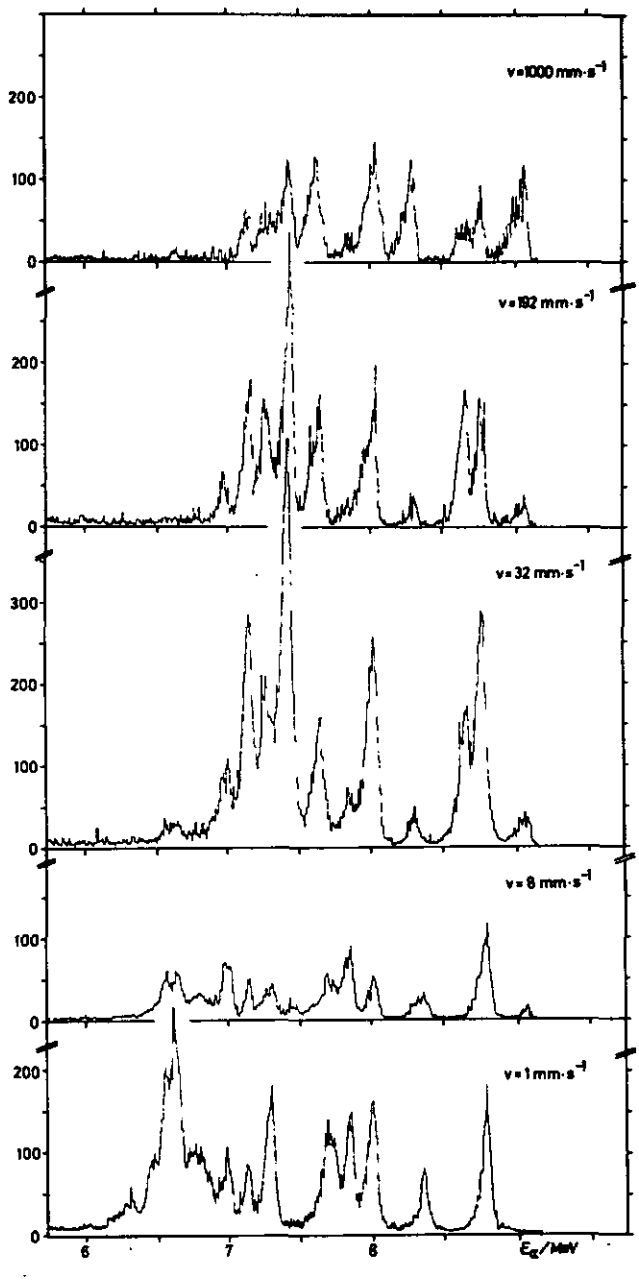


*Figure 2:*
*BANDIT α-spectra with five different tape velocities at an α-projectile energy of 130 MeV normalized to a charge of 1 mC.*

*In order to widen the range of detectable half-lives up to several* weeks also many foil stacks were irradiated consisting of thorium targets and aluminium catcher foils. As for the Mylar tape of BAN-DIT the recoils (E ≤ 2 MeV) are stopped within 1 μm reducing the line-broadening compared to that of the targets (d ≤ 5 μm). In addition, one gets rid of the natural α-activity of thorium. A preliminary analysis shows that the long-lived isotopes $^{222}Rn$, $^{223}Ra$, $^{224}Ra$, and $^{225}Ac$ are produced in $^{232}Th$ + α at $E_\alpha$ ≤ 160 MeV. The evaluation of absolute cross sections and an investigation of the underlying reaction mechanism is in progress.

*) University of Bonn

## References


[1] R. Ibowski et al., Annual report 1976, Institut für Kernphysik, KFA Jülich, KFA-IKP 10/77, p. 41
[2] A. Hardt et al., Nuclear Instruments and Methods 143 (1977) pp. 519-523
[3] W. Seelmann-Eggebert et al., chart of the nuclides, Karlsruhe 1974

## 1.20. Extensions of the Hybrid-Model of Pre-Equilibrium Decay

H. Machner

The success of the hybrid-model[1] in describing angular integrated nucleon spectra in the intermediate region between compound and direct reactions has led us to extend this model to complex particle emission. The emission of a cluster β with $P_\beta$ nucleons could occur during the equilibration process when equal or more than $P_\beta$ nucleons are excited and the $P_\beta$ nucleons have the right momentum distribution to condensate to a cluster. For the calculations we have approximated the inverse cross sections by the following formula

$$\sigma_\beta(\epsilon_\beta) = (R + \lambda\!\!\!^{-})^2 \frac{\hbar\omega}{2\epsilon_\beta} \ln\left\{1 + \exp[2\pi(\epsilon_\beta - V_c)/\hbar\omega]\right\}$$

with the radius R, coulomb-barrier $V_c$ and the frequency $\omega = [d^2V(r)/dr^2|_R/\mu]^{1/2}$. V(r) is the effective potential for the reaction, μ the reduced mass. $\lambda\!\!\!^{-}$ denotes the De Broglie wavelength. The calculations of angular integrated spectra show satisfactory agreement with experimental data. In the figure we compare data[2] (histogram) with calculations (solid line) and calculations from a different approach (dashed)[3]. In our calculations we have approximated the compound part by the Weiskopf-Ewing-formula[4]. At the high energy part the calculations do not describe the data, because direct reactions are not included in the model.

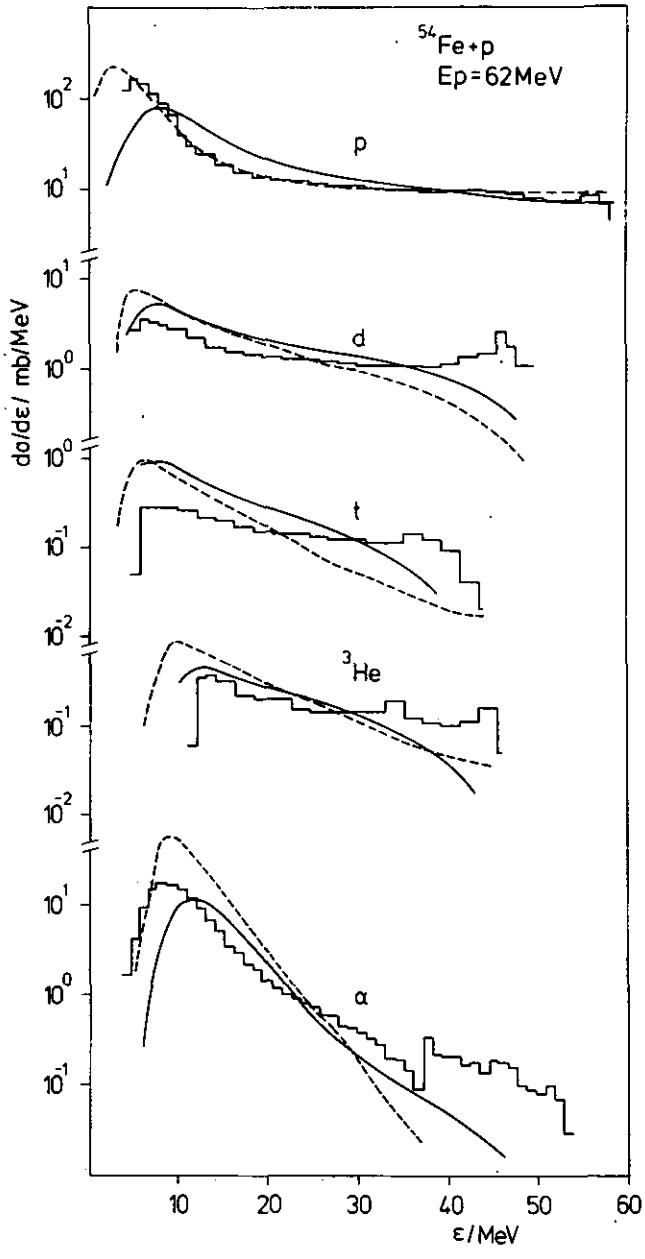


*Figure 1:*
*Experimental [2] and calculated angular integrated charged particle spectra from 62 MeV protons incident on $^{54}$Fe. The histogram shows the data calculated results are presented by dashed lines[3] and solid lines (this work).*

### References

[1] M. Blann, Phys. Rev. Lett. 27 (1971) 337
[2] F.E. Bertrand, R.W. Peelle, Phys. Ref. C8 (1973) 1045
[3] C.K. Cline, Nucl. Phys. A193 (1972) 417
[4] V.F. Weisskopf, D.H. Ewing, Phys. Rev. 57 (1940) 472

## 1.21. Continuous Charged Particle Spectra from Deuteron Induced Reactions

U. Bechstedt, H. Machner, C. Alderliesten, O. Bousshid, A. Djaloeis, P. Jahn, and C. Mayer-Böricke

Measurement of p, d, t, $^3$He and α spectra from deuteron induced reactions on $^{27}$Al, $^{93}$Nb and $^{197}$Au targets has been performed at the Jülich Isochronous Cyclotron JULIC at incident energy $E_d$ = 80 MeV. The light charged reaction products were detected by means of a ΔE-E telescope consisting of 400 μm ΔE silicon surface barrier and 28 mm Ge(Li)[1] detectors, respectively. Particle identification was accomplished making use of the energy range relationship[1]. Angular distributions as well as angle integrated spectra have been obtained from the continuous part of the measured particle spectra. A broad bump centered at energy E ≃ 1/2 $E_d$ was observed in the angle integrated proton spectra for all target nuclei measured. This bump, which has a forward peaked angular distribution, is due to protons originating from deuteron break-up.

Fig. 1 shows angle integrated proton spectra from $^{27}$Al, $^{93}$Nb and $^{197}$Au targets and their comparison to geometry-dependent hybrid model (GDH) predictions[3]. A 2p-1h initial configuration was assumed. Agreement between theory and experiment (excluding the break-up component) is reasonable. Analysis of the break-up bump is in progress.

For $^{93}$Nb target the deuteron spectra and angular distributions have been compared with an inelastic scattering model developed by G. Baur and H. Lenske[4]. The excited states of $^{93}$Nb are assumed to have only (1p-1h) structures. Excitations of a nucleon from closed subshells (with $^{90}$Zr as core) to those up to $3p_{1/2}$ were considered. This gives a total number of 435 transitions to possible

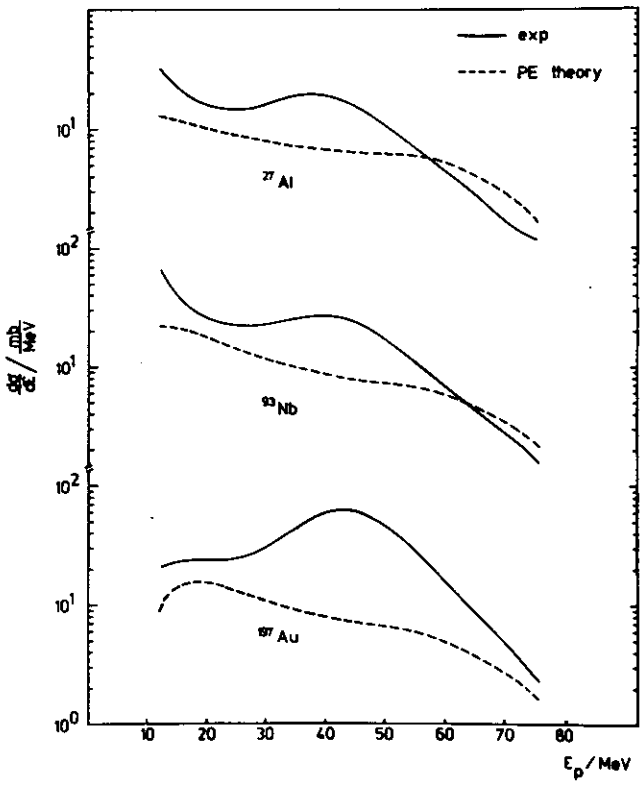


*Figure 1:*
*Angle integrated proton spectra from the reactions $^{27}Al$ (d,px), $^{93}Nb$(d,px) and $^{197}Au$(d,px) in comparison with preequilibrium theory.*

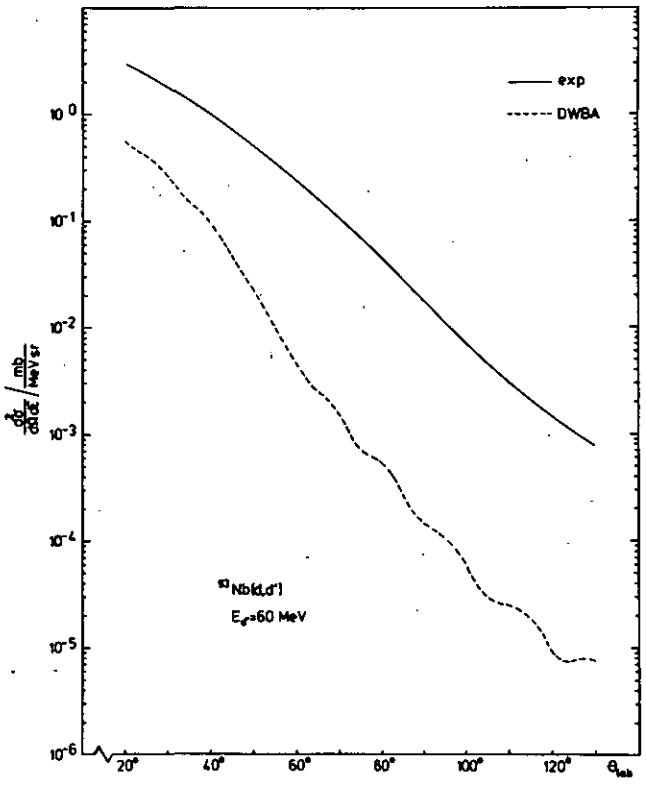


*Figure 2:*
*Angular distribution of 60 MeV deuterons from reactions of 80 MeV deuterons with $^{93}Nb$. Comparison of experimental data with one-step DWBA calculation.*

$(1p\text{-}1h)_J$ intermediate states. The single particle energies were approximated by data for $^{90}Zr$[5]. The deuteron optical model parameters were those from the work of Perey and Perey[6].

Fig. 2 shows a comparison between experiment and theoretical predictions to $^{93}$Nb(d,d') reactions with energy $E_{d'} = 60$ MeV. The theoretical cross sections are too small by nearly one order of magnitude at forward angles and even two orders of magnitude at backward angles. For lower $E_{d'}$ (i.e. higher excitation energy of the target nucleus) the fit gets worse.

The disagreement between theory and experiment may be partly due to the neglect of low lying collective states as well as multi-step p-h excitations.

### References


[1] G. Riepe, D. Protic, Nucl. Instr. 101 (1972), 77
[2] Goulding, Harvey, Ann. Rev. Nucl. Science 25 (1975) 167
[3] M. Blann, Ann. Rev. Nucl. Science 25 (1975) 123
[4] G. Baur, H. Lenske, Proceedings of Varenna Conference (1977), and private communication
[5] S. Krewald, Jül. Rep. 1315 (1976)
[6] C.M Perey and F.G. Perey, Atomic and Nucl. Data Tab. 13 (1974) 294


## 1.22. Investigation of the Continuous Part of Charged-Particle Spectra from τ-Induced Reactions


O. Bousshid, H. Machner, C. Alderliesten, U. Bechstedt, A. Djaloeis, P. Jahn, and C. Mayer-Böricke


The hybrid model of preequilibrium decay[1] has been successfully used to describe the high-energy tails in the excitation functions of (particle,ypxn) reactions[2]. So it was possible to describe the data for $^{197}$Au(τ,ypxn) reactions with bombarding energies up to 135 MeV[3] in terms of this model. It is the purpose of this work to compare the experimental angle-integrated charged-particle spectra with the prediction of this model.

Therefore we have measured proton spectra from τ-reactions on $^{27}$Al, $^{56}$Fe, $^{59}$Co, $^{93}$Nb, $^{197}$Au and $^{209}$Bi at bombarding energies of 68, 90 and 120 MeV. The experimental set up consisted of a ΔE-E telescope with a silicon surface-barrier and a Ge(Li)[4] as ΔE and E detectors, respectively. Particle identification was done in the Landis-Goulding method. Spectra were taken at angles from 13° to 160° in steps of about 10°. From these data we have extracted double-differential cross sections, angular distributions in 10 MeV wide bins and angle-integrated spectra. As an example, angle-integrated τ and proton spectra are shown in fig. 1 and 2, respectively. There is a broad bump at about one third of the incident energy with a FWHM of 24–30 MeV, which is due to protons from the break up of the τ-particle. The dependence of the cross section on A or Z is clearly demonstrated. In fig. 3–4 we compare the data with

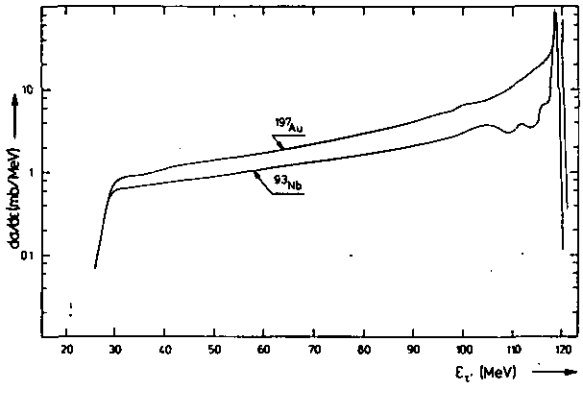


*Figure 1:*
*Angle-integrated τ-spectra from τ-induced reactions at $E_\tau$ = 120 MeV.*

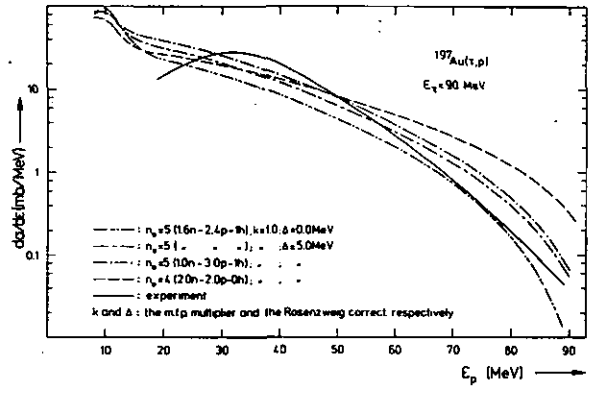


*Figure 3:*
*Comparison of the hybrid model calculation with experimental data at $E_\tau$ = 90 MeV.*

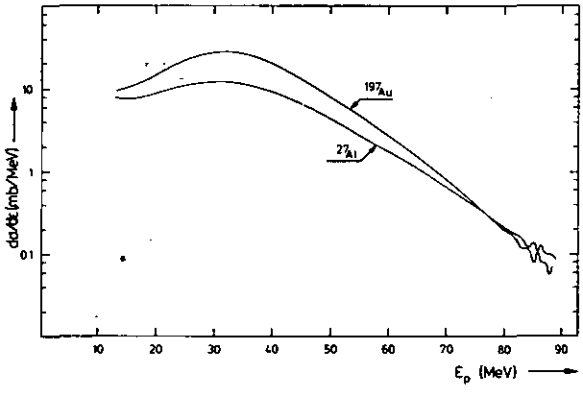


*Figure 2:*
*Angle-integrated proton spectra from τ-induced reactions at $E_\tau$ = 90 MeV.*

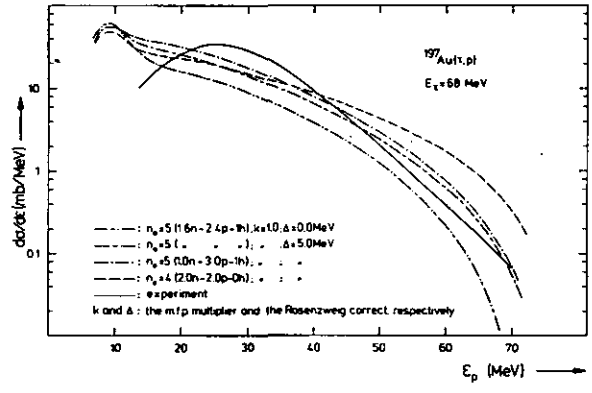


*Figure 4:*
*Comparison of the hybrid model calculation with experimental data at $E_\tau$ = 68 MeV.*

a hybrid-model calculation using the same input parameters as in ref. 3. The agreement between theory and experiment is satisfactory with respect to the high energy part of the spectra.

**References**


[1] M. Blann, Phys. Rev. Lett. 27 (1971) 333
[2] M. Blann, Ann. Rev. Nucl. Sci. 25 (1975)
[3] O. Bousshid et al., see contribution to this annual report
[4] G. Riepe and D. Protic, Nucl. Instr. Meth. 101 (1972) 77


## 1.23. Description of Continous Particle Spectra Including Angular Distributions


H. Machner


The concept of pre-equilibrium decay in nuclear reactions[1] was extended by the group from Heidelberg[2] so that the calculation of angular distributions of emitted nucleons became possible. In a later formulation[3] the approach was brought into the frame of the hybrid-model[1]. Because our extension of the hybrid-model to complex particle emission[4] gave encouraging results we have tried to incorporate the ideas of ref. 3 into our model. The basic assumption is that in a nucleon-nucleon collision the fast particle has information of its incoming direction in mind. Furthermore we assume that transfered nucleons have zero momentum. This seems to be a good approximation at the average as long as the nucleon-nucleon-interaction in nuclear matter could be taken as to be isotropic.

In fig. 1 we compare double differential cross sections from $^{54}$Fe (p,d) reactions with $E_p$ = 62 MeV. The experimental data[5] show good agreement with the calculations (dashed line) at different angles. The calculation fails in the hard component because of direct reactions which are not included in the model.

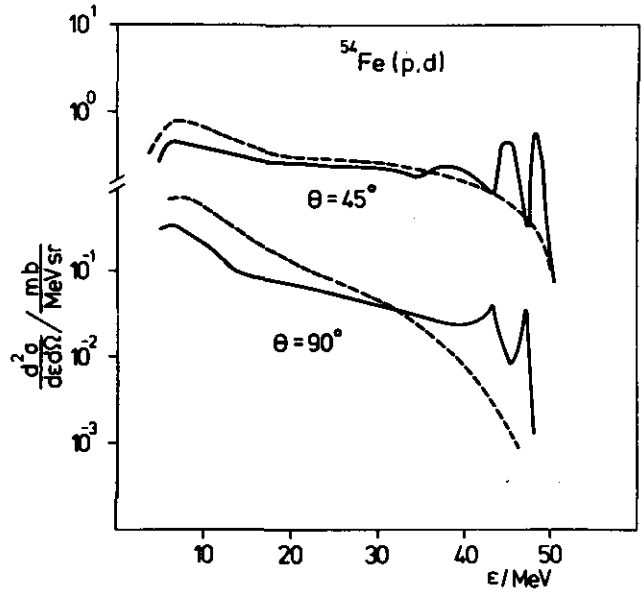


*Figure 1:*
*Spectra of (p,d)-reactions with incoming 62 MeV protons of $^{54}$Fe. Solid line shows the data and dashed line the calculations.*


## References

[1] M. Blann, Ann. Rev. Nucl. Sci. 25 (1975) 123 and references therein
[2] D. Agassi, H.A. Weidenmüller, G. Mantzouranis, Phys. Reports 22C (1975) 147; G. Mantzouranis, D. Agassi, H.A. Weidenmüller, Phys. Lett. 57B (1975) 220
[3] G. Mantzouranis, Phys. Lett. 63B (1976) 25 and private communication
[4] H. Machner, contribution to this Annual Report
[5] F.E. Bertrand, R.W. Peelle, Oak Ridge National Laboratory Report ORNL-4469 (1970)


## 1.24. Energy and Mass Distribution of Fragments after α-Bombardment of Ca Isotopes at $E_\alpha$ = 100 MeV**)


H. Löhner*), H. Eickhoff*), D. Frekers*), G. Gaul*), K. Poppensieker*), and R. Santo*)


The investigation of reaction products from 100 MeV α-particle bombardment of $^{40}$Ca and $^{44}$Ca (see Annual Report 1976) has further been completed. The results are shown in fig. 1–3. The energy spectra and in particular the asymmetric angular distributions indicate that a mechanism other than the normal compound nuclear evaporation takes place. Instead, a striking similarity exists between spectra and fragment distribution in the present data and the results of relativistic nucleus-nucleus interactions[1]. Therefore, the simple classical models of relativistic heavy ion physics have been applied to parametrize the data.

The coalescence model[1] has been used to calculate the energy spectra of the heavy fragments from the experimental p-spectrum. Attempts to fit the low-energy part of the p-spectrum by a Maxwellian distribution lead to a rather high temperature of T ≈ 14 MeV (for a normal compound nucleus T = 6 MeV is expected). Furthermore, the angular distrubutions indicate that the emission of fragments occurs from a system with velocity intermediate between projectile and compound system velocity.

The Maxwellian fits to proton spectra and their low energy extrapolation have subsequently been used as „experimental p-spectra" in coalescence model calculations.

It is seen that with the only free parameter $P_o$ (which has the meaning of a momentum space radius including binding energy effects) a rather good description of the energy spectra of heavy fragments is obtained (fig. 1).

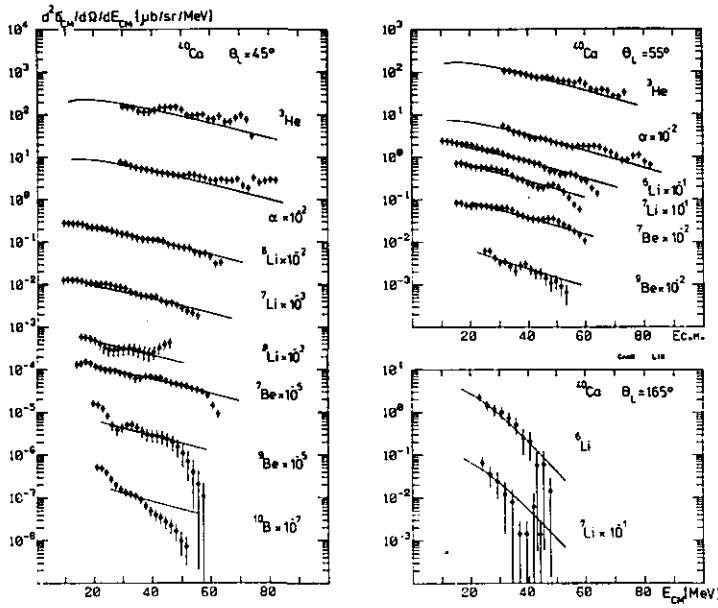


*Figure 1:*
*Fragment spectra from $^3$He to $^{10}$B at different angles together with coalescence-model-calculations. For calculating the proton spectra a Maxwellian has been used with temperature T = 14 MeV assuming nucleon emission from a system moving with velocity v/c = 0.11.*

The observation of high temperature and velocity is typical for the „fireball" hypothesis[2] where a highly excited system of few nucleons in the projectile-target overlap moves with a characteristic velocity different from the compound system. Therefore a calcula-

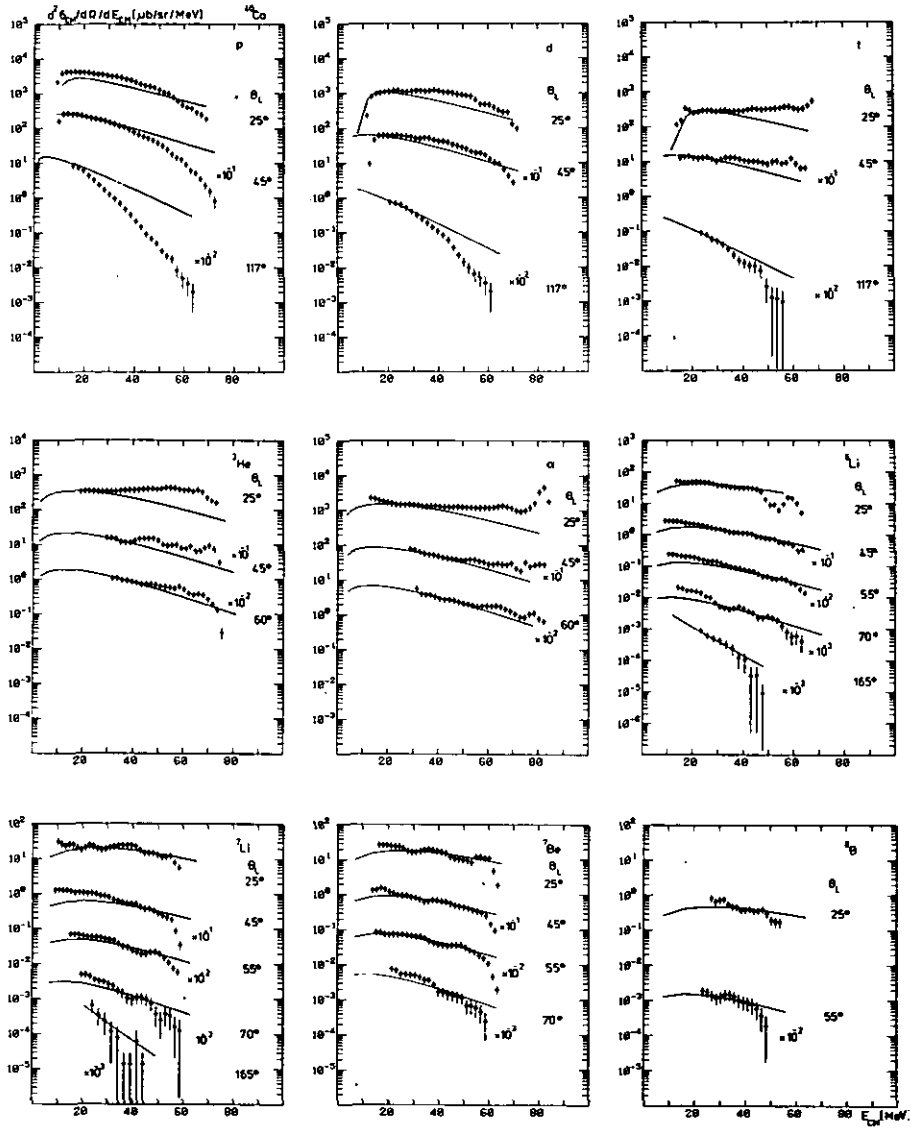

*Figure 2:*
*Fragment spectra from p to $^{8}B$ at different angles. The curves have been calculated using the fireball-formalism together with the coalescence-model for composite-particle-spectra.*

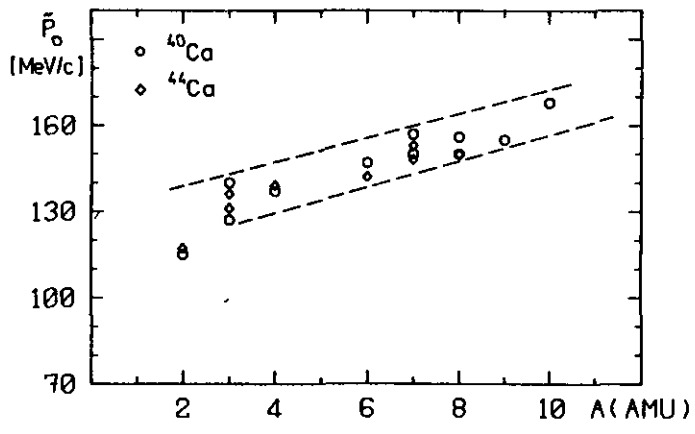


*Figure 3:*
*Momentum space radius $\tilde{P}_o$ versus fragment mass number A. The fragment dependent normalizations $P_o$ of the coalescence model have been corrected for spin statistics and binding energy to obtain $P_o$-values.*

tion according to ref. 2 has been performed, where the temperature and velocity of the geometrical projectile-target overlap is obtained by integrating over all impact parameters.

The coalescence model has then again been applied to obtain the spectra of the complex fragments (fig. 2). Using the equivalence of the coalescence and thermodynamical model[3] corrected $P_o$ values have been evaluated (fig. 3) showing a smooth behaviour with fragment mass number. Additional data at higher energies and smaller angles have to be performed in order to investigate the applicability of the various alternative concepts of nuclear fragmentation.

*) Institut für Kernphysik, Universität Münster, Germany
**) Supported in part by the Bundesminister für Forschung und Technologie

## References

[1] H.H. Gutbrod et al., Phys. Rev. Lett. 37 (1976) 667
[2] G.D. Westfall et al., Phys. Rev. Lett. 37 (1976) 1202
[3] A. Mekjian, Phys. Rev. Lett. 38 (1977) 640

## 1.25. Determination of the Charge Distribution of Fission Products from $^{197}$Au(α,fission)

S.M. Sahakundu, C. Alderliesten, P. Jahn, H.-J. Probst and C. Mayer-Böricke

The experimental yields for the production of $^{95}$Nb (independent) and $^{95}$Zr (cumulative) by fission of $^{197}$Au with α-particles in the energy range 65 MeV ≦ $E_\alpha$ ≦ 155 MeV[1] have been found to be consistent with the assumption of a charge distribution width parameter c = 0.95[2]. This value had been determined earlier in other experiments on different fissioning systems, mostly at lower excitation energies. The data[1] are not sufficient to derive a value for c; it is necessary to measure the yields for three members of a mass chain, namely one cumulative and two independent yields. This cannot be done in a stacked-foil experiment[1] because of the background of (α,xnyp)-reaction products which does not permit the measurement of short-lived isotopes. Therefore catcher-foil arrangements were irradiated at different α-particle energies.

The target arrangement consisted of a stack of three identical gold foils and an aluminium catcher foil forming a cylinder around the beam at backward angles. Three irradiations were performed at each of the α-particle energies of 90, 105, 120 and 140 MeV. At each energy two of the catcher foils were processed radiochemically, the third one was measured without any further treatment. As the mass chains A = 95 and A = 105 appeared to be the most useful ones for this off-line investigation, the chemical separations were designed to improve the conditions of measurement for $^{95}$Y ($T_{1/2}$ = 10.9 min) and $^{105}$Tc ($T_{1/2}$ = 7.7 min) by removing the bulk of other fission products. The aluminium catcher foils were dissolved in presence of appropriate carriers. Yttrium was precipitated as yttrium oxalate; technetium was carried over rhenium and was precipitated as tetraphenylarsoniam perrhenate. The chemical yields were determined after finishing the γ-ray spectrometry. The middle gold foil was measured for the determination of the total number of fissions using longer-lived fission products; it can also provide a check of the beam current integration using known (α,xn)-reaction[3] cross sections. The insertion between two other gold foils compensates escape losses of fission fragments and recoil nuclei. The γ-ray spectra of the activities were taken using a conventional Ge(Li) spectrometer. The data reduction is still in progress.

### References

[1] H.-J. Probst, C. Alderliesten, P. Jahn and C. Mayer-Böricke, Annual Report 1974, Institut für Kernphysik, KFA Jülich, KFA-IKP 10/75, p. 49
[2] P. Jahn, Annual Report 1976, Institut für Kernphysik, KFA Jülich, KFA-IKP 10/77, p. 25
[3] A. Djaloeis, P. Jahn, H.J. Probst and C. Mayer-Böricke, Nucl. Phys. A 250 (1975) 149

## 1.26. $^4$He-Induced Spallation of $^{45}$Sc and Evidence for a Fission-Like Process

P. David*), J. Debrus*), H. Fahlbusch*), J. Schulze*), K.A. Eberhard**)

The investigation of reaction products observed after the bombardment of light nuclei is continued[1]. The nucleus $^{45}$Sc was bombarded with $^4$He-particles of T($^4$He) = 150 MeV. The residual nuclei were idendified by the activation analysis technique applied to the γ-activity of the foil. In Figure 1 the results are displayed together with spallation cross sections calculated with a CDMD Rudstam formula. The excess yield for $^{24}$Na is studied in a wider context. Published cross sections are compared with the values from this work and from ref. 2 in fig. 2. Curves are drawn through the experimental points of the same excitation function. It is seen for all kinds of projectiles, photons, pions, protons and $^4$He-particles that the cross section is higher for heavier particles and lower for

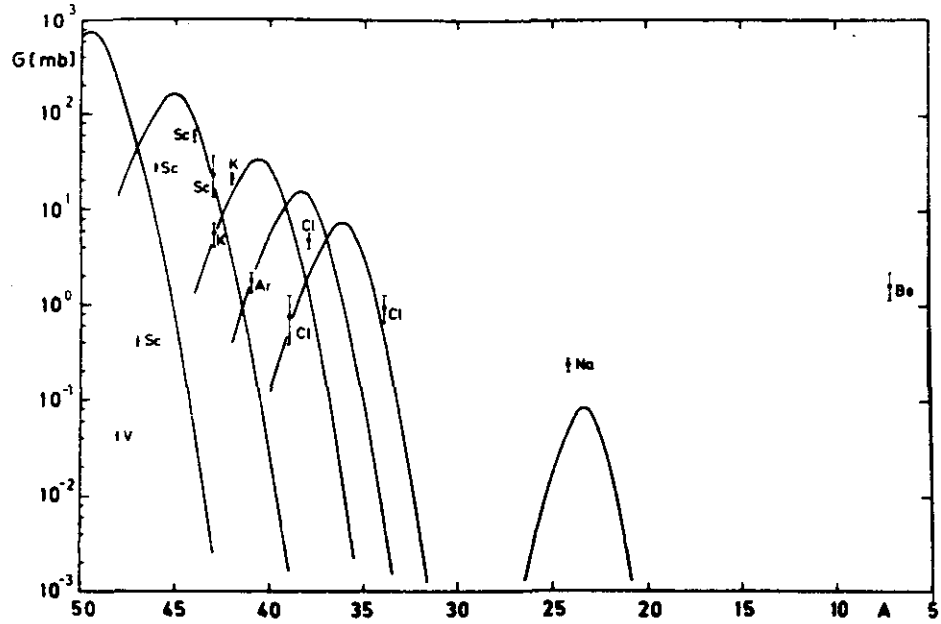


*Figure 1: See text*

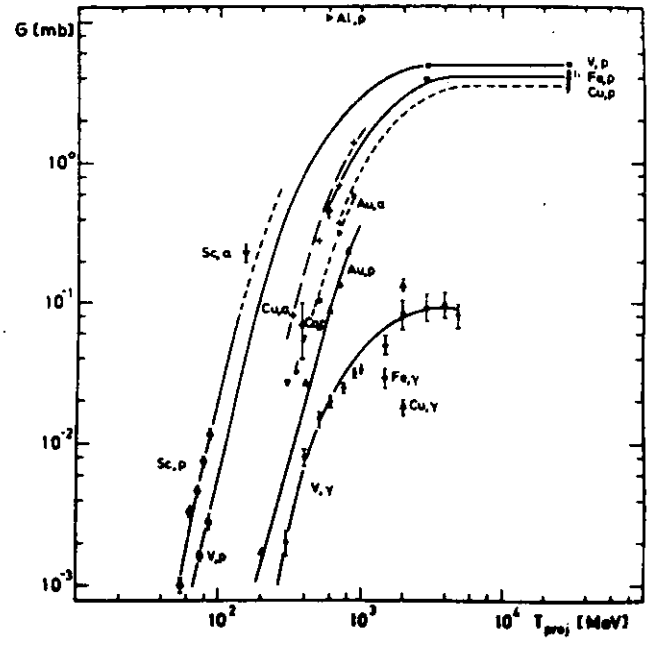


*Figure 2:*
*See text.* ▽ $^{45}Sc + {}^4He$ *this work,* △ $^{45}Sc$, *Cu + ref. 2,* ▽ *Au +* π, *ref. 5.*

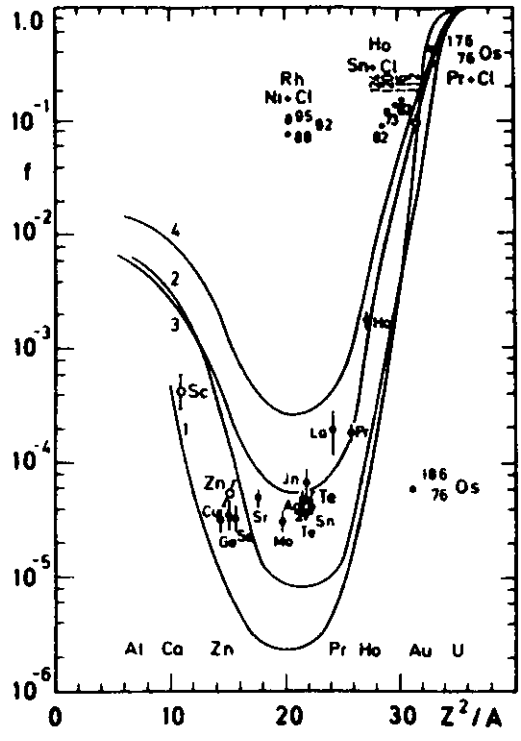


*Figure 3:*
*See text, points in the upper part are from heavy ion reactions.*

heavier target nuclei. The excitation curves for $^{24}Na$ production for $^{45}Sc$ with protons and $^4He$ rise just above the fission threshold for this nucleus. Since the spallation channels $^{45}Sc(p;xn,yp)^{24}Na$, $^{45}Sc(^4He;xnyp)^{24}Na$ have very high negative Q-values a fission-like process may be present ($B_f \sim 46$ MeV). The $^{24}Na$ excess over the calculated spallation yield was taken as fission cross section. The isomeric ratio $\sigma(^{44m}Sc(271\ keV))/\ \sigma(^{44}Sc(O.O\ keV))$ from the $^4He$ experiment is larger by a factor of 5 compared to the ratio of the photon experiment[2], indicating different amount of angular momentum transferred in either reaction. The experimental fission probabilities are compared with fission probabilities as calculated with the program ALICE for $^4He$-induced fission at $T(^4He) = 150$ MeV. The curves are displayed in fig. 3 together with our experimental results and data from ref. 3. Curve 1 is from ref. 4. Curve 2 is for excitation energy $E_x = T_{cm} + B(^4He) + B_f$, curve 3 for $E_x = T_{cm} + B(^4He)$, $B_f \times 0.7$, curve 4 for $E_x = T_{cm} + B(^4He) + B_f$, $B_f \times 0.7$.

This work was supported by the Bundesminister für Forschung und Technologie.

*) Institut für Strahlen- und Kernphysik der Universität Bonn
**) Sektion Physik der Universität München, Garching

## References

[1] P. David, G. Engels, K.A. Eberhard, Annual Report, Institut für Kernphysik der Kernforschungsanlage Jülich, 1975, p. 35
[2] N.M. Bachschi, P. David, J. Debrus, F. Lübke, H. Mommsen, R. Schönmackers, G.G. Jonsson, K. Lindgren, Nucl. Phys. A264 (1976) 493
[3] B.D. Pate, J. Peter, Nucl. Phys. A173 (1971) 520
[4] J.R. Nix, E. Sassi, Nucl. Phys. 81 (1966) 61
[5] N.T. Porile, B.J. Dropesky, R.A. Williams, Phys. Lett. 67B (1977) 43

# 2. Nuclear Spectroscopy

## 2.1. Hyperfine Shifts of Xe K X-Ray Energies Following Electron Capture

P.G. Hansen*), G.L. Borchert, B. Jonson*), H.L. Ravn*), P. Tidemand-Petersson*), O.W.B. Schult

The lifetimes of K holes are short relative to those of low lying states in heavy nuclei. The energies of the X-rays following electron capture will therefore depend on the static properties of the populated nuclear levels. The expected atomic 1 s state energy shifts due to the nuclear volume effect or the magnetic hyperfine splitting are only $10^{-2}$ to $10^{-3}$ of the natural line width. Their measurements require strong sources, high resolution of the spectrometer and special precautions to eliminate systematic errors.

Mono-isotopic sources up to 1 Ci were produced at ISOLDE 2 at CERN. Their K X-radiation was measured with a DuMond type diffractometer. Photons were recorded from two different sources placed at short distance, one above and one below the focal circle and behind a rotating shutter. Reflections were measured at positive and negative Bragg angles. This measurement procedure allowed the determination of relative K X-ray energies with an accuracy which was essentially limited only by the counting sta tistics.

*Table 1:*
*Energy shifts of xenon K X-rays*

| X-ray | Source 1 | Source 2 | $E_1-E_2$ (meV) |
|---|---|---|---|
| $K\alpha_1$ | $^{127}Cs$ | $^{129}Cs$ | - 12 ± 9 |
| $K\alpha_1$ | $^{127}Cs$ | $^{131}Cs$ | -132 ± 20 |
| $K\alpha_1$ | $^{127}Cs$ | $^{132}Cs$ | 36 ± 20 |
| $K\alpha_1$ | $^{129}Cs$ | $^{131}Cs$ | -108 ± 21 |
| $K\alpha_1$ | $^{129}Cs$ | $^{132}Cs$ | 53 ± 12 |
| $K\alpha_1$ | $^{131}Cs$ | $^{132}Cs$ | 112 ± 11 |
| $K\alpha_2$ | $^{131}Cs$ | $^{132}Cs$ | 170 ± 40 |
| $K\beta_1$ | $^{131}Cs$ | $^{132}Cs$ | 120 ± 60 |

The results are listed in Table 1 where $E_1 - E_2 = E(K\,X\text{-ray, source 1}) - E(K\,X\text{-ray, source 2})$. They reveal large shifts between the K X-ray energies from the different sources. These shifts appear too large to be explained on the basis of the nuclear finite size effect. Furthermore, shake off effects and chemical shifts are believed to be negligible, since the sources consist of the same element implanted into identical backings. The magnetic hyperfine effect[1] leads to shifts $A\,I/2$ and $A(I+1)/2$ for the states with $F=I+1/2$ and $F = I-1/2$, respectively. For allowed or first forbidden electron capture, a transition with $\Delta I = \mp 1$ populates only one hyperfine level with $F = I \pm 1/2$, whereas a transition with $\Delta I = 0$ feeds both hyperfine states in the non-statistical ratio $I/(I+1)$ leading to a shift of $-A/2$.

Because of the simplicity of the decay schemes for $^{131}Cs$ and $^{132}Cs$ with $^{131}Cs$ ($I^{\pi}=5/2^+$) $\rightarrow$ $^{131}Xe$ ($I^{\pi}=3/2^+$, $\mu=0{,}692\ \mu_N$) and $^{132}Cs$ ($I^{\pi}=2^+$) $\rightarrow$ $^{132}Xe$ ($I^{\pi}$(668 keV) $= 2^+$, $\mu = 0.74 \pm 0.10\ \mu_N$[2], a calculation of the magnetic hyperfine shifts is feasible. We find[3] + 75 meV for $^{131}Cs$ and -38 ± 6 meV for $^{132}Cs$ as sources so that $E_K(^{131}Xe) - E_K(^{132}Xe)$ is expected to be 113 ± 6 meV which compares well with the measured value of 116 ± 11 meV.

We are grateful to J.U. Andersen for drawing our attention to the F selection rule.

*) CERN Geneva, Switzerland

### References

[1] H. Kopfermann, Kernmomente (Academic Press, N.Y. 1958) p. 129-131
[2] A. Arnesen, K. Johansson, E. Karlsson, T. Noreland, L.-O. Norlin and S. Ogaza, Uppsala Univ. Inst. of Physics report UUIP-950 (1977)
[3] G.L. Borchert, P.G. Hansen, B. Jonson, H.L. Ravn, O.W.B. Schult, P. Tidemand-Petersson (CERN Preprint), submitted to Physics Letters A

## 2.2. Shifts in the Energies of Gold K X-Rays and the Role of the Excitation Mechanism

G.L. Borchert, P.G. Hansen*), B. Jonson*), I. Lindgren*), H.L. Ravn*), O.W.B. Schult, P. Tidemand-Petersson*)

The large widths of K X-rays conceal unresolved satellite lines associated with outer-shell excitations caused by the primary excitation mechanism. These satellites lead to a line shift which occurs superimposed on a contribution from the coupling to the nuclear spin (magnetic hyperfine splitting: hfs). Energy shifts from the latter effect have recently been observed[1] in electron-capture beta decay (EC). In the present study, we exploit the near-absence of outer-shell excitations during the formation and decay of the $1s_{1/2}$ hole in EC beta decay. The reason for this is the almost complete screening of the nuclear charge by the 1s electrons, so that the simultaneous disappearance of a proton and of a 1s electron should leave the wave functions of the outer electrons essentially unchanged. Thus, allowing for the hfs shift, a comparison of the energies of K X-rays from EC beta decay and from photo-ionization (PI) should reveal the contribution of unresolved satellite lines.

The high intensities of the radioactive beams of mercury at the ISOLDE facility at CERN made an experiment with gold (Z = 79)

attractive, and resulted in a statistical precision of $3 \times 10^{-4}$ of the natural line width for $K\alpha_1$.
The radio isotope $^{197}$Hg (64 h), produced in the ISOLDE on-line mass separator, was implanted in an aluminium backing in a spot of a few mm$^2$. The K X-rays emitted from this source originate predominantly in the ($1/2^- \rightarrow 1/2^+$) EC transition to the 77.3 keV level, which is below the K threshold so that only 0.77 % of the K X-rays result from internal conversion in gold. The photo-ionization source consisted of a 0.05 mm gold foil supported on aluminium and located at a distance of 0.5 mm from a 40 Ci $^{169}$Yb source. The energies of the $K\alpha_1$, $K\alpha_2$ and $K\beta_1$ lines from both sources were compared by scanning their Bragg reflections in second order with a bent-crystal spectrometer[1] equipped with an adjustable shutter which allowed to optimize the counting strategy, and with a micrometer screw for an easy and accurate alignment of the two sources. The instrumental asymmetry was found to be $0.93 \times 10^{-6}$ E for a transition of energy E.

The results corrected for the instrumental asymmetry are given in column 3 of Table 1. The effect of the asymmetric line shape was taken into account through a proper method of determination of the line position[2]. The anaysis is complicated slightly by the presence of the 24 h $^{197m}$Hg together with the 64 h $^{197g}$Hg. The Hg $K\alpha_2$ X-ray line from the isomeric transition is so close to the Au $K\alpha_1$ line that its tail gives rise to an additional shift $\varepsilon_{Hg}$, which can be calculated (column 5 of Table 1) from the known intensity and shape of the Hg X-ray reflection. A measurement of the Au $K\alpha_1$ line after the 24 h activity had died away (last line in Table 1) confirms that this correction is precise enough. The short-lived isomer furthermore contributes to the hyperfine shift (column 4 of Table 1) through a weak branch to the 11/2$^-$ level in $^{197}$Au, which was assumed to have $\mu/\mu N = 6.3$.

*Table 1:*
*Shifts $\Delta E = E_{PI} - E_{EC}$ in the energies of gold K X-rays*

| Line | mid-time of measurement after 78 h (h) | ΔE observed shift (meV) | Calculated contribution $\varepsilon_{hfs}$ [2] | $\varepsilon_{Hg}$ [a] | $\Delta E_{corr} = E - \varepsilon_{hfs} - \varepsilon_{Hg} - \varepsilon_{is}$ |
|---|---|---|---|---|---|
| $K\alpha_1$ | 20 | 286±42[b] | 330 | -224 | 168±42[b] |
| $K\alpha_1$ | 47 | 413±25 | 350 | -130 | 181±25 |
| $K\beta_1$ | 75 | 605±52 | 362 | - | 231±52 |
| $K\beta_1$ | 101 | 560±73 | 371 | - | 177±73 |
| $K\beta_1$ | 126 | 670±76 | 373 | - | 285±76 |
| $K\alpha_2$ | 159 | 569±40 | 378 | - | 179±40 |
| $K\alpha_2$ | 189 | 564±57 | 378 | - | 174±57 |
| $K\alpha_1$ | 238 | 568±27 | 378 | 0 | 178±27 |

a) Contribution to the Au $K\alpha_1$ shift from the tail of the Hg $K\alpha_2$ line from the 24 h isomer.

b) The experimental errors are statistical errors only.

The contributions $\varepsilon_{hfs}$ from magnetic hfs can be calculated from the expressions given in Ref. 1, if the branching of multipole order 0 to multipole order 1 in the dominant $1/2^- \rightarrow 1/2^+$ EC transition is taken into account[2].

*Table 2:*
*Caculated contributions $\Delta_{ose}$ from outer-shell excitations; comparison with experiment*

| Line | $\Delta_{ose}$ [a] (meV) | $\Delta E_{corr}$ (meV) | | |
|---|---|---|---|---|
| | | b) | c) | d) |
| Au $K\alpha_1$ | 180 | 178 | (±17) | (±36) |
| Au $K\alpha_2$ | 180 | 177 | (±33) | (±46) |
| Au $K\beta_1$ | 440 | 230 | (±37) | (±50) |

a) The value given is essentially the increase in energy of the X-ray due to photo-ionization, the contribution from EC being 100 times smaller.

b) Weighted mean (Table 1).

c) Error due to counting statistics.

d) Total error including a contribution from the asymetry correction ( ± 15 meV) and from the bias correction[2] (± 0.05 ΔE).

The atomic excitation processes are considered as instantaneous. The K X-rays emitted on a time scale of $10^{-17}$ s will not be influenced by subsequent atomic rearrangements. The intensities of the satellites, expected to be different for the PI and the EC processes, may be obtained in the sudden approximation. Calculations of vacancy probabilities have been performed by Nestor et al.[3]. The satellite energies were calculated in the relativistic Hartree-Fock (Dirac-Fock) scheme, using the programme of Lindgren and Rosen[4]. In the first approximation „frozen orbitals" can be used. Somewhat higher accuracy is achieved, if self-consistent wave functions are used for the different hole states, which means that the relaxation effect is taken into account. This was done for the innermost holes, where this effect is significant.

Our experiments on gold K X-rays show that in addition to the hyperfine shift[1] one finds a shift of 200 meV which we tentatively interpret as the contribution from satellite lines originating in the photo-ionization process. The agreement with a simple calculation is excellent for $K\alpha_1$ and $K\alpha_2$, while less good for $K\beta_1$ (Table 2). We note in this connection that the $K\beta_1$ contribution comes predominantly from the outer electrons, for which the sudden approximation is less precise.

*) CERN, Geneva, Switzerland

## References

[1] G.L. Borchert, P.G. Hansen, B. Jonson, H.L. Ravn, O.W.B. Schult and P. Tidemand-Petersson, Phys. Letters 63A (1977) 15
[2] G.L. Borchert, P.G. Hansen, B. Jonson, I. Lindgren, H.L. Ravn, O.W.B. Schult and P. Tidemand-Petersson, Phys. Letters A (to be published)
[3] C.W. Nestor, T.C. Tucker, T.A. Carlson, K.D. Roberts, F.B. Malik and C. Froese, ORNL- 4027 (1966)
[4] A. Rosen and I. Lindgren, Phys. Rev. 176 (1968) 114

## 2.3. High Precision Measurement and Calculation of the Hypersatellite $K\alpha_1^h$ X-Ray Energy for Z=80

K. Schreckenbach*), H.G. Börner, J.P. Desclaux**)

For inner shell energies of high Z atoms, corrections to the predominant electrostatic terms, i.e. magnetic interactions, retardation and Lamb-shift, become important, and it is necessary to check the level of accuracy to which these corrections can be calculated from first principles. The shift between an X-ray and its hypersatellite provides a good test for the magnetic interaction.

The hypersatellite line is due to double ionisation of the K electron shell. The probability of the creation of this situation in radioactive decay processes like K-capture and internal conversion is very small in comparision to the ordinary single K ionisation[1]. For higher Z it is only in the order of $10^{-5}$.

We have performed a measurement of the hypersatellite $K\alpha_1^h$ X-ray in Hg, following the decay of $^{199}$Au by means of the curved crystal spectrometer GAMS 1 at the high flux reactor of the ILL in Grenoble. A gold wire of 0.12 mm diameter and 40 mm length was activated in a flux of $8 \times 10^{14}$ n/cm$^2$s. The isotope $^{199}$Au is produced by double neutron capture. After $\beta^-$-decay double ionisation of the K-shell of $^{199}$Hg is caused by a 208 keV conversion electron transition.

The measurement of the corresponding hypersatellite line was performed after the shut-down of the reactor. The sum over the first 91 scans (4 days) is plotted in fig. 1a. Assuming a smooth curvature of the background a clear peak is visible. The background is due to the tail of the $K\alpha_1$ X-ray and to $\gamma$-radiation from the target and from the reactor hall.

In fig. 1b the best fit of the line to a Lorentzian line shape is given. The line has the following characteristics: confidence, taken over the half width: 99.75 % (3 x$\sigma$); shift with total error: 1145±12 eV; half width: 80±20 eV; intensity relative to the main $K\alpha_1$ X-rays $(2.8 \pm 1.1) \times 10^{-5}$; intensity relative to the 208.2 keV branch in the $^{199}$Au decay: $(7.8 \pm 3.1) \times 10^{-5}$. In table 1 the value of the shift calculated at various levels of approximation is listed[3]. The experiment gives a value which is 39±12 eV lower than the predicted energy difference.

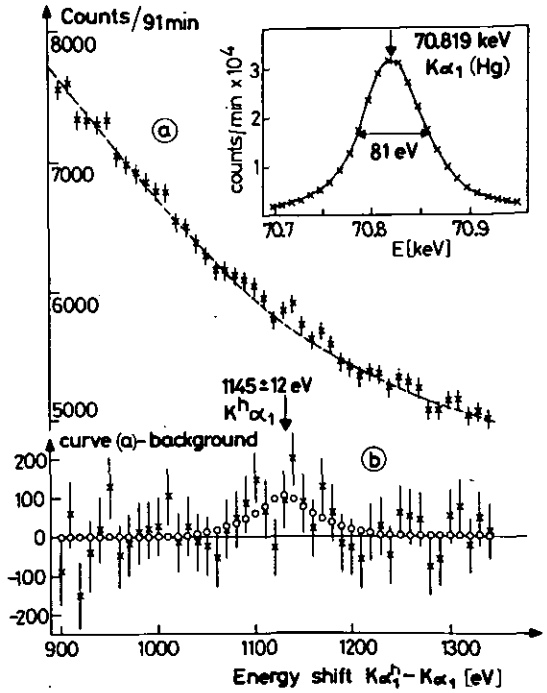


*Figure 1:*
*Sum of 91 runs of 1 min. per point*
*a) The background is denoted (——)*
*b) The best fit of the line (background substracted) is given by (ooo). The inset shows the $K\alpha_1$ line (observed half width 81 eV, natural line width: 65 eV).*

*Table 1:*
*Shift between the $K\alpha_1$ X-ray and its hypersatellite for Z=80 (in eV).*

| | |
|---|---|
| Unperturbed Dirac-Fock | 992 |
| + Magnetic interaction | 1179 |
| + Magnetic interaction and retardation | 1184 |
| above correction + Lamb shift | 1182 |
| all above correction + mixing with $^1P_1$ | 1184 |
| experimental value | 1145±12 |

*) Institut Laue-Langevin, Grenoble, France
**) CEA, Grenoble, France

### References

[1] T. Mukoyama and S. Shimizu, Phys. Rev. C13 (1976) 377
[2] S.I. Salem and P.L. Lee, Atomic and Nucl. Data Tab. 18 (1976) 233
[3] K. Schreckenbach, H.G. Börner, J.P. Desclaux, Phys. Lett. 63A (1977) 330

## 2.4. Evidence for a $10^+$ Isomer in $^{134}$Ce

M. Müller-Veggian, H. Beuscher, D.R. Haenni, R.M. Lieder, C. Mayer-Böricke

The light Ce nuclei, with mass number A = 128–134 (ref. 1,2), display well developed rotational bands up to spin $I^\pi = 16^+, 18^+$. These nuclei show pronounced backbending effects at the critical angular momentum $I_c = 10$. Considering the experimental result that in the neighbouring odd-proton nuclei the $h_{11/2}$ proton bands do not show backbending, Ward et al.[2] concluded, invoking blocking arguments, that the backbending in the Ce region is due to the $h_{11/2}$ protons. Recently in the heavier nuclei $^{136}$Ce, $^{138}$Ce $10^+$ isomeric states were observed[3], the configuration of which is $\nu[h_{11/2}]^{-2}$. Therefore it seemed interesting to search for such an isomer also in the lighter Ce nuclei. The nucleus $^{134}$Ce was studied by in-beam $\gamma$ and $e^-$ spectroscopy using the $^{134}$Ba)$\alpha$,4n) reaction at 60 MeV. In the nucleus $^{134}$Ce a long lived isomer was observed

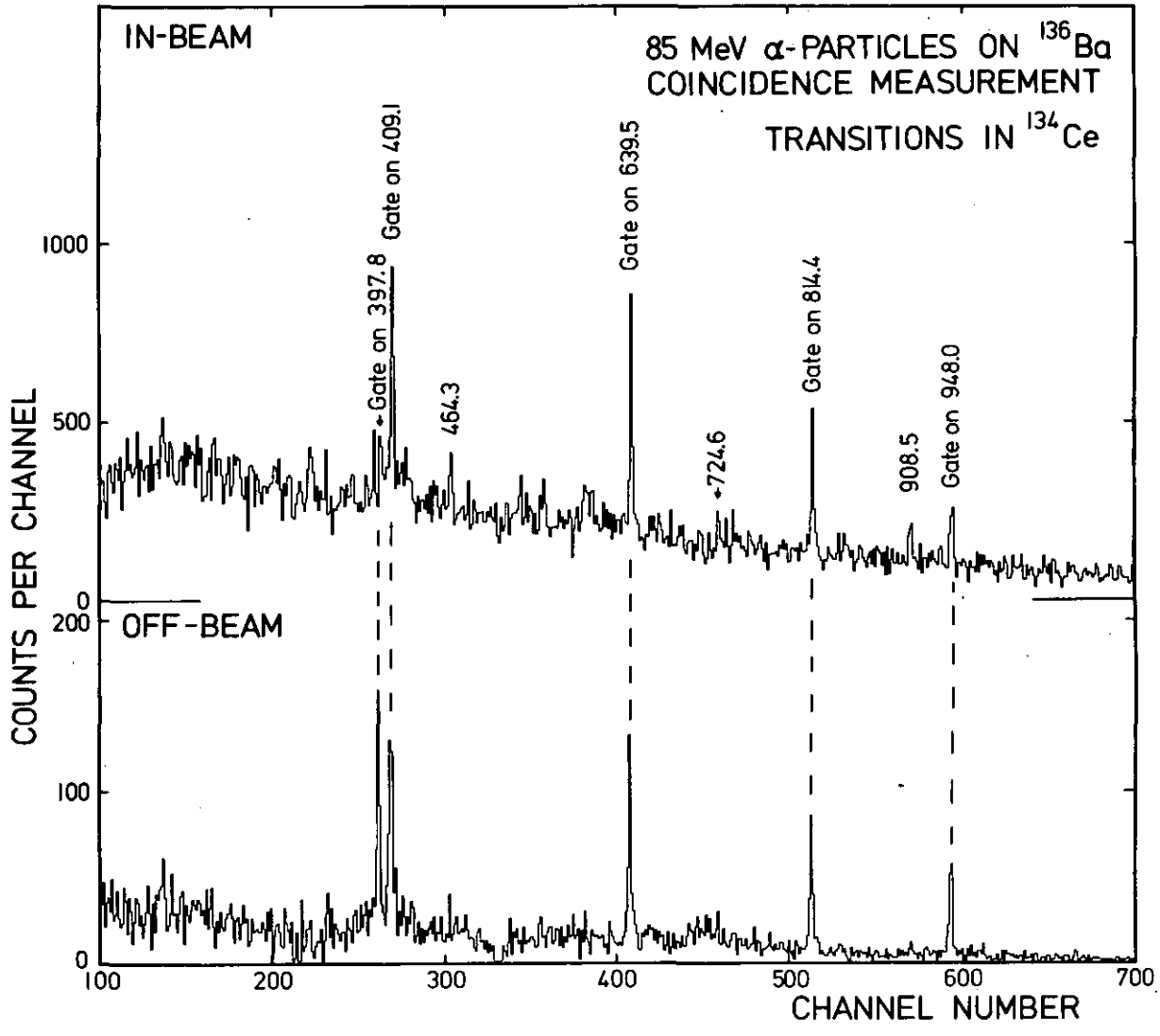


*Figure 1:*
*In-beam and off-beam γ-γ coincidence spectra resulting form summing spectra gated on the 397.8 keV, $2^+ \rightarrow 0^+$, $4^+ \rightarrow 2^+$, $6^+ \rightarrow 4^+$ and $8^+ \rightarrow 6^+$ transitions.*

| | |
|---|---|
| $\frac{I_\gamma(409,2)}{I_\gamma(397.5)}$ | 1 a) |
| $\left[\frac{I_K(409.2)}{I_K(397.5)}\right]_{exp}$ | 1.0 ± 0.1 |
| $\left[\frac{I_{KE2}(409.2)}{I_{KE1}(397.5)}\right]_{th}$ | 2.94 |
| $\left[\frac{I_{KE2}(409.2)}{I_{KE2}(397.5)}\right]_{th}$ | 0.9176 |
| $\left[\frac{I_{KE2}(409.2)}{I_{KM1}(397.5)}\right]$ | 0.647 |

*Table 1:*
*Intensity ratios for the 409.2 keV and 397.5 keV lines in the γ and e⁻ off-beam spectra*

a) In the decay of the isomer both lines have the same γ intensity.

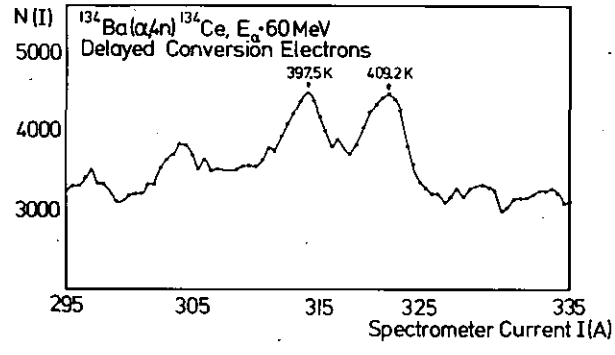


*Figure 2:*
*Delayed conversion electron spectrum.*

with a half life $T_{1/2} > 200$ ns. As can be seen from the spectrum shown in fig. 1, this isomer feeds into the $8^+$ state of the ground state band. In fact in the in-beam spectrum, obtained by summing all the spectra gated on the 397.8 keV, $2^+ \rightarrow O^+$, $4^+ \rightarrow 2^+$, $6^+ \rightarrow 4^+$ and $8^+ \rightarrow 6^+$ transitions, the other members of the ground state band as well as further lines are seen. In the off-beam spectrum, obtained by summing the spectra gated on the 397.8 keV, $2^+ \rightarrow O^+$, $4^+ \rightarrow 2^+$, $6^+ \rightarrow 4^+$ and $8^+ \rightarrow 6^+$ transitions, only the states populated

by the 397.8 keV isomeric transition are seen. In order to assign spin and parity to this new isomeric state in $^{134}$Ce, conversion electron spectra were measured. Figure 2 shows a delayed conversion spectrum, obtained setting an off-beam window on the $t_{e^-RF}$ time spectrum. The $2^+ \rightarrow 0^+$ transition of 409.2 keV and the 397.5 keV lines appear with comparable intensities. In table 1 the experimental results for this measurement are compared to ratios of theoretical conversion coefficients. It can be clearly seen that only when the 397.5 keV transition is assumed to have an E2 multipolarity, this ratio fits the experimental data. From this experimental evidence it was concluded that the new isomer observed in $^{134}$Ce has spin and parity $10^+$.

## References


[1] W. Dehnhardt, S.J. Mills, M. Müller-Veggian, V. Neumann, D. Pelte, G. Poggi, B. Povh and P. Taras, Nucl. Phys. A225 (1974) 1
[2] D. Ward, H. Bertschat, P.A. Butler, P. Colombani, R.M. Diamond and F.S. Stephens, Phys. Lett. 56B (1975) 139
[3] M. Müller-Veggian, Y. Gono, R.M. Lieder, A. Neskakis and C. Mayer-Böricke to be published


## 2.5. High-Spin Isomer in $^{137}$Ce


M. Müller-Veggian, Y. Gono*), R.M. Lieder, A. Neskakis**), C. Mayer-Böricke


In the odd-neutron nucleus $^{137}$Ce an isomer with spin (31/2) with a half life of 5 ns was observed at an excitation energy of 4.254 MeV. This nucleus has neutron numer 79. In fig. 1 the level scheme, as resulting from our experiments, is shown. The sequence of states with spins and parities $11/2^-$, $15/2^-$, $19/2^-$ has been interpreted to form a decoupled sequence based on the $11/2^-$ isomer of $h_{11/2}$ neutron-hole configuration[1]. The state with spin and parity $21/2^{(+)}$ may result from the coupling of a $h_{11/2}$ neutron to the $5^-$ state in $^{138}$Ce, which has a $[\nu h_{11/2}^{-1}\, \nu d_{3/2}^{-1}]_5$ configuration (ref. 1). The $(23/2^+)$ state, which is deexcited by the 734.9 keV into the $21/2^{(+)}$ level, may originate from the coupling of the $h_{11/2}$ neutron to the I=8 state in $^{138}$Ce of $[\pi h_{11/2}\pi g_{7/2}]_8$- or $[\pi h_{11/2}\pi d_{5/2}]_8$- structure.

In $^{138}$Ce an isomer with spin and parity $10^{(+)}$ was observed[1]. This *isomer, which has been observed*[2] *at a similar excitation energy* in the N=80 isotone $^{144}$Gd, has been interpreted to have a $[\nu h_{11/2}^{-2}]$ configuration[1]. The state with spin (27/2) therefore may originate from the coupling of the $h_{11/2}$ neutron to the $10^{(+)}$ state in $^{138}$Ce yielding a $[\nu h_{11/2}^{-3}]$ configuration. This state was not found to be isomeric, since it is deexcited by dipole transition of 287.2 keV to the I=(25/2) state, whereas the $10^{(+)}$ state in $^{138}$Ce is depopulated by a quadrupole transition of 430.0 KeV, which may have a M2 multipolarity. The interpretation of the (31/2) isomer depends on the configuration assigned to the (27/2) state. This high-spin isomer can have a three-particle configuration since its excitation energy is comparable to the energy $4\Delta$, necessary to break two pairs. Assuming that this state with I=(31/2) has a three-particle configuration only one possibility exists.

In fact the spin I=31/2 could be obtained by coupling a $h_{11/2}$ neutron hole with two $h_{11/2}$ protons. The 552.1 keV $\gamma$ ray depopulating the I=(31/2) state is a stretched quadrupole transition. Assuming an E2 character for this transition, the hindrance of a factor about 5 with respect to Weisskopf units[3] can be understood considering the above configurations assigned to the I=(31/2) and I=(27/2) states. If five particle configurations are used to interprete this state then, due to the lo cation of the Fermi surface for neutrons and protons, the candidates are:

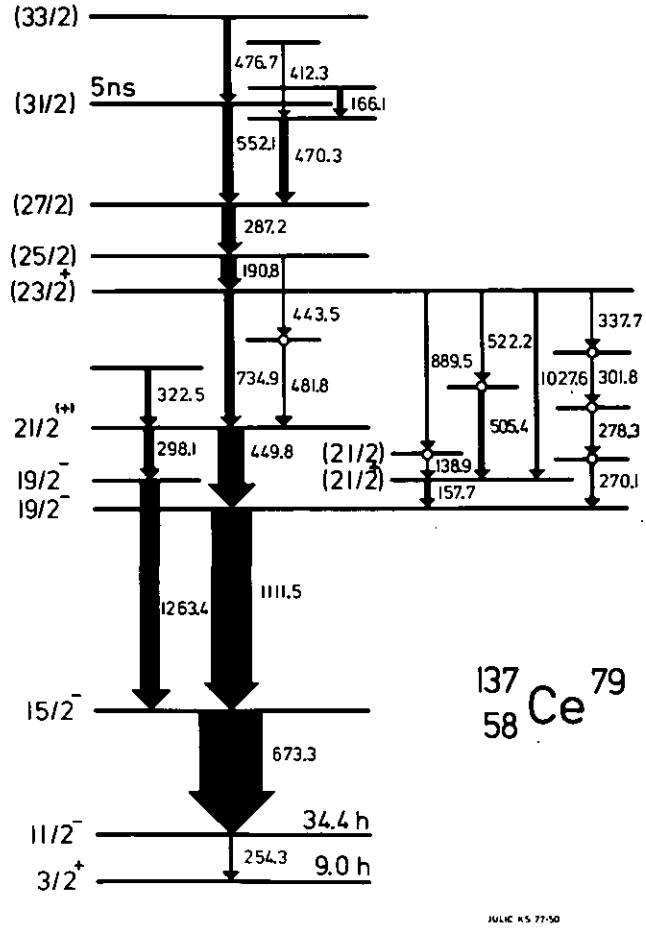


*Figure 1:*
*Level scheme of $^{137}$Ce.*

(i) in case of negative parity

1) $[(\nu h_{11/2})\otimes(\nu h_{11/2}\nu h_{11/2})\otimes(\nu d_{3/2})\otimes(\nu s_{1/2})]_{31/2^-}$

2) $[(\nu h_{11/2})\otimes(\pi g_{7/2}\pi g_{7/2})\otimes(\pi g_{7/2})\otimes(\pi d_{5/2})]_{31/2^-}$

3) $[(\nu h_{11/2})\otimes(\pi g_{7/2}\pi d_{5/2})\otimes(\pi g_{7/2})\otimes(\pi d_{5/2})]_{31/2^-}$

(ii) in case of positve parity

1) $[(\nu h_{11/2})\otimes(\nu h_{11/2}\nu s_{1/2})\otimes(\pi d_{5/2})\otimes(\pi g_{1/2})]_{31/2^+}$

2) $[(\nu h_{11/2})\otimes(\pi h_{11/2}\pi g_{7/2})\otimes(\nu d_{3/2})\otimes(\nu s_{1/2})]_{31/2^+}$

3) $[(\nu h_{11/2})\otimes(\pi h_{11/2}\pi d_{5/2})\otimes(\nu d_{3/2})\otimes(\nu s_{1/2})]_{31/2^+}$

*) Present address: Institut für Kernphysik, Technische Hochschule Darmstadt, 6300 Darmstadt, West Germany

**) Present address: State University of New York, Stony Brook, New York 11794, USA

## References


[1] M. Müller-Veggian, Y. Gono, R.M. Lieder, A. Neskakis, C. Mayer-Böricke to be published

[2] M.A.J. Mariscotti, H. Beuscher, W.F. Davidson, H.M. Jäger, R.M. Lieder, M. Müller-Veggian, A. Neskakis, D.R. Zolnowski, to be published

[3] C.M. Lederer, J.M. Hollander, I. Perlman in Table of Isotopes 6th Edition, New York (1967)


## 2.6. Systematics of $1O^+$ Isomers in the N = 78 Nuclei


M. Müller-Veggian, H. Beuscher, Y. Gono*), D.R. Haenni, R.M. Lieder, A. Neskakis**), and C. Mayer-Böricke


The transitional nuclei which are located near the closed shells are expected to have properties connected to the collective degrees of freedom as well as to the intrinsic motion of the nucleons. Therefore it seems interesting to study these nuclei in order to investigate the competition of these two different types of nuclear motion. Furthermore these transitional nuclei seem to provide valid tests for the predictions of theoretical models. In fact it is just in these regions where models, based on spherical and deformed basis should overlap. The N = 78 isotones are expected to exhibit collective as well as single-particle porperties. Therefore the even-mass nuclei $^{136}$Ce, $^{138}$Nd, $^{140}$Sm were investigated using in-beam spectroscopy at our laboratory using the following reactions: $^{136}$Ba(α,4n) at 61 MeV, $^{140}$Ce(α,6n) at 85 MeV and $^{142}$Nd (α,6n) at 90 MeV. The level schemes of these nuclei, as resulting from our experiments are shown in fig. 1. These isotones have very similar ground state bands. In all three nuclei isomers are observed. The half life decreases with increasing proton number. These isomers were found to have spin and parity $1O^+$. They are interpreted as $[\nu h_{11/2}]^{-2}$ states. In fact the Fermi surface for neutrons lies very close to the $h_{11/2}$ orbital. On the other hand there is also the possibility that protons may be excited into the $h_{11/2}$ orbital. The interpretation that the neutrons are responsible for the configuration of the $1O^+$ isomer, in $^{136}$Ce, $^{138}$Nd and $^{140}$Sm, gains support form the fact that the excitation energies of these $1O^+$ isomers in the N = 78 nuclei agree within 75 keV, thus indicating that the level structure does not change very much with proton number. These nuclei show similar collective states up to $6^+$. The $6^+$ states are well reproduced by the VMI model[1,2]. The two parameters of the VMI model[1] are found to be $\mathcal{J}_o \cong$ O.OO2 [keV]$^{-1}$ and $\sigma \simeq 1O$ for these isotones. These values imply small deformations. The predicted energies of the $8^+$ states in $^{138}$Nd and $^{140}$Sm are in fair agreement with the experimental ones [1,2]. In case of $^{136}$Ce an excitation energy of 3226 keV was predicted for the collective $8^+$ state (ref. 1). The experimental energy of the $8^+$ state was found to be 299O.O keV. This difference suggests that the $8^+$ state in $^{136}$Ce may be dominated by the $[\nu h_{11/2}]^{-2}$ configuration. In $^{138}$Nd and $^{140}$Sm the $8^+$ states contain more collectivity. These assumptions may provide an understanding of the experimental B(E2) values of the $1O^+ \rightarrow 8^+$ isomeric transitions in $^{136}$Ce, $^{138}$Nd and $^{140}$Sm as given in table 1. The B(E2)

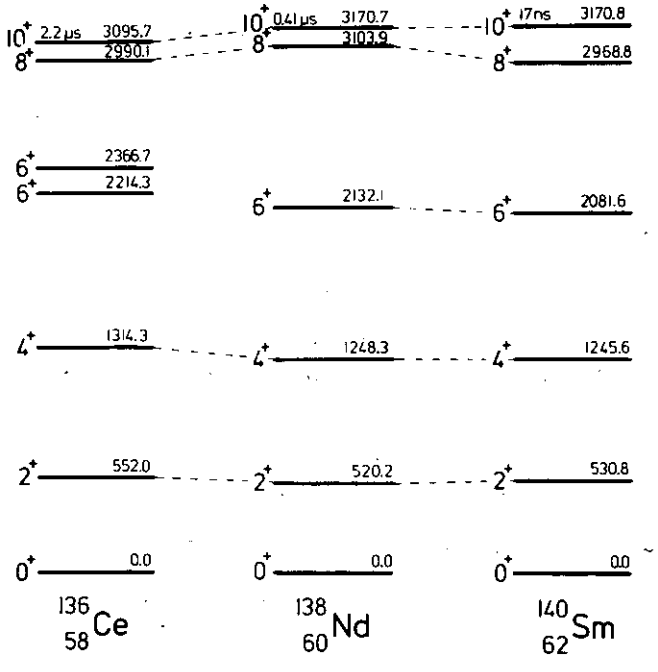


*Figure 1:*
*Level structure for the N = 78 isotones.*

*Table 1:*
*B(E2;$10^+ \rightarrow 8^+$) values for the N = 78 isotones*

| Nucleus | $E_\gamma(10^+ \rightarrow 8^+)$ | $T_{1/2}$ | $B(E2;10^+ \rightarrow 8^+)$ | $\frac{B(E2;10^+ \rightarrow 8^+)}{B(E2)\ w.u.}$ |
|---|---|---|---|---|
| $^{136}$Ce | 105.7 [keV] | 2.2 [μs] | $7.35\times10^{-4}$ [$e^2b^2$] | 0.18 |
| $^{138}$Nd | 66.8 [keV] | 0.41 [μs] | $1.05\times10^{-2}$ [$e^2b^2$] | 2.5 |
| $^{140}$Sm | 202.0 [keV] | 17 [ns] | $8.16\times10^{-3}$ [$e^2b^2$] | 1.88 |

value of the $1O^+ \rightarrow 8^+$ transition in $^{136}$Ce is reduced by a factor of about 6 with respect to single particle units[3] indicating rather pure single particle configurations: In the cases of $^{138}$Nd and $^{140}$Sm the B(E2) strengths were found to be slightly enhanced by a factor of

about 2 and 1.5, respectively, in comparison to single particle units[3], probably due to the collectivity of the $8^+$ states.

*) Present address: Institut für Kernphysik, Technische Hochschule Darmstadt, 6300 Darmstadt, West Germany
**) Present address: State University of New York, Stony Brook, New York 11794, USA

## References


[1] M.A.J. Mariscotti, G. Scharff-Goldhaber, B. Buck, Phys. Rev. 178 (1969) 1864
[2] M.A.J. Mariscotti, H. Beuscher, W.F. Davidson, R.M. Lieder, A. Neskakis and H.M. Jäger, Z. Physik A279 (1976) 169
[3] C.M. Lederer, J.M. Hollander, I. Perlman in Table of Isotopes 6th Edition, New York (1967)


## 2.7. Gamma-ray Multiplicities in α-Induced Compound and Precompound Reactions


M. Ogawa*), P. Kleinheinz, S. Lunardi, M. Fenzl**), and O.W.B. Schult


Many gamma-ray multiplicity measurements have been conducted, primarily for the investigation of the angular momentum transfer in charged particle induced reactions. Their emphasis has been the study of the deexcitation of the compound systems resulting mostly from heavy ion fusion processes. Relatively little is known, however, about the angular momentum transfer at much higher projectile velocities, where extensive excitation function studies have indicated that precompound processes are important.

Multiplicity measurements in reactions with high velocity $^{12}C$[1] and $^{40}Ar$[2] ions have recently been carried out. However, highly complex reactions occur with these heavy projectiles. We have therefore used α-beams of various energies to study the angular momentum associated with compound as well as precompound reactions through a γ-ray multiplicity measurement. Very recently similar experiments have been initiated by a group at Osaka[3].

In our measurements a self supporting metallic target of 2 mg/cm² $^{150}Sm$ enriched to 95.4 % was bombarded with α-particles from our cyclotron. A 74 cm³ true coaxial Ge(Li) detector was used for selection of the exit channel. The coincident photons with energies greater than 170 keV were detected in a 7.6 cm diameter x 7.6 xm NaI(Tl) scintillation counter which was located at 40 cm distance from the target in order to discriminate against neutrons. Both detectors were oriented at 125° to the beam direction. Further details about the measurement and the detector calibration are given elsewhere[4]. Our results are plotted in Figure 1. The multiplicities shown are those through the entire γ-ray cascade down to the ground state including the gating transition. They were obtained from the ratio of the coincidence to singles rates for each gate. Gates were set on two or three strong low-lying γ-transitions in each residual nucleus produced in the different (α,xn) reactions (x = 4 – 8). The statistical errors given in Figure 1 become quite large in those energy regions where the respective exit channel is fed with very small cross section. The ordinate scale is accurate to ≅10 %.

In contrast to the expectation for compound nuclear reactions we find that with increasing bombarding energy the multiplicity rises to a maximum and then decreases at still higher energies. This can be attributed to the increasing contribution of precompound processes where the outgoing particles can remove more angular momentum than in case of evaporation following compound nucleus formation. The resulting maximum in the multiplicity is found about 12–18 MeV above the maximum of the excitation function for the respective exit channel. These excitation functions were obtained simultaneously with the multiplicity measurements. The increase in multiplicity for the lower bombarding energies follows the prediction for compound nucleus formation. However, until now it was not clear how high in the bombarding energy this trend would prevail. Our data give the quantitative result for (α,xn) reactions.

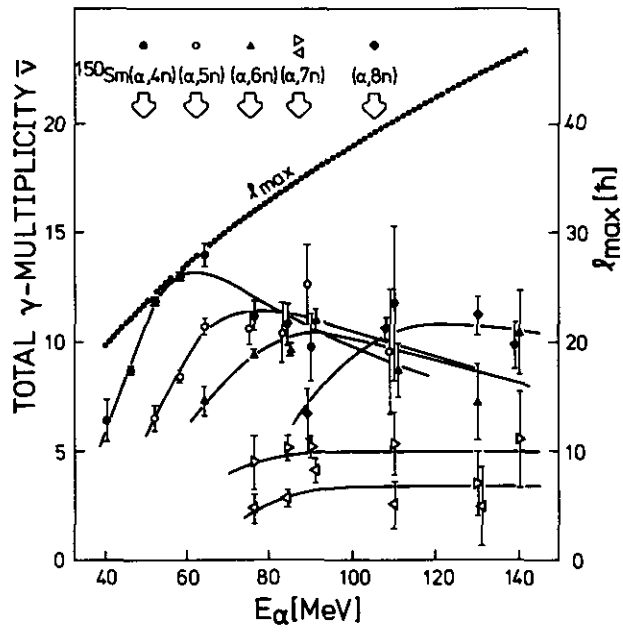


*Figure 1:*
*Total γ-ray multiplicities for various nuclei produced in compound and precompound (α,xn) reactions. The curves for the individual exit channels drawn to guide th eye. For the (α,7n) reaction the upper curve is obtained with the gate on the 1491 keV line, the lower curve with the 997 keV transiton in $^{147}Gd$[10]. The dotted curve gives the maximum angular momentum calculated for compound-nucleus formation (right hand ordinate scale). The arrows at the top indicate the positions of the maxima of the excitation functions.*

The relative importance of precompound contributions is also obvious from a comparison of the maximum multiplicity in e.g. the 4n and 8n reactions. Again, compound-nucleus formation should give higher angular momentum transfer in the (α,8n) reaction than in (α,4n), whereas the measured result shows the opposite.

In Figure 1 we have also drawn the curve for the expected maximum angular momentum transferred. From the comparison of the measured $\nu_{(\alpha,4n)}$ points with the $\ell_{max}$ curve it becomes clear that the assumption of an average angular momentum transfer of $2/3\,\ell_{max}$ and $\Delta I=2$ per γ-transition is incompatible with our results. For (α,4n) data at E≅60 MeV we expect that the transferred angular momentum is more than $2/3\,\ell_{max}$ as we are above the maximum of the (α,4n) excitation function where a fractionation of the angular

momentum should occur for the different exit channels[5]. In a similar way we estimate an average angular momentum transfer of 23 ħ for the (α,4n) process at 64 MeV. From the known level scheme of $^{156}$Gd[6] we find a $\Delta I \cong 1.7$ per yrast transition. In addition, studies of the statistical γ-cascade[7-9] suggest the emission of three transitions in the pre-yrast cascade. This leaves 10 γ-transitons for the yrast cascade which remove 17 ħ. The remaining 6 ħ for the 4 neutrons plus the 3 statistical photons agree with what is expected if one interpolates the results of [7] and [9].

Whereas the multiplicities for the 4n, 5n, 6n and 8n channels show a systematic behaviour, the results for the 7n channel appear to be totally irregular. This can be simply understood[4] from the presence of several isomers in $^{147}$Gd[10]. In $^{148}$Gd which is populated in the (α,6n) reaction the γ-decay proceeds partially through a 17 ns isomer[11]. Due to this isomer the measured multiplicities given in Figure 2 are somewhat lower than the actual ones. From detailed in-beam level scheme studies[6,10,11] we know that the multiplicities measured for the other final nuclei are not affected by the occurrence of isomers.

*) Alexander von Humbold fellow 1976/77, on leave from Tokyo Institute of Technology
**) Physik Department E 17, Technical University Munich.

## References


[1] K.A. Geoffroy, J.B. Natowitz, Phys. Rev. Lett. 37 (1976) 1198
[2] J.O. Newton, I.Y. Lee, R.S. Simon, M.M. Aleonard, Y. El Masri, F.S. Stephens, R.M. Diamond, Phys. Rev. Lett. 38 (1977) 810
[3] H. Ejiri, H. Sakai, Y. Nagai, T. Itahashi, T. Shibata, S. Nakayama, T. Kishimoto, K. Maeda, M. Hoshi, Annual Report 1976, Research Center for Nuclear Physics, Osaka University, p. 181
[4] M. Ogawa, P. Kleinheinz, S. Lunardi, O.W.B. Schult, M. Fenzl, Z. Physik A284 (1978) 271
[5] P.O.Tjøm, F.S. Stephens, R.M. Diamond, J. de Boer, W.E. Meyerhof, Phys. Rev. Lett. 33 (1974) 593
[6] D.R. Haenni, T. Sugihara, Phys. Rev. C16 (1977) 120
[7] O.W.B. Schult, B.P.K. Maier, U. Gruber, R. Koch, Z. Physik 185 (1965) 295
[8] J.R. Grover, J. Gilat, Phys. Rev. 157 (1967) 814
[9] C.F. Williamson, S.M. Ferguson, B.J. Shepherd, I. Halpern, Phys. Rev. 174 (1968) 1544
[10] P. Kleinheinz, M.R. Maier, S. Lunardi, M. Ogawa, R. Broda, Contribution to the Int. Conf on Nucl. Structure, Tokyo (1977) p. 865, and separate contribution to this report
[11] S. Lunardi, M. Ogawa, M.R. Maier, P. Kleinheinz, Institut für Kernphysik, KFA Jülich, Annual Report 1976, p. 40; and P. Kleinheinz, M.R. Maier, unpublished data


## 2.8. The 3⁻ State in the Doubly Closed Shell Nucleus $^{146}_{64}Gd_{82}$


P. Kleinheinz, S. Lunardi, M. Ogawa, and M.R. Maier*)


In the N=82 nucleus $^{146}_{64}Gd_{82}$ the $g_{7/2}$ and $d_{5/2}$ proton shells are completed. One therefore expects in that nucleus the 3⁻ state at rather low energy, since the lowest-lying neutron as well as proton particle-hole excitations ($\nu s^{-1}_{1/2}\, \nu f^{+1}_{7/2}$ and $\pi d^{-1}_{5/2}\, {}_{p}h^{+1}_{11/2}$) will contribute to such a state.

Previous studies of $^{146}$Gd[1-4] gave conflicting results on the 3⁻ level. We have therefore reinvestigated this nucleus in an in-beam γ-ray experiment using the $^{148}$Sm(α,6n) reaction at $E_\alpha$ = 82 MeV. Our coincidence results confirm the previous level scheme below 3 MeV except for a weak 1074 - 1585 keV parallel cascade to the ground state which is incompatible with our data. This cascade had been tentatively suggested in ref.[2] but was contested in the subsequent radioactivity study[4].

However we disagree with the previous spin and parity assignments for the excited states in $^{146}$Gd. Our data establish the 1579 keV ground state transition as E3, in contrast to the previous E2 assignment. Fig. 1 gives the angular distributions for the three lowest yrast transitions in $^{46}$Gd. The $A_2$-values of the ground state transition is 1.7 times larger than the $A_2$-values for the two preceding transitions, a result which it totally unusual for a 6→4→2→0 stretched E2 sequence as was previously suggested. Furthermore, in contrast to the negative $A_4$-values of the two preceding E2 transitions, the 1579 keV ground state transition has a slightly positive $A_4$, conflicting with an E2-, but in agreement with an L=3 assignment. In the middle of fig. 1 the measured $A_2$ values are compared with the theoretical coefficients. Whereas a 6→4→2→0 assignment for $^{146}$Gd gives an unreasonably increased $\alpha_2$-value for the ground state transition, the alternate 7→5→3→0 sequence results in a regularly decreasing $\alpha_2$ as is generally found for yrast transition sequences from (α,xn) angular distribution data. The short half life of the 1579 keV level (cf. separate contribtuion to this

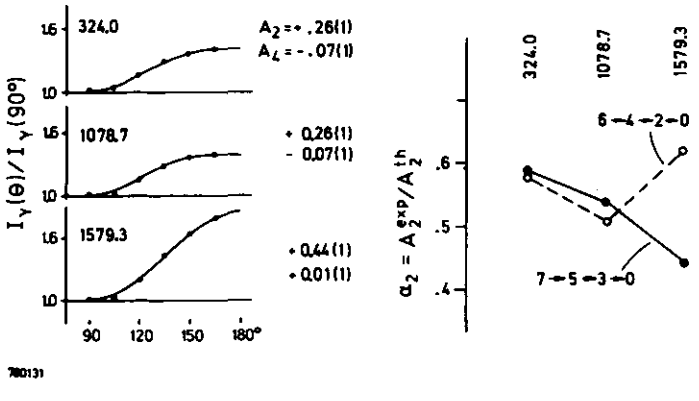


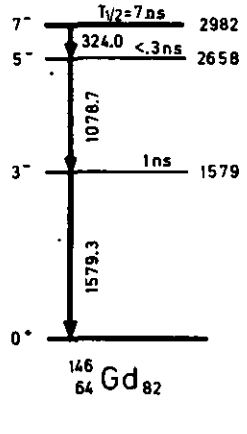


*Figure 1:*
*Angular distributions for the three lowest yrast transitions in $^{146}$Gd. The errors of $A_2$ and $A_4$ are purely statistical.*

report) excludes M3 multipolarity, but is in agreement with an enhanced E3 transition. Spin and parity 3⁻ are therefore assigned to the 1579 keV first excited state in $^{146}$Gd, in accordance with simple shell model expectations. The existence of lower-lying $0^+$ or $2^+$ levels is almost certainly excluded since they should definitely have been observed in the previous[1,2] experiments. Thus $^{146}$Gd is besides $^{208}$Pb the only doubly even nucleus with a 3⁻ first excited state.

*) Physik Department, TU München, D-8046 Garching, Germany, now LBL Berkeley


**References**

[1] B. Spoelstra, Nucl. Phys. A174 (1971) 63
[2] J. Kownacki, H. Ryde, V.O. Sergejev, and Z. Sujkowski, Nucl. Phys. A196 (1972) 498
[3] K. Krien, F. Djadali, R.A. Naumann, H. Hübel, and E.H. Spejewski, Phys. Rev. C7 (1973) 2484
[4] E. Newman, K.S. Toth, C.D. Hensley, and W.-D. Schmidt-Ott, Phys. Rev. C9 (1974) 674


## 2.9. The $\alpha_K$-value of the 1579 keV E3 Ground State Transition in $^{146}$Gd

P. Kleinheinz, M. Ogawa, R. Broda, P.J. Daly, H. Beuscher, and D. Haenni

The 1579 keV first excited state in $^{146}$Gd, which previously had been assigned as $I^\pi = 2^+$ has been shown to be the 3⁻ octupole excitation on the basis of γ-ray angular bution measurements[1]. We have performed conversion electron measurements[2] which confirm this 3⁻ assignment.

The experiment was carried out with the high transmission iron free orange spectrometer[3] which is placed at 90° to the beam direction of the cyclotron at this institute. A self supporting metallic 1.2 mg/cm² 97.7 % enriched $^{149}$Sm target was bombarded with 90 MeV α-particles where the (α,6n) and (α,7n) reactions leading to $^{147}$Gd and $^{146}$Gd are dominant. In fig. 1 the relevant portions of the conversion electron spectrum are shown, together with the γ-ray spectrum measured under identical conditions with a 65 cm³ coaxial Ge(Li) detector placed at 125° to the beam direction. The figure also shows the relevant portions of the level schemes. For normalizing γ- and e⁻ intensities the known[4] E2 and E3 multipolarities

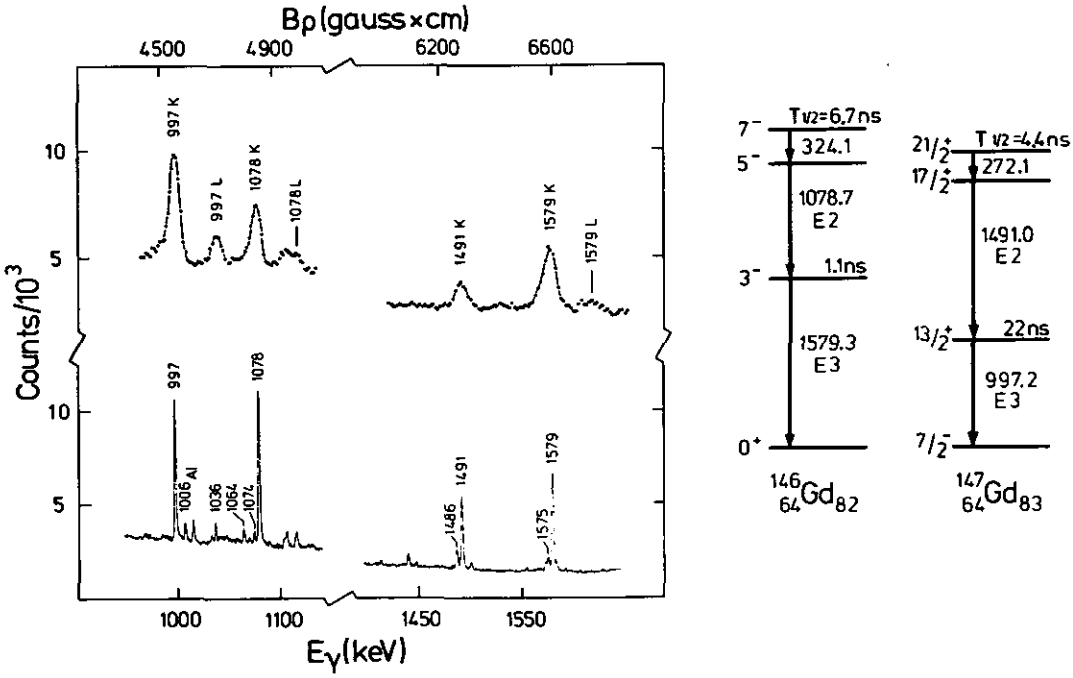


*Figure 1:*
*Conversion electron and γ-ray spectra from the $^{149}$Sm(α,6n) and (α,7n) reactions at 90 MeV. Relevant portions of the level schemes for the $^{147}$Gd and $^{146}$Gd final nuclei are shown to the right. The weak peaks in the γ-ray spectrum labelled with energies occur in various neighbouring nuclei. Where necessary the $\alpha_K$ values were corrected for contributions from these transitions.*

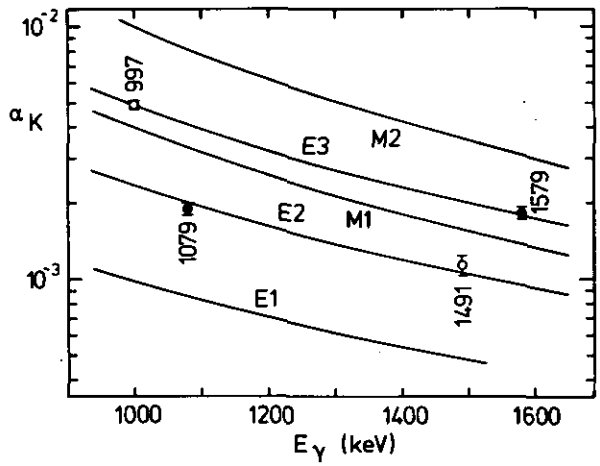


*Figure 2:*
*Comparision of measured conversion intensities with theoretical values of Hager & Seltzer. The 1491 keV E2 and 997 keV E3 transitions were used for normalization.*

of the 1491 and 997 keV transitions in $^{147}$Gd, respectively, were used. For the two $^{146}$Gd transitions the conversion coefficients

$$\alpha_K(1079) = 1.87(11) \times 10^{-3} \text{ and}$$
$$\alpha_K(1579) = 1.79(9) \times 10^{-3}$$

result. The influence of the $e^-$ angular distribution on the $\alpha_K$ values is calculated to be $<2\,\%$. The comparison with theoretical values (fig. 2) gives E2 and E3 multipolarity for the 1079 and 1579 keV transitions, respectively. Thus the conversion electron measurements fully confirm the $3^-$ character for the first excited state of $^{146}$Gd indicated from the angular distribution data.


**References**

[1] P. Kleinheinz, S. Lunardi, M. Ogawa, and M.R. Maier, Z. Phys. A284 (1978) 351, and separate contribution to this report
[2] P. Kleinheinz, M. Ogawa, R. Broda, P.J. Daly, D. Haenni, H. Beuscher, and A. Kleinrahm, Z. Phys. A286 (1978) 27
[3] H. Beuscher et al., Institut für Kernphysik Annual Report 1976, p. 124
[4] P. Kleinheinz, M.R. Maier, R.M. Diamond, F.S. Stephens, and R.K. Sheline, Phys. Lett. 53B (1975) 442, and separate contribution to this report.


## 2.10. The B(E3) value of the $3^-$ First Excited State in $^{146}$Gd


P. Kleinheinz, M. Ogawa, R. Broda, P.J. Daly, and A. Kleinrahm*)


A half-life determination of the 1579 keV $3^-$ level in $^{146}$Gd is complicated by the fact that the level in (α,xn) reactions is populated almost entirely through the 7 ns 2982 keV $7^-$ isomer. The 1579 keV state half-life therefore cannot be determined from measurements of singles γ-ray spectra delayed with respect to the beam burst. Instead the time distribution between consecutive transitions has to be measured in a coincidence experiment.

An initial half-life determination utilized the four parameter list mode data of a standard γγ-coincidence experiment with two 70 cm$^3$ true coaxial Ge(Li) detectors in an (α,6n) experiment at $E_\alpha = 76$ MeV. The 1579 keV state half life could be extracted from a centroid analysis of the $t_{\gamma\gamma}$ time distributions associated with coincidence events which involve full energy absorption in both detectors. Results are shown in fig. 1. By comparing the two time distributions of a particular pair of transitions but with reversed gate settings in the two detectors systematic errors can be largely excluded. The analysis of the data of fig. 1 gives the result $T_{1/2} = 0.97 \pm 0.25$ ns, where the error is assigned from the scatter of the four possible individual measurements given in fig. 1.

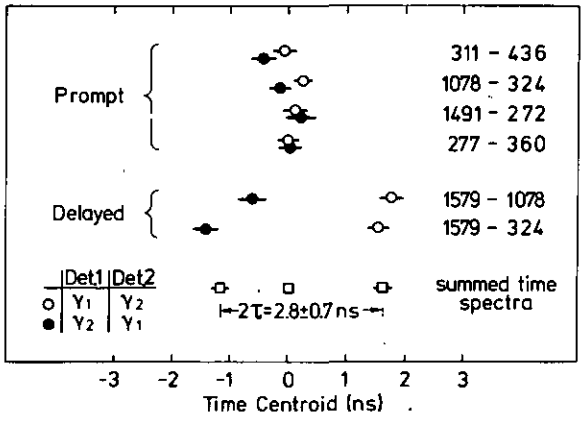


*Figure 1:*
*Half-life determination for the 1579 keV $3^-$ first excited state in $^{146}$Gd from γγ-coincidence data using two 70 cm$^3$ Ge(Li) detectors. The 277–360 keV prompt transition pair occurs in $^{147}$Gd, which is also produced in the experiment through the (α,5n) reaction.*

An independent $e^-\gamma$ half-life measurement utilized the much superior timing properties of plastic scintillation detectors. The experiment was carried out with the orange Spectrometer[1] at the University of Bonn cyclotron. The $^{144}$Sm (α,2n) reaction at 30 MeV was used in this measurement since it gives a much less complex γ-ray spectrum where the energy region above 1 MeV is strongly dominated by only the 1079 keV $5^- \rightarrow 3^-$ and the 1579 keV $3^- \rightarrow 0^+$ transitions. In the coincidence experiment the electron spectrometer was set on the 324 K-line and a 3.8 cm thick × 3.8 cm diameter NE 104 plastic scintillator at 4 cm distance from the target detected high energy γ-rays. The time distributions of fig. 2 were ob-

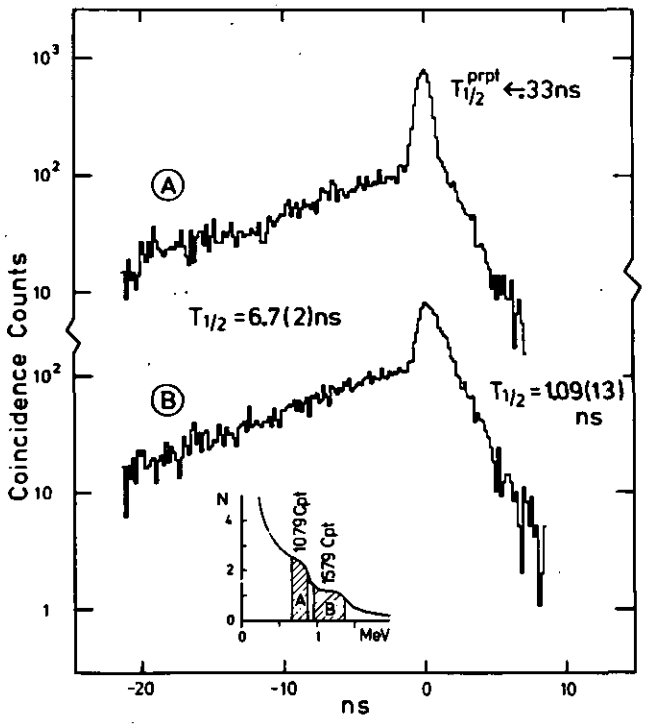


*Figure 2:*
*Time distributions from the 324K-γ coincidence measurements. The gate settings for the γ-ray detector are shown in the insert.*

tained from the two-parameter list mode data with 660 to 860 keV and 960 to 1360 keV windows on the γ-detector. The left hand slopes reflect the 6.7 ns half life of the 2982 keV $7^-$ state. In the case of the lower energy gate on the γ-detector (curve A), the right hand slope shows the presence of a prompt component from the 1079 keV E2 transition, and of a delayed component from the

1579 keV line. The higher energy gate contains no events from the 1079 keV transition and therefore shows the 1579 keV $3^-$ state half life alone. The half life extracted from these data is $T_{1/2} = 1.09 \pm 0.13$ ns, in good agreement with the $\gamma\gamma$-coincidence result. The weighted mean of the two measurements, $T_{1/2} = 1.06 \pm 0.12$ ns, corresponds to

$$B(E3,3\rightarrow 0) = (4.7\pm0.5)\times10^4 e^2fm^6.$$

Comparison with the single particle estimate[2] gives

$$\frac{B(E3,3\rightarrow0)_{^{146}Gd}}{B(E3,3\rightarrow0)_{SP}} = 37$$

which is an unusually large enhancement for a $3^-$ state in an even nucleus and comparable to the octupole strength found in the Pb region. For example, the corresponding enhancement factor for the octupole state at 2.614 MeV in $^{208}Pb$ is also 37.

*) Institut für Strahlen- und Kernphysik der Universität Bonn

**References**

[1] W.D. Schneider and K.H. Gonsior, Nucl. Instr. & Meth. 130 (1975) 165
[2] K.E.G. Löbner, Chapt. 5 of Nuclear Spectroscopy, Amsterdam 1975, p. 149

## 2.11. A Successful Search for the Lowest $2^+$ State in $^{146}Gd$

M. Ogawa, R. Broda, P.J. Daly, P. Kleinheinz, P. v. Brentano*), and K.O. Zell*)

As described in a separate contribution, the 1579 keV first excited state in $^{146}Gd$, earlier assigned as $I^\pi_\upsilon = 2^+$, has now been shown to be the $3^-$ octupole state instead. This result naturally raised the question of the true location of the lowest $2^+$ level, as there were no likely candidates among the known energy levels of 146 Gd. Since the $2^+$ energy would provide an indication of the shell closure at Z=64, and would be valuable in interpreting the level structure of neighbouring nuclei, a separate experiment with the specific aim of locating that state was undertaken.

The search for the $2^+$ state was performed with the $^{144}Sm(\alpha,2n\gamma)^{146}Gd$ reaction using $\alpha$-particle beams from the Köln University Tandem accelerator. The energy threshold estimated from mass tables for populating the $^{146}Gd$ ground state is $E_\alpha = 20.4$ MeV. Therefore, in order to scrutenise the levels of $^{146}Gd$ in the 1.5–3.5 MeV excitation energy region, detailed excitation function measurements were carried out using eight different bombarding energies spanning the range $E_{\alpha\upsilon} = 22.4$–25.1 MeV. $\gamma$-ray spectra up to 3.5 MeV were recorded at each bombarding energy with two 70 cc Ge(Li) detectors placed at 125° and 90° to the beam direction.

The $\gamma$-ray spectra obtained showed, in a quite dramatic way, the successive appearance in order of the 1579, 1079, 324 and 311 keV known $^{146}Gd$ transitions as the beam energy was increased

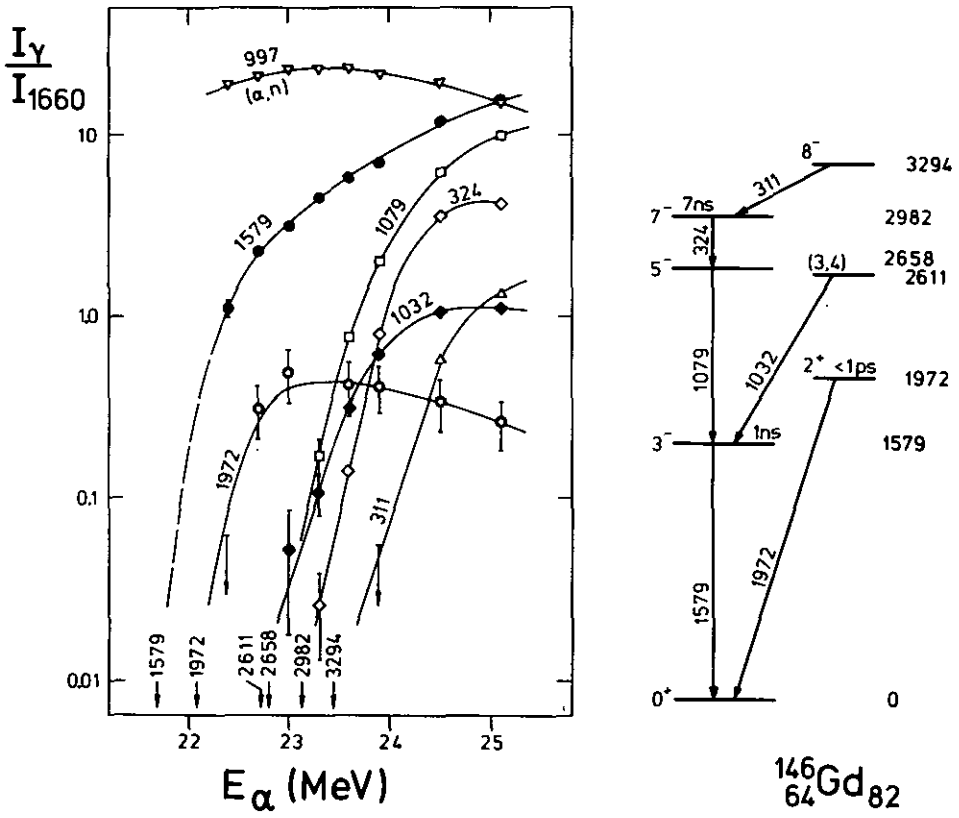


*Figure 1:*
*Excitation functions for various $\gamma$-rays in Gd populated through ($\alpha$,2n). Also shown are data for the 997 keV transition of $^{147}Gd$. Approximate thresholds for individual levels of $^{146}Gd$ are indicated as arrows. Placements of the observed $^{146}Gd$ transitions are shown in the level scheme.*

above the thresholds for population of the $3^-$, $5^-$, $7^-$ and $8^-$ states, respectively. The excitation functions for these transitions and for two other γ-rays of 1972 and 1032 keV, which must also belong to $^{146}$Gd, are shown in fig. 1; the results for the 997 keV γ-ray of $^{147}$Gd are included for comparison. The 1660 keV transition induced by the (α,α′) process has been used for normalization since the (α,α′) cross section is almost independent of energy in this range. The excitation function of the 1972 keV γ-ray unambiguously marks it as a ground state transition from a level at 1972 keV. The 1032 keV line, previously observed in radioactive decay[1], is placed between a level at 2611 keV and the $3^-$ level. Extrapolation of the excitation functions towards lower energies yields threshold energies for population of the individual $^{146}$Gd levels which agree within 0.3 MeV with the thresholds estimated from mass tables.

The measured anisotropy for the 1972 keV γ-ray gave a positive $A_2$ angular distribution coefficient consistent with stretched E2 character and definitely excluding ΔI=1 for the transition. In the 125° spectra at the lower bombarding energies the main portion of the 1972 keV peak was observed to be shifted towards lower energies by 3.5 keV. This is interpreted as a Doppler shift effect indicating for the 1972 keV state a lifetime shorter than the stopping time of recoiling $^{146}$Gd nuclei in the Sm target. Indeed a short measurement with the detector at 55° showed a similar shift in the opposite direction (fig. 2). The size of the energy shift agrees well with the value calculated from the reaction kinematics. By considering the stopping times of Gd ions in Sm, a safe upper limit of $10^{-12}$ s can be placed on the half-life of the 1972 keV state. This short half-life excludes M2 and higher multipolarities for the 1972 keV transition.

Von Oertzen et al.[1] have studied the $^{144}$Sm($^{16}$O,$^{14}$C)$^{146}$Gd reaction, and observed the population of only two excited states below 2 MeV in $^{146}$Gd, at 1.58 and 1.95 MeV. It is now evident that the lower state is the 1579 keV $3^-$ octupole state, and almost certainly the 1.95 MeV level is identical with the 1972 keV state reported here. The excitation function, angular distribution and lifetime data obtained in the present study, as well as the two-proton transfer result, lead to a firm identification of the 1972 keV state as the lowest $2^+$ state in $^{146}$Gd. The location of this state more than 300 keV higher than the first excited $2^+$ state in any other N=82 nucleus pro-

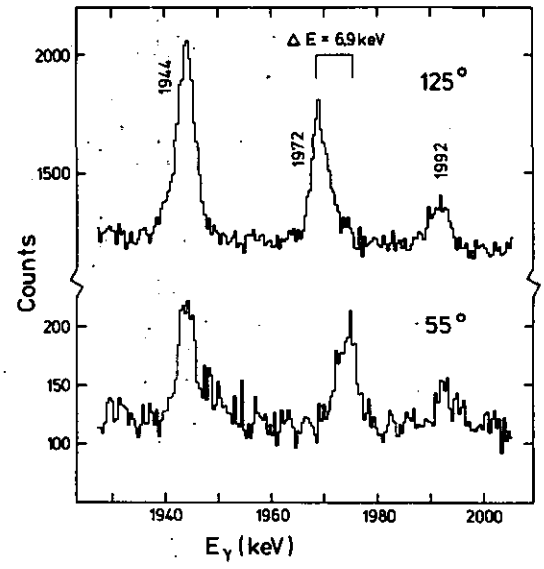


*Figure 2:*
*Portions of the γ-ray spectra recorded at 125° and 55° to the beam direction at $E_\alpha$ = 23.6 MeV. The data illustrate the Doppler shift of the 1972 keV line.*

vides the most compelling and direct spectroscopic evidence obtained thus far for a pronounced energy gap at Z=64. In contrast there is no indication of a similar gap at N=64; specifically, the $2^+$ energies in the even Sn nuclei, including the N=64 nucleus $^{114}$Sn, are essentially constant.

*) Universität Köln

**References**


[1] E. Newman, K.S. Toth, D.C. Hensley, and W.-D. Schmidt-Ott, Phys. Rev. C9 (1974) 674
[2] W. von Oertzen, H. Homeyer, B.G. Harvey, D. Hendrie and D. Kovar, Z. f. Phys. A279 (1976) 357


## 2.12. High Spin Levels in $^{146}$Gd and $^{147}$Gd


P. Kleinheinz, R. Broda, M. Ogawa, P.J. Daly, S. Lunardi, and J. Blomqvist*)


The (α,5n) and (α,6n) reactions have been used to study high-spin level structures in the doubly closed $^{146}$Gd nucleus and in the one particle nucleus $^{147}$Gd. Partial level schemes have previously been reported for these nuclei. However our recent finding that the 1.6 MeV first excited state in $^{146}$Gd has $I^\pi = 3^-$ (rather than $2^+$) requires a change in $I^\pi$ assignments for all the $^{146}$Gd excited states, and it also has far-reaching consequences in the structural interpretation of the excited states of both nuclei. In the present investigation metallic self supporting >98 % enriched $^{148}$Sm and $^{149}$Sm targets were bombarded with α-beams from 70 to 82 MeV. The experiments included γ-ray angular distribution-, excitation function-, and γγ-coincidence measurements, as well as lifetime determinations between beam bursts and with a μs-pulsed beam. Supplementary conversion electron and γ-ray spectra were measured with 30 MeV α's at the University of Bonn Cyclotron.

The results establish the $^{146}$Gd level scheme shown in fig. 1. For the levels below 4 MeV, the experimental results are particularly clearcut and complete, and the level properties can be naturally and convincingly explained using the shell model. The strongly populated $0^+$ level at 3.86 MeV is interpreted as the lowest lying twoparticle–twohole yrast state with the configuration $(\pi h_{11/2}^2)_{0^+} \times (\nu j^{-2})_{0^+}$, and the lower lying negative parity states are interpreted as one particle one hole excitations of $\pi h_{11/2}^{+1}\, \pi d_{5/2}^{-1}$ or $\pi h_{11/2}^{+1}\, \pi g_{7/2}^{-1}$ type. Theoretical excitation energies have been estimated using empirical single particle energies and interactions, and the results, shown to the left of fig. 1, are in very good agreement with the experimental energies.

The $^{146}$Gd level scheme above the 3.86 MeV $0^+$ level is not complete since several moderately strong transitions have not yet been placed. However, the levels shown in the figure are based on firm evidence. The $0^+$ state of $^{146}$Gd can be considered as coupling of two $h_{11/2}$ protons to the ground state of the $^{144}$Sm two proton hole core. Correspondingly, the six positive parity levels with spins 11 to 16 located between 5.0 and 6.4 MeV can be attributed to the

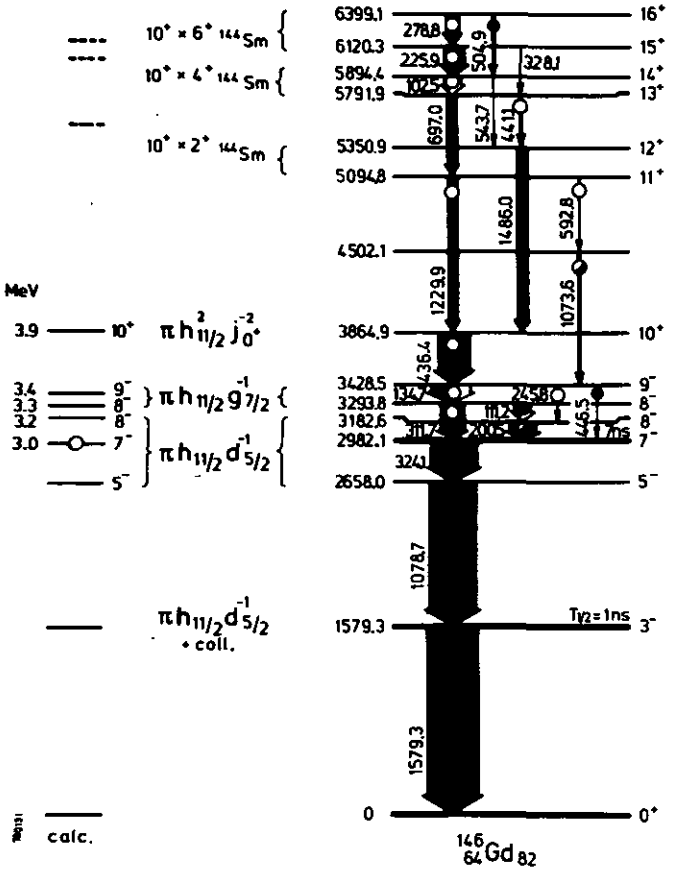


*Figure 1:*
*High spin states in the doubly closed shell nucleus $^{146}$Gd. Theoretically estimated level energies for the states with I ≤ 10 are shown for comparison. Gamma intensities shown as observed at $E_\alpha$ = 82 MeV in (α,6n). Dots (or nothing) indicate $A_2 > 0$, bubbles $A_2 < 0$.*

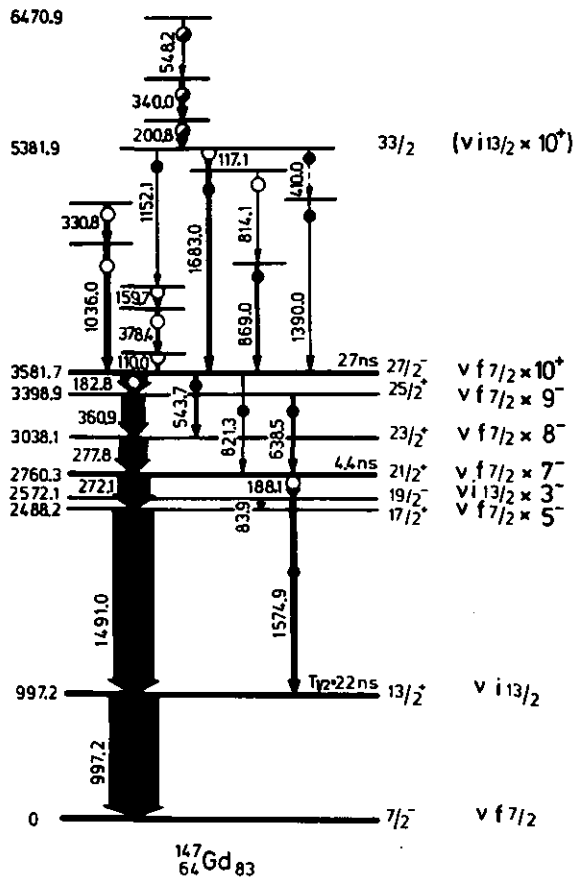


*Figure 2:*
*High spin states in the single neutron nucleus $^{147}$Gd. Gamma intensities at $E_\alpha$ = 70 MeV in (α,5n). Angular distributions characterized as in fig. 1. Many transitions connecting high-lying states are not shown here.*

coupling of the $(\pi h_{11/2}^2)_{10^+}$ excitation and the known $2^+$, $4^+$ and $6^+$ states of $^{144}$Sm.

The energy levels of $^{147}$Gd, up to the $27/2^-$ state at 3.58 MeV, very naturally resemable the $^{146}$Gd core states and can be interpreted as coupling of the $f_{7/2}$ valence neutron to the two proton core states. The much lower energy of the E3 ground state transition demonstrates that the 997 keV level is mainly the $\nu i_{13/2}$ state rather than the $(\nu f_{7/2}^{+1} \times 3^-)_{13/2^+}$configuration. This conclusion is supported by the observation of a 1575 keV E3 transition to that state from the 2572 keV $19/2^-$ state of $(\nu i_{13/2}^{+1} \times 3^-)_{19/2^-}$ character.

The high spin level scheme of $^{147}$Gd below 3.6 MeV is similarly complete and well understood as that for $^{146}$Gd below the $10^+$ level. Above 3.6 MeV a highly complicated level scheme emerges, characterized by many γ-ray deexcitation paths (not all shown in the figure) from a level at 5.38 MeV. The data clearly indicate an $I^\pi$ value of ≤33/2 for the 5.58 MeV state which is fed through a cascade of two intense $\Delta I < 2$ transitions, establishing $I^\pi \leq 37/2$ for the highest level (6.47 MeV) shown in fig. 2. From the excitation energy one might interpret the 5.26 MeV state as the $(\nu i_{13/2}^{+1}(\pi h_{11/2}^2)_{10^+})$ excitation. For the other high lying states in $^{147}$Gd however configuration assignments become in creasingly difficult since higher order core excitations and valence neutron excitations compete.

*) AFI Stockholm

## 2.13. Production of High Multiplicity Yrast Isomers in $^{147}$Gd and $^{146}$Gd in α-Particle Induced Reactions

R. Broda, M. Ogawa, S. Lunardi, M.R. Maier*), P.J. Daly and P. Kleinheinz

The results of a recent extensive search for yrast traps[1] using heavy ion beams from the UNILAC accelerator have stirred considerable interest. According to that work an island of high spin isomers with multiplicities between 8 and 18 and half-lives ranging from 1 to 700 ns has been observed in the region near N=82. However, neither the excitation energies nor the spins of these isomers could be extracted from the data, and the isotopic identification was only possible in the cases of $^{147}$Gd and $^{146}$Gd where the results of (α,xnγ) studies[2,3] were available.

In the course of our studies of $^{147}$Gd and $^{146}$Gd using 70 to 90 MeV α-beams (cf. preceding contribution to this report) we have identified in both nuclei isomers with properties resembling those re-

ported in ref. 1. We have determined their precise half-lives and our detailed level scheme investigations give approximate excitation energies and spins for these isomers.

The half-life of the $^{147}$Gd isomer was measured with a pulsed beam to be 560±60 ns (fig. 1), and in its decay essentially all the γ-rays of fig. 2 of the preceding contribution were observed. The isomeric decay feeds the 6.47 MeV level through a cascade of three transitions of undetermined multipolarity, which locates the isomer at 7.5 MeV and gives an upper limit of 49/2 for the isomeric spin. The population of the isomer at $E_\alpha$ = 90 MeV is about 3 % of the total (α,6n) cross section.

The high spin isomer of $^{146}$Gd lies above the 6.4 MeV $16^+$ level shown in fig. 1 of the preceding contribution. Its half-life was obtained as $T_{1/2}$ = 4.1±0.3 ns from the time distributions of several strong high-lying transitions with respect to the beam burst (fig. 2).

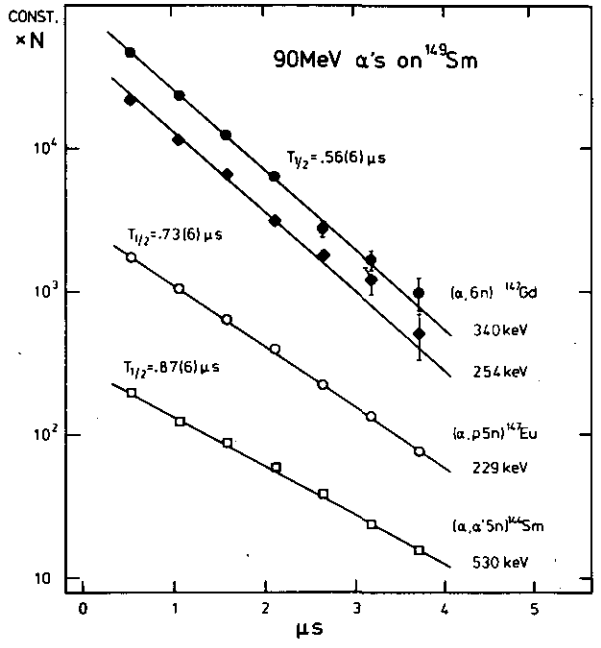


*Figure 1:*
*Half-life measurement of the 7.5 MeV high spin isomer in $^{147}$Gd using a μs beam pulsing system. Decay curves for γ-rays deexciting previously observed isomers in neighbouring nuclei, which are also produced at 90 MeV bombarding energy, are included.*

A cascade of two transitions in the isomeric decay feeding the $16^+$ level can clearly be identified in the γγ-coincidence data, and one of them, showing no prompt component, could be the isomeric transition. Both transitions have negative $A_2$ values, indicating a probable isomeric spin of ≤ 18. It is possible that an additional low energy transition in the isomeric decay may not have been observed, but in any case the excitation energy cannot exceed 8.2 MeV and the isomeric spin must be ≤ 20. At $E_\alpha$ = 82 MeV, the isomeric population is ≈ 10 % of the total (α,6n) cross section.

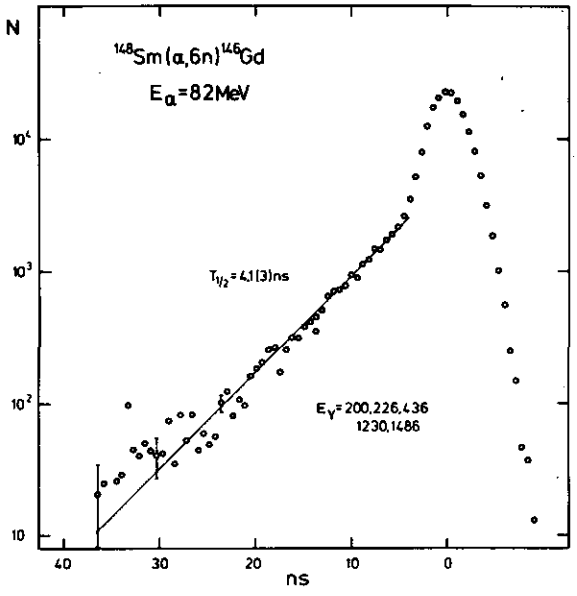


*Figure 2:*
*Half-life of the high spin isomer in $^{146}$Gd from a between-beam-burst timing measurement, derived from the time distributions of five intense high-lying $^{146}$Gd γ-transitions.*

It is an interesting question whether the isomers characterized here are identical with those seen[1] in the $^{50}$Ti and $^{40}$Ar induced reactions. The results of our level scheme studies appear to be entirely consistent with the multiplicity values given in ref. 1, but the rough half-life estimates of ref. 1 are three to six times smaller than the half-lives determined in the present measurement. It is however scarcely likely that the ($^{50}$Ti,xn) reactions should not have populated the longer lived high spin isomers observed in the α-induced reactions. Moreover, in the case of $^{147}$Gd there is detailed agreement between the large number of γ-rays[4] attributed to the 100 ns isomer of ref. 1 and those occurring in the 560 ns isomeric decay. It therefore seems to us very probable that the isomers seen in both experiments are indeed the same. If this conclusion is correct it follows that the isomers in $^{147}$Gd and $^{146}$Gd cannot be the very high spin deformed yrast traps predicted for this region in several[5] recent theoretical studies. Instead, it appears more natural to interpret these isomers as spherical shell model states of seniorities 4 and 5 as has been done for similar high spin isomers observed in the lead region.

*) Physik Dept. Tu München, now LBL Berkeley

## References


[1] J. Pedersen et al., Phys. Rev. Lett. 39 (1977) 990
[2] P. Kleinheinz, M.R. Maier, S. Lunardi, M. Ogawa, R. Broda, Proc. Int. Conf. Nucl. Struct. Tokyo 1977, p. 865, and priv. comm. to G. Sletten
[3] J. Kownacki, H. Ryde, V.O. Sergejev, Z. Sujkowski, Nucl. Phys. A196 (1972) 498
[4] G. Sletten, private communication
[5] cf. e.g. T. Døssing, K. Neergård, K. Matsuyanagi, Hsi-Chen Chang, Phys. Rev. Lett. 39 (1977) 1395; A. Faessler, M. Ploszajczak, R.K. Sandhya Devi, M. Wakai, Proc. Int. Conf. Nucl. Struct. Tokyo 1977, Vol. II in press

## 2.14. Picosecond Half-Lives in $^{153}$Dy

A.M. Stefanini, G. Batistuzzi*), M. Morando*), M. Neiman**), and P. Kleinheinz

In an earlier study[1] we had investigated the high spin level structures of the N=87 isotones $^{149}$Sm, $^{151}$Gd, and $^{153}$Dy. The principal result of this work was the identification in each isotone of a strongly populated $\Delta I=2$ yrast band built on the $i_{13/2}$ particle state and of a weakly fed $\Delta I=1$ band associated with the $h_{11/2}$ single hole excitation. From an analysis of the level energies we attributed strong prolate deformation to the $h_{11/2}$ band ($\beta=.29$) and weak triaxial deformation to the $i_{13/2}$ configuration ($\beta=.21, \gamma=30°$). To obtain independent data on the nuclear shapes we have measured absolute transition probabilities in $^{153}$Dy, which from the isotones investigated is the only one accessible in a (HI,xn) reaction suitable to carry out recoil distance measurements.

A 59 MeV $^{12}$C beam from the NBI Super-FN-Tandem accelerator has been used for a recoil distance measurement with the $^{144}$Nd($^{12}$C,3n)$^{153}$Dy reaction. The 270 $\mu$/cm$^2$ thick $^{144}$Nd target was evaporated on a 550 $\mu$g/cm$^2$ Au foil which was spanned in the target holder of a plunger[2] with a .7 mm thick Bi stopper which stopped the recoil nuclei and the $^{12}$C beam. The minimum target-stopper distance that could reliably be reached was 3±1 $\mu$m. Gamma rays were observed in a 60 cm$^3$ GeLi counter at 0°, ≃5 cm distant from the target.

The computer analysis of the decay curves obtained in these measurements gave the results indicated in the level scheme of fig. 1. Examples of decay curves are given in fig. 2. Of particular interest are the B(E2) values for the three lowest yrast transitions of the 13/2$^+$ band (fig. 2), where the third transition (25/2 → 21/2) has a very irregularly large enhancement. As shown in fig. 3 such an irregular increase of this B(E2) value is indeed predicted from the theory[4] for an odd-A triaxially deformed rotor in the region of $\gamma\simeq 30°$. This irregularity arises from a realignment of the total an-

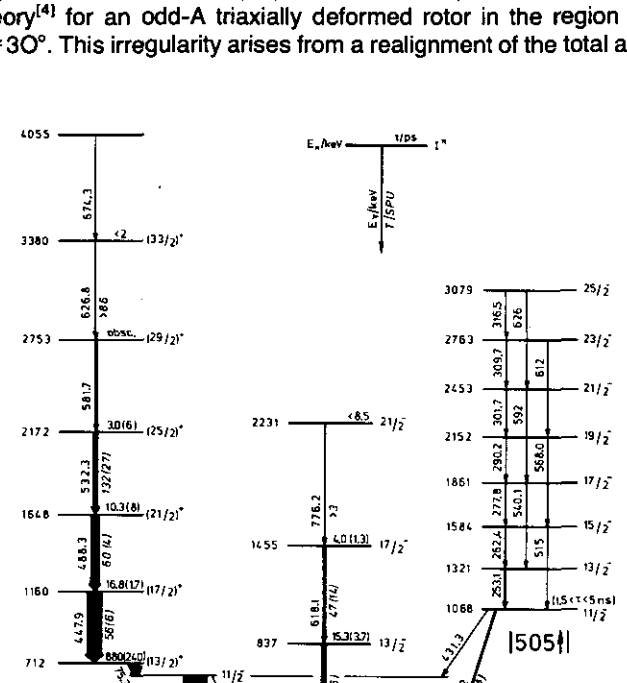


*Figure 1:*
*High spin states in $^{153}$Dy. Measured mean-lives (in ps) are given above the level; the corresponding enhancement factors[3] are indicated (in italics) with the respective deexcitation transition.*

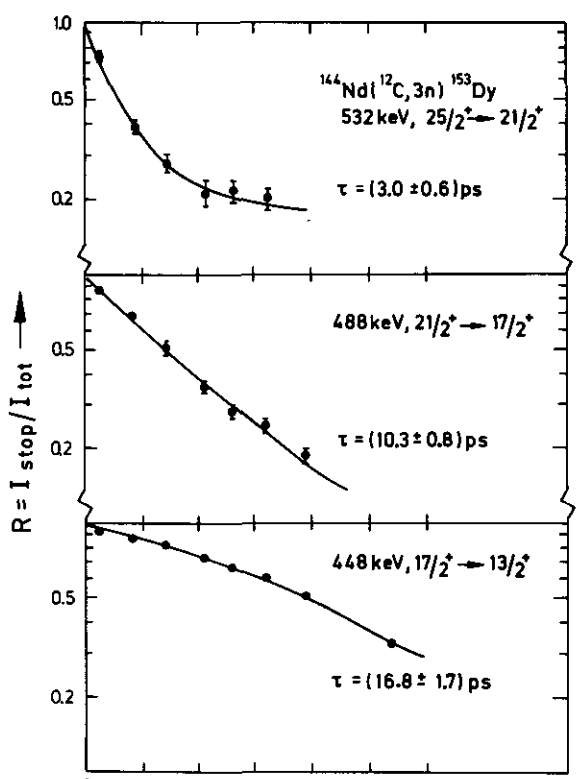


*Figure 2:*
*Decay curves for the 3 lowest yrast transitions feeding the 13/2$^+$ intrinsic state.*

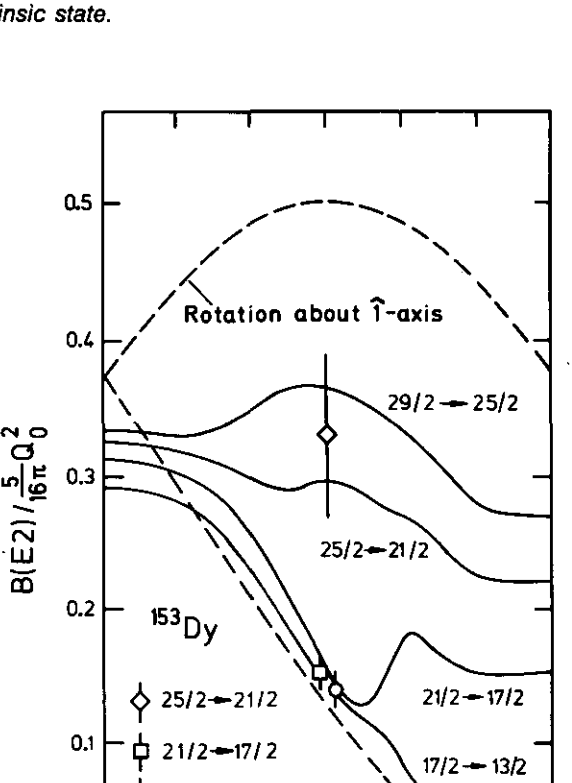


*Figure 3:*
*Comparision of measured B(E2) values with predictions from the theory[4] for a single particle coupled to a rigid triaxial rotating core. The dashed lines give the classical limits for B(E2).*

gular momentum of the system. For the low cascade members the total angular momentum localizes around the $\hat{2}$ axis of the triaxial core where the overlap between core and particle is maximum, whereas for the states with $I > 25/2$ the angular momentum tends to align with the $\hat{1}$ axis which has the largest moment of inertia in the triaxial region. Although the curves of fig. 3 are calculated for $j=11/2$ and one particle in the shell, the principal results remain[4] unaltered with $j = 13/2$ and 3 particles in the shell, which is valid for $^{153}$Dy. To compare our experimental results with theory we used the relation $Q_o = (3/\sqrt{5\pi})R_o^2 Z\beta$, with $R_o = 1.2 \times A^{1/3}$ and $\beta = 0.21$ as obtained from the analyses of the level energies. To our knowledge the present results are the first experimental evidence of this realignment of the total angular momentum in an odd-A triaxial rotor.

Unfortunately it was not possible to get half-lives of collective transitions in the strongly deformed band, since the crossover E2's are too weak and the cascade transitions have large negative $A_2$ and could not be observed at 0°.

However there is some indication of an exceptionally large retardation for the 772.2 keV M1 transition deexciting the $|505\uparrow|$ bandhead, which would be the shape isomeric transition. The data give clear evidence that its mean life is much longer than that of the close-lying 776.2 keV $h_{9/2}$ intraband ($21/2^- \rightarrow 17/2^-$) E2 transition of similar intensity, where only a flight peak was observed. Due to poor statistics for these lines only a range of 1.5 to 5 ns can be specified for the $|505\uparrow|$ bandhead mean life. With pure M1 multipolarity, which is indicated from the measured angular distribution, this result gives a retardation factor of the order of $10^5$.

*) Padova University and INFN Padova
**) NBI Copenhagen

## References

[1] P. Kleinheinz et al. Nucl. Phys. A283 (1977) 189
[2] G. Batistuzzi et al. Nucl. Instr. 146 (1977) 481
[3] A. De-Shalit and M. Feshbach, Theoretical Nucl. Phys. (Wiley 1974) Vol. 1, p. 702
[4] P.A. Butler et al., Phys. Lett. 56B (1975) 453

## 2.15. Side Bands in $^{172}$Hf

D.R. Haenni, Y. Gono*), H. Beuscher, R.M. Lieder, M. Müller-Veggian, C. Mayer-Böricke, D.R. Zolnowski**), T.T. Sugihara**)

The $^{176}$Hf isotope is well known for its high-K isomers and strongly-coupled rotational bands while $^{168}$Hf exhibits backbending which presumably results from a decoupled band structure. We have undertaken the present study of $^{172}$Hf to see what features belong to a nucleus intermediate to these two regions.

Levels in $^{172}$Hf have been populated primarily by the $^{172}$Yb($\alpha$,4n) reaction at both the Texas A&M University and Jülich Cyclotrons. Standard $\gamma$-ray and conversion-electron measurements have been performed. After the first set of experiments using relatively large volume Ge(Li) detectors, it was found that several low energy transitions must exist which play an important role in constructing the level scheme. A second $\gamma$-$\gamma$ coincidence measurement was made using two high-resolution planar Ge(Li) detectors. Angular distributions for these low-energy $\gamma$ rays are not yet measured.

The level scheme for $^{172}$Hf is shown in Fig. 1. A large number of side bands are observed as well as several isomeric states. It is interesting to note that only two of the side bands show the characteristics of strongly coupled bands while the rest have a $\Delta I = 2$ spacing. One of the $\Delta I = 2$ bands is the $\beta$ band which has been identified primarily by strong $I_\beta \rightarrow I_g$ transitions in the conversion-electron spectra.

The character of the remaining $\Delta I = 2$ side bands is not obvious, the bands at 1968 and 2034 keV have dipole crossover transitions to the groundstate band. Perhaps one of them is a negative parity band such as is found in the 88-neutron isotones. The character of the remaining band starting possibly on the 1418 keV level is somewhat more difficult to establish. Except for the 1418 keV level, the band prefers to deexcite via low energy transitons to intermediate states which in turn feed the ground-state band. As mentioned, the angular distributions of these low-energy transitions including the one at 179 keV were not well determined in the first distribution measurement. Therefore the $I^\pi$ assignments to the members of this band are not certain. Indeed even the inclusion of the 1418 keV level as a member of the band is presently based more on systematics than on experimental evidence. Future angular-distritution measurements should help to clarify these points.

The 1418, 1503, and 1684 keV levels in $^{172}$Hf were also reported in the decay[1] of $^{172}$Ta, however, some disagreements about the decay properties of these levels exist. To help clarify these difference, we have also begun a limited study of the $^{172}$Ta decay. Thus far $\gamma$-$\gamma$ coincidences and portions of the conversion-electron spectrum have been obtained. From a preliminary analysis of these data, the 1418 keV level is common to the decay and in-beam studies while the 1684 keV levels are different. The results for the 1503 keV level are not yet conclusive. The 875 keV transition depopulating the 1503 keV level not reported in the pervious decay study[1] has been identified. However, a strong 427 keV transition from the same level, which has not been found in the in-beam results, appears to be multiple in our decay coincidence data. Thus its previously reported intensity[1] may be too large. This problem may be resolved when better decay singles spectra are obtained.

Very recently we have learned of a concurrent study[2] of $^{172}$Hf by a group in Canberra, Australia using (HI,xn) reactions. This group

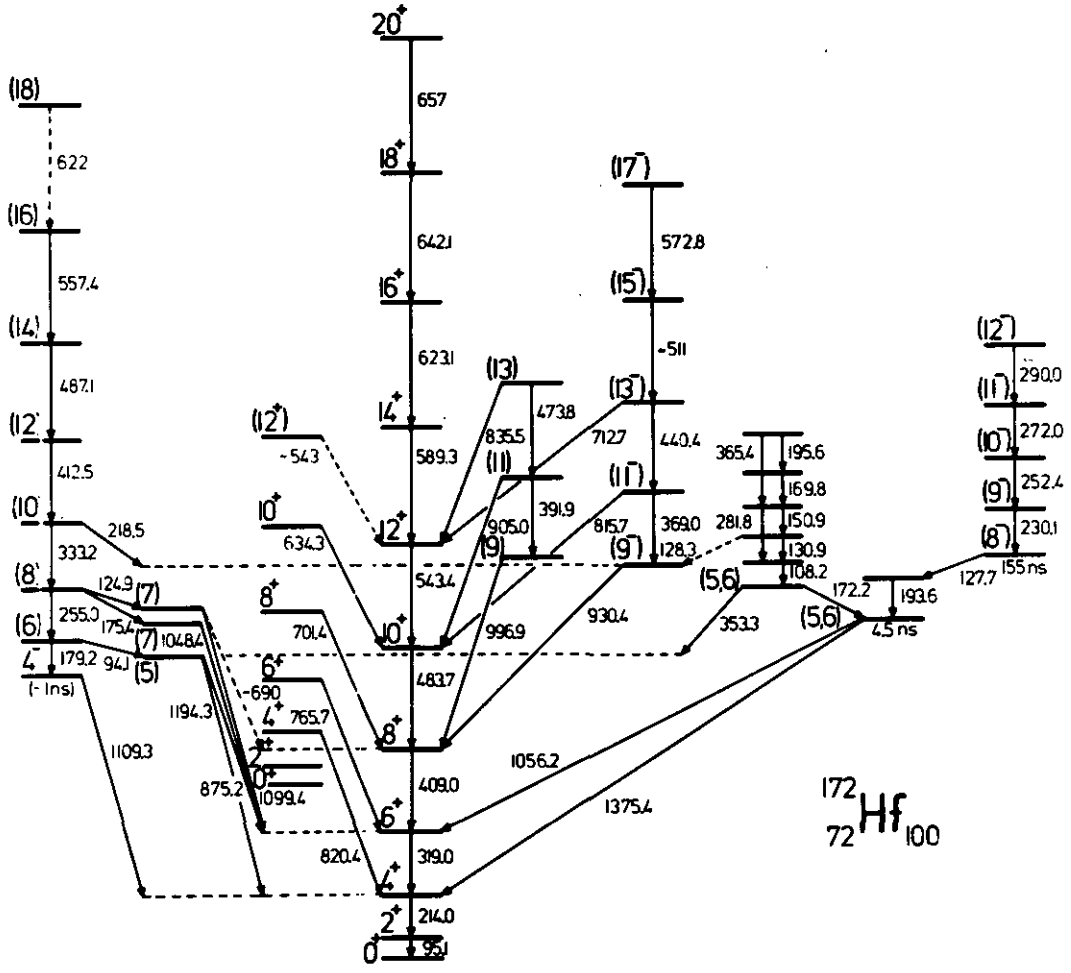


*Figure 1:*
*Level scheme for $^{172}$Hf. The lower two members of the β band are taken from ref.[1].*

has also studied levels in $^{173,174,176}$W where they observe even- and odd-spin side bands which they interpret as a negative-parity decoupled band. From systematics, they propose that this band also exists in $^{172}$Hf. The cascade on the 1418 keV level represents the even-spin sequence of this decoupled band while the cascade on the 1968 keV level together with the 1503 and 1725 keV levels form the odd-spin sequence. This interpretation, however, is heavily based on systematics, since in a preprint of their results almost no angular distributions are reported for transitions below ~ 300 keV. It would seem worthwhile to test this interpretation of the levels in $^{172}$Hf with more experimental data.


*) Present address: Institut für Kernphysik, Technische Hochschule Darmstadt, 6100 Darmstadt, W. Germany
**) Cyclotron Institute, Texas A&M University. College Station Texas 77843, USA


### References


[1] M.H. Cardoso, P.F.A. Goudsmit, and J. Konijn, Nucl. Phys. A205 (1973) 121
[2] P.M. Walter, G.D. Dracoulis, and A Johnston, to be published and private communication


## 2.16. Backbending Behavior and Decay of a High-Spin Isomer in $^{179}$W


F.M. Bernthal**), B.B. Back*), O. Bakander*), J. Borggreen*), J. Pedersen*), G. Sletten*), H. Beuscher, D.R. Haenni, and R.M. Lieder


The high spin features of the tungsten isotopes provide an unusual opportunity to study the competing influences of rotation-aligned and of high-K „deformation-aligned" structures on the yrast sequence of states. Above tungsten, in $^{182-186}$Os, rotation alignment of a pair of high-j nucleons is thought to be reponsible for the appearance of backbending behaviour[1,2], whereas below tungsten, in $^{176-178}$Hf, high spin multiquasiparticle isomers intrude into the yrast sequence[3].

At Risø the ($^{13}$C, 4n) reaction was used to populate high spin states in $^{179}$W, and a new 710ns isomer with I=37/2 or 39/2 was identified[4]. The 7/2$^-$[514] ground band sequence was identified to spin 37/2 and the 9/2$^+$[624] band to 33/2. In a separate experiment, 58 MeV α-particles from the Jülich cyclotron were used in the $^{180}$Hf(α, 5n) reaction to identify the $i_{13/2}$ band at least to spin 39/2.

Two aspects of the high spin features of $^{179}$W are of special interest: 1) The contrasting behaviour of the 7/2$^-$[514] and 9/2$^+$[624] rotational bands, and 2) The unusually short half life and decay path of the 710 ns isomer. It is noteworthy that the second observation may be closely related to the first and presents new, rather direct evidence for the existence of higher seniority components in states in the backbending region.

The explanation for the reappearance of strong backbending behaviour in the yrast sequence of $^{180}$W and $^{182,184,186}$Os has been a subject of some controversy. Blocking experiments in $^{181}$Os and $^{181}$Re carried out by the Jülich group[2] seemed to argue for the dominant role of $h_{9/2}$ protons in $^{182}$Os and perhaps also $^{184}$Os backbending, but recent data for $^{183}$Ir from the Grenoble-Swierk group rather seemed to implicate $i_{13/2}$ neutrons[5]. In $^{180}$W, isotonic with $^{182}$Os, the Michigan State group[6] has suggested that the $i_{13/2}$ neutrons are primarily responsible for the backbending behaviour. The combined ($^{13}$C, 4n ) and ($\alpha$, 5n ) experiments reported here provide data which are consistent with the interpretation of Ref. 6. The 7/2$^-$[514] band in $^{179}$W displays backbending behaviour very similar to that observed in $^{180}$W, while the $i_{13/2}$, 9/2$^+$[624] band shows no evidence for such behaviour up to spin 39/2, suggesting the odd $i_{13/2}$ neutron indeed blocks the rotation-alignment effects postulated to be responsible for backbending in the g.r.b. and, by implication, in $^{180}$W.

A particularly intriguing aspect of the backbending in the 7/2$^-$[514] g.r.b. of $^{179}$W is its possible influence on the decay of the 710 ns isomer. The striking feature of the isomeric decay is its small hindrance for feeding into the ground band. Such a transition should be 14 times K-forbidden if the isomer is similar in structure to the 51-min $K^\pi = 37/2^-$ isomer identified in $^{177}$Hf by Chu et al.[7]. Instead, it displays a half life consistent with a total hindrance $< 10^2$, and perhaps as small as unity, depending on the multipolarity of the thus-far unobserved isomeric transition. Clearly, such a short lifetime cannot be understood within the framework of the usual rules governing K-forbidden transitions in deformed nuclei, where hindrance factors of 10-100 per unit of K-forbiddance are normally observed.

The exact structure of the isomeric state is at this time unknown, but the key factor determining the short isomeric lifetime appears to be the special structure in the backbending region into which the isomer decays. The $^{179}$W data would thus appear to offer some of the most direct evidence thus far for the proposed[8] higher-seniority configuration thought to dominate that region.

*) Niels Bohr Institute, Riso, Denmark
**) Niels Bohr Institute and Michigan State University, USA

## References

[1] R.A. Warner, et al., Phys. Rev. Lett. 31 (1973) 835
[2] A. Neskakis, et al., Nucl. Phys., A261 (1976) 189
[3] T.L. Khoo, et al., Phys. Rev. Lett. 37 (1976) 823
[4] O. Bakander, J. Borggreen, J. Pedersen, and G. Sletten, to be published
[5] jnS. Andre, et al., Phys. Rev. Lett. 38 (1977) 327
[6] F.M. Bernthal, et al., Phys. Lett. 64B (1976) 147
[7] Y.Y. Chu, P.E. Haustein, and T.E. Ward, Phys. Rev. C6 (1972) 2259
[8] F.S. Stephens and R.S. Simon, Nucl. Phys. A183 (1972) 257

## 2.17. Particle-Hole Symmetry Observed in the Angular Distributions of $\gamma$-Rays in $^{189,191,193}$Au

Y. Gono, R.M. Lieder, M. Müller-Veggian, A. Neskakis, C. Mayer-Böricke

Levels in $^{189,191,193}$Au have been studied by in-beam $\gamma$-ray spectroscopic techniques. Interesting features of the high-spin states in these nuclei obtained in this study such as the three-quasi particle states resulting from the $(\pi h_{11/2})^{-3}$ configuration were reported last year[1]. Systematical trends of the bands based on the proton $h_{9/2}$ and $h_{11/2}$ orbitals were also discussed previously[2] within a triaxial-rotor-plus-particle model[3]. In the course of the study positive and negative $A_2$ coefficients of the angular distribution function were obtained for the $\Delta I=1$ transitions between the unfavoured and the favoured states in the $h_{11/2}$ and $h_{9/2}$ bands, respectively. They are listed in table 1. The positive values of $A_2$ for these transitions in the $h_{11/2}$ bands in $^{191,193}$Au are comparable to those of the stretched E2 transitions and cause some difficulties for the spin parity assignment. However the spin parity of the 13/2$^-$ states of the $h_{11/2}$ bands in $^{191,193}$Au could be obtained uniquely combining the informations of the present $\gamma$-ray angular distribution data and the internal conversion coefficients and the logft values which were known from the previous activity studies[4]. Relatively large negative $A_2$ values for these transitions of the $h_{9/2}$ bands in $^{189,191}$Au result only from the mixed dipole-quadrupole transitions for $I+1\rightarrow I$ transitions. The attenuation factors of the angular distribution coefficients were obtained comparing the theoretical $A_2$, $A_4$ values with the experimental ones for the stretched E2 transitions listed in table 1. The E2/M1 mixing ratios $\delta$ for the $\Delta I=1$ transitions were calculated taking these attenuation factors into account. It is clearly seen in the table that the positive and negative values $\delta$ are obtained corresponding to the positive and negative $A_2$ values for the $\Delta I=1$ transitions in the $h_{11/2}$ and $h_{9/2}$ bands, respectively. The sign of $\delta$ for these transitions has been discussed theoretically by Meyer-ter-Vehn[3] within a framework of a triaxial-rotor-plus-particle model. His calculation shows that the $\delta$-values of these $\Delta I=1$ transitions in the bands originating from high-j proton orbitals are always negative. However the $h_{9/2}$ and $h_{11/2}$ proton orbitals lie above and below the Fermi level, respectively, in Au isotopes, namely, the $h_{9/2}$ and the $h_{11/2}$ states in these nuclei are the particle and the hole states, respectively. Considering the particle-hole

*Table 1:*
*Gamma-ray energies ($E_\gamma$), relative intensities ($I_\gamma$), angular distribution coefficients ($A_2/A_0$,$A_4/A_0$), and E2/M1 mixing ratios ($\delta$) in $^{189,191,193}$Au. Experimental errors are given in brackets.*

| $E_\gamma$ (keV) | I | $I_i \rightarrow I_f$ | $A_2/A_0$ | $A_4/A_0$ | $\delta$ |
|---|---|---|---|---|---|
| $^{189}$Au | | | | | |
| 321.3 | 12(3) | 13/2$^-$ → 9/2$^-$ | 0.21(5) | -0.03(7) | |
| 387.5 | 4(2) | 11/2$^-$ → 9/2$^-$ | -0.31(16) | -0.01(22) | -5.53<$\delta$<-0.03 |
| 434.6 | 100(7) | 15/2$^-$ → 11/2$^-$ | 0.22(2) | -0.05(3) | |
| 459.3 | 11(1) | 17/2$^-$ → 13/2$^-$ | 0.28(3) | -0.09(4) | |
| 565.5 | 10(2) | 13/2$^-$ → 11/2$^-$ | 0.03(1) | 0.03(3) | 0.17<$\delta$< 0.19 |
| 730.3 | 93(7) | 19/2$^-$ → 15/2$^-$ | 0.20(2) | -0.05(3) | |
| $^{191}$Au | | | | | |
| 274.1 | 10(2) | 9/2$^-$ → 11/2$^-$ | 0.00(1) | -0.02(2) | |
| 356.9 | 4(1) | 11/2$^-$ → 9/2$^-$ | -0.48(13) | -0.04(18) | -1.97<$\delta$<-0.34 |
| 371.0 | 6(1) | 13/2$^-$ → 9/2$^-$ | 0.26(4) | -0.10(6) | |
| 420.1 | 100(7) | 15/2$^-$ → 11/2$^-$ | 0.29(2) | -0.06(3) | |
| 439.9 | 1(1) | 15/2$^-$ → 13/2$^-$ | -0.55(33) | 0.20(46) | -5.95<$\delta$<-0.05 |
| 519.4 | 5(1) | 17/2$^-$ → 13/2$^-$ | 0.30(7) | -0.06(10) | |
| 578.5 | - | 13/2$^-$ → 11/2$^-$ | - | - | |
| 690.4 | 3(1) | 17/2$^-$ → 15/2$^-$ | 0.35(13) | -0.28(18) | 0.35<$\delta$< 0.81 |
| 725.1 | 86(12) | 19/2$^-$ → 15/2$^-$ | 0.29(4) | -0.07(6) | |
| $^{193}$Au | | | | | |
| 407.6 | 100(7) | 15/2$^-$ → 11/2$^-$ | 0.28(2) | -0.03(3) | |
| 572.9 | 6(2) | 13/2$^-$ → 11/2$^-$ | 0.18(6) | 0.08(8) | or $^{0.29<\delta<0.43}_{3.18<\delta<6.51}$ |
| 674.8 | 6(1) | 17/2$^-$ → 15/2$^-$ | 0.25(5) | 0.05(7) | |
| 720.9 | 79(8) | 19/2$^-$ → 15/2$^-$ | 0.27(3) | -0.02(4) | 0.33<$\delta$< 0.44 |

conjugation with which the sign of the E2 operator changes while the sign of the M1 operator does not, the opposite sign of $\delta$ for the $\delta$ I = 1 transitions in the $h_{9/2}$ and the $h_{11/2}$ bands can be understood as resulting from the particle-hole symmetry.


**References**

[1] Y. Gono et al., Annual Report IKP der KFA Jülich (1976)
[2] Y. Gono et al., Proc. Int. Symposium on Collectivity of Medium and Heavy Nuclei, Tokyo, 1976, ed. Y. Shida
[3] J. Meyer-ter-Vehn, Nucl. Phys. A249 (1975) 111 and 141; H. Toki and A. Faessler, Nucl. Phys. A253 (1975) 231
[4] H. Beuscher et al., Z. Physik 247 (1971) 383; Z. Plajner et al., Z. Physik 233 (1970) 122


## 2.18. Bandstructure in $^{190,192}$Au


H. Beuscher, A. Neskakis*), Y. Gono**), D.R. Haenni, R.M. Lieder, M. Müller-Veggian and C. Mayer-Böricke


The odd-odd nuclei $^{190,192}$Au have been studied by in-beam $\gamma$-spectroscopy. The levels in these nuclei have been populated by irradiating $^{191,193}$Ir targets with 63 MeV $\alpha$ particles from the Jülich isochronous cyclotron. So far $\gamma$-$\gamma$ coincidences, $\gamma$-ray angular distributions and $\gamma$ spectra time related to the cyclotron beam bursts have been measured. From these experiments the promptly decaying yrast states possibly situated above a long living isomer could be established.

Spin and parity of the lowest state in $^{190}$Au as well as in $^{192}$Au which is assumed to be a long lived isomeric state could not be determined from the data so far. That the observed structure starts on a long lived high-spin isomer has been deduced in the following way. In an ($\alpha$,5n) reaction one can normaly observe levels up to spin 18 or 20 $\hbar$. Since levels up to about I + 8 are found in $^{190,192}$Au this suggests that the lowest observed state has a spin of the order of 10 $\hbar$. Since it was not possible to see transitions below the lowest state in the delayed ($\gamma$-$\gamma$) coincidences the halflife of this state has to be $T_{1/2} >> 1$ µs.

Further experiments, especially conversion electron measurements are required since the isomers in $^{190,192}$Au decay via low-energy transitions which are not necessarily observable in the $\gamma$-spectrum. Yates et al[3] report that the 420 ms isomer in $^{194}$Au has spin 10 or 11. Romanij et al[4] determined that the ms isomers in $^{192,194}$Au were 11$^-$. It is not certain, however, that the observed levels are built on this 11$^-$ isomer.

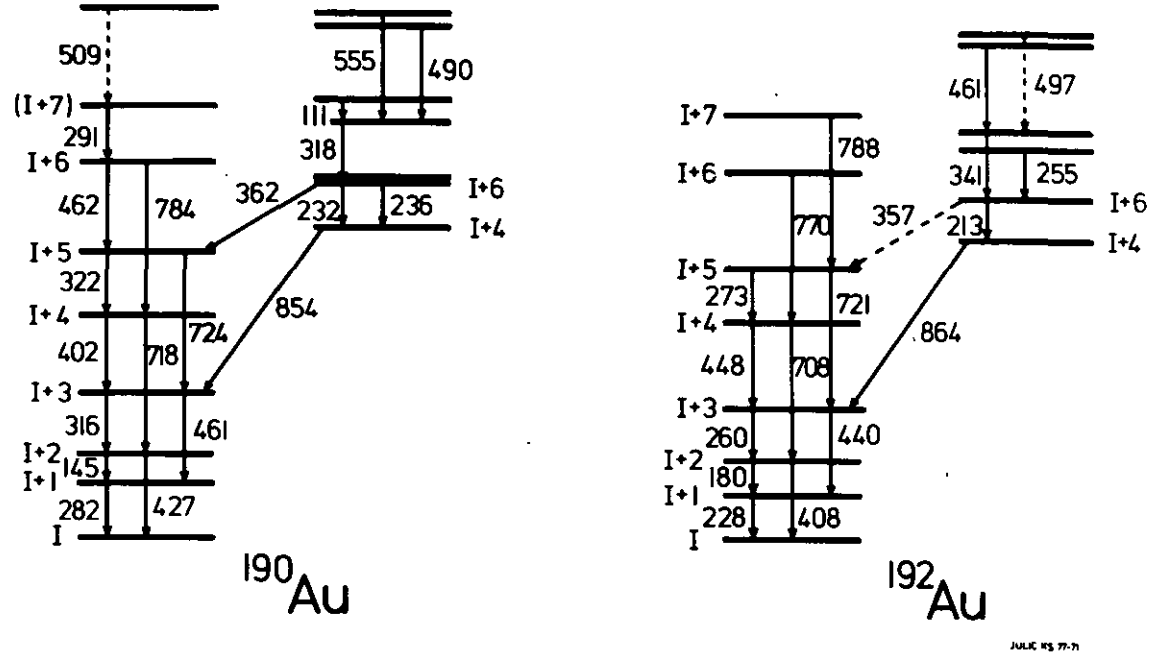


*Figure 1: Partial scheme of promptly decaying levels for $^{190,192}$Au.*

The level schemes are very similar in both nuclei. A well developed strongly coupled band with fairly strong crossover quadrupole transitions is observed. In addition a side band is observed which probably has different parity than the main band. This has been deduced from the angular distributions of the 855 and 864 keV interband transitions in $^{190,192}$Au, respectively, which indicate pure dipole character for these transitions. The same conclusion about a parity change was made for the neighbouring Hg isotopes[1] where also conversion electron data are available[2]. Levels of these side bands form the yrast states at higher spins. The strongest transitions observed in the in-beam $\gamma$ spectrum in $^{192}$Au are the 213, 864, 260 and 408 keV transitions.

The lowest-energy bands in the odd-odd nuclei $^{190,192}$Au are not decoupled bands like in the neighbouring odd-mass Au[5] and Hg[1] nuclei but have strongly coupled structures. A possible decoupled state in $^{190,192}$Au could be a 12$^-$ state consisting of a $h_{11/2}$ proton hole which is decoupled in the odd-mass Au[5] isotopes and a $i_{13/2}$ neutron hole which is decoupled in the odd-mass Hg isotopes[1].

The fact that no decoupled band is observed indicates that the band head is probably not this 12⁻ state. Toki et al[6] made a calculation for $^{194}$Au using the asymmetric-rotor model including the softness of the core assuming that the odd particles occupy the high spin states $h_{11/2}$ (proton) and $i_{13/2}$ (neutron). The result is a decoupled structure on the 12⁻ decoupled state as the lowest lying sequence. This is not in agreement with our experimental results for $^{190,192}$Au. The reason for this disagreement may be that the 12⁻ ($\nu i_{13/2}$, $\pi h_{11/2}$) decoupled state is not an yrast state and therefore not observed in our in-beam experiment. To make this comparison more meaningful, it seems necessary to determine spin and parity of the isomeric band head in each of the nuclei $^{190,192}$Au.

*) Present address: State University of New York, Stony Brook, New York 11794, USA
**) Present address: Institut für Kernphysik, Technische Hochschule Darmstadt, 6300 Darmstadt, West Germany

## References


[1] R.M. Lieder, H. Beuscher, W.F. Davidson, A. Neskakis, and C. Mayer-Böricke, Nucl. Phys. A248 (1975) 317
[2] R.F. Petry, R.A. Naumann, and J.S. Evans, Phys. Rev. 174 (1968) 1441
[3] S.W. Yates and F.J. Lynch, Phys. Rev. C12 (1975) 1080
[4] I.A. Romanij, A.P. Klutchariev, W.A. Lutsik, J.N. Rakivnenko, Proceedings of the International Conference on Selected Topics in Nuclear Structure, Dubna (1976) 63
[5] Y. Gono, R.M. Lieder, M. Müller-Veggian, A. Neskakis, and C. Mayer-Böricke, Phys. Rev. Letters 37 (1976) 1123
[6] H. Toki, H.L. Yadav, and A. Faessler, Phys. Letters 66B (1977) 310


## 2.19. In-Beam γ-Spectroscopic Investigation of $^{196}$Tl


A.J. Kreiner*), M. Fenzl*), W. Kutschera*), R.M. Lieder, H. Beuscher, Y. Gono, D. Haenni, M. Müller-Veggian and C. Mayer-Böricke


The reactions $^{197}$Au(α,5n) at $E_\alpha \simeq 65$ MeV and $^{194}$Pt ($^6$Li,4n) at ≃ 44 MeV were used to produce the residual nucleus $^{196}$Tl. The subsequent prompt and delayed decay was studied by means of γ-spectroscopic techniques. The resulting level scheme is shown in fig. 1. The most interesting finding is a „rotational-like" structure based on an isomeric state at 739 keV ($I^\pi = 8^-$, $T_{1/2} \simeq 21$ nsec). A similar band has been already found in $^{198}$Tl[1] in an investigation carried out using the $^{197}$Au(α,3n) reaction. The aim of the present work was to go a step further towards the systematic knowledge of these features in doubly odd Tl nuclei. As expected, the higher bombarding energy allows us to populate states of significantly higher angular momentum compared to the (α,3n) case. Special care was put in the investigation of the γ-spectrum lying below the Tl X-rays. For that purpose an X-γ coincidence experiment was performed utilizing a large volume Ge(Li)-(140 cm$^3$, 27 % effic.) and a planar intrinsic Ge-detector. This measurement sets an up-

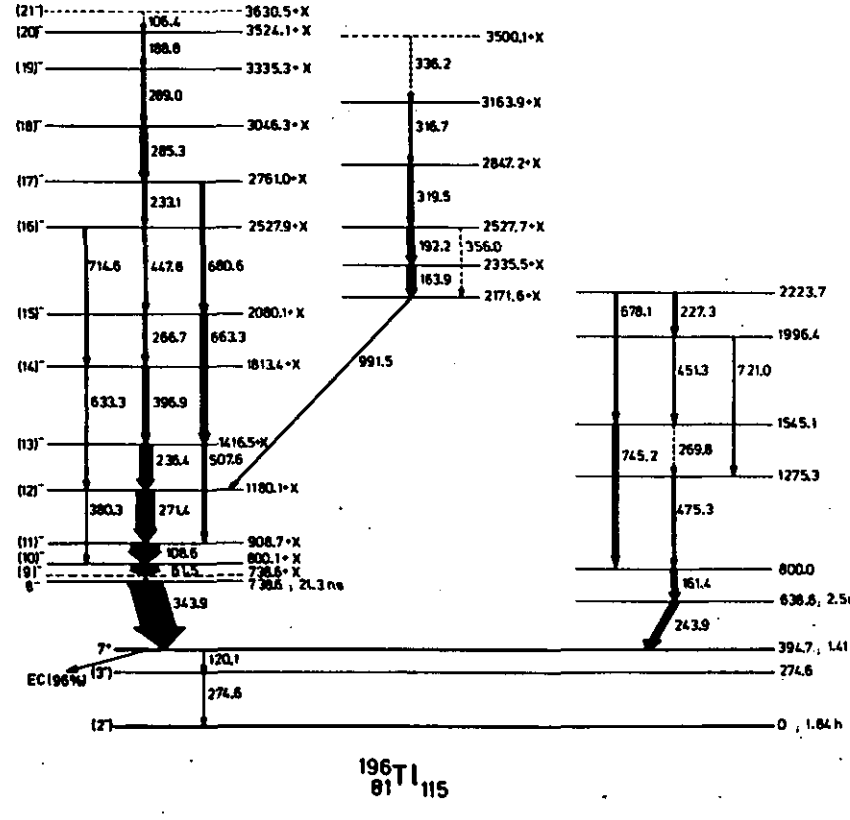


$^{196}_{81}Tl_{115}$

*Figure 1:*
*Level scheme of $^{196}$Tl.*

per limit for eventually unobserved cascade transitions at ≃ 35 keV. These low energy lines represent a general problem in γ-ray spectroscopy, especially on complex heavy nuclei. Due to the strong conversion the deexcitation will no longer proceed through γ emission below a certain energy. Therefore from a purely experimental point of view spins and level energies cannot be assigned unambiguously. There are, however, theoretical reasons which lead us to believe that there exists a single additional cascade transition. In fact, the analogous band in $^{198}$Tl has been successfully interpreted in the framework of a model of two noninteracting quasiparticles coupled to an axially symmetric rotor as based on the $\tilde{\pi}h_{9/2}$ $\tilde{\nu}i_{13/2}$ intrinsic state[1]. A further theoretical study[2] has shown that the model is able to reproduce all the special qualitative features found in the experiment, in particular the staggering in the excitation energies of even-and odd-spin states; the nonexistence of the transition mentioned above would imply that the calculated and observed staggerings are opposite in phase. The definitive clarification of this point remains as a challenging experimental problem. In addition, the structure of the band is seen to change above the $(17)^-$ state. The quenching of the levels is connected with the irregularity in the gsb of the core nucleus $^{194}$Hg, where the $8^+$ and $10^+$ states, which lie very close together, have been interpreted as aligned members of the $\pi h_{11/2}^{-2}$ multiplet[3]. An analogous phenomenon has already been described in $^{195,197}$Tl[4]. Our band probably terminates at the $(21)^-$ state in a completely aligned 4 quasiparticle $[(\pi h_{9/2} \otimes \pi h_{11/2}^{-2}) \otimes \nu i_{13/2}^{-1}]_{21}$- state.

*) Fachbereich Physik E 17, Technische Universität München, D-8046 Garching, Germany

### References


[1] A.J. Kreiner, M. Fenzl, S. Lunardi and M.A.J. Mariscotti, Nucl. Phys. A282 (1977) 243
[2] A.J. Kreiner, Preprint, Technische Unversität München, Sept. 1977 (to be published)
[3] D. Proetel, R.M. Diamond and F.S. Stephens, Nucl. Phys. A231 (1974) 301
[4] R.M. Lieder, Int. Symp. on collectivity of medium and heavy nuclei, Tokyo, 1976; R.M. Lieder, A. Neskakis, M. Müller-Veggian, Y. Gono, C. Mayer-Böricke, S. Beshai, K. Fransson, C.G. Linden and Th. Lindblad, to be published


## 2.20. B(E2) Ratios of Cascade and Crossover Transitions in $^{195,197}$Tl

R.M. Lieder, A. Neskakis*), M. Müller-Veggian, Y. Gono**), C. Mayer-Böricke, S. Beshai***), K. Fransson***), C.G. Linden****), Th. Lindblad****)

In the nuclei $^{195,197}$Tl strongly-coupled bands built on $9/2^-$ isomers have been observed up to $27/2^-$ and $29/2^-$, respectively[1,2]. The excitation energies of the band members in $^{195,197}$Tl can be reproduced up to the $21/2^-$ states in the framework of the triaxialrotor-plus-particle model[3] by coupling a $h_{9/2}$ proton to the corresponding Hg core nuclei $^{194,196}$Hg (ref.[1,2,4]. The closely spaced $23/2^-$, $25/2^-$, $27/2^-$ and $29/2^-$ states in $^{195,197}$Tl have been interpreted as resulting from the coupling of the $h_{9/2}$ proton to the $(\pi h_{11/2}^{-2})$ configurations of the $8^+$ and $10^+$ states in $^{194,196}$Hg (ref.[1,2]).

A sensitive test for the applicability of the triaxial-rotor-plus-particle model is the comparision of experimental and theoretical ratios of B(E2) values of crossover and cascade transitions. The experimental ratios have been deduced for the $9/2^-$ bands in $^{195,197}$Tl taking into account the transition probabilities $T_\gamma$ of the cascade and crossover transitions and the E2/M1 mixing ratios δ of the cascade transitions as deduced from their γ-ray angular distributions[2]. The Equation

$$\frac{B(E2,I\to I-2)}{B(E2,I\to I-1)} = \left[\frac{E(I\to I-1)}{E(I\to I-2)}\right]^5 \cdot \frac{T_\gamma(I\to I-2)}{QT_\gamma(I\to I-1)}$$

has been used, were $Q = \delta^2/(1+\delta^2)$. The theoretical B(E2) ratios have been calculated by Toki[4] in the framework of the triaxial-rotor-plus-particle model for a deformation parameter $\beta = 0.13$ and an asymmetry parameter $\beta = 37°$. In fig. 1 the experimental and theoretical B(E2) ratios have been compared for the transi-

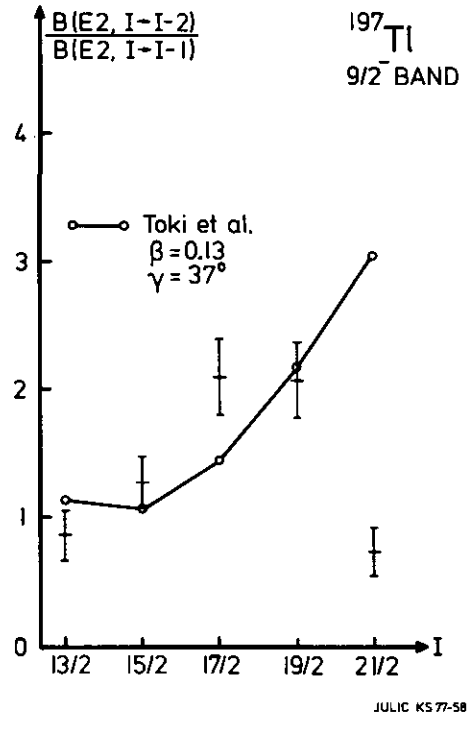


*Figure 1:*
*Experimental and theoretical B(E2) ratios of crossover and cascade transitions in the $9/2^-$ band of $^{197}$Tl.*

tions in the 9/2⁻ band of $^{197}$Tl. A reasonable agreement has been obtained up to the 19/2⁻ state. It should be pointed out that the B(E2) ratios depend in a sensitive manner on the asymmetry parameter γ. For a change of γ by 3° the theoretical B(E2) ratio changes by about a factor of two[3].

The deviation between the experimental B(E2) ratio and the theoretical prediction for the 21/2⁻ state in $^{197}$Tl may be understood by a change of the intrinsic configuration of the 9/2⁻ band at high-spin states. As mentioned in the beginning such a change in structure becomes evident in the excitation energies of the states lying above the 21/2⁻ level. It seems plausible to assume that the configuration of the 21/2⁻ state in $^{197}$Tl contains a contribution of the $(\pi h_{9/2} \pi h_{11/2}^{-2})$ configuration, which is most probably the predominant one for the 23/2⁻ state. Similar results have been obtained for $^{195}$Tl (ref.[2]).

*) Present address: State University of New York, Stony Brook, New York 11974, USA
**) Present address: Institut für Kernphysik, Technische Hochschule Darmstadt, 6100 Darmstadt, W. Germany
***) Institute of Physics, University of Stockholm, Stockholm, Sweden
****) Research Institute of Physics, S-10405 Stockholm 50, Sweden

### References


[1] R.M. Lieder, in Proc. Int. Symposium on Collectivity of Medium and Heavy Nuclei, Tokyo, 1976, ed. Y. Shida, p. 459
[2] R.M. Lieder et al., Nucl. Phys. to be published
[3] J. Meyer-ter-Vehn, Nucl. Phys. A249 (1975) 111 and 141
[4] H. Toki, private communication; H. Toki, A. Faessler, Nucl. Phys. A253 (1975) 231


## 2.21. Cross Sections and Isomer Ratios for $^{211,212}$Po


R.M. Lieder, J.P. Didelez*), H. Beuscher, D.R. Haenni, M. Müller-Veggian and C. Mayer-Böricke


It is known since a long time that high-spin isomers exist in $^{211,212}$Po (ref.[1]) which decay predominantly by α emission. The half lives are 25 and 45 s, respectively. The competing γ branches are < 0.2 % for $^{211}$Po$^{m}$ and < 1.5 % for $^{212}$Po$^{m}$. Spins and parities of (25/2⁺) and (18⁺) have been proposed for $^{211,212}$Po$^{m}$, respectively. The (18⁺) isomer in $^{212}$Po has been considered by Faessler et al. as an example of an yrast trap produced by the MONA mechanism[2]. It seemed worthwhile, therefore, to study the features of $^{211,212}$Po$^{m}$. We have measured the cross sections for the ground states $\sigma_g$ and the isomers $\sigma_m$ in these nuclei and determined the resulting isomer ratios $\sigma_m/\sigma_g$ as a function of bombarding energy for α-induced reactions.

The final nuclei $^{211,212}$Po have been produced by the $^{208}$Po(α,n)$^{211}$Po, the $^{209}$Bi(α,pn)$^{211}$Po and the $^{209}$Bi(α,p)$^{212}$Po reactions. The α-beam energy ranged between 45 MeV and 172.5 MeV. The first reaction was previously studied up to 27 MeV (ref.[3]) and the latter two reactions up to 59.2 MeV (ref.[4]).

In the present experiments the α-decay of the final nuclei has been measured using Si surface barrier detectors. The target thickness was 700 μg/cm² for $^{208}$Pb and 600 μg/cm² for $^{209}$Bi. The targets were irradiated for 560 ms. After a delay of 40 ms the α-spectra were measured for 480 ms. After a further delay of 40 ms the next irradiation was started. This cycle was repeated for 5 to 6 hours of beam time in order to collect sufficient statistics. The experimental set-up is described in more detail in contribution 2.22 of this annual report.

In fig. 1 the cross sections for $^{211,212}$Po$^{m}$, as obtained in the bombardment of the $^{209}$Bi target are plotted vs. beam energy. The low-energy results of Chulick and Natowitz[4] are also included. It can be seen, that the cross section decreases exponentially with energy for $^{212}$Po$^{m}$ but less than exponentially for $^{211}$Po$^{m}$. This may be due to the fact that the reaction mechanism is direct in case of $^{212}$Po, whereas several reaction mechanisms may play a role in case of $^{211}$Po. The latter nucleus can be produced by the (α,np) or the (α,d) reaction, so that compound, pre-compound as well as direct reactions may take place.

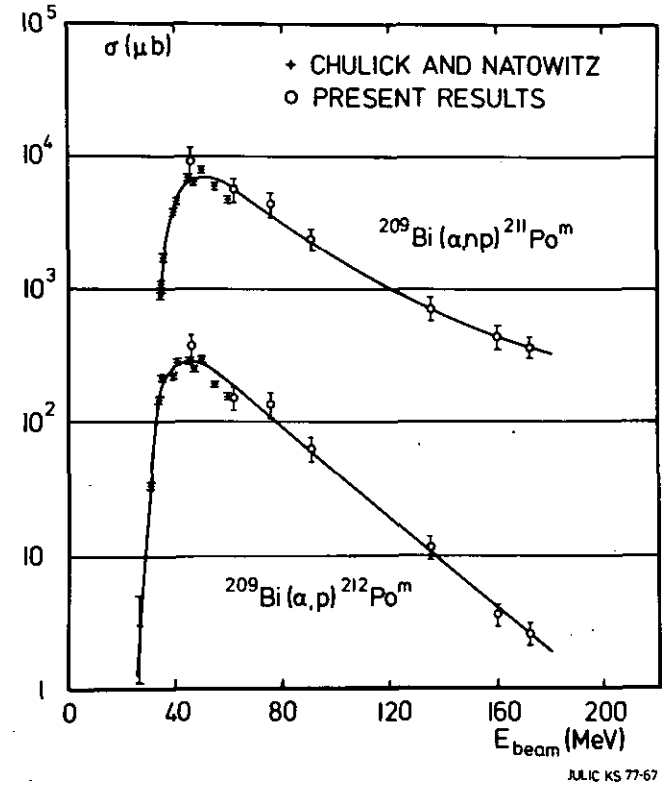


*Figure 1:*
*Cross sections of the $^{209}$Bi(α,p)$^{212}$ Po$^{m}$ and $^{209}$Bi(α,np) $^{211}$Po$^{m}$ reactions vs. beam energy.*

In fig. 2 the isomer ratio for the reaction $^{208}Pb(\alpha,n)^{211}Po$ is plotted vs. beam energy. The low-energy results of Barnett and Lilley[3] are also included. The isomer ratio increases very strongly at low beam energies but much more slowly at high beam energies. This behaviour seems to be characteristic for the direct mechanism. It deviates significantly from that of a compound nucleus reaction. There the isomer ratio shows a maximum at a beam energy close to that at which the cross section has its maximum[5]. The isomer ratio will be measured for $^{212}Po$ as well in order to find out whether its energy dependence is affected by the angular momenta of the states involved.

*) Present address: Institut de Physique Nucleaire, Fac. des Sciences de Paris, B.P. n. 1, F-91406 Orsay, France

### References


[1] I. Perlman et al., Phys. Rev. 127 (1962) 917
[2] A. Faessler, et al., Phys. Rev. Letters 36 (1976) 1028
[3] A.R. Barnett and J.S. Lilley, Phys. Rev. C9 (1974) 2010
[4] E.T. Chulick and J.B. Natowitz, Nucl. Phys. A173 (1971) 487
[5] J.W. Meadows, R.M. Diamond and R.A. Sharp, Phys. Rev. 102 (1956) 190


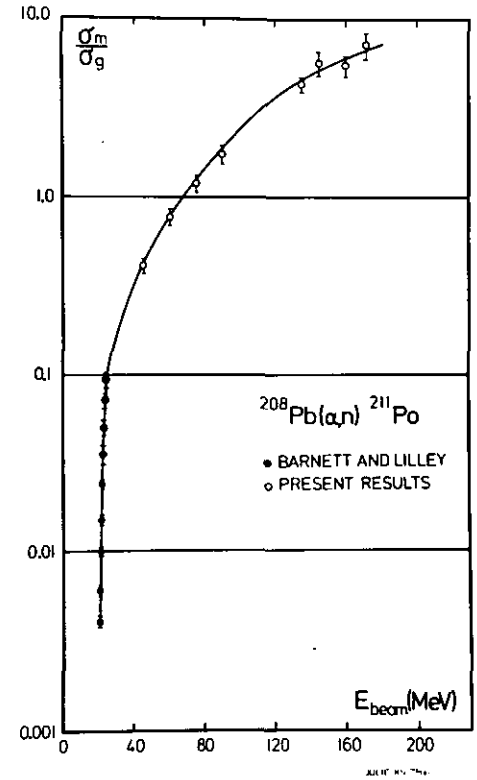


*Figure 2:*
*Isomer ratio of the $^{208}Pb(\alpha,n)^{211}Po$ reaction vs. beam energy.* ▶

## 2.22. Search for Yrast Traps through the Study of the α-Decay after (α,xn) Reactions


R.M. Lieder, J.P. Didelez*), H. Beuscher, Y. Gono**), D.R. Haenni, H.J. Jäger, M. Müller-Veggian, C. Mayer-Böricke


The search for yrast traps has been continued studying the α decay of final nuclei produced in the bombardment of target nuclei with alpha particles. An incident alpha-beam energy of 145 MeV has been used. In the framework of the sharp cut-off model then an angular momentum of ~ 39 ħ is transferred to the final nuclei. The α particles have been detected with Si surface barrier detectors. In order to obtain sufficient sensitivity, the following technique involving the slow pulsing system of the cyclotron has been applied. The targets were irradiated for a certain time. Subsequently eight spectra of 2048 channels have been taken in the multi-spectrum-scaling mode of the analyzing system. The counting time was chosen to be approximately equal to the irradiation time. During the irradiation the detector was closed by means of a mechanical device so that large beam currents of up to ~ 1 μA could be used. This mechanical device consists of a conical shielding between detector and target and a wheel in front of the cone. On the wheel are 8 holes and spaces of same sizes as the opening of the cone equally distributed at the circumference. The wheel is driven by a stepping motor, which is controlled by the pulsing system so that the detector is closed during irradiation but open during the counting time. The device could make reliably not more than 10 stepts per second. Therefore the search for yrast traps was limited to half lives longer than 10 ms. On the other hand states produced with cross sections as small as 80 nb could be detected.

The targets used in these experiments were $^{152,154}Sm$, $^{154,156}Gd$, $^{172,174}Yb$ and $^{194,196}Pt$. The targets were self-supporting metal foils of 1.0 to 1.5 mg/cm$^2$ thickness. The rare earth oxide powders have been reduced either with La or in case of Gd with Zr instead of Th to avoid contaminant α-radiation of the Th(α,xn) reaction products. The irradiation and counting times varied between 100 ms and 20 min. The known ground state α-decay of the final nuclei $^{148}Gd$, $^{150,151}Dy$ was observed in these experiments. However no α-decay of isomers with half lives $T_{1/2} \gtrsim 10$ ms and produced with yields larger than 80 nb have been observed in these experiments.

*) Present address: Institut de Physique Nucleaire Fac. des Sciences de Paris B. P. n. 1. 91406 Orsay, France
**) *Present address: Institut für Kernphysik, Technische Hochschule Darmstadt,* 6100 Darmstadt, West Germany

## 2.23. Status of In-Beam Experiments with the Orange-β-Spectrometer

H. Beuscher, D.R. Haenni, Y. Gono*), R.M. Lieder, M. Müller-Veggian, C. Mayer-Böricke

During the past year, a considerable effort has been made to upgrade the performance of the orange-β-spectrometer so that it could be used for routine conversion-electron measurements. Basically this involved increasing the resolution of the system and reducing the amount of non-electron background observed by the plastic scintillator electron detector. Sufficient improvements have been made to permit the acquisition of some useful data.

At the beginning of the year, the typical in-beam resolution of the spectrometer was ~ 1.2 %. Now this has been improved to ~ 0.7 % and under optimum condition 0.55 %. This was accomplished by redetermining the optimum target location for in-beam measurements (i.e. parallel to the spectrometer axis). The spectrometer was then moved such that this target position corresponded to the optimum position for focusing the beam. Now it is possible to produce well defined beam spots of 2-4 mm diameter at the target position.

In addition to improving the resolution, the peak to background ratio had to be increased. Since a large portion of this background results from γ rays interacting with the plastic scintillator, it was useful to reduce its size to the minimum required to stop the incoming electrons. Increased shielding of the Faraday cup, better beam optics, and a new beam collimator to reduce the amount of stray beam hitting the beam pipe near the spectrometer were also helpful. Further improvement was obtained by counting pulses from the dynode rather than the anode of the photomultiplier. Since the dynode signal provides energy information, it was possible to select by means of a single channel analyzer (SCA) those events whose energies corresponded to electrons of interest. While this does reduce the observed background, it does not provide a correction for the background inside the SCA window. Since the dynode spectrum consists of a single electron peak and a smooth background, it should be possible to obtain an even greater background reduction by recording the dynode spectrum for each spectrometer current setting and a subsequent computer analysis of each spectrum to obtain the area of the conversion-electron peak.

It was found that the β-spectrometer-control circuit (described in the 1976 annual report) could be easily modified to include the external control of a multichannel analyzer. Thus it is possible to automatically acquire and record on magnetic tape a spectrum for each spectrometer current setting. In addition to singles dynode spectra, it is also possible to acqire 2-dimensional dynode vs. RF timing spectra which provide the opportunity to acquire both prompt and delayed electron spectra.

A computer program for the analysis of these data is now under development. Such a program is complicated somewhat by the requirement that it must be capable of processing singles and 2-dimensional spectra (up to 16 k channels) on an equal basis. At present the program provides for the analysis of the dynode spectra in an 'SCA' mode which is analogous to using a hardware SCA on the dynode signal for the singles spectra or two SCAs on the dynode and timing signals for the two-parameter spectra. A second mode of analysis provides for a simple linear or exponential background subtraction. The background regions on either side of the electron peak in the dynode spectrum are selected by the user. Since the position of the dynode peak moves as a function of the spectrometer current, it is possible to enter the background regions at the beginning and end of a series of spectrometer currents. The program then interpolates to find the background regions for intermediate currents.

As an example, fig. 1 shows a portion of the electron spectrum for the decay of 37 min $^{172}$Ta. The source was obtained by irradiating a 1 mg/cm$^2$ Lu target in the spectrometer for 40 min with 0.5 A of 90 MeV $^4$He. The spectrum was acquired for 40 min following the irradiation. The upper spectrum was derived from the integral dynode counting rate. The middle spectrum shows the improvement which can be obtained from a 'SCA' window selected from inspection of the total dynode spectrum (summed over all spectrometer counts). The lower spectrum results from the application of the background analysis. The insert shows the dynode spectrum resulting from the sum of 20 points in the middle of this electron spectrum. The position of the background windows is also indicated. While the background analysis provides a suitable reduction of the background in the electron spectrum, it was found to be very sensitive to the choice of the background regions. Inappropriately chosen background regions can effect the relative detection efficiencies of successive points. At lower electron energies other problems occur since the electron peak is located on a rather steep background which is not always describable as a simple linear or exponential function.

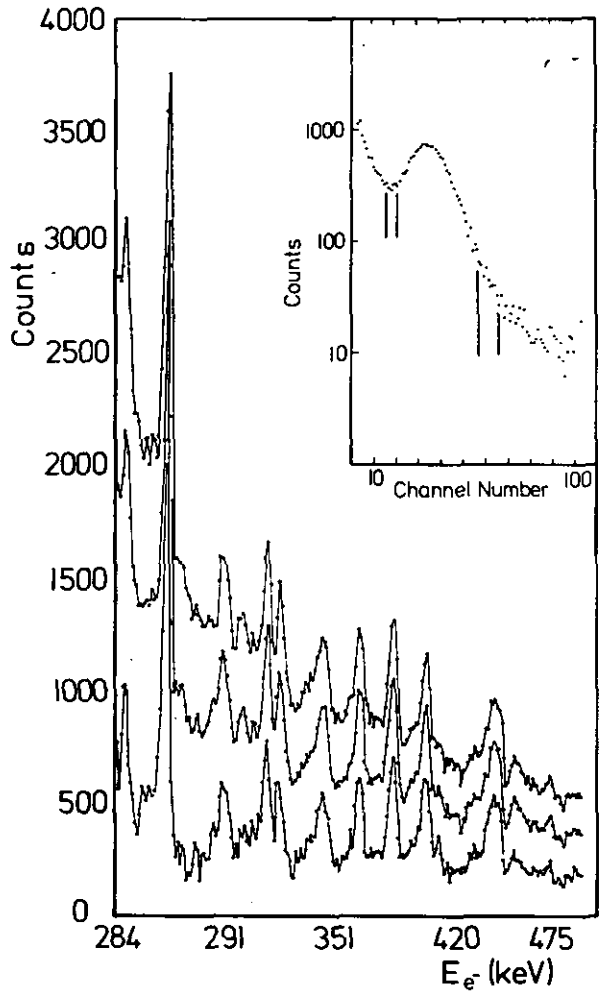


*Figure 1:*
*Part of the conversion electron spectrum from the decay of $^{172}$Ta, showing the effect of different methods of background analysis. The insert shows the dynode spectrum summed over 20 points in the middle of the spectrum.*

A better method of analysis would entail determining the experimental electron response function of the scintillator and the shape of the background spectrum. These could then be fit to the observed dynode spectrum to obtain the appropriate electron counting rates. The electron response functions are relatively easy to

obtain, however, the background shape must be determined during the measurement. Background spectra can be obtained by recording the dynode spectrum with the detector slit closed. Since the background is not necessarily time independent one would have to acquire such spectra after a certain number of dynode spectra are aquired with the slit open. Implementation of such a data acquisition and reduction system is being considered.

Useful electron singles data have been obtained for delayed transitions in $^{134}$Ce (see contribution 2.4 ) and for prompt transitions in $^{146}$Gd (see contribution 2.9 ). The former study was difficult because of low transition intensities and the lack of suitable metallic Ba targets while the latter required that the power supply be modified to extend the spectrometer range to ≃ 1.8 MeV electron energy. A further problem with in-beam measurements results from the necessity of making electron angular distribution corrections. As can be seen in fig. 2, the acceptance of the spectrometer in terms of the reaction angle covers a large angular range and is not constant.

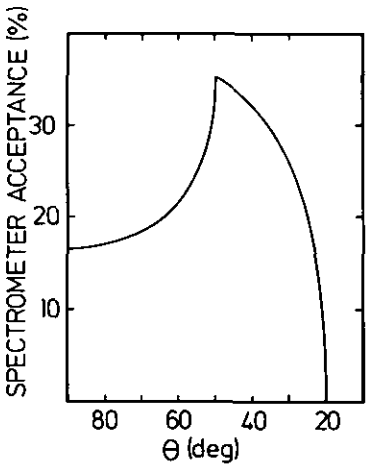


*Figure 2:*
*Acceptance of the Orange-β-Spectrometer. The angle Θ is the reaction angle in the plane of the beam and the spectrometer axis. No correction for the shadow of the coils is included.*

The large transmission of the spectrometer (up to 16 % of 4π) allows one to use it also for coincidence measurements. It should be particularly useful for measuring delayed coincidences since one can make use of the relatively good timing characteristics of the plastic scintillator for determining if the events are in- or off-beam. Fig. 3 shows a coincidence γ-ray spectrum gated by the K-conversion line of the 397 keV isomeric transition in $^{134}$Ce (see contribution 2.4 ). This spectrum is at least of comparable quality to similar data from γ-γ coincidence measurements in spite of the fact that the conversion coefficient of this transition is 1.7 %. The Ge(Li) detector for this measurement was located 4.5 cm from the target, had an active volume of 79 cm$^3$ and a resolution of 2.5 keV at $^{60}$Co. This same detector has been used for an in-beam coincidence measurement with the $^{176}$Yb(α,8n)$^{172}$Hf reaction at 100 MeV. The γ-ray coincident with the K-line from the 409 keV $8_q^+ \rightarrow 6_q^+$ transition ($\alpha_K$ = 0.024) is shown in fig. 4. The ground state band up to $20^+$ is observed. A large amount of γ-background is still observed due to the enormous amount of yrast feeding in the (α,8n) reaction. From these test measurements it would seem that the orange-β-spectrometer can be useful in coincidence measurements where the transitions being gated have either short lifetimes or a conversion coefficient greater than about 5 %.

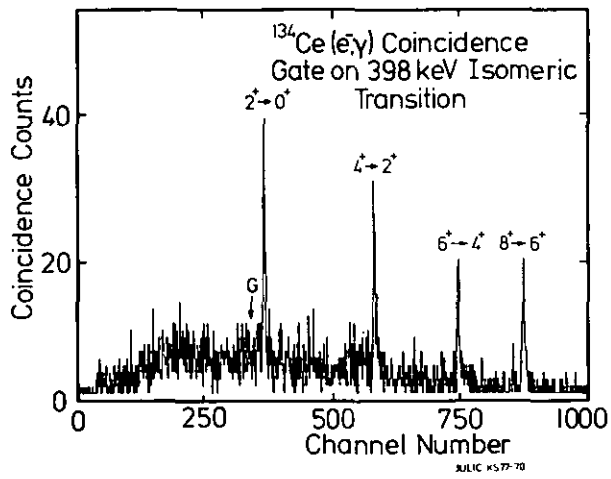


*Figure 3:*
*The off-beam (e⁻,γ)-coincidence spectrum for $^{134}$Ce.*

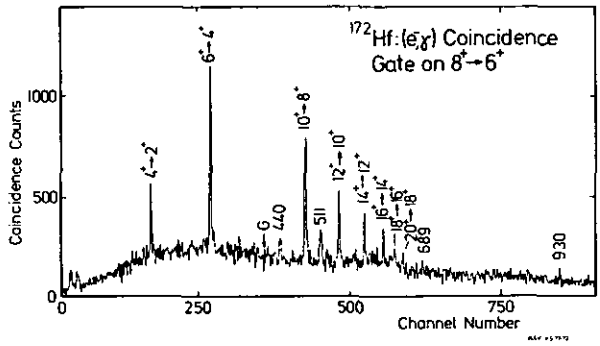


*Figure 4:*
*In-beam (e⁻,γ)-coincidence spectrum for $^{192}$Hf.*

*) Present address: Institut für Kernphysik, Technische Hochschule Darmstadt, 6300 Darmstadt, West Germany

## 2.24. The β-Decay of $^{100}$Y

T.A. Khan, W.-D. Lauppe, K. Sistemich, H. Lawin, G. Sadler, H.A. Selič

The β-decay of $^{100}$Y has been investigated by means of the gas-filled recoil separator JOSEF. The assignment of the γ- and conversion electron lines was carried out by measuring their intensity as a function of the magnetic rigidity of the separator and then comparing the position of the maximum with the calibration curves obtained previously. In addition X,γ- and X,ce-coincidences were performed to establish the charge of the emitting nucleus, thus allowing an unambiguous assignment of the conversion electron and γ-lines[1] (see figure 1).

The lifetime of the β-decay was measured by recording the intensity of the γ- and conversion electron lines as a function of time after each activity transport event. Two β-decay modes of lifetimes O.55 s and O.94 s were found to exist in $^{100}$Y. The lowest lying $O_2^+$ state was discovered in the daughter nucleus $^{100}$Zr, at 331.3 keV. It was found to be principally populated by the O.55 s β-decay mode.

The β-branch to the ground state of $^{100}$Zr was measured by a new technique[1] which showed a strong preference by the O.55 s mode for decay to the $O_1^+$ ground state compared to the $O_2^+$ state.

The present results have been analysed in the framework of the Gneuss and Greiner model[2] and suggest[1] that $^{100}$Zr may have an asymmetric second minimum in its nuclear potential energy surface (see fig. 2).

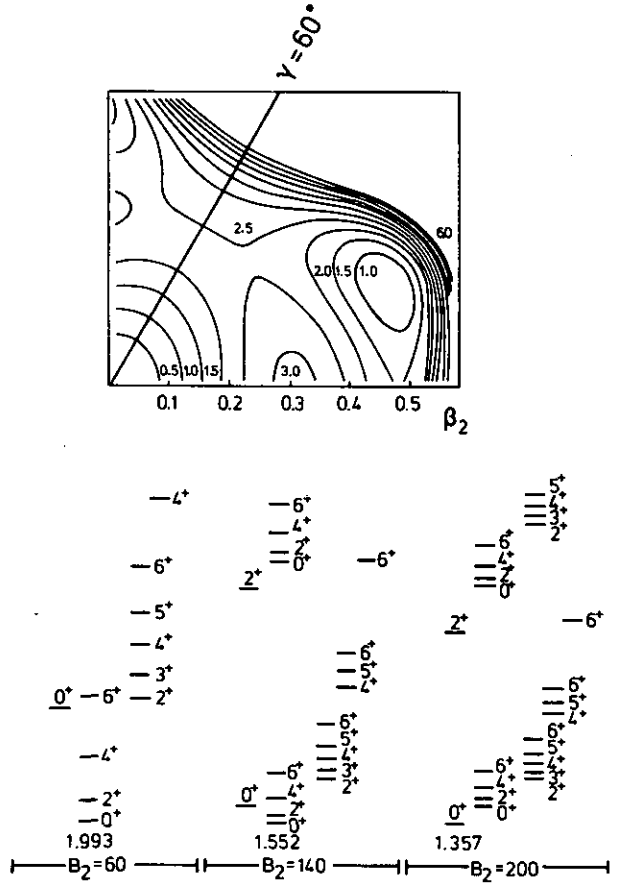


*Figure 2:*
*One of the potential energy surfaces in the β-γ plane generated in ref.[2] and the resulting level structure. The variations in the relative positions of the "vibrational" levels are due to the different zero point energies.*

### References

[1] T.A. Khan, W.D. Lauppe, K. Sistemich, H. Lawin, G. Sadler, H.A. Selič, Z. Physik A283 (1977) 105
[2] G. Gneuss, W. Greiner, Nucl. Phys. A171 (1971) 449

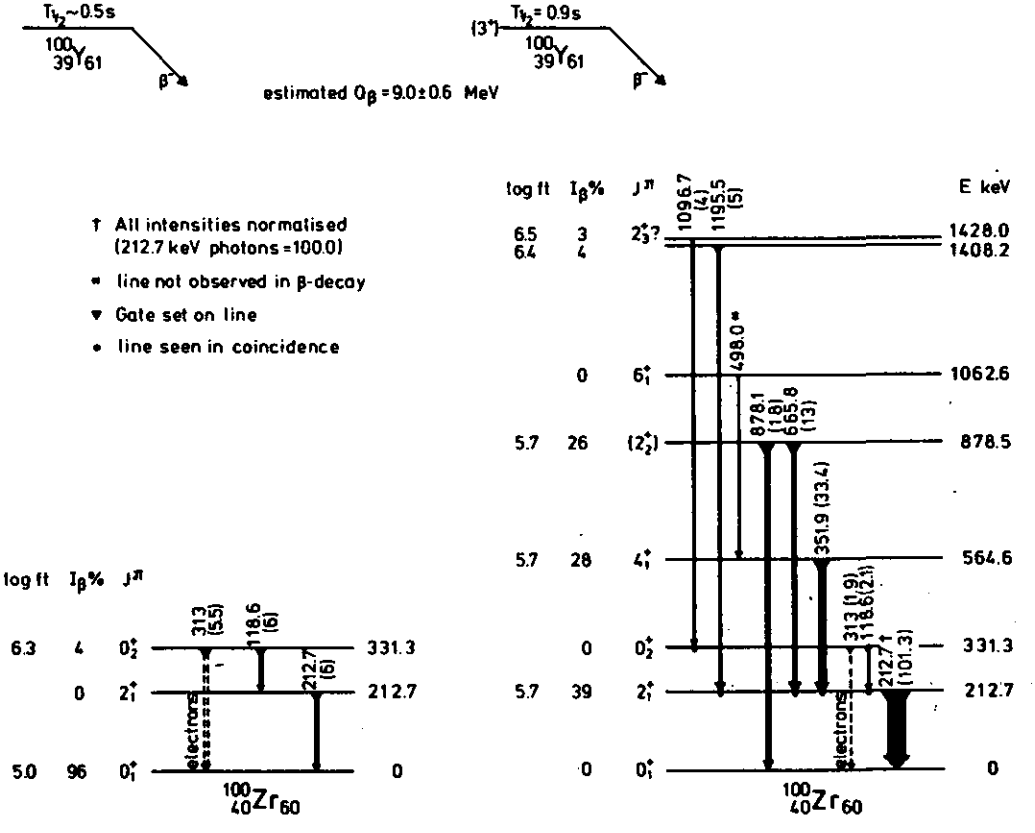


*Figure 1:*
*The decay scheme $^{100}$Y.*

## 2.25. Confirmation of the 331 keV $O^+$-State in $^{100}Zr$

H.A. Selič, W.-D. Lauppe, H. Lawin, K. Sistemich, W. Borgs

Studies of the ß-decay of $^{100}Y$ and the subsequent γ- and ce⁻-transitions in $^{100}Zr$ at the fission product separator JOSEF led to the conclusion that an extremely low lying excited $O_2^+$-state exists in $^{100}Zr$ (ref. [1,2,3]). This level was supposed to decay by conversion electrons into the ground state and by a weak γ transition of 118 keV into the first excited $2^+$ state at 213 keV. In order to prove this part of the level scheme angular correlation measurements were undertaken for the 118-213 keV γ,γ-cascade which should show the very specific anisotropy of a $O^+ \rightarrow 2^+ \rightarrow O^+$ spin sequence.

The experimental procedure for angular correlation measurements at JOSEF with the necessary beam concentration by means of an air-jet system has been described in ref.[4]. An intrinsic Ge(Li)-detector of 3 $cm^2$ × O.7 cm was fixed at a distance of 5 cm from the source while a Ge(Li)-diode of 148 $cm^3$ was moved around the source at a distance of 11.2 cm. The activity was transported (t = O.18s) with a discontinuously moving tape device from the accumulation position to the measurement position in front of the detectors.

The result is shown in fig. 1. The data have been corrected for beam instability with the use of the singles γ-ray spectra of the

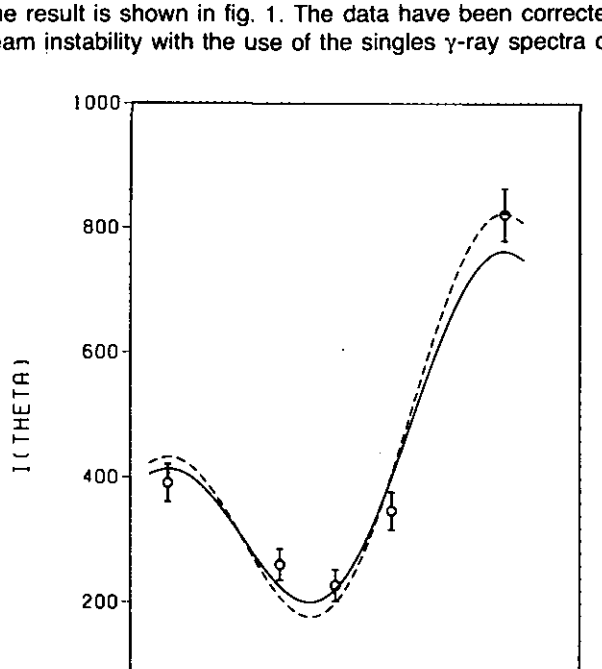


*Figure 1:*
*γ,γ angular correlation of the measured 118/213 keV cascade*
——— *with uncorrected $A_{22} = 0.2795 \pm 0.09$ and $A_{44} = 0.9979 \pm 0.11$ fit*
- - - - - *corrected with $Q_{22}$ and $Q_{44}$ to solid angle.*

movable detector which were recorded by a ND 5O/5O-system in equal periods of 78OOs during the measurements. The solid line shows the least squares fit through the data while the dashed line results from solid angles corrections for the finite size of the detectors. The deduced coefficients for the directional-correlation function W(Θ) are $A_{22}$ = O.29 ± O.O9 and $A_{44}$ = 1.17 ± O.11. The complete agreement with the theoretical values of $A_{22}$ = O.357 and $A_{44}$ = 1.14 (ref.[5]) for a O(2)2(2)O γ,γ-cascade confirms the spin assignments in $^{100}Zr$.

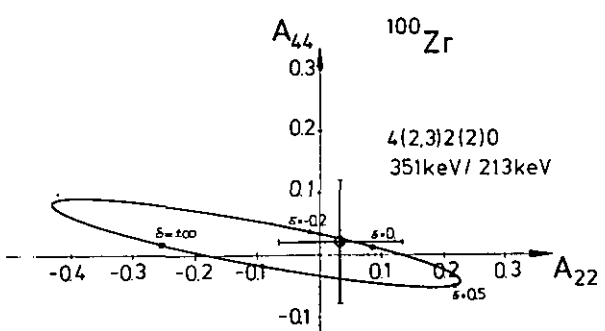


*Figure 2:*
*$A_{44}$ vs. $A_{22}$ parametergraph of the 4-2-0 cascade with the resulted correlation coefficients.*

The 351-213 keV γ,γ-cascade is hard to observe but the evaluation of the data yields coefficients of $A_{22} = 0.026 \pm 0.101$ and $A_{44} = 0.028 \pm 0.11$ depicted in fig. 2. This is also consistent with the supposed spin assignments of $4^+(2,3)2^+(2)0^+$ for the 565 keV and 213 keV levels (ref.[3]), respectively.

### References

[1] T.A. Khan, W.D. Lauppe, K. Sistemich, H. Lawin, G. Sadler and H.A. Selič, Z. Physik A283 (1977) 1O5
[2] T.A. Khan, W.D. Lauppe, K. Sistemich, H. Lawin and H.A. Selić, Z. Physik A284 (1978) 313-317
[3] Contribution of this annual report (1977) p. 55
[4] H.A. Selič, W. Borgs, T.A. Khan, W.D. Lauppe, H. Lawin, G. Sadler, K. Sistemich, Jül-Report KFA-IKP 1O/77, p. 45; H.A. Selič, Thesis, University of Cologne D38 (1977)
[5] H. Frauenfelder and R.M. Steffen, Alpha, Beta and Gamma Ray Spectroscopy, Ed. by K. Siegbahn, North-Holland Publ. Co. Amsterdam 1966

## 2.26. Lifetime of the 331.3 keV excited $O^+$ state in $^{100}Zr$

T.A. Khan, W.-D. Lauppe, H. Lawin, H.A. Selič, K. Sistemich

The discovery of the lowest lying exited $O^+$ state in $^{100}Zr$ has led again to the speculation that rotational and vibrational modes coexist in this nucleus. The lifetime of this $O_2^+$ state has been measured at the gas-filled recoil separator JOSEF[1]. By observing the delayed coincidences between the β-particles populating the $O_2^+$ level and the EO conversion electrons from its decay, a half life of 3.37 ± O.3O ns has been obtained (see fig. 1). From the measured lifetime and the relative intensities of the $O_2^+ \rightarrow O_1^+$ and $O_2^+ \rightarrow 2_1^+$ transitions, values of O.493 ± O.O15 for the EO strength parameter ρ and 16 s.p.u. for B(E2, $2_1^+ \rightarrow O_2^+$) have been obtained.

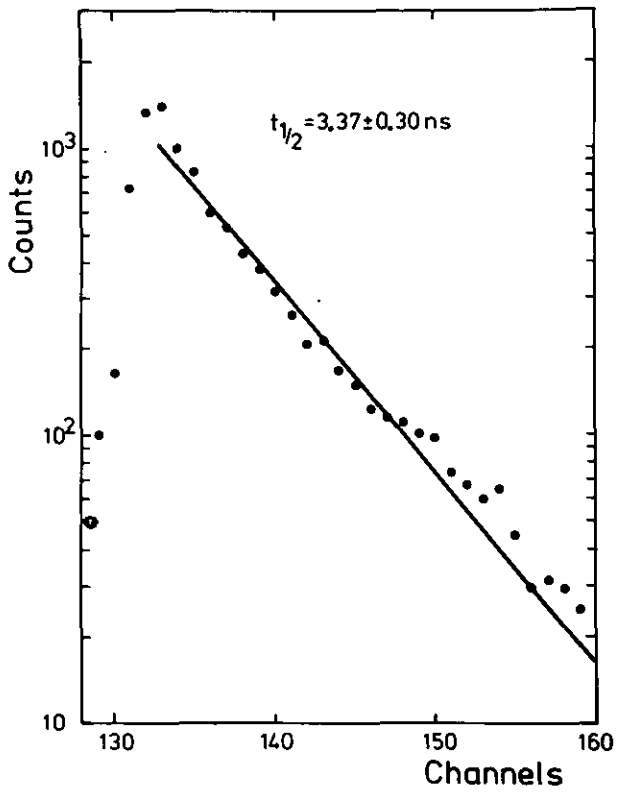


*Figure 1:*
*The delayed β-conversion electron coincidence for the 331.3 keV $0_2^+$ state in $^{100}Zr$.*

The surprisingly large value of ρ (see fig. 2) suggests that the $O_1^+$ ground state is mixing with the $O_2^+$ excited state to accelerate the transitions. Evidence for this mixing is also provided by the VMI model which predicts an energy of the $6_1$ state from the measured $E_4+/E_2+$ ratio 44 keV below the observed value, suggesting that the $O_1^+$ ground state has been pushed downwards from its unperturbed position.

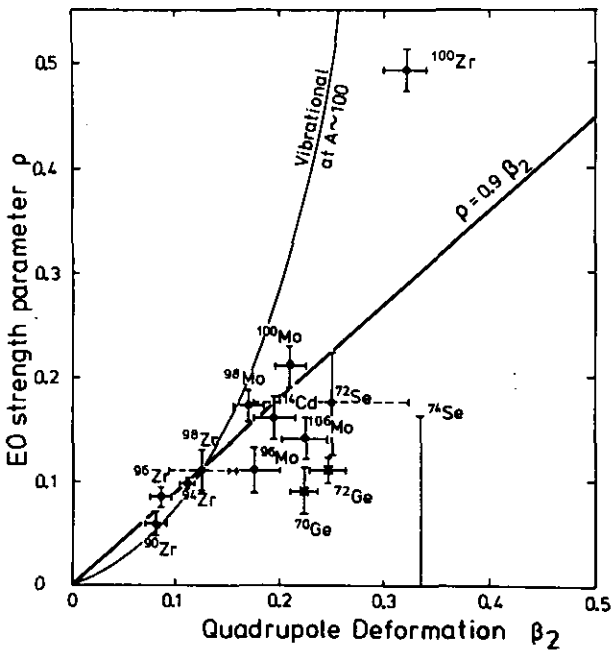


*Figure 2:*
*The ρ versus $\beta_2$ distribution for nuclei with 50 < A < 130.*

The asymmetric VMI model[2] has been used to analyse this shift and obtain a value for the mixing of the two $O^+$ states[1]. Values of $a^2$ = O.82 and $b^2$ = O.18 were obtained for the postulated wave functions

$$|O_1^+> = a|O_{rot}^+ > + b\,|\,O_{vib}^+ >$$
$$|O_2^+> = \beta\,|O_{rot}^+ > + a\,|\,O_{vib}^+ >$$

for the two states at a γ deformation of 17°.

To compare the prediction with experiment, the values of B(E2, $2_1^+ \rightarrow O_1^+$) of 62 s.p.u.[3] and of B(E2, $2_1^+ \rightarrow O_2^+$) of 16 s.p.u. were used to obtain $a^2$ and $b^2$ and gave $a^2$ = O.79 and $b^2$ = O.21. The good agreement between theory and experiment confirms the postulated mixing of the two $O^+$ states and suggests that $^{100}Zr$ is a triaxial nucleus in its ground state.

### References

[1] T.A. Khan, W.D. Lauppe, K. Sistemich, H. Lawin, H.A. Selič, Z. Physik A284 (1978) 313
[2] H. Toki, A. Faessler, Z. Physik A276 (1976) 35
[3] R.C. Jared, H. Nifenecker, S.G. Thompson, Proc. IAEA symposium on fission, Rochester 1973

## 2.27. The Level Scheme of the Doubly Magic Nucleus $^{132}Sn$

W.-D. Lauppe, K. Sistemich, T.A. Khan, H. Lawin, G. Sadler, H.A. Selič, O.W.B. Schult

Doubly magic nuclei are of special interest since they allow tests of the basic concepts of the shell model. Among these nuclei, the only one with two closed mayor shells which is experimentally accessible in the wide mass region between $^{56}Ni$ and $^{208}Pb$ is $^{132}_{50}Sn_{82}$. It is very neutron rich and can only be produced in fission.

Our study of $^{132}Sn$ has been carried out at the fission product recoil separator JOSEF[1], which permits prompt investigations within 1 μs after fission. It serves for the determination of both the mass and the nuclear charge of the radiating nuclei.

We found that

- The γ-transition of 4041 keV which has tentatively been assigned[2] to the β-decay of $^{132}In$ is indeed emitted from $^{132}Sn$.
- It is observed not only in the β-decay of $^{132}_{49}In_{83}$ with a half-life of 0.12 s, ref.[2], but also in the γ-deexcitation of an isomer in $^{132}Sn$ ($t_{1/2}=1.7 \pm 0.3$ μs which is fed drectly in fission.
- Additional γ-transitions of 132.3 keV (60 % relative intensity), 299.2 keV (125), 374.3 keV (100) and 4415.7 keV (25) exist in $^{132}Sn$.
- A γ,γ-coincidence measurement[3] lead to the level scheme given in fig. 1.
- The upper limits for any γ-intensity of transitions from the 4714 and 4847 keV levels to the ground state are 5 %.

The relative position of the 132.3 and 299.2 keV lines is deduced from the fact that the higher lying line must account for the isomerism. For the 132.3 keV line E2 multipolarity is suggested since its γ-ray intensity indicates a total conversion coefficient of 1. Then this transition must be hindered 10 times compared to single particle units which is not unusual in that region. If the 299.2 keV line would cause the isomerism then hindrance factors of $10^8$, $10^6$ and $10^2$ would be required for the possible multipolarities of E1, M1 or E2.

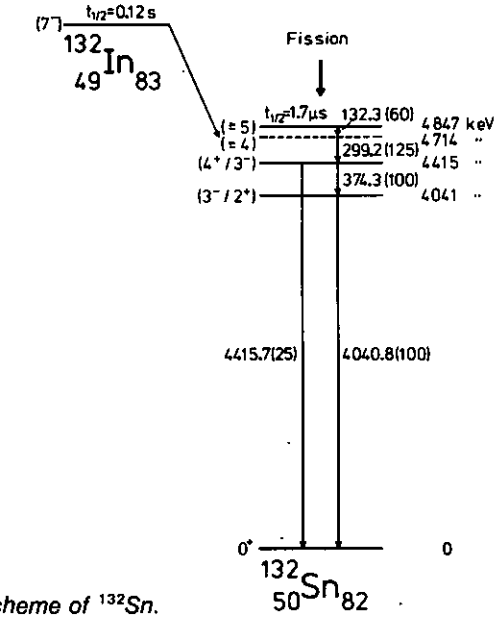


*Figure 1: Tentative level scheme of $^{132}Sn$.*

The proposed spin and parity assignments are deduced from the deexcitation pattern. The should be compared to the predictions of ref. [4].

### References

[1] H. Lawin, J. Eidens, J.W. Borgs, R. Fabbri, J.W. Grüter, G. Joswig, T.A. Khan, W.D. Lauppe, G. Sadler, H.A. Selič, M. Shaanan, K. Sistemich, P. Armbruster, Nucl. Instr. Meth. 137, 103 (1976)
[2] A. Kerek, G.B. Holm, L.-E. De Geer, S. Borg, Phys. Lett. 44B, (1973) 252
[3] W.D. Lauppe, K. Sistemich, T.A. Khan, H. Lawin, G. Sadler, H.A. Selič, O.W.B. Schult, Proc. I.U.P.A.P. Conf. on nuclear structure, Tokyo 1977, invited papers, in press
[4] S. Dehesa, J. Speth, contribution to this annual report, p. 70

## 2.28. The Level Scheme of $^{133}Sb_{82}$

K. Sistemich, W.-D. Lauppe, T.A. Khan, J.W. Grüter, H. Lawin, H.A. Selič, J.P. Bocquet*), R. Sellam*), E. Monnand**), F. Schussler**)

Nuclei adjacent to a doubly magic isotope provide infor mation about the single particle energies. Thus the knowledge of the level scheme of $^{133}Sb$ with one proton outside the doubly closed $^{132}Sn$ core gives the energies of the single proton states in this region.

The nucleus $^{133}Sb$ is a neutron rich fission product. The only information about its level scheme stems from the observation[1] of a β-decay with a half-life of 1.47 ± 0.04 s in the A=133 chain which was assigned to the decay of $^{133}Sn$, and of one 963 keV γ-transition coincident with the β-particles. This transition was attributed to the depopulation of the first excited state in $^{133}Sb$ with the probable spin and parity of $5/2^+$.

The recoil fission product separators JOSEF[2] and LOHENGRIN[3] have been used for more detailed studies of the level scheme of $^{133}Sb$. The following results were obtained:

- The 963 keV transition belongs indeed to $^{133}Sb$. A half-life of $1.37 \pm 0.07$ s was found for the decay of $^{133}Sn$. The mean value of $t_{1/2}=1.42$ s is adopted.
- Two isomeric states ($t_{1/2}=3 \pm 1$ and $16.0 \pm 1.5$ μs) exist in $^{133}Sb$ above 4 MeV. They are not fed in the γ-decay of $^{133}Sn$ but directly in fission.
- Four γ-transitions of 61.7 keV (30 % rel. intens.), 162.5 keV (70), 1510.1 keV (100) and 2792.1 keV (100) depopulate the isomeric states.
- The γ,γ-coincidence results show that the γ-lines form a stretched cascade.
- These data, the absence of crossover transitions (< 5 % rel. intens.) and the systematics of the N = 82 single proton energies[4] suggest the scheme, see below.

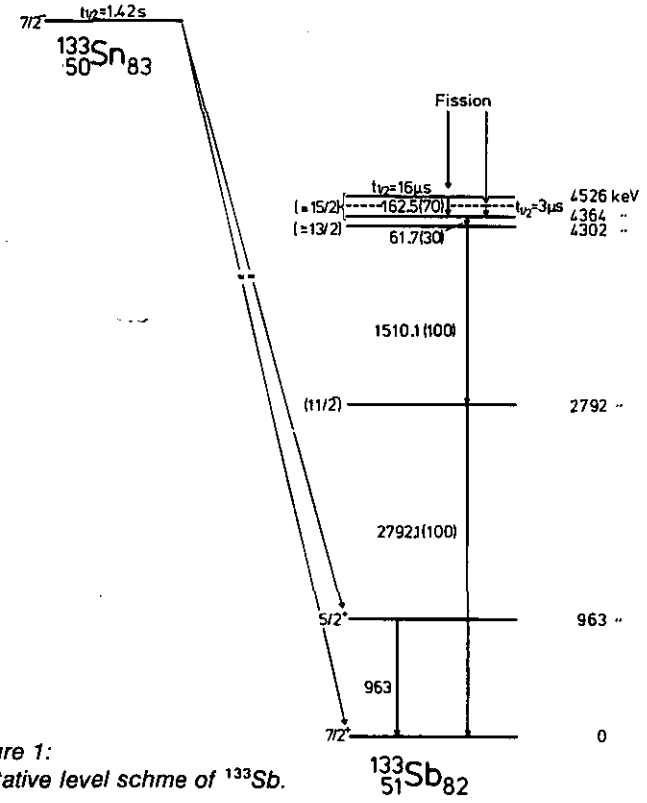


*Figure 1:*
*Tentative level schme of $^{133}Sb$.*

O The total internal conversion coefficients of the 61.7 and 162.5 keV lines as deduced from the relative γ-intensities are about 2.3 and $<0.4$, respectively. The probable multipolarities of the lines are M1 and M1, E1 or E2.

The energy of the 3 µs level is unknown as no γ-transition feeding the 4364 keV state has been observed. This transition might be highly converted. The level at 2792 keV is most probably the $h_{11/2}$ single proton state. The levels above 4 MeV are presumably due to particle-core coupling as $^{132}Sn$ has several states at this energy[5].

*) Institut Laue-Langevin, Grenoble, France and D.R.F. C.E.N. Grenoble, France
**) D.R.F. C.E.N. Grenoble, France

### References

[1] S. Borg, G.B. Holm, B. Rydberg, Nucl. Phys. A212 (1973) 197
[2] H. Lawin, J.W. Borgs, R. Fabbri, J.W. Grüter, T.A. Khan, W.D. Lauppe, G. Sadler, H.A. Selič, M. Shaanan, K. Sistemich, Nucl. Instr. Meth. 137 (1976) 103
[3] E. Moll, H. Schrader, G. Siegert, M. Asghar, J.P. Bocquet, G. Bailleul, J.P. Gautheron, J. Greif, G.I. Crawford, C. Chauvin, H. Ewald, H. Wollnik, P. Armbruster, G. Fiebig, H. Lawin, K. Sistemich, Nucl. Instr. Meth. 123 (1975) 615
[4] B.H. Wildenthal, E. Newman, R.L. Auble, Phys. Rev. C3 (1971) 1199
[5] W.D. Lauppe, K. Sistemich, T.A. Khan, J.W. Grüter, H. Lawin, G. Sadler, H.A. Selič, O.W.B. Schult, Proc. of the Int. Conf. on Nuclear Structure – Invited Papers, Tokyo, Japan (in press)

## 2.29. The Study of the (n,α) and (n,γα) Reactions on $^{143}Nd$

L. Aldea, B. Kardon*), O.W.B. Schult, H. Seyfarth, N. Wüst

In the last years studies of the (n,α) reaction induced by thermal or resonant neutrons have been performed in order to obtain information about the α-decay mechanism and also about the structure of highly excited states. In favourable cases the competition between α and γ decay allows the observation of the two-step (n,γα) reaction. In this process, an α particle follows the emission of a low-energy γray to a bound state. The α spectrum from the (n,γα) process was expected to consist of broad and smooth continua (bumps) on the low-energy sides of the discrete (n,α) peaks.

A similar smooth energy dependence has been expected for the population of highly excited states in α-transfer heavy-ion reactions. However, a selective population has been observed among other for the $^{140}Ce(^{16}O,^{12}C)^{144}Nd$ reaction[1] involving states in $^{144}Nd$ at excitation energies of 8 MeV. Consequently it is of interest to find out, whether this selectivity also occurs in the $^{143}Nd(n,\gamma\alpha)^{140}Ce$ process. The (n,γα) cross sections have been measured for several nuclei[2,3,4]. However, the values reported by various authors differ by a factor of about 4 in case of the $^{143}Nd(n,\gamma\alpha)^{140}Ce$ reaction. We have therefore studied again and under improved experimental conditions the α spectrum following thermal neutron capture in $^{143}Nd$[5].

The measurements were performed at the Bi-filtered thermal neutron beam of the FRJ-2 (DIDO) reactor. The targets were placed at an angle of 15° toward the n beam ($1.3 \cdot 10^6$ n/cm²s) so that they fully covered the beam area of $2.4 \times 0.5$ cm². For detection of the α particles a surface-barrier detector with 100 µ depletion depth and 100 mm² area was placed at a distance of 1.5 cm in front of the target (100 µg/cm² Nd enriched in $^{143}Nd$ to 88.4 %). Special care was taken for a reliable determination of the background.

One of the α spectra obtained in the present experiment is depicted in fig. 1. The well resolved peaks above 7.3 MeV correspond to α-transitions to the ground state and first excited states of $^{140}Ce$. In table 1 the cross sections are listed for these transitions and for the unresolved group of transitions with energies between 6.9 and 7.2 MeV as obtained from the α spectrum of fig. 1. For comparison also the cross sections refs. 3 and 4 are included.

Fig. 1 shows the existence of a relatively broad α peak between 8 and 9 MeV. This peak is attributed to the two-step reaction (n,γα). In fig. 2 the spectrum is plotted which results after subtraction of the properly normalized background and of the discrete peaks from the experimental spectrum. A simple summation of counts in the spectrum of fig. 2 gives a value of $1.04 \pm 0.03$ mb for the cross section of the $^{143}Nd(n,\gamma\alpha)^{140}Ce$ reaction in good agreement with the data from refs. 3 and 4, but approximately 3 times the value given in ref. 2. The normalization is based on[2] $\sigma(n,\alpha_0) = 21.28$ mb. A surprising feature of the (n,γα) spectrum consists in its structure, revealing two maxima.

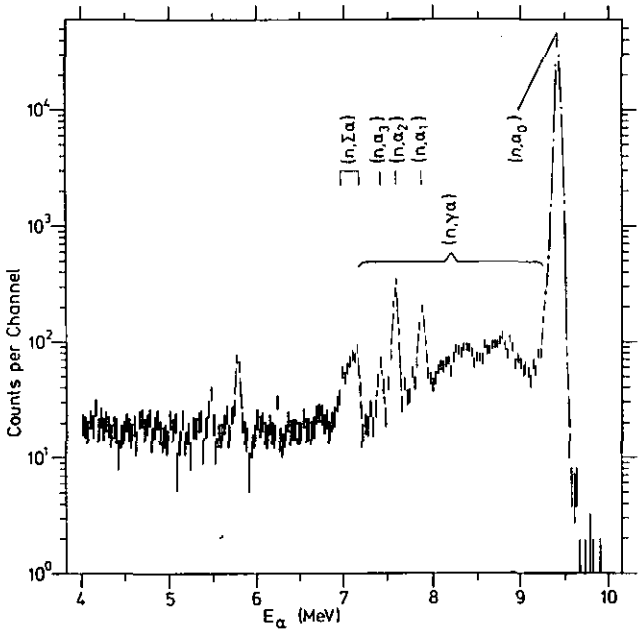


*Figure 1:*
*Alpha-particle spectrum from the reactions $^{143}Nd(n,\alpha)^{140}Ce$ and $^{143}Nd(n,\gamma\alpha)^{140}Ce$. The peaks at 5.5 and 5.8 MeV are due to the backing material. The channel width corresponds to 29.4 keV.*

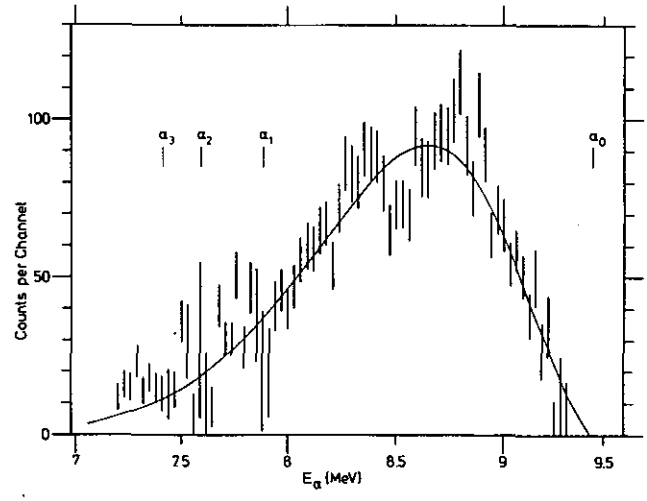


*Figure 2:*
*The $(n,\gamma\alpha)$ spectrum, obtained from the spectrum of fig. 1 after subtraction of background and discrete peaks the position of which is indicated. The solid line shows the spectral shape which is predicted by the extreme statistical model. On the ordinate 100 counts correspond to 28.2 μb.*

In order to compare the spectrum from fig. 2 with what is predicted by a pure statistical model description, a least square analysis of the data has been performed. A parametrization of the theoretical

*Table 1:*
*Partial cross sections (μb) of the $^{143}Nd(n_{th},\alpha)^{140}Ce$ reaction*

| Peak | $E_{ex}$ (MeV) | $E_\alpha$ (MeV) | Ref. 3 | Ref. 4 | Present work |
|---|---|---|---|---|---|
| $\alpha_0$ | 0 | 9.44 | 21,280[a] | 22,000±2000 | 21,280[a] |
| $\alpha_1$ | 1.60 | 7.89 | 140±20 | 95±15 | 101±9 |
| $\alpha_2$ | 1.90 | 7.59 | 230±20 | 180±20 | 190±10 |
| $\alpha_3$ | 2.08 | 7.40 | 100±20 | 60±10 | 30±6 |
| $\Sigma\alpha$ | 2.3-2.6 | 6.9-7.2 | 160±30 | 90±20 | 125±9 |

a) For normalization this value was taken from ref.[2]

shape of the spectrum $S_\alpha$ can be accomplished introducing $E_\alpha^{Max}$ as the energy where the $(n,\gamma\alpha)$ spectrum reaches its maximum $S_\alpha^{Max}$. With $E^o$ as the energy of the $\alpha_o$ transition one obtains

$$S_\alpha = S_\alpha^{Max}\left[\frac{E_\alpha^O - E_\alpha}{E_\alpha^O - E_\alpha^{Max}}\right]^3 \exp\left\{\frac{6E_\alpha^{Max}}{E_\alpha^O - E_\alpha^{Max}}\left[1-\left[\frac{E_\alpha^{Max}}{E_\alpha}\right]^{1/2}\right]\right\}$$

The values of $S_\alpha^{Max}$ and $E_\alpha^{Max}$ were obtained from the least-squares fit. The $\chi^2$ test allowing only for the statistical errors in each channel excludes at a confidence level of 99.5 % the randomness of the observed structure in the $(n,\gamma\alpha)$ spectrum. The actual data are, however, expected to be affected by the Porter-Thomas fluctuations of the partial γ-radiation widths and the α widths in the two-step $(n,\gamma\alpha)$ process. The full line in fig. 2 represents the calculated curve corresponding to the fit performed after quadratic addition of the expected variance due to Porter-Thomas fluctuations and the statistical errors for each channel. The result of the least-squares fit shows that at the present stage of the statistics in the experimental $(n,\gamma\alpha)$ spectrum the observed structure can be explained through Porter-Thomas fluctuations of both γ and α widths. However, the surprising selectivity in population of states observed in direct α-transfer reactions justifies the tentative assumption that the α decay of states which are involved in the $(n,\gamma\alpha)$ process is of direct character and that therefore the α widths are not affected by Porter-Thomas fluctuations. Together with the summation over two channels this assumption yields at a confidence level of 95 % a discrepancy between the observed double-humped structure of the $(n,\gamma\alpha)$ spectrum and what is expected from the extreme statistical model.

*) Present address: Central Research Institute for Physics, Hungarian Academy of Sciences, Budapest

## References


[1] W. v. Oertzen, H.G. Bohlen, B. Gebauer, Nucl. Phys. A207 (1973) 91
[2] N.S. Oakey, R.D. MacFarlane, Phys. Lett. 26B (1968) 662
[3] J. Kvitek, Z. Kosina, Yu.P. Popov, Rep. UJF 3303-F (1974)
[4] A. Emsallem, M. Asghar, Proc. 2nd Int. Symp. Neutron Capture Gamma Ray Spectroscopy and Related Topics, Petten/The Netherlands 1974, Edt.: RCN Petten (1975), p. 395
[5] L. Aldea, B. Kardon, O.W.B. Schult, H. Seyfarth, N. Wüst, Z. Physik A283 (1977) 391

## 2.30. Low-Lying Levels of $^{196}$Pt: A Possible Example of the O(6) Symmetry Group

J.A. Cizewski*), R.F. Casten*), G.J. Smith*), M.L. Stelts*), W.R. Kane*), H.G. Börner, W.F. Davidson**)

The reaction $^{195}$Pt(n,γ) was studied at the Grenoble High Flux Reactor with the bent crystal spectrometers Gams 1 and Gams 2/3. The primary purpose of the experiment was to complement existing data from Brookhaven in which primary and secondary γ-rays following thermal and resonance capture were studied along with γ-γ coincidence measurements and study of the primary E1 transitions following average resonance capture. Specifically, the Brookhaven data, obtained with Ge(Li) detectors, were rather insensitive to low energy transitions which are weak in intensity but which, corresponding to transitions between high lying states, represent the dominant decay modes of these states. The GAMS spectrometers are particularly powerful here and also provide far superior overall energy resolution and multiplet decomposition for γ rays up to an energy of ∼1200 keV.

corresponding to the SU(5), SU(3) and O(6) subgroups of the SU(6) group. The first two limits correspond to the familiar anharmonic vibrator and deformed rotor, respectively, for both of which numerous empirical examples are known. The exact geometrical analogue of the third, O(6), limit is not yet established although it appears that the displaced γ-unstable model is the closest approximation to it. $^{196}$Pt provides the first empirical manifestation of this limit. The correspondence between experimental results and the O(6) predictions are shown in the accompanying figure in which all low spin positive parity levels below the pairing gap are shown along with their γ-ray decay branches. The first numbers on the transition arrows are the relative observed deexcitation B(E2) values (assuming pure E2 multipolarities). The second numbers are the predictions of the model. The predicted energy levels are given to the left of each set of experimental levels along with the model quantum numbers (σ, τ and νΔ). The agreement is remarkable. All observed levels have analogues in the model and vice versa. All γ-ray transitions predicted to be strong are in fact the strongest observed from the given level and all strong γ-ray branches are predicted to be strong. The only exception to this is the decay of the

*Figure 1:*
*Level scheme of $^{196}$Pt.*

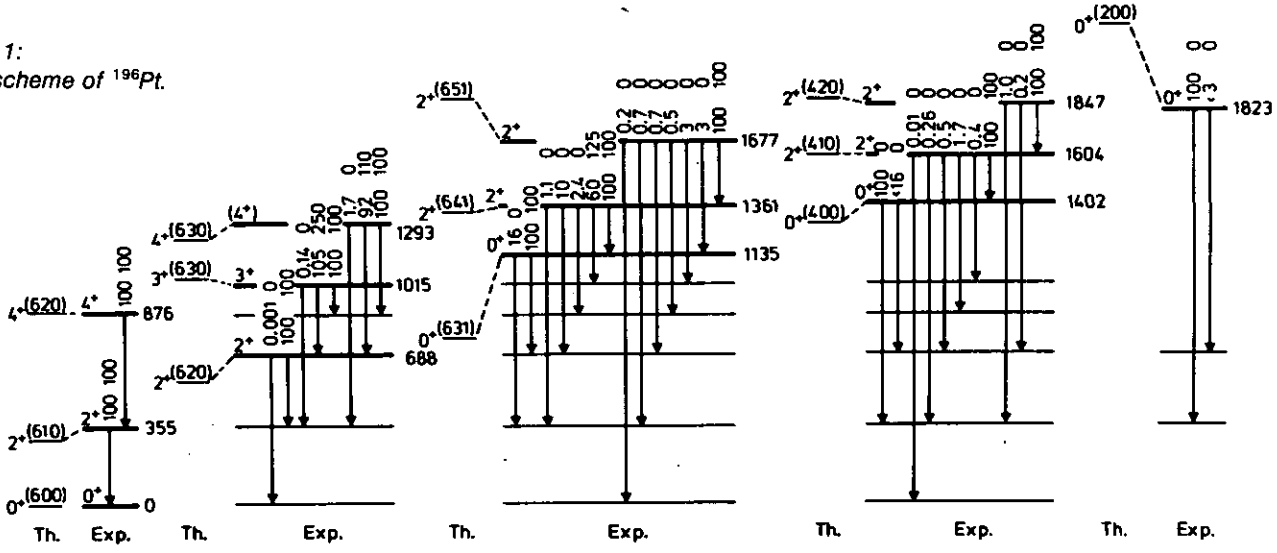


The ILL and Brookhaven data have been combinded to generate a detailed level scheme up to 2500 keV, the most important feature of which is the interpretation of all observed positive parity levels below the pairing gap(∼1800 keV) in terms of the O(6) limit of the Interacting Boson Model of Arima and Iachello. This model treats all heavy even-even nuclei (except for those very close to closed shells) in terms of interactions among bosons which can occupy s(L=0) and d(L=2) states. Three natural limits arise in this model, higher lying $0^+$ states and this can be readily explained in terms of very small σ-breaking interactions. Given the results for $^{196}$Pt, an effort is now underway to determine if one can treat the series of even-even Os and Pt nuclei in terms of systematically varying departures from the O(6) limit.

*) Brookhaven National Laboratory, Upton, New York 11973
**) Institut Laue-Langevin, 38042 Grenoble, France

# 3. Applied Nuclear Physics

## 3.1. Production of $^{48}Cr$ via α- and $^{3}He$-Particle Induced Reactions on Titanium

H.J. Probst, R. Weinreich*), S.M. Qaim*)

Investigations started last year[1] on the production of $^{48}Cr$ via α- and $^{3}He$-particle induced nuclear reactions on titanium of natural isotopic composition were carried further and are now about to be completed. Fig. 1 shows the effective cross sections for the production of $^{48}Cr$ as a function of the incident particle energy. Since for applications in the life sciences the yield and purity of an isotope are very important, we investigated the production of $^{48}Cr$ from these two aspects. The yields for both the α- and $^{3}He$-particle induced reactions are shown in Fig. 2 (left hand scale). Also shown in

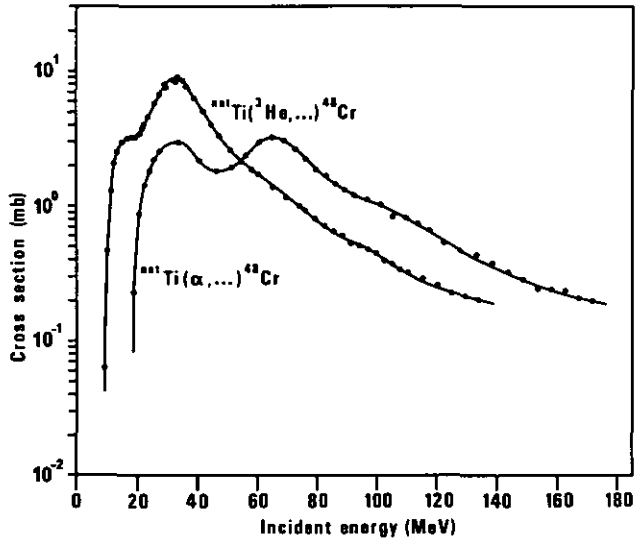


*Figure 1:*
*Effective cross sections for the formation of $^{48}Cr$ from natural titanium as a function of the incident particle (α or $^{3}He$) energy.*

Fig. 2 are the relative contributions in the two reactions of the invariably accompanying undesired $^{51}Cr$ impurity (right hand scale). It was chosen to plot the ratio of the intensities of the two main γ-lines 320 keV ($^{51}Cr$) and 308 keV ($^{48}Cr$) as a function of the incident

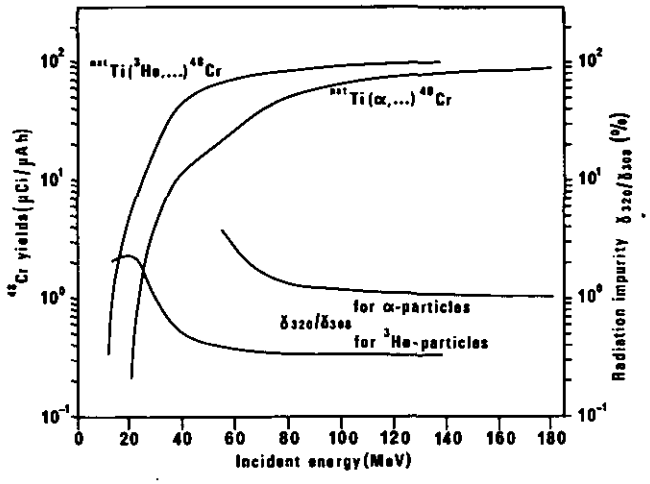


*Figure 2:*
*Yields of $^{48}Cr$ and the ratio $^{51}Cr/^{48}Cr$ in the irradiations of natural titanium with α- or $^{3}He$-particles.*

particle energy. If a limit on the maximum acceptable contamination from $^{51}Cr$ is placed at 1 %, in routine production via α-particle irradiations (primary energy: 120 MeV; beam current: 15 A; target thickness: 2.2 mm) 0.8 mCi $^{48}Cr$/h and via $^{3}He$-particle irratiations (primary energy: 135 MeV; beam current 15 μA; target thickness: 4.5 mm) 1.5 mCi $^{48}Cr$/h are produced.

Besides $^{51}Cr$, irradiations of titanium with α- or $^{3}He$-particles give rise to a few other impurities as well. These reaction products are essentially the same as those produced in the deuteron induced reactions on vanadium, a report on which was given last year[2]. For applications in life sciences $^{48}Cr$ would be needed in a pure and carrier-free from. A method for the chemical separation of carrier-free $^{48}Cr$ has therefore been worked out.

*) Institut für Chemie I (Nuklearchemie), KFA Jülich

**References**

[1] H.J. Probst, R. Weinreich and S.M. Qaim, Annual Report 1976 of IKP, KFA-IKP 1O/77, p. 58
[2] H.J. Probst, S.M. Qaim and R Weinreich, Annual Report 1976 of IKP, KFA-IKP 1O/77, p. 58/59

## 3.2. On the Anomalous Diffusion Behaviour of β-Zirconium

C. Herzig*) and H. Eckseler*)

The anomalous diffusion behaviour of some bcc metals could not be, reliably explained up to now. The most important metals, which belong to this group, are β–Zr, β–Ti, β–Hf and γ–U. The diffusion parameters of these metals, i.e. the prexponential factor and the activation enthalpy, have unusual small values as compared to normal fcc and bcc metals. Furthermore, the Arrhenius plots of their diffusion coefficients are continuously curved in the total temperature range of the bcc phase as far as this can be examined within the limits of accuracy of the diffusion measurements. The common property which probably can explain the peculiar diffusion behaviour of these anomalous bcc metals is the fact, that all of these metals have one or more phase transitions between room temperature and the melting point. The bcc phase is the high temperature phase.

Since there existed no experimental results with additional information about the diffusion mechanism in these metal, we investigated the isotope effect for self-diffusion mechanism. For measuring the isotope effect E the diffusion of two radioisotopes a and b of

the element is examined simultaneously. the corresponding diffusion coefficients $D_a$ and $D_b$ are somewhat different because of the different masses $m_a$ and $m_b$ of the isotopes.

$$B = (D_a/D_b) - 1 \quad / \sqrt{m_b/m_a} - 1$$

Following a diffusion anneal the penetration plots of both isotopes have to be determined with high precision by separating the radioactive radiation of both isotopes.

In our measurements we used $^{95}Zr$ and $^{88}Hr$, which was produced in the isochronous cyclotron of the KFA Jülich by the process $^{89}Y$ (d,3 n) $^{88}Zr$. Allowing for the decay of the coproduced $^{89}Zr$ no radioactive impurity could be detected besides the daughter nuclide $^{88}Y$. For measuring the isotope effect first of all $^{88}Zr$ had to be separated for the Y-target. Then it was necessary to remove the daughter nuclides $^{88}Y$ and $^{95}Nb$ from $^{88}Zr$ and $^{95}Zr$, respectively. This radiochemical separations were performed with assistance of the Institute of Nuclear Chemistry of the KFA.

Results

Diffusion measurements were performed in UHV between 926° C and 1727° C. The results are in very good agreement with data from literature and confirm the anomalous behaviour of self-diffusion in β-Zr. The isotope effect experiments yielded the surprising result of an increase of E with increasing temperature, which was not yet observed in any normal metal investigated so far.

A preliminary interpretation of the results shows that the monodivacancy model or diffusion via grain boundaries or dislocations at low temperatures can be excluded to explain the curvature in the Arrhenius plot of the diffusion coefficients.

*) Institut für Metallforschung der Westfälischen Wilhelms-Universität, 4400 Münster/W.

## 3.3. Investigation on the Diffusion of the Radioactive Isotopes $^{57}Ni$ and $^{64}Cu$ in Copper-Nickel Alloys

Th. Heumann*) and R. Damköhler*)

Within the framework of diffusion studies in the copper-nickel system up to 20 atomic % Ni, the tracer diffusion coefficients at different Ni-concentrations and a temperature of 1273 K were measured with the aid of the isotopes $^{57}Ni$ and $^{64}Cu$ by the standard sectioning technique.

From the results obtained to date the tracer diffusion coefficient of Ni can be given by the following arithmetic expression:

$$D^*_{Ni} = 6.21 \cdot 10^{-10} \exp(-5.84\, N_{Ni})\ [cm^2/s]$$
$N_{Ni}$: 0 to 0.2 atomic fraction Ni, 1273 K

Since the measurements have not been completed small changes can still show up. For the tracer diffusion coefficient of Cu a decrease with increasing Ni-concentration was found, in agreement with data given by other authors.

It is the aim of the investigations to examine theoretical concepts for the diffusion in fcc alloys at extreme dilution[1,2] and also at high concentrations[3], with the aid of the determined tracer diffusion coefficients as well as measurements of the interdiffusion coefficient and intrinsic diffusion coefficients.

*) Institut für Metallforschung der Westfälischen Wilhelms-Universität, 4400 Münster/W.

### References

[1] R.E. Howard and A.B. Lidiard, Reports in Progress in Physics, 27 (1964) 161
[2] J.R. Manning, Phys. Rev., 139 (1965) A 2027
[3] J.R. Manning, Acta Met., 15 (1967) 817

## 3.4. Investigation of Clayey Sediments to Determine their Depositional Environments

K. Brinkmann*), L. Aldea, H. Seyfarth

In contrast of the knowledge of the deposits underlying the Rhenish soft coal there is relatively little known about the environment in which the overburden has been deposited. Generally these overlying strata are considered to be terrestrial (freshwater) sediments. Some sedimentological criterions and results of geochemical analyses of iron sulfides in the overburden showed, however, that it cannot be excluded that these Tertiary layers of upper Miocene (about 12 million years old) and lower Pliocene age were deposited in an environment affected by the sea[1,2]. Subject of the investigations which are made now is to examine whether the above mentioned presumption can be proved. If it is right the consequence would be that the Upper Tertiary shore lines of the „North Sea" would have been located much further southwards than assumed until now.

Concentrations of different elements and ratios of elements in sedimentary rocks have been used to determine the depositional environment of these rocks. Mostly the results were contradictory. Most of the authors agree, however, that higher contents of boron can be an indicator for a sea depositional environment. Boron is mainly bound to clay minerals, especially to illites whereas kaolinites, chlorites, and montmorillonites have up to ten times lower contents. Clayey sediments have the following contents[3]: Saliniferous clays up to 2000 ppm B, marine clays some 100 ppm B, lake clays about 50 ppm B.

In the opencast mine at Frechen (Rhenish soft coal field) in the overburden samples were taken in a profile from the bottom to the

top of the Tertiary layers. The fraction $< 2\,\mu$ which consists predominantly of clay minerals was separated. The mineralogical composition was analysed by X-ray diffraction, the contents of Fe, Co, Ni, and Zn were checked by X-ray fluorescence. Complete chemical analyses are carried out at present.

The thermal neutron-capture reaction $^{10}B(n,\alpha)^{7}Li^{*}$ is very well suited to determine the contents of boron due to the high reaction cross section (20 % natural abundance of $^{10}B$, 3588 b for formation of $^{7}Li$ in the first excited state at 478 keV) contrary to the main elements of the clayey sediments (O, Si, Al, Fe) which do not contribute to the (n,α) reaction. The α spectra have been measured in the target-detector arrangement described in another contribution to this report[4]. To avoid changes in the chemical composition the targets have been prepared as follows:

in the dilution of commercial gelatine in warm water a homogeneous suspension of clay was achieved by ultrasonic treatment. Immediately after homogenization part of the suspension was dropped onto a 2.5 μ Al foil and dried slowly to avoid splintering of the gelatine-clay layer. Details of three targets from different clay samples are given in table 1 together with the boron contents resulting from the recorded α spectra. Absolute values have been determined through a measurement with a pure boron target of known thickness. After these first measurements further investigations have to be performed to check whether the described method of target preparation yields reproduceable results within the given errors.

*) Geologisches Institut der Universität zu Köln

*Table 1:*
*Experimental details and boron content of three clay samples determined through the $^{10}B(n,\alpha)^{7}Li^{*}$ reaction*

| Sample | Target diameter (mm) | Target thickness ($\mu g/cm^2$) clay+gelatine | clay | Measuring time (h) | Boron content[a] (mass ppm) |
|---|---|---|---|---|---|
| 1 | 28 | 121.3 | 79.3 | 6.1 | 351 ± 4 |
| 2 | 27 | 131.9 | 84.4 | 14.6 | 97 ± 3 |
| 3 | 29 | 136.2 | 88.1 | 3.3 | 148 ± 5 |

a) the given errors only include statistical erros in the determination of the α peaks.

## References


[1] K. Brinkmann, Braunkohle 28 (1976) 448
[2] K. Brinkmann, Neues Jahrbuch Mineralogischer Abhandlungen 129 (1977) 333
[3] H. Harder (1960), cited in K. Krejci-Graf, Freiburger Forschungshefte C224 (1966) 1
[4] this report, contribution 2.29, p. 57

# II. Theoretical Nuclear Physics

## 4. Nuclear Structure

### 4.1 Selfconsistent Theories

#### 4.1.1. A Unifying View of Collective Theories

K. Goeke, A.M. Lane*), J. Martorell*))

For the description of nuclear small and large amplitude collective motion there is presently used a multitude of collective theories (cranking, double constraint HF, ATDHF, GCM) together with a multitude of collective paths. In this context the purpose of the present paper[1] is to provide a formalism[2,3] which allows to unify these approaches. To this end a family of particle-hole operators $Q_n$ is constructed from a chosen Q (e.g. multipole op.) by $Q_n = [iH,Q_{n-1}]_{ph}$ where the index ph denotes the projection on the particle-hole subspace with respect to the HF minimum, and $Q_o = Q_{ph}$. The vector $\underline{Q}_n$ of the ph-elements of $Q_n$ is given by $i(A+(-)^{n+1}B)\underline{Q}_n = \underline{Q}_{n-1}$ where A and B are the well known RPA matrices with respect to the HF wavefunction. For the $Q_n$ the energy weighted odd RPA moments $m_k(Q_n) = \Sigma (E_\alpha - E_o)^k |<\alpha|Q_n|O>|^2$, defined in terms of the RPA states $|\alpha>$ and corresponding energies $E_\alpha$, are formally very simple, e.g.

$$m_{2n+1}(Q_m) = \tau^n \tilde{\underline{Q}}_m (A-(-)^m B)(A+(-)^m B)...A+(-)^m B)$$

$$(A-(-)^m B)\underline{Q}_m$$

and can be derived from each other: $m_{2n+1}(Q_m) = m_{2(n-k)+1}(Q_{m+k})$. The $Q_n$ have the remarkable property that if the collective path is constructed by the CHF solution of $H+\lambda_n Q_n$, then the usually used collective paths, e.g. ordinary CHF or scaling, are just special cases referring to a particular n. In the small amplitude limit ($\lambda_n \to O$) the generator $C_n$ of the collective path, defined by $|\lambda_n+\delta\lambda_n> = |\lambda_n> + \delta\lambda_n \Sigma C_n^{ph}|ph>$, is equal to $-iQ_{n-1}$. For small amplitudes ($\lambda_n \to O$) the collective masses from the cranking approach, the double projection method and from ATDHF are all identical and equal to $M_n(\lambda_n) = 2m_{-3}(Q_n) = 2m_{2n-3}(Q_o)$. The resulting harmonic collective energies are of the form $E_n = (m_n/m_{n-2})^{1/2}$ with $n = \pm1,\pm3,...$ Hence even in case of a broad RPA distribution each $E_n$ has a clear physical significance given to it by the RPA moments. On the other hand each odd RPA moment can be reproduced by any of the collective theories. The collective mass resulting from the GCM can be expressed rather simply by RPA although not in terms of moments.

$$M_n^{GCM}(\lambda_n) = 2h^2 \frac{\{\underline{Q}_n (A+B)^{-2} \underline{Q}\}^2}{\tilde{\underline{Q}}_n (A+B)^{-1}(A+B)(A+B)^{-1}\underline{Q}_n} < 2h^2 m_{2n-3}(Q_o)$$

For n=O a generalization to large amplitudes is possible. One obtains identical expressions for the RPA moments, taken locally. The collective masses are no more expressible in terms of these moments, but one obtains

$$M_o(\lambda_o) = 2h^2\, \underline{Q}_o (A+\lambda_o Q_o+B)^{-1}(A-B)\,(A+\lambda_o Q_o+B)^{-1}\,\underline{Q}_o$$

where all quantities are defined with respect to the CHF solution of $H' = H-\lambda_o Q_o$ assuming $Q_o$ to have only ph elements.

*) Theoret. Physics Div., AERE Harwell, England
**) Department of Physics, University of Madrid, Spain

**References**

[1] K. Goeke, A.M. Lane and J. Martorell, to be published
[2] O. Bohigas, J. Martorell and A.M. Lane, Phys. Lett. 64B (1976) 1
[3] K. Goeke, Nucl.Phys. A265 (1976) 301

#### 4.1.2. Time Dependent Hartree-Fock and Classical Motion

K. Goeke and P.G. Reinhard*)

The purpose of this note[1] is to show that the time dependent Hartree-Fock equation (TDHF) is equivalent to a set of classical canonical equations. To this end we introduce a certain appropriate representation of the Slater determinants met during the time evalution: We define coordinate like operators $Q_\alpha$ and momentum like operators $P_\alpha$ with respect to $\Psi(t)$ by

$$Q_\alpha = \frac{1}{\sqrt{2\lambda_o}} (b_\alpha^+ + b_\alpha) \quad P_\alpha = i\sqrt{\lambda\alpha/2}\,(b_\alpha^+ - b_\alpha) \qquad (1)$$

with $b_\alpha^+ = a_p^+ a_h$. The $\lambda_\alpha$ are arbitrary such can be chosen at convenience. Any p-h operator can be represented as

$$A = i \sum_\alpha Q_\alpha <[P_\alpha,A]> - i \sum_\alpha P_\alpha <[Q_\alpha,A]> \qquad (2)$$

The Thouless theorem suggests to label each Slater determinant by coordinats $q_\alpha$, $p_\alpha$, $=1,2...$ such that $Q_\alpha$ and $P_\alpha$ enter as infinitesimal generators:

$$|\underset{\sim}{q} + \delta\underset{\sim}{q}, \underset{\sim}{p} + \delta\underset{\sim}{p}> = (1 + i \sum_\alpha \delta p_\alpha Q_\alpha - i \sum_\alpha \delta q_\alpha P_\alpha)\,|\underset{\sim}{q}, \underset{\sim}{p}> \qquad (3)$$

or equivalently

$$Q_\alpha \mid \underset{\sim}{q}\,\underset{\sim}{p}> = -i\,\partial_{p_\alpha} \mid \underset{\sim}{q}\,\underset{\sim}{p}>,\quad P_\alpha \mid \underset{\sim}{q}\,\underset{\sim}{p}> = i\,\partial_{q_\alpha} \mid \underset{\sim}{q}\,\underset{\sim}{p}>. \qquad (4)$$

One is tempted to map out the space of Slater determinants by means of the Thoules representation with respect to one given determinant. However this is not very satisfying since the $Q_\alpha$, $P_\alpha$ are no larger infinitesimal generators at large amplitudes, and then the equations of motion will have no canonical form. This is not the case in the present formalism: The TDHF equation[2] is the projection of the time dependent Schrödinger equation $(H-i\partial_t)/\Psi = 0$ into the p-h subspace. According to (2) this is equivalently

$$<\Psi \mid [Q_\alpha, H-i\partial_t] \mid \Psi> = <\Psi\,[P_\alpha, H-i\partial_t] \mid \Psi> = 0 \qquad (5)$$

Since $i\partial_t \mid \Psi> = i\partial_t \mid \underset{\sim}{q}\,\underset{\sim}{p}> = \sum_\beta (\dot{q}_\beta P_\beta - \dot{p}_\beta Q_\beta) \mid q\,p>$

and since $<[Q_\alpha, Q_\beta]> = <[P_\alpha, P_\beta]> = 0$

and $<[Q_\alpha, P_\beta]> = i\delta_{\alpha\beta}$

one obtains with $<\underset{\sim}{q}\,\underset{\sim}{p} \mid H \mid \underset{\sim}{q}\,\underset{\sim}{p}> = H(\underset{\sim}{q}\,\underset{\sim}{p})$

and

$$<\underset{\sim}{q}+\delta\underset{\sim}{q}, \underset{\sim}{p}+\delta\underset{\sim}{p} \mid H \mid \underset{\sim}{q}+\delta\underset{\sim}{q}, \underset{\sim}{p}+d\underset{\sim}{p}> = H(\underset{\sim}{q},\underset{\sim}{p}) + \sum_\alpha Q_\alpha \partial_{q_\alpha} H + \sum_\alpha P_\alpha \partial_{p_\alpha}$$

the final form of the TDHF equations

$$\dot{p}_\alpha = -\partial_{q_\alpha} H \quad \dot{q}_\alpha = \partial_{p_\alpha} H$$

These are obviously classical Hamiltonian equations with the canonical coordinates $q_\alpha$ and $p_\alpha$.

*) Institut für Kernphysik, Universität Mainz

**References**

[1] P.G. Reinhard and K. Goeke, to be published
[2] K. Goeke and P.G. Reinhard, Annals of Physics (1978), to be published

## 4.1.3. Theory for Initial Conditions in Time Dependent Hartree-Fock

K. Goeke

In recent years it has become possible to perform numerical time dependent Hartree-Fock (TDHF) calculations. Those calculations provide the nuclear many body wave function $\varnothing(t)$, assumed to be a Slater determinant, for all times t, if one assumes $\varnothing(t)$ at a certain time $t_o$ (initial condition). Usually $\varnothing(t)$ is noticeably dependent on the initial condition. The question arises, how one has to chose $\varnothing(t_o)$ in order to ensure that $\varnothing(t)$ describes a certain desired collective motion. The answer to such a question may help to find the proper initial conditions in order to describe e.g. fission, soft vibrations, etc. Those processes are often well characterized by one or several collection parameters, q(t), and there are many attempts to describe the dynamics of the motion by means of a collective Hamiltonian, i.e. a Schrödinger equation in terms of q. Such a description is only justified if during the process collective and intrinsic motion are well decoupled, or, if the intrinsic motion adjusts to the collective one. Obviously not any TDHF trajectory fulfils this condition. A sufficient condition could be, that the time even part of the trajectory does not change, if the system moves with different velocity, $\dot{q}$. This means that $\dot{q}(t)$ should be treated as a free parameter, which is only subjectedto the condition that it is small, since usually collective motion is only well established for slow motion. Hence one has to formulated an adiabatic perturbation expansion[1] for the TDHF equation in terms of $\dot{q}$ and must treat the various orders in $\dot{q}$ separately. Writing for the single particle density matrix $\rho(t) \simeq \rho_o(q) + \dot{q}\bar{\rho}_1(q)$ one obtains the following equations:

$$i\frac{\partial \rho_o}{\partial q} = [W_o, \bar{\rho}_1] + [\bar{W}_1, \rho_o]$$

$$[W_o - \frac{\partial V}{\partial q}\,Q, \rho_o] = 0 \qquad V(q) = \mathrm{Tr}\,T\rho_o + \frac{1}{2}\,\mathrm{Tr}\,\mathrm{Tr}\,\rho_o v \rho_o$$

$$Q = \frac{i}{M(q)}\,[\rho_o, \bar{\rho}_1] \qquad M(q) = i\,\mathrm{Tr}\left\{[\rho_o, \bar{\rho}_1]\,\frac{\partial \rho_o}{\partial q}\right\}$$

These equations determine simultaniously the collective mass M(q), the collective potential V(q), the constraining operator in CHF, i.e. Q(q), and most important $\rho_o(q)$ and $\bar{\rho}_1(q)$. This solution can be used for two purposes: First, one can set up a classical Hamiltonian, from which by proper quantization a Schrödinger equation can be extracted[1]. Second and for the problem more important: Suppose one choses proper values of q and $\dot{q}$ and constructs the density matrix $\rho(t_o) = \rho_o(q) + \dot{q}\,\bar{\rho}_1(q)$. This one can be used as initial condition at $t \geq t_o$ for TDHF. The resulting, trajectory has then the property, that its time even part equals $\rho_o(q(t))$ and the time odd part equals $\rho_1(q(t))$. Obviously by construction $\rho_o(q)$ is independent on $\dot{q}$ and therefore to a large extend intrinsic and collective motion are decoupled. Hence one has derived an initial condition which leads to the desired collective motion.

**References**

[1] K. Goeke and P.G. Reinhard, Annals of Physics (1978), to be published

## 4.1.4. Reality Conditions of Classical Motions Along Collective Paths

K. Goeke and P.G. Reinhard

Microscopic theories of collective motion usually employ classical concepts. Using a deformation path $|q>$, one has already put in a classical imagination. In particular, the group of theories based on time dependent Hartree-Fock (TDHF), which embraces e.g. adiabatic TDHF (ATDHF), local harmonic approach (LHA) and cranking, makes extensive use of a classical Hamiltonian function and the classical motion along the collective path. It is not guaranteed, however, that this motion will take place along real values for the collective parameters. In this paper we focus our attention on the collective paths which are given by constraint Hartree-Fock (CHF). Thereby we confine the considerations to the case of one collective degree of freedom, described with a two parameter basis $|q,p>$, where q corresponds to a static deformation and p represents the momentum.

The „classical" description of collective motion is introduced by considering an explicitly timedependent state vector $|\psi(t)>$, which is restricted to follow the collective path. That means, the time evolution of $|\psi>$ is determined exclusively by the time evolution of the collective parameters q and p,

$$|\psi(t)> = N(t)e^{i\Phi(t)}\,|q(t),p(t)> \qquad (1)$$

where, N and $\Phi$ are real parameters which serve to guarantee norm conservation and the right phase oscillations. The EoM for q and p are determined by the least action principle,

$$\delta \int_{t_1}^{t_2} dt\ <\psi(t)|\,\hat{H}-i\partial_t\,|\psi(t)> = 0. \qquad (2)$$

Explicit evaluation of (2) and splitting q and p into real and imaginary components gives

$$\begin{aligned}
\dot{q}_r &= \Delta^{-1}\,[i<[Q,H]>-<\{Q,H\}><\{Q,P\}>+2<Q^2><\{P,H\}>]\\
\dot{p}_r &= \Delta^{-1}\,[i<[P,H]>+<\{P,H\}><\{Q,P\}>-2<P^2><\{Q,H\}>]\\
\dot{q}_i &= \Delta^{-1}\,[2i<P^2><[Q,H]>-i<[P,H]><\{Q,P\}>+<\{P,H\}>]\\
\dot{p}_i &= \Delta^{-1}\,[2i<Q^2><[P,H]>-i<[Q,H]><\{Q,P\}>-<\{Q,H\}>]\\
\Delta &= 4<P^2><Q^2>-<\{Q,P\}>^2-1.
\end{aligned} \qquad (3)$$

There we have introduced $P|q,p> = i\partial_p|q,p>$ and $Q|q,p> = -i\partial_p|q,p>$ in view of the application to CHF, ATDHF and LHA.

In general, these EoM allow the system to move in the whole complex planes for q and p. The system might try to gain better dynamics by driving out to imaginary paths, if the basis is not properly optimized. In the reverse, a reasonable basis should yield a motion which evolves along a real path by its own dynamics, without imposing further constraints. That means, the EoM should predict no deviation to imaginary parts, if the initial conditions are on the real path, i.e.

$$\dot{q}_i = 0,\ \dot{p}_i = 0 \quad \text{if} \quad q_i = 0,\ p_i = 0. \qquad (4)$$

We call this the reality condition.

In CHF the collective path is determined by employing the microscopic Hamiltonian H and two constraints, Q for fixing the deformation and P for the momentum. From the Ritz variational principle one obtains the CHF equations

$$<q,p|\,[A_{ph},H-xQ-yP]\,|q,p> = 0 \qquad (5)$$

where $A_{ph}$ can be any 1p-1h operator about $|q,p>$ and x and y are chosen to give the desired deformation and momentum.

Before studying in detail the reality condition for CHF paths, we shortly want to expose the 1p-1h algebra as it simplifies the subsequent considerations. Every Slater determinant defines an algebra of 1p-1h excitations which serves as an expansion basis for small amplitude motion about just this Slater determinant. It is advantageous to couple the elementary 1p-1h excitations $a_n^+a_i$ to coordinate and momentum like operators $Q_\alpha = (a_n^+a_i + a_i^+a_n)/\sqrt{2\lambda}$ and $P_\alpha = (a_n^+a_i - a_i^+a_n)i\sqrt{\lambda/2}$, where the label $\alpha$ combines here n and i and the width $\lambda$ is chosen at convenience. This basis $Q_\alpha$, $P_\alpha$ can even be thought more general, e.g. as a result of an orthogonal transformation with in the states $\alpha$. For convenience, we assume in the following a labeling in which $\alpha = 0$ describes the collective channel, $Q_o = Q$ and $P_o = P$. The Q and P set up an orthogonal,

$$<[Q_\alpha,P_\beta]> = \delta_{\alpha\beta},\ <[Q_\alpha,Q_\beta]> = <[P_\alpha,P_\beta]> = 0 \qquad (6)$$

and complete

$$A_{ph} = i\sum_\alpha Q_\alpha\ <[P_\alpha,A_{ph}]> - i\sum_\alpha P_\alpha\ <[Q_\alpha,A_{ph}]> \qquad (7)$$

system of 1p-1h excitations. Thus in eq. (5) the $A_{ph}$ can be replaced by any $Q_\alpha$ and $P_\alpha$. With eq. (7) a formulations equivalent ot CHF is found to be

$$<q,p|\,[Q_\alpha,H]\,|q,p> = 0, <q,p|[P_\alpha,H]\,|q,p> = 0 \text{ for } \alpha \neq 0. \qquad (5b)$$

Although $Q_\alpha$ and $P_\alpha$ provide a complete and orthonormal set of 1p-1h operators, they only produce a redundant set of state vectors if they act on $|q,p>$. That means, every vector $Q_\alpha|q,p>$ can be expanded into $\sum_\beta c_{\alpha\beta}P_\beta\,|q,p>$ and reversely. In particular, we can represent the collective operators (i.e. the CHF constraints) as

$$\begin{aligned}
P\,|q,p> &= i\sum\lambda_\alpha Q_\alpha\,|q,p>,\ Q\,|q,p>\\
&= -i\sum 1/\mu_\alpha P_\alpha\,|q,p>
\end{aligned} \qquad (8)$$

where especially $\lambda_o = 2<P^2>.\ 1/\mu_o = 2<Q^2>$. Using this representation, we can transform the anticommutators in eq. (4) into commutators, e.g. $<\{P,H\}> = i2<P^2><|Q,H|>$. Together with the CHF eq. (6b) we obtain

$$\begin{aligned}
&<P,H> = -2i<P^2><[Q,H]>,\ <Q,H>\\
&= 2i<Q^2><[P,H]>
\end{aligned} \qquad (9)$$

$$\text{and} \quad <\{P,Q\}> = 0.$$

Inserting this into eq. (4) clearly shows, that the reality condition is fulfilled for CHF paths.

### References

[1] P.G. Reinhard and K. Goeke, Phys. Rev. ( (1978) to be published

## 4.1.5. The Influence of a Self-Consistent Model Space on the Folded Diagram Expansion of Nuclear Effective Interactions

J. Shurpin*), H. Müther, T.T.S. Kuo*), A. Faessler

Intensive studies have been performed to derive the effective NN interaction $V_{eff}$, which should be used in a shell-model calculation, from the free NN interaction[1,2] in a perturbation expansion. The investigation of Schucan and Weidenmüller[3] cast some doubt on the convergence of this expansion. Leinaas and Kuo[4] have shown that an improvement of the convergence may be achieved using a Hartree-Fock (HF) single-particle basis for the model space. With this choice a part of the NN force is put into the self-consistent field, which weakens the residual interaction. It is the aim of the present work to investigate this influence of the self-consistent choice of the model space on the convergence property of the expansion of $V_{eff}$ in a realistic calculation.

For the calculation of $V_{eff}$ the Folded Diagram (FD) technique of Kuo, Lee and Ratcliff[5] is used. For the Q-box, containing all diagrams without folds, we take into account the diagrams displayed in figure 1. In this figure the wiggly lines stand for the G matrix calculated in the numerical example for the Reid soft core interaction. The effective interaction $V_{eff}$ is then defined to be the two-body part of these diagrams plus all the folded diagrams built with these Q-box diagrams. This calculation of $V_{eff}$ has been done assuming for the single-particle states oscillator wavefunctions or self-consistent Brueckner HF, Renormalized Brueckner HF or Density dependent HF wavefunctions[6]. To make a comparison of the results obtained in the oscillator basis and in a self-consistent basis meaningfull, the oscillator length has been chosen such that the overlap of the self-consistent hole state wavefunctions and the corresponding oscillator wavefunctions is as large as possible. With this choice the oscillator potential localizes the particle states at smaller radii than the self-consistent potential. This yields larger average distances for two particles in the self-consistent particle states than for the oscillator basis. Since the NN interaction is of short range this means smaller values for the G matrix elements in the diagrams of figure 1. This can be seen from a comparison of the typical values for

$$W = \sum_{J,T} \langle d_{5/2}, d_{5/2} | W | d_{5/2}\, d_{5/2} \rangle_{JT}$$

for the different diagrams in the oscillator basis and the Brueckner HF basis in table 1. In this table $F_i$ stands for the contribution to $V_{eff}$ from all diagrams with i folds. It can be seen that the contribution from the different core-polarization diagrams is reduced in the self-consistent basis. In addition the contribution from the folded Diagrams is reduced. All these results indicate a better convergence in the self-consistent basis. Similar results are also obtained for the other self-consistent choices (RBHF, DHF).

Shell-model calculations for the mass 18, 19 and 20 systems yield spectra which are too compressed and which have too little groundstate binding energy relative to $^{16}O$ if one uses the HF model space. The good agreement found in the past as well as here using the oscillator basis therefore seems to be somewhat fortuitos. One should not expect to get enough binding energy in a shell-model calculation relative to $^{16}O$ if for the same NN force $^{16}O$ itself is underbound by 4 MeV per nucleon.

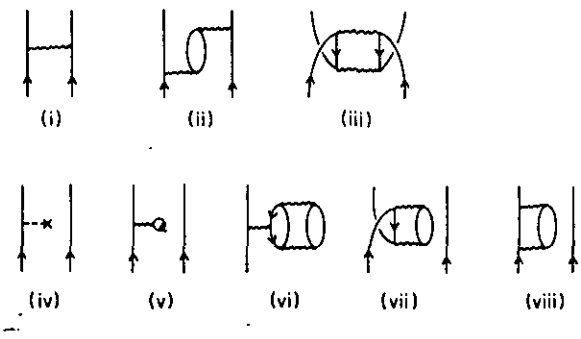


*Figure 1:*
*Diagrams included in Q-box.*

*Table 1:*
*Average Matrix Elements*

| | Osc. | BHF |
|---|---|---|
| Fig. 1 i) | -81.53 | -74.33 |
| Fig. 1 ii) | 8.79 | 2.59 |
| Fig. 1 iii) | - 1.95 | - 1.68 |
| $F_0$ | -74.69 | -73.42 |
| $F_1$ | 10.77 | 7.07 |
| $F_2$ | 0.13 | - 0.86 |
| $F_3$ | 0.76 | 0.08 |
| $F_4$ | 0.25 | 0.08 |

*) SUNY at Stony Brook, New York, USA

### References

[1] T.T.S. Kuo, Ann. Rev. Nucl. Sci. 24 (1974) 101
[2] B.R. Barrett and M.W. Kirson, Advances in Nuclear Physics, ed. E. Vogt, M. Baranger, Vol. 6 (Plenum Press, N.Y. 1972)
[3] T.H. Schucan and H.A. Weidenmüller, Ann. of Phys. 73 (1972)108
[4] J.M. Leinaas and T.T.S. Kuo, Phys. Lett. 62B (1976) 275
[5] R.K. Tripathi, A. Faessler and H. Müther, Phys. Rev. C10 (1974) 2080

## 4.1.6. Variational Definition of the Single-Particle Potential in the Brueckner-Hartree-Fock Approach

A. Faessler, T.T.S. Kuo*), H. Müther

The choice of the optimal single-particle potential, to be used in a Brueckner calculation of finite nuclei, has often been discussed in the literature[1-4]. It is the aim to choose the single-particle potential such, that one minimizes the effects of higher order terms in the Brueckner perturbation expansion, which cannot be taken into account explicitly. If correlations between particles can be neglected, the variational definition of the single-particle potential is justified by the Rayleigh-Ritz variational principle and leads to the Hartree-Fock approach. In the Brueckner expansion two-particle correlations are considered already in lowest order by using the solution of the Bethe-Goldstone equation

$$G(W) = V + V \frac{Q}{W - H_o} G \qquad (1)$$

as an effective interaction. Since this effective interaction G depends on the single-particle states, via the Pauli operator ($Q = (1-\rho)(1-\rho)$) and the starting energy ($W = \varepsilon_1 + \varepsilon_2$), a variational definition yields more terms, the so called rearrangement terms, for the single-particle Hamiltonian

$$h_{\alpha\beta} = \frac{\partial E(\rho)}{\partial \rho_{\alpha\beta}} = \langle \alpha | t | \beta \rangle + \sum_j \langle \alpha j | G | \beta j \rangle \rho_j - \sum_{ijk} \langle ij | G | k\beta \rangle \times$$

$$\frac{(1-\rho_k)}{\epsilon_i + \epsilon_j - H_o} \langle k\alpha | G | ij \rangle \rho_i \rho_j + \sum_{ij} \langle ij | \frac{\partial G}{\partial W} | ij \rangle \frac{\partial \epsilon_i}{\partial \rho_{\alpha\beta}} \rho_i \rho_j \qquad (2)$$

Since the $\varepsilon_i$ are the diagonal elements of h in the self-consistent basis, the derivative $\partial\varepsilon_i/\partial\rho_{\alpha\beta}$ in the last term of eq (2) leads to an infinite set of terms. If one neglects second derivatives $\partial^2\varepsilon/\partial^2\rho$, the $\partial\varepsilon/\partial\rho$ are obtained as a solution of an inhomogeneous system of linear equations. In figure 1 we display the Brueckner-Goldstone diagrams of the usual Brueckner-Hartree-Fock (BHF) terms (1a), of the Pauli rearrangement term (1b) and of a few lowest order starting energy rearrangement terms. The terms represented by figures 1a, c, d, e are considered by Brandows self-consistent occupation probabilities in a Renormalized BHF calculation. From the diagrammatic representation one can see that the variational definition of the single-particle potential leads to overcounting terms. For example the diagrams 1g and 1h contain insertions of the form displayed in fig. 1c and should therefore not be considered. In a numerical calculation for $^{16}O$ it turns out, however, that the effects of these terms are small. Results for the binding energy and radius of $^{16}O$ using diagrams of figure 1 in the definition of the single-particle potential, as indicated in the first row, are given in table 1. For the nucleon-nucleon interaction V the Reid soft-core potential has been used. One can see that the sum of all terms in addition to RBHF yields small effects only. This is due to a large cancellation of the contributions of different terms.

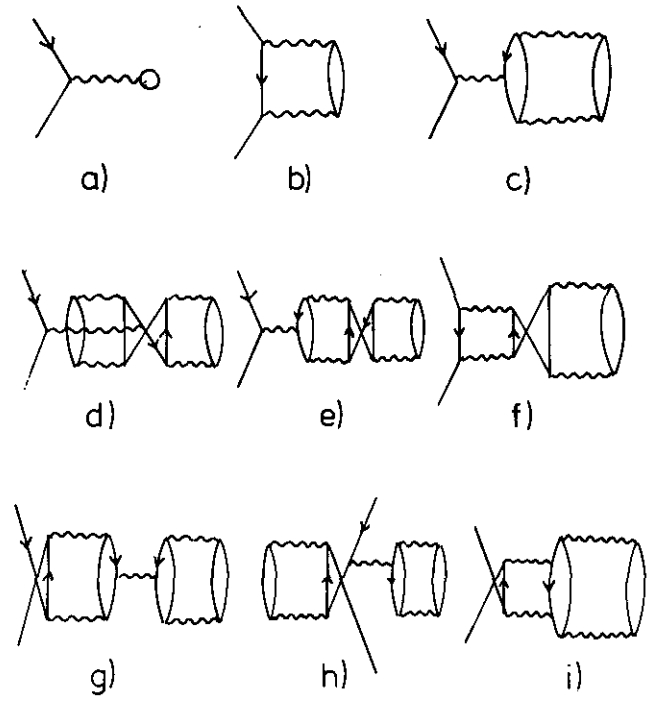


*Figure 1:*
*Graphical representation of the single-particle potential.*

*Table 1:*
*Results for $^{16}O$ using different single-particle potentials*

| considered diagrams | a) | a,c,d,e) | a) - i) |
|---|---|---|---|
| E/A [MeV] | -3.76 | -4.12 | -4.05 |
| $R_{ch}$ [fm] | 2.45 | 2.55 | 2.50 |

*) Department of Physics, State University of New York at Stony Brook, USA

### References

[1] H.S. Köhler, Phys. Rep. 18C (1975) 217
[2] M.W. Kirson, Nucl. Phys. A115 (1968) 49
[3] B.H. Brandow, Ann. Phys. 57 (1970) 214
[4] L. Schäfer and H.A. Weidenmüller, Nucl. Phys. A215 (1973) 493

## 4.1.7. Coulomb Energy Differences of Mirror Nuclei

R. DiStefano*), T.T.S. Kuo*), H. Müther, A. Faessler

Calculations of Coulomb energy differences of mirror nuclei usually gave values about 10 % smaller than the experimental values[1]. This failure may be due to one or both of the following two reasons. (a) The nuclear wave functions and the many-body approximations used in the calculation are not accurate enough. (b) The nucleon-nucleon (N-N) interaction employed may have some defects. For many cases, these two reasons are in fact related to each other. If one considers (b) to be the more likely reason, then one will have to modify the N-N interaction. Several authors[2,3] in fact suggested some charge symmetry breaking interactions in order to obtain correct Coulomb energy differences. We feel that there is need to investigate (a) more carefully. For example, in a recent calculation[4] only few low-order diagrams were included and some important core polarization diagrams were apparently ignored. Furthermore, no folded diagrams were included.

Using Brueckner-Hartree-Fock self-consistent wave functions, we are calculating the $^{17}F - {}^{17}O$ Coulomb energy differences using a fold-diagram theory for effective operators[5]. We use the Reid N-N potential.

Terms with one to four folds are included, as illustrated by diagram (a). Note that each terms has only one Coulomb vertex (denoted by - - - - - ), and it can be in any of the Q-boxes. For each Q-box, we include terms through second order in G-matrix (denoted by ∿∿∿∿). Because the long range nature of the Coulomb interaction, diagram (b) appears to be the dominant core-polarization diagram. This diagram was apparently not included in earlier calculations. Since the n-p interaction is generally stronger than the p-p interaction, this diagram will enhance the calculated Coulomb energy difference. The derivative method[6], with minor modifications, will be used to calculate the folded terms.

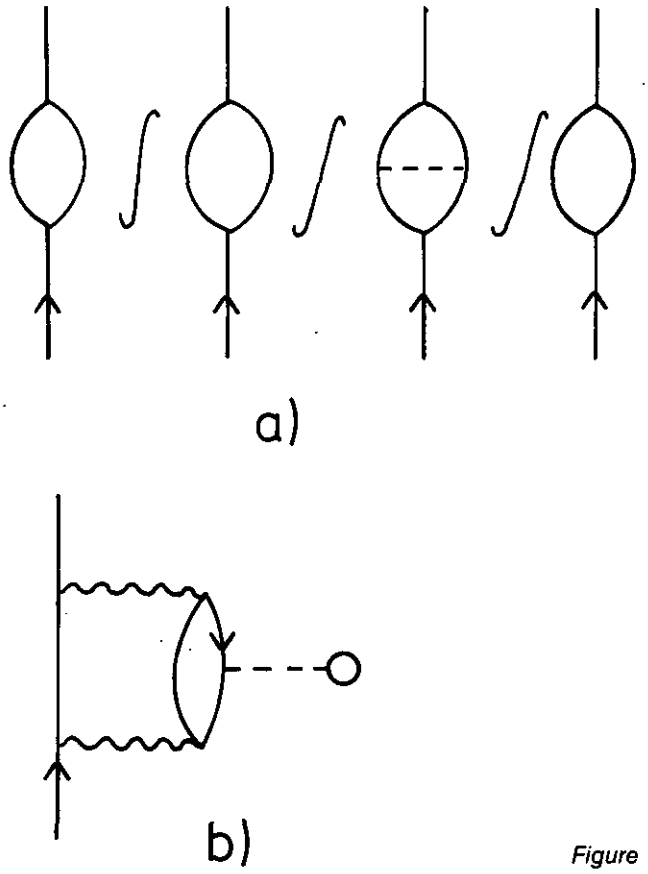


*Figure 1*

*) Department of Physics, SUNY at Stony Brook, USA

### References

[1] J.A. Nolen, Jr. and J.P. Schiffer, Ann. Rev. Nucl. Sci. 19 (1969) 527
[2] J.W. Negele, Nucl. Phys. A165 (1971) 305
[3] H. Sato, Nucl. Phys. A269 (1976) 378
[4] A. Barroso, Nucl. Phys. A281 (1977) 267
[5] E.M. Krenciglowa and T.T.S. Kuo, Nucl. Phys. A240 (1975) 195
[6] 6) J. Shurpin, D. Strottman, T.T.S. Kuo, M. Conze and P. Manakos, Phys. Lett. 69B (1977) 395

## 4.1.8. Third-Order Q-Box Diagrams

J. Shurpin*), R. DiStefano*), T.T.S. Kuo*), H. Müther, A. Faessler

In the so-called Q-box effective interaction theory, diagrams are grouped according to number of folds. For example, all diagrams with three folds are grouped together, denoted as $\hat{Q}\int\hat{Q}\int\hat{Q}\int\hat{Q}$ where $\hat{Q}$ represents a $\hat{Q}$-box and the symbol $\int$ represents a generalized folding. In an sd shell calculation using the Reid potential, Shurpin et al.[1] found that the folded-diagram effective interaction series appears to converge very rapidly; terms with more than four folds can be safely ignored. This calculation involves no

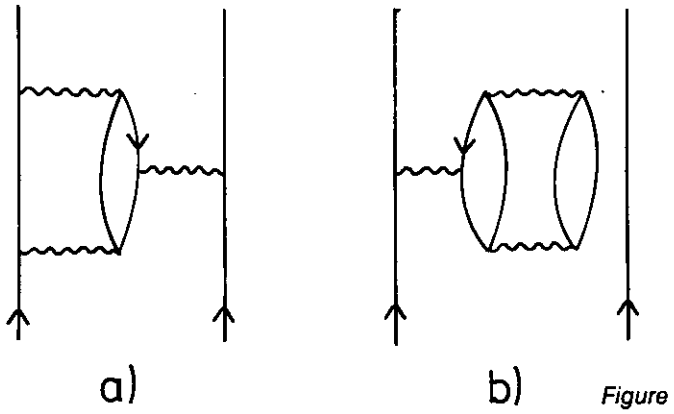


*Figure 1*

serious approximations except for the truncation of the $\hat{Q}$-box after second order in interaction (G-matrix). How reliable is this truncation? To answer this question, we are extending the above calculation to include all the Q-box diagrams third order in G such as those shown in the figure. Note that (b) is a one-body $\hat{Q}$-box diagram, but it can be a part of a two-body diagram when folded with a two-body $\hat{Q}$-box diagram such as (a)-fold-(b). There is a rather large number of such diagrams[2]. We are calculating these diagrams using an essentially exact G-matrix, with off-shell effects included. $\hat{Q}$-box diagrams using oscillator wave functions and those using BHF wave functions[3] will both be considered. It will be of interest to examine the effect of the third-order $\hat{Q}$-box diagrams on the energy derivatives $d^n\hat{Q}/d\omega^n$, since the convergence of the folded-diagram series is directly related to these derivatives.

*) Department of Physics, SUNY at Stony Brook, USA

### References


[1] J. Shurpin, D. Strottman, T.T.S. Kuo, M. Conze and P. Manakos, Phys. Lett. 69B (1977) 395
[2] B.R. Barrett and M.W. Kirson, Nucl. Phys. A148 (1970) 145
[3] J. Shurpin, H. Müther, T.T.S. Kuo and A. Faessler, see p. 66 of this progress report


## 4.1.9. The Landau-Recipe for the Particle-Hole Interaction and the Random Phase Approximation


A. Faessler, H. Müther


In the framework of Landau theory[1,2] one considers an energy functional $E(\rho)$ depending on the single particle density $\rho$. The first derivative of this energy functional $\partial E/\partial\rho$ defines a self-consistent single particle field and the residual particle-hole interaction is obtained from the second derivative. It is the aim of the present note to study this Landau recipe if the energy functional $E(\rho)$ is approximated by that obtained in Brueckner theory in a certain order[2,3]. For that reason we translate the formal derivatives $\partial/\partial\rho$ into the language of Goldstone diagrams. In this framework applying the derivative to the energy contribution from a certain diagram means that one considers all the diagrams which are obtained by cutting one internal particle or hole line. Depending, if one considers a derivative with respect to a particle hole (ph) or a hp matrixelement of the density matrix, the two parts of this cutted line are turned into 2 external lines as it is indicated in figure 1. For the second derivative the procedure has to be repeated. To study the irreducibility of the resulting terms of the particle-hole interaction, it is sufficient to analyse diagrams consisting of two parts which are linked by 2 particle and 2 hole lines like e.g. the left diagram in figure 2. Diagrams,

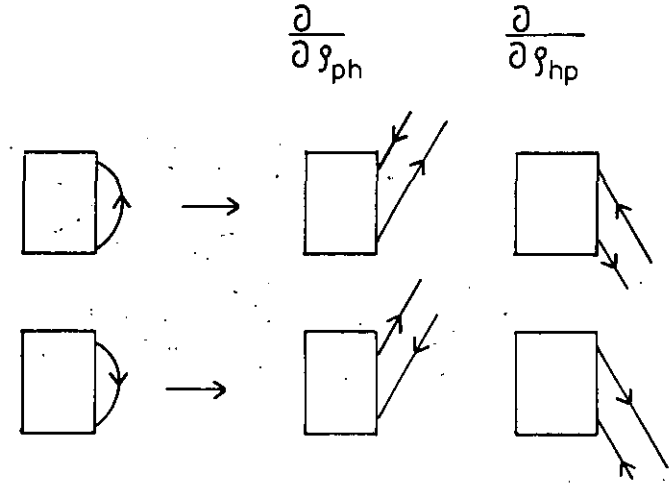


*Figure 1*

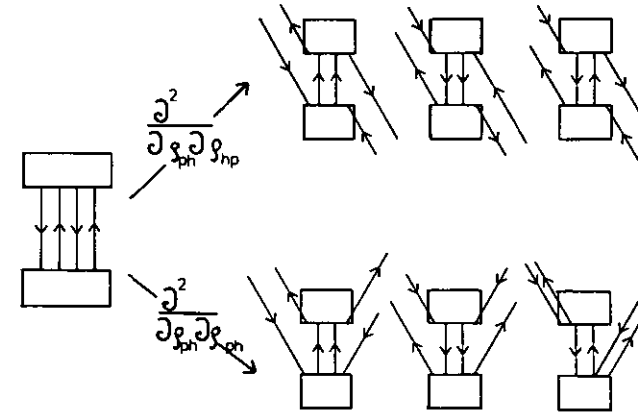


*Figure 2*

*which are linked by 1 particle and 1 hole line only, do not occur in* the Brueckner expansion for the energy, because they are canceled by corresponding diagrams with single particle field insertions, if the single particle field is defined by $\partial E/\partial\rho$. The matrixelements of the particle-hole interaction which are used in the Tamm Dancoff Approximation (TDA) are obtained from $\partial^2 E/\partial\rho_{ph\ hp}$. Therefore, if one considers in the graphical representation only the application of the derivatives to the lines drawn explicitly in figure 2, one takes into account for the residual interaction of TDA the irreducible diagrams in the first row of figure 2. In the Random Phase Approximation (RPA) also the matrixelements obtained by $\partial^2 E/\partial\rho_{ph}\,\partial\rho_{ph}$ are used. They are displayed in the second row of figure 2, and one can see that also diagrams wich are reducible with respect to RPA are obtained (like e.g. the last one in figure 2). The arguments can easily be extended to other diagrams than those displayed in figure 2. Therefore we conclude that the application of the Landau recipe for the derivation of the ph interaction in TDA yields irreducible diagrams only. In RPA, however, one also obtains reducible diagrams which lead to an overcounting. Numerically this overcouting seems to be small but not negligible. For the RPA energy of the lowest $3^-$ in $^{16}O$, for example[3], it turned out to be about 0.3 MeV.

### References


[1] L.D. Landau, Sov. Phys. JETP 8 (1959) 70.
[2] G.E. Brown, Rev. Mod. Phys. 43 (1971) 1
[3] H. Müther, Y.R. Waghmare, A. Faessler, Phys. Lett. 64B (1976) 125

## 4.2 Theories Including Residual Interactions

### 4.2.1. On an Overlooked Term in Two-Particle Matrix Elements of the Tensor Force

V. Klemt

The use of realistic forces, especially the tensor force, in nuclear structure calculations of heavy nuclei has been frequently limited by computational capacities. Whereas this seems to be true up to now in the general case, at least two treatments of special cases should be numerically tractable.

The method of Horie and Sasaki[1] exploits the special properties of harmonic-oscillator wave functions to get fairly simple expressions for two-particle matrix elements of realistic forces with arbitrary radial dependence. Whereas this method can be extended to more general bound-state wave functions (which can be expanded into harmonic oscillators) scattering wave functions cannot be handled in this way.

The method of Buttle and Goldfarb[2] is complementary to the above one insofar as it makes use of the special radial dependence of the Yukawa and tensor force, the latter having the form of a spherical Hankel function with imaginary argument

$$V_T(r) = h_2^{(1)}(i\mu r),$$

where $\mu$ is the pion mass,

whereas the radial form of the wave function is arbitray and may well be of scattering type.

It turned out that actual calculations with the second method[3] ran into difficulties unless the tensor force had been „regularized":

$$V_T^{reg}(r) = h_2^{(1)}(i\mu r) - (\tfrac{\nu}{\mu})^3 h_2^{(1)}(i\nu r) \text{ with } \nu > \mu .$$

In the following it will be shown that the reason for these difficulties is a term of the same order of magnitude as the others which has been overlooked by Buttle and Goldfarb in their formula.

The tensor force can be represented as follows:

$$V_T(r)\, S_{12} = \sqrt{\tfrac{8\pi}{15}}\,[\sigma\times\sigma']^{(2)} \cdot h_2^{(1)}(i\mu r)\, \hat{Y}^{(2)}(\Omega)\,, \qquad (1)$$

where $\hat{Y}^{(2)}$ is a tensor of rank two, the components of which are the spherical harmonics $Y_{2m}(\Omega)$. Both methods use the following identity (in obvious notation):

$$h_2^{(1)}(i\mu r)\, Y_{2m}(\Omega) = -\frac{8}{\mu^3\sqrt{5}} \sum_{k_1 k_2} (-1)^{k_2}\, i^{k_1-k_2} \langle k_1 \| Y^{(2)} \| k_2 \rangle \qquad (2)$$

$$[Y^{(k_1)}(\Omega_1) \times Y^{(k_2)}(\Omega_2)]^{(2)}_m \int_0^\infty j_{k_1}(pr_1) j_{k_2}(pr_2)\, \frac{p^4}{p^2+\mu^2}\, dp$$

Now Buttle and Goldfarb give a formula which they obtained by contour integration:

$$\int_0^\infty j_{k_1}(pr_1) j_{k_2}(pr_2)\, \frac{p^4}{p^2+\mu^2}\, dp = \begin{cases} \frac{\pi}{2}\mu^3 h_{k_1}^{(1)}(i\mu r_1)\, j_{k_2}(i\mu r_2) \text{ for } r_1 > r_2 \\ \frac{\pi}{2}\mu^3 j_{k_1}(i\mu r_1)\, h_{k_2}^{(1)}(i\mu r_2) \text{ for } r_1 < r_2 \end{cases} \qquad (3)$$

It is true that this formula is correct as it stands, but it turns out that for $r_1 = r_2$ the integral does not exist, since its semicircle contribution in the complex p-plane is proportioanl to its radius. Since the divergence is limited to one point, it is obvious that it must be of $\delta$-function type. A short calculation gives the result that on the right hand side of eq. (3) one has to add the term

$$i^{k_1-k_2}\, \frac{\pi}{2}\, \frac{\delta(r_1-r_2)}{r_1 r_2} .$$

#### References


[1] H. Horie, K. Sasaki, Prog. Theor. Phys. 25 (1961) 475
[2] P.J.A. Buttle, L.J.B. Goldfarb, Nucl. Phys. 78 (1966) 409
[3] C. Wong, J.D. Anderson, V.A. Madsen, F.A. Schmittroth, M.J. Stomp, Phys. Rev. 5C (1971) 1904


### 4.2.2. Structure Calculations for the Double Magic Nucleus $^{132}$Sn

J.S. Dehesa, J. Speth

Since very recently some experimental informations on the double magic nucleus $^{132}$Sn are available (see contribution to this report). We have performed nuclear structure calculations within the random-phase-approximation. From similar investigations in $^{208}$Pb[1] we know that the knowledge of the single particle energies is of crucial importance. Unfortunately, one only knows experimentally a few levels in $^{133}$Sb (proton particles) and $^{131}$Sn (neutron holes). No corresponding results are known for $^{131}$In (proton holes) and $^{133}$Sn (neutron particles). This lack of information introduces severe uncertainities in our calculation. The theoretical results shown in fig. 1 and fig. 2 have been calculated using two different sets of single particle energies, both justified by different extrapolation procedures. In both cases one is able to explain the isomeric state at $E_{exp} = 4847$ keV in a nearly quantitative way. All the other known experimental results are in much better agreement with the theoretical results shown in fig.1. Nevertheless this should not intepreted as a final decision. More experimental informations are necessary in order to check them with our theoretical predictions.

#### References


[1] P. Ring and J. Speth, Nucl. Phys. A235 (1974) 315; J. Speth, E. Werner and W. Wild, Phys. Rev. 33C (1977) 127
[2] J. Blomqvist, private communication

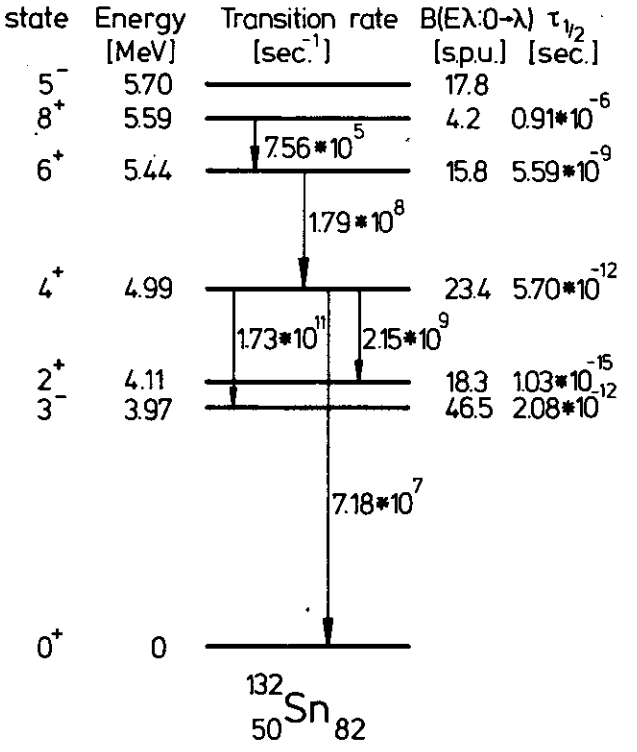


*Figure 1:*
*The theoretical level scheme. The transition rates and half-life values have been calculated by using the experimental energies.*

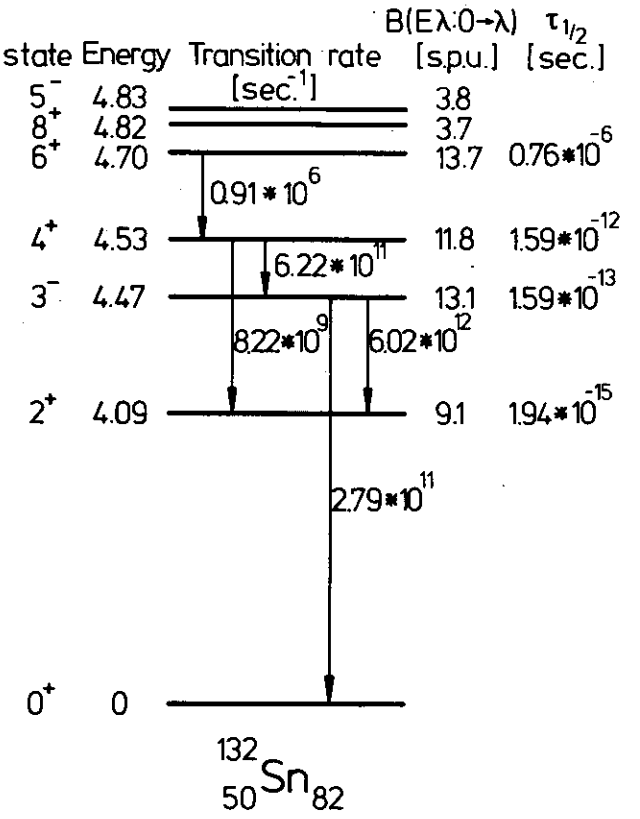


*Figure 2:*
*The same as in fig. 1. Here we have used a different set of single particle energies, proposed by Blomqvist[2].*

## 4.2.3. The Influence of 2ħω-Excitations on the Low Energy Spectra of Nuclei

K.W. Schmid, H. Müther

In the angular momentum projected deformed particle-hole model (PTD)[1] the states of open shell nuclei are approximated as linear combinations of the angular momentum projected HF-vacuum and the projected and isospin coupled selfconsistent particle-hole states with respect to it:

$$|d;IMT> = C^{IT}_{o,d}\, p^{IM}\,[|i>]_T + \sum_{\substack{\alpha \lesseqgtr F \\ M>F}} C^{IT}_{\alpha M;d}\, p^{IM}\,[a^{\dagger}_{M} a_{\alpha}|>]_T \qquad (1)$$

The configuration mixing degrees of freedom C are determined by solving the following matrix equation:

$$(H^{IT} - E^{IT} N^{IT})\, C^{IT} = 0 \qquad (2)$$

Note, that performing the angular momentum projection before the variation (2) is essential out of two reasons: first, only in this way the possible angular momentum dependence of the correlations as well as K-mixing and the renormalization of the HF-field can be taken into account. Second, and this is even more serious, only by projection before variation of the multideterminantal wave function rotational spurious admixtures can be avoided.

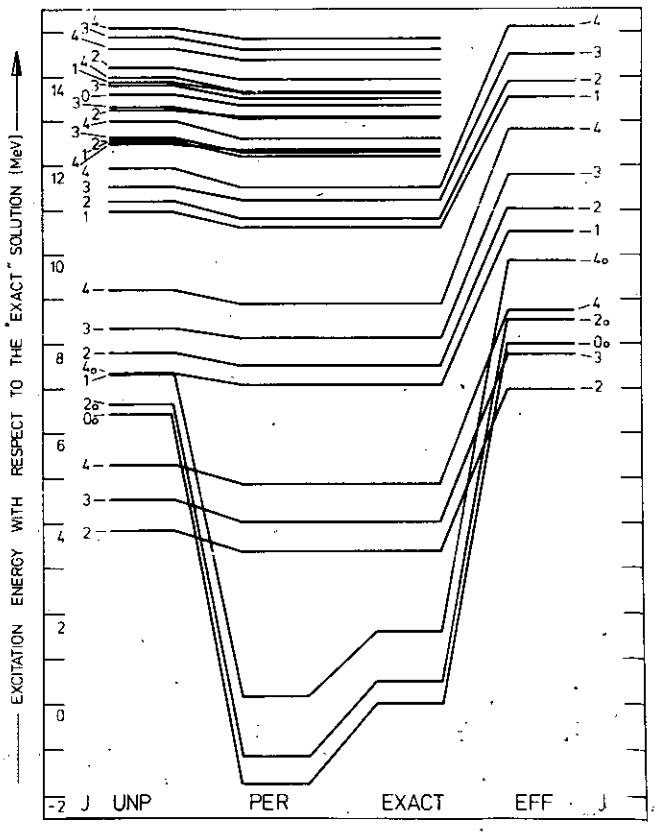


*Figure 1*

The above model has been used to study the influence of collective $2\hbar\omega$-excitations on the low lying positive parity states of some sd-shell nuclei. For this purpose first a PTD-calculation in a 3 major shell basis (Op, 1sOd, 1pOf) has been performed („Exact" Solution). For the nucleon-nucleon interaction the G-matrix elements for the Hamada-Johnston potential have been used. Switching off the interaction between the Op to 1pOf and the 1sOd to 1sOd excitations the full space was then splitted into two orthogonal subspaces, in which „unperturbed" solutions (UNP) could be obtained. Coupling the Op to 1pOf excitations to the 1sOd to 1sOd ones we have then calculated „perturbed" solutions (PER), which contain the effects of the $2\hbar\omega$-collective excitations in first order perturbation theory. Finally, it has been tried to include the effects of the $2\hbar\omega$-excitations via an „effective" force (EFF) resulting from the summation of core polarization diagrams.

*The results*[2] *(for the case of* $^{24}$*Mg an example is given in the Figure) show, that while the many-body perturbation theory (PER), though overshooting since being the first term of an alternating series, reproduces the full space results (EXACT) not too badly, the effective force (EFF) being based on an expansion which tries to include the effects of the excitation of the spherical* $^{16}$*O-core completely fails to do so. It is hence hopeless to try to include the effects especially of the highly collective* $2\hbar\omega$*-excitations by simply summing up core polarization diagrams, unless very high orders would be included.*

*The results help to understand the large discrepancies between the microscopically calculated and the recently by large scale shell model calculations fitted effective sd-shell interactions.*

**References**


[1] K.W. Schmid, G. Do Dang, Phys. Rev. C15 (1977) 1515
[2] K.W. Schmid, H. Müther, Phys. Rev. C16 (1977) 2050


## 4.2.4. A Study of the Ground State Energy of $^{40}$Ca


H.A. Mavromatis


We set up the energy matrix for $^{40}$Ca in an oscillator basis including the closed shell (n = O), the 5 1p-1h states and the 170 2p-2h states which arise to $2\hbar\omega$ in oscillator excitations (n = 1...175). The Hamiltonian used (following the notation of references 1 and 3) is:

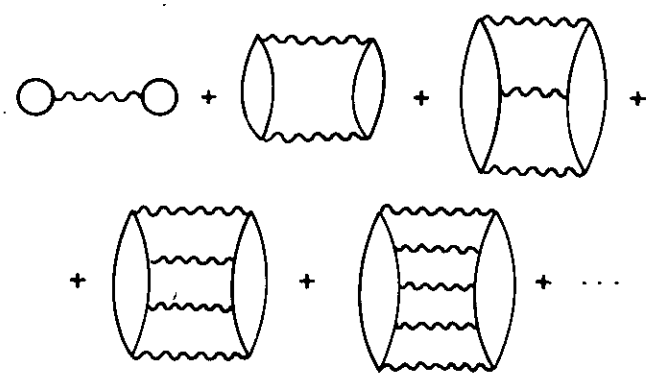

*Figure 1:*
*Linked series (where each graph represents all graphs of that order).*

$$H = (H_{osc} + \Lambda) + V$$

where

$$\Lambda = \sum_{n\ell} \lambda_{n\ell} |n\ell\rangle\langle n\ell| \qquad (1)$$

and

$$\hat{V} = V_s + G_c - (U_{osc} - R^2) - \Lambda = V_s + G_c - \frac{m\omega^2}{2A} \sum_{i<j} r_{ij}^2 - \Lambda$$

One notes that the matrix elements of $(V_s + G_c)$ reduce to the original Sussex Matrix Elements (SME)[2] if the core (c) used to obtain $G_c$ by reaction methods is set equal to zero. The $\Lambda$ modify the oscillator single-particle spectrum if $\lambda_{n\ell} \neq 0$, and the $R^2$ center of mass operator is added in order that spurious and nonspurious states do not mix in this mixed space calculation.

In diagonalizing the resulting matrix we get the usual linked series of figure 1, plus unlinked graphs[4] for the ground state.

To obtain only the linked graph expansion from this matrix we calculate the quantity Q (analogous to the quantities calculated in the Q box expansion of Kuo and coworkers[5] for more complex systems) where

$$Q = v^{+} G v \qquad (2)$$

and

$$G = (H_{00}\ I\text{-}H)^{-1}$$

Here v is the n component row matrix

$$(\hat{V}_{01}, \hat{V}_{02} \ldots \hat{V}_{0n})$$

| | Diagonalization | | Inversion | $E_0 + E_1 - 3/2\hbar\omega$ | Linked Graphs | | | | | 2nd, 3rd + 4th | 2nd, 3rd 4th, 5th + 6th |
|---|---|---|---|---|---|---|---|---|---|---|---|
| | G. State | Ist exc state | | | 2nd 0 | 3rd 0 | 4th 0 | 5th 0 | 6th 0 | | |
| A | −25.59 | 18.60 | −69.41 | −288.65 | −52.11 | −6.47 | −10.65 | 3.55 | −6.24 | −69.23 | −71.92 |
| B | −13.51 | 17.01 | −24.07 | −220.61 | −21.90 | 2.00 | − 5.45 | 3.33 | −3.82 | −25.35 | −25.84 |
| C | −13.51 | 17.01 | −24.07 | −220.61 | −14.60 | −3.98 | − 2.64 | −1.20 | − .75 | −21.22 | −23.17 |

*Table 1:*
*(b = 2 fermis)*
*Diagonalization, Inversion and Order by Order Results in MeV*

where $\hat{V}_{oi}$ connects the states O and i. (Thus v is the first row of the n+1 dimensional energy matrix except that the first entry is missing). I is the idendity matrix, $H_{oo}$ is the first entry of the energy matrix and H the energy matrix minus the first row and first column.

We consider three situations:

A. $G_c = O, \lambda_{n\ell} = O$. This is the crudest approach and corresponds to using the original unsaturating SME and the oscillator single-particle spectrum in this calculation.

B. $G_c \neq O$ (c = .3 fermis, $\bar{\omega}_r = n + 1.5 + 2\bar{\lambda}$, where $\bar{\lambda} = 5.8$[3] such that the SME saturate, but n = O so one is still using an oscillator single-particle energy spectrum.

C. $G_c \neq O$ and $\lambda_{n\ell} = \lambda(n + /2)\hbar\omega$. With $\lambda = 1$ this corresponds roughly to the single-particle spectrum chosen in ref. 1.

Results are listed in Table 1 for these three situations for b = 2 fermis, where the sum of the linked graphs (eq. 2) is labelled 'Inversion'.

Important conclusions from this work are that for $^{40}$Ca 1) Neither the original SME nor the Saturating SME converge in an order by order linked graph expansion in this model space if oscillator single particle energies are used. 2) Order by order convergence is possible for a reasonable choice of unperturbed single particle energies. 3) With the saturating SME the all order result for the g.s. energy is not very sensitive to the oscillator size parameter one uses in one's calculation.

### References


[1] R.K. Tripathi, E.A. Sanderson and J.P. Elliott, Nucl. Phys. A278 (1977) 78
[2] J.P. Elliott, A.D. Jackson, H.A. Mavromatis, E.A. Sanderson and B. Singh, Nucl. Phys. A121 (1968) 241
[3] E.A. Sanderson, J.P. Elliott, H.A. Mavromatis and B. Sing, Nucl. Phys. A219 (1974) 190
[4] H.A. Mavromatis, Nucl. Phys. A206 (1973) 477
[5] E.M. Krenciglowa and T.T.S. Kuo, Nucl. Phys. A235 (1974) 171


## 4.2.5. The Cranking Approximation in Isospin Space


H. Müther, A. Faessler, Hsi-Tseng Chen*)


For schematic few level models with isospin structure it has recently been shown, that for the BCS approximation particle number- and isospin projection are indispensible to obtain reliable results[1]. Especially the isospin projection, however, leads to computational difficulties, because it requires a 3 fold integration. This makes it quite attractive to look for reliable approximations. If the nucleon-nucleon interaction is approximated by a pairing interaction, which is not to weak, the ground state energies of states with different isospin form an almost pure rotational band. This can also be seen from figure 1, which displays exact solutions for 8 particles in a 2 level model ($\varepsilon_1 = O$, $\varepsilon_2 = 1$, $j_1 = j_2 = 3/2$, pairing strength g = 1) and shows a linear dependence of the energy on T(T+1). Therefore it is very tempting, to treat the rotation in isospin space by a kind of cranking approximation, which tries to describe a collective rotation around the x axis in isospin space. This is achieved by constructing the BCS solution for the modified Hamiltonian

$$\hat{H}' = \hat{H} - \omega \hat{T}_x \,. \qquad (1)$$

For the resulting wave functions ($|BCS(\omega)>$ we calculate the total energy and the expectation value of $\hat{T}^2$, and present these results for different values of $\omega$ in the energy versus T(T+1) plot in figure 1 (results denoted by crosses. If one projects from the wave functions $|BCS(\omega)>$ the components with particle number N = 8, and calculates the energy and expectation value of $\hat{T}^2$ for these projected wave functions, the results denoted by the open circles are obtained. These results are in quite a good agreement with the exact solution. This agreement is slightly improved, if wave functions with proton- and neutron particle number $N_\pi = N_\nu = 4$ are projected from $|BCS(\omega)>$ (see the full dots in figure 1). In this approximation states with small expectation values for $<T^2>$ are obtained, because the simultaneous projection of proton- and neutron particle number yields wave functions with $T_z = O$. Instead of using the cranking model one may also construct BCS wave functions with different expectation value for $<T^2>$ by using instead of eq. (1) the modified Hamiltonian[2]

$$\hat{H}'' = \hat{H} - \lambda \hat{T}^2 \,. \qquad (2)$$

The wave functions obtained with this method yield results which are quite similar to those discussed above. For other strengths of the pairing interaction one also obtains similar results. Therefore we conclude that the yrast state energies for isospin bands may be calculated from the energies obtained for wave functions with different expectation value for $T^2$, like e.g. those from the cranking approach. The results are in good agreement with the exact solution if a particle number projection is performed.

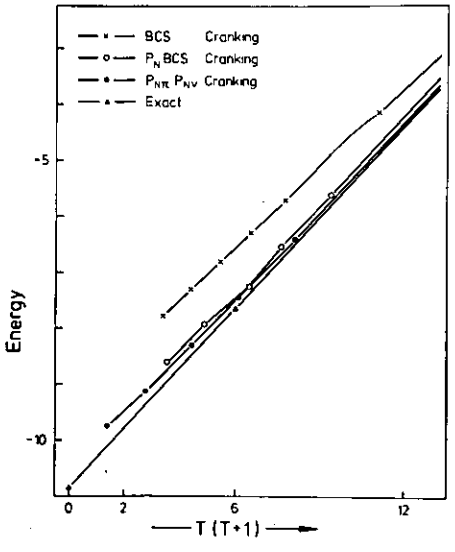


*Figure 1: Isospin bands in a 2 level model.*


*) Instituto de Fisica, Universidade de Sao Paulo, Brazil


### References


[1] H.T. Chen, H. Müther and A. Faessler: 'Pairing Vibrational and Isospin Projected Generator Coordinate Method' Preprint (see also this report)
[2] P. Camiz, A. Covello and M. Jean, Nuov. Cim. 62B (1966) 199

## 4.2.6. Pairing Vibrational and Isospin Rotational States in a Particle Number and Isospin Projected Generator Coordinate Method

Hsi-Tseng Chen*), H. Müther, A. Faessler

In recent years the Generator Coordinate Method (GCM) has been used to describe pairing vibrational states[1]. Following the phenomenological picture these states are described by a superposition of wave functions with different amount of pairing correlations and therefore the ansatz

$$|\Psi_{T,N}> = \int d\Delta\, f_{T,N}(\Delta)\, |\phi_{T,N}(\Delta)>$$

is used. In contrast to earlier calculations[1] we consider proton-proton, neutron-neutron and proton-neutron (T=1) pairing correlations simultaneously and the generator coordinate $\Delta$ stands for 3 variables which describe these correlations. The wave functions $|\phi_{T,N}(\Delta)>$ are obtained from generalized BCS wave functions with different amount of pairing correlations

$$|\phi_{T,N}(\Delta)> = P_T P_N\, |BCS(\Delta)>.$$

To allow a comparison with physical states $P_T$ and $P_N$ are projection operators for states of good isospin T and particle number N, which restore the symmetries violated by the BCS wave function. To study the usefulness of this GCM we apply it to a 2 level model ($\varepsilon_1 = 0$, $\varepsilon_2 = 1$, $j_1 = j_2 = 3/2$) of protons and neutrons interacting by the schematic pairing interaction, which can be solved exactly[2]. We also investigate the importance of isospin and particle number projection by comparing the energies resulting for BCS, $\hat{P}_N$ BCS, $\hat{P}_T$ BCS, $\hat{P}_N\hat{P}_T$ BCS, and $\hat{P}_{N\pi}\hat{P}_{N\nu}$BCS (proton and neutron particle numbers are projected separately) with the exact solution. In figure 1 results are shown for the ground state energies of the system with T = 0 and N = 8 assuming different strengths g for the pairing interaction. The figure shows, that particle number and isospin projection are indispensible to obtain a reasonable agreement. It can also be seen, that, especially in the limit of strong interaction, particle number and isospin projected BCS($\hat{P}_N\hat{P}_T$ BCS) is a rather good approximation to the exact solution. The GCM using $\hat{P}_N\hat{P}_T\,|BCS(\Delta)>$ as generator wave functions yields for all values of g such a good agreement with the exact solution, that the results cannot be distinguished in figure 1. Similar results are also obtained for the other yrast states of the isospin band. But also the second and third lowest energies of charge symmetric states are still very reliable. This can be seen from table 1, which shows results of a four level model corresponding to the A = 52 system with

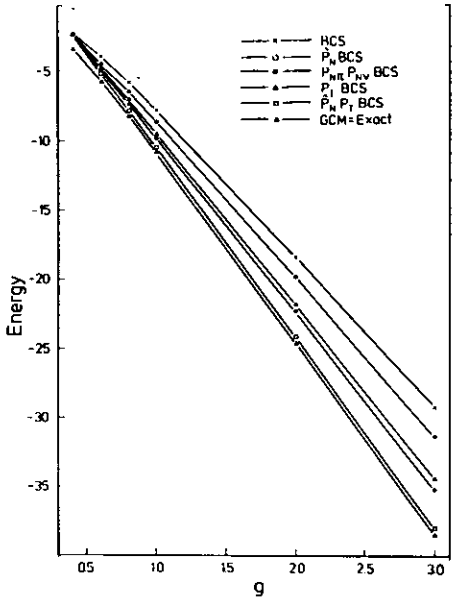


*Figure 1: Ground state energy in the 2 level model as a function of the pairing strengths g for different approximations.*

| T | GCM | Exact |
|---|---|---|
| 0 | −10.75 | −10.84 |
| | − 7.00 | − 6.62 |
| | − 2.81 | − 2.58 |
| 2 | − 7.52 | − 7.65 |
| | − 2.95 | − 3.81 |

*Table 1: Energies for A = 52 nuclei in a 4 level*

12 active nucleons in the pf shell. Some GCM states yield more binding energy than the charge symmetric exact solution because the GCM wave functions also contain charge intermediate symmetric components.

*) Instituto de Fisica, Universidade de Sao Paulo, Brazil

### References

[1] A. Faessler, F. Grümmer, A. Plastino and F. Krmpotic, Nucl. Phys. A217 (1973) 420

[2] H.T. Chen and R.W. Richardson, Nucl. Phys. A212 (1973) 317

## 4.3 Giant Resonances

### 4.3.1. Breathing Mode in $^{208}$Pb

J. Wambach, V.A. Madsen, G.A. Rinker, J. Speth

In recent years a large amount of data on giant multipole resonances has been accumulated. Among those resonances, of which the giant dipole and quadrupole resonances are now well established, the isoscalar monopole resonance (breathing mode) is of special interest. The excitation energy of this mode gives direct information about the nuclear compressibility $k_n$ through

$$E^{0^+} = \sqrt{\hbar^2 k_n / m}\ \frac{\pi}{3R}$$

R: nuclear radius, m: nucleon mass.

The wide range of theoretical predictions of this mode in $^{208}$Pb from 8 – 22 MeV shows the extreme sensitivity on the effective force used.

With a parametrization of the effective p-h force used in RPA-calculations[1] which includes adjustment to the isotope shifts and thus directly tests the monopole part of the interaction, one gets a monopole strength concentration at around 14 MeV.

In order to check consistency of these predictions with various experimental data in $^{208}$Pb we calculated spectra for inelastic (e,e'), ($\alpha,\alpha'$) and (d,d') scattering[2].

The transition densities were obtained from improved RPA wavefunctions in a $3\hbar\omega$-configurations space. A strong argument against the existence of monopole strength at 14 MeV comes from the fact, that in inelastic (e,e') scattering monopole strength exhausting 100 % of the EWSR should give equally large contributions to the cross-section, as the isovector dipole, which lies almost at the same energy. This is obviously not the case, since the dipole alone gives already good agreement to the data. However this analysis depends strongly on the choice of the collective transition density (G-T or S-J). With the same BE1-value S-J gives a larger (e,e') cross-section than G-T. Our calculations favour G-T transitions in that energy region and the actual mixing G-T/S-J is 4. Therefore our theoretical (e,e') cross section is too small allowing only for E1 strength (80 % of EWSR) and additional E0 strength (82 % of EWSR) is needed (Fig. 1). From a discrete RPA-calculation we do not get information about the width of the various resonances. Using Breit-Wigner resonance shapes, they were fitted to the known experimental ones. The splitting of the E2 resonance was taken from recent 2p-2h calculations of J.S. Dehesa, which are in agreement with experiment.

Figure 2 and 3 show inelastic ($\alpha,\alpha'$) and (d,d') cross-sections obtained with the same densities used in (e,e'). To get form factors they were folded with an effective projectile-target force based on a phenomenological n-n force. Details are described in Ref. [2]. In ($\alpha,\alpha'$) the monopole appears as a shoulder on the quadrupole, while in (d,d') it is excited much stronger, due to the larger spacial extend of the projectile.

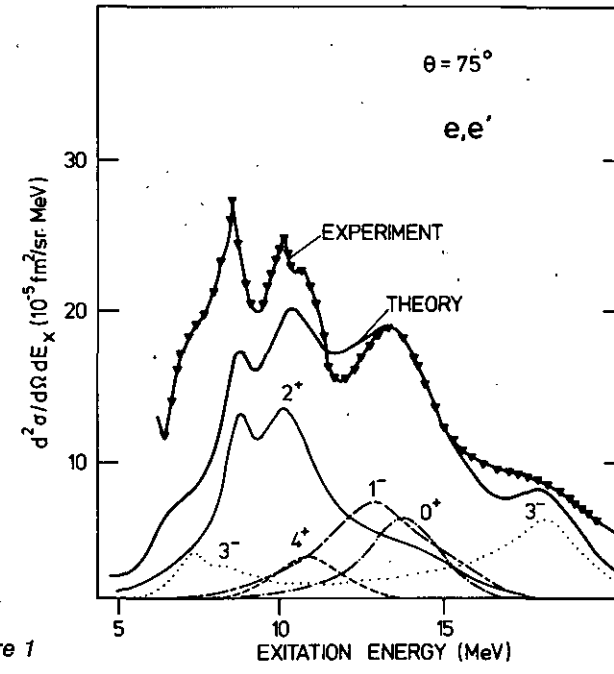


*Figure 1*

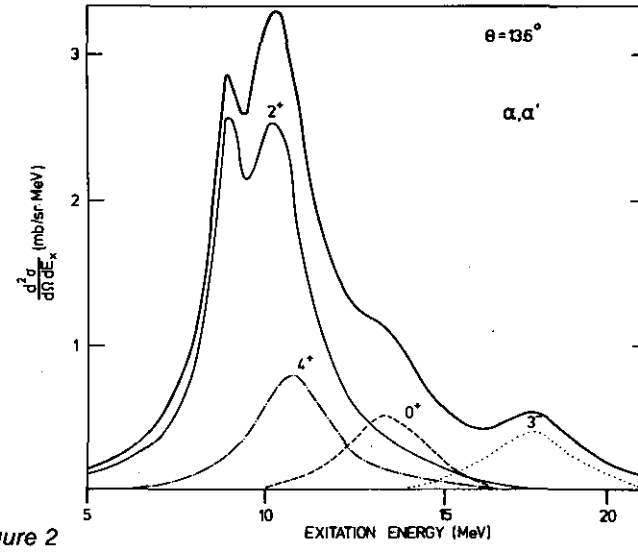


*Figure 2*

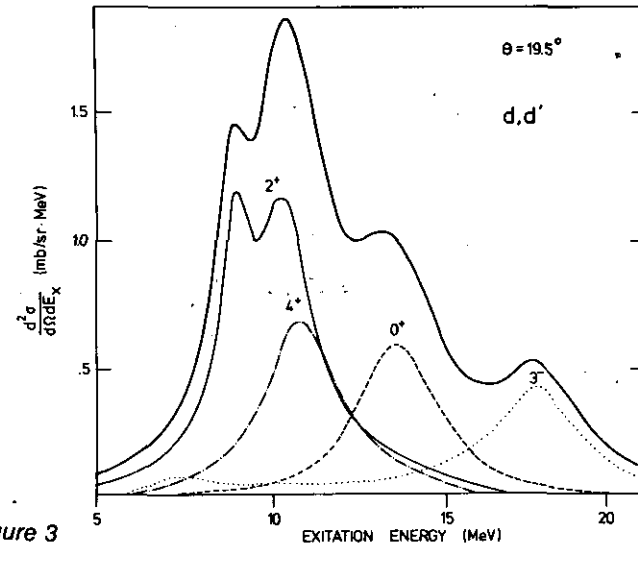


*Figure 3*

#### References

[1] P. Ring and J. Speth, Nucl. Phys. A235 (1974) 315; J. Speth et al., Nucl. Phys. A232 (1974) 1

[2] J. Wambach et al., to be published in Phys. Rev. Lett.

## 4.3.2. On the Monopole and Quadrupole Resonances in $^{90}Zr$

J.S. Dehesa, J. Speth and Amand Faessler

Here we present (1p-1h) and (2p-2h) RPA calculations of E0 and E2 resonances in $^{90}Zr$. This is done in the frame work of the core-coupling-random-phase-approximation[1,2].

The distribution of the monopole and of the quadrupole strength is shown in Figures 1 and 2 respectively. In the upper part of Figure 1, we find two giant (1p-1h) T = O EO states at 15 MeV and a stronger isoscalar monopole state at 20.7 MeV. As shown in the lower part of the figure, the inclusion of the 2p-2h excitations strongly fragments all the three isoscalar resonances. A similar situation is observed for the quadrupole resonances in Figure 2.

The portion of E0 and E2 strength which locate at different energy ranges below 35 MeV is shown in Table 1. Therein one can notice that both strength distributions strongly overlap. In particular, about 20 % of the isoscalar E0 sum rule and 48 % of the isoscalar E2 sum rule locate together between 12.5 and 15.0 MeV. In the 20.0-to-22.5 MeV energy range lies down 42.5 % of the T = O E0 sum rule. And between these two energy regions, 22 % and 9 % of the isoscalar E2 and E0 sum rules respectively are found.

### References

[1] J.S. Dehesa, Ph. D. thesis, University of Bonn, June 1977
[2] J.S. Dehesa, J. Speth and A. Faessler, Phys. Rev. C15 (1977) 1858
[3] J.S. Dehesa, J. Speth and A. Faessler, to be published

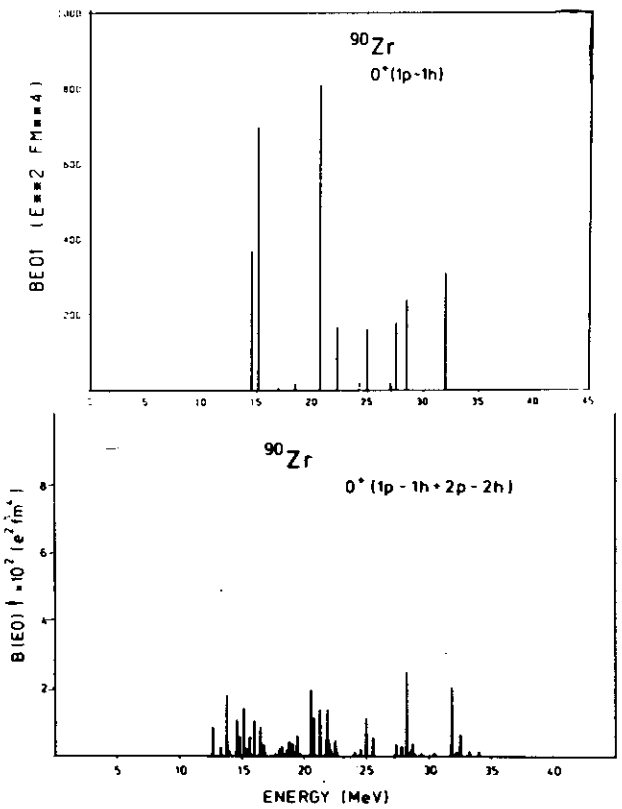


*Figure 1*

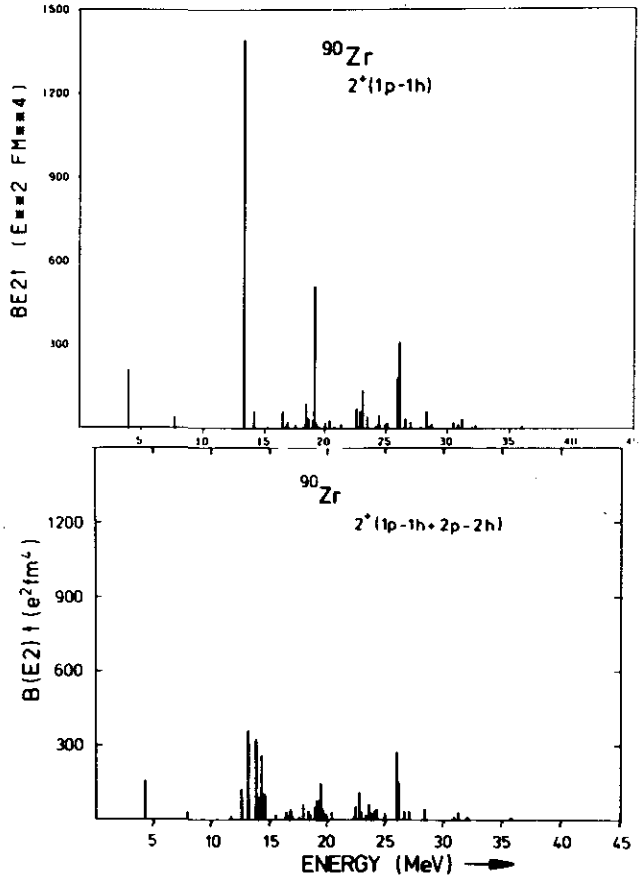


*Figure 2*

*Table 1:*
*Distribution of E0 and E2 Strength in $^{90}Zr$*

| Eλ / Energy Interval (MeV) | E0 | | E2 | |
|---|---|---|---|---|
| | % (T=0+T=1) EWSR | % T=0 EWSR | % (T=0+T=1) EWSR | % T=0 EWSR |
| 0- 5 | - | - | 1 | 1.8 |
| 5-10 | - | - | 0.5 | 0.8 |
| 10-12.5 | - | - | 0.3 | 0.6 |
| 12.5-15 | 10.2 | 19.7 | 26.4 | 47.7 |
| 15-17.5 | 13.5 | 16.3 | 3.6 | 0.8 |
| 17.5-20 | 7.1 | 8.7 | 20.2 | 22.0 |
| 20-22.5 | 25.4 | 42.5 | 3.9 | - |
| 22.5-25 | 6.7 | 2.6 | 4.0 | - |
| 25-30 | 20.1 | 8.1 | 24.6 | 0.5 |
| 30-35 | 15.5 | - | 4.7 | - |

## 4.3.3. Microscopic Calculation of the Electric Dipole- and Quadrupole-Parts of the $^{19}F$ Proton Radiative Capture Cross Section

K.W. Schmid and G. Do Dang*)

About a year ago we had proposed[1] a microscopic model for the description of the giant multipole resonances (GMR) in light deformed nuclei and their excitation via radiative capture reactions. This model had then been applied to the giant dipole part (GDR) of the GMR in $^{20}Ne$ as seen via the $^{19}F$ $(p,\gamma)^{20}Ne$ reaction. The results had been in surprisingly good agreement with the experimental data. However, besides being restricted to the GDR, these calculations had made use of a couple of approximations which were not completely satisfying.

In the meantime[2] most of these approximations have been removed. So, the groundstate correlations due to the mixing of the angular momentum projected Hartree-Fock vacuum and the projected particle-hole configurations have been included and no more restriction on the K-quantum numbers of the intrinsic configurations has been made. Furthermore the one body decay terms[3] due to the orthogonalization of the continuum with respect to the bound states have been taken into account and additionally to the GDR also the giant quadrupole part (GQR) of the GMR has been studied.

All these improvements do have considerable effects on the quantitiative results. However, the qualitative features of both the cross sections as well as the angular distributions obtained in ref. 1 remained unchanged. Fig. 1 compares the theoretical results for the 90°-yield curves of the $^{19}F$ $(p,\gamma_0)^{20}Ne$(g.s.) reaction with experiment[4]. While the full curve (IRA) has been calculated using the isolated resonance approximation, i.e. assuming a diagonal propagator in the T-matrix, the dashed curve (MIA) results from an inversion of the full propagator at all considered energies. In both calculations the final state interaction term (FSI) of the T-matrix has been included and E1- as well as E2-transitions have been taken into account. It is seen that the theoretical results are at least qualitatively in good agreement with the experimental data. However, especially in the upper part of the spectrum, a quantitative agreement could not be obtained. These quantitative discrepancies can most probably not be explained by the shortcomings of the model, but there are strong hints that they are mainly due to an improper choice of the effective nuclear interaction. Further improvements can hence only be expected, if some more reliable information about this interaction can be obtained.

Considering our results for the GQR in $^{20}Ne$ (Fig. 2 shows the total E2-cross section for the $^{19}F(p,\gamma_0)$ $^{20}Ne$(g.s.)-reaction), it is seen, that although a couple of isospin zero $J = 2^+$ states with large groundstate B(E2)-values are available in the region between 15 and 25 MeV excitation energy (i.e. ~ 2 to 12 MeV proton energy), the isoscalar GQR in $^{20}Ne$ is only weakly excited in the capture reaction. This result resolves at least qualitatively the puzzle why inelastic α-scattering experiments on certain light nuclei see sometimes an E2-strength distribution, which looks rather different from that one obtained via the corresponding radiative capture reactions. It is obvious that the (α,α') experiments do excite all those states with a large transition density. Hence all the isoscalar $2^+$ states with strong groundstate B(E2)'s will be strongly excited whatever their individual structure may be. On the other hand the (p,γ) reactions are much more selective on the specific structure of the states involved. In the special case of $^{19}F$ because of the $J^\pi = 1/2^+$ target spin only d-waves can couple with the target to yield $J^\pi = 2^+$ states. Our numerical results show, that such configurations do only weakly couple to intermediate states of predominantly $(p^{-1}$ pf) structure at least via the conventional nuclear interaction we have used. Hence at least the $(p^{-1}$ pf) part of the GQR in $^{20}Ne$ is only weakly excited via proton radiative capture.

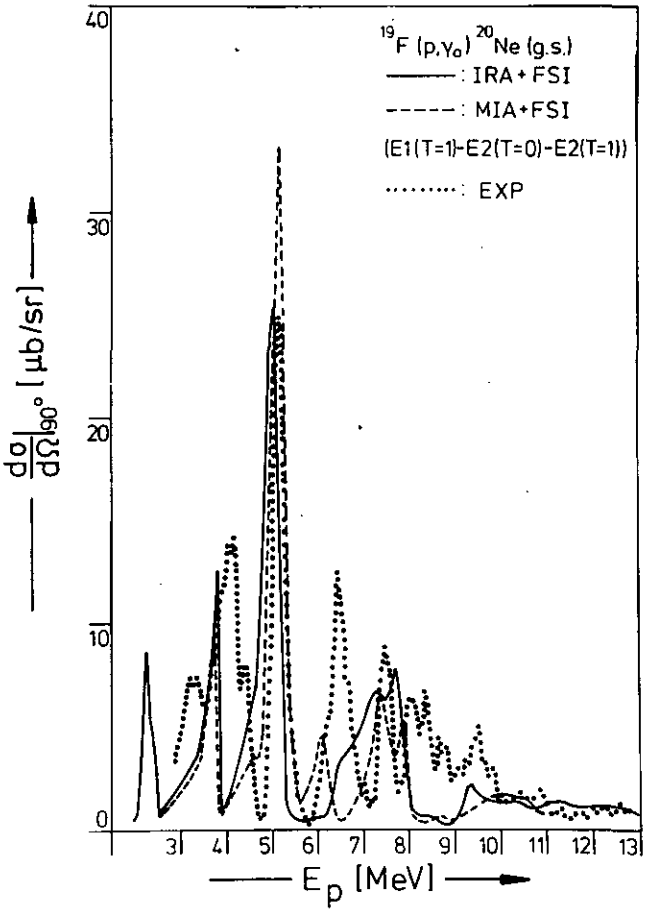


*Figure 1*

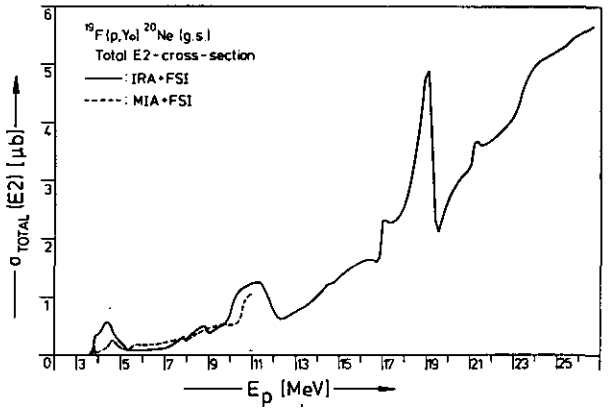


*Figure 2*

*) Laboratoire de Physique Theorique et Hautes Energies, Orsay, France

### References

[1] K.W. Schmid, G. Do Dang, Phys. Rev. C15 (1977) 1515
[2] K.W. Schmid, G. Do Dang, to be published
[3] M. Micklinghoff, to be published in Nucl. Phys.
[4] R.E. Segel et al., Nucl. Phys. A93 (1967) 31

## 4.3.4. Excitation of Giant Resonances in $^{208}$Pb by Inelastic Electron Scattering

J. Wambach, J. Speth, G.A. Rinker

Now a lot of low momentum transfer inelastic electron scattering data with medium and high resultion are available. In order to interpret those data in $^{208}$Pb especially at excitation energies larger than 20 MeV we made a microscopic analysis of the (e,e')-spectrum using RPA-transition densities. As modellspace we used p-h configurations of 3 $\hbar\omega$Since transverse components in the cross-sections were neglected up to now, we only get information about natural-parity states and the accuracy of the predictions are limited to forward-angle scattering ($\Theta < 90^{\circ}$). Beside the well studied resonances below 20 MeV we find resonance structure of different multipolarities (Fig. 1). The spectrum is calculated at an incident electron energy of 90 MeV under a scattering angle of 75°. Experimental hints for isoscalar E3 and isovector E2 strength[1] concentration between 15 and 25 MeV are supported. In addition to that we find E3, E1 and E4 isovector strength above 25 MeV. Since the continuum is not included explicitly in the calculation, but folded in afterwards, the resonacne width for energies larger than 20 MeV is only to be taken as an estimation.

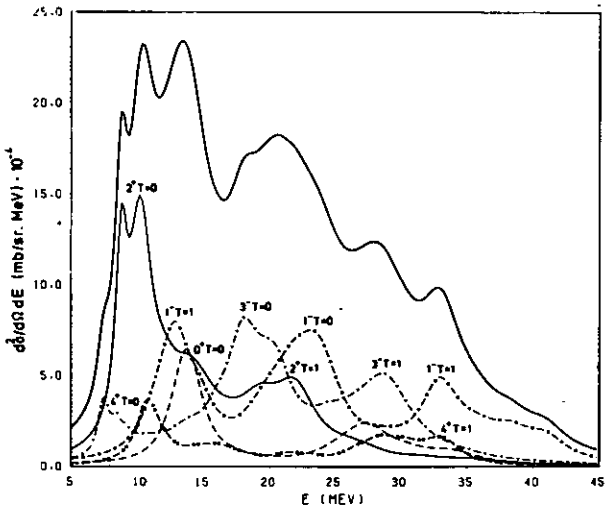


*Figure 1*

The isovector component of the breathing mode is found at a centroid energy of 28 MeV. Fig. 2 shows the transition densities of this resonance for protons and neutrons. One of the most striking features of the calculation is the strong E1 T = 0 excitation at 23 MeV, which is predominantly built up by 3-$\hbar\omega$ p-h configurations. Fig. 3 shows the form factors of this state compared to the 1⁻ T = 1 form factor at 13 MeV. Since it is hard to project spurious admixtures to the E1 mode either out of the wavefunction or the excitation-operator, we don't get a quantitative estimation of the spurious contributions. However they should not be too large because of the 3$\hbar\omega$-nature of the resonance.

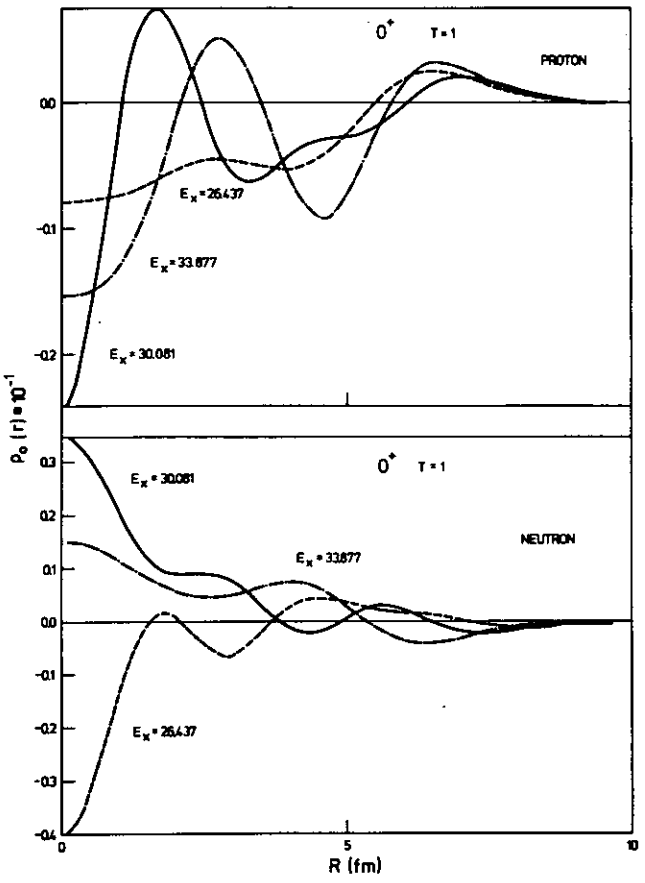


*Figure 2*

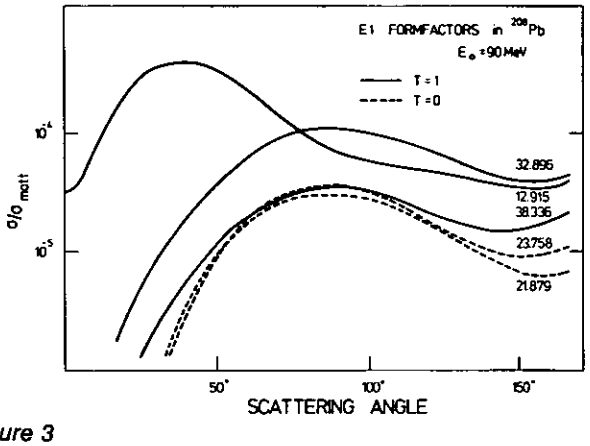


*Figure 3*

### References

[1] R. Frey et al., Proceedings to the International Conference on Nuclear Structure, Tokyo, Japan, 5-10 Sept. 1977

## 4.3.5. Forward Angle Analysis of the Monopole in $^{208}$Pb by Inelastic α-Scattering

J. Wambach, V.A. Madsen, J. Speth

Using α-particles as projectiles in inelastic scattering one excites selectively T = O transitions, since α-particles have isospin O and can not produce isospin flip. In the giant resonance region of $^{208}$Pb α-scattering projects out expecially the isoscalar quadrupole and monopole transitions, while the isovector dipole is strongly suppressed since Coulombexcitation is expected to be small at higher incident bombarding energies. In lowest order the (α,α')-form factor is given by

$$F^{0^+\to J^\pi}(r) = \int V^{\alpha n}(r,r')\rho^{0^+\to J^\pi}(r')\, r'^2 dr'$$

where $V^{\alpha n}(r,r')$ is the effective α-n interaction and $O^+\to J^\pi$ (r) the groundstate transition density, which in $^{208}$Pb is well described by RPA p-h correlations. $V^{\alpha n}$ is obtained from folding an effective n-n interaction with the groundstate wave function of the α-particle, choosing a reasonable projectile rms-radius.

Fig. 1 shows the (α,α') cross-sections for different multipoles in the giant resonance region from 5-20 MeV in $^{208}$Pb. The form factors of the strongest RPA-states were taken. Between 8 and 15 MeV mainly 2⁺, O⁺ and 4⁺ contribute to the spectrum (Fig. 2). As in electron scattering it turns out, that the cross-sections of 2⁺- and O⁺-states are rather similar, except that the diffraction minima of the O⁺ are deeper. Nevertheless there is one clear distinction between 2⁺ and O⁺ angular distributions. At around 4° the monopole shows an extremely deep minimum, which does not occure in the 2⁺ cross-section and at angles smaller than 2° the monopole distribution is strongly enhanced (Fig. 2). This feature was recently used[1] to support experimentally monopole strength-concentration at 13 MeV. Another interesting result of our investigations is, that it should be possible to measure the 4⁺-contribution to the α-excitation function in $^{208}$Pb.

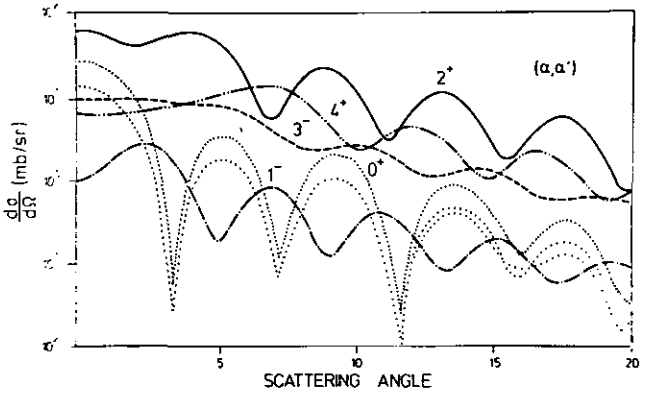


*Figure 1*

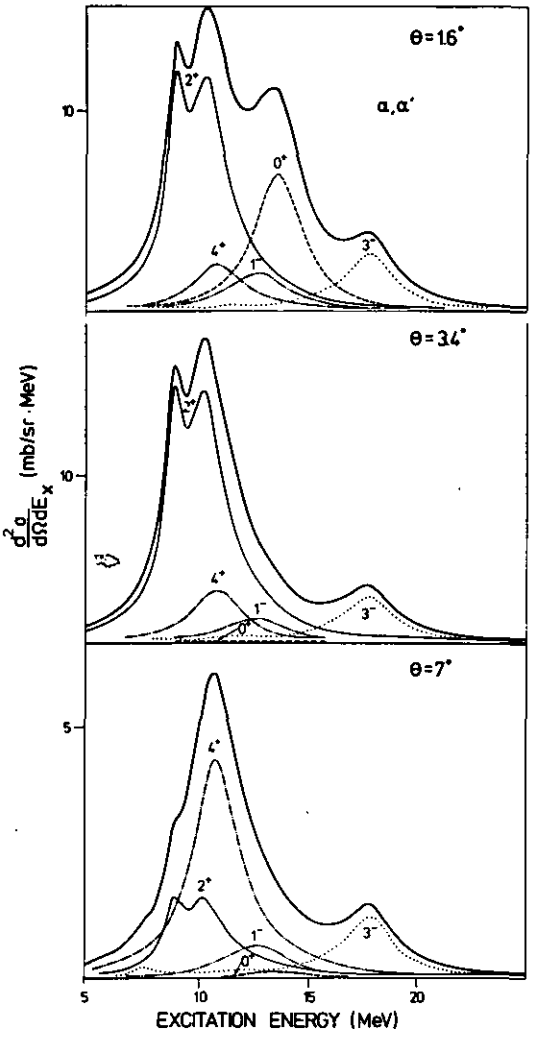


*Figure 2*

Since the 4⁺ lies just under the quadrupole peak (Fig. 2) there exsists an angular region (≃ 7°, Fig. 1) where the 4⁺ cross-section is larger than the quadrupole. Measuring the excitation function under that angle, one should see a peak, which is predominantly 4⁺ (Fig. 2).

### References

[1] D.H. Youngblood et al., Phys. Rev. Lett. 39, 1188 (1977)

## 4.3.6. Distribution of the Magnetic Dipole Strength in $^{90}$Zr

J.S. Dehesa, J. Speth and A. Faessler

In the present note the influence of the 2p-2h excitation for the microscopic discription of the magnetic dipole states in $^{90}$Zr is shown. The core-coupling-random-phase-approximation[1], which has been proved to be very successful in studying electric[2] and magnetic[3] multipole resonances in light and heavy nuclei, is used.

The (1p-1h) RPA and (2p-2h) RPA results are shown in Figure 1. Only one (1p-1h) 1⁺ level at 9.8 MeV with B(M1) value of 5.44 $\mu_o^2$ (if we use the effective magnetic operator) or 11.11 $\mu_o^2$ (if we use the bare magentic operator) is observed. Its structure is exclusively built up by the particle-hole $(g^1_{9/2}-g_{7/2})$ excitation.

Due to the coupling of the core excitations, the single-hole states $g_{9/2}$ weakly splits in such a way that the main strength (90.75 %) remains at the experimental energy –11.75 MeV. There are other three relatively important pieces at –14.66 MeV (with 3.17 %), at

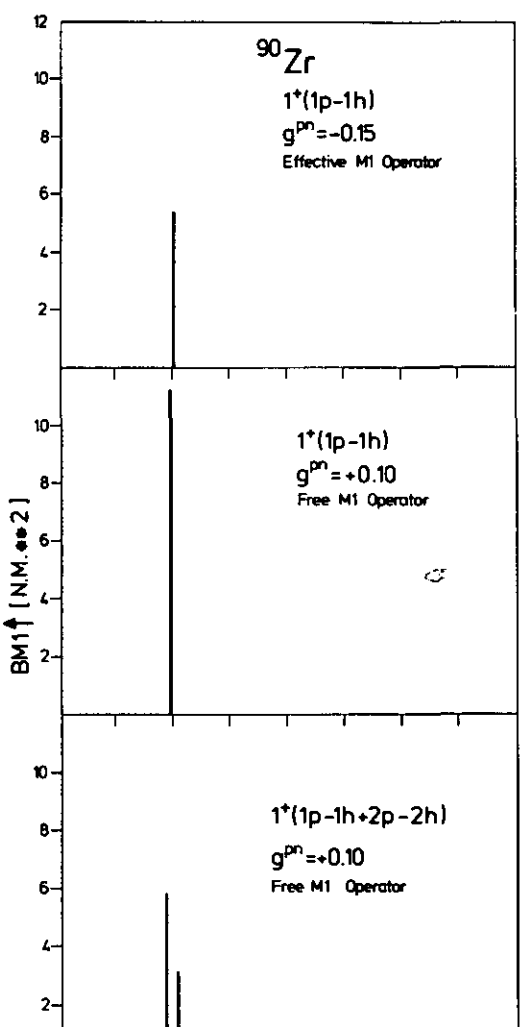


*Figure 1*

–19.81 MeV (2.94 %). Many other fragmented $g_{9/2}$ pieces with very small strengths also appear. As a consequence of the splitting of this hole state, one expects fragmentation of the (1p-1h) M1 resonance due to the inclusion of the (2p-2h)-configurations. The bare M1 operator has been used. This is seen in the lower part of Figure 1 where we mainly notice four narrow peaks of relatively important B(M1) value, and many other $1^+$ states with very small strength. It is interesting to remark that the reduction of the strength undergone by the (1p-1h) M1 resonance and the structure of the two other strongest M1 states at 10.5 and 11.1 MeV are mainly due to the following admixtures

$$1g_{7/2} \times (2^+ \times 1g_{9/2}) \text{ and } 1g_{7/2} \times (4^+ \times 1g_{9/2})$$

From an experimental point of view, the location of M1 strength is still very unclear although there are indications due to Fagg[4] and to Torizuka[5] in recent inelastic electron scattering which locates it about 9 to 10 MeV.

### References


[1] J.S. Dehesa, Ph. D. thesis, University of Bonn, 1977
[2] J.S. Dehesa, J. Speth and A. Faessler, Phys. Rev. C15 (1977) 1858
[3] J.S. Dehesa, J. Speth and A. Faessler, Phys. Rev. Lett. 38 (1977) 208
[4] L.W. Fagg, Rev. Mod. Phys. 47 (1975) 683
[5] Y. Torizuka in Colloque Franco-Japonais sur Spectroscopie Nucleaire et Reactions Nucleaires, Dogashima, Japan, September 1976


## 4.3.7. Comparison of Microscopic and Phenomenological Transition Charge Densities


G.A. Rinker, J. Speth


We have used our improved RPA wavefunctions[1] to calculate the corresponding transition charge densities. In all cases shown below, the RPA results contain the proton form factor folded in. The RPA densities shown in the figures are properly normalized, but the phenomenological ones not. In fig. 1 the theoretical transition charge density of the lowest $3^-$ state in $^{208}$Pb (full line) is compared with the error band of a previous electron scattering experiment[2]. The agreement between the RPA and experimental densities is remarkably good, both in shape and normalization. This gives us confidence also for the other theoretical densities.

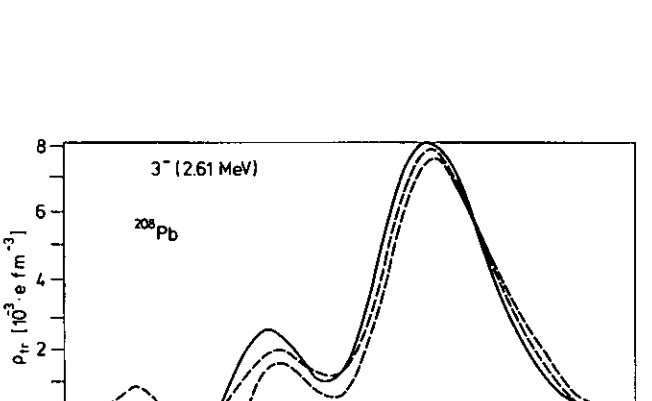


*Figure 1*

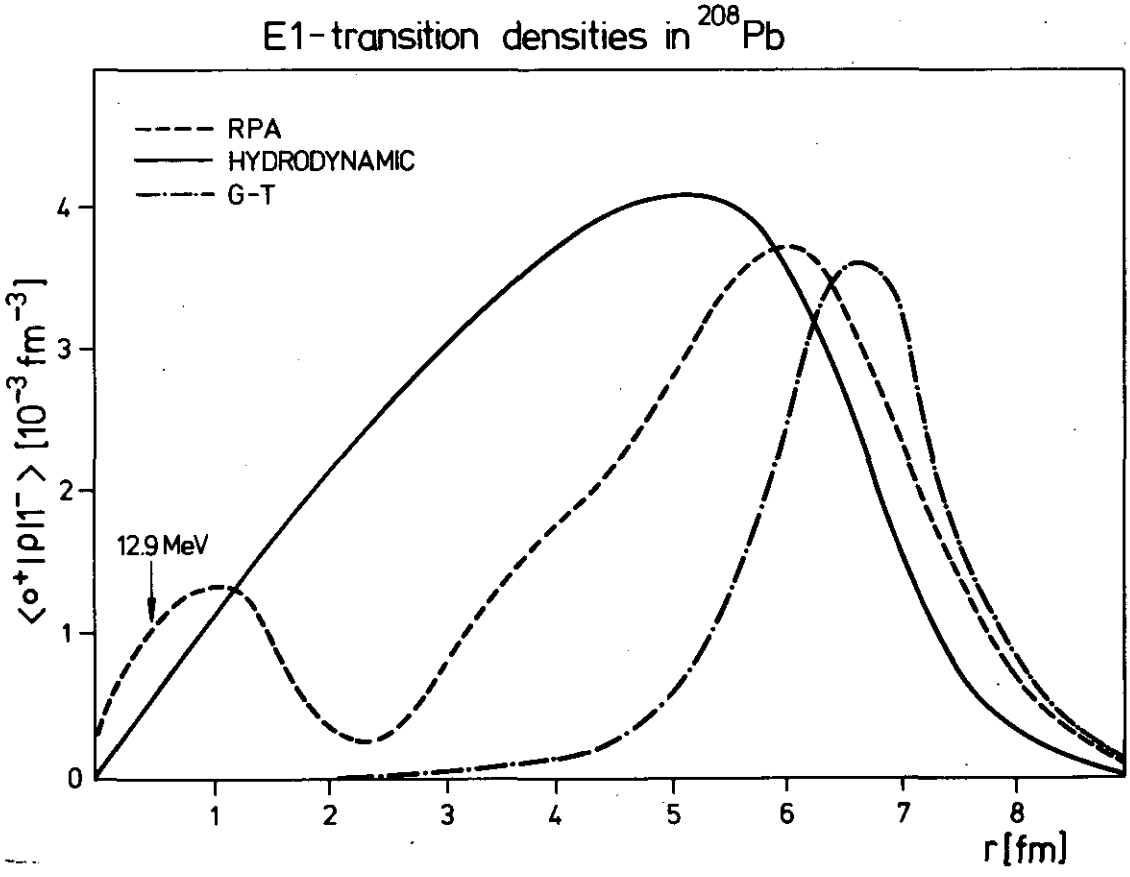


*Figure 2a*

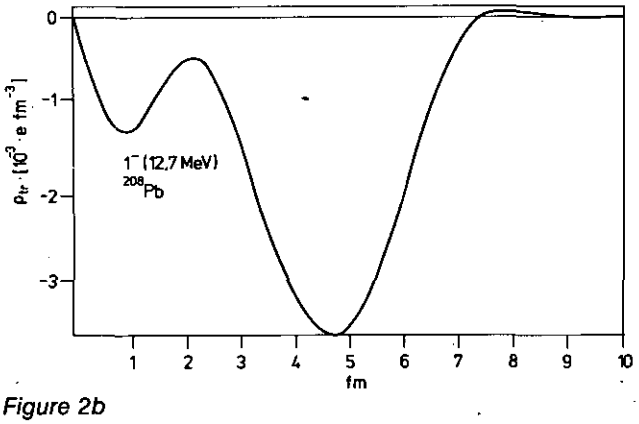


*Figure 2b*

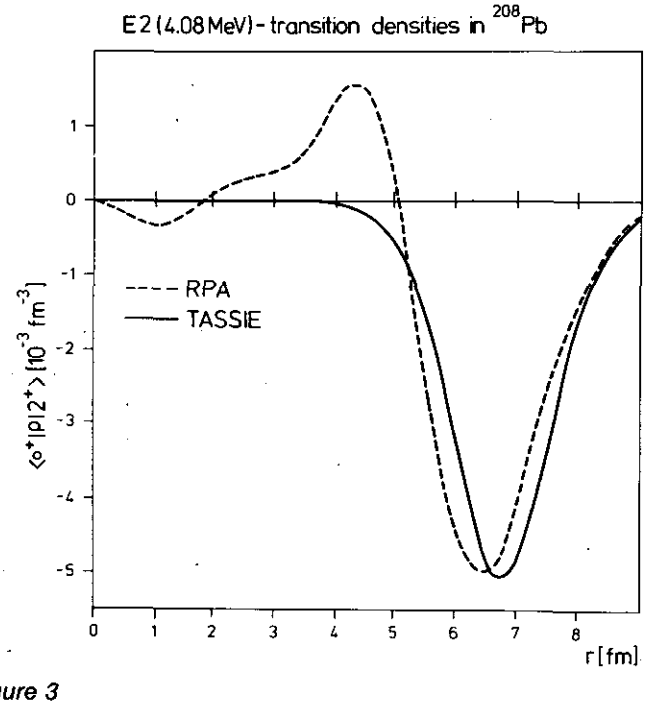


*Figure 3*

Figs. 2a and 2b exhibit dipole excitations. The dashed curve in fig. 2a and the curve in fig. 2b are RPA results. The state at 12.9 MeV exhausts nearly 50 % of the $\tau = 1$ EWSR, whereas the state at 12.7 MeV bears only 8 %. Neither the hydrodynamical model nor the Goldhaber-Teller model adequately dexcribes the strong RPA state, although the weaker transition is somewhat similar to the hydrodynamic model. By inspecting the transition densities of all stronger states we found that only a few levels, which exhaust together about 20 % of the EWSR, possess a transition density similar to the hydrodynamic model. In figure 3 the strong 2$^+$ state at 4.08 MeV along with the Tassie model is shown. Also here the interior is not well-represented by the simple Tassie form, but near the surface the agreement is much better.

**References**


[1] G.A. Rinker and J. Speth, preprint
[2] H. Rothaas et al. Phys. Letters 51B (1974) 23

## 4.3.8. Monopole-Vibrations in the ATDHF Model

K. Goeke, B. Castel*)

There are many microscopic calculations of the isoscalar giant monopole resonance (GMR) in the literature. These approaches include the Thomas-Fermi model, the cranking approximation, the adiabatic time dependent Hartree-Fock theory (ATDHF), hyperspherical harmonics and the generator coordinate method and finally the random phase approximation. The purpose of this note is to study the GMR in the framework of ATDHF using self-consistently determined Slater determinants[1,2] in contrast to previous approaches.

In ATDHF[3] one derives a classical collective Hamiltonian for the dilatational motion in terms of the collective coordiante $q = (\langle r^2\rangle/A)^{1/2}$

$$H_c = \frac{1}{2} M(q)\,\dot{q}^2 + V(q)$$

The collective potential V(q) and the mass M(q) are determined from an appropriately determined set of Slater determinants $|q\rangle$ with varying rms-radius q. Explicitly $V(q) = \langle q|H|q\rangle$, and M(q) is given in terms of the density matrix $\rho_o(q)$ corresponding to $|q\rangle$ by

$$M(q) = i\,\mathrm{Tr}\left\{[\rho_o,\bar{\rho}_1]\ \frac{\partial \rho_o}{\partial q}\right\}$$

The $\bar{\rho}_1$ is determined by

$$[W_o,\bar{\rho}_1] + [\bar{W}_1,\rho_o] = i\frac{\partial \rho_o}{\partial q}$$

where $W_o = T + \mathrm{Tr}\,v\,\rho_o$ and $\bar{W}_1 = \mathrm{Tr}\,v\,\bar{\rho}_1$. In the present calculation the collective path $|q\rangle$ (or $\rho_o(q)$) is constructed by means of constrained HF with $\delta\langle q|H-\lambda\Sigma r_i^2|q\rangle = 0$. The results for doubly magic nuclei are given in table 1. The excitation energies are calculated in the harmonic limit and the force is the Skyrme-3 interaction

*Table 1:*

| | $^{16}O$ | $^{40}Ca$ | $^{90}Zr$ | $^{208}Pb$ |
|---|---|---|---|---|
| M | 23.3 | 50.9 | 98.1 | 228.0 |
| Mc | 22.2 | 47.1 | 86.4 | 197.1 |
| K | 130 | 176 | 214 | 215 |
| Ec | 23.6 | 24.8 | 22.4 | 17.3 |
| E | 23.1 | 22.4 | 21.0 | 16.1 |

*M and Mc are the collective masses for ATDHF and cranking. $K_A$ is the compression moduls in excitation energies. The units are MeV and nucleon masses, respectively.*

The difference between M and Mc is made by the neglect of the residual interaction in the calculation of Mc. This depends on the force and is proportional to (1 - m/m*). The energies are all slightly higher than those which seem to emerge from experiments, probably due to the interaction. The results can also be interpreted[4] in terms of energy moments of the RPA strength distribution

$$m_k(r^2) = \sum_{\alpha>o} (E_\alpha - E_o)^k\ |\langle \alpha\,|\,r^2\,|\,o\rangle|^2$$

According to ref. 4) the ATDHF mass at the HF minimum $q_o$ is given by

$$M = 2\hbar^2\, m_{-3} \left(\frac{A q_o}{m_{-1}}\right)$$

and the excitation energy

$$E = \left(\frac{m_{-1}}{m_{-3}}\right)^{1/2}$$

If the collective path is constructed by means of scaling operations rather than CHF the excitation energy is then $E' = (m_3/m_1)^{1/2}$. The difference $\Delta E = [E-E']$ may serve as a quantitative measure for the width of the resonance. This number together with $m_{-3}$ [$fm^4$ $MeV^{-3}$] is given in table 2. (The units are $MeV^{-3}$ $fm^4$ and MeV respectively.)

*Table 2:*

| | $^{16}O$ | $^{40}Ca$ | $^{90}Zr$ | $^{208}Pb$ |
|---|---|---|---|---|
| $m_{-3}$ | 0.02 | 0.12 | 0.64 | 7.25 |
| $\Delta E$ | 11.4 | 6.1 | 2.4 | 1.8 |

Obviously the width of GMR decreases with increasing mass number A, a trend which is reproduced also by the collective masses whose deviation from the total mass decreases with increasing A.

The ATDHF theory is mainly designed to describe large amplitude collective processes. The methods for solving the equations in such a case can reliably be studied in the small amplitude limit and obviously turn out to be useful and applicable.

*) Queen's University, Kingston, Canada

### References

[1] K. Goeke, Phys. Rev. Lett. 38 (1977) 212
[2] K. Goeke and B. Castel, Phys. Rev., to be published
[3] K. Goeke and P.-G. Reinhard, Annals of Physics, to be published
[4] K. Goeke, A.M. Lane and J. Martorell, Nucl. Phys., to be published

## 4.4 Mesonic Degrees of Freedom in Nuclei

### 4.4.1. Mesonic and Isobar Degrees of Freedom in the Ground State of the Nuclear Many-Body System

M.R. Anastasio, A. Faessler, H. Müther, K. Holinde*) and R. Machleidt*)

One shortcoming of most microscopic nuclear structure calculations arises from the use of a phenomenological NN interaction which is taken to be the same in both the two-body and many-body systems. However, it is now generally accepted that the NN interaction is mediated by the exchange of various mesons[1]. This implies that if the many-body problem is solved in a Hilbert space containing only nucleons, then the NN interaction must be modified to account for the effect of the virtual mesons. These extra mesonic degrees of freedom (MDF) have been studied previously[2,3] in the framework of a one boson exchange (OBE) potential and found to be very important. Another feature of the NN interaction which leads to modifications in the many-body system is the explicit inclusion of possible excitations of the nucleon into the important $\Delta(1236)$ resonance. These isobar degrees of freedom (IDF) have also been studied previously[4,5] and lead to significant effects in the many-body system.

The aim of this work is to study in $^{16}O$ and nuclear matter the interplay of the MDF with other features of the NN interaction. To do this three new potentials are fit to the NN scattering and bound state data. The first two potentials combine the MDF and IDF and the resulting NN interaction has the following form in the many-body system

$$V_{eff}(z)=V_{OBE}(z)+V_{N\Delta}(z)\frac{Q}{z-H_0}V_{N\Delta}(z)+V_{\Delta\Delta}(z)\frac{1}{z-H_0}V_{\Delta\Delta}(z) \quad (1)$$

where $V_{OBE}$, for example, has the form

$$V_{OBE}(z)=W\frac{1}{z-H_0}W \quad (2)$$

with W representing the NN-meson vertex and z is the starting energy. For $V_{N\Delta}$ and $V_{\Delta\Delta}$, either one or both W must be replaced by the N$\Delta$-meson vertex. It is clear that eqs. 1 and 2 are different from the interaction in the two-body system due to dispersion effects in the propagators and Pauli effects. The first potential MDFP 1 is given by eq. 1 and includes only the $N\Delta\pi$ vertex while the second potential MDFP 2 also includes the $N\Delta\rho$ vertex. The third new potential MDFPE is a OBE potential with MDF (given by eq. 2), but uses the eikonal form factor, which approximately sums a certain class of higher-order diagrams, to regularize divergencies instead of the standard phenomenological form factor of the dipole type.

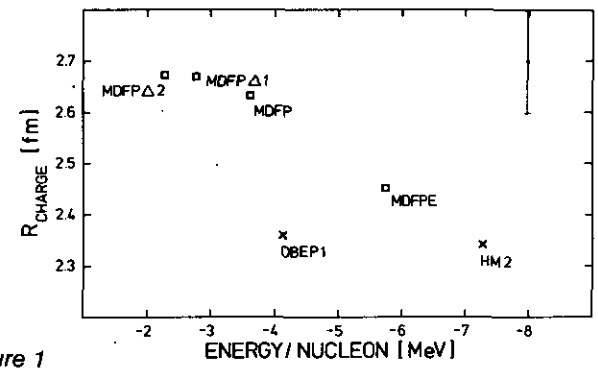


*Figure 1*

The results from a Brueckner-Hartree-Fock (BHF) calculation in $^{16}O$ are shown in the figure. Here, an improved technique is used which involves the direct solution of the BHF equations instead of using the local density approximation as in previous work[2,4]. In addition to the results from the new potentials described above, results from three others are included for comparison: 1) OBEP1, a standard OBE potential, 2) HM2, a OBE potential with eikonal form factor and 3) MDFP, a OBE potential with MDF. Although the results are not shown, calculations are also made in infinite nuclear matter.

There are three main conclusions that can be drawn: 1) The MDF are found to play a significant role by introducing additional density dependence which yields a large improvement of the radius in $^{16}O$ with only a small change in the binding energy. 2) When IDF are added to the MDF, repulsion is obtained in $^{16}O$ with a corresponding increase in radius. 3) The use of the eikonal form factor results in attraction and this persists when it is used in a potential that includes MDF.

*) University of Bonn

#### References

[1] G.E. Brown and A.D. Jackson, The Nucleon-Nucleon Interaction (North-Holland, Amsterdam, 1976)
[2] A. Faessler, H. Müther, R. Machleidt and D. Schütte, Nucl. Phys. A262 (1976) 389
[3] K. Kotthoff, R. Machleidt and D. Schütte, Nucl. Phys. A264 (1976) 484
[4] K. Holinde, R. Machleidt, A. Faessler and H. Müther, Phys. Rev. C15 (1977) 1932
[5] K. Holinde and R. Machleidt, Nucl. Phys. A280 (1977) 429

### 4.4.2. Isobar Contributions to the Two-Nucleon Interaction Derived from Non-Covariant Perturbation Theory

K. Holinde*), R. Machleidt*), M.R. Anastasio, A. Faessler and H. Müther

One of the main reasons for explicitly including isobar degrees of freedom in the two-nucleon interaction is to allow modifications of this interaction due to the presence of other nucleons. These isobar degrees of freedom arise, e.g. from the excitation of a $\Delta$-resonance through a meson exchange and then its de-excitation through a second meson exchange. It is already known that such many-body effects play a large role in relatively dense systems such as nuclear matter[1] and even in light nuclei like $^{16}O$[2]. There are also good reasons to believe that the empirical saturation point in nuclear matter cannot be reached without such density dependent modifications.

The isobar contributions are included by starting from a semitheoretical one-boson-exchange potential and replacing part of the $\sigma$-meson, describing the intermediate range attraction, by

twice-iterated transition potentials with both $\pi$ and $\rho$-meson exchange. Both the contributions from the NN → NΔ and NN → ΔΔ transitions are included. Previously, the transition potentials have been considered with a simple pion-range propagator. However, the transition potential approach can handle those time-ordered diagrams which have purely baryonic intermediate states, i.e. the first 4 of the possible 12 diagrams shown in the figure for NN → NΔ and it is a matter of some controversy whether the simple pion-range propagator can provide a realistic description. Estimates based on dispersion theory indicate that the use of this propagator overestimates the isobar contribution by a factor of 2 or 3.

It is clear that the reason that an explicit calculation of the time-ordered diagrams has been avoided is the difficulty in analytically transforming into r-space the expressions for the propagators which are defined in momentum space. Since our work is done in momentum space these difficulties are avoided. Furthermore, the use of time-ordered perturbation theory provides a well defined procedure for going from the two-body to the many-body problem[3].

In this work, a study is made of the inclusion of $\rho$-exchange in the transition potentials and of the use of the exact time-ordered propagators. The results show that both effects strongly reduce the isobar contribution with pion range found previously[1]. This allows the use of cutoff parameters at the NΔπ vertex that are in a much more reasonable range. The use of the simple pion-range (or rho-range) propagator instead of the time-ordered one seriously overestimates the isobar contribution by as much as a factor of 3. Since these calculations are made in momentum space, the effects of taking the static limit (also necessary in r-space calculations) can also be studied and this leads to an underestimation of roughly a factor of 2. Consequently, the combined use of simple pion-range propagators and the static limit in the transition potentials overestimates the isobar contribution relative to the relativistic case with time-ordered propagators by a factor of 2, a similar result to that

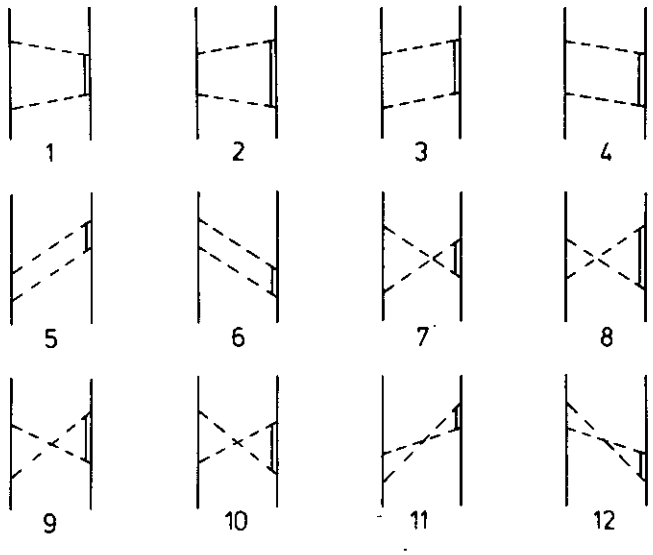


*Figure 1*

obtained with dispersion theory. However, this effect is different in different partial waves so that it cannot be adequately mocked up by a simple change of parameters. This is true as well for the inclusion of $\rho$-meson exchange which leads to an improvement of the description of $^3$P partial waves.

*) University of Bonn

### References


[1] K. Holinde and R. Machleidt, Nucl. Phys. A280 (1977) 429
[2] K. Holinde, R. Machleidt, A. Faessler and H. Müther, Phys. Rev. C15 (1977) 1432
[3] D. Schütte, Nucl. Phys. A221 (1974) 450


## 4.4.3. Modification of the Migdal Interaction by the One-Pion-Exchange Potential


V. Klemt, J. Speth, J. Wambach


The density dependent zero range residual ph interaction of the form:

$$F^{ph}(\vec{r},\vec{r}') = C_0\,\delta(\vec{r}-\vec{r}')\;\{f_0(\rho) + f'_0(\rho)\,\vec{\tau}\cdot\vec{\tau}' + g_0\,\vec{\sigma}\cdot\vec{\sigma}' + g'_0\,\vec{\sigma}\cdot\vec{\sigma}'\,\vec{\tau}\cdot\vec{\tau}'\} \qquad (1)$$

originally proposed by Migdal, has been applied very sucessfully to many nuclear structure problems[1]. Since the one pion exchange potential (OPEP) is long range it seems important[2] to take into account this part of the interaction explicitly. As long as we restrict ourself on the direct term, one only gets a contribution to the $\sigma\cdot\sigma'$ $\tau\cdot\tau'$-part of eq. 1, of the form:

$$g'_0\,\delta^3(r) \rightarrow g'_0\,\delta^3(r) - C_Y + c_Y\,\frac{m_\pi^3}{4\pi}\left[V_Y(r)+V_T(r)\right] \qquad (2)$$

Here $V_Y(r)$ is the Yukawa force, V the tensor force and $C_Y$ a parameter.

| force | $E_1$ | $E_2$ | $B_1$(M1) | $B_2$(M1) | $h_{9/2}h^{-1}_{11/2}$ $i_{11/2}i^{-1}_{13/2}$ first state | | $h_{9/2}h^{-1}_{11/2}$ $i_{11/2}i^{-1}_{13/2}$ second state | |
|---|---|---|---|---|---|---|---|---|
| a | 7.41 | 7.85 | 3.10 | 15.12 | 0.92 | -0.42 | 0.42 | 0.92 |
| b | 7.26 | 7.56 | 12.87 | 6.20 | 0.99 | 0.11 | -0.11 | 0.99 |
| c | 6.38 | 7.55 | 0.64 | 11.99 | 0.78 | -0.63 | 0.63 | 0.78 |

*Table: Energies [MeV], B(M1)-values [(nm)²] and amplitudes of the lowest two 1⁺ level in $^{208}$Pb calculated with different forces.*

a) Purce δ-force b) *δ-force + Yukawa + tensor (direct term only)* c) *δ-force* + tensor (direct + exchange term)

The influence of the OPEP on magnetic dipole resonances in $^{208}Pb$ is shown in the table. From these results one notices appreciable changes compared to the original δ-force. More detailed investigations are in progress.


**References**

[1] J. Speth, E. Werner and W. Wild, Phys. Rep. 33C (1977) 127
[2] M.R. Anastasio and G.E. Brown, Nucl. Phys. A285 (1977) 516


## 4.4.4. Influence of the Finite Range and Tensor Part of the ph-Interaction on M2-Resonances


V. Klemt, J. Speth, J. Wambach


In connection with the pion-condensation in nuclei it has been argued that the one-pion-exchange (OPEP) part of the ph-interaction should be taken into account explicitely. Therefore we have modified Migdal's density dependent zero range force by including this part of the interaction explicitely. Because of selection rules the magnetic resonances are only influenced by the spin dependent parameters. Therefore they provide an excellent tool to investigate the influence of the OPEP contribution. In the following table we show the preluminary results of our investigation using different ph-interactions:

(i) In the first row the original result[1] using a pure δ-force is shown. The B(M2)-strength around 7.5 MeV is concentrated mainly in one state (the strength of the other states in that energy range is at least two orders of magnitude smaller).

(ii) In the second row the direct term of the OPEP is taken into account. Here we only get a change in the $\sigma \cdot \sigma' \tau \cdot \tau'$-channel (see eq. 2 of the preceeding article) and the $g'_0$ is effectively reduced.

(iii) If we include also the exchange contribution of the OPEP (third row) than one obtains drastically changes. The $2^-$-resonance is split into 4 strong states. This is due to the exchange term which reduces the $g_0$-parameter and increases the $g'_0$-parameter. We have now the situation that effectively $g_0$ and $g'_0$ are no longer roughly equal as one would expect from the analysis of magnetic moments. More detailed investigations are in progress.

*Table 1:*
*M2-strength distribution in $^{208}Pb$ around 7.5 MeV calculated with different forces*

| force | energy | B(M2) [(fm n.m.)$^2$x10$^4$] |
|---|---|---|
| δ-force | 7.49 | 1.015 |
| δ-force | 7.46 | 0.996 |
| + Yukawa + tensor | | |
| (direct term only) | 7.93 | 0.104 |
| δ-force | 6.23 | 0.130 |
| + Yukawa + tensor | 7.35 | 0.292 |
| (direct + exchange) | 7.49 | 0.464 |
| | 7.94 | 0.233 |


**References**

[1] P. Ring and J. Speth, Phys. Lett. 44B (1973) 477


## 4.4.5. Pion Condensation in a TDHF-Approach


S. Krewald, J.W. Negele*), E.J. Moniz*)


A phase transition in nuclear matter at high densities has been suggested in several nuclear matter calculations. The attractive P-Wave part of the One-Pion-Exchange-Potential (OPEP) will make a spin-isospin fluctuation in the new ground state („Pion Condensate") at about twice normal nuclear matter density. One of the characteristic observable consequences of this phase transition is the emission of pions, knocked out of the coherent condensate on the mass shell by a nuclear Compton effect. The advent of relativistic heavy ion beams has made possible the experimental investigation of nuclear matter under densities probably high enough for a phase transition.

Since all existing calculations are restricted to infinite systems, it has to be analysed, whether a phase transition would not be suppressed by finite time effects in an actual reaction. A unique opportunity to describe both the mechanism of a heavy ion reaction and the dynamical onset of the phase transition simultaneously is given by the Time-Dependent-Hartree-Fock (TDHF) theory. Once the initial conditions, i.e. the relative velocity of the two heavy ions, are given, the reaction process is fully determined. The signal for the onset of a phase transition is the sudden growth of spin-isospin waves. This is information enough to determine a characteristic signature in the spectrum of outgoing pions. In order to describe the evolution of the condensed phase, one would have to extend the TDHF-theory to include correlations.

The interaction in the spin-isospin channel is taken from nuclear matter calculations. It consists of the OPEP-potential and a repulsive point-coupling. In nuclear matter estimates, the $\Delta_{33}$-resonance was shown to counteract drastically the inhibiting effects of nuclear correlations. It can be effectively included by using a renormalized coupling strength $f^2_{eff} = 1.8\, f^2$, as suggested by Brown and Weise. The correlation parameter $g'_0$ is taken from the calculation of Speth et al. The TDHF-equations are solved in coordinate

space using a Pade-approximation to the evolution operator exp (−iHt).

With the present Hamiltonian, nuclei are found to be very soft against condensation. This is a discrepancy between nuclear matter predictions and finite nuclei. In nuclear matter, translational invariance requires the single particle states to be plane waves, whereas in a finite nucleus, the wavefunctions are entirely free to change their shapes, which results in an earlier onset of the instability.

The influence of various approximations, such as the omission of the $\rho$-meson exchange potential, have to be tested, before definite conclusions can be drawn.

*) MIT, Cambridge, Mass., USA

## 4.4.6. On Pion Condensation in Finite Nuclei

J. Meyer-ter-Vehn

The critical pionic mode leading to pion condensation is investigated for finite nuclear systems. The critical density and the critical angular momentum are calculated for some closed-shell nuclei and are compared with infinite nuclear matter results based on the same model[1].

The model treats the infinite system of nucleons as a Fermi gas and the finite system as an harmonic oscillator. For the pion self-energy in the nuclear medium, only the lowest order diagram shown in fig. 1 is taken into account with bare, non-relativistic, p-wave $\pi$-nucleon coupling. This model neglects important physical effects such as isobar excitation and repulsive baryon interactions and is clearly insufficient to calculate the absolute value of the critical density. In fact, the critical density for symmetric nuclear matter is obtained to be $\rho_{crit}^{N.M.} \cong 0.27\ \rho_0$ ($\rho_0 = 0.5\ m_\pi^3$) and the critical momentum $k_{crit} = 1.9\ fm^{-1}$. However, the model may provide a reasonable estimate for the ratio of the critical densities in infinite and finite systems and for the angular momentum $L_{crit}$.

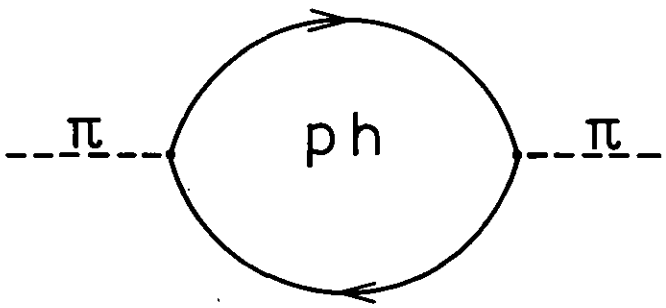


*Figure 1:*
*Diagram for the pion selfenergy of the model.*

For the finite nuclear system, the Klein-Gordon equation takes the form

$$(m_\pi^2 - \nu^2)\,\Psi^\pi(r) - \int d^3r' \cdot \Pi^{(o)}(r,r';\omega,\rho)\Psi^\pi(r') = \omega^2\Psi^\pi(r) \qquad (1)$$

Here, the selfenergy diagram in fig. 1 appears as a nonlocal potential $\Pi^{(o)}(r,r';\omega,\rho)$. The single nucleon states are described by harmonic oscillator (H.O.) wave functions

$$\phi_{n\ell m}(r) = b^{-3/2}\,\varphi_{n\ell}\left(\frac{r}{b}\right) Y_{\ell m}(\Omega) \qquad (2)$$

with energies $E_N = \hbar\omega_o\,(N + 3/2)$. The oscillator length is $b^2 = \hbar/m\omega_o$. The critical pionic wave function $\psi^\pi(r)$ is also expanded in the H.O. basis

$$\Psi^\pi_{LM} = \sum_N C_N^{(L)}\ \phi^\pi_{NLM} \qquad (3)$$

Equation (1) then comes down to the diagonalization problem

$$\sum_{N_2} \langle \phi^\pi_{N_1 L} | m_\pi^2 - \nu^2 - \Pi^{(o)}(\omega,\rho) | \phi^\pi_{N_2 L}\rangle C^{(L)}_{N_2} = \omega^2 C^{(L)}_{N_1} \qquad (4)$$

The p-wave potential is obtained as

$$\langle \phi^\pi_{N_1 L} | \Pi(\omega = 0) | \phi^\pi_{N_2 L}\rangle = 4\left(\frac{f}{m_\pi}\right)^2 \frac{m_N}{b^3}\, V(N_1, N_2, L) \qquad (5)$$

with

$$V(N_1, N_2, L) = 2 \sum_{\substack{m > \nu_F \\ i < \nu_F}} \frac{\langle \phi_m | b^{5/2}\nu\phi_{N_1 L} | \phi_i^*\rangle \langle \phi_m | b^{5/2}\nu\phi^\pi_{N_2 L} | \phi_1\rangle}{(N_m - N_i)} \qquad (6)$$

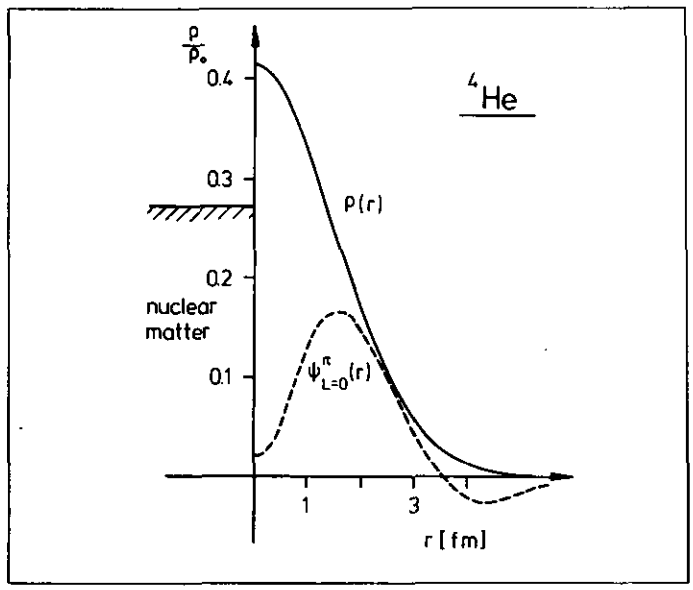


*Figure 2:*
*The density of nuclear matter (left side) and the nuclear density distribution of the A = 4 system (right side) at threshold to ion condensation in units $_o = 0.17\ fm^{-3}$. The broken line shows the critical pionic wave function.*

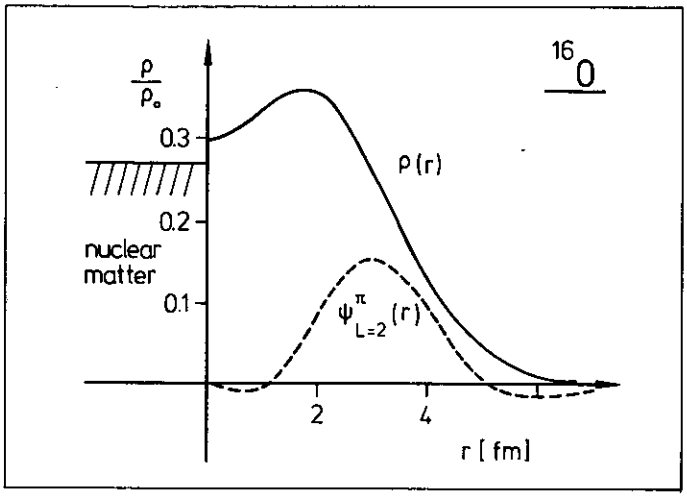


*Figure 3:*
*Same as fig. 2, but for the A = 16 system.*

*Table 1*

| | L [h] | $b^{(L)}_{crit}$ [fm] |
|---|---|---|
| A=4 | 0 | 2.16 |
| ($^4$He) | 2 | 1.30 |
| | 1 | 1.35 |
| A=16 | 2 | 2.43 |
| ($^{16}$O) | 0 | 2.37 |
| | 1 | 2.10 |
| | 4 | 1.65 |
| A=40 | 0 | 3.11 |
| ($^{40}$Ca) | 2 | 2.86 |
| | 1 | 2.69 |
| | 4 | 2.68 |
| | 3 | 2.53 |

Critical oscillator lengths for pion condensation in closed-shell systems with different particle number A and different angular momenta of the critical pionic state.

The critical pionic mode is characterized by a lowest eigenvalue $\omega^2 = 0$ of eq. (4), and the critical density is the lowest density for which this happens. Since the nuclear density varies with radius in the finite system, we use the oscillator length b as a measure for the overall density ( $\rho \sim b^{-3}$). The pionic mode with largest $b^{(L)}_{crit}$ (lowest overall density) represents the condensation mode and defines the critical angular momentum $L_{crit}$.

Results for closed-shell systems with 4, 16 and 40 nucleons are shown in table 1 and fig.s 2, 3. In table 1, critical values of the oscillator length are given for different angular momenta of the pionic state. For the A = 4 system, the most critical pionic mode has L = 0. The corresponding nuclear density distribution at $b^{(L=0)}_{crit}$ is shown in fig. 2 and is compared with the critical density of nuclear matter (left side) calculated within the same model. The critical pionic wave function $\psi_{L=0}$ is also shown. Pionic modes with L = 1, 2 become critical only at higher nuclear density. For the A = 16 system (fig. 3), the L = 2 mode turns out as most critical, closely followed by the L = 0 mode. For A = 40, L = 0 comes first, followed by L = 2, 1, and 4. The relative suppression of the L = 1 mode is a shell effect. Due to parity selection, odd L modes cannot couple to 1 $\hbar\omega$ nucleon particle hole states and are therefore unfavoured. Higher L modes are suppressed since they do not fit into the finite geometry.

The present model calculation suggests the following conclusions: (1) The critical density for pion condensation in finite nuclear systems is close to that of nuclear matter already for small particle numbers. Within the model, the central density of $^4$He at $b_{crit}$ is 50 % larger than $\rho_{crit}$ in nuclear matter, and the central density of $^{16}$O at $b_{crit}$ is 10 % larger. Apparently, the nuclear surface region has little influence on $\rho_{crit}$. (2) Concerning angular momentum, pionic modes with $L < R_c \cdot k_{crit}$ tend to become critical simultaneously. Here, $k_{crit}$ is the critical momentum for pion condensation in nuclear matter and $R_c$ is the radius of the central region of the nucleus. However, odd-L modes are suppressed in light closed-shell systems due to shell effects. (3) Already in light systems such as $^{16}$O, the L = 2 mode is as critical as the L = 0 mode. To check how close (or far) normal nuclei are from threshold to pion condensation, one should therefore consider $2^-$ nuclear states as well as $0^-$ states.

The author acknowledges helpful discussions with the SIN theory group and with W. Weise.

**Reference**

[1] J. Meyer-ter-Vehn, submitted to Z. Physik

## 4.5 High and Very High Spins

### 4.5.1. Angular Momentum Fluctuations in the Cranking-Model

F. Grümmer, K.W. Schmid, A. Faessler

The two most important methods for the description of rotational states in nuclei are the angular momentum projection techniques[1] and the selfconsistent crancing-model[2,3]. The shortcoming of angular momentum projection from a single HFB-wavefunction is the fact that one misses the degree of freedom connected with rotational alignment (RAL), which becomes important in the „backbending"-region. Using the selfconsistent cranking-model one can include this degree of freedom by breaking all symmetries except of the symmetry under rotations $e^{i\pi j_x}$. One of the conditions for the validity of the cranking-model is, however that the corrections due to the angular momentum fluctuations should not vary very much within the rotational band. Recently Hamamoto[4] pointed out that this is not the case if one describes a region where two bands are crossing. Since in this paper a simple particle plus rotor model for $i_{13/2}$ neutrons was used, we reinvestigated this effect using more realistic cranking-wave functions like in ref. 2. In addition we performed a more detailed analysis of these wavefunctions using angular momentum projection. We calculated the quantities

$$n^J_{KK'} = \frac{2J+1}{8\pi^2} \int d\Omega\, D^{J*}_{KK'}(\Omega) \cdot \langle \phi | R(\Omega) | \phi \rangle$$

and

$$n^J = \sum_{KK'} n^J_{KK'} \cdot \delta_{KK'}$$

As a first step we analyzed cranking-wavefunctions for $^{162}$Er with fixed deformations $\beta = 0.3$, $\gamma = 0.0$ and paring gaps $\Delta_p = \Delta_n = 0.9$ MeV. Fig. 1 shows the expectationvalues $\langle J_x \rangle$ and $\langle (\Delta J)^2 \rangle$ as a function of the cranking frequency $\omega$. Between $\omega = 0.28$ and 0.30 a rapid increase of $\langle J_x \rangle$ due to the rotational alignment of two $i_{13/2}$ neutrons is accompanied by a sharp peak in the angular momentum fluctuation. The second peak at $\omega \simeq 0.45$ is connected with the rotational alignment of two $h_{9/2}$ protons. Fig. 2 shows the angular momentum distributions of the cranking-wavefunctions corresponding to the average expectation values $\langle J_x \rangle = \sqrt{I(I+1)}$, where I is the number at each curve. In this figure one sees clearly the reason for the increase of the angular momentum fluctuation in the backbending region. Up to spin 12 more average angular momentum is gained by shifting the maximum of the distribution slowly to higher angular momentum and broadening of the distribution. The maximum width is reached for spin 14. Beginning with spin 16 more angular momentum is obtained by having more strength again in the components with higher spin which is an indication for the change of the structure of the wavefunction.

Preliminarily one may say that also with realistic cranking-wavefunctions one runs into difficulties in the band-crossing region, since the angular momentum fluctuations are much larger there than in the other parts of the rotational band. But more detailed investigations have to be performed, in order to say wether the cranking-model is able to describe the backbending region or not.

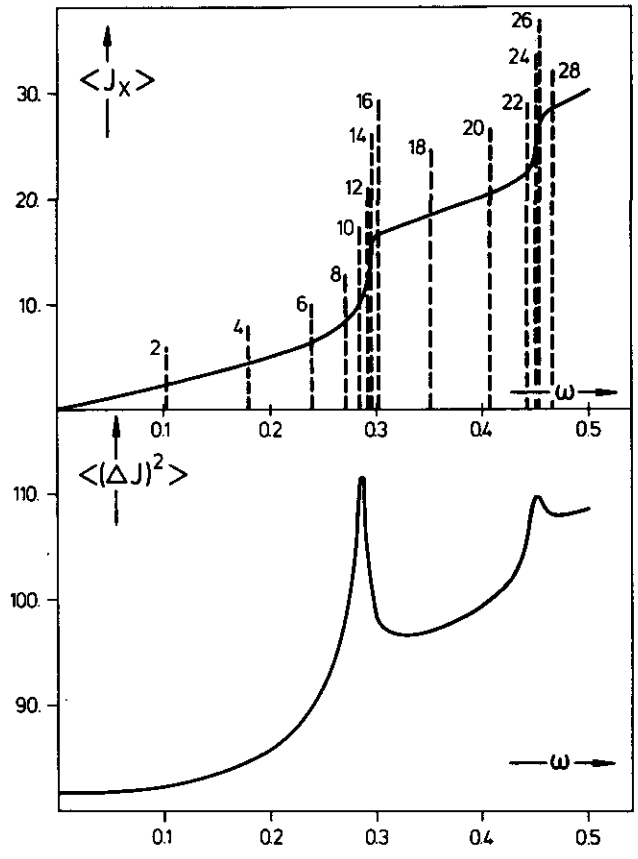


*Figure 1*

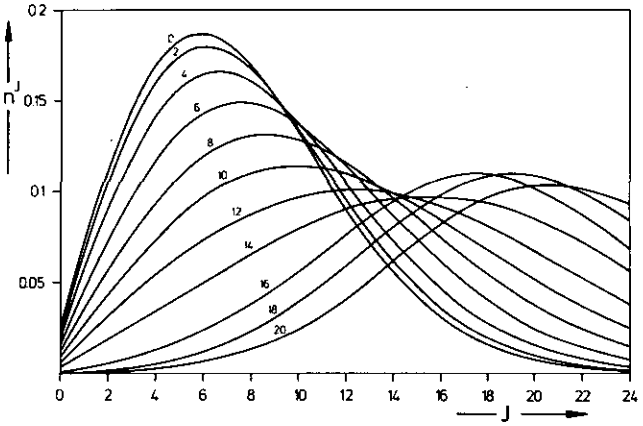


*Figure 2*

### References

[1] F. Grümmer, K.W. Schmid, A. Faessler, Nucl. Phys. A239 (1975) 289
[2] A. Faessler, K.R. Sandhya Devi, F. Grümmer, K.W. Schmid, R. Hilton, Nucl. Phys. A256 (1976) 106
[3] B. Banarjee, H.J. Mang, P. Ring, Nucl. Phys. A215 (1973) 266
[4] I. Hamamoto, Nucl. Phys. A271 (1976) 15

to zero the cyclotron frequency has to be adjusted by the aid of the time spectra. The spectrum on the top shows a result for a frequency detuned by $\Delta f/f = 7.5 \cdot 10^{-5}$. The spectrum in the middle shows the result of the optimized frequency. Since we intend to cut the phase width of the beam in the next future, we hope to get a better reproducibility in the beam fall time. To cover, however, the lacking time range between 100 and 1000 ns an external pulsing system will be developed.


**References**

[1] Annual Report 1974, KFA-IKP 1O/75, p. 345
[2] R. Brings, G. Lürken, P. Wucherer, Annual Report 1975, KFA-IKP 1O/76, p. 248
[3] N. Dolfus, Work for Examination as Engineer 1977
[4] P. Kleinheinz, this Report, p. 39
[5] J. Linz, this Report, p. 123


### 7.6. Status of Beam Quality Improvement


W. Bräutigam, J. Linz, J. Reich, and P. Wucherer


1. Coherent amplitude correction

During the last shut-down time harmonic coils[1] have been built in near the cyclotron center together with new isochronous trim coils[2]. The first tests showed, that any radial coherent amplitude of $A_c \leq 5$mm generated during the first revolutions can be compensated directly at small machine radii. Before having the full benefit of the minimization of the coherent amplitude by the inner harmonic coils, asymmetries in the main magnetic field, which lately have been observed as excentricities of the beam at all radii, have to be analysed and corrected. The observed asymmetries can generate coherent amplitudes especially at larger radii, which therefore cannot be compensated by the inner harmonic coils.

2. Phase optimization

An iterative procedure for phase optimization is now working reliably in the complete energy range of JULIC[3]. The corresponding necessary phase measurements are carried out by intercepting the beam with an internal probe and measuring the time distribution of prompt $\gamma$'s. For a quicker access to the phase data a new non intercepting phase measuring equipment[4] is getting completed and will be installed in 1978.

3. Axial phase selection

Calculations have been carried out to find the optimum possible location of two slits near the cyclotron center for axial phase selection. The results show, that it should be possible to reduce the present phase width of the beam ($\Delta\Psi = 24^\circ$ RF) by a factor of two. The corresponding axial phase slits, which have been developed, are now ready for use and will be built in and tested in the near future.


**References**

[1] R. Brings, J. Linz, P. Wucherer, Annual Report 1976, KFA-IKP 1O/77, p. 122
[2] W. Bräutigam, R. Fiedler, W. Klein, U. Rindfleisch, P. Wucherer, Annual Report 1975, KFA-IKP 1O/76, p. 246
[3] J. Linz, this report, p. 123
[4] W. Bräutigam, M. Herschbach, K. Kannepohl, J. Reich, Annual Report 1976, KFA-IKP 1O/77, p. 123


# 8. Magnet Spectrometer

### 8.1. The Magnet Spectrometer BIG KARL


A. Hardt, W. Huerlimann, M. Koehler*), S. Martin, J. Meissburger, A. Retz, T. Sagefka, and O.W.B. Schult


1. Status of the magnet spectrometer BIG KARL

During the last period the following components have been built or installed at the BIG KARL[1,2] experimental area:

- The beam line design has been completed and the components are ready.
- The instrumentation of the whole system is nearly completed. This includes the cooling water system, the cables for power and electronic signals, the air pressure system for moving the support and the CAMAC installations for connection to the online computer PDP 11/40.
- Computer control of all components such as power supplies and field measuring devices is available through a package of modular test and service routines at Fortran level. Complete programs and a file handler with user defined Fortran interface allow easy data acquisition and processing.
- The power supplies of the 5 magnets and the 24 correction elements have been tested.
- Magnetic measurements on different antimagnetic material have been performed[3]. The effects of Ht field correction windings have been studied and found to be in good agreement with the theoretical model.
- The scattering chamber and the vacuum box for the detector system are assembled and mechanically tested.
- The magnets Q1, Q2 and D1 have been assembled in their final positions on the support.
- The magnetic field measurements for the dipole magnets D1 and D2 are going on. The D2 magnet has been assembled in a separate place in the experimental area.
- The vacuum tests using cryo pumps have been carried out for the scattering chamber and the detector box.
- A measurement of the inelastic alpha-scattering at $^{12}C$ using the multi-wire proportional chamber in a small QDQQ magnet spec-

## 7.5. Extension of the Internal Macroscopic Beam Pulsing into the μ sec-Region

R. Brings, N. Dolfus, P. Wucherer

At JULIC fast and slow pulsing devices are in operation acting both on an internal axial deflector[1,2]. Between the time ranges corresponding to the fast (microscopic) and the slow (macroscopic) pulsing existed a lacking time region[2] from ≃ 130 ns to ≃ 500 μs. The lower limit of this region cannot be highered using internal deflection[1] but the upper limit can be lowered into the μs-region. This upper limit depends on the time spread caused by different energy gains of the particles during accelleration. The accelleration time is different for the particles within a beam burst (caused by the cosinelike accelleration voltage) and also for different beam bursts (caused by rf-resonator noise). At present the phase width for 99 % of the beam is $2\Delta\psi_b \simeq 24^\circ$ rf. The resonantor noise causes a phase jitter at extraction radius of $2\Delta\psi_j \simeq 1^\circ$ rf. To get a figure for the necessary voltage rise and fall times of the planned pulse generator the minimum possible beam fall time, $\Delta t_b$, has to be estimated from

$$\Delta t_b \simeq t_{0/2}(\Delta\psi_b^2 + \Delta\psi_b \cdot \Delta\psi_j + \Delta\psi_j^2/3).$$

Since the accelleration time $t_o$ is approx. 60 μs the result is $\Delta t_b \simeq$ 2 μ sec.

The electronics of the experiments in nuclear spectroscopy have dead times of about 10 μs. Therefore the repetition frequency, $f_r$, which determines the required power of the pulse generator, can be $< 10^5$ Hz.

The principal elements of the push-pull generator (see fig. 1) are two pairs of tubes, which serve as fast switches. The internal deflector is switched to a positive or negative deflection voltage, U, or to ground, respectively. The spectrum of the available tubes shows a lack in the medium range of > 50 Watts. After some lifetime tests with higher power but additional air cooling we decided to use the cheap pentode „PL 519" which normally should operate below 50 Watts. At the maximum energy of JULIC a deflection voltage of U ≃ 4 kV is needed. If we limit the power to P = 400 Watts - i.e. 100 Watts per tube - the lifetime of the tubes is 3 to 4 days at a repetition frequency of $f_r = P/(C \cdot U^2) = 80$ kHz (loading capacity C = 300 pF). At the lowest α-energy, which at present is mostly used for spectroscopy experiments, $f_r$ can be raised to > 100 kHz and the tubes live for weeks.

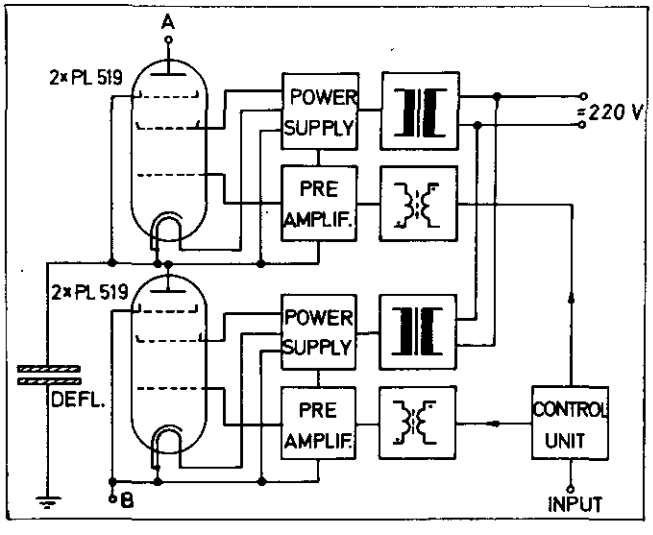


*Figure 1:*
*Schematic diagram of the pulse generator*

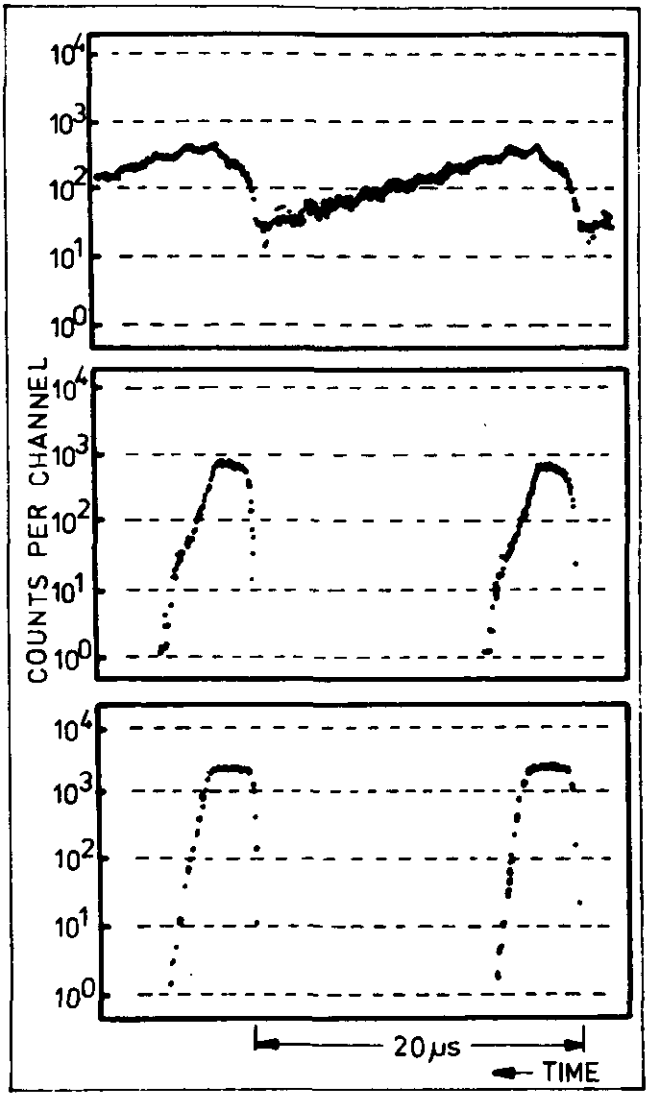


*Figure 2:*
*Time spectra of external beams of α-particles, top: 90 MeV α, cyclotron-rf detuned by 7.5 · 10⁻⁵; middle: 90 MeV α, cyclotron-rf optimized, bottom: 106 MeV α, beam fall time to 1 % amounts to 1.6 μs.*

The rise and fall time of the pulse is given by $\Delta t_p = C \cdot U/I \leq 250$ ns (pulse current for two tubes I = 5 A) which has to be compared with the beam intensity fall time $\Delta t_b \simeq 2$ μs from Eq (1). Fig. 1 shows the schematics of the electronics[3]: The control grids of the tubes are triggered via two separate preamplifiers by a common control unit, which mainly controls the push-pull operation. Both, the power supplies and the preamplifiers are DC-decoupled from the line and the control unit, respectively. This enables a free choice of the sign of the deflection voltage: If a positive voltage results in an easier beam suppression point A is connected to a positive DC-voltage and point B to ground. In the opposite case point B is connected to a negative DC-voltage and point A to ground.

Fig. 2 shows as results with the macroscopic internal pulsing, time spectra on log scale of 90 MeV (the upper two) and 106 MeV α-particles (bottom). At 106 MeV the best result up to now has been achieved: The beam fall times from 90 % to 10 % and to 1 % of the maximum intensity are 0.5 and 1.6 μs, respectively. During this run a lifetime of 560 ns could be measured[4]. One of the presuppositions to reach the theoretical limit of equation (1) is a nearly zero beam phase along the radius. These results therefore became possible for the first time after the iterative optimization of the beam phase was realized[5]. To bring the averaged phase exactly

The control matrix C can be calculated from the trim coil vectors $\vec{\pi}_j$, which again can be calculated either from field measurements or phase measurements with the cyclotron beam. The determination of the control matrix is afflicted with errors, especially due to the poor reproducibility of the trim coil fields because of hysteresis effects. This fact might influence the convergence of the control scheme severely as is illustrated in fig. 1 in a two dimensional subspace. In both cases (A) and (B) a desired vector $\vec{r}_d$ is to be composed from two base vectors $\vec{\pi}_1$ and $\vec{\pi}_2$. In both cases we also assume, that because of errors the real base vector $\vec{\pi}_{2r}$ differs from the calculated vector $\vec{\pi}_2$ by the same angle of rotation $\Theta$. It is clearly to be seen, that in case (B) the achieved vector $\vec{r}_a$ differs much less from the desired vector $\vec{r}_d$ than in case (A). This is due to the fact, that in case (B) the calculated base vectors are orthogonal, whereas in case (A) they are far from orthogonality.

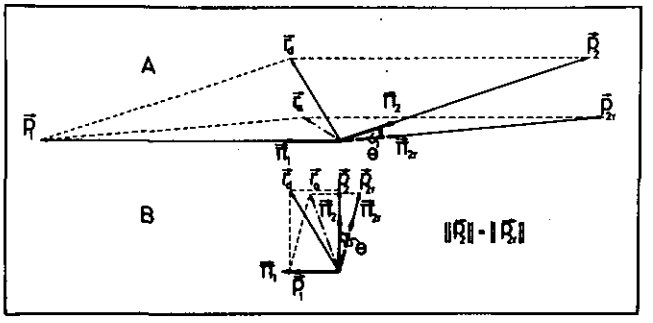


*Figure 1:*
*Difference between desired and achieved vector ($\vec{r}_d$,$\vec{r}_a$, resp.) to be composed from two base vectors ($\vec{\pi}_1$,$\vec{\pi}_2$) either being far from orthogonality (A) or being orthogonal (B), in case the determination of the base vector $\vec{\pi}_2$ is afflicted with an error.*

Therefore it is necessary to choose the „most orthogonal" set of trim coil vectors. The first two „most orthogonal" vectors $\vec{\pi}_k$ and $\vec{\pi}_l$ are found from the minimum of the inner product of all pairs of the coil vectors

$$\min_{i,j} \left| \frac{\vec{\pi}_i \cdot \vec{\pi}_j}{||\vec{\pi}_i|| \; ||\vec{\pi}_j||} \right| \Rightarrow a_{k\ell} \qquad (5)$$

The next „most orthogonal" vector $\vec{\pi}_q$ with respect to $\vec{\pi}_k$ and $\vec{\pi}_l$ is found by looking at the maximum of the inner products of all possible linear combinations of $\vec{\pi}_k$ and $\vec{\pi}_l$ and any other vector $\vec{\pi}_j$ and taking the minimum of the set of maxima

$$\min_{j\neq k,\ell} \left( \max_{\lambda_k,\lambda_\ell} \left| \frac{(\lambda_k\vec{\pi}_k+\lambda_\ell\vec{\pi}_\ell)\cdot\vec{\pi}_j}{||\lambda_k\vec{\pi}_k+\lambda_\ell\vec{\pi}_\ell|| \cdot ||\vec{\pi}_j||} \right| \right) \Rightarrow c_q \qquad (6)$$

This is carried on with the 3 vectors $\vec{\pi}_k$, $\vec{\pi}_\ell$, $\vec{\pi}_q$, and any other vector $\vec{\pi}_j$ and so forth. The process is stopped in case the values of the inner product get „too close" to one. What „too close" means, has to be estimated from the accuracy in determining the trim coil vectors $\vec{\pi}_j$.

At JULIC the phase is measured at n = 12 different radial positions (see equation (2)). The distance between each two positions covers about the same number of turns (38). m = 7 trim coils are used in the control scheme.

So far we did not talk about the fact that the mean field level $\bar{B}$ has to be changed when variing the energy. In general the control matrix C is depending in a non-linear manner on the field level $\bar{B}$. Nevertheless, a good iterative phase optimization in less than 4 steps was achieved at any filed level just by multiplying the one control matrix $C_o$ in the following manner:

$$C_{new} \approx \frac{\bar{B}_{new}}{\bar{B}_o} C_o \,. \qquad (7)$$

The matrix $C_o$ was calculated from phase as well as field measurements performed at $\bar{B}_o$ = 12.8 kG. Fig. 2 shows results of the iterative phase optimizations for 3 different main field values $\bar{B}$, distributed in the region covered at JULIC.

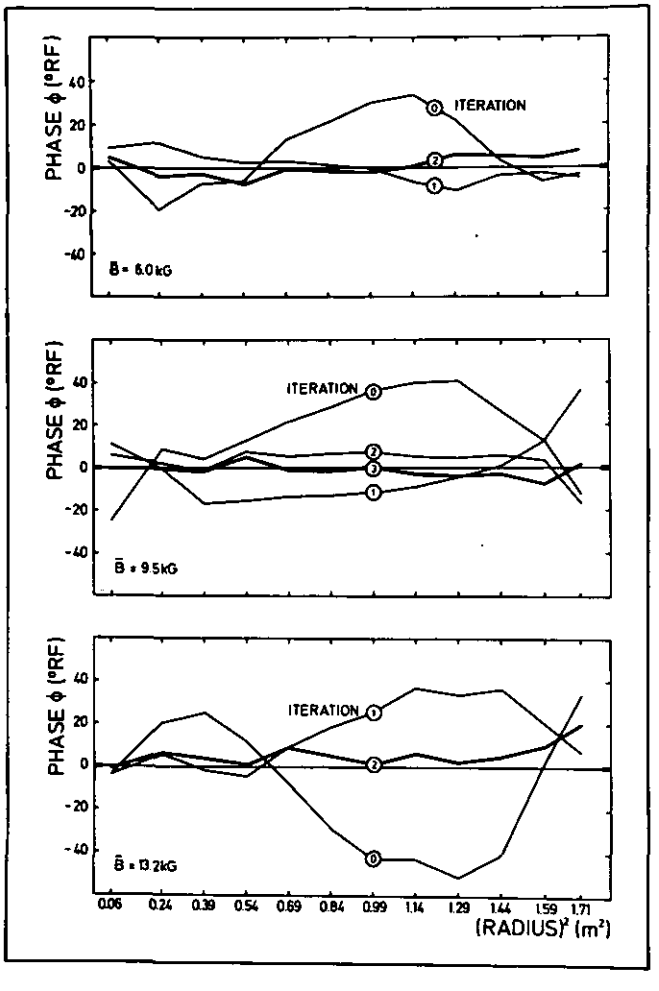


*Figure 2:*
*Iterative optimization of the beam phase performed at three different field levels $\bar{B}$ in the JULIC tuning range (for protons of 35 MeV and α-particles of 90 and 172.5 MeV, respectively).*

The author acknowledges the good cooperation with G.C.L. van Heusden[1] and W. Schulte from the Eindhoven University of Technology (EUT) cyclotron laboratory.

**Reference**

[1] G.C.L. van Heusden, EUT Thesis (1976)

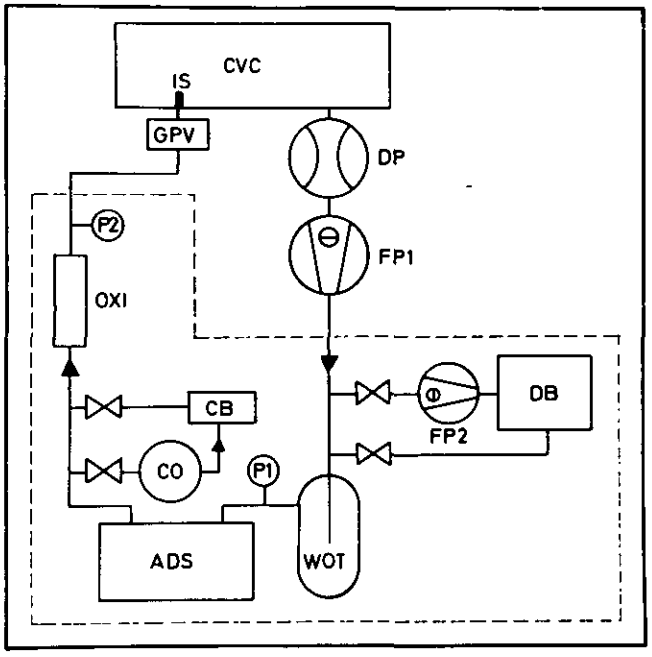


*Figure 1:*
*Schematic diagram of the $^3$He-recovery system:*
*CVC cyclotron vacuum chamber, DP diffusion pump, FP fore pump, WOT water oil trap, P pressure gauge, ADS adsorber (molecular sieves), OXI oxygen adsorber, GPV Granville Phillips pressure regulating valve, IS ion source, DB dirty buffer, CB clean buffer, CO compressor.*

Without complications and costs it was not possible to keep the volume between FP1 and GPV lower than 30 l. Therefore, in closed loop operation the system is operated at a rather low pressure of 50 mbar. To keep a $^3$He-pressure of 50 mbar before the valve GPV, the system has to be loaded with approximately 1 bar l of $^3$He. After a $^3$He-run in closed loop operation the pure $^3$He is stored in the clean buffer CB by using the compressor CO. In case of $^3$He-beam times shorter than 10 hours the system is operated for convenience in the following way: The trap ADS is not cooled, the ion source is fed with $^3$He from the buffer CB and the gas, which is exhausted from the cyclotron, is stored in the „dirty" buffer DB. At the end of each run either in closed or open loop operation the system is pumped out by a helium-leak proved forepump FP2 into the buffer DB as well.

The actual recovery system, which is surrounded by a dotted line in figure 1, can be manipulated during the beam time. Therefore the system is operated by hand according to a check list. Only the pressures P1 and P2 as well as the cooling status of the traps WOT and ADS are displayed in the control room.

1977 the cyclotron was used with $^3$He-beam for 403 hours. More than 150 bar l $^3$He passed the system. With no recovery system the corresponding costs would have amounted to 50 kDM. Since on the other side only 1.2 kDM had to be payed for the liquid nitrogen and $^3$He losses, the $^3$He operation costs are now at a level, which is negligible in comparison to the total cyclotron operation costs.

## 7.4. Beam Phase Optimization Using a Mathematical Procedure

J. Linz

To have the full benefit of beam qualities achievable with a cyclotron, the internal beam should be accelerated at the maximum energy gain per turn at all radii. The deviation from the maximum energy gain corresponds to the deviation from the maximum of the cosine like accelerating voltage, is measured in RF-degrees and called phase. Phase optimization means to bring it close to zero by a systematic alteration of the trim coil currents.

The phase shift $\Delta\Phi$ per turn is given by

$$\Delta\Phi = -N \cdot 2\pi \cdot \overline{\Delta B}/\overline{B} \qquad (1)$$

where N=harmonic number (=3 at JULIC) and $\Delta B/B$ is the relative deviation from the isochronous field averaged over one orbit. Since typically $\overline{\Delta B}/\overline{B} < 1$ %, $\overline{\Delta B}$ is a linear function of any trim coil current change $\Delta I$. For small current changes the relation between phase shift and current variation I can then be taken as linear in the following form

$$\vec{\Phi} = \begin{pmatrix} \Delta\Phi_1 \\ \vdots \\ \Delta\Phi_n \end{pmatrix} = \sum_{j=1}^{m} \vec{\pi}_j \, \Delta I_j \qquad (2)$$

where $\Delta\Phi_i$ are the phases measured at n different radial positions and the $\Delta I_j$ are the current changes at m different trim coils. Each vector $\vec{\pi}_j$ represents the phase vector $\vec{\Phi}$ when changing the current of coil number j by 1 Ampere. The $\vec{\pi}_j$ are therefore called the trim coil vectors. Arranging the $\vec{\pi}_j$ as columns of a matrix B and the $\Delta I_j$ as elements of a vector $\vec{I}$ equation (2) becomes

$$\vec{\Phi} = B \cdot \begin{pmatrix} \Delta I_1 \\ \vdots \\ \Delta I_m \end{pmatrix} = B \cdot \vec{I} \, . \qquad (2.1)$$

For this equation small variations in the trim coil currents were presupposed. Developing an iterative procedure, we apply this equation also in case of large changes in phase or current, respectively, which are normal at a real cyclotron.

In case of a non optimized phase vector $\vec{\Phi}_1$ we can now ask for a vector $\vec{I}$, which describes the current change necessary to bring the phase vector as close as possible to the zero vector:

$$| |\vec{\Phi}_1 + \vec{\Phi}| | = | |\vec{\Phi}_1 + B \cdot \vec{I}| | \equiv \min \qquad (3)$$

If $n \geq m$ and the columns of matrix B, i.e. the trim coil vectors $\vec{\pi}_j$, are linearly independant, a general solution of the problem is given by

$$\vec{I} = -(B^T \cdot B)^{-1} \, B^T \, \vec{\Phi}_1 = C \cdot \vec{\Phi}_1 \, , \qquad (4)$$

where $B^T$ is the transpose of B and C is the so called control matrix.

## 7.2. Modification of Target Area M4 for In-Beam-γ-Spectroscopy Experiments

J. Reich, A. Retz, G. Schlienkamp

The in beam-γ-spectroscopy experiments carried out in the past at station C were pretty much affected by the varying γ-background after experiments at the three other stations in the same target area M2. Therefore in 1976 the final decision was made to enlarge target area M4 and to modify the corresponding beamline to be suited for the variety of in beam-γ-spectroscopy experiments.

The modification of the beam line includes the installation of a Be-wedge-energy degrader at slit AS2 and of a dispersive slit DS4 preceeded by a ZnS-screen and followed by a beam stop, the conversion of the former quadrupole doublet into the triplet QA1 and the addition of the quadrupole doublet QA2, which focuses the beam into the Faraday cup, shielded way back in the wall.

For the beam at target station A the double monochromator[1] is operated in achromatic mode supplying a non dispersed focus at the achromatic outlet slit AS2. With the energy degrader at this position an energy variation below the cyclotron energy range will be possible. In the case of an energy degradation for instance from 90 down to 50 MeV α-particles the energy width E/E(FWHM) of the degraded beam will be around 3 to 4 % because of energy loss straggling in the Be-wedge[2]. The angular straggling will add to the beam divergence after the degrader in the order of 1 degree[3]. Both effects blow up the phase space much more than the following beam line can accept. Also, the large energy width of the beam would prohibit a clean focusing at the target. The necessary cut in beam divergence can be made with the slit DS2 (i.e. outlet slit of the double monochromator in dispersive mode). The necessary cut in energy width can be made with a focus condition at slit DS4. The dispersion of the magnet SM3 will then supply an energy resolution of 3 $10^{-3}$ for 6.0 mm slit width at DS4. For this energy resolution and for the above described energy degradation ray tracing calculations result in a transmission of typically 1 % with respect to the beam intensity at the cyclotron exit in comparison to 100 % transmission, when the energy degrader is removed.

The beam can be focused at a target either on position A1 or A2. A gantry in the target area will allow at these positions a quick change or modification of the following experimental equipment for in beam-γ-spectroscopy:

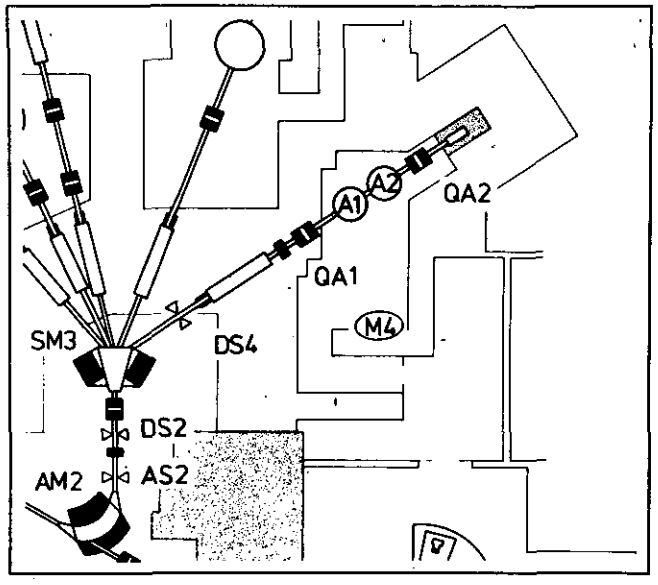


*Figure 1:*
*Layout of the beam line to the modified target area M4.*

Angular distribution, γ-γ-coincidence and α-decay chambers, g-factor magnet, multiplicity set-up and sum spectrometer.

The modification of the beam line in the cyclotron vault up to the quadrupole triplet QA1 was carried out in the past shut down time. By the end of the year the target area M4 was again ready for moving in. The installation of the rest of the beam line and the experimental equipment will start in January 1978.

### References

[1] J. Reich, C. Mayer-Böricke, S. Martin, K.L. Brown, F.E. Johnson, AIP Conference Proceedings No. 9 (1972) p. 401
[2] H. Münzel et al., Nucl. Instr. Meth. 74 (1969) 103
[3] D. Ingham, private communication 1973

## 7.3. Operation Experience with the $^3$He-Recovery System

R. Fiedler, U. Rindfleisch, P. Wucherer

A $^3$He-recovery system saves costs, being today typically in the range of 100 DM per running hour. In 1976 with increasing demand of $^3$He beam time the old $^3$He-recovery system, which was bought from a manufacturer, caused severe beam-time and as well $^3$He losses, mainly because of two reasons:

Firstly, the system was operated at a pressure of $\geq 1$ bar and therefore was using a large gas volume in terms of normalliters. Secondly, the system was not failsafe against the rather drastic changes in the level of water vapour in the cyclotron vacuum chamber, which cannot be avoided. The system was therefore completely reconfigurated in 1976. Fig. 1 shows the systematics of the system (for simplicity most of the valves and gauges are not shown). The cyclotron vacuum chamber CVC is evacuated by diffusion pumps DP and forepumps FP1. The water-oil trap WOT is cooled down to $-12^{\circ}$C and prevents the following adsorber trap ADS from ice obstructions caused by water-vapour as already mentioned. The trap ADS is filled with molecular sieves (1.5 kg), cooled down to liquid-nitrogen temperature and can work properly for about 200 hours of $^3$He-beam time. The oxigen trap OXI indicates by its changing colour, when the trap ADS starts to get completely loaded, and prevents the ion source from oxigen overflow. The ion source IS is fed with pure $^3$He through the Granville Phillips valve GPV, which regulates the gas pressure in the ion source.

# III. Technical Development

## 7. Isochronous Cyclotron

### 7.1. Cyclotron Operation and Improvement

H.G. Böge, W. Bräutigam, R. Brings, R. Fiedler, C. Mayer-Böricke, J. Reich, A. Retz, U. Rindfleisch, G. Schlienkamp, H. Schwan, P. Wucherer

In 1977 the cyclotron was in 21 shifts per week operation during 45 weeks. The cyclotron was available for experiments during 6313 hours, which amounts to 85 % of the scheduled operating time (see table 1). This is the best result obtained since the existence of the variable energy cyclotron JULIC. In evaluating this it has to be taken into account that about 240 energy and particle changes are usually made per year.

*Table 1:*
*Cyclotron time distribution in 1977*

| | | |
|---|---|---|
| Cyclotron Operation | | |
| Beam time for experiments | 6313 h | 85.0 % |
| Scheduled maintenance | 254 h | 3.4 % |
| System failures | 858 h | 11.6 % |
| Scheduled operating time | 7425 h | 100.0 % |
| Beam Time Distribution | | |
| Guest scientiests (U. Bonn, KFKI Budapest, U. Hamburg, MPI Heidelberg, U. Köln, T.U. München, U. Münster, U. Tübingen) | 1199 h | 19.0 % |
| Scientists of KFA excluding IKP (IFF;ICH-1-IME,-ARA;ZCH;ZEL) | 877 h | 13.9 % |
| Scientists of IKP | 4237 h | 67.1 % |
| Beam time for experiments | 6313 h | 100.0 % |

The increase in beam time for experiments of 471 hours in comparison to 1976 is for a large part a result of the development and installation of new extraction elements[1,2] (compensated channels, septum deflector) during the past years. Correspondingly, the failure time of the extraction system decreased by 311 hours in comparison to 1976 (see table 2). A remarkable decrease in failure time appeared also for the RF-system (95 hours).

*Table 2:*
*Component failure time distribution in 1977*

| | | |
|---|---|---|
| CYCLOTRON | | |
| Radio frequency system | 356 h | 41.5 % |
| Ion source (including all changes) | 120 h | 14.0 % |
| Extraction system (including waiting time because of high radiation level) | 110 h | 12.8 % |
| Water cooling system | 71 h | 8.3 % |
| Magnet power supplies | 38 h | 4.4 % |
| Vacuum system | 34 h | 4.0 % |
| Pulsing system | 25 h | 2.9 % |
| Internal targets | 19 h | 2.2 % |
| Personell safety system | 15 h | 1.7 % |
| Others | 29 h | 3.4 % |
| BEAM HANDLING SYSTEM | 41 h | 4.8 % |
| Total | 858 h | 100.0 % |

Several additional efforts have been made to improve the cyclotron, which mainly were carried out during the shut-down time of 7 weeks in August and September:

1. Installation of new redesigned isochronous trim coil plates with imbedded harmonic coils near the cyclotron center.
2. Magnetic field mapping carried out over a complete sector, expecially to get data about the main field at very high excitation and about the azimuthal distribution of the trim coil fields.
3. Installation of an auxiliary mechanism to guide the dees during the insertion in the vacuum tank especially in the critical phase, when the dee-tips lock together.
4. Replacement of the non-reliable original electrostatic steerer by a magnetic steerer following the focusing channel in the fringe field.
5. Modification and extension of the beam handling system with respect to the magnetspectrograph „Big Karl" and the enlarged target area M4 for in beam-γ-spectroscopy.

#### References

[1] Annual Report 1975, KFA-IKP 1O/76, p. 245
[2] Annual Report 1976, KFA-IKP 1O/77, p. 135

The muon capture strength goes most strongly into 2⁺ (28 %) and 1⁺ (20 %) states. This is expected since the muon is captured from a 1s atomic orbit. Considerable E2 capture strength is concentrated near $E^{ex}$ = 5 MeV in $^{208}$Tl. This indicates that the isovector E2 resonance, which has been discussed in the context of $(\pi^-,\gamma)$[1] is specifically ex cited in $(\mu^-,\gamma)$. Its energy lies slightly above the neutron threshold (3.82 MeV in $^{208}$TL), and it might be possible to identify the resonance experimentally by its decay products. The outstanding 1⁻ level at 3.1 MeV is an almost pure (π h (11⁻¹/2), ν i 11/2) state. It is more strongly excited in $(\mu^-,\gamma)$ than in $(\pi^-,\gamma)$ due to the vector part in the weak interaction.

The capture rate for $(\pi^-,\gamma)$ summed over all states form O to 15 MeV excitation energy in $^{208}$Tl is obtained

$$\Lambda_\pi^{theor}\ (0-15) = 9.6 \cdot 10^{15}\text{sec}^{-1}$$

which is about a factor 2 larger than the measured value. On the other hand, the $(\pi^-,\gamma)$ rate is obtained

$$\Lambda_\mu^{theor}\ (0-15) = 134 \cdot 10^{5}\text{sec}^{-1}$$

in excellent agreement with the measured total rate $\Lambda_\mu^{exp}$(total) = (129.8 ± 1.0) · $10^5$/sec. For a more detailed discussion see ref. 1.

In conclusion, we have shown that the $(\pi^-,\gamma)$ reaction excites a broad mixture of multipole states with emphasis on 4⁻, 5⁺, 6⁻, and 7⁺ levels. It leads to no pronounced structure except for a gap in the excitation spectrum between $E^{ex}(^{208}\text{Tl})$ = 6–9 MeV. Muon capture, however, shows a concentration of E2 strength near 5 MeV.

*) TU München, 8046 Garching, BRD

### References


[1] K. Ebert and J. Meyer-ter-Vehn, submitted to Phys. Letters.
[2] H.W. Baer, K.M. Crows, and P. Truöl, Adv. Nucl. Phys. 9 (1977) 177
[3] J. Alder et al., contribution to Int. Conf. on High-Energy Physics and Nuclear Structure, Zürich, 1977, abstract vol., p. 4
[4] A. Fujii and H. Primakoff, Nuov. Cim. 12 (1959) 327
[5] R. Bauer, K. Ebert, P. Ring, W. Theis, E. Werner and W. Wild, Z. Physik A274 (1975) 41; K. Ebert, thesis, TU München 1976


## 6.2 Muonic Atoms

### 6.2.1. A Resolution of the Nuclear Polarization Anomalies in $^{208}$Pb

G.A. Rinker, J. Speth

We have calculated nuclear polarization energy shifts e.g.[1] for muonic $^{208}$Pb using the renormalized random-phase approximation to describe the nuclear excitations. We find smaller energy shifts than previously calculated, in disagreement with several empirical determinations of these effects.

In table 1 we show our theoretical nuclear polarization binding energy shifts in [keV]. The indices ℓ and τ denote the different nuclear angular momentum and isospin, whereas the indices in the first column denote the muon states. In the last column we show the total energy shift due to all different nuclear excitations. Through a more critical examination of the experimental data of muonic $^{208}$Pb, we argue[2] that the previous empirical determinations are incorrect, and we point out other likely sources for the remaining discrepancies.

*Table 1:*
*Nuclear Polarization Binding Energy Shifts (keV)*

| State \ ℓτ | 00 | 01 | 11 | 20 | 21 | 30 | 31 | ℓ>3 | Total |
|---|---|---|---|---|---|---|---|---|---|
| $1s_{1/2}$ | 0.884 | 0.358 | 1.327 | 0.583 | 0.249 | 0.106 | 0.239 | 0.239 | 3.967 |
| $2s_{1/2}$ | 0.300 | 0.093 | 0.201 | 0.061 | 0.023 | 0.024 | .0.011 | 0.021 | 0.734 |
| $2p_{1/2}$ | 0.060 | 0.026 | 0.774 | 0.411 | 0.108 | 0.043 | 0.043 | 0.108 | 1.670 |
| $2p_{3/2}$ | 0.035 | 0.015 | 0.734 | 0.393 | 0.100 | 0.130 | 0.040 | 0.096 | 1.543 |
| $3p_{3/2}$ | 0.014 | 0.006 | 0.271 | 0.139 | 0.030 | 0.042 | 0.011 | 0.029 | 0.542 |
| $3d_{3/2}$ | 0.000 | 0.000 | 0.066 | 0.032 | 0.008 | 0.122 | 0.000 | 0.006 | 0.234 |
| $3d_{5/2}$ | 0.000 | 0.000 | 0.055 | 0.026 | 0.007 | -0.071 | 0.000 | 0.005 | 0.022 |
| $4f_{5/2}$ | 0.000 | 0.000 | 0.055 | 0.002 | 0.000 | 0.000 | 0.000 | 0.000 | 0.007 |
| $4f_{7/2}$ | 0.000 | 0.000 | 0.004 | 0.001 | 0.000 | 0.000 | 0.000 | 0.000 | 0.005 |

### References


[1] M.Y. Chen, Phys. Rev. C1 (1970) 1167; G.A. Rinker, Phys. Rev. A14 (1976) 18
[2] G.A. Rinker and J. Speth, preprint (Jülich 1977)

## 6.1.3. Radiative Pion and Muon Capture on $^{208}$Pb

K. Ebert*), J. Meyer-ter-Vehn

*Partial and total rates for the $(\pi^-,\gamma)$ and $(\mu^-,\nu)$ capture reactions on $^{208}$Pb have been calculated within RPA[1]. Radiative pion capture on heavy nuclei is almost unexplored. Beyond $^{40}$Ca, experiments have been performed only for Bi and Pb. The results are contradictory. The first study of $^{209}$Bi$(\pi^-,\gamma)$ $^{209}$Pb[2] had suggested a sharp resonance in the photon spectrum near $E^{ex}$ = 7.9 MeV in $^{209}$Pb. Tentatively, it had been interpreted as an isovector E2 resonance. Recent $(\pi^-,\gamma)$ experiments on $^{209}$Bi and $^{208}$Pb, however, do not show the resonance structure[3]. The identification of isovector giant resonances in $(\pi^-,\gamma)$ and $(\mu^-,\nu)$ capture reactions – be it of M1, E2 or higher multipole character – would be of considerabe interest for nuclear structure physics. In this paper, we concentrate on the question which multipoles are favoured in the two processes and by which mechnisms.*

The simultaneous consideration of $(\pi^-,\gamma)$ and $(\mu^-,\nu)$ turns out to be very illuminating. For light nuclei, the two processes have often been compared showing their similarity due to similar vertex structure and momentum transfer. For $^{208}$Pb, however, the comparison will accentuate an important difference:

whereas capture of the weakly interacting muon proceeds from the 1s orbit, the strongly interacting pion is captured from the 4f orbit.

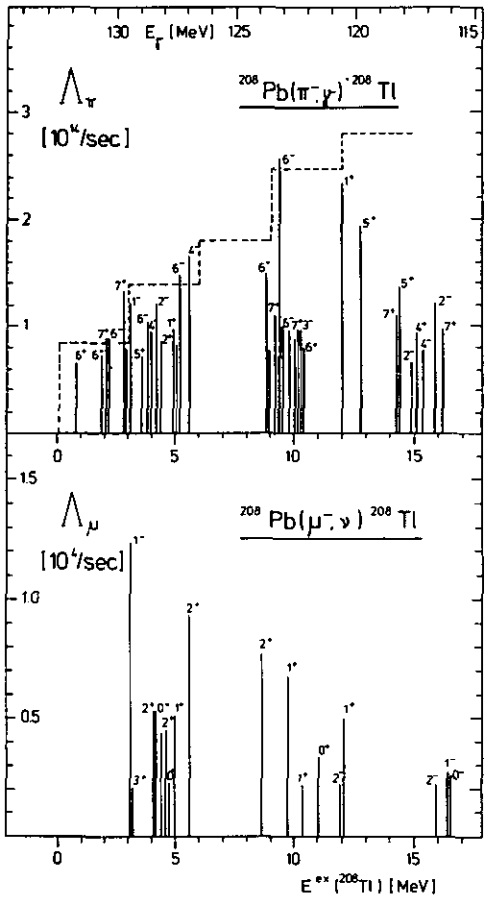


*Figure 1:*
*Calculated excitation spectra of $^{208}$Tl after radiative pion capture (upper part) and muon capture (lower part) on $^{208}$Pb. Only strongly excited states and their multipolarity are shown. For $(\pi^-,\gamma)$, the photon energy E is given gy the top scale; the $^{208}$Tl groundstate corresponds to E = 132.5 MeV. The dashed line shows the measured photon spectrum average over 3 MeV intervals in units $10^{15}$/(sec · MeV).*

This leads to very different excitation spectra and illustrates the importance of the entrance channel.

The present calculation is based on the standard form for the $(\pi^-,\gamma)$[2] and $(\mu^-,\nu)$[4] vertices and RPA wave functions[5]. Results for the distribution of capture strength over energy and different multipoles are presented in Fig. 1 and Table 1. Radiative pion capture excites a broad mixture of multipole states, ranging from $1^+$ to $7^+$. The strong excitation of high angular momentum states, in particular unnatural parity states $J^\pi = 4^-, 5^+, 6^-, 7^+$, is an outstanding feature. These states correspond to the coupling of the initial pion angular momentum $\ell_\pi = 3\,\hbar$ and a dominant photon partial wave with $\ell_\gamma = 3\,\hbar$. Higher photon partial waves are cut off, since $k_\gamma \cdot R \cong 4\,\hbar$ with the Pb radius R = 6.7 fm.

*Table 1*

| $J^\pi$ | $\Lambda_\pi$ (%) | $\Lambda_\mu$ (%) |
|---|---|---|
| $0^+$ | 0.0 | 4.8 |
| $0^-$ | 0.2 | 4.7 |
| $1^+$ | 7.1 | 20.2 |
| $1^-$ | 2.2 | 13.1 |
| $2^+$ | 4.5 | 27.8 |
| $2^-$ | 4.6 | 5.8 |
| $3^+$ | 6.7 | 7.6 |
| $3^-$ | 5.9 | 8.8 |
| $4^+$ | 3.6 | 1.3 |
| $4^-$ | 9.5 | 4.6 |
| $5^+$ | 9.2 | 0.7 |
| $5^-$ | 7.5 | 0.1 |
| $6^+$ | 6.5 | - |
| $6^-$ | 13.0 | - |
| $7^+$ | 8.4 | - |
| $7^-$ | 4.4 | - |
| $8^+$ | 0.9 | - |
| $8^-$ | 4.4 | - |
| $9^+$ | 1.1 | - |
| $9^-$ | 0.2 | - |

Distribution of radiative pion an dmuon capture strength over different J multipole transitions. Rates, summed over $E^{ex}(^{208}Tl)$ = 0 – 15 Mev, are given in per cent of $A^{theor}(0-15)$.

The results are given in table 1 for $(OsOp)^{-2}$ configurations for the A = 14 residual nuclei. The ratio R = W(nn)/W(np) is 12.5. This is larger than the observed value $3.8 \pm 1.0$[4]. However, in view of the fact that the ratio R observed by Nordberg et al.[4] was low by a factor of three possibly because of the contamination from heavier hydrogen isotopes[5], these two values are quite consistent. The total absorption rate is $6.5 \times 10^{15}$ $sec^{-1}$ and is in good agreement with experiment[6] which is $7.1 \times 10^{15}$ $sec^{-1}$.

In conclusion, the p-wave rescattering terms play a dominant role even in a bound pion absorption in $^{16}O$, and can solve some long standing problems.


**References**

[1] [1] K. Shimizu and A. Faessler, to be published
[2] D.S. Koltun and A. Reitan, Phys. Rev. 141 (1966) 1413
[3] B. Goplen et al., Phys. Rev. Lett. 32 (1974) 1012
[4] M.E. Nordberg et al., Phys. Rev. 165 (1968) 1090
[5] J.P. Castleberry et al., Phys. Lett. 34B (1971) 57
[6] H. Koch et al., Phys. Lett. 29B (1969) 140


## 6.1.2. Two Nucleon Emission Following Bound Pion Absorption


K. Shimizu, A. Faessler


It has been well known that the absorption of a bound negative pion most often leads to two nucleon emission because a large amount of energy is brought into the nucleus with very little momentum[1]. Since the two emitted nucleons have a large relative momentum, the relative motion of the nucleon pair at small distances plays a very important role in this process. Thus a detail study of the pion absorption is expected to provide us with important information on short range nucleon-nucleon correlations as well as two hole states in nuclei.

We have performed the calculation of the absorption of a bound 2p pion in $^{16}O$ with the emission of two fast nucleons leading to low excitation of the residual nucleus. In our calculation, the following important effects have been considered simultaneously: (i) Correlations in the initial nuclear wave function are treated on the basis of the Brueckner theory, (ii) the mutual final state scattering of the emitted pair and (iii) the nucleon-nucleon scattering are taken into account by the use of eikonal model wave function together with the T-matrix in momentum space. The absorption operator is taken to be a non-relativistic reduction of the pseudovector interaction without rescattering.

Fig. 1 shows the angular distributions between two emitted neutrons for the three states of $J^P = 1^+$, T = 0 in $^{14}N$. Here we have used the Cohen and Kurath's wave function to describe the initial and final nuclei. Experimentally a peak at the 3.9 MeV state in $^{14}N$ has been observed[2] and the recoil momentum distribution of the residual nucleus at this 3.9 MeV state has been shown to have the c.m. angular momentum L = 0 patterns. Our result is consistent with the experiment. Table 1 shows the total absorption rates of

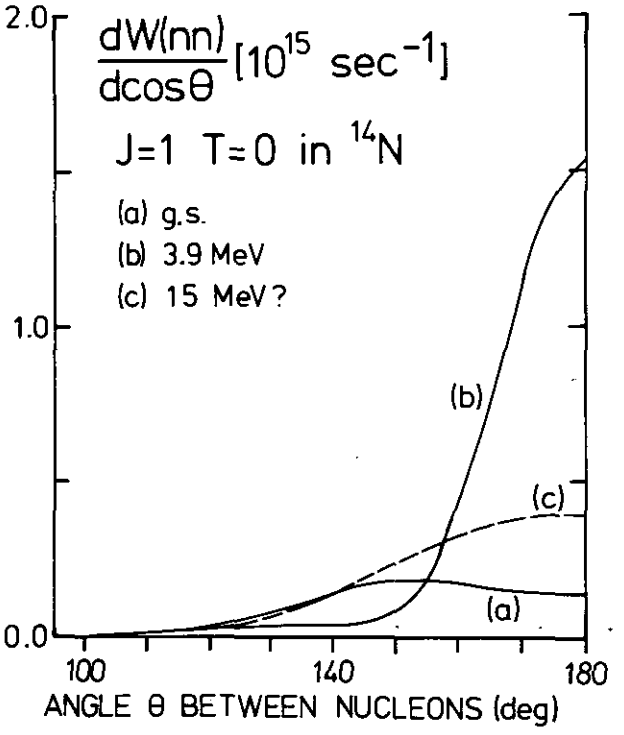


*Figure 1:*

*Table 1*

| | W(nn) $10^{13}$ sec$^{-1}$ | W(np) $10^{13}$ sec$^{-1}$ |
|---|---|---|
| $0s^{-2}$ | 8.71 | 8.87 |
| $0s^{-1}0p^{-1}$ | 43.23 | 46.60 |
| $0p^{-2}$ | 58.69 | 67.22 |
| Sum | 110.63 | 122.69 |

n-n and n-p emission from $Os^2$, Os Op and $Op^2$ configurations. From this table we obtain the total absorption rate for two nucleon emission $W = 2.3 \times 10^{15} sec^{-1}$ and the ratio of n-n to n-p emission R = W(nn)/W(np) = 0.9, whereas experimentally these are $W_{exp} \sim 7.1\ 10^{15} sec^{-1}$ and $R_{exp} = 3.9 \pm 1.0$[3]. The dependence of R on the initial and final state correlations has been studied in details. It is found that the initial state correlation increases the ratio R while the final state correlation decreases it. Thus we obtain R ~ 1.0 after we include both initial and final state correlations. In order to resolve consistently the discrepancies discussed above, we emphasize that a more careful examination of the absorption mechanism itself is necessary. Rescattering of the pion from a nucleon before absorption could be an important effect to overcome the above difficulties.


**References**

[1] D.S. Koltun, Adv. in Nucl. Phys. 3 (1969) 71; J. Hüfner, Phys. Rep. 21C (1975) 1
[2] H.D. Engelhardt and H. Ullrich, private communication
[3] H. Koch et al., Phys. Lett. 29B (1969) 140; M.E. Nordberg et al., Phys. Lett. 34B (1971) 57

# 6. Medium Energy Physics

## 6.1 Pionic Atoms

### 6.1.1. Rescattering Effect in Bound 2p-Pion Absorption

K. Shimizu, A. Faessler

We had shown that direct absorption (see (a) in fig. 1) cannot explain the measured ratio of n-n to n-p emission following a 2p-bound pion absorption in $^{16}O$ even if we include the initial and final state correlations[1].

Here we would like to show that this problem can be solved by introducing p-wave rescattering terms shown in (b) of fig. 1.

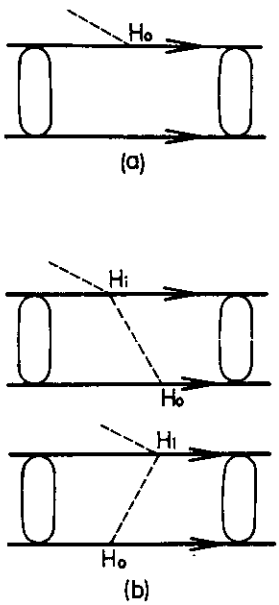


*Figure 1*

It has been already pointed out that the s-wave rescattering terms are very important for s-wave pion absorption[2]. Goplen et al.[3] investigated the p-wave rescattering terms in the pion absorption by the deuteron and found that it has a large contribution even for a low energy pion.

In a bound pion absorption problem, the pion has very little momentum. Therefore, the p-wave rescattering terms seem to be less important. We must, however, notice the following points. (a) The absorption operator which is a non-relativistic reduction of the pseudovector $\pi$1NN interaction has itself a linear momentum dependence. (b) In the rescattering process, the pion is emitted by the first nucleon and absorbed by the second nucleon with a rather large momentum because both nucleons must obtain large momenta 300 MeV/c. Because of this situation, the absorption with p-wave rescattering is of the same order of magnitude as the absorption without rescattering.

Now we evaluate the rescattering terms. For simplisity, we take only the p-wave part of the absorption operator $H_o$.

$$H_0 = i\sqrt{4\pi}\, f\, \mu^{-1}\, \sigma\tau \cdot q\phi$$

The p-wave scattering-vertex operator $H_3$ and $H_4$ are taken[3] as

$$H_3 = -4\pi\, \lambda_3\, \mu^{-3}\, q\phi \cdot q\phi$$

$$H_4 = -4\pi\, \lambda_4\, \mu^{-3}\, \sigma\tau \cdot (q\phi \times q\phi)$$

where $\mu$ is the pion mass, q is the pion momentum and $\emptyset$ and $\pi$ are pion field operators. The dot-cross product is understood to apply to coordinate and isospin simultaneously. The $\lambda$'s are chosen to reproduce the measured pion scattering lengths. Evaluating the graphs (b) in fig. 1, we obtain the following terms in the nucleon-nucleon coordinates for the p-wave rescattering.

$$T_3 = \frac{2}{3} G_3 N\, (\tau_1\sigma_1 + \tau_2\sigma_2)\, Y_0(r)$$

$$-\frac{2\sqrt{10}}{3} G_3 N\, [C^{(2)} \times (\tau_1\sigma_1 + \tau_2\sigma_2)]^{(1)}\, Y_2(r)$$

$$T_4 = -\frac{8}{3} G_4 N\, [\tau_1 \times \tau_2]^{(1)}\, [\sigma_1 \times \sigma_2]^{(1)}\, Y_0(r)$$

$$-\frac{4\sqrt{10}}{3} G_4 N\, [\tau_1 \times \tau_2]^{(1)}\, [C^{(2)} \times [\sigma_1 \times \sigma_2]^{(1)}]^{(1)}\, Y_2(r)$$

where the pion wave function $\chi(r_\pi) = Nr_\pi$ is used and coupling constants and radial functions are

$$G = \frac{\mu^3}{\lambda_3} G_3 = \frac{\mu^3}{\lambda_4} G_4 = \sqrt{\frac{4\pi}{2\mu^3}}\, f$$

$$Y_0(r) = a^2 \frac{e^{-ar}}{r}$$

$$Y_2(r) = a^2 \left(1 + \frac{3}{ar} + \frac{3}{a^2 r^2}\right) \frac{e^{-ar}}{r},\quad a = \frac{\sqrt{3}}{2}\mu$$

Here r is the relative coordinate of two nucleons. When we include the cutoff range parameter[3], the radial function $Y_o(r)$ and $Y_2(r)$ must be properly modified. We have used the cutoff range parameter $\beta$ = 300 MeV/c suggested by Goplen et al.[3]. Initial and final state correlations are included in the same manner as in ref. 1.

*Table 1*

| | W(nn) | W(np) |
|---|---|---|
| $0s^{-2}$ | 0.618 | 0.004 |
| $0s^{-1}0p^{-1}$ | 2.310 | 0.189 |
| $0p^{-2}$ | 3.086 | 0.288 |
| Sum | 6.014 | 0.481 |
| Total theor. | 6.495 | |
| Total exp. | 7.1 | |

In units of $10^{15}$ sec$^{-1}$.

## 5.5 Continuous Particle Spectra

### 5.5.1. Direct Components in Continuous Particle Spectra. „Elastic" and „Inelastic" Break-up Modes

G. Baur, M. Pauli*), F. Rösel*), D. Trautmann*)

The typical spectrum of a nuclear reaction at medium energies shows a broad distribution between the low energy end, which is dominated by evaporation processes, and the high energy end, which corresponds to the excitation of discrete states in the residual nucleus. In nucleon induced reactions, the bulk of the intermediate region is explained in terms of multistep compound and multistep direct precompound processes[1]. For composite particles, on the other hand, a substantial part of these intermediate spectra is due to fragmentation processes; e.g. the total break-up cross section of the deuteron induced reaction on $^{208}$Pb and $E_d$ = 70 MeV is estimated[2] to be 910 mb, as compared to the total reaction cross section of 2100 mb. It is the purpose of this work to study the break-up components of these spectra.

Of course, in certain cases it is still possible to study the transition to individual resonances. Then the study of the line shape of these resonances is especially interesting. This has been done recently for charged particle transfer reactions on $^{12}$C with the (d,n) and ($^3$He,d) reaction. The region of the first $s_{1/2}$, $d_{5/2}$ and $p_{3/2}$ resonances including the background region could be described consistently[3]. This example is a particularly suitable test for the theory of transfer reactions into the continuum, because the corresponding proton elastic scattering phase shifts – the input of our theory – are very well known.

In order to understand inclusive type spectra A + d → p + anything in general it is necessary to extend the theory of deuteron break-up[4] A + d → p + A + n to those cases where the unobserved part of the system (n+A) does not decay back into n + A(groundstate), but where further inelastic processes may happen. If the interaction of the neutron with the target in the final state is responsible for these inelastic processes, those contributions can be obtained under certain assumptions directly from the „elastic break-up T-matrix" which is given by

$$T^+_{\ell m} = D_0 \int d^3R\, \chi_p\, f_\ell\, Y_{\ell m}\, \chi_d \qquad (1)$$

where the $\chi$'s denote the distorted waves and f is the neutron elastic scattering wave function. We obtain for the inclusive cross section the formula

$$\frac{d^2\sigma}{d\Omega\, dE}\ (\text{inclusive}) \quad \propto \sum_{\ell m} \left(|T_{\ell m}|^2 + \frac{\sigma_\ell^{\text{reaction}}}{\sigma_\ell^{\text{elastic}}} \cdot |T_{\ell m} - T^0_{\ell m}|^2\right) \qquad (2)$$

where $T^0_{\ell m}$ is the „free break-up" matrixelement, i.e. the wave function $f_\ell$ in eq. (1) is replaced by the regular spherical Bessel function $j_\ell$. The total reaction and elastic scattering cross section for n – A scattering of the $\ell$-th partial wave are denoted by $\sigma_\ell^{\text{reaction}}$ and $\sigma_\ell^{\text{elastic}}$ respectively.

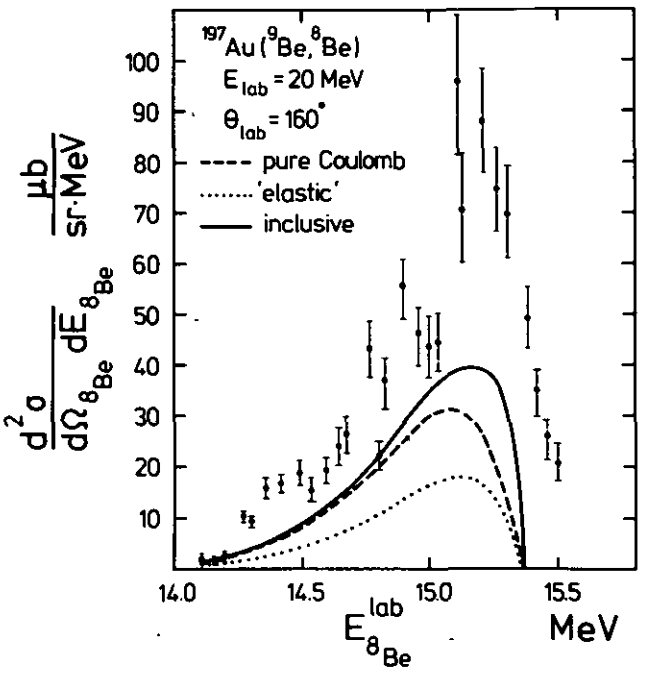


*Figure 1:*
*Comparison of $^8$Be spectra in the $^{197}$Au($^9$Be,$^8$Be) reaction with the "inclusive break-up" theory.*

This theory has been applied to (d,p) spectra with $E_d$ = 25.5 MeV on various target nuclei. First results were reported at the Tokyo conference[5]. Another very loosely bound nucleus next to the deuteron is $^9$Be. The semiclassical break-up theory[6] has been applied to $^9$Be break-up measurements[7] on an $^{197}$Au target. There it was found[7] that, using the „elastic" break-up mode only, the shape of the $^8$Be(→α+α) spectra are given quite well, but not the absolute magnitude. By adding the „inelastic" break-up mode, according to eq. (2), satisfactory agreement between the theory and experiment is obtained, as can be seen in Fig. 1. Also for strongly bound particles the fragmentation process is important. It accounts for the bump observed in the continuous $^{62}$Ni(α,$^3$He) spectrum at $E_L$ = 172.5 MeV recently measured in Jülich (A. Budzanowski et al., see this annual report p. 10).

*) Institut für theoretische Physik der Universität Basel

#### References


[1] H. Feshbach, Conference on Nuclear Reaction Mechanisms, Italy 1977, preprint
[2] J.R. Wu, thesis, University of Maryland, 1977, unpublished, p. 47, 300
[3] G. Baur, F. Rösel and D. Trautmann, Journal of Physics G, February 1978
[4] G. Baur, D. Trautmann, Physics Reports 25C (1976) 293
[5] J. Pampus, J. Ernst, T. Mayer-Kuckuk, J. Rama Rao, G. Baur, F. Rösel and D. Trautmann, Contribution to the Tokyo conference, 1977, p. 571
[6] G. Baur, M. Pauli and D. Trautmann, Nucl. Phys. A224 (1974) 477
[7] J. Lang, R. Müller, E. Ungricht and J. Unternährer, contribution to the Heavy Ion Conference in Caen, 1976, p. 48

## 5.4.2. Monte-Carlo Description of Particle Emission and Gamma-Multiplicities in Heavy-Ion Fusion Reactions

A. Faessler, M. Wakai

In (heavy ion, xn) fusion reactions the energy and the angular momentum brought into the compound system are spread over a large number of nucleons. The greater part of the excess angular momentum is carried away by γ-rays and the multiplicity of the γ-cascades is strongly related to the excitation energy, the distribution of the angular momentum in the compound system and the relative strengths of electro-magnetic probabilities with different multipolarities. The experimental data of the γ-multiplicity and related quantities provide, therefore, important informations on the validity of the compound nucleus picture. We performed calculations of such quantities for the reactions $^{150}$Nd($^{16}$O,4n) $^{162}$Er and $^{148}$Nd($^{18}$O,4n)$^{162}$Er[1] by using the statistical model of nuclear reactions. We applied the Monte Carlo method[2], which gives a very intuitive picture of the multiple particle- and γ-emissions. Emission of different particles and E1-, M1- and E2-transitions are taken into account. The E1-ransitions are restricted to high-energy and high-angular momentum regions. The E2-transitions between states belonging to the same ratational band are specially considered, since these transitions are very strong in the case of deformed nuclei. Some of theoretical results are presented in figs. 1 and 2 to be compared with experimental data[1]. The figure 1 shows good agreement between the theoretical and experimental data of the side feeding intensities. To obtain this agreement one is forced to introduce strong E2-transitions between states in the same rotational bands as mentioned above. A good agreement is found also for the γ-multiplicities in fig. 2. In conclusion we can say that the statistical model is a powerful tool to analize statistically the -ray emission after heavy ion fusion reactions.

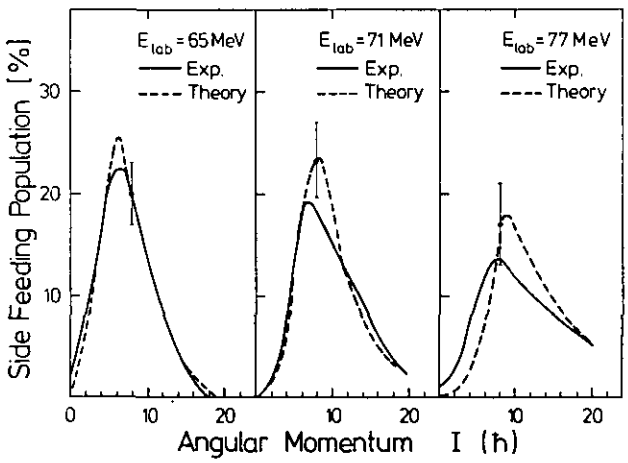


*Figure 1:*
*Ratios of side feeding populations to the ground states band in $^{162}$Er after the reaction $^{150}$Nd($^{16}$O,4n)$^{162}$Er for three bombarding energies.*
*The agreement between the theoretical and experimental results are fairly good. The shift of the angular momentum giving the maximum value with the bombarding energy is qualitatively reproduced.*

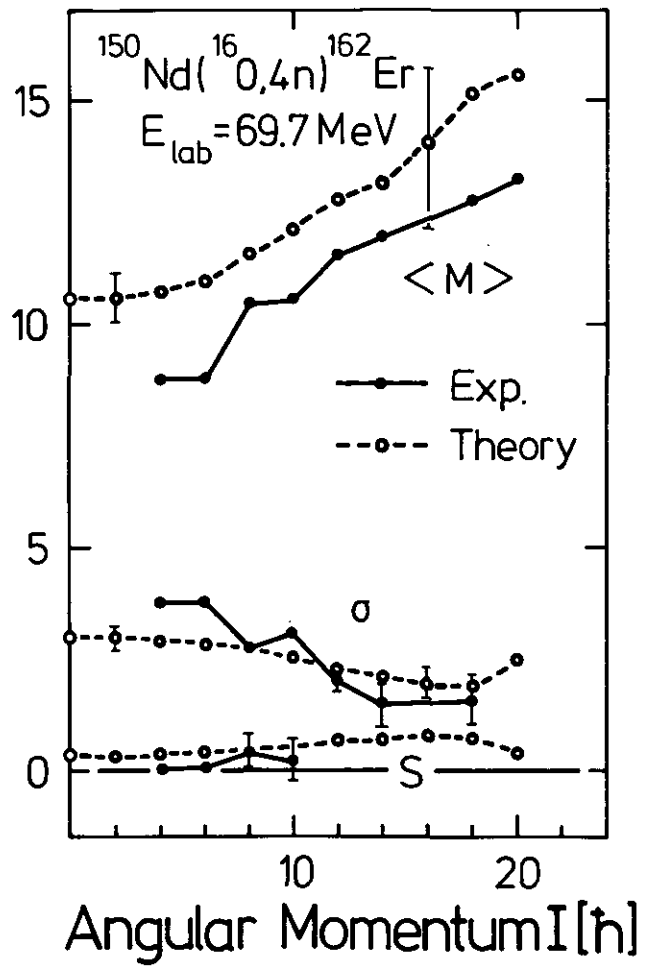


*Figure 2:*
*The avarage multiplicity <M> of the γ-ray cascades proceeding through a definite ground state rotational band angular momentum in $^{162}$Er for the reaction $^{150}$Nd($^{16}$O,4n)$^{162}$Er, $E_{lab}$ = 69.7 MeV. The standard deviation σ and the skewness s are also plotted. The experimental trends for the angular momentum dependence are well reproduced by the theoretical calculation.*

### References

[1] G.B. Hageman et al., Nucl. Phys. A245 (1975) 166; R. Broda et al., Nucl. Phys. A248 (1975) 356; C. Anderson et al., preprint
[2] D.G. Sarantites, B.D. Pates, Nucl. Phys. A93 (1967) 545

## 5.4 Heavy Ion Reactions

### 5.4.1. Excitation of the Lowest 1⁻ State in $^{18}O$ by Scattering from $^{16}O$

J. Carter*), R.G. Clarkson*), V. Hnizdo*), F. Osterfeld, A. Richter**) and J.P.F. Sellschop*)

Excitation of low lying states in $^{18}O$ was studied by scattering $^{18}O$ from $^{16}O$ at $E_{lab}$=35 MeV[1]. The $^{18}O$ beam was accelerated by the Witwatersrand University EN tandem onto a self-supporting $S_iO_2$ target, and a kinematic coincidence method employing a position sensitive detector was used to separate the events of interest. Of particular interest was the 1⁻ (4.45 MeV) state, the excitation of which in heavy ion scattering has so far received little attention.

In the collective model, meaningful description of low lying 1⁻ states requires a two-step excitation mechnism. Thus coupled channel calculations were performed assuming the 1⁻ level to be either a quadrupole/octupole 2-phonon state, reached via the 2⁺(1.98 MeV) state, or an octupole/quadrupole state, fed via the 3⁻ (5.09 MeV) level. The resulting fits for the two coupling schemes are shown in the figure, and the optical potential with the deformation lengths are given in the table.

The lowest 2⁺ and 3⁻ excitations in $^{18}O$ are fitted well and the deformation lengths $\delta_\ell$ of the 2⁺ and 3⁻ states are in good agreement with published results of both alpha ($\delta_2=\beta_2R$=0.86, $\delta_3=\beta_3R$=1.25)[1] and heavy ion scattering ($\delta_2$=1.08, $\delta_3$=0.83)[2]. On the other hand, as seen in table I, quite different deformation length are needed if the 1⁻-state is interpreted as a quadrupole/octupole or octupole/quadrupole phonon state, respectively. From these comparisons one may question the plausibility of a two-step excitation mechanism.

Therefore a microscopic analysis of the $^{16}O$ induced 1⁻ cross section was performed in DWBA with a microscopic form factor and with distorted waves generated by the optical potential as given in table I. The nucleon-nucleon force was assumed to have the commonly used Gaussian form with a range and strength adjustable to fit the data. By folding this two-body force with the internal wave function of the $^{16}O$ nucleus (we assumed all p-shell nucleons to be active) an effective interaction with an $^{18}O$ nucleon was obtained. For the ground state and 1⁻ level of $^{18}O$ the weak-coupling model wave functions of Zuker[3] were employed. The results of the microscopic model calculations are also shown in the figure. It should be stressed that a realistic value of 62 MeV for the strength of the nucleon-nucleon force was required while the force range was fixed at 1.75 fm. This value is also in good agreement with results obtained for $^{18}O(\alpha,\alpha')^{18}O(1^-)$-scattering where a value of 43 MeV has to be used in order to fit the data of ref. 4).

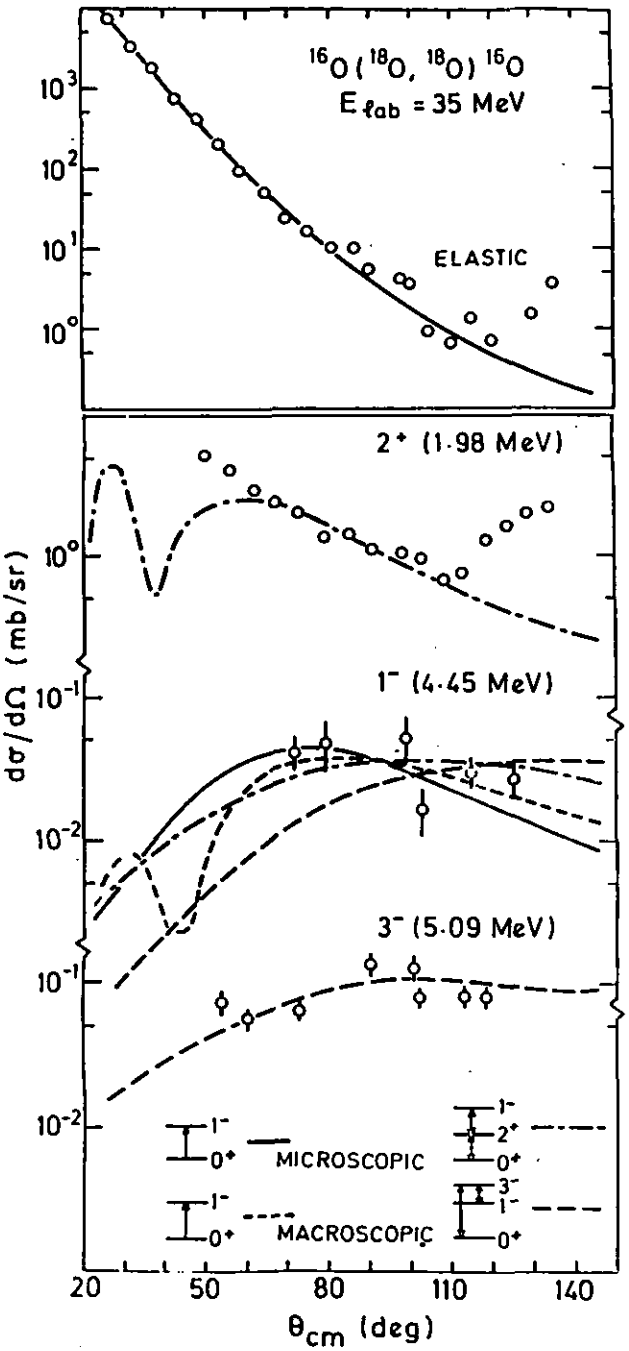


*Figure 1:*
*Experimental and theoretical angular distributions for $^{18}O$ + $^{16}O$ at $E^{lab}$ = 35 MeV.*

*Table 1: Optical parameters and deformation lengths $\delta_\ell = \beta_\ell R$. Energies in MeV, lengths in fm*

| | V | $r_o$ | $a_o$ | W | $r_I$ | $a_I$ | $\delta_1$ | $\delta_2/\delta_3$ | $\delta_3/\delta_2$ |
|---|---|---|---|---|---|---|---|---|---|
| $^{18}O+^{16}O$ | 100 | 1.20 | 0.49 | 40[a] | 1.20 | 0.49[b] | 0.34 | 1.08/0.66 | 0.64/2.00 |

*a) Reduced to 25 MeV in CC calculations* *b) Reduced to 0.20 fm in CC calculations*

*) Nucl. Physics Research Unit, University of the Witwatersrand
**) Technische Hochschule Darmstadt

**References**

[1] H.F. Lutz, S.F. Eccles, Nucl. Phys. 81, 423 (1966)
[2] R. Vandenbosch, W.N. Reisdorf, P.H. Lau, Nucl. Phys. A230, 59 (1974)
[3] A.P. Zuker, Phys. Rev. Lett. 23, 983 (1969)
[4] B.G. Harvey et al., Phys. Rev. 146, 712 (1966)

## 5.3 Transfer Reactions

### 5.3.1. An Analysis of (d,p) Reactions

K.A. Gridnev*), V.M. Semjonov*), E.F. Hefter**)

In a foregoing analysis of the reaction $^{14}N(d,p)^{15}N$ applicability of the conventional DWBA and the impulse approximation (IA) have been discussed[1]. These results will be supplemented by calculations based on the adiabatic approximation (AD)[2] employing some approximate formulae[3]. For practical purposes this model is reduced to a prescription of how to construct from nucleon potentials the appropriate deuteron potential. In the approximate version employed, the radii are not altered and the depth of the spin-orbit potential is simply taken to be the sum of the nucleon potentials. The parameters for the transferred neutron and the global potentials for neutrons and protons in the continuum are taken to be the same ones as previously.

Fig. 1 shows experimental points for $E_d$ = 12 MeV, 32 MeV and 52 MeV and results of calculations with the DWBA and the IA. The dotted curves correspond to computations with the adiabatic approximation. In line with our experience with the IA[1] an energy dependence assigned to the imaginary part of the optical potential is seen to remove a good deal of the discrepencies between theory and experiment, cf. full curves. The numerical material shows that already the simplified version of the AD leads to results, which are no worse than the ones of the IA. Relative to the DWBA both markedly improve the correspondence to experiment, esp. for higher energies. However, the problem associated with the computations point to the need for a better knowledge of the optical model potentials for light nuclei and of consistent methods of how to treat their energy dependence when employing them within the IA or the AD.

*) Phys. Res. Institute, Leningrad State University, USSR
**) Institut für Theor. Pysik der TU Hannover

#### References

[1] E.F. Hefter, E.T. Boschitz, V. Heidt, Ch. Wed digen, Nucl. Phys. A275 (1977) 212
[2] R.C. Johnson et al., Phys. Rev. C1 (197O) 976; Nucl. Phys. A234 (1974) 56; G.H. Rawitscher, Nucl. Phys. A241 (1975) 365; Phys. Rev. C11 (1975) 1152
[3] G.R. Satchler, Phys. Rev. C4 (1971) 1485 G.L. Wales and R.C. Johnson, Nucl. Phys. A274 (1976) 168

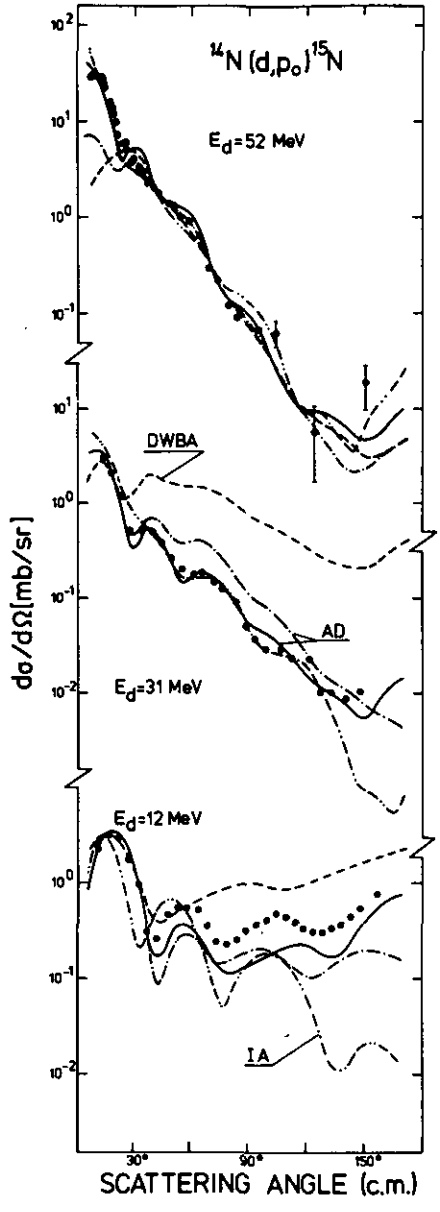


*Figure 1:*
*For different deuteron energies experimental and theoretical (d,p) angular distributions are shown. (DWBA-convertional DWBA, IA-impulse approximation; AD-adiabatic approximation, cf. tents).*

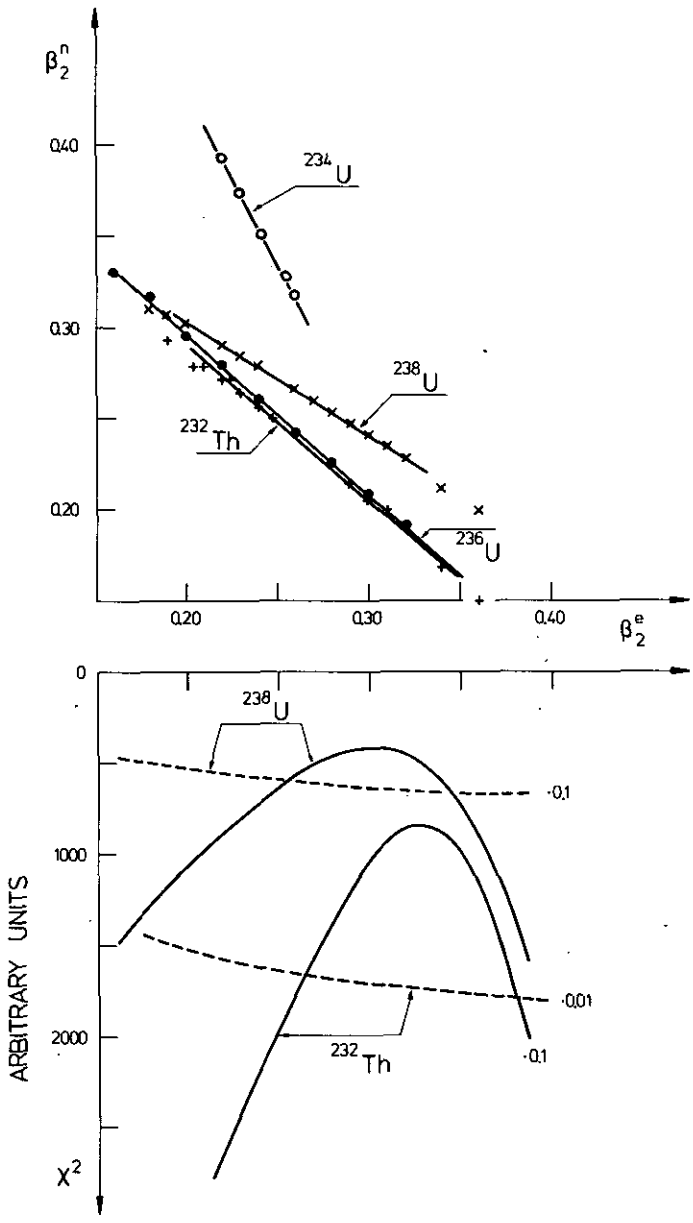


*Figure 1:*
*The dependence of the potential deformation, $\xi_2$, on the charge deformation, $\beta_2$, is illustrated. For the nuclei $^{232}Th$ and $^{238}U$ the corresponding $j4c^2$-minima are situated at $\beta_2 = 0.33$, $\beta_2 = 0.18$ and at 0.3, 0.24, respectively (of lower part of the figure, the broken lines refer to the ground state).*

$\beta_2^n(\chi^2)$ show that there exist definite ninima for some of the isotopes.

However, the corresponding values for $\beta_2^e$ and $\beta_2^n$ (of fig. 1) markedly differ from the ones obtained in the preceeding work[1].

Because of the use of average optical model parameters the present results have only the character of model calculations. They are consistent with the interpretation attributing different shapes to the nucleus when looking at it in differently coulered light (i.e. employing different projectiles). Similar relations as for $\beta^e$–$\beta^n$ are observed for the deformations of the real and imaginary parts of the transition potential. These findings seem to suggest that the task of determining the „true" deformation encounters additional obstacles when considering targets with strongly correlated states.

*) ISKP der Universität Bonn
**) FHP der Forschungsgesel. für angew. Naturw., 5307 Wachtberg
***) Institut für Theor. Physik der TU Hannover

## References

[1] P. David, J. Debrus, H. Essen, F. Lübke, H. Mommsen, R. Schoenmackers, W. Soyez, H.V. von Geramb and E.F. Hefter, Z. Physik A278 (1976) 281

Isospin violation can now happen in two ways. First, the states $\Phi_i$ themselves can be of mixed isospin. Following ref. 2 we assume two-state mixing for the states $^{12}C$ (15.11, 1$^+$) and $^{12}C$ (12.71, 1$^+$):

$$\phi^{1^+}_{15.11} = \sqrt{1-\epsilon^2}\ \phi^{1^+}_{T=1} + \epsilon\ \phi^{1^+}_{T=0}$$
$$\phi^{1^+}_{12.71} = \sqrt{1-\epsilon^2}\ \phi^{1^+}_{T=0} - \epsilon\ \Phi^{1^+}_{T=1} \qquad (9)$$

where the mixing parameter $\epsilon$ in first order perturbation theory is related to the Coulomb-matrix element by

$$\epsilon = \frac{< \phi^{1^+}_{T=0} | V_c | \phi^{1^+}_{T=1} >}{E_1 - E_0} \qquad (10)$$

$$E_1 - E_0 = 2.4\ \text{MeV}$$

where $V_c$ is the coulomb-interaction between the target nucleons. If the mixing in the target states were the only source of isospin-mixing a measurement of the differential cross sections leading to the 15.11 MeV-state and 12.71 MeV-state would determine the desired $\epsilon$. However, secondly there are effects of the same order of magnitude due to $V_{el}$ („polarization"). Because of the unnatural parity transition $0^+ \rightarrow 1^+$ only magnetic interaction can be involved in a direct transition. But these can be safely neglected.

But there are second order processes of the type

$$(O^+, T=O)\ V^+_{el}\ (J^\pi, T=1)\ V^+_n\ (1^+, T=1)$$
$$(O^+, T=O)\ V^+_n\ (J^\pi, T=O)\ V^+_{el}\ (1^+, T=1) \qquad (11)$$

In second order DWBA, the T-matrices for these processes can be written as

$$T^{(2)}_{fi,m} = \int d^3R\, d^3R'\ \chi_f(\vec{R}') < \phi_f | V_{fm} | \phi_m > G_m(\vec{R},\vec{R}')$$
$$\times\ < \phi_m | V_{im} | \phi_i > \chi_i(\vec{R}) \qquad (12)$$

$\Phi_m$ is the intermediate target state with $(I_m M_m; T_m T^3_m = O)$ $V_{im}$, $V_{fm}$ are the relevant parts of the effective interactions which cause the transitions and $G_m(\vec{R},\vec{R}')$ is the Greens-function in the intermediate channel m at the energy $E_m = E-\varepsilon_m-\varepsilon_d$.

There is a remarkable similarity to the direct amplitude which proceeds through the internal mixing alone:

$$T^{(1)}_{fi} = \int d^3R \chi_p(\vec{R})\ < \phi^{1^+}_{T=1} | V_c | \phi^{1^+}_{T=0} > \frac{1}{E_1 - E_0}$$
$$\times < \phi^{1^+}_{T=0} | V | \phi^{0^+}_{T=0} > \chi_i(\vec{R})$$
$$E_1 - E_0 = 2.4\ \text{MeV}$$

By comparing eq. (12) and eq. (13) we see that the „polarization" of the target wavefunction by the incoming projectile admixes isospin violating parts into the reaction amplitude comparable in magnitude to the mixing in the target itself. Furthermore these two amplitudes add up coherently showing the sensitivity of the cross section to isospin violating parts in the reaction mechanism. We suppose that the T=1, 1$^-$ (giant resonance) states are the most important intermediate states.

A coupled channel programm is presently set up to test quantitatively these ideas. (Of course, all orders of magnitude are taken into account but the 2$^{nd}$-order effects are the most important ones). The giant resonance is described as a RPA-state, the 1$^+$-states are taken as a pure $p^{-1}_{3/2}\ P_{1/2}$-configuration.

Furthermore, also the importance of the contributions of the deuteron intermediate states will be studied.

**References**


[1] Isospin in Nuclear Physics, Wilkinson (ed.), Amsterdam 1969
[2] W.J. Braithwaite, J.F. Bussoletti, F.E. Cecil, G.T. Garvey, Phys. Rev. Lett 19 (1972) 376
[3] J.M. Lind, G.T. Garvey, R.E. Tribble, Nucl. Phys. A276 (1977) 25
[4] F. Iachello, P.P. Singh, Phys. Lett. 48B (1974) 81
[5] L.A. Charlton, P.D. Kunz, Phys. Lett. 72 B (1977) 7
[6] T. Tamura, Rev. of Mod. Phys. 37, 679 (1965) V.A. Madsen, Nucl. Spectr. and Reac. Part D, Academic Press Inc. San Francisco, New York, London 1975


## 5.2.6. A Study of Correlations between Deformation Parameters


P. David*), H. Essen**) and E.F. Hefter***)


One of the unresolved problems in collective model analysis of inelastic scattering experiments is the determination of the absolute deformation. A glance into the published literature shows that investigations employing different projectiles (or simply considering different energies of the projectile) yield in general different answers.

In a previous analysis[1] of ($\alpha,\alpha'$) experiments on Th and U isotopes correlations between the charge and potential deformations ($\beta^e_2$ and $\beta^n_2$) were observed. In the limited range of values considered, the correspondence to experiment was of the same order of magnitude for all pairs $\beta^e_2 - \beta^n_2$. The ambiguity was resolved by adjusting $\beta^e_2$ to approved values as taken from literature. In here the interrelation $\beta^e_2 - \beta^n_2$ is to be looked at more closely. Our aim is to explore the possibility of obtaining on grounds of a consistent analysis unique values for the $\beta^n_j$; i.e. without resorting to results of other studies. Numerical investigations of the functions $\beta^e_2(\chi^2)$ and

Satchler et al.[8] by fitting to inelastic scattering to bound states in the Ca-region, our calculations would be of the same order of magnitude as the experimental results.

Finally let us relate our work to other approaches in the literature. A formal general theory of „multi-step-direct" processes has recently been given by Feshbach[2]. Our calculations correspond to the first step contribution to the „hierarchy" of states, e.g. excitations of increasing complexity introduced by Feshbach.

Recently, a calculation of the (p,p')-reaction in first and second order DWBA was done by the Austin Group[9]. They get impressive agreement with experiment. In principle, our calculations for (d,d') correspond to their first order contribution. The advantage of the present approach is that the form factors for specific transitions are each calculated separately introducing less assumptions as compared to multi-step calculations of (p,p) reactions by Tamura et al.[9] using an averaged form factor valid for all ph excitations.

We thank Profs. J. Ernst and V.A. Madsen for very stimulating and helpful discussions.

## References


[1] M. Blann, Ann. Rev. of Nucl. Sci. 25 (1975)
[2] H. Feshbach, Proceedings, Varenna-Conference, Varenna 1977
[3] J. Ernst, J. Bisplinghoff, T. Mayer-Kuckuk, J. Pampus, J. Rama-Rao, G. Baur, H. Lenske, F. Rösel, D. Trautmann, Proceedings of the Varenna Conference, Varenna 1977
[4] S. Krewald, Jül-Report 1315, Jülich 1976
[5] H. Horie, K. Sasaki, Prog. of Th. Phys. 25 (1961) 475
[6] M. Abramowitz, I.A. Stegun, Handbook of Mathematical Functions, Dover Publ. Inc., New York
[7] C.M. Perey, F.G. Perey, Atomic Data and Nuclear Data Tables, 13 (1974) 294
[8] T.A. Belote, J.H. Bjerregard, O. Hansen, G.R. Satchler, Phys. Rev. 138 (1965) B1067
[9] T. Tamura, T. Udagawa, D.H. Feng, K.K. Kan, Phys. Lett. 66B (1977) 109


## 5.2.5. Investigation of the Role of Isospin in Nuclear Reactions

G. Baur and H. Lenske

One of the fundamental assumptions of nuclear physics is the charge independence or at least charge symmetry of nuclear interactions. However, because of the presence of the charge symmetry breaking electromagnetic interactions a test of this hypothesis in the nuclear many-body system is extremely difficult[1]. If there are charge dependent nuclear interactions they are of the same magnitude or less[1] than the Coulomb-interaction. Therefore, one has to describe the Coulomb-effects in nuclei very properly. One way to investigate isospin mixing in nuclear states is to study isospin violation in nuclear reactions.

As an example of our general approach we study the inelastic scattering of deuterons on $^{12}C$ leading to the T = 1, 1⁺ level at 15.11 MeV in $^{12}C$[2,3]. Clearly, this excitation is forbidden in the absence of isospinviolating forces because of the T = O groundstates of d and $^{12}C$. The weak, but long range static Coulomb interaction between the two constituents can polarize both nuclei resulting in an admixture of T = 1 components into the wavefunctions of the deuteron and the $^{12}C$ target. The magnetic interactions are less important in the measured energy region (E ≤ 40 MeV).

Therefore, we expand the total wavefunction of the system in the following way

$$\psi(\vec{R},\vec{r},\vec{\rho}) = \Sigma_i \phi_i(\vec{\rho})\chi_i(\vec{R})\psi_d(\vec{r}) + \sum_{\nu,i} \phi_i(\vec{\rho})\int d\vec{q}\,\chi^{\nu}_{\vec{q}}(\vec{R})\psi^{\nu}_{\vec{q}}(\vec{r}) \qquad (1)$$

Here, $\Phi_i(\vec{\rho})$ denote states in the $^{12}C$ system (i=o:$^{12}C$ g.s.), $\chi_i(\vec{R})$ is the c.m. wavefunction of relative motion of $^{12}C$ and d, and $\psi_d(\vec{r})$ is the internal wavefunction of the deuteron in the groundstate. $\psi^{\nu}_{\vec{q}}(\vec{r})$ is the wavefunction of the broken up n-p system with $\vec{q}$ the wavevector of the relative motion of n and p, $\chi^{\nu}_{q}(\vec{R})$ denotes the c.m. wavefunction of the unbound p-n system. The indices i = ($\varepsilon_i$, T $T_3$, I $M_I$) and ν = ($T_d T_d^3$ I $M_I$) denote all internal quantum numbers as excitation energy $\varepsilon_i$ of the target, isospin T, total angular momentum and parity $I^{\pi}$ and the projections $T_3$,$M_I$ of target and projectile. In the following we will neglect the second term of eq. (1). We assume that states in which both subsystems are mutually excited have reduced overlap relative to the simpler case in which only one subsystem is excited.

In contrast to the stripping-pick-up mechanism considered by Iachello and Singh[4] our ansatz, eq. (1), is in principle a complete expansion of the total wavefunction. Also it avoids the appearance of non-orthogonal channels and no problems with finite range effect[5] arise.

Furthermore we obtain a simple physical interpretation of the isospin violating part of the reaction mechanism.

Inserting eq. (1) into the Schrödinger-equation

$$(H - E)\psi = 0 \qquad (2)$$

and integrating over all coordinates except R, the c.m.-coordinate of the relativ motion, one gets coupled equations for the wavefunctions $\chi_i(R)$:

$$(K + U_i(\vec{R}) - E_i)\chi_i(\vec{R}) = -\sum_{j\neq i} V_{ij}(\vec{R})\chi_j(\vec{R}) \qquad (3)$$

When $\varepsilon_i$ is the excitation energy of the target and $\varepsilon_d$ the binding energy of the deuteron ($\varepsilon_d$<O), then

$$E_i = E\text{-}\varepsilon_i\text{-}\varepsilon_d \qquad (4)$$

and K is the kinetic energy operator. As usual[6] for the diagonal potentials $U_i$ we take optical potentials at the energy $E_i$. The coupling potentials $V_{ij}$ are given by

$$V_{ij}(\vec{R}) = \langle \phi_i(\vec{\rho})\psi_d(\vec{r})|V(\vec{\rho},\vec{r},\vec{R})|\psi_d(\vec{r})\phi_d(\vec{\rho})\rangle \qquad (5)$$

and

$$V(\vec{\rho},\vec{r},\vec{R}) = V_n(\vec{\rho},\vec{r},\vec{R}) + V_p(\vec{\rho},\vec{r},\vec{R}) + V_{el}(\vec{\rho},\vec{r},\vec{R}) \qquad (6)$$

is the sum of elementary nucleon-nucleon interactions of the type (x = n,p)

$$V_x(\vec{\rho},\vec{r},\vec{R}) = g_x(\vec{\rho},\vec{r},\vec{R})\,(a_o + a_\sigma\,\vec{\sigma}_x\vec{\sigma}_i + \vec{\tau}_x\vec{\tau}_i(a_\tau + a_{\tau\sigma}\vec{\sigma}_x\vec{\sigma}_i)) \qquad (7)$$

and the charge dependent electromagnetic interactions $V_{el}$. By folding V with the d-groundstate an effective deuteron-nucleon interaction is derived:

$$V_{eff}(\vec{\rho},\vec{R}) = \langle \psi_d(\vec{r})|V|\psi_d(\vec{r})\rangle \qquad (8)$$

## 5.2.4. Inelastic Scattering into the Continuum Region as Particle-Hole Excitations

H. Lenske and G. Baur

In the last years, several attempts have been made, to explain the broad distribution of inelastically scattered projectiles into the continuum region by the preequilibrium mechanism. The statistical models like the Hybrid-Model of Blann[1] are able to explain the spectra of the inelastically scattered projectiles, but there are some discrepancies or inabilities to give the angular-distributions in a similar good agreement with experiments as the angle integrated spectra. We view the excitation of the nucleus as a sequence of p-h-excitations of the DWBA-type, i.e. we take into account explicitly the shell-structure of the nucleus. It was our aim to calculate the first order contributions to the preequilibrium-cross-section. The inclusion of second and higher order effects would become increasingly difficult and non-transparent. However, simplifications of the resulting expressions can be done due to statistical assumptions, as it was shown recently by Feshbach[1], so that the multistep direct processes are in principle calculable, too.

As a first example, we investigate the reaction $^{63}$Cu(d,d') at 24.7 MeV bombarding energy, which was recently measured in Bonn[3].

At this energy a total number of 96 single proton or neutron p-h-excitations are open, disregarding spin-flip. Furthermore, only excitations from closed sub-shells are taken into account. The shell-model s.p.-energies were taken from the $^{90}$Zr-Region[4]. In order to have the calculations as transparent as possible we choose for the NN-interaction a Gaussian, which was folded with the Deuteron-ground-state wavefunction, to give an effective Deuteron-Nucleon-Interaction of the form

$$V_{dN} = -V_o^{eff} \exp\left[-\mu_{eff}^2 (\vec{R}_d - \vec{r}_N)^2\right] \qquad (1)$$

Here, $\vec{R}_d$ is the c.m.-coordinate of the Deuteron relative to the nucleus and $\vec{r}_N$ the nucleon-coordinate. The deuteron groundstate was taken as a 1s harmonic oscillator state with an oscillator-constant of $b_D$ = 2.488 fm corresponding to the mean-square-radius of the deuteron. The derived values for $V_o^{eff}$ and $\mu_{eff}$ are $V_o^{eff}$ = 15 MeV, $\mu_{eff}^{-1}$ = 2.0 fm corresponding to a Yukawa type interaction of 1 fm range.

Also the single-particle wavefunctions were taken as harmonic-oscillator functions. Then, the form factor

$$F_{IM}(\vec{R}) = \langle IM|V|O^+\rangle \text{ for a } O^+ \to (j_i^{-1}\, j_f)\, I^\pi M$$

transition can be calculated analytically[5] as

$$F_{IM}(\vec{R}) = V_o\sqrt{4\pi}\,\hat{j}_i\;\hat{j}_f\; I \begin{pmatrix} j_i & j_f & I \\ 1/2 & -1/2 & 0 \end{pmatrix}$$

$$\cdot (\sqrt{i})^{4l+1}\;\frac{1}{(b\beta)^3}\left(\frac{\mu_{eff}^2 R}{\beta}\right)^l \exp\left|-\mu_{eff}^2\,\frac{\beta^2-\mu_{eff}^2}{\beta^2}\,R^2\right|$$

$$\cdot M(n_i\ell_i,n_f\ell_f)^{-1/2} \sum_{m=\ell_i+\ell_f}^{\ell_i+\ell_f+2(n_i+n_f)} a_m(n_i\ell_i,n_f\ell_f)$$

$$\cdot 2^{m/2}\;\frac{1}{(b\beta)^m}\left(\frac{m-l}{2}\right)!\, L_{\frac{m-l}{2}}^{(l+1/2)}\left(-\frac{\mu_{eff}^2 R}{\beta}\right) Y_{lM}(R)$$

i.e. the radial integrals are given by an expansion of generalized Laguerre-Polynomials $L_k^{(\mu)}$[6]. The $M(n_i\ell_i,n_f\ell_f)$ and $a_m(n_i\ell_i,n_f\ell_f)$ are normalization constants[5] and $\hat{j} = (2j+1)^{1/2}$, $\beta^2 = (1+b^2\mu_{eff}^2)/b^2$, b the oscillator constant.

This form factor is inserted in the standard DWBA-code DWUCK to compute the T-matrix elements

$$T_{IM} = \int d^3R\, \chi_f^{(-)}(\vec{k}_f,\vec{R})^*\, V_{IM}(\vec{R})\, \chi_i^{(+)}(\vec{k}_i,\vec{R}) \qquad (3)$$

where the $\chi$'s are the distorted waves of the deuteron, generated by standard optical potentials as given by Perey and Perey[7].

The differential cross-sections for a specific p-h-excitation i of angular momentum $l_i$ is given by

$$\frac{d\sigma^{l_i}}{d\Omega} = \frac{2\pi\hbar}{v_d} \sum_{M_i} |T_{l_iM_i}|^2\, \rho_f(E_{d'}) \qquad (4)$$

In reality, these states will be smeared out due to coupling to the continuum and more complicated states. To take this in some way into account we introduce a smearing function $f(E_{l_i}-E_{d'})$ of Gaussian type

$$f(E_{l_i}-E_{d'}) = \frac{2}{\Gamma\sqrt{\pi}} \exp\left[-\frac{4(E_{l_i}-E_{d'})^2}{\Gamma^2}\right] \qquad (5)$$

The summation over all degenerate p-h excitations leads to the double-differential cross section

$$\frac{d^2\sigma}{d\Omega\, dE_{d'}} = \sum_{i,l_i} \frac{d\sigma^{l_i}}{d\Omega} f(E_{l_i}-E_{d'}) \qquad (6)$$

In Fig. 1 the results for the angular distribution of the reaction $^{63}$Cu(d,d') for several final energies of the deuterons are shown and can be compared with the experimental results. We choose $\Gamma$ = 5 MeV for all states. Most of the cross-section stems from $\Delta L$ = 1 transitions. As the experimental ones the theoretical angular distributions show strong forward peaking, but the former show less structure at low energies due to isotropic evaporation contributions. With our choice of 15 MeV for the effective D-N-Interaction we are too low by about an order of magnitude. We remark that using a strength of $V_o^{eff}$ = 65 MeV, a value which was obtained by

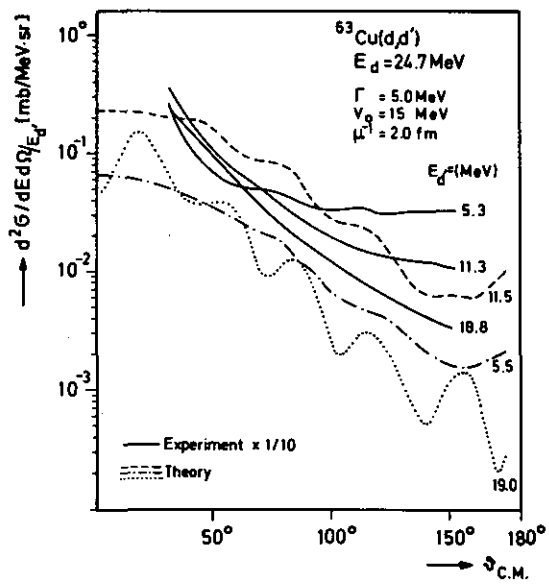


*Figure 1:*
*Comparison of the calculated and experimental cross-section for $^{63}$Cu(d,d') for three energies $E_d$, of the outgoing Deuteron.*

## 5.2.3. Microscopic Theory of the Imaginary Inelastic Transition Form Factor[1]

G. Baur, V.A. Madsen*), F. Osterfeld

It has long been recognized that a complex interaction is needed to describe the elastic scattering of a projectile from a nucleus when one uses a one-body Schrödinger equation. However, for inelastic scattering very little is known about the imaginary part of the form factor from a microscopic point of view. In the collective model, the inelastic form factor is simply proportional to the derivative of the optical potential and therefore has a real and imaginary part. The problem with the microscopic approach has to do with the nature of the intermediate states. In elastic transitions, any strong intermediate state n contributes in the second order transition i → n and n → i with the same phase. For inelastic scattering the intermediate state should have substantial coupling to the initial and final state; but, since the two matrix elements i → n and n → f are different, there is no guarantee that the phases of the various n terms are constructive. They could be random and therefore destructive[2]. We show however, that there is no randomness of phase and that substantial imaginary interaction is expected. We assume that the initial and final nuclear states are related as follows,

$$\phi_f = \sum_{\bar{m}\underline{n}} A_{\bar{m}\underline{n}}\ a^{+}_{\bar{m}}\ a_{\underline{n}}\ \phi_i \qquad (1)$$

where m refers to an unoccupied state (particle) an n an occupied state (hole) based on the target. Eq. (1) would hold for TDA collective states as well as simple single particle transitions. The intermediate states are simple particle hole doorway states. Thus we find two types of important intermediate states for each particle-hole configuration mn: there are the 'particle scattering' type and the 'hole scattering' type shown in Figs. 1a) and 1b) respectively. From the Fermion anti-commutation relations it follows that the two contributions 1a) and 1b) have opposite sign.

In our calculations of the imaginary part of the inelastic transition form factor Im $F^{(2)}$ in second order we have used a zero range projectile nucleon interaction. The intermediate projectile Green's function was calculated using a complex Saxon Woods potential. Furthermore a local approximation has been introduced[3]. Our result in that Im $F^{(2)}$ can be written as

$$\mathrm{Im}\ F^{(2)} = F^{(1)} < \mathrm{Im}\ \tilde{G} > \qquad (2)$$

where $F^{(1)}$ is the real part of the first order transition form factor and G is a local function[1]. Calculations have been carried out for $^{40}$Ca(n,n')$^{40}$Ca ($3^-$,3.73 MeV) and $^{17}$O(n,n')$^{17}$O($1/2^-$,.86VMeV) at 3O MeV incident energy. Fig. 2 shows a comparison of our microscopic results with the collective model. The magnitude surface peak comes at too small a radius. This may be due to the use of a zero range force. In summary we have shown that the real and imaginary form factors are related in strength and that the hole scattering term subtracts from the particle term giving rise to a peak at or beyond the nuclear surface.

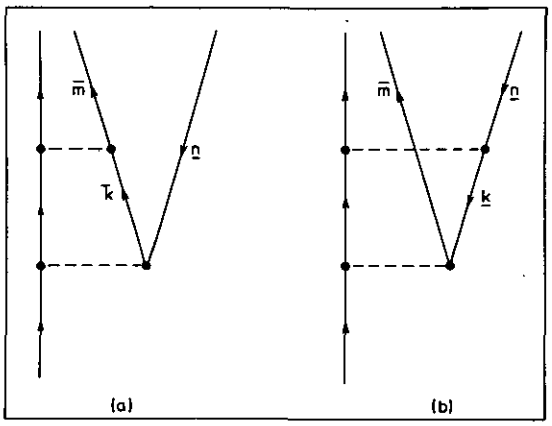


*Figure 1:*
*Diagrams showing the (a) particle-scattering and (6) hole-scattering second-order interactions contributing to the imaginary inelastic form factor.*

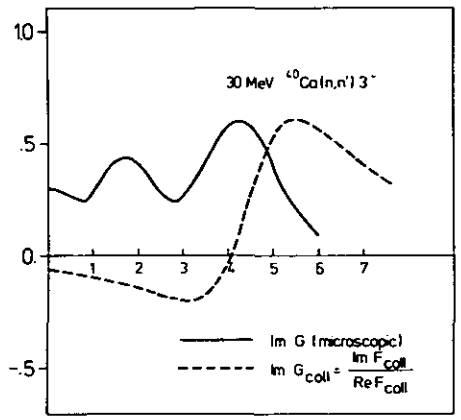


*Figure 2:*
*Microscopic and collective functions G relating approximately real and imaginary form factors (see text).*

### References

[1] G. Baur, V.A. Madsen and F. Osterfeld, Pyhs. Rev. C, in press
[2] N.K. Glendenning, Proceedings of the International School of Physics Enrico Fermi Course XL, eds. M. Jean and R.A. Ricci (Academic press, New York 1969) p. 332; A. Sevgen, Nucl. Phys. A216 (1973) 429
[3] N. Vinh Mau and A. Bouyssy, Nucl. Phys. A257 (1976) 189

*) Permanent address: Oregon State University, Corvallis OR, 97331, USA

## 5.2.2. Two-Step Processes in Inelastic Proton Scattering

E.F. Hefter*), H.V. von Geramb**), F. Osterfeld, T. Udagawa***)

Calculations within the microscopic antisymmetrized DWBA (MADWBA) showed the necessity of suppelementing the real nucleon nucleon interaction by imaginary contributions[1,2]. The additional terms are said to take care of intermediate multistep processes, which are not treated explicitly. The simplest possible intermediate configuration with a complex particle in the continuum corresponds to the formation of a virtual deuteron in its groundstate (S=1). Our aim is to study the significance of such (p-d-p') processes with the transition amplitude $T^{(2)}$, in the building up of the final transition amplitude, T.

$$T = T^{(1)} + T^{(2)}$$

$T^{(1)}$represents the contribution of the direct process computed via the MADWBA. To minimize the uncertainties associated with the microscopic description, we choose the targets $^{16}O$ and $^{40}Ca$, which have been thoroughly discussed in literature. The parameters employed to generate $T^{(1)}$ are in accord with ref. 2). The ones for $T^{(2)}$ are selected to comply with the requirements of a consistent description applying the adiabatic approximation to the single-particel transfers.

Some numerical results for the target nucleus $^{16}O$ are displayed in fig. 1. The two-step process is about an order of magnitude smaller than the direct process, which in turn underestimates experiment for small angles by a factor of two. For larger angles it is of the same magnitude or even larger than experiment. The total cross-section is about 20 % larger than the one based on $T^{(1)}$ only. However, it shows only very little additional structure. The improvement relative to experiment is restricted to forward angles and larger energies.

It appears premature to name with sorbidence the reasons for the remaining disagreement with experiment; but, besides possible inaccuracies due to the optical model potentials and the nucleon-nucleon interaction, it is obvious that the S=O state of the deuteron and other intermediate multistep processes could well give rise to additional terms being of the same order or even larger than $T^{(2)}$.

*) Institut für Theor. Physik der TU Hannover
**) I. Inst. für Experimentalphysik der Univ. Hamburg
***) permanent address: Dept. of Physics, Univ. of Texas, Austin, Texas 78712, USA

### References

[1] G.R. Satchler, Phys. Letters 35B (1971) 279 Y. Terrien, Nucl. Phys. A199 (1973) 65
[2] H.V. Geramb and P.E. Hodgson, Nucl. Phys. A246 (1975) 173

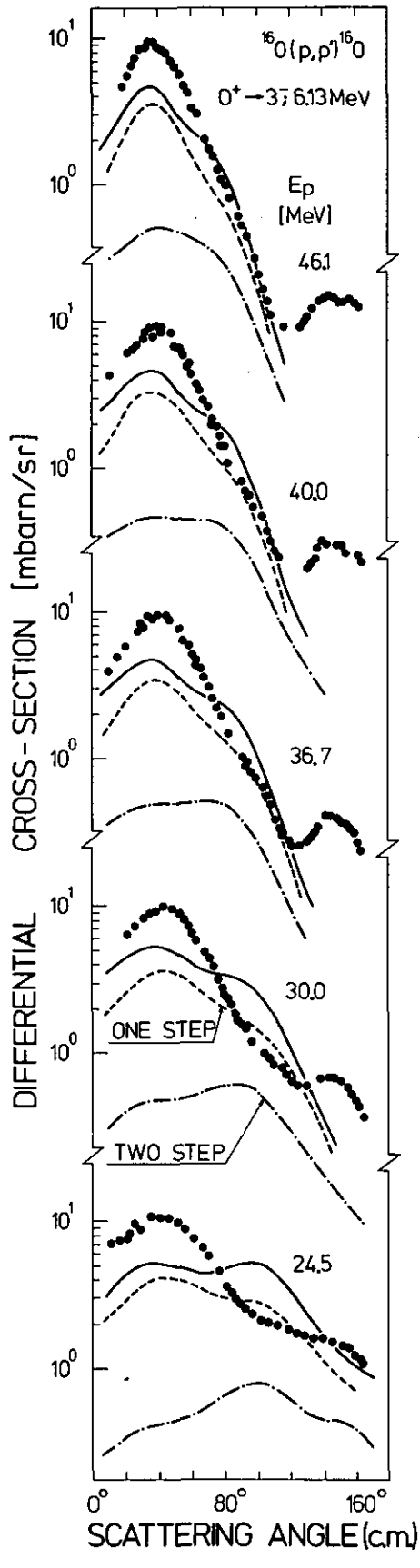


*Figure 1:*
*The full points correspond to inelastic proton scattering experiments on $^{16}O$ leaving the residual nucleus in its excited $3^+$ state at 6.13 MeV. The broken lines correspond to MADWBA calculations, the dotted ones give the contributions of the two-step process alone and the full curves represent the final results based on $T = T^{(1)} + T^{(2)}$.*

where the exchange potential is given by

$$V^{EXCH}(1,0) = V(\vec{r}_o,\vec{r}_1)\delta^3(\vec{r}_1-\vec{r}'_o)\delta^3(\vec{r}_o-\vec{r}'_1)P_\sigma(0,1)P_\tau(0,1) \quad (3)$$

The coordinate of the incident nucleon carries the index O and the target nucleon the index 1. $P_\sigma$ and $P_\tau$ are the spin and isospin exchange operators, respectively. $V(r_o,r_1)$ is assumed to be a finite range force with central and tensor parts. Following the notations of Tamura[2] the bracket matrix element in (2) can be written as

$$<Bb|V^{EXCH}|Aa> = \sum_{JLS} (-)^{J_A-M_A+s_b-m_b+s+m_s}$$

$$(J_A M_A J_B - M_B | j\ m_j)(s_a m_a\ s_b - m_b | s m_s)(j m_j\ s m_s | l - m_l) \quad (4)$$

$$f^{l_a,l_b}_{jls}(r_o,r'_o)\ [Y_{l_a}(\hat{r}_o)\ Y_{l_b}(\hat{r}'_o)]_{lm_l}$$

with the non-local exchange form factor

$$f^{l_a,l_b}_{jls}(r_o,r'_o) = (-)^{s_a-s_b-s}\ \frac{\hat{j}}{2} \sum_{\lambda l_1 l_2} \rho^{l_1,l_2}_{\lambda sj}(r'_o,r_o)$$

$$\times \sum_{na_1a_2} v^n_{a_1a_2}(r'_o,r_o)(-)^{j-s+l_1}\ \hat{n}\hat{j}\ W(\lambda l s s, n j)$$

$$\times i^{-l_a-l_b}\ \frac{1}{4\pi}\hat{\lambda}\hat{a}_1\hat{a}_2\hat{l}_a\hat{l}_b(a_2 0 l_b 0|l_1 0)(a_1 0 l_a|l_2 0) \quad (5)$$

$$\begin{Bmatrix} a_1 & a_2 & n \\ l_b & l_a & L \\ l_2 & l_1 & \lambda \end{Bmatrix}$$

Here, $\rho^{l_1,l_2}_{\lambda sj}(r_o,r_o)$ denotes the non-local transition density and the coefficients $v^n_{a_1a_2}$ arise from the multipole expansion of the central (n=O) and tensor (n=2) parts of the nucleon-nucleon interaction. A program has been written to evaluate the non-local form factor $f^{l_a,l_b}_{jls}(r_o,r_o)$. Since the non-local form factor is strongly peaked at the diagonale ($r_o=r'_o$) in ($r_o,r'_o$)-space and falls off quickly as one goes away from the diagonale, it has to be known only for points near the diagonale in order to carry out the 6-dimensional integral in (2). This fact has been incorporated into the program Saturn-Mars of Tamura and Low[3] where we put in the form factor given in (5). By also making use of the interpolation facilities of the Saturn-Mars program the calculations can be sped up tremendously, so that, for instance a ADWBA-calculation for the reaction $^{208}$Pb (p,p') $^{208}$Pb (3$^-$, 2.6 MeV) with 3 $\hbar\omega$-RPA wave functions takes less than 2 minutes on the IBM 365-168.

*) Permanent address: Oregon State University, Department of Physics, Corvallis, Oregon, USA

## References


[1] V.A. Madsen, in Nuclear Spectroscopy and Reactions, Part D, 1975, Academic Press, New York, p. 249
[2] T. Tamura, Phys. Reports 146 (1974) 61
[3] T. Tamura, K.S. Low, Comp. Phys. Commun. 8 (1974) 349

### 5.1.2. Microscopic Calculation of the Imaginary Part of the Optical Potential

V.A. Madsen, F. Osterfeld, J. Wambach

In second order perturbation theory the imaginary part of the nucleon-nucleus potential is given by[1]

$$W(\vec{r},\vec{r}') = \mathrm{Im} \sum_N <\Phi_o|V|\Phi_N> G_N(\vec{r},\vec{r}') <\Phi_N|V|\Phi_o>$$

where $\Phi_o$ and $\Phi_N$ are the ground and excited states of the target nucleus, respectively. $G_N$ is the Green's function for the intermediate propagating nucleon. Note that W is non-local and has to be made local in order to be compared with phenomenological potentials. In the work of Vinh Mau and Bouyssy[2] W has been calculated with the following assumptions:

1. V is a δ-type force
2. $G_N$ is the free particle Green's function
3. the $\Phi_N$ are RPA-states
4. Exchange effects between the incident nucleon and target nucleons are taken into account.

Vinh Mau and Bouyssy obtain results which are in reasonable agreement with the imaginary part of phenomenological potentials, especially they obtain surface peaking. We have repeated their calculations using a „realistic" finite range force[3] and an improved Green's function (optical model Greens function), but neglecting exchange effects (exchange effects are difficult to include with a finite range force). For the intermediate states $\Phi_n$ we used either simple particle-hole doorway states or collective RPA-wave functions with very similar results:
In both cases we get pure volume absorption and no surface peaking appears. This can be seen from fig. 1 where we compare our potential with that of ref. 1 and with the phenomenological potential of Becchetti and Greenless[4]. From our calculations and that of ref. 1 we must conclude that only exchange effects are producing a surface peaking in the imaginary part of the optical potential. While a δ-force produces the peak at to a small radius, it could be possible that the peak would be shifted to larger radii if a finite range force is used. Therefore it seems to be desirable to perform a calculation with finite range forces and with inclusion of exchange effects.

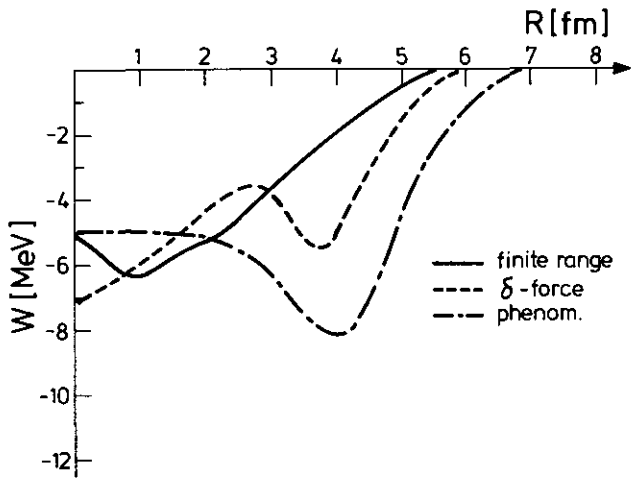


*Figure 1:*
*Imaginary part of the optical potential for 30 MeV neutrons scattered from $^{40}Ca$. The full curve shows our results obtained with intermediate particle-hole doorway states and the dotted curve is the phenomenological potential of Becchetti and Greenless [4].*

**References**

[1] H. Feshbach, C.E. Porter, V.F. Weisskopf, Phys. Rev. 96, 448 (1954)
[2] V. Vinh Mau, A. Bouyssy, Nucl. Phys. A257, 189 (1976)
[3] H. Eikemeier, H.H. Hakenbroich, Nucl. Phys. A169 (1971) 407
[4] F.D. Becchetti, J.W. Greenless, Phys. Rev. 182, 1190 (1969)

## 5.2 Inelastic Light Ion-Scattering

### 5.2.1. Non-Local DWBA-Code and Rapid Exchange Calculations

F. Osterfeld, V.A. Madsen*)

A difficulty with the use of inelastic nucleon scattering for nuclear spectroscopy is that calculations of inelastic cross sections become very long and tedious when large basis wave functions have been used to obtain the nuclear states. On the other hand, these large basis functions are absolutely necessary to produce inelastic transition strengths and form factors. There is no difficulty with the direct form factor but the calculation of exchange amplitudes can become very long and time consuming. Here, we present a method for calculating these exchange amplitudes in a very rapid way.

The antisymmetrized DWBA-transition amplitude ($T^{ADWBA}$) can be written as

$$T^{ADWBA} = T^{DIR} + T^{EXCH} \qquad (1)$$

where $T^{DIR}$ is the usual direct transition amplitude and $T^{EXCH}$ is the exchange amplitude. Here, we are especially interested in $T^{EXCH}$.

It is known[1] that exchange in inelastic nucleon scattering can be treated as direct DWBA with a non-local form factor. Denoting the initial and final channels by α = (a+A) and β = (b+B), respectively, the exchange amplitude can be written as

$$T^{EXCH} = \int d\vec{r}_o' \int d\vec{r}_o \, \chi_\beta(-)^* (\vec{r}_o') <Bb|V^{EXCH}|Aa> \chi_\alpha^{(+)}(\vec{r}_o) \qquad (2)$$

# 5. Nuclear Reaction

## 5.1 Elastic Scattering

### 5.1.1. Elastic Scattering below the Coulomb Barrier Static and Dynamic Polarization Effects

G. Baur, F. Rösel*), D. Trautmann*)

In the elastic scattering of heavy ions deviations from the Rutherford cross section $\sigma_R$ can occur even below the Coulomb barrier. These deviations[1,2] are mainly due to atomic screening, vacuum polarization and the Coulomb excitation of nuclear levels. Vacuum polarization, which is known from quantum electrodynamics, can be accurately taken into account by the usual Uehling form. It is calculated by a new and economic method[1]. In Ref. 1 we mainly investigated the influence of virtual (dipole) excitations. These excitations have usually a rather high excitation energy, which means that the adiabaticity parameter $\zeta$ is larger than 1. In this case the effect can be represented by a real potential which depends on the polarizabilities $\alpha$ of the two nuclei. The nuclear dipole polarizability is connected with the total photoabsorbtion cross section $\sigma$ by

$$\alpha \equiv 2 \sum_{n \neq 0} \frac{|\langle n|D_z|0\rangle|^2}{E_n - E_0} \leqslant \frac{\hbar c}{2\pi^2}\, \sigma_{-2} \equiv \frac{\hbar c}{2\pi^2} \int \frac{\sigma(E)}{E^2}\, dE, \qquad (1)$$

where the z-component of the dipole operator is denoted by $D_z$. The calculation of the deviation $\Delta = (\sigma - \sigma_R)/\sigma_R$ from Rutherford scattering can now be done either exactly by solving the radial Schrödinger equation, by first order quantum mechanical perturbation theory or by classical mechanics (exactly or in first order). Because of the large Coulomb parameter $\eta$ and the smallness of the additional potentials $V_{vac\ pol}(R) + V_{pol}(R)$ all methods yield practically the same result[1]. Thus we have for the effect of the polarizability:

$$\Delta(\Theta) = -\frac{E^3}{e^6 (Z_1 Z_2)^4}\, P^*\, g(\Theta) \qquad (2a)$$

with

$$P^* = \alpha_1 Z_2^2 + \alpha_2 Z_1^2 \qquad (2b)$$

*The function g depends only on the scattering angle $\Theta$ and is given* analytically in Ref. 1. Thus precise measurements of elastic scattering could determine nuclear polarizabilities in a new and independent way.

The excitation of nuclear levels characterized by $\zeta < 1$ leads to another effect: while the virtual excitation of nuclear levels leads to deviations from the Rutherford orbit by a change of the real potential, the real excitation of nuclear levels takes flux out of the elastic channel while the ions stay practically on the Rutherford orbit. Semiclassically, the elastic scattering cross section is given by[1,2]

$$\frac{\sigma}{\sigma_R} = P_0 = 1 - \sum_{i=0} P_i \qquad (3)$$

where $P_i$ denotes the excitation probability of the i-th level (0 = ground state).

Quite recently[3] a local potential was constructed to second order in the interaction coupling the two ions. (Because $\zeta < 1$ in their cases, their potential is mainly imaginary). In our approach, which is essentially exact for $\eta >> 1$, we can of course take coupling to all orders into account. In Fig. 1 we compare our calculations with the results of Ref. 3. We use 3 different coupling schemes: $0^+ \leftrightarrow 2^+$ *without (1a) and with (1b) reorientation and* $0^+ \leftrightarrow 2^+ \leftrightarrow 4^+$ *coupling* in a rotational model (1c). While for $\Theta \lesssim 50^\circ$ our calculations with the 3 coupling schemes agree quite well with each other and also with the (numerically much more elaborate) approximations of Ref. 3, for $\Theta > 50^\circ$ higher order effects become very important. This means that the assumption of Ref. 3 (second order coupling) will break down for larger angle scattering and the construction of a local potential will become even more difficult. But the semiclassical theory of Coulomb excitation can still be applied straightforwardly.

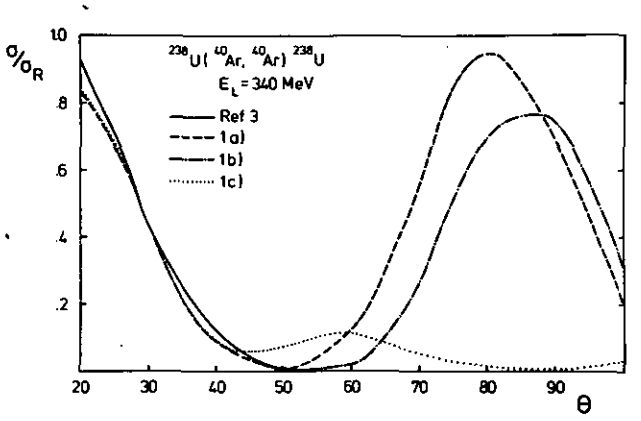


*Figure 1:*
*Comparison of semiclassical Coulomb excitation calculations with the optical model calculations of ref.[3]. Note that no nuclear effects are included in the Coulomb excitation calculations, this becomes unrealistic for* $\Theta \gtrsim 50^\circ$.

*) Institut für theoretische Physik der Universität Basel

**References**

[1] G. Baur, F. Rösel and D. Trautmann, Nucl. Phys. A288 (1977) 113
[2] K. Alder and A. Winther, Electromagnetic Excitation, North-Holland, Amsterdam (1975)
[3] W.G. Love, T. Terasawa and G.R. Satchler, Phys. Rev. Lett. 39 (1977) 6

## 4.6.2. Hermitian Operator Method for pf Shell Nuclei

H. Müther, K. Allaart*)

In recent years the Generator Coordinate Method (GCM) appeared to be a suitable method to describe those excitations of pf shell nuclei which correspond to collective degrees of freedom[1]. The GCM has been extended to include two-quasiparticle excitations[2]. Due to the large numerical effort, however, in this extended GCM (GCM+QP) one only can consider a few specific single particle excitations. It is the aim of the present investigation to search for a method, which considers the GCM correlations for the ground state, but allows for a more explicit treatment of single-particle excitations. This may be done assuming that the excited state results from a one-body excitation operator acting on the GCM ground state wave function

$$|\omega> = O^+ |GCM>. \tag{1}$$

Assuming the condition

$$O\,|GCM> = O\,, \tag{2}$$

this leads to the open-shell RPA. For low-lying states in nuclei with open shells the condition (2) is to restrictive. It has been argued[3] that, for the description of these states, one should better make the assumption that the excitation operator is a Hermitian one-body operator

$$O^+ = O\,. \tag{3}$$

This leads to the equation of the Hermitian Operator Method (HOM)

$$\begin{aligned} &<GCM|\,[R,[H,O^+]]|GCM> \\ &= \omega\,<GCM|RO^+ + O^+R|GCM> \end{aligned} \tag{4}$$

with R representing a complete set of one-body operators. Both sides of eq. 3 can easily be calculated using the one- and two-body density matrices for the GCM ground state. Results for the nucleus $^{54}$Fe using HOM and GCM+QP are displayed in figure 1 and compared to experimental data. For the calculations the whole pf shell is used as the model space. The Hamiltonian is the same as in ref. 2). One may notice from the figure that for this example, $^{54}$Fe, the excitation energies of the yrast states are considerably lower in HOM than in GCM+QP. The HOM results are also in a better agreement with experimental data. This shows, that, although the GCM description of these states is improved by adding K = O two-quasiparticle states in GCM+QP, a further improvement can be obtained by including also K ≠ O two-quasiparticle states in

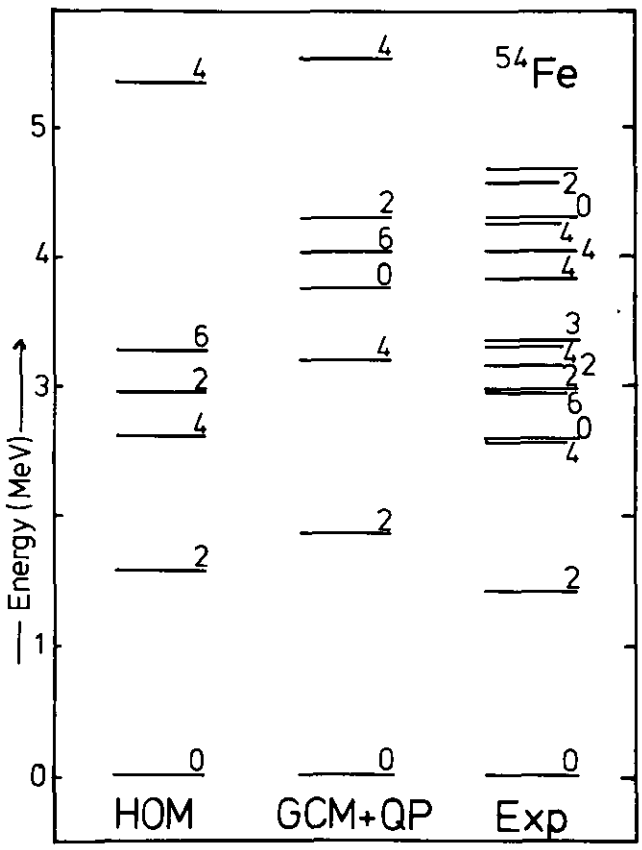


*Figure 1:*

HOM. The nuclei with N ≠ 28 exhibit more collective experimental excitation spectra and the lowest $4^+$ and $6^+$ states may be interpreted as vibrational or rotational states. The one-body excitations of the HOM therefore can describe the lowest $2^+$ but not the $4^+$ and $6^+$ states which are 2- and more phonon states. These collective states are described by GCM. Therefore we conclude that the HOM is a useful method to describe single-particle excitations. It is important, however, to use good approximations for the ground state wave function in HOM like e.g. those obtained from a GCM calculation.

*) Natuurkundig Laboratorium, Vrije Universiteit, Amsterdam

### References

[1] H. Müther, K. Allaart, K. Goeke and A. Faessler, Nucl. Phys. A298 (1975) 451
[2] H. Müther, K. Goeke, K. Allaart and A. Faessler, Phys. Rev. C15 (1977) 1467
[3] M. Bouten, P. van Leuven, M.V. Mihailovic and M. Rosina, Nucl. Phys. A202 (1973) 127

namely, $(4_2^+, 5_1^+)$, $(6_2^+, 7_1^+)$ ... This has been an outstanding difficulty of the Davidov-Filippov model. However, it is remarkable that the γ-deformations extracted from the extensive study[3] of the odd-mass transitional nuclei are quite consistent with the values obtained from the $E_{2_2}^+/E_{2_1}^+$ ratio predicted by the Davydov-Filippov model for the even-even mass nuclei.

Recently it has been shown[4] that in the description of the ground band of the even-even mass transitional nuclei using the deformed rotor model, the coupling of the Oqp and the 2qp excitations plays a very important role. Indeed we have found that due to this coupling the deformed rotor Oqp states (which lie high in the Davydov-Filippov model) are pushed down to be in close agreement with the experimental energies.

Encouraged with this success in describing the ground band we have employed the deformed rotor model which includes the O-2qp coupling, for studying the γ-band. It is extremely gratifying that this model provides the correct bunching of the states in the γ-band. The details of the Hamiltonian describing the system having O- and 2-qp excitations, and the basis wave functions employed in the calculations have been described in Ref. 4.

A detailed study shows that the effect of O-2qp coupling is larger for even spin states than that for the odd ones. And due to this the even spin states are pushed down much more than the odd spin states. As a consequence the bunching $(4_2^+, 5_1^+)$, $(6_2^+, 7_1^+)$ in the Davydov-Filippov model is destroyed, and in fact the lowering of the even spin states may be so large as compared to the odd ones (which depends on the γ-deformation) that just an opposite bunching is produced as seen in the experiments.

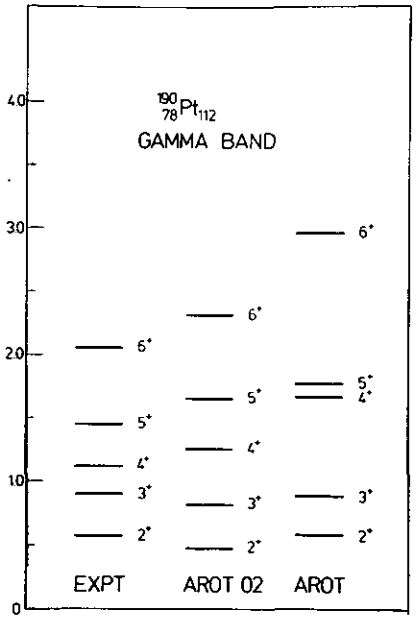


*Figure 1: Experimental and calculated results for the γ-band in $^{190}Pt$. Excitation energies have been plotted in units of MeV.*

As a representative case of such calculations we have shown the results for $^{190}Pt$ in Fig. 1. The results including the O-2qp coupling have been labeled AROTO2. We have also given the results for the deformed rotor model of Davydov-Filippov (AROT) for the purpose of comparison. The parameters used in the calculations are those employed in the description of the ground band[4]. It is evident from Fig. 1 that AROTO2 results are in fairly good agreement with the data. A comparison of AROTO2 with AROT shows how drastically the bunching in AROT is destroyed due to the O-2qp coupling.

Similar calculations for the other isotopes of Pt and for the Hg and Os isotopes have been performed. Throughout we witness similar results as described above. More interesting is the fact that the γ-deformations for the even-even mass nuclei and those used in the odd mass studies are found to be consistent. This provides a strong evidence supporting the existence of γ-deformation as opposed to the microscopic calculations.

The above results can be understood in a simple manner as explained in what follows: The O-2qp coupling is due to the Coriolis term $((\vec{I}\cdot\vec{j})\hbar^2/2\Theta_0)$ which is maximum when the core and particle angular momenta point in the same direction. Keeping this in mind we analyse for a given γ-deformation what are the favourable directions of the core and particle motions. As an example, let us consider $\gamma = 30^\circ$ which is simple as in this case the core motion can be described analytically. For $\gamma = 30^\circ$, the Hamiltonian for the core motion is given by $H \alpha [R_1^2 + 4(R^2 - R_1^2)]$ where $R_1$ is the projection of the core angular momentum R along the 1-axis which is the symmetry axis. $R_1$ being a good quantum number, it is straightforward to see that the even spin states of the γ-band have larger components along the 2-3 plane than the odd spins. This means that for $\gamma = 30^\circ$ the core motion favours the 2-3 plane in case of even spin states. Further, we examine the favoured direction of the particle motion. The particle-core coupling force can be written as

$$H_p \alpha \frac{1}{j(j+1)} \left\{(\sqrt{3}\sin\gamma - \cos\gamma)j_1^2 + (-\sqrt{3}\sin\gamma - \cos\gamma)j_2^2 + 2\cos\gamma\, j_3^2\right\}$$

which shows that for $\gamma = 30^\circ$ the particle motion favours the 2-axis. Thus, it is seen that in the case of even spin both the core and the particle angular momenta have the maximum overlap giving rise to a stronger O-2qp coupling as compared to that for odd spin states in the γ-band. A similar analysis can be made to understand the structure of the γ-band for γ-values away from $30^\circ$.

## References


[1] A.S. Davydov and G.F. Filippov, Nucl. Phys. 8 (1958) 237.
[2] H. Toki and A. Faessler, Z. Physik A276 (1976) 35
[3] J. Meyer-ter-Vehn, Nucl. Phys. A249 (1975) 111, 141 H. Toki and A. Faessler, Nucl. Phys. A253 (1975) 231
[4] H.L. Yadav, H. Toki and A. Faessler, Phys. Rev. Lett. 39 (1977) 1128

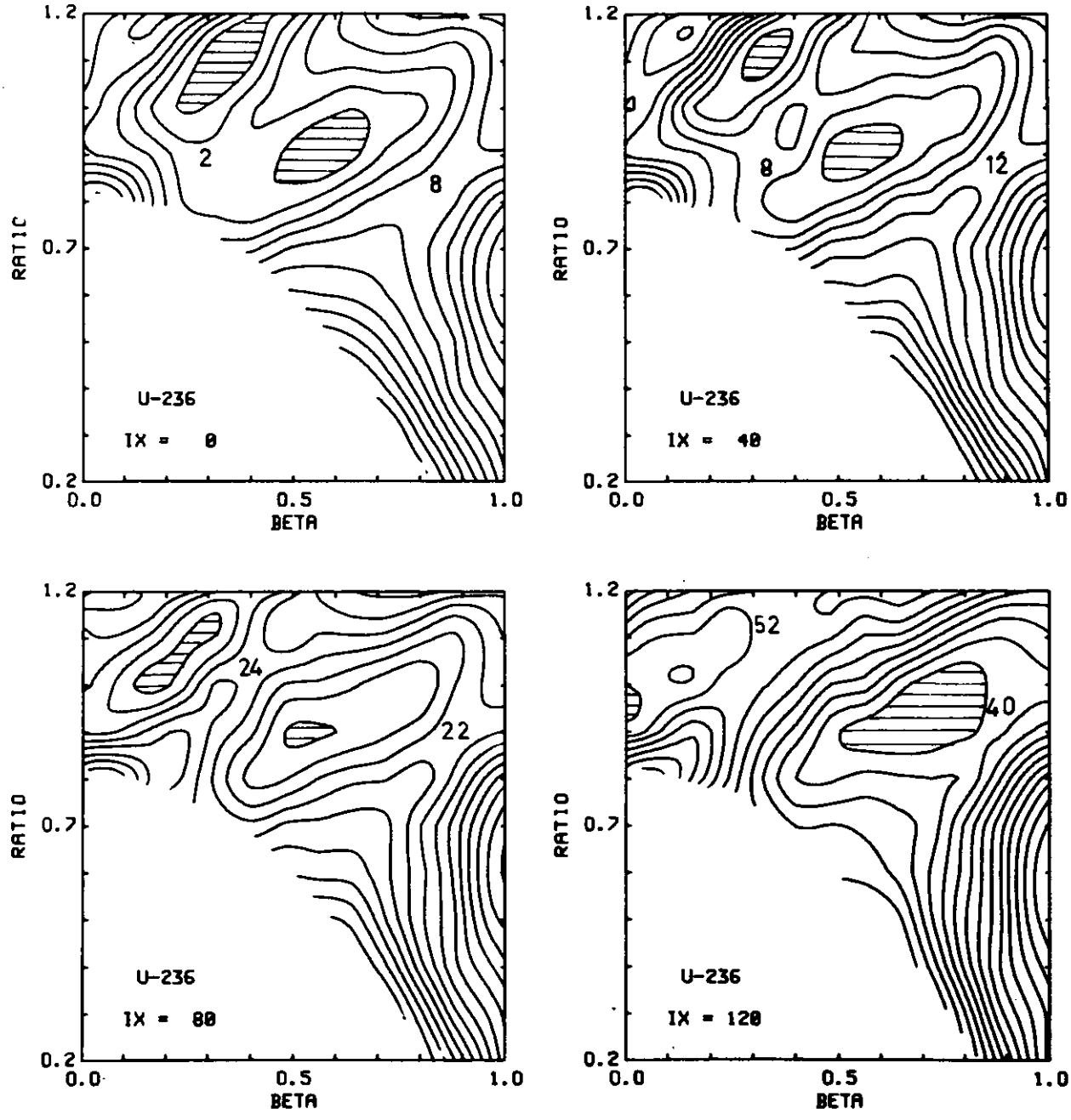


*Figure 1:*
*Deformation energy surface of $^{236}U$ for different angular momenta $I_x$. The minima are shadowed.*

## 4.6 Transitional Nuclei

### 4.6.1. Gamma Band in Transitional Nuclei

H.L. Yadav, H. Toki, A. Faessler

The asymmetric rotor model of Davydov and Filippov[1] has been extensively used in the past for studying the even-even mass nuclei. Recently Toki and Faessler[2] have carried out a systematic study of the ground and the γ-bands in the even mass transitional nuclei wherein the softness of the core has been taken into account phenomenologically through an extension of the variable moment of inertia (VMI) model. It has been pointed out in Ref. 2 that this description provides a nice agreement with the data for the ground band, but fails often in case of the γ-band as elaborated below. Experimentally one finds in many nuclei bunching of the $(3_1^+, 4_2^+)$, $(5_1^+, 6_2^+)$ ... states in the γ-band whereas calculations using the Davydov-Filippov model always produces opposite bunching,

(see 'theory $\gamma = 0^{\circ\prime\prime}$ fig. 2) which is intersecting with the ground state rotational band at around J = 10 and forms the yrast line above that angular momentum. An other way to generate this 'band' of band heads is to crank directly around the prolate symmetry axis. (In the calculation we allow for $\gamma$ deformations. But it turns out to be small ($|\gamma| \leq 6°$) and not essential for the results.) These calculations are also shown in fig. 2 ('theory = 120°'). Again this 'band' intersects the ground state rotational band at around J = 10 and forms for higher angular momenta the yrast line. Together with the selection rule $|\Delta K \leq \lambda$ ($\lambda$ = multipolarity of $\gamma$ transition) this leads with a high probability to yrast traps since the $\gamma$ transition operator is a one body operator and can connect only nqp states which differ at most by the nature of two quasi particles.

The reasons why one finds just in $^{176}$Hf so many K isomers which lie even lower than the yrast line, may be the following: (i) Near the Fermi surface at proton number 72 and neutron number 104 many Nilsson levels with $\Omega = j$ or $\Omega\ j-1$ are situated. They rotate around the waist of the prolate deformed nucleus and are concentrated near the equator. It is therefore possible without too much energy to build a large angular momentum along the symmetry axis. (ii) These qp states are further lowered in energy due to smaller pairing gaps than in neighbouring nuclei. (iii) Since the quasi particles are concentrated near the equator their overlap is increased and one gains additional energy by the increased overlap[6] (Maximization of the operlap of nucleonic wave functions by alignment of angular momenta = MONA).

*) Now at Institute of Nucl. Phys. Cracow, Poland

### References


[1] A. Bohr, B.R. Mottelson, Physica Scripta 10A (1974) 13
[2] R.G. Helmer, C.W. Reich, Nucl. Phys. A114 (1968 649
[3] T.L. Khoo, F.M. Bernthal, R.G.H. Robertson, R.A. Warner, Phys. Rev. Lett. 37 (1976) 823
[4] A. Faessler, K.R. Sandhya Devi, F. Grümmer, K.W. Schmid, R.R. Hilton, Nucl. Phys. A256 (1976) 106 and Nucl. Phys. A286 (1977) 101
[5] P. Ring, H.J. Mang, B. Banerjee, Nucl. Phys. A225 (1974) 141
[6] A. Faessler, M. Ploszajczak, K.R. Sandhya Devi, Phys. Rev. Lett 36 (1976) 1028


## 4.5.13. The Deformation Energy Surface of Necked Actinide Nuclei at Very High Angular Momentum


M. Faber*), A. Faessler, M. Ploszajczak, H. Toki


Cohen et al.[1] predicted within the liquid drop model that the fission barriers of beta stable actinides vanish at a critical spin value of about 60h. We studied the effects of shell structures on the defission barriers for axially and mirror symmetric fissioning nuclei. The single particle energies were calculated from a single particle Hamiltonian including a Saxon-Woods potential for the necked shapes of fissioning nuclei. To compare the total energy of largely different shapes a Strutinsky renormalization to the liquid drop average behaviour is necessary. The Strutinsky shell corrections $\delta E$ in the rotating case have to take into account both the level density and the angular momentum density

$$\delta E = \delta R + \omega \delta I.$$

To discuss the interplay between the rotational and the deformation energy in the Strutinsky renormalized total energy

$$E_{total} = E_{1d}(\omega=0) + \omega^2 \Theta_{geom}/2 + \delta R + \omega \delta I$$

we show in fig. 1 the energy surface of $^{236}$U for four angular momenta. The surfaces are parametrized by the ratio of the neck cross section to the cross section of the corresponding ellipsoid with the same volume and the same length of the symmetry axis. The deformation of the corresponding axially symmetric ellipsoid is parametrized by $\beta$. The energies are calculated with respect to the energy of a non rotating spherical liquid drop. The distance between the equienergy lines is 2 MeV. The ground state for low angular momenta is given by the first minimum, for angular momenta above 50h by the second minimum. Because of the shell effects the fission barrier vanishes slowly with increasing rotational angular momentum $I_x$ around the x-axis. The critical angular momentum with respect to fission[2] is very high in comparison to the critical value calculated with the liquid drop model.

Strutinsky calculations of non rotating nuclei show that further deformation degrees of freedom like axially asymmetric and mirror asymmetric deformations modify the second barrier. Since for high angular momenta the second barrier is the important one it will be interesting to extend the calculations to these shapes also for rotating nuclei.

*) TU Vienna, Australia

### References


[1] S. Cohen, F. Plasil and W.J. Swiatecky, Annals of Physics 82 (1974) 557
[2] M. Faber, A. Faessler, M. Ploszajczak, H. Toki, Phys. Lett., 70B (1977) 399

## 4.5.12. Yrast Traps in $^{176}$Hf

Amand Faessler, M. Ploszajczak*)

The possibility of the existence of isomeric states at very high spins has been linked to the rotation around a symmetry axis of an oblate shape[1]. But the same arguments lead to the possible existence of yrast traps for a rotation of a prolate nucleus around the symmetry axis. This mode of rotation and the possible yrast traps connected with it has not been stressed since it seemed very unlikely that a nucleus prefers to rotate along the yrast line (lowest energy for a given angular momentum) around the axis with the smallest classical moment of inertia. But an analysis of old data[2] shows that the $K^{\pi} = 16^{+}$ isomer at 2.45 MeV formed by four quasi particles with a half-life of 31 years in $^{178}$Hf is exactly of that nature. More recently a group from Michigan State University[3] published in $^{176}$Hf a measurement of a series of yrast traps with life times in the nanosecond region which seem to be of this nature.

This note wants to analyse these states in $^{176}$Hf theoretically: The method used[4] is a cranked Hartree-Fock-Bogoliubov (HFB) approach with particle number projection before the variation of the deformation and the pairing degrees of freedom. The total angular momentum is conserved in average by cranking around the x axis

$$H - \omega J_x \qquad (1)$$

which lies perpendicular to the prolate symmetry axis. The yrast traps are probably formed by four (4qp) and six (6qp) quasi particle states.

$$a^{+}_{\alpha} = \sum_{a} \left( A_{a\alpha} C^{+}_{a} + B_{a\alpha} C_{a} \right)$$
$$|nqp\rangle = a^{+}_{\alpha_1} \ldots a^{+}_{\alpha_n} \prod_{a \| \alpha} a_{\alpha} |0\rangle \qquad (2)$$

It was first shown by Mang and coworkers[5] and used in ref. [4] that the nqp state can be written as a HFB vacuum

$$|HFB\rangle = \prod_{a \| \alpha} \tilde{a}_{\alpha} |0\rangle \qquad (3)$$

if for the nqp states the coefficients A and B are exchanged for the definition of $\tilde{a}_{\alpha}$.

Table 1 shows a listing of the nature of the 4 and 6 qp states used in the calculation. Fig. 1 shows the energies of the different K isomeric states compared with the experimental data[3]. The agreement is surprisingly good apart of the $K^{\pi} = 22$ band head. If one connects the energies of the K = J band heads one finds a 'band'

*Table 1:*
*Nature of 4 and 6 quasi-particle states in $^{176}_{72}Hf_{104}$*

| K | E [kev] | quasi-particle states ($\Omega^{\pi}_{\tau}$) | | | | | |
|---|---|---|---|---|---|---|---|
| $14^-$ | 2866 | $7/2^+_p$ | $9/2^-_p$ | $7/2^-_n$ | $5/2^-_n$ | | |
| $15^+$ | 3080 | $7/2^+_p$ | $9/2^-_p$ | $9/2^+_n$ | $5/2^-_n$ | | |
| $16^+$ | 3266 | $7/2^+_p$ | $9/2^-_p$ | $7/2^-_n$ | $9/2^+_n$ | | |
| $19^+$ | 4377 | $7/2^+_p$ | $9/2^-_p$ | $7/2^-_n$ | $9/2^+_n$ | $5/2^-_n$ | $1/2^-_n$ |
| $20^-$ | 4766 | $7/2^+_p$ | $9/2^-_p$ | $7/2^-_n$ | $9/2^+_n$ | $7/2^+_n$ | $1/2^-_n$ |
| $22^-$ | 4864 | $7/2^+_p$ | $9/2^-_p$ | $7/2^-_n$ | $9/2^+_n$ | $7/2^+_n$ | $5/2^-_n$ |

The first column lists the angular momentum projection K of these bands to the symmetry axis. K is a relatively good quantum number for small total angular momenta only. The second column gives the experimental energies of the band heads. In addition we list the angular momentum projection Ω (only approximately good for small J), the parity π and the charge τ for the quasi-particle states which form the different K bands. Of the two different $\Omega^{\pi}_{\tau} = 7/2^{\pi}_{n}$ qp states one is of $h_{9/2}$ (93 %) and the other is of $i_{13/2}$ (93 %) nature mainly.

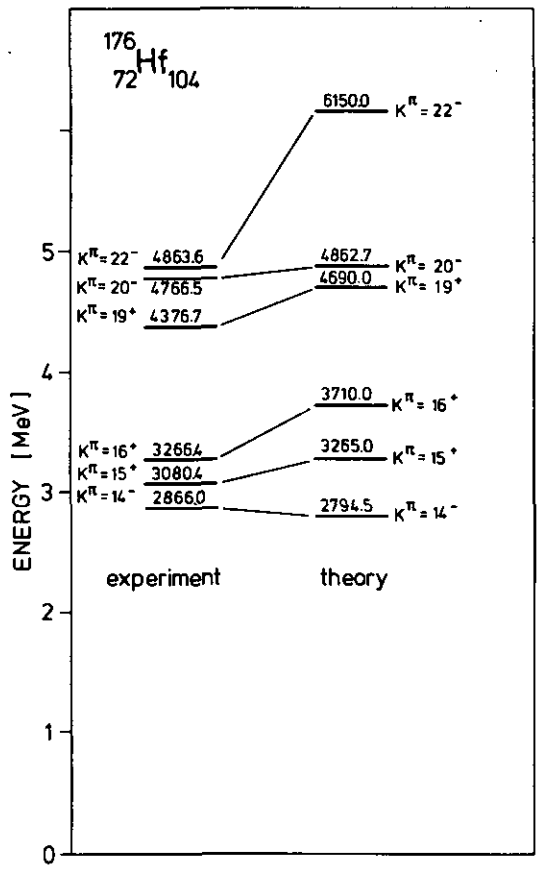


*Figure 1:*
*Experimental and theoretical K = J band head energies for the four and six quasi particle states in $^{176}$Hf characterized in table 1.*

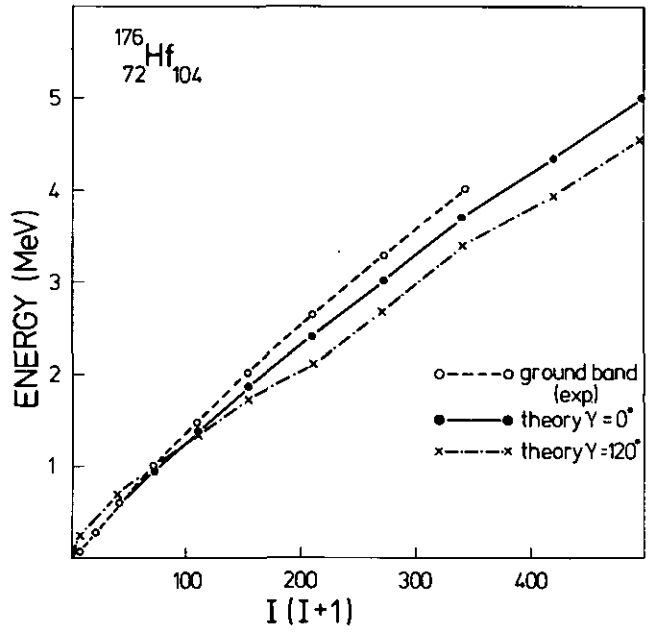


*Figure 2:*
*Excitation energy of the experimental (dashed line) and theoretical ground state rotational band (solid line) for $^{176}$Hf. the theoretical rotational band (γ = 120°; dashed dotted line) for a rotation around the prolate symmetry axis is also given. The "band" corrospinds to the K = J band heads on each of wich a rotational band is built. The K = J "band" is constructed by cranking around the prolate symmetry axis. Keeping the constraint $-\omega J_x$ this corresponds to a γ deformation of 120 degrees. One sees that the K = J "band" crosses the ground state band at around angular momentum 10 and forms for higher J the yrast states.*

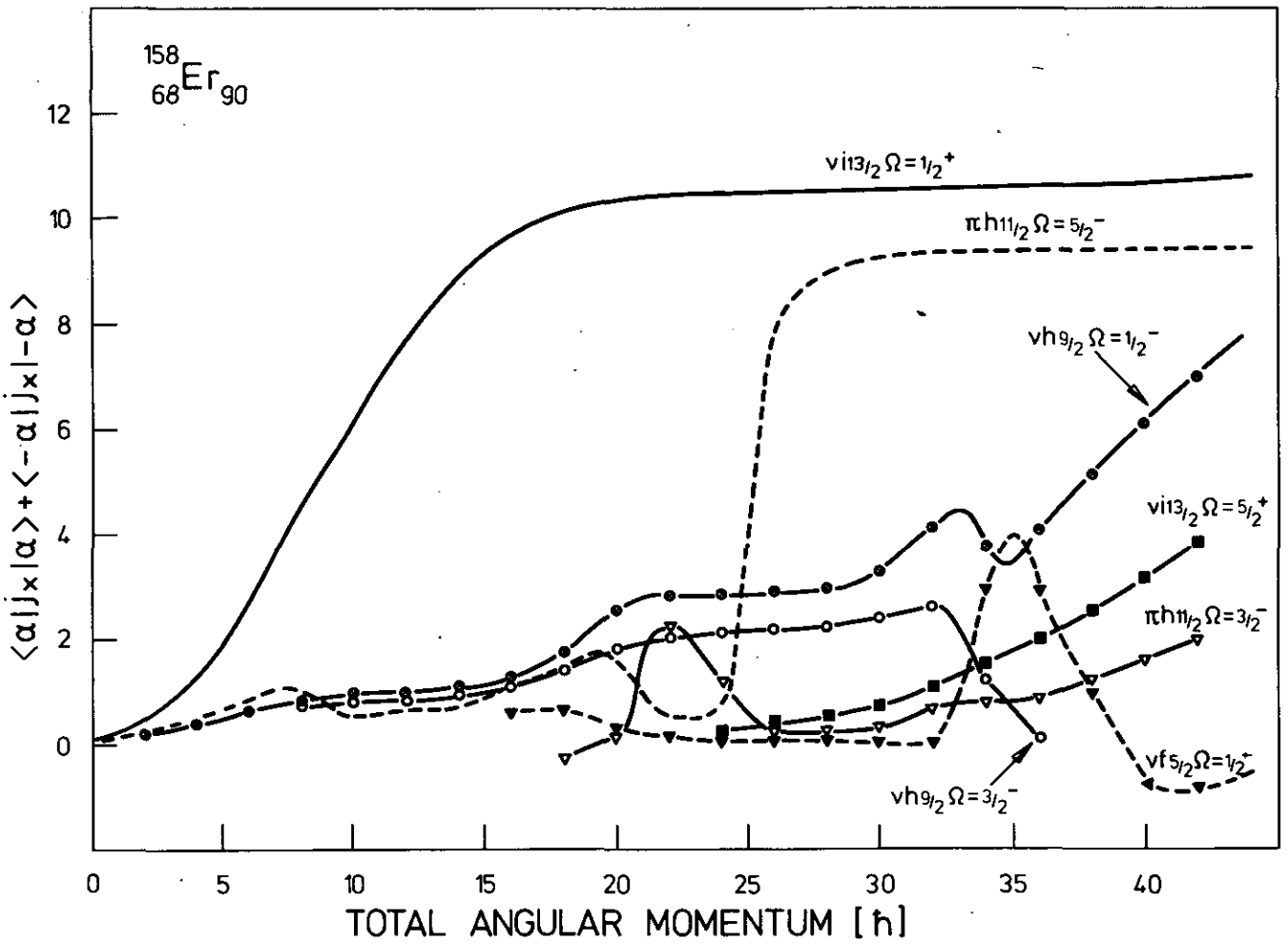


*Figure 2:*
*Rotational alignmant (RAL) plot for $^{158}Er$. The angular momentum expectation values $<\alpha|j_x|\alpha> + <-\alpha|j_x|-\alpha>$ for different pairs of nucleons are plotted against the total angular momentum. Backbending at $I \cong 14$ is due to RAL of an $i_{13/2}$ neutron pair. The anomaly at $I \cong 28$ is probably connected with the alignment of an $h_{11/2}$ proton pair.*

The wave function $|J> = |\beta, \gamma; \Delta_P, \Delta_N; J>$ is found for an average angular momentum J by minimizing the expectation value (1) in a class of HFB trial functions[3].

Figure 1 shows the result of the calculation for slightly different proton pairing force parameters $G_P$. The theoretical curve shows backbending at a too low value of the angular momentum.

This is due[4] to the omission of higher multipole pairing forces in the many body Hamiltonian H. Calculations with inclusion of a quadrupole pairing force show that about half of the discrepancy can be explained in this way[4]. Fig. 2 shows that the first anomaly is as expected connected with the alignment of an $i_{13/2}$ neutron pair (RAL).

The theory yields also a strong second anomaly at J = 22 to 24 which is too strong and lies at a too low angular momentum compared to the Berkeley data[1]. But keeping in mind that quadrupole pairing shifts also this second anomaly to higher angular momenta we may tentatively identify this second anomaly with the experimental upbending found at J = 26 and 28. The alignment plot in fig. 2 shows that this second anomaly is connected with the alignment of a $h_{11/2}$ proton pair. The next pair to align is a $h_{9/2}$ neutron pair and only then comes the second $i_{13/2}$ neutron pair.

In conclusion the theoretical calculations seem to indicate that the second anomaly of the moment of inertia in $^{158}Er$ is connected with the alignment of a $h_{11/2}$ proton pair.

*) Now at Institute of Nucl. Phys. in Krakow, Poland

## References


[1] I.Y. Lee, M. Aleonort, Y. El Masri, U.O. Newton, R. Simon, D. Diamond, F. Stephens, Phys. Rev. Lett.
[2] H. Beuscher, W.F. Davidson, R.M. Lieder, C. Mayer-Böricke, Phys. Lett. 40B (1972) 449
[3] A. Faessler, K.R. Sandhya Devi, F. Grümmer, K.W. Schmid, R.R. Hilton, Nucl. Phys. A256 (1976) 106
[4] M. Wakai, A. Faessler, Jülich preprint 1977 and this annual report

The purpose of this report is to study with a cranked Hartree-Fock-Bogoliubov (HFB) theory including particle number projection[1,2] this question. We construct a HFB trial wave function $|> = \beta,\gamma,\beta_4,\Delta_P,\Delta_N,J>$ for an average angular momentum J

$$<J_x> = \sqrt{J(J+1)} \qquad (1)$$

from the trial Hamiltonian

$$h_t = \sum_{i=1}^{A} [h_{Nil}(i,\beta,\gamma,\beta_4) - \omega j_x(i) + h_{Pair}(i,\Delta P,\Delta_N)] \qquad (2)$$

with the help of the HFB approach. The final solution is found by minimizing the particle number projected ($P_N$) expectation value of the many body Hamiltonian H with pairing and quadrupole force.

$$\frac{<HP_N>}{<P_N>} = E_J(\beta,\gamma,\beta_4,\Delta_P,\Delta_N) \qquad (3)$$

as a function of the shape parameters $\beta$, $\gamma$, $\beta_4$ and the pairing gaps $\Delta_P$ and $\Delta_N$. (Some of the parameters are kept constant to the value, which minimizes the energy in the intrinsic system, if test calculations showed that the results are not essentially influenced by this approximation.)

The theoretical calculations seem to be less reliable in this mass area than in Yb due to uncertainties of the Nilsson levels caused mainly by the lack of reliable information on the $\beta_4$ deformation. But they indicate clearly that the upbending found theoretically for $^{162}$Os is due to alignment of two $i_{13/2}$ neutrons. The dominant role of the $i_{13/2}$ neutrons stems from $\beta_4$ deformation which lifts even the $\Omega = \pm 1/2\, \upsilon i_{13/2}$ level near to the Fermi surface. The cranking term supports this further by cranking one of the $\Omega = \pm 1/2$ levels in the same direction.

The fact that one finds backbending in the $\upsilon i_{13/2}$, $\Omega = 9/2$ band experimentally and theoretically (see fig. 2) can be explained in the following way: Blocking of the $\upsilon i_{13/2}$, $\Omega = 9/2$ level prevents alignment of an $i_{13/2}$ neutron pair for low angular momenta. At higher angular momenta the $\Omega = 3/2$ level is cranked near to the Fermi surface and the corresponding neutron pair is rapidly aligned and produces backbending.

We find no backbending for $\pi h_{9/2}$, $\Omega = 1/2$ band in $^{181}$Re (see fig. 3) since the down sloping $h_{9/2}$ hole state induces a smaller deformation ($\beta_2 = 0.227$ see fig. 3). The Coriolis force is therefore increased and alignment of an $i_{13/2}$ neutron pair starts already at low angular momenta but in a smooth way, so that one obtains no backbending. The deformations for the $\pi h_{11/2}$, $\Omega = 9/2$ ($\beta_2 = 0.235$ see fig. 3) and the $d_{5/2}$, $\beta = 5/2$ ($\beta_2\Omega = 0.235$) are larger, so that the Coriolis force is only strong enough at higher angular momenta to aligne an $i_{13/2}$ neutron pair. This alignment is then quite rapid and produces backbending.

In conclusion we can say that backbending is also in the Os region caused by the alignment of an $i_{13/2}$ neutron pair.

*) Now at Institute of Nucl. Physics, Cracow, ul. Radzikowskiego 152, Poland
**) Now at Schuster Laboratory, Manchester University, England

### References


[1] A. Faessler, K.R. Sandhya Devi, F. Grümmer, K.W. Schmid, R.R. Hilton, Nucl. Phys. A256 (1976) 1O6
[2] A. Faessler, K.R. Sandhya Devi, A. Barroso, Nucl. Phys. A286 (1977) 1O1
[3] A. Neskakis, R.M. Lieder, M. Müller-Veggian, H. Beuscher, W.F. Davidson, C. Mayer-Böricke, Nucl. Phys. A261 (1976) 189


## 4.5.11. A second anomaly of the moment of inertia in $^{158}$Er


Amand Faessler, M. Ploszajczak*)


Recent experiments at Berkeley[1] have extended the angular momenta measured in the ground state rotational band in $^{158}$Er in Jülich[2] up to $J^{\pi} = 32^+$. The exciting fact in this measurement is a second anomaly of the moment of inertia above the backbending region around angular momentum J = 26 (see fig. 1).

Ever since it has been established that backbending is due to the Coriolis antipairing (CAP) or the rotational alignment (RAL) effect one has been speculating about a possibility of a second backbending due to the proton pairing collaps in the CAP effect or due to the alignment of a second $i_{13/2}$ neutron pair (RAL).

In this note we want to report on a theoretical analysis of the second anomaly found in $^{158}$Er and try to identify their nature. The theoretical analysis is based on a cranked Hartree-Fock-Bogoliubov (HFB) theory with particle number projection ($P_N$) before the variation of the essential degrees of freedom ($\beta$, $\gamma$, $\Delta_P$, $\Delta_N$).

$$E_J(\beta,\gamma;\Delta_P,\Delta_N) = \frac{<J|HP_N|J>}{<J|P_N|J>} \qquad (1)$$

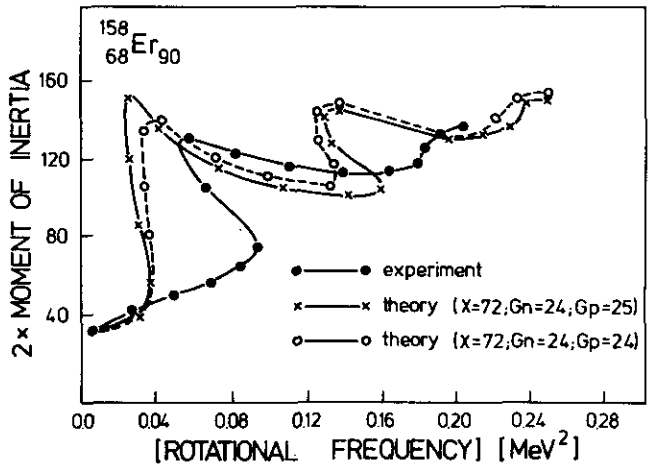


*Figure 1:*
*Twice the moment of inertia against the square of the rotational frequency for $^{158}$Er. The experimental data from Berkeley[1] and the theoretical results for two sets of the pairing force constants ($G_P A = 24$ MeV) and the quadrupole force ($\chi = 72$ MeV) are plotted. The experimentally found anomaly is explained as an RAL of an $h_{11/2}$ proton pair.*

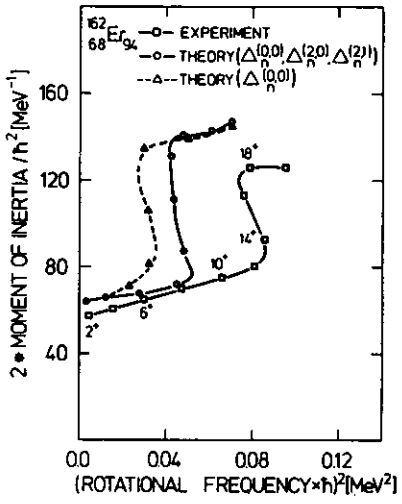


*Figure 2:*
*Backbending plot for $^{162}Er$ with inclusion of the monopole-, $Y_{21}$- and $Y_{20}$-pairings (open circles) and the monopole pairing only (triangles). The quadrupole pairing shifts the backbending point to hogher values.*

(3) The $Y_{20}$- and $Y_{21}$-pairings give a better agreement with the experimental data concerning the backbending point by shifting it to higher angular momentum (see fig. 2).
(4) The $Y_{22}$-pairing is negligible.

### References


[1] A.B. Migdal, Nucl. Phys. 13 (1959) 655; S.T. Beliaev, Nucl. Phys. 24 (1961) 322; I. Hamamoto, Nucl. Phys. A232 (1974) 445
[2] jnA. Faessler et al., Nucl. Phys. A256 (1976) 1O6


## 4.5.10. Cause of Backbending in the Os Region


Amand Faessler, M. Ploszajczak*), K.R. Sandhya Devi**)


In the Er and Yb region it seems to be well established that backbending is caused by the alignment of an $i_{13/2}$ neutron pair[1,2]. The situation is not so clear in the Os region. The Coriolis matrix element $[j(j+1)-\Omega(\Omega\pm1)]^{1/2}$ for the $i_{13/2}$ neutrons is getting smaller since the angular momentum projection quantum number Ω is increasing to Ω = 9/2. This arguments seem to be supported by recent experimental data from Jülich[3]. The dominant role of the alignment of an $i_{13/2}$ pair in backbending is demonstrated in the Yb region by the fact, that blocking of an $\nu i_{13/2}$ level by an odd neutron prevents backbending. Figure 1 shows a strong experimental backbending for $^{182}Os$ (the experiment in $^{180}Os$ shows only a slight upbending). Removal of a neutron from a $\nu i_{13/2}$ level does not prevent backbending (see fig. 2). But if one removes from $^{182}Os$ a $\pi h_{9/2}$, Ω = 1/2 proton, then one finds in $^{181}Re$ no backbending (see fig. 3). One could therefore conclude from these data that the $h_{9/2}$ protons are responsible for backbending in the Os region.

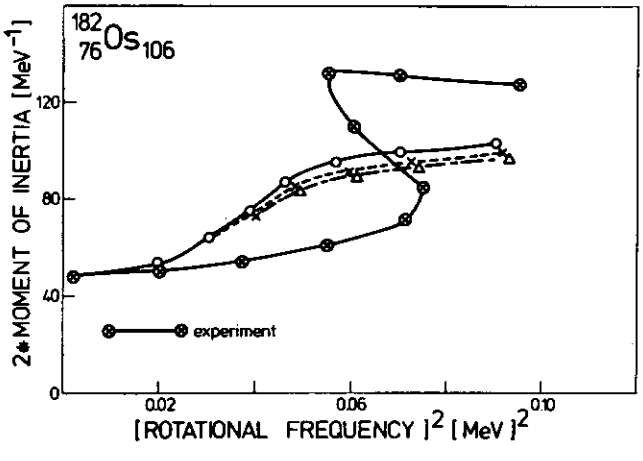


*Figure 1:*
*Twice the value of the moment of inertia as a function of the square of the rotational frequency in $^{182}Os$. The data are indicated by the crossed circles. The other curves give theoretical results for slightly modified forces.*

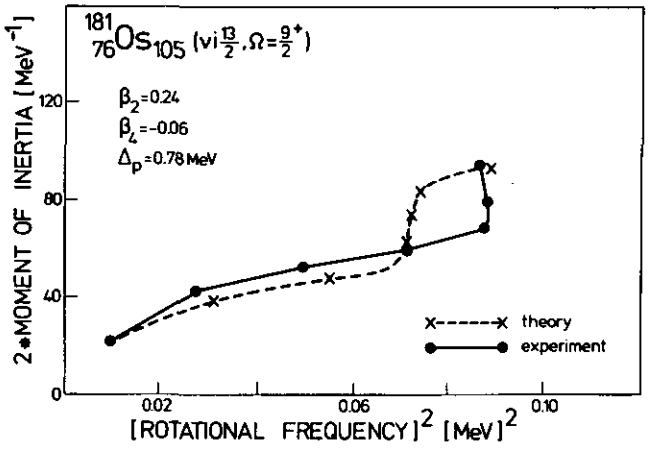


*Figure 2:*
*Backbending plot for the $i_{13/2}$, Ω = 9/2 band in $^{181}Os$. The solid line is the experiment[3] and the dashed line the theory.*

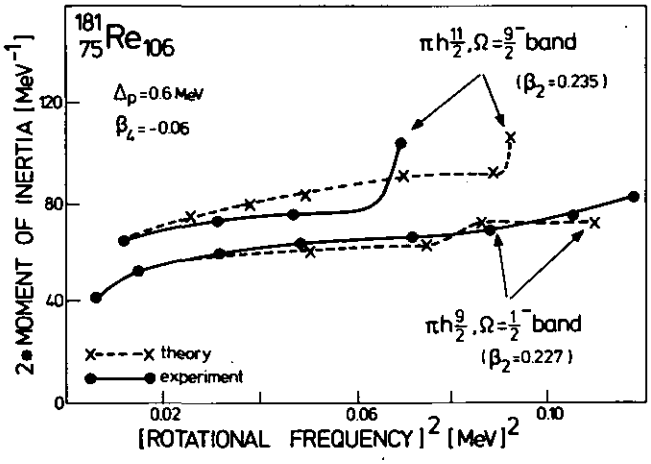


*Figure 3:*
*Backbending plots for the $\pi h_{11/2}$, Ω = 9/2 and the $\pi h_{9/2}$, Ω = 1/2 bands in $^{181}Re$.*

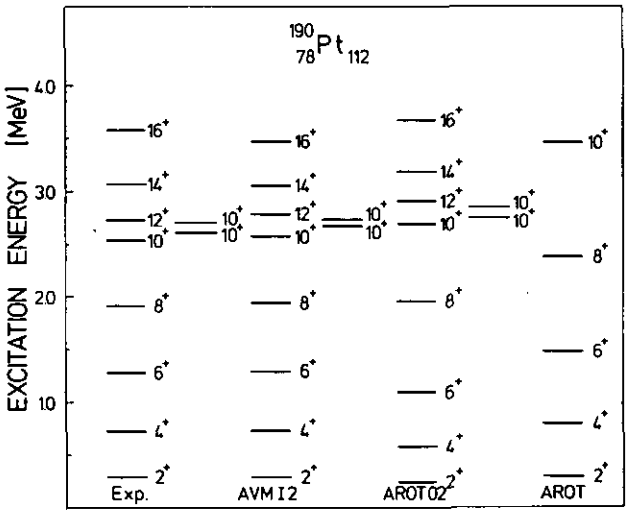


*Figure 2:*
*Experimental and calculated results for the positive parity states in $^{190}$Pt. Here the second and third $10^+$ states have been shown beside the yrast band in each case. The parameters are $\beta = 0.155$, $\gamma = 30^\circ$, $\lambda_p = 43.43$ MeV, $\lambda_n = 48.76$ MeV, $\Delta_p = 0.80$ MeV, $\Delta_n = 1.10$ MeV.*

velocity can be described in the simple deformed rotor model in terms of the coupling of the Oqp and 2qp bands.

The experimental spectra of the Hg isotopes are similar in structure up to A = 196. Beyond A = 196 the spacing between $1O^+$ and $12^+$ states is substantially reduced. We find that this change in the structure of the spectrum for A = 198 is due to the fact that beyond A = 196 the neutron 2qp energies are lower than the proton ones. The lowering of the $(\nu i^2_{13/2})$ excitation energy in the case of $^{198}$Hg is partly due to the position of the neutron Fermi energy ($\lambda_n$) very close to the highest Nilsson levels and partly due to the decrease of the pairing energy ($\Delta_n$). Our calculations show that for the Hg isotopes the states up to spin $6^+$ are Oqp states, whereas $8^+$, $1O^+$ and $12^+$ etc. are essentially 2qp states of proton nature for $A \leqslant 196$ and of neutron nature for $A \geqslant 198$. Similar calculations in Pt isotopes show that the yrast states up to spin $8^+$ belong to the Oqp band. In $^{186}$Pt states up to $14^+$ are found to be Oqp states. In $^{188\text{-}194}$Pt isotopes the yrast $1O^+$ state is of $(\pi h_{11/2})$ configuration whereas $12^+$ and $14^+$ states are due to neutron excitation. Furthermore, our calculations provide three close lying $1O^+$ states in agreement with experiment.

### References


[1] C. Günther et al., Phys. Rev. C15 (1977) 1298; H. Beuscher et al., Phys. Rev. Lett. 32 (1974) 843; M. Piiparinen et al., Phys. Rev. Lett. 34 (1975) 1110; S.A. Hjorth et al., Nucl. Phys. A262 (11976) 328

[2] H. Toki, K. Neergard, P. Vogel and A. Faessler, Nucl. Phys. A279 (1977) 1


## 4.5.9. Influence of Quadrupole Pairing on Backbending


A. Faessler, M. Wakai


The backbending (BB) phenomenon is attributed to the Coriolis antipairing (CAP) and the rotational alignment (RAL) effects. We can consider both effects simultaneously by applying the cranked Hartree-Fock-Bogoliubov (HFB) thoery to the description of the rotational motion of nuclei. In usual treatments of the backbending, however, only the monopole pairing force is considered and pairing forces of other types are neglected. This may be the main reason for starting of the backbending at a too small total angular momentum in theoretical results.

Some authors[1] pointed out the importance of the quadrupole pairing force. They considered mainly the $Y_{21}$-pairing force by using the perturbational approach of the lowest order. The purpose of this study is to investigate the influence of the quadrupole pairing force on the backbanding by fully solving the cranked HFB equation with particle number projection. We choose for the total Hamiltonian the monopole-quadrupole pairing plus quadrupole force Hamiltonian. The connection between the monopole and quadrupole pairing forces is given by the surface delta interaction. All the components of the quadrupole pairing force, $Y_{20}$-, $Y_{21}$- and $Y_{22}$-pairing forces, are taken into account. A rotational state is described by an HFB wave function which is a function of the deformation parameters $\beta$, $\gamma$, the monopole pairing gap $\Delta^{(o,o)}$ and quadrupole pairing gaps $\Delta^{(2,m)}$ (m = O, 1,2). These parameters are determined by minimizing the particle number projected energy expectation[2]. To see the influence of the quadrupole pairing force on

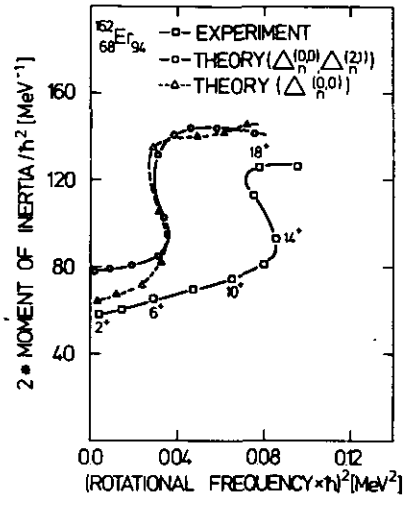


*Figure 1:*
*Backbending plot for $^{162}$Er. theoretical values are obtained by inclusion of the monopole- and $Y_{21}$-pairings (open circles) and the monopole-pairing only (triangles). The $Y_{21}$-pairing is influential only at angular momenta below the backbending region.*

rotational states clearly, we fixed the values of $\beta$, $\gamma$ and the monopole pairing gap of protons $\Delta_p^{(o,o)}$ and ignored the quadrupole pairing force between protons. We did calculations for $^{162}$Er and got the results summarized as follows:

(1) The $Y_{21}$-pairing, which increases the moment of inertia at low spin states by 2O %, does not affect the backbending (see fig. 1).

(2) The $Y_{2O}$-pairing brings on the reduction of the moment of inertia by about 2O %, which just cancels the increase by the $Y_{21}$-pairing.

shell corrections, respectively, which have been discussed in ref. [1]. With increasing angular momentum of the system the lowest minimum shifts to larger β-deformation with γ = –60° from β 0.1 to β 0.3 at I = 50 ħ and goes to β 0.6 at I = 70 ħ, which happens already at a little lower value of the angular mometum than in the case of RLDM. At I 80 h the lowest minimum becomes triaxial. A similar behaviour can be seen in the other nuclei in this mass region. Generally, nuclei in the transitional region have a tendency to rotate around the oblate symmetry axis. This may make them favourable candidates for yrast traps. However, as pointed out in ref. [3] the yrast traps in the rare-earth nuclei are rather infrequent above I~40 ħ due to the large slope of the yrast line. This slope is reciprocally proportional to $J_{rig} \alpha A^{5/3}$. Thus, the slope in the mass region around A = 120 is about 1.6 time larger than that at the beginning of the rare earth region (A = 160) and at I ≅ 25 ħ the slope in the transitional region is same to that at I ≅ 40 ħ in the beginning of the rare earth region. Therefore, we expect that the yrast traps in the transitional (A 120) region should correspond to a region of a relatively low angular momentum (I ≲ 15 ħ) though the lowest minimum has γ = –60° even at much higher I.

### References


[1] K. Neergard, H. Toki, M. Ploszajczak, A. Faessler, Nucl. Phys. A287 (1977) 48
[2] M. Ploszajczak, H. Toki, A. Faessler, to be published in J. Physics G /1978/
[3] M. Ploszajczak, A. Faessler, G. Leander, S.G. Nilsson, to be published in Nucl. Phys.


## 4.5.8. Positive Parity States in Pt and Hg Isotopes


H.L. Yadav, H. Toki, A. Faessler


Anomalies in the recent experimental spectra[1] for the positive parity states of the Pt and Hg isotopes are explained in the gamma deformed rotor model using two different descriptions for the energy of the core. (i) In the first description we extend the asymmetric rotor model of Davydov to include the coupling between O and 2 qp states (referred to as AROTO2). As a reference we shall give also the results of the simple asymmetric rotor (AROT) model of Davydov. (ii) In the alternative case (AVMI2) we neglect the interaction between the O and 2 qp states. Instead we allow for an increase of the moment of inertia of the rotor with growing angular momentum using the VMI model.

For the description of the O and 2qp excitations the Hamiltonian is written as

$$H = H_{sp} + H_{Rot} + H_{Res}$$

Here $H_{sp}$ is the single quasipartilce Hamiltonian, $H_{Rot}$ is the Hamiltonian of the rotating core and $H_{Res}$ is the residual interaction which is taken to be a Surface Delta Interaction. The total wave function of the system is written using the basis

$$|(j_1 j_2 J)\ R\alpha; IM> = \frac{1}{\sqrt{1+\delta_{j_1 j_2}}} \sum_{M_J M_R} (JM_J RM_R|IM)\ |(j_1 j_2)JM_J>\ |R\alpha M_R>$$

in which $|(j_1 j_2)JM_J>$ is the antisymmetrized wave function of the 2qp and $|R\alpha M_R>$ is the core eigenfunction. The essential formulation relevant to the present calculations is given in ref. 2. In these calculations the moment of inertia parameter is fitted to the $2_1^+$ energy. The deformation γ(60° for Hg and 30° for Pt isotopes) are taken to be that employed in the study[2] of the negative parity states in Pt and Hg isotopes. The stiffness parameter of the AVMI2 model is adjusted by the $4_1^+$ energy. For the single particle configuration we have considered only the $\pi h_{11/2}$ and $\nu i_{13/2}$ spherical subshells. The other parameters λ and Δ have been indicated in the figure captions. The spurious components in the description of the 2qp states arising due to the nonconservation of the number of particles have been removed by Schmid's orthogonalization method.

In Figs. 1 and 2 we have shown the results for the $^{196,198}$Hg and $^{190}$Pt isotopes as the representative examples. On comparison it is evident that AROTO2 and AVMI2 give similar results and both are in good agreement with the experimental data. However, the difference between the two results at high spins ($14^+$, $16^+$ etc.) indicates that one has to take into account also the admixture of the 4qp states to the 2qp states. A comparison of the results for the core energy with and without O-2qp coupling (AROTO2 and AROT) shows a remarkable lowering of the core energy (Oqp energy) providing a nice agreement with the data. This indicates an underlying relationship between the VMI model and the O-2-qp coupling. Moreover, this leads us to believe that the Coriolis antipairing (CAP) effect which is supposed to be responsible for the increase in the moment of inertia with the square of the angular

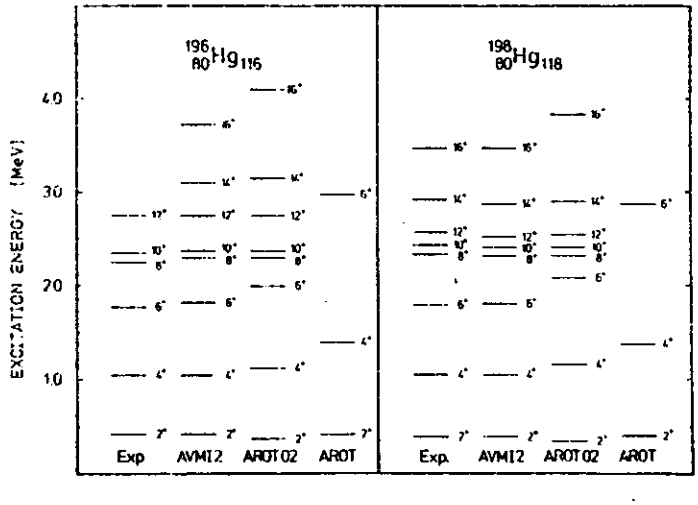


*Figure 1:*
*The experimental and calculated results for the positive partity states in $^{196,198}$Hg. The parameters used are β = 0.116, γ = 60°, $\lambda_p$ = 42.20 MeV, $\lambda_n$ = 48.05 MeV, $\Delta_p$ = 0.90 MeV and $\Delta_n$ = 1.24 MeV for $^{196}$Hg, and β = 0.990, γ = 60°, $\lambda_p$ = 42.04 MeV, $\lambda_n$ = 48.18 MeV, $\Delta_p$ = 0.90 MeV and $\Delta_n$ = 1.12 MeV for $^{198}$Hg.*

60° (oblate shape) both contribute to expand the spectrum. The calculated result using $\gamma = 40°$ as an example, which is suggested from the adjacent odd mass nuclei, is compared with the experimental and the calculated spectra for the oblate shape in Fig. 1.

Physically this system is understood as follows: If the core rotation is small $R \simeq 0$, spins of the particles tend to be perpendicular to each other. This yields the band head spin around 8. As the core rotation increases the strongly coupled particle $\pi h_{9/2}$ starts to be aligned to the core rotational axis. This would correspond to the mechanism of the alignment of many particles at very high spin states.

*) It seems there is still an ambiguity concerning the spin assignment, since experimentally one knows only the nature of the transitions.

## References


[1] A.J. Kreiner, M. Fenzl, S. Lunardi and M.A.J. Mariscotti, Nucl. Phys. A282 (1977) 243

[2] H. Toki, H.L. Yadav and A. Faessler; Phys. Lett. 71B (1977) 1


## 4.5.7. Very High Spin States in the Transitional Region (A ≅ 120)


*M. Płoszajczak, H. Toki, A. Faessler*


The phenomenon „yrast traps" may be related with the axially symmetric nuclear shape rotating around its symmetry axis. Intensive studies of the nuclei in the rare earth region, using the Saxon-Woods potential as the average field to calculate the shell correction[1] show that there only exist nuclei with such a configuration in the neutron deficient nuclei at the beginning of the rare earth region. Here we attempt to find such shapes in the region of A 120 (Te-Sm)[2]. The total energy in the rotating frame in the Strutinsky approach is given as described in ref. [1]. The RLDM energy in the β,γ plane is given in Fig. 1 together with the trajectory of the deepest energy minimum as a function of the total angular momentum for $^{124}$Te. The lowest minimum moves along the $\gamma = -60°$ line (disc shape) increasing its β-deformation and at I = 92ħ for $^{124}Te_{72}$ it starts to deviate from $\gamma = -60°$. Results including the shell corrections to the RLDM are shown in Fig. 2. At I ≈ 30ħ in addition to the energy minimum favoured by the RLDM there appears a minimum at $\gamma = -60°$, $\beta = 0.55$ and a maximum at $\gamma = 0°$, $\beta = 0.75$. This is due to the strong negative and positive

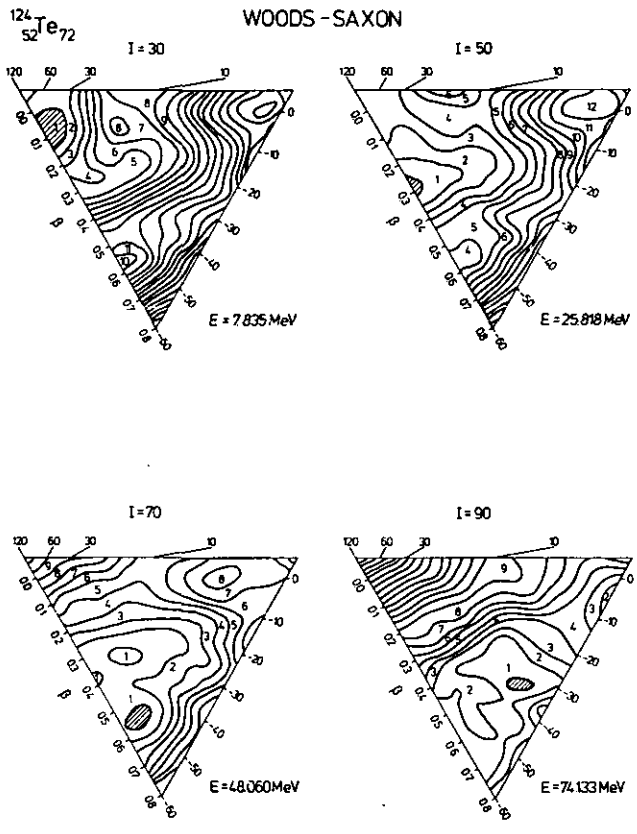


*Figure 1:*
*The RLDM energies of $^{124}_{52}Te_{72}$ as a function of the β, γ deformation for various angular moments. The shaded area indicates the deepest miminum in the energy plane and the spacing between the contours is 1 MeV. The trajectory of the lowest minimum as a function of I is also shown in the right – lower part.*

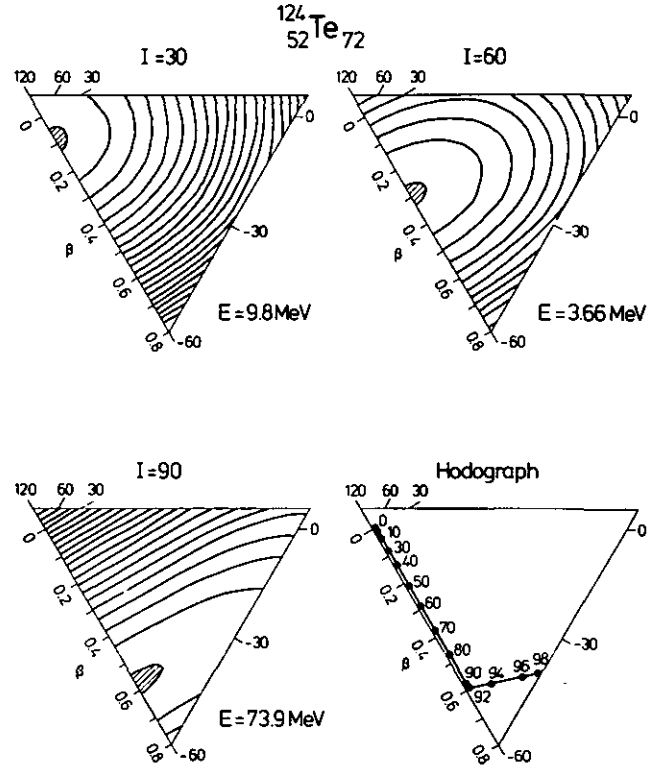


*Figure 2:*
*Deformation energy surfaces for various angular momenta using the Saxon-Woods potential for the shell corrections.*

parameters would be: β deformation, γ deformation (triaxiality), Fermi energy of proton $\lambda_p$ and neutron $\lambda_n$.

A series of graphs will be published in the near future[2]. As an example of these graphs, let us show here the γ-dependence of the spectrum of $\pi h_{9/2}$–$\nu i_{13/2}$ system with $\lambda_p$ on the lowest, $\lambda n$ on the highest Nilsson states. This corresponds to the so-called conflicting case, where one of the particles favours decoupling, whereas the other strong coupling. The so-called peaceful case has already been discussed in ref.[3].

The interesting thing to note is that in the peaceful case, the resultant spin J of the two particle spins $j_p$ and $j_n$ stays as a good quantum number and this fact allows us to group the states into bands specified by J. One may consider then each band for a specific J to correspond to band in odd mass nuclei. In the conflicting case, one does not find such a quantum number. But a simple analysis of the system yiels the band head spin and the nature of the sequential spectrum.

The experimental studies of odd-odd mass nuclei in light of the systematic studied here will give necessary information for the values of the important parameters.

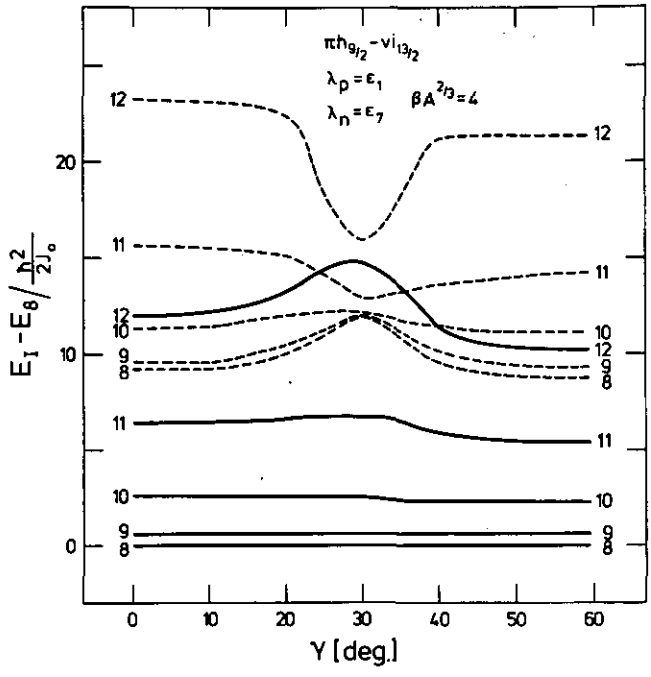


*Figure 1:*
*Excitation energies of $\pi h_{9/2}$–$\nu i_{13/2}$ system as a function of γ deformation. The solid lines denote the first spin states and the dotted ones the second.*

**References**


[1] A.J. Kreiner, M. Fenzl, S. Lunardi and M.A.J. Mariscotti, Nucl. Phys. A282 (1977) 243
[2] H. Toki, H.L. Yadav and A. Faessler, to be published
[3] H. Toki, H.L. Yadav and A. Faessler, Phys. Lett. 66B (1977) 310


## 4.5.6. Decoupled and Strongly Coupled Particles System in Odd-Odd Mass Nuclei


H. Toki, H.L. Yadav, A. Faessler


The decoupling and the strong coupling structures have been studied in details for the odd mass nuclei in the transitional mass region. To understand the interplay between the particles and the core motions and also to go further to the many particle system with a deformed field (very high spin states), one of the most interesting problems would be to study the two particles system where one particle favours decoupling and the other favours strong coupling. More specifically this is the case if one is of particle nature and the other of hole nature.

Such a system has been investigated experimentally by Kreiner et al.[1] for the $\pi h_{9/2}$–$\nu i_{13/2}$ particle-hole system in $^{198}$Tl. From the spectra of the adjacent odd mass nuclei, one can clearly see that $\pi h_{9/2}$ particle favours strong coupling and $\nu i_{13/2}$ hole decoupling. The spectrum seen shows a sequential increase of the spin by one as the excitation energy increases and the band head is I = 8*.

The calculated spectrum assuming the core is oblate (axially symmetric shape) seems entirely compressed compared to the experiments. We have studied this system allowing also the axially asymmetric shape (triaxial), which is concluded to be extremely important in this mass region[2]. The result is that the increase of the β deformation and the decrease of the γ deformation from γ =

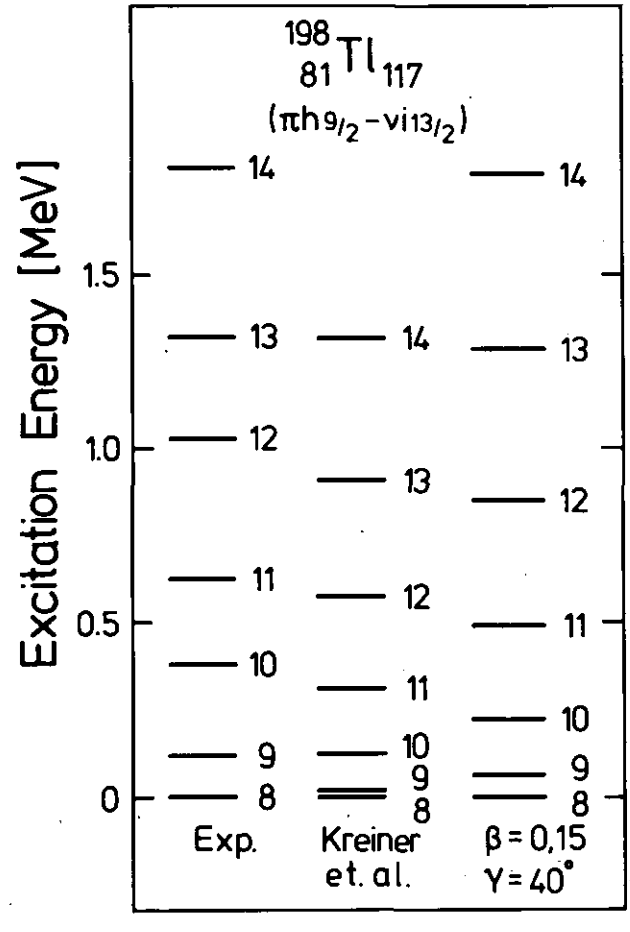


*Figure 1:*
*Experimental and theoretical excitation energies for the $\pi h_{9/2}$–$\nu i_{13/2}$ system in $^{198}$Tl.*

## 4.5.4. Unified Description of the Yrast Traps at Very High Angular Momenta

M. Ploszajczak, A. Faessler, G. Leander*), S.G. Nilsson*)

We give a unified microscopic description based on the CHFB theory for the formation of the yrast traps whereby the MONA traps and the statistical traps appear as special cases[1]. The method is based on Hartree-Fock (HF) trial wave functions and a many-body Hamiltonian with a quadrupole-quadrupole (QQ) and a hexadecapole-hexadecapole (HH) force. The trial wave function parametrized by the deformations $\beta$, $\gamma$, $\beta_{40}$ is a Slater determinant built by cranked M.O. single particle functions. The total energy of the system for a given angular momentum I has been obtained by minimizing the sum of the Coulomb energy and the expectation value of the many-body Hamiltonian with respect to the deformation parameters. For details see Ref.[1]. Using a Slater determinant of the energetically lowest single particle wave functions we describe only states with I corresponding to a sloping Fermi surface („optimal configuration"). States inbetween the „optimal" states have been constructed by 1p-1h, 2p-2h excitations over the straight sloping Fermi surface. The application of this method is restricted to nuclei for which calculations[2-4] indicate that they rotate around the symmetry axis.

For both above mentioned mechanisms for the formation of yrast traps it is essential that no collective rotation is possible. The results for $^{148}_{62}$Sm and $^{198}_{82}$Pb are shown in Figs. 1 and 2. We define traps marked by encircled „+" or „–" (+ (–) denote the positive (negative) partiy states) as yrast states which cannot decay by an E1, M1, E2 or M2 transition. The points in squares correspond to the „optimal" configuration. In almost all isomeric configurations, increase of the quadrupole or hexadecapole moment is not large. Therefore one can exclude in almost all cases in the neutron deficient rare earth nuclei the MONA mechanism as an explanation for the formation of the isomeric states. Generally traps above I = 40 ħ are rather infrequent. This is probably due to the large slope of the yrast line above I ~ 40 ħ, which reduces the importance of the shell fluctuations.

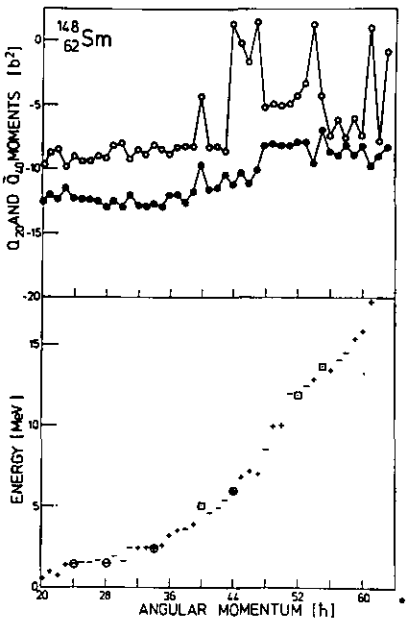


*Figure 1:*
*The excitation energies as well as the quadrupole $Q_{20}$ (solid circles) and the hexadecapole $Q_{40}$ moment (open circles) of the yrast states are shown as a function of the total angular momentum for $^{148}$Sm at $\gamma = -60°$. $\chi \sim 0$.*

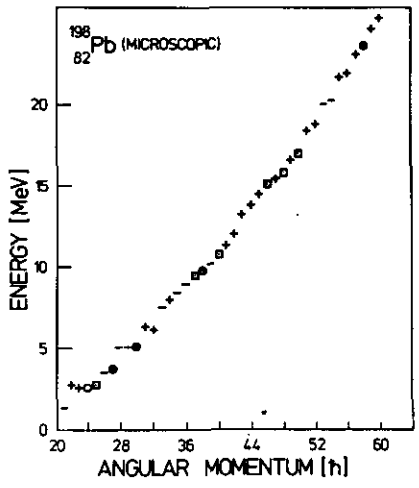


*Figure 2:*
*The excitation energies of the yrast states at $\gamma = 120°$ are shown as a function of the total angular momentum for $^{198}$Pb.*

*) Lund Institute of Technology, Lund, Sweden

### References

[1] M. Ploszajczak, A. Faessler, G. Leander, S.G. Nilsson, to be published in Nucl. Phys.
[2] M. Ploszajczak, K.R. Sandhya Devi, A. Faessler, Z. Physik A282 (1977) 267
[3] M. Ploszajczak, H. Toki, A. Faessler, to be published in Nucl. Phys.
[4] K. Neergard, H. Toki, M. Ploszajczak, A. Faessler, Nucl. Phys. A287 (1977) 48

## 4.5.5. Systematic Study of Transitional Odd-Odd Mass Nuclei

H. Toki, H.L. Yadav, A. Faessler

The selectivity of the $\gamma$ ray spectroscopy after the bombardment of the nuclear system with heavy ions or $\alpha$ particles enables us to study the low lying high spin states in odd-odd mass nuclei, the level density of which is extremely high. Theoretically this is a very interesting system to understand the interplay between the intrinsic particles and between the particles and the deformed core. Furthermore, since this system can be treated easily, it may help to understand the mechanisms or physics of very high spin states.

Upto now, however, only one piece of experimental data is reported in the literature[1]. But there will be a bunch of data coming for various odd-odd mass nuclei in the near future. Thus, the thing to be done theoretically is to study the systematics of such a system with the various parameters in a reasonable range. Those

## 4.5.3. Very High Spin States in Transuranic Nuclei (Strutinsky Approach)

M. Ploszajczak, H. Toki, A. Faessler

Deformation energy surfaces at very high spins of the nuclei in the transuranic (Po-Th) region are calculated as a function of β and γ deformations in terms of the Strutinsky approach using the Sax-on-Woods single particle potential. The total energy in the rotating frame is given by:

$$R(\beta,\gamma;\omega) = E_{LD}(\beta,\gamma) + \frac{1}{2} J_{rig}(\beta,\gamma)\omega^2 + \delta R(\beta,\gamma;\omega) \qquad (1)$$

where

$$R(\beta,\gamma;\omega) = \sum_{\substack{\text{protons}\\ \text{neutrons}}} [\Sigma_i \epsilon_i(n_i - \tilde{n}_i)]$$

The cranking frequency ω in the above expression is related with the total angular momentum I as:

$$I(\beta,\gamma;\omega) \approx J_{rig}(\beta,\gamma)\omega + \delta I(\beta,\gamma;\omega) \qquad (2)$$

where

$$\delta I(\beta,\gamma;\omega) = \sum_{\substack{\text{protons}\\ \text{neutrons}}} [\Sigma_i \langle j_x \rangle_{ii} (n_i - \tilde{n}_i)]$$

Furthermore the total energy in the laboratory frame is given through (1) and (2) as:

$$E(\beta,\gamma;I) = R(\beta,\gamma;\omega(I)) + \hbar\omega I \qquad (3)$$

The LD-energy entering eq. (1) is given in Ref.[1]. The RLDM energy along with its trajectory for $^{208}$Rn is given in Fig. 1. The β deformation of the lowest minimum increases with increasing angular momentum and it starts to deviate from the disc shape at I = 80 ħ. The maximum β-deformation for the disc shape is in this case β ~ 0.3 (γ = –60°). Adding the shell correction to the RLDM energy, one obtains the deformation energy surfaces as shown in Fig. 2. There are essentially two minima seen; one is at β ~ 0 and the other is at γ = 0° and β = 0.7. These two minima are competing. When I is small, the energy minimum at β ~ 0 is the lowest one and at I ~ 60 ħ, the energy minimum at β ~ 0.7, γ = 0° becomes lower. The minimum at β ~ 0.7, γ = 0° remains as a distinct deep minimum throughout. Such a large change in the shape at I ~ 60 ħ may be seen as „giant backbending" in the plot of the moment of inertia against the angular frequency. The minimum at β ~ 0, which is seen also in other nuclei in this region ($_{84}$Po, $_{86}$Rn, $_{88}$Ra, and $_{90}$Th), could give rise to high spin isomers[2]. Such states have been recently reported by Blomquist et al.[3] in Pb-isotopes.

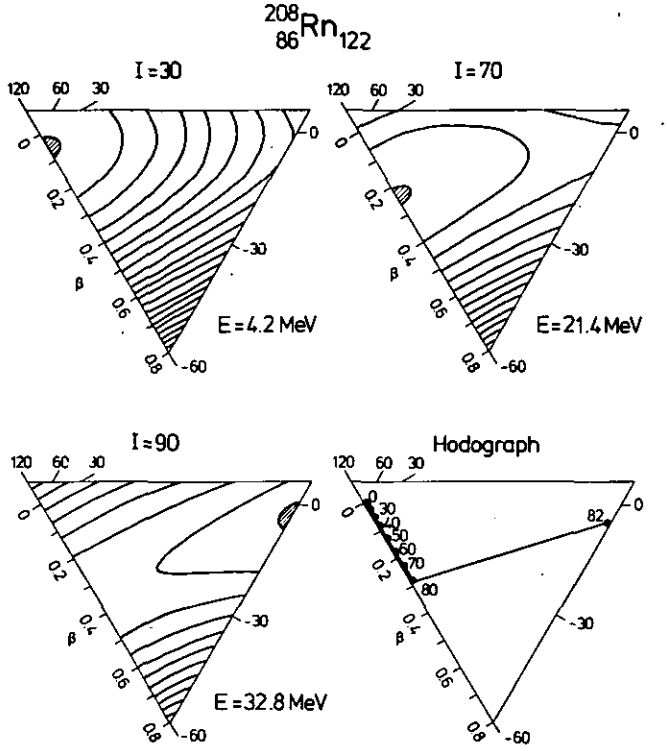


*Figure 1:*
*The rotating liquid drop (RLDM) energies and their trajectory of $^{208}$Rn$_{122}$. The energy given beside each figure is the excitation energy of the deepest minimum in the plane relative to the spherical liquid drop energy with spin zero.*

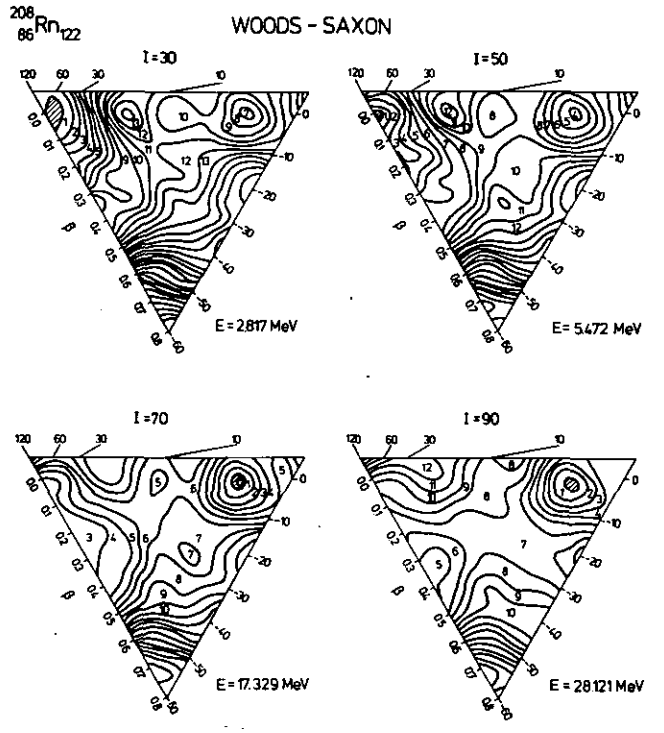


*Figure 2:*
*Deformation energy surfaces of $^{208}$Rn$_{122}$ for various angular momenta using the S-W potential for the shell corrections.*

### References

[1] Neergard et al., Nucl. Phys. A287 (1977) 48
[2] M. Ploszajczak et al., to be published in J. Physics G (1978)
[3] J. Blomquist et al., Phys. Rev. Lett. 38 (1977) 534

## 4.5.2. Description of Negative Parity Yrast States in $^{156}Er$

M. Ploszajczak, A. Faessler

High spin states with negative partiy have been observed recently in several rare earth nuclei[1]. These states are often found to be located close to the positive parity yrast states in the backbending region. The 2 q.p., negative parity states cannot mix with the positive parity g.s.b. Therefore, without going into the elaborate calculations including the interaction between O q.p. and 2 q.p. bands, the studies of these bands in the same nucleus provide the opportunity for a better understanding of the phenomena in the critical region. The mathematical approach used which allows for the simulatneous des cription of g.s. rotational band as well as the excited configurations is given by the cranking-HFB theory[2].

Fig. 1 shows the theoretical as well as the experimental blot of moment of inertia vs. rotational frequency squared for the g.s.b. The theoretical moment of inertia exhibits backbending at lower angular momenta than observed experimentally. This small stability of the pairing field is rather common for all theoretical approaches used at high spins and can be partially removed if the higher multipoles in the short range component of the nucleon-nucleon forces are taken into account[3]. The theoretical moment of inertia shows once more the rapid increase at J = 22 h which is not seen experimentally up to J = 24 h. Since the theory predicts the first backbending at too low angular momentum, one might expect that the second anomaly of the moment of inertia appears also at higher J.

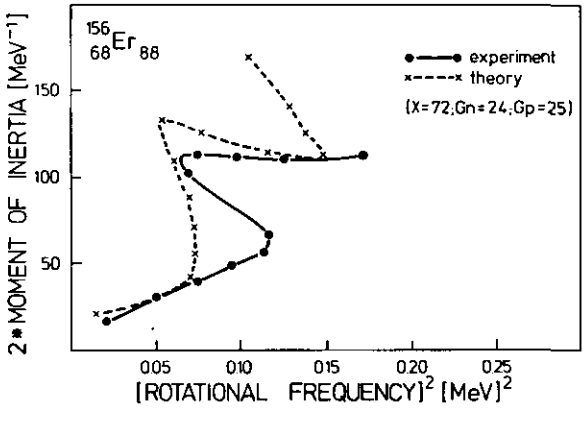


*Figure 1:*
*Backbending plot for the positive parity yrast states in $^{156}Er$.*

Fig. 2 shows the energy of the odd spin rotational levels corresponding to the lowest band heads. The lowest states ($J^\pi = 1^-, 3^-, 5^-$) belong to the rotational band built on the 1-ı state. At $J^\pi = 7^-$ the structure of the odd-spin yrast line is drastically changed since the proton 2 q.p. state ($J^\pi = 7^-$) has lower excitation energy than the $7^-$ state in the $1^-$ band. The $7^-$ state corresponds to the 2 q.p. proton excitation with respect to the $O^+$-HFB vacuum whereas the dominating contribution in the $5^-$ level is the neutron 2 q.p. excitation. One can, therefore, expect that the $7^-$ state will be isomeric and the transition to the lower odd-spin negative parity state will be difficult to detect experimentally. The yrast line is once more mod-

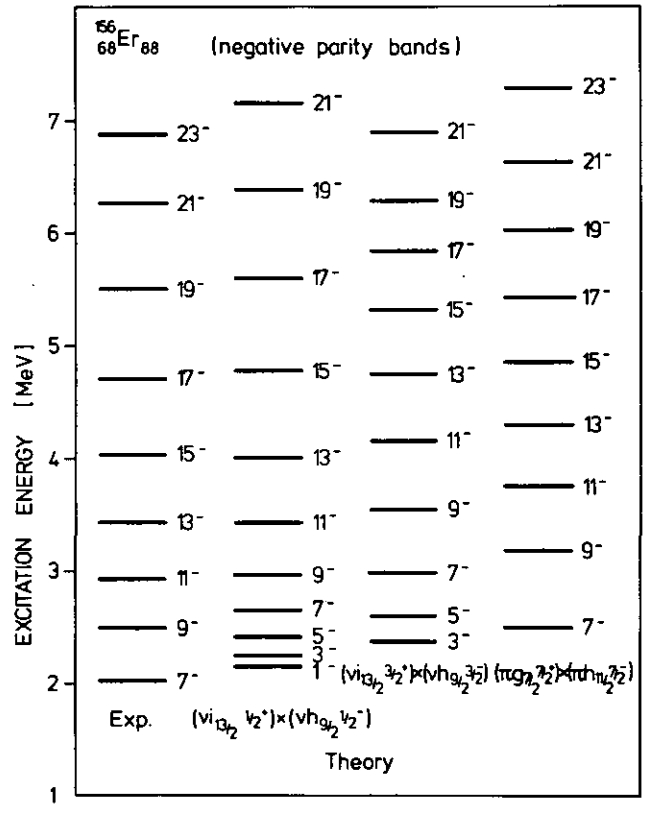


*Figure 2:*
*Experimental negative parity yrast energies in $^{156}Er$ compared with different theoretical negative parity bands built on the 2 q.p. states indicated in the figure.*

ified at $J^\pi = 9^-$ since the $9^-$ member of the $1^-$ band has lower excitation energy than the $9^-$ state in the $7^-$-band. At $8^+$ the q.s. band contains already large admixtures of the blocked $\nu i_{13/2}$, $\Omega = 1/2^+$ configuration. Therefore, the transition with emission of E1-quanta from the $9^-$ state to $8^+$ member of the g.s.b. would be favoured over the transition $9^-$ [$1^-$ band] $\rightarrow 7^-$ [$7^-$ band]. (This is also true for the transition $11^-$ [$1^-$ band] $\rightarrow 10^-$ [g.s.b.].) Indeed, this retardation is also observed experimentally[4]. At $J^\pi = 17^-$ we may see in Fig. 2 the intersection of the $1^-$-band with a $7^-$-band which has a larger moment of inertia. Moreover, at J = 17 and 19 ħ the neutron pair $i_{13/2}$, $\Omega = 1/2^+$ is broken and aligned along the symmmetry axis. This sudden alignment is responsible for the further reduction of the energy of $19^- \rightarrow 17^-$ transition with respect to the transition $17^- \rightarrow 15^-$. Our results alow us to understand qualitatively and in some cases also quantitatively the experimental data for the negative parity bands, namely spin of the band head, anomalous decrease of the transition energies between the $11^- \rightarrow 9^-$ and $23^- \rightarrow 21^-$ states and preference of the $9^- \rightarrow 8^+$ transition over the $9^- \rightarrow 7^-$.

### References

[1] R.M. Lieder, H. Ryde, Jülich report (1977)
[2] M. Ploszajczak, A. Faessler, Z. Physik A283 (1977 349
[3] M. Wakai, A. Faessler, to be published
[4] H. Beuscher, et al., Z. Physik 263 (1973) 201

trometer has shown besides its reliablility a position resolution of better than O.4 mm.

2. Field measurements on dipole D1

In order to obtain the field characteristics of D1 the following three methods are used (Fig. 1):

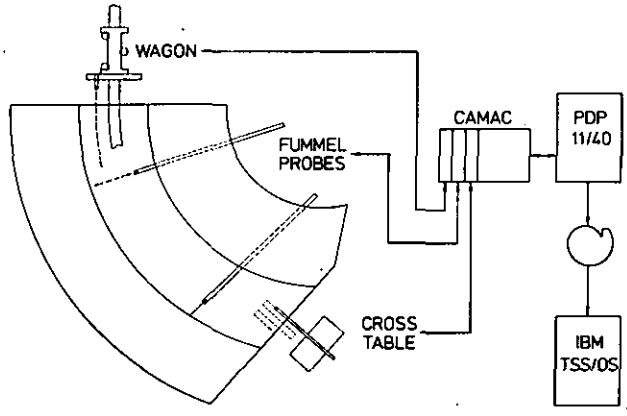


*Figure 1:*
*Field measurement devices.*

a) Wagon:
The measuring device is a wagon which is moved in azimuthal direction through the magnet along a rail. Either coils or NMR-probes can be mounted on the wagon in several positions.

b) Fummel-probes:
*The radial field shape is obtained by inserting two tubular probes* through the inner side-yoke; each probe contains a coil and a NMR-probe to measure field gradients and the absolute field.

c) Crosstable:
The fringing fields at the magnet entrance and exit are measured by scanning along two perpendicular directions relative to the magnet. The measuring arm mounted on the table contains two coils for gradient measurements, one Hall-plate and one NMR-probe used for matching the fringing field region to the homogeneous region.

Control and data aquisition for all measurements are carried out by a PDP11/4O-CAMAC-System as de scribed below.

Results:
a) Fig. 2 shows a field map of the homogeneous region obtained by wagon-NMR-measurements (plotted is the field difference to 8765 Gauss at 35 % of the main current). A homogeneity of better than O.1 % has been found.

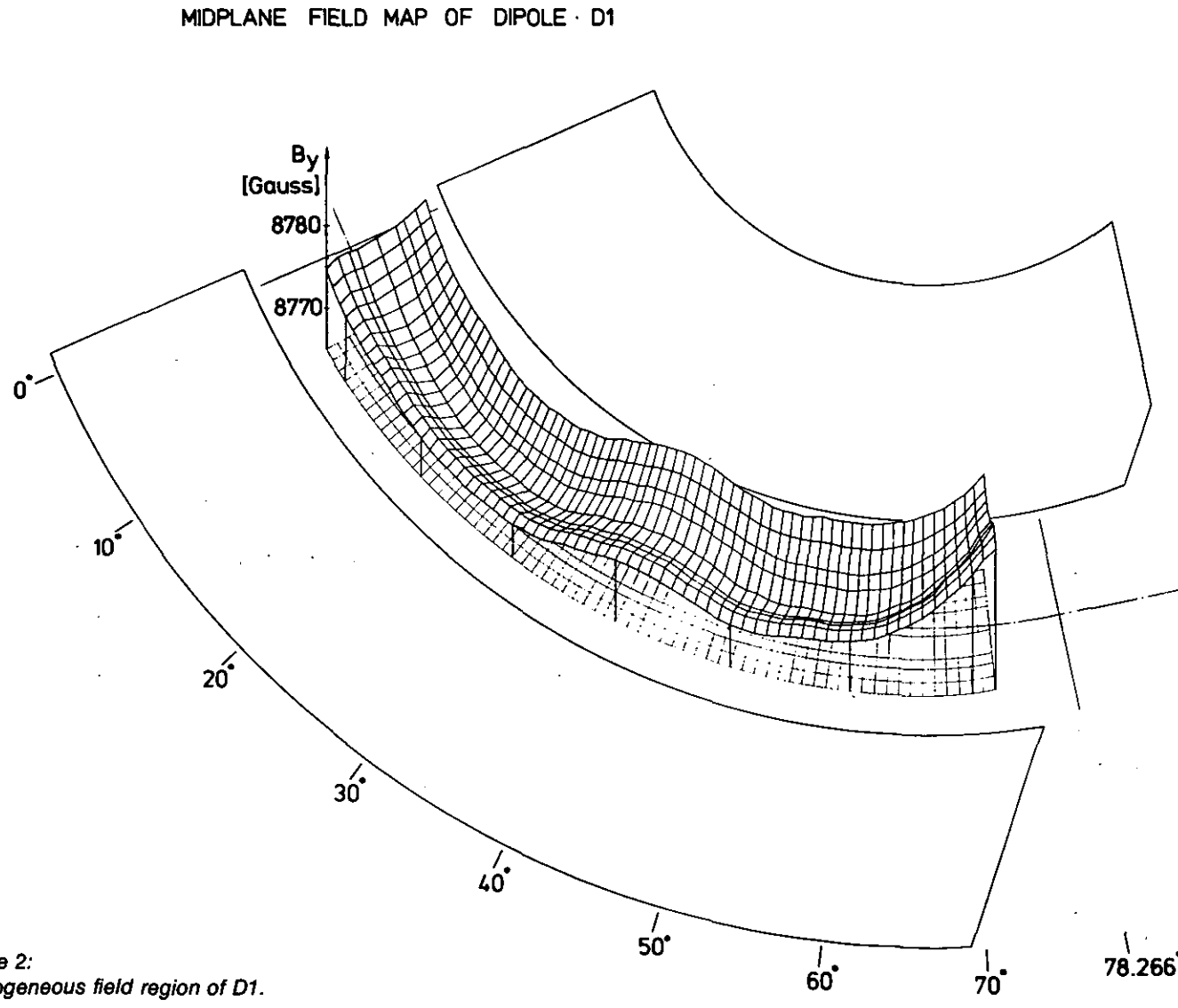


*Figure 2:*
*Homogeneous field region of D1.*

b) Fummel-measurements have delivered not only the radial field shape (Fig. 3) but also the time dependence of the field (Fig. 4) which reveals a high reproducibility of about O.OO2 %.

c) From crosstable measurements which are carried out at present the following parameters of the fringing field will be deduced:
- the geometry of the virtual field boundary (VFB)
- the entrance and exit angles
- the outer range of the fringing fields.

As a first result Fig. 5 shows a comparison between a fitted model calculation and the measured fringing field along the central trajectory at the exit of D1.

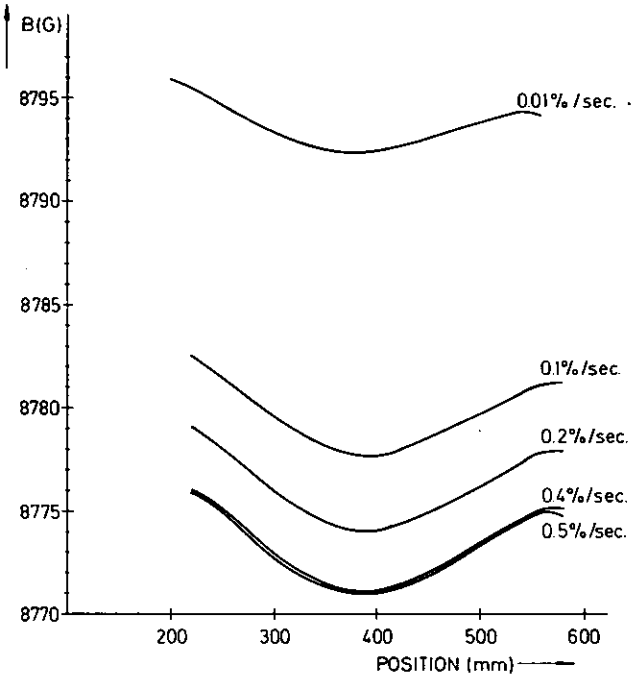


*Figure 3:*
*Radial variation of field form for different rate of change of current.*

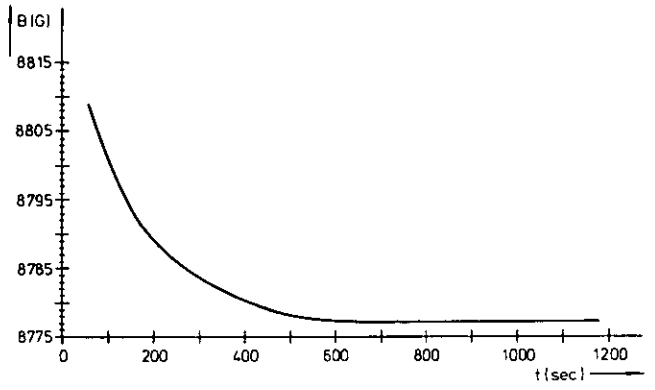


*Figure 4:*
*Stabilization time of the D1 field. t = O is reckoned after the current has reached a preset value.*

## 3. Test of the detectorsystem

The prototype detector is a multi-wire proportional chamber (MWPC) with a 3OO mm × 4Omm sensitive area[4]. The two coordiantes X and Y of an ionizing particle are measured. The MWPC contains 5 wire planes, seen by the incoming particle in the following order: Cathode K1, anode A1, separation cathode MK, anode A2, cathode K2. The wires of the planes K1, K2 are perpendicular to the anode wires A1, A2 respectively and the wires of A1 are perpendicular to the wires of A2. All wires except those of MK have an angle of 0-45 degree to the horizontal base line. The readout is accomplished by delay lines on the cathode wires. It was important to optimize[5] the band width and the dispersion (this means the delay time as a function of the frequency) of the delay line. The spatial resulution has been tested using a collimated e-source of $^{90}$Sr. In both directions (X and Y) the spatial resolution under different conditions of gas pressure, high voltage, gas mixture, and wire spacing has been measured to be better than O.5 mm (FWHM). This is a worst case measurement because the $^{90}$Sr electrons are minimum ionizing particles.

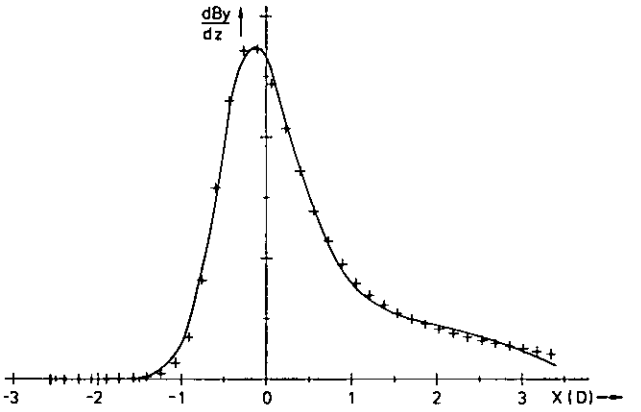


*Figure 5:*
*Theoretical description of the fringe field (solid line) and comparison with measured values (crosses).*

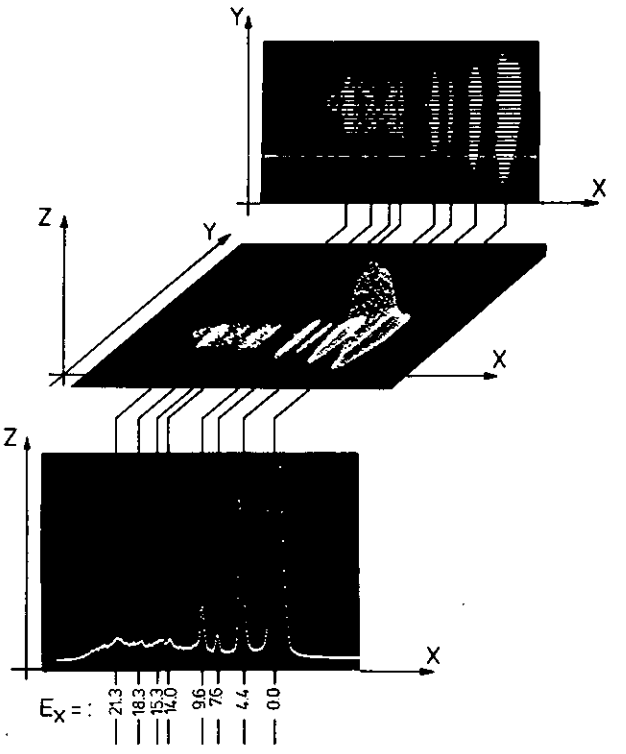


*Figure 6:*
*Spectrum from the inelastic α-scattering in single parameter, isometric, and 2-dimensional representation.*

For measuring the spatial resulution under experimental conditions the reaction $^{27}Al(\alpha,\alpha')^{27}Al$ has been studied with a small magnet spectrometer[5]. The measured line width was 0.4 mm FWHM. The dispersion and the energy resolution of the test spectrometer were:

$$D = \Delta X/(\Delta E/E \cdot 100) = 0.29 \text{ cm/\%}$$

and

$$\Delta E/E = 1.5 \cdot 10^{-3}$$

The time resolution was extracted by measuring the time difference between the signal from the sepa ration cathode and a coincident scintillator signal using a time to amplitude converter[5]. The scintillator was located behind the chamber. The efficiency of the chamber is defined as the five-fold coincidence signal of the four delay line signals with the signal from the separation cathode divided by the number of the scintillator signals. The true efficiency derived from that measurement was about 90 %[5]. The nonlinearity of the position calibration for X and Y is given by the nonlinearity of the delay lines. The nonlinearity of both delay lines has been measured using the collimated $^{90}Sr$ e-source. It is less than 1.33 mm for a 260 mm region of the delay line and it can easily be corrected by software.

Fig. 6 shows a spectrum from the inelastic alpha scattering on $^{12}C$.

4. Computer control

A PDP 11/40 computer controls and supervises all relevant spectrometer functions through a two crate CAMAC system. One disk drive, a 9-channel magnetic tape unit and either a DEC-writer or a graphic display with hardcopy facility complete the system. The software is presently running under DOS with 28 k of memory.

The following functional blocks are served by the CAMAC system:
a) The 5 main power supplies and later on the power supplies feeding an additional multipole are controled by dual storing output registers. The 24 Ht power supplies accept data through a common bus from one CAMAC module thus only requiring a second special module to deliver 24 strobe pulses. A programmable clock module serves as an interrupt source and provides a flexible means of timing for various magnet cycling and measurement purposes.
b) The actual magnet currents and the error status of all power supplies are processed by an external ADC-multiplexer system and fed into the computer using interrupt control; reading a single channel with a 0.001 % resolution takes about 60 msec after a computer request.
c) Position control of the Fummel-probes, the cross table and the collimator slits is accomplished through static I/O driver modules.
d) A Spectromagnetics NMR unit, a medium speed ac/dc voltmeter and 5 integrating digital voltmeters (0.001 % resolution) are connected to I/O registers with handshake features. A special trigger arrangement allows to synchronise the reading of the five DVMs using only one interrupt request.
e) Additional isolated digital and analogue I/O channels as well as two serial asynchroneous interfaces provide the user with further control capabilities.

*) KFA-ZEL

**References**


[1] S. Martin, C. Mayer-Böricke, Internal Report IKP-403 (1972)
[2] A. Abdel Gawad, A. Hardt, S. Martin, J. Reich, K.L. Brown, K. Halbach, Proc. of 5th Int. Conf. on Magnet Technology, Roma (1975), p. 45
[3] K. Ehrhard, Juel-1427 (1977)
[4] M. Koehler, K.D. Mueller, M. Teske, IEEE Trans. Nucl. Sci., NF-22 (1975) 272
[5] M. Koehler, Thesis, Univ. of Bonn, to be published (1978)


# 9. Solar Energy

## 9.1. Outline of the Solar Energy Activities


J.W. Grüter, O. Schult, H.J. Stein


Solar energy is expected to be an essential option to contribute to future energy needs of mankind. Since 1974, renewed interest in research and technological development in all areas related to solar energy has become a matter of national programs[1] and international co-operation[2] all over the world.

In 1975 activities on solar energy have been started at the Institut für Kernphysik. Experimental studies on thermal applications are being carried out since summer 1976.

Short-term aims of these activities are
- testing of solar collectors, including thermal performance as well as reliability and durability, and the
- development of instrumentation for solar radiation and solar-system data acquisition.

Middle-term aims consist in the application of
- theoretical models to describe the interaction of solar radiation and climatic conditions with a specified collector in a specific system, and the
- amendment of such models based on new measurements.

With the help of actual data and better models it will be possible to contribute to the basic question of a broad-scale application of solar energy, i.e. economics. Economics should be studied from two points of view
- economics based on usual cost-benefit arguments
- economics based on energy investment and energy pay-back time of a solar energy system.

The latter point of view has become highly controversial in the field of nuclear reactors[3,4]. Recently, such considerations have also been transferred to solar energy[5,6].

*Figure 1:*
*View of the solar collector test station at the Institut für Kernphysik.*


**References**

[1] Programm Technologien zur Nutzung der Sonnenenergie 1977-1980, Ed.: Minister of Science and Technology, Bonn 1977, ISBN 3-88135-050-0
[2] Cf., International Energy Agency and Commission of the European Community
[3] P. Chapmann, The ins and outs of nuclear power, New Scientist, Vol. 64, No. 928, p. 866 (1974)
[4] G. Kolb, F. Niehaus, St. Rath-Nagel, A. Voss, Der Energieaufwand zum Bau und Betrieb von Kernkraftwerken, KFA-Jülich, Report No. Jül-1230, Aug. 1975
[5] W. Seifritz, Sonnenenergie unrentabel – Ein großes Sonnenenergieprogramm würde die kommende Ölkrise noch verschärfen, Der Bund, Bern, 20.7.1977
[6] H.J. Wagner, R. Turowski, Contribution to IIASA Solar Energy Group, Nov. 1977


## 9.2. Instrumentation and Data Acquisition at the Solar Energy Test Facility at KFA-IKP


J.W. Grüter, H.J. Stein


The solar energy test station being under construction at KFA-IKP will include several facilities for testing solar collectors, and a selectively sophisticated instrumentation to measure solar and other meteorological data which are relevant for solar energy applications. Several test rigs for short and long term testing as well as test stands for collector storage combinations will be constructed. The solar meteorological equipment consists of a standard arrangement to measure energy exchange of sensible and latent heat fluxes in the so called Prandtl layer of the earths surface together with radiation balances. An assembly of pyranometers, pyrheliometers and pyrgeometers measures global, direct, diffuse and infrared radiation from the sun and the atmosphere under different conditions. For the different measurement tasks individual data acquisition systems are foreseen.

The meteorological data are processed by two MADAS[1] data systems, one for the energy exchange data, the other for the radiation data. For long term collector and system tests a commercially available data logger will be used. This system has no internal intelligence but it comprises all necessary transducers to take data from thermocouples or thermopiles and resistance thermometers (Pt 100). Short term test data have until now been recorded by strip chart recorders. In a later stage a MADAS will be used.

Each individual data acquisition station will be coupled to a PDP11/10 minicomputer with 28 kbyte memory running under the Real Time Executive System RSX11S modified for operation with a flopy disc as system and data device. The modification work was done by the data handling group of the institute. The coupling of the different systems together with standard data input output devices, as paper tape and magnetic tape cassette, will be done by asynchroneous serial line interfaces. This local data acquisition system is installed hardwarewise and will go into operation in spring 78.

**Reference**

[1] See next chapter.

## 9.3. MADAS, a Microprocessor Aided Data Acquisition System

J.W. Grüter, K.P. Kruck, H. Labus

The sensors used in solar radiation and solar system measuring equipment can electronicwise be characterized by a voltage or a current source if they are active, or a resistor if they are passive. By applying appropriate transducers the physical quantities to be measured are transformed to potentials which, by an ADC, are converted to digital information. Most of such quantities, e.g. solar radiation or wind, are to be averaged over a certain measuring period. Usually, this is performed by hardware integrators.

Our Microprocessor Aided Data Acquisition System (MADAS) is based on CAMAC using the intelligent crate controller MACAMAC[1], a development of the central electronic division of KFA in collaboration with Borer SA, Solothurn. MACAMAC is a fully interrupt-driven stand-alone system. The program language is BASIC. For digital conversion a dual-slope scanning ADC is used. For the existing prototype version, individual transducers for each specific sensor have been developed by the electronic division of the institute. For an amended second version transducers and ADC will be integrated within a single CAMAC module. The types of sensors which are adaptable to this combined module are restricted to active sensors with voltage outputs $\geqq$ 100 microvolts.

A constant current source is available via the multiplexer to passive sensors.

The averaging process in the MADAS is done by software. The sensors are scanned by the ADC with a frequency of 0.1 sec/channel. After digital conversion the values are transferred to an integration program. Calculation of the first and second momentum of the data is performed simultaneously. Using BASIC for the integration program, the total scanning time is $\simeq$ 10 $\hat{s}$ for 32 channels. A time of 3-4 s can be achieved by according ASSEMBLER routines, fast enough for solar energy applications. Sensors having a pulse output can be fed into a fourfold CAMAC scaler module. All modules are under BASIC program control.

The mass storage device is optional; all devices with TTY 20 mA passive current loop are applicable. A connection by CCITT-V24 norm is under development.

The hardware costs of the MADAS are about 25 TDM.

### References

[1] Interner Bericht ZEL-NE-406/76 „CAMAC 8080 Microcomputer Hardware and Operating system (Borer „MACAMAC" 1521)"

## 9.4. Solar Collector Testing

H.P. Pohl, R. Schröer, H.J. Stein

A specific aim of collector testing at the KFA Jülich is to investigate the usability of mixed indoor/outdoor tests in comparison to the NBS method[1]. Not being completely novel in its principle, the ASE[2] procedure introduces one important addition, that is the ventilation of the collector front cover during the $\eta_o$ determination.

The general principle of mixed indoor/outdoor testing is a point in dispute since plate temperatures are different in indoor and outdoor conditions, and therefore the heat losses will be different. From a simplified theoretical point of view it can be shown that the heat losses determined in an indoor thermal-loss measurement are the same as they are determined from the slope of a NBS curve. Provided that all heat-transfer coefficients are reversible and constant with temperature, this is exactly correct for any F' factor[3]. Unfortunately, in reality heat-transfer coefficients may strongly vary with temperature. Nevertheless, it is hoped that this effect is tolerable small for typical flat-plate collectors. In any case, ASE tests will have the great advantage of being more reproducable and much easier to be carried out.

First results on a collector which is used in a worldwide round-robin test[4,5] show a surprisingly good agreement between NBS and ASE data, Fig. 1. It is interesting to note that this collector seems to

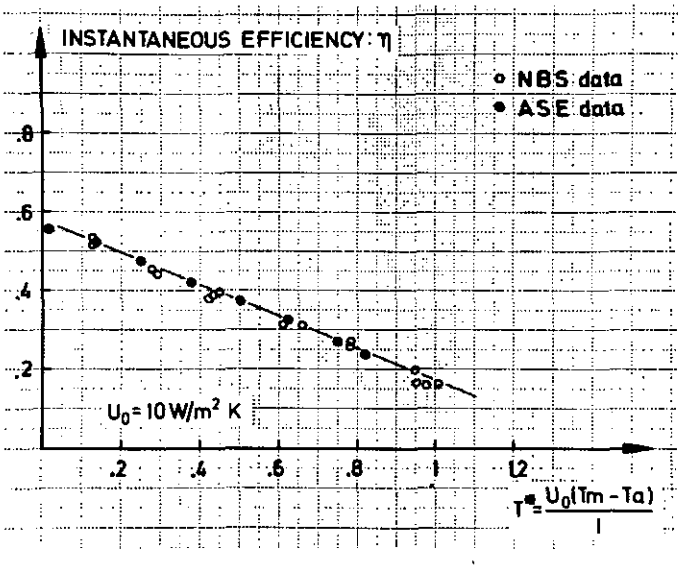


*Figure 1:*
*Measured efficiency curve of a collector. The efficiency is plotted versus a reduced temperature T* given by the temperature difference ΔT of mean fluid and ambient temperature divided by the intensity I of the incoming solar radiation. For convenience ΔT/I is multiplied by an arbitrry value $U_o$ having the dimension of a heat-transfer coefficient.*

have a relatively bad fin efficiency, i.e. the collector has a bad heat conductance from the solar-radiation absorbing plate into the heat extracting fluid. Measurements of thermal losses indoors and outdoors under varying conditions[6] have shown that infrared radiation from the atmosphere may be important for the efficiency of a solar collector. Therefore, infrared measurements should be introduced, e.g. by a direct determination, or by following the idea of Ployart et al.[7] who propose to measure the „effective" temperature comprising air, „sky" and „wind" temperature.

## References


[1] J.E. Hill, T. Kusuda, Method of Testing Solar Collectors Based on Thermal Performance, NBS- Report No. NBSIR 74-635, 1974
[2] Birnbreier et al., Wirkunsgradtest an Solarkollektoren, working document of Arbeitsgemeinschaft Solarenergie e.V., Essen, Sept. 1977
[3] R. Schröer, Vergleich zweier Testmethoden zur Bestimmung des Wirkungsgrads thermischer Flachkollektoren. Grad. eng. thesis, Jülich, Oct. 1977
[4] IEA Implementing Agreement for a Programme to Develop and Test Solar Heating and Cooling Systems, Paris, Dec. 20, 1976
[5] E. Aranovitch, The Joint Solar Collector Testing Programme of the European Community, UK-ISES Conference, April 1977, ISSN No. 0306-7874
[6] H.P. Pohl, Messungen des Wirkungsgrads thermischer Flachkollektoren. Grad. eng. thesis, Jülich, Jan. 1978
[7] R. Ployart, J. Colomes, B. Devin, Integration of Infrared, Ambient Temperature and Wind Condition in Flat Collector Performance Prediction, private communication


## 9.5. Instrumentation for Energy Exchange Measurements in the Prandtl Layer


K. Maßmeyer, J.W. Grüter


During the installation of a teststand for solar collectors a meteorological station has been built up simultaneously. The meteorological quantities to be measured are listed in the following table:

| height (m) | 0.25 | 0.5 | 1 | 2 | 4 | 8 |
|---|---|---|---|---|---|---|
| wind velocity | x | x | x | x | x | x |
| wind direction | | | x | | x | x |
| dry bulb temperature | x | x | x | x | x | x |
| wet bulb temperature | x | x | x | x | x | x |
| radiation balance 0.3-3 µm | | | | x | | |
| radiation balance 0.3-60 µm | | | | x | | |

soil temperatures in 5 depths (2, 5, 10, 20, 50 cm).

The data from this system enable the computation of the energy balance of the earths surface in the surrounding of the collector test station. These data are basic input parameters for the energy exchange problem of a thermal solar collector with its environment. The energy exchange is described by the following equation:

$$Q_K = H + E + B$$

where $Q_k$ is the net all wave radiation
H is the turbulent transfer of sensible heat
E is the contribution of latent heat of evaporation
B is the heat transfer into the collector.

This equation indicates a dependence of B from the following meteorological parameters:
- short wave radiation from sun and sky
- long wave radiation received by the surface from the atmosphere (counter radiation)
- wind velocity.

During a period of 1 or 2 years the meteorological variables in different heights in the vicinity of the collectors will be measured. With appropriate statistical methods the description of the thermal losses of the collector caused by atmospheric conditions will be possible.

Additional measurements of the angular distribution of direct and diffuse solar radiation give information about the optimum arrangement of the collectors.

The work is being carried out in collaboration with Institut für Geophysik und Meteorologie of University of Cologne.

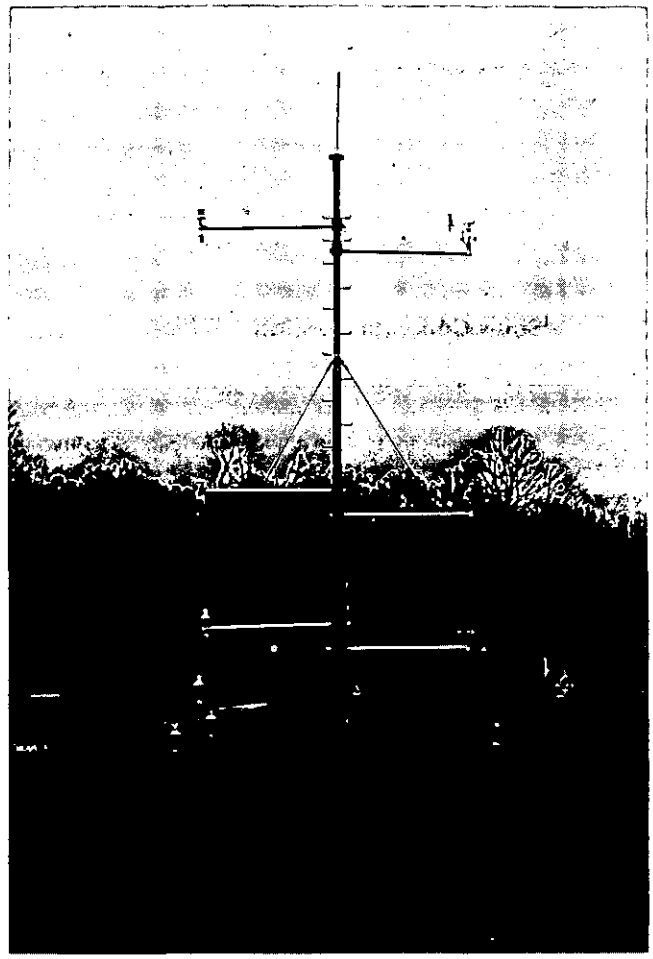

*Figure 1:*
*Meteorological tower for measurement of sensible and latent heat transfer in the lower Prandtl layer.*

# 10. Detector- and Target-Laboratory

## 10.1. Target-Laboratory

J. Pfeiffer, G. Riepe

For various experiments at the cyclotron, at the reactor, and in university laboratories approximately 150 targets (with and without backing) were produced from 30 different elements or enriched isotopes. Depending on the starting material various technologies had to be investigated until reproducible procedures could be used. In many cases these procedures are applicable only to a certain range of target thicknesses. The most often used technologies were: evaporation (sometimes heating by electron gun), cold-rolling (especially after the reduction of an oxide), and sputtering.

## 10.2. Semiconductor Detectors for Charged Particle Spectroscopy

A. Hamacher, T. Künster, E. Lawin, K. Nicoll, D. Protić, G. Riepe, H. Spanier

To be used for charged particle spectroscopy and particle discrimination in nuclear reaction experiments (IKP and visiting groups) the following detector systems were kept available: 15 telescope cryostats equipped with side-entry Ge(Li) detectors (which had been produced in the laboratory) and commercial silicon ΔE detectors, and 3 special cryostats designed for being mounted inside a large scattering chamber, each of which housing two Ge(Li) detectors. To ensure optimum operation during experiments, several detector parameters were checked in all stages. 50 radiation damaged Ge(Li) detectors had to be regenerated or replaced by new ones. ΔE detectors and collimators were exchanged according to experimental requirements.

The technology of fabricating charged particle detectors from high-purity germanium (HPGe) could be improved significantly, especially concerning the realization of thin $n^+$-contacts, sustaining fields of more than 5 kV/cm, by ion-implantation.

The problem of making good ohmic contacts to the implanted layers was solved. Several planar HPGe detectors with areas of up to 27 $cm^2$, both contacts made by ion-implantation, were fabricated according to this technology. Typical overvoltages of more than 1000 V could be applied to diodes of 15 mm thickness.

Since this detector type offers the advantage of thin dead layers (appr. 0.2 μm) on both contact sides, a stack arrangement of 5 detectors inside a single cryostat will be investigated in the near future. The total thickness of 55 mm will provide stopping of 160 MeV protons. Processing of coincidence signals from each detector not only leads to energy information but also to particle identification and to the reduction of the nuclear reaction tail.

As two companies fabricating detectors showed interest in the technology of producing thin $n^+$-contacts on HPGe, negotations were begun with the aim of an agreement concerning the transfer of technological know-how.

## 10.3. A Position-Sensitive HPGe Detector for Gamma Rays

A. Hamacher, T. Künster, R. Kurz*), D. Protić, R. Reinartz*), G. Riepe, W. Triftshäuser**)

Due to the above mentioned improvements in the HPGe technology the project of a digitally position-sensitive gamma-detector to be used as a positron-camera (Solid State Physics Department) could be completed. Many detail problems had been investigated on several prototype detectors.

The final detector with an active area of 5 x 6 $cm^2$ consists of two planar HPGe diodes with implanted contacts on both sides. The dimensions of each diode are 9 x 3 x 1 $cm^3$.

As seen in fig. 1, 32 stripe-electrodes on the $p^+$-side and 25 orthogonal ones on the $n^+$-side are connected to individual amplification channels. The periodicity of the stripes is 1.9 mm, the etched grooves between them being about 0.2 mm.

Well-defined position information results from coincidences between individual x- and y-stripes, dual and triple events being excluded by one-and-only-one circuits. All the necessary electronics was developed in the Central Electronic Laboratory.

Unfortunately, at this stage about 20 % of the 800 image points cannot be used because of broken connections to several stripe-electrodes.

Preliminary measurements showed a typical energy resolution for 1.33 MeV ($^{60}Co$) of 6 keV fwhm for an individual image point.

*) KFA-ZEL
**) KFA-IFF

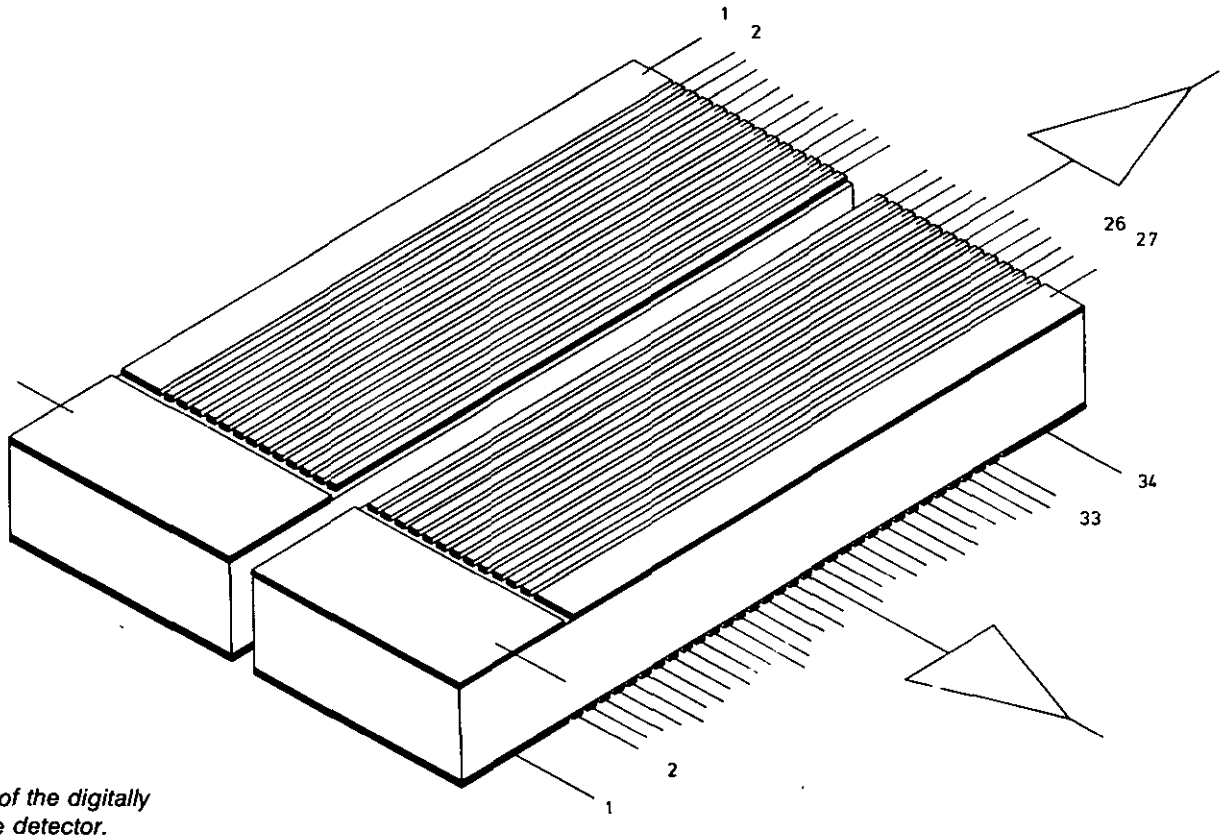


*Figure 1:*
*Schematic view of the digitally position-sensitive detector.*

# 11. Computer Development

## 11.1. IKPNET: Current IKPNETwork Configuration with Extended Online Support

J. Siefert, M. Karnadi, J. Klaes, B. Schmid

The hard- and software configuration of the PDP-11/ PDP-15-based resource sharing network IKPNET[1,2] were altered for the following reasons:

- The former PDP-15/30 system was replaced by a new PDP-11/T34 system with currently 64K (words) MOS memory, 1 RK05-F fix/exchangeable disk system, 1 additional RK05 exchangeable disk, 4 DL11-E asynchronous, serial line interfaces, 3 terminals (LA36, VT55, TEKTRONIX 4010), 1 DR11-C used as interprocessor link to a PDP-11/10-based CAMAC multi-channel analyzer (MCA), 1 CAMAC crate interfaced by a 1533A BORER SCC to the 11T34 UNIBUS. The new system runs under RSX-11M/V3 and is prepared at present[3] as the future ONLINE master of a PDP-11-based online data aquisition network for PHA and listmode experiments with new nodes and fast communication links (SCORPIO 3204 from CANBERRA and ND6660 from NUCLEAR DATA), replacing obsolete hardware components.

Parts of the replaced PDP-15/30 system (CPU with I/O processor, 16K core memory, BORER 2200 CAMAC branch driver with 1 CAMAC crate and 1 CC-A) together with the fast, program-controlled DMA DB99 interprocessor buffer were installed with additional hardware components (interprocessor link DA15-E, memory multiplexor MX15-A), realizing fast communication channels for the PDP-15-based network and extending the ONLINE functional capabilities of the PDP-15/50-system, running under the resource sharing executive RSX-IKP[4].

- A PDP-11/10-CAMAC-based MCA with 28K (words) core memory for ONLINE data-taking: with currently four 100 MHz ADCs from NUCLEAR DATA are interfaced by double buffers CAMAC input modules, a CAMAC DMA-controller[5] and a 1533A SCC from BORER to the PDP-11/10. The DMA-controller supports a maximal count rate of 125 Kevent/s in DMI- (singles) and 1 Mevent/s in DMA-mode (listmode). A NIM/CAMAC-based DMA hardware memory display controller[5] is used for live time display applications. The CAMAC front-end MCA with no mass storage devices is linked via a 16 bit/word parallel DR11-C to the PDP-11/T34 master and by a 24 bit/word parallel CAMAC link (JRE10/JRS10 I/O registers from SCHLUMBERGER) to the

# 12. Electronics Division

*H. Labus and J. Bojowald*

The following devices, already announced in the annual report 1976, have been set into operation:

1. The control electronics for the scattering chamber (with target position and rotation) and for the entrance slit (with four independent movable parts) of the magnetspectrograph BIG KARL have been installed and can now be remote controlled by CAMAC and manually from different places.
(H. Diesburg, G. Brittner)

2. The electronics to control the movements of a cross table for field measurements in the fringing field region of big spectrometer magnets have been redesigned and new installed.
(H. Diesburg, G. Brittner)

3. Hardware and software of the computer controlled curved crystal spectrometer with interferometric angle measurements have successfully been tested in the laboratory. After being installed on line the instrument was disturbed by mechanical vibrations induced by large cooling water pumps. They could be partly compensated by a closed loop control with adjustable PID-characteristic acting on a piecocrystal, which is able to perform fast displacements of the curved crystal.
(A. Hillers, H. Labus)

4. A data acquisition system for solar radiation and related meteorological data has been set up. 32 independent transducers have been developed for sensors which act as current or voltage sources or as resistors. The transducer outputs are fed to a CAMAC based data acquisition system consisting of a scanner with dual slope ADC (JOERGER-AM1) and a BASIC programmable intelligent crate controller (MACAMAC-BORER). Main advantages of this system compared with conventional data loggers are economic on line data reduction, as evaluation of time integrals, variances, normalisations etc. and flexible system configurations.
(P. Kruck, W. Ernst)

5. The curved crystal spectrometer at the ISOLDE II facility at CERN has been equipped with a linear source chopper. The slit system is accelerated and retarded between two opposite magnets in such a way that small switching times are combined with small mechanical shocks. The main advantage compared with a formerly used rotating chopper with fixed duty cycle is the switch selectable chopper frequency and duty cycle. Interfacing this linear chopper with the existing electronics and developing a new motor driver have been further activities.
(P. Kruck, W. Ernst)

6. The high voltage pulse generator for the internal macroscopic beam pulsing using axial deflection near the cyclotron center has been installed. To control the high voltage unit a NIM pulse generator has been developed with switch selectable beam on and beam off times in the range from $10^{-7}$ to $10^{+5}$ sec which itself is controlled by the ND-3300 on line data acquisition system. The complete beam pulsing system showed reliable operation during three periods.
(J. Bojowald, N. Dolfus, H. Labus, R. Nellen)

7. A peak stabilizer for time-to-pulse-height converters (TPC)[1] has been further developed for time measurements at pulsed beam accelerators at countrates far below 100 Hz. The existing device has a voltage controlled delay unit (VCD) between detector time pick off and TPC start. The control voltage is derived from two single channel analysers (SCA), each covering one half of a significant peak in the TPC output spectrum, one SCA charging and the other SCA discharging an analog integrator. Stabilisation is good at countrates greater some 100 Hz. The new device has a fast VCD with < 8 nsec recovery time which acts between cyclotron – RF and the stop input of an auxiliary TPC whereas TPC start is taken from an auxiliary detector, e.g. PM-tube with plastic-scintillator which can run at high countrates. Control voltage is derived as described above but a digital integrator with pure I-behaviour consisting of an up-down counter for the SCAs output pulses followed by a DAC is taken instead of an analog integrator. In steady-state condition the fast VCD output is strongly correlated in time with the beam pulses independent from cyclotron RF-phase and serves as stop signal for the main TPC which is started by time signals from the main detector, whose count rate has no influence on the stabilization quality. To take up operation properly after beam break down an automatic search run is initiated at countrates < 100 Hz of the auxiliary detector.
(H. Labus, G. Lürken)

Current activities are concentrated to the following subjects:

1. To get better economy and flexibility the 32 transducers of the data aquisition system mentioned above will be replaced by a CAMAC module which includes a FET-Scanner for 32 analog inputs, a current source for resistor sensors which is switched in phase with the first 16 inputs, a monolithic dual slope integrator and 64 word RAM's which control switches for individual offset and sensitivity of each input channel before conversion is performed. Thus the module can be adapted by programs to optio nal sensor configurations by loading the RAM's with specific information before each measurement cycle.
(H. Labus, K. Kruck, W. Ernst)

2. A long time integrator for solar radiation with mechanical display is tested in various configurations to find a low cost and fail safe circuit. A special wired up monolithic dual slope integrator seems to be superior to conventional techniques using voltage to frequency converters.
(R. Nellen, H. Labus)

3. For life time measurements in the msec region a high voltage pulse generator is built to switch the inner conductor of the fission product guide of the seperator JOSEF from –30 kV to +10 kV with rise and fall times < 100 s. The principle of operation is the same as used at the internal macroscopic cyclotron beam pulsing: Two tetrodes 4PR 250C are cascaded and both supplied by high voltage pulse and line transformers to operate between arbitrary levels within their maximum ratings.
(G. Lürken, N. Dolfus, H. Labus)

4. For the further extension of the microscopic beam pulsing with external deflection a 12 kV RF oscillator is developed whose resonance can be tuned from 1.75 to 3.3 MHz.
(N. Dolfus, H. Labus)

**Reference**

[1] W. Scheck, A. Hillers, H. Labus, Time pick off from pulsed beam accelerators, Nucl. Instr. and Meth. 128 (1975) 581–582

allows up to 128 simple or overlapping 2K gates (or 64 4K gates) to be sorted on a fix-head disk, using 32K memory. The sort consists of complex overlay segments, written in FORTRAN and assembler. More than 20 program functions, called by a special command syntax, are supported. The overlay program system is saved together with the DOS executive into a reserved save area on disk prior to the actual sort of a listmode tape and restored after sorting. This technique was implemented to use as much memory as gate buffers as possible of the available 32K memory to accelerate the tape sorting. The sort nucleus consists of a 4K assembler written segment. It is loaded from disk after memory saving into the lowest memory page and controls the gate buffer allocation, the parameter dependent sorting and the gate buffer overflow handling. Fast drivers for input of raw listmode data records from magtape (7 track, 556 bpi: ND330O output format) and for read/write of the sorted gate spectra on the fix-head disk are implemented. The sort nucleus also restores the saved memory image from disk after one tape sort and restarts the DOS system and the overlay system just after the CALL for tape sorting. The sort of a large listmode tape (760 m) with 4 parameters and average statistics for maximal 128 specified gates lasts about 30 minutes. The sorted gates may be written file-oriented and MTPIP compatible with maximal 128 gate spectra/file onto magtapes or saved together with the DOS system, user- and system programs as DOSSAVE-file by MTPIP onto disk-packs or magtapes. SORT output files may be mixed with DOSSAVE-files on magtapes. SORT V3D also allows the online plotting of monitor spectra with defined gates via the DB99 interprocessor link on the electrostatic STATOS plotter at the PDP-15/30/50 system. Monitor spectra of listmode ADCs, accumulated either in the PDP-11/10-based CAMAC MCA or the ND330O MCA may be read via the JRE10/JRS10 CAMAC-links[2] under SORT control for gates setting. A similar SORT V4A was realized with data input from a 9-track/800bpi magtape with records of 3.5 K words. Tapes may be generated with this data format by MTCOPY. This program condenses ND330O output tapes (7-track/ 556 bpi, 1K data records), saving considerably magtype space (9-track 800 bpi, 3.5K records, about a factor of 2.3) and sorting time because of the reduced number of magtapes. A normal SORT V3D run sorts about 50 large tapes, SORT V4A only about 22 tapes. A very fast vector SORT V3V for 7-track tapes and SORT V4V for 9-track tapes was realized. These SORTs use a new gate check algorithm: a vector of as many channels as the size of a gate spectrum contains either the address pointers to allocated gate buffers in memory (according to the specified gates) or zeroes, if no gate definitions were specified for these channels. The VECTOR-SORTs sort only non-overlapping gates but accelerate the tape sorting from about 30 min/large tape down to about 18 min inclusive tape rewinding (the physical read/write time of a tape on a TU10 drive is 15 min).

A general purpose graphic package CPKV (with currently about 50 standard routines) for comfortable, interactive use of the graphic capabilities of a KV15 storage display with cursor was realized for DOS/V3B. CPKV was written mainly in FORTRAN and uses an assembler written KV15 driver. The package was implemented CALL-compatible with the corresponding CPTEK graphic package for a TEKTRONIX 4010 under RSX-11M/V3[3]. The character generation for the KV15 is performed by software and generates a 5x7 dot matrix for any terminal character.

The CALCOMP driver for the CALCOMP software under DOS/V3B was extended to support optional IOT-spooling onto DEC-tapes or disks as spooler files. They may be transferred to a disk pack of the PDP-15/30/50 system by a simple TRA-command and then spooled to the CALCOMP plotter. This option was realized by implementing a new XYPLT spooler task, processing the IOT-records from the spooler files, and by modifying our XY.... CALCOMP plothandler task for appropriate IOT-processing.

The new configured PDP-15/30/50 double-processor system with a DB99 interprocessor link, a DA15-E interprocessor interrupt link and a shared 8K memory bank by a multiplexor MX15-A for the front-end PDP-15/304)ı was supported by a new communication handler task DL.... with spooler facilities and sub-tasking together with an extension DBLINK V4D for the resource sharing executive RSX-IKP[1]. The assembler written DBLINK services all DMA-transfers via the DB99 link and all DA15-E interrupts in the PDP-15/30 front-end. This communication executive is loaded from the system disk-pack DP0 by a new network initialization MCR-task ...NET. Very simple boot procedures for the PDP-15/30 and PDP-15/50 system parts were implemented: a simple MCR NET command initializes the network and boots a fresh copy of the communication executive DBLINK into the 15/30 front-end. The RSX-IKP system may be booted now directly either from DP0 by means of a papertape bootstrap without booting DOS first, or may be booted simply via the switch register if the 15/30 front-end was initialized. The idle and/or busy status of both CPUs are displayed by rotating lights in the console AC-register display lights.

### References


[1] J. Siefert, RSX-PLUS-IKP EXECUTIVES FOR ONLINE NUCLEAR DATA ACQUISITION AND ANALYSIS, European DECUS Proceedings, 1976, p. 307-312

[2] J. Siefert, IKPNET: A PDP-11/PDP-15-BASED RESOURCE SHARING NETWORK, European DECUS Proceedings, 1977, p. 101-107

[3] J. Siefert, B. Schmid, PDP-11 SOFTWARE DEVELOPMENT, contribution of this report, p. 137

[4] J. Siefert, M. Karnadi, J. Klaes, B. Schmid, CURRENT CONFIGURATION OF IKPNETWORK WITH EXTENDED ONLINE SUPPORT, contribution of this report, p. 134

coded to binary or string arguments, using a second subroutine PARAMS.

For optimization of the phase angle between the internal cyclotron beam pulses and the accelerating RF voltage an interactive RSX-11M/V3 program was written, using an iterative procedure[4]. For on-line magnetic field measurements with the PDP-11/T34, performed during the 1977 cyclotron shut down period[5], a field measurement DOS/VO9 program was written, supporting an interactive, operator synchronized data-taking with a FLUKE DVM and CAMAC I/O modules together with a flexible data-taking by means of direct-access files on RKO5 disks.

A DR11-C link between the memories of the PDP-11/T34 master and the PDP-11/1O CAMAC-based MCA was supported under DOS/VO9 as interprocessor link for IKPNETwork device-, file- and program-sharing as well as down-line system loading. A special MCA supervisor task ADCS under control of the CAMOS executive[2] was realized for servicing the parameter setup of the ADCs and CAMAC modules, the online data-taking of 4 ADCs in DMI-mode and the data transmission via a parallel CAMAC link (JRE1O/JRS1O) to the PDP-15/35 as master for online data storage and analysis. The CAMOS executive together with the ADC-S-supervisor task may be booted from the PDP-11/T34 master into the PDP-11/1O slave either via the DR11-C or a 96OO baud, opto-coupled, serial DL11-E link.

Available resource sharing facilities of the RSX-11M/ PDP-11 and RSX-IKP/PDP-15 time-sharing executive for the IKPNETwork are currently implemented in new PDP-11 user application programs. Further extensions of supported network functions (device-, file-, program- and terminal-sharing, program loading,...) for the DL11-E, DR11-C and CAMAC-links on system level (RSX-11M/V3, RSX-11S/V2, RT-11/V2C) for a new PDP-11 network supervisor task NET are in progress.

### References


[1] Digital Equipment, RSX-11M Version 3 Documentation Kit, 1976; RSX-11S Version 2 Documentation Kit, 1977
[2] J. Siefert, CAMOS, A FAST REAL-TIME CAMAC EXECUTIVE WITH GRAPHIC SUPPORT, European DECUS PROCEEDINGS, 1976, p. 259-264; Annual IKP Report 1976, p. 132-133
[3] Digital Equipment, IAS/RSX-11 I/O Operations Reference Manual, 1976
[4] J. Linz, this report, p. 123
[5] P. Wucherer, R. Brings et al., this report, p. 121


## 11.3. New User Applications and System Resource-Sharing Functions for PDP-15 Systems


J. Siefert, M. Karnadi, J. Klaes


A new magtape file-handling program MTPIP was realized for DOS/V3B. MTPIP allows the transfer of data files or system images to/from 7-(MT7) or 9-track (MT9) file-directory structured magtapes, to/from DEC-tapes (DTO,...DT3) or fix-head disks (DK) or via the online DB99 interprocessor link to disk packs (DPO, DP1) or the line printer (LP) at the PDP-15/5O/3O double-processor system, running under the resource sharing executive RSX-IKP[1]. Complete fix-head disk images, containing the DOS system together with user and system programs and data files may be saved/restored as named files onto/from MT7, MT9 or via the DB99 online link onto DPO or DP1. A DOSSAVE restore or save of 2 DK disks (512 K words) via the DB99 link from/to DPO or DP1 needs only 2 min. Sorted gate spectra from listmode magtapes by SORT runs may be listed on the LP via the DB99 link. The syntax of the MTPIP commands, their operands and optional default values may be explained at run-time by MTPIP itself. The MTPIP syntax corresponds to the standardized command syntax, introduced for all new developed IKP-programs for PDP-15-and PDP-11-systems. This command syntax is independent of the used, very different operating systems as RSX-IKP, DOS/V3B for PDP-15-systems and DOS/VO9, RT-11/V2C, RSX-11M/V3 and RSX-11S/V2 for PDP-11-systems. The new command syntax uses an easy-to-learn mnemonic, but flexible command formats with optional defaults for command operands. Only the first three letters of a command or operand are used for syntax checks. The available explanations of MTPIP may be listed e.g. on TT1, a LA3O at the PDP-15/35, by the command EXP ALL TT1 after the prompting symbol PIP . The DOS[SAVE]command syntax may be explained at the system console by EXP DOS[SAVE]. A named 2-DK DOSSAVE-image (e.g. the file SORT V3D) may be restored via the online link from DPO by the command DOS DK,DPO SORT V3D. A 9-track tape may be scratched, labelled (e.g. DATA) and formatted with a new file-directory by NEW MT9 DATA. Sorted gate spectra (e.g. gates 3O to 5O) may be listed from MT7 files (e.g. GATES UNF) on the LP via the DB99 link by the command TRA LP,MT7 GATES 3O 5O.

The new command syntax was introduced also for some older program systems. All new developed PDP-11 and PDP-15 programs handle command explanation files on disk. These files are edited by the corresponding EDIT utilities, supported by the operating systems. They contain all available command explanations which may be requested interactively at program run-time by the EXP[LAIN] command. The TRA[NSFER] command handles all file operations of supported I/O devices. E.g., the complex overlay program system SPT (DOS/V3B) for spectra analysis may access the following input/output devices by simple TRA-commands of the format TRA OUT,IN FILE (or ADC) EXTension (or TAG-word). OUT-devices are MT7, MT9, the memory MM, the CALCOMP plotter XY, and via the DB99 link the LP or STATOS plotter XP at the PDP-15/3O/5O system. Supported IN-devices are: CA, the PDP-11/1O-based CAMAC MCA for single transfers via CAMAC links, ND, the ND33OO MCA via CAMAC links, MT7 or MT9 and DK. Spectra, displayed on the KV15 storage display may be dumped to the XY and XP plotter with linear or logarithm coordinates by a simple TRA command.

A new, general magtape utility MTDUMP was realized for DOS/V3B. MTDUMP uses the new command syntax and allows by specifying a TRA-command with appropriate operands to convert and/or condense input tapes with different formats (7- or 9-track, 556 or 8OO bpi, different physical/logical record structures), written by different computer systems (e.g. SIGMA 3 at MPI-Heidelberg, DECsystem 1O at Munic, ...) into standard tape formats, used by IKP-programs, e.g. SORT programs for listmode data tapes.

Existing SORT programs for the PDP-15/35 system, running under DOS/V3B, were considerably extended. A new SORT V3D program system for 2-, 3- and 4-parameter sorts of listmode data

## 11.2. PDP-11 Software Development

J. Siefert, B. Schmid

The real-time executive RSX-11M/V3[1] from DEC was introduced as time- and resource-sharing executive for the new installed PDP-11/T34 system, which is at present prepared as future PDP-11 master for online data storage and analysis as well as PDP-11-network host. RSX-11-S/V2[1] from DEC with boot and data file support for RX11-Dual Floppy disks was introduced for a slave PDP-11/10 system with basic MCR, online task loader support OTL from a floppy disk and the system save image processor SIP. Several RSX-11M/S system generations were performed to generate configuration-dependent mapped RSX-11M and unmapped RSX-11S systems with appropriate resident device handlers and partition layouts. Most of the available RSX-11M executive and terminal driver options, as e.g. round robin scheduling or system-controlled partition support were selected for different system generations to estimate the core and execution time overhead and to tune the system parameters and performance to our PDP-11/T34 configuration with tolerable executive overhead for an online system. As the DEC-supplied system generation procedures, together with the DEC RKO5 distribution-kits, use complicated, time and disk space wasting algorithms, we re-organized the distribution disks and wrote fast executable batch files for RSX-11M system generations, using the very flexible structure of the RSX-11M batch command language.

A set of fast executable, FORTRAN FUNCTION callable routines for a multi-crate CAMAC support was realized for RSX-11M/V3. The process-variable oriented CAMAC CNAF processing supports all I/O requests and status functions without LAM-handling for CAMAC modules with crates interfaced by 1533A BORER single crate controllers (SCC). The FUNCTION-CALL mnemonic is very simple and closely related to CAMAC terms. A CAMAC operation must be first translated by a CAMVAR=CNAF(C,N,A,F,MODE) DOUBLE PRECISION FUNCTION call into a process variable, named by the user (CAMVAR). The time-consuming CALL parameter checking is done by the CNAF-FUNCTION as well as the generation of a binary code, optimized according to core amount (maximal 4 words) and execution time. The code sequence is stored in the user supplied process variable. This CAMAC variable may be executed by a FORTRAN or MACRO written task with minimal execution overhead by the INTEGER FUNCTION call CSR=CAMAC(CAMVAR,DATA) with an optional DATA address pointer for I/O transfers. The CNAF execution time of 30-45 µs is of the same order as the time needed by an in-line, assembler coded statement sequence, using registers for time minimization. The SCC control and status bits, correlated with a CAMAC-CALL, are available and may be stored by the user as integer variable (CSR) for later processing. The CSR-bits may be tested for a Q and/or X or ORED LAM by the logical FUNCTIONs Q(CSR), X(CSR), LAM(CSR). All FUNCTIONs may be called by one FORTRAN statement, e.g. IF (Q(CAMAC(CAMVAR,DATA))) GOTO ... All SCC--functions are available as normal CNAFs, using N24 as station number and appropriate F-codes together with AO. E.g., CN24AOF10 clears a missing Q-LAM, CN24AOF9 generates a Z, ..etc. Currently the tests for a fast LAM-interrupt handling by a privileged CAMAC LAM-supervisor task with front-end LAM-service in kernel mode and data communication via a shared COMMON data region on an intertask receive/send communication level with CAMAC application tasks in a system-controlled partition are in progress. A context switch-time of only about 100 µs to a LAM-synchronized interrupt service routine in a mapped RSX-11M system was realized. The LAM supervisor will service LAMs with standardized and optional user-supplied, MACRO-written interrupt service routines.

A general purpose graphic package CPTEK (with currently about 35 standard routines) for easy but full, interactive use of the graphic capabilities of a TEKTRONIX 4010 display terminal was realized for RSX-11M/V3. CPTEK was written mainly in FORTRAN and was derived from a similiar graphic package, used since 2 years already for application tasks, running under the CAMOS[2] or DOS/V09 operating system. The package was designed very modular. It supports a comfortable, interactive graphic representation and analysis of spectra in point-, line- or histogram mode in cartesian, semi-log or log-log coordinates with axis labelling and scaling of distinct curves in the same or different coordinates. The package offers four functional levels for different skilled users and applications. On the highest level, plotting with a series of default conditions may be performed with a minimum of effort. E.g., the plot of a data vector y versus a vector x with n elements each, with x- and y-axis, appropriate tic marks and data symbols is performed by a CALL CPDIAG (X,Y,N), using default values for specific graphical variables. All available options may be explicitly defined by setting corresponding COMMON variables. Graphic coordinates for peak-, background-definitions, .. may be specified interactively at run-time, using the graphic cross-hair cursor by e.g. CALL CPCURS (KEY,IX,IY). This CALL transmits to the caller the cross-hair coordinates in absolute, adressable raster units together with the ASCII value of the key depressed after cursor positioning. The cursor coordinates may be transmitted by a CALL CPINXY (KEY,X,Y) in scaled, rotated user units relative to the origin of an underlying coordinate system. On the next lower levels down to the physical I/O level for character I/O in alphanumeric, bit-transparent mode, light or dark vector generation in graphic mode, screen erase or hardcopy, a full set of routines is available. They allow an experienced experimentalist to use only those functions he needs to develop his own set of specialized graphic functions. Functional extensions of the package are in progress: a flexible, sub-task oriented plot command handler for interactive request of pre-defined or user-written graphic functions at run-time with display file handling,...

A set of MACRO written, FORTRAN callable subroutines (currently about 25) for terminal I/O was realized for RSX-11M/V3. They support unformatted binary and formatted ASCII data output with FORTRAN equivalent slash, X, L, O, I, F, E, A, H and string format specifications at task run-time, allowing a much more dynamical and flexible data formatting than the corresponding FORTRAN FORMAT statements, and using available memory by far more economical than the DEC-supplied FORTRAN library modules. Read routines for characters and unformatted terminal input (numeric and command/ string arguments) are also supported. E.g., a user-specified maximal number of characters may be read into a user-supplied buffer as response to an optional, user-defined prompting symbol from any terminal by a CALL CTREAD and decoded into command (strings) and/or binary numeric arguments. The number and the type of each decoded argument is supplied for command dispatcher purposes too.

A general magnetic tape transfer program was written for RSX-11M/V3 for data interchange of magnetic tapes between PDP-11 systems (running under control of DOS/V09, RT-11/V2, RSX-11M/V3) and an IBM 370/168 system with a TSS time-sharing monitor in the ZAM-institute. The tape transfer program uses the support of ANSI magnetic tape standard[3], available since V3 of RSX-11M together with FLX-utility file-transfer capabilities for DOS and RT-11 files. The FILES-11 file structures single-file-single-volume and multifile-single-volume with standard ANSI volume-, file-header- and end-of-file, end-of-volume labels are supported on magtape. Data must be written as formatted ASCII records of fixed length onto tape. These ANSI tapes may be referenced (OPEN, READ, CLOSE) by the TSS file-control system by specifying an appropriate DDEF with file generation number. Records from a DDEF-specified file may be read by TSS FORTRAN program, calling a simple subroutine MTLINE. The EBCDIC converted, formatted characters supplied by MTLINE may be de-

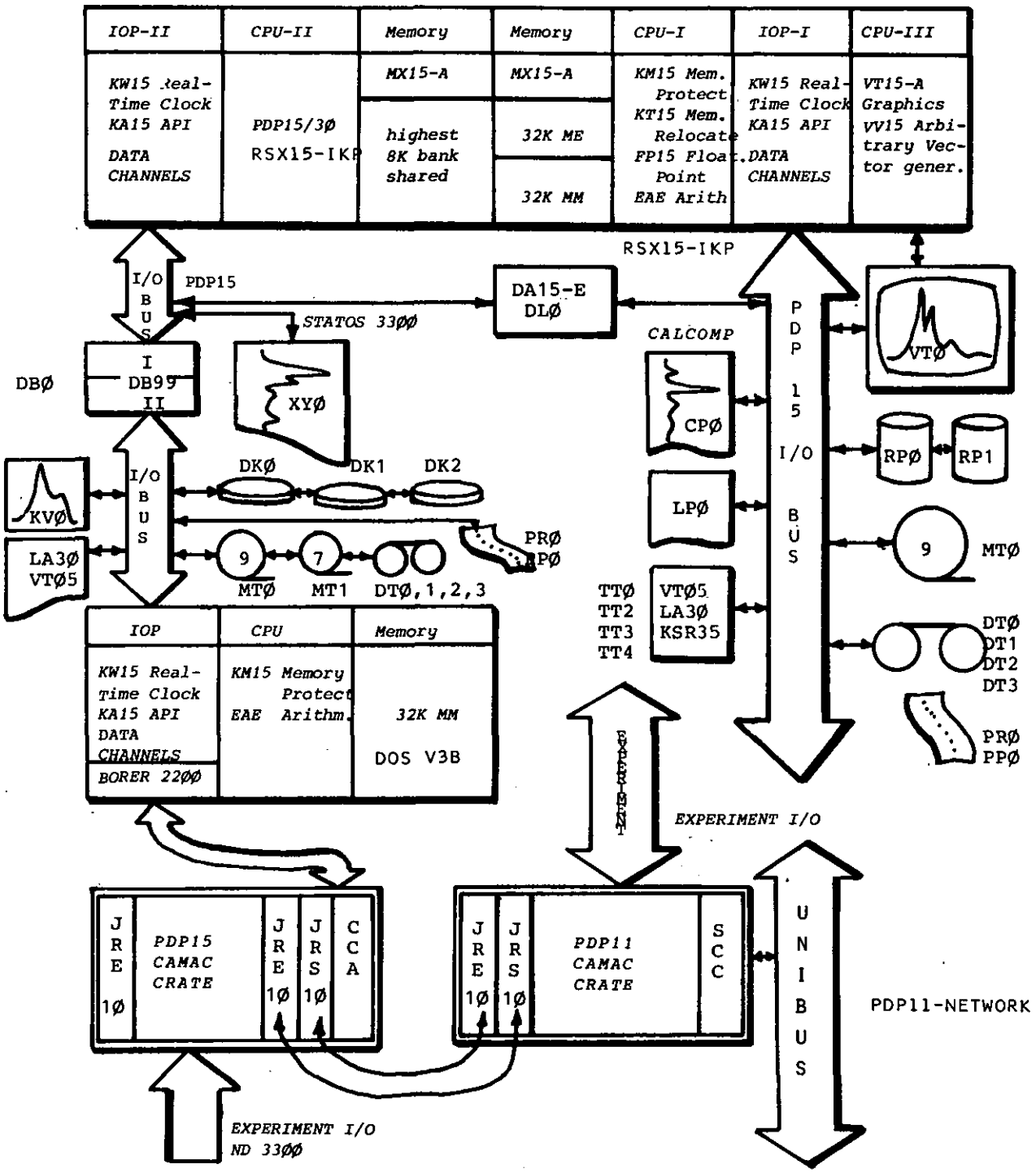


*Figure 2:*
*Triple PDP-15 computer configuration of PDP-15 IKPNETwork.*

## References


[1] J. Siefert, IKPNET: A PDP-11/PDP-15-BASED RESOURCE-SHARING NETWORK, European DECUS Proceedings, 1977, p. 101-107

[2] J. Siefert, M. Karnadi, J. Klaes, COMPUTER DEVELOPMENT, IKP Annual Reports 1975, 1976

[3] J. Siefert, B. Schmid, PDP-11 SOFTWARE DEVELOPMENT, contribution of this report, p. 137

[4] J. Siefert, M. Karnadi, RSX-PLUS-IKP EXECUTIVES FOR ONLINE NUCLEAR DATA ACQUISITION AND ANALYSIS, European DECUS Proceedings, 1976, p. 307-312; J. Siefert, M. Karnadi, COMPUTER DEVELOPMENT, IKP Annual Reports 1975, 1976, 1977

[5] J. Siefert, A CAMAC-BASED MCA, RUNNING UNDER CAMOS, IKP Internal Report, 1977; K. Zwoll, W. John et al., CAMAC DMA- und NIM/CAMAC Display Controller für PDP-11 Systeme, KFA-ZEL-NE, Internal Reports, 1974

[6] Digital Equipment, PDP-9 Interprocessor Data Buffer DBO9A, DB99 Interface Manuals, 1969; DA15-E Interprocessor Interrupt Link Manual, 1971 MX15-A Memory Multiplexor Manual, 1971

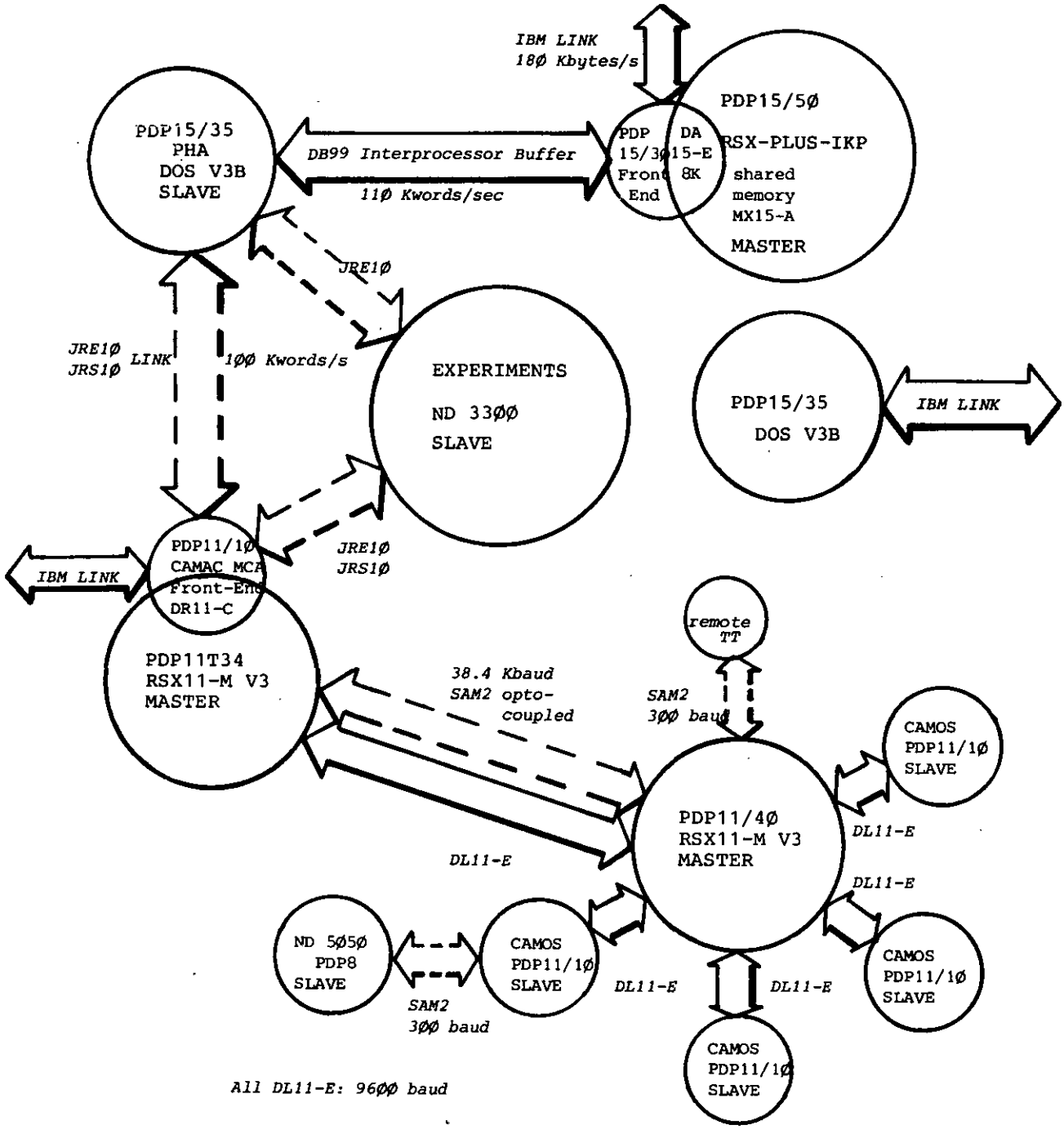


*Figure 1:*
*Current IKPNETwork configuration.*

PDP-15/35 of the PDP-15-network. These fast communication channels support the online storage and analysis of accumulated data on both hosts.

The current configuration of the IKPNETwork, the realized communication channels, the linked systems and the used operating systems are shown in figure 1[1,2]. Details of the PDP-15/35--PDP-15/3O--PDP-15/5O triple-computer system are shown in figure 2. The program-controlled DB99 interprocessor buffer[6] is now used as fast DMA link between the memories of a PDP-15/35 and a double processor system PDP-15/5O with a PDP-15/3O as front-end. The DMA data transfer rate is 11OK 18-bit/words parallel. The front-end PDP-15/3O is linked via a DA15-E interprocessor interrupt link[5] to the master PDP-15/5O and shares the upper 8K memory bank of the master's total 64 K words of core memory via a MX15-A memory multiplexor[6]. The PDP-15/35 system, running under DOS/V3B, is used day and night mainly for extensive sort runs of listmode γγ-coincidence data (about 5O large magtapes per run) and ONLINE PHA-analysis of accumulated single spectra from either the PDP-11/1O-based CAMAC- or ND33OO-MCA. The PDP-15/5O/3O double-processor system runs under the resource sharing executive RSX-IKP and is used for extensive interactive, graphical analysis of spectra (graphics processor with lightpen, electrostatic STATOS plotter, CALCOMP plotter) and concurrent program development for all PDP-15-systems in a time-sharing environment[4].

# 13. Radiation Protection

*H.J. Probst*

Beside the routine duties, the activities of the radiation protection were mainly concentrated in fulfilling the obligations of the new radiation protection ordinance valid from April of this year:

1) Application for the licence for the operation of the isochronous cyclotron JULIC was proposed.
2) Several existent radiation protection measuring and warning devices were reconstructed, and defect indicators were installed.
3) Above the doors to the controlled as well as the restricted areas appropriate signs, which could be switched on and off by a remote control were prepared. Their application by the personnel safety system was investigated.
4) For the low-level area M4 the reconstruction of an ionization chamber was planned so that at an increased radiation level (for that the relatively thin shielding is not sufficient) a delayed cyclotron shut down is made.
5) The air monitoring system was completed installing an air flow meter in the chimney. Now air activity concentration at various measuring areas and air flow in the chimney are monitored.

In 1977 the radiation exposure in the institute was less than in 1976. Using the new electrostatic deflector in the cyclotron, a trend-turning for the man-rem-dose could be realized as desired and a strong decrease of the radiation exposure took place. This can be seen from the exposure values of the last three years: 27.6 rem (1975), 3O.O rem (1976), 24.3 rem (1977). Considering that some components of the new deflector still are to be improved, a further decrease of the radiation exposure can be expected in 1978.

Furthermore the shielding thicknes of the measuring area M5 was tested by the „technical supervision association". The result was essentially in agreement with the calculations.

# 14. Engineering Office and Mechanical Workshops

*W. Briell, K.H. Ramacher, A. Retz, U. Rindfleisch, H. Schwan*

The activities of the engineering office and the mechanical workshops were concentrated on maintenance and improvement of the accelerator, beam line and experimental equipment. New correction coils, a new septum deflector and the mechanical equipment for a phase measuring facility were prepared and installed during the annual shut down period. The septum deflector and the compensated channel installed in 1976 met the requirements and improved the reliability of the accelerator. Spare parts for these elements are now under construction.

A new scattering chamber with irradiation target and a chopper was designed and is now being constructed for measurements of α and γ high spin states (Fig. 1). The design of the experimental equipment for the experimental areas A1 and A2, a g-factor magnet and a natrium cristal detector has been started. The scattering chamber with the target exchange valve, the variable collimator and the detector box for the magnet spectrometer Big Karl were testet and are now ready for installation. All components of the beam line system to the experimental areas A1 and A2 and to the magnet spectrometer are ready. Installation and alignment started at the end of the year.

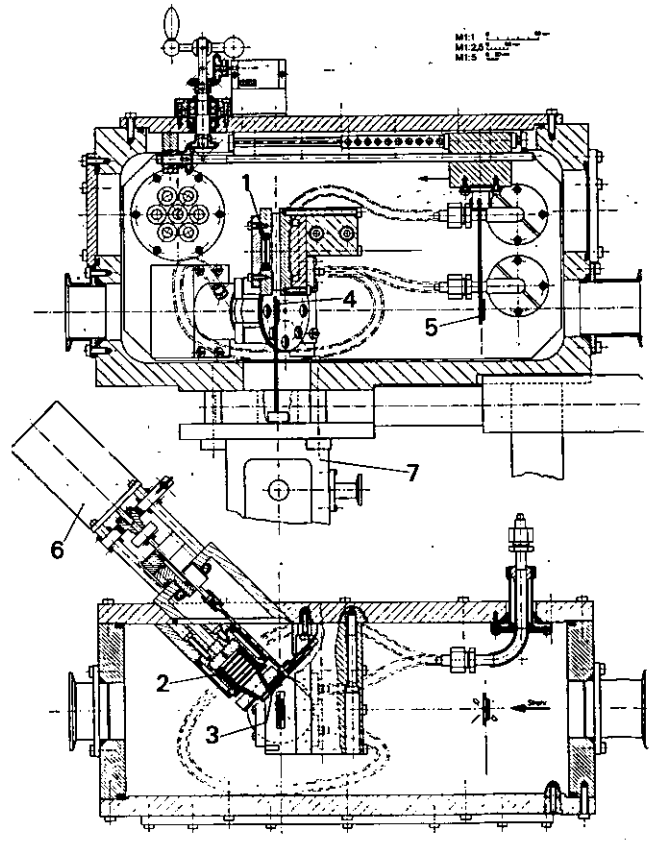


*Figure 1:*
*1.+2. Refrigerated Si-surface barrier detector*
*3. Tantal chopper*
*4. Catcher target*
*5. Target*
*6. 22,5° Stepping motor*
*7. Target exchange valve*

# IV. Scientific Advisory Council of the Institute of Nuclear Physics

| | |
|---|---|
| Prof. Dr. K. Alder | University of Basel |
| Prof. Dr. R. Bock | Chairman, GSI Darmstadt |
| Prof. Dr. P. von Brentano | University of Köln |
| Dr. F. Führ | KFA Jülich |
| Prof. Dr. P.G. Hansen | CERN, Genf, Switzerland |
| Prof. Dr. H.-J. Mang | TU München |
| Prof. Dr. T. Mayer-Kuckuk | University of Bonn |
| Prof. Dr. H. Neuert | University of Hamburg |
| Prof. Dr. B. Povh | MPI Heidelberg |
| Prof. Dr. K. Wildermuth | University of Tübingen |

# V. External Committee for Guest Experiments

| | |
|---|---|
| Prof. Dr. R. Bock | GSI Darmstadt |
| Prof. Dr. P. von Brentano | University of Köln |
| Prof. Dr. K. Wildermuth | University of Tübingen |

# VI. Personnel

**Institute for Nuclear Physics:**

| | |
|---|---|
| Dr. A. Fäßler | Director of the Institute for Nuclear Physics (Theory)<br>Professor of Physics at University of Bonn |
| Dr. C. Mayer-Böricke | Director of the Institute for Nuclear Physics (Experiment I)<br>Professor of Physics at University of Bonn |
| Dr. O. Schult | Director of the Institute for Nuclear Physics<br>Managing director of the Institute for the year 1977<br>Professor of Physics at University of Köln |

## Scientific Staff:

DP L. Aldea (E2)
Dr. M.R. Anastasio (Th)
Dr. C. Alderliesten (E1)
Dr. A. Ansari (Th)
Dr. G. Baur (Th)
Dipl. U. Bechstedt (E1)
Dr. M. Behar (E2)
Dr. H. Beuscher (E1)
Dr. H. Börner (E2)
DP J. Bojowald (Ec)
Dr. G. Borchert (E2)
DP O. Bousshid (E1)
DI W. Bräutigam (Cy)
Dr. J.R. Broda (E2)
Dr. H. Bromme (E2)
Dr. P.J. Daly (E2)
(Professor at the
Purdue University, West
Lafayette, Indiana, USA)
DP W.H. Dickhoff (Th)
Dr. J.P. Didelez (E1)
Dr. A. Djaloeis (E1)
Prof. Dr. A. Fäßler (Th)
Dr. K. Göke (Th)
(Privat Dozent at the
University of Bonn)
Dr. Y. Gono (E1)
Dr. F. Grümmer (Th)
Dr. J.W. Grüter (E2)
Dr. D.R. Haenni (E1)
Dr. A. Hardt (Ms)
Dr. E.F. Hefter (Th)
DM W. Hürlimann (Ms)
Dr. P. Jahn (E1)
Dr. B.D. Kern (E2)
(Professor at the
University of Kentucky,
Lexington, USA)
Dr. T.A. Khan (E2)
Dr. P. Kleinheinz (E2)
Dr. V. Klemt (Th)
Dr. H.R. Koch (E2)
Dr. S. Krewald (Th)
Dr. D. Kucheida (E2)
Dr. H. Külz (E2)
Dr. H. Labus (Ec)
DP W.D. Lauppe (E2)
Dr. H. Lawin (E2)
DP H. Lenske (Th)
Dr. R.M. Lieder (E1)
DP J. Linz (Cy)
DP S. Lunardi (E2)
Dr. H. Machner (E1)
Dr. V.A. Madsen (Th)
(Professor of the Oregon
State University, USA)
Dipl. M. Manko (E1)
Dr. S. Martin (Ms)
Dipl. K. Maßmeyer (E2)
Prof. Dr. C. Mayer-Böricke (E1)
Dr. J. Meißburger (Ms)
Dr. J. Meyer-ter-Vehn (Th)
Dr. H.P. Morsch (E1)
Dr. M. Müller-Veggian (E1)
Dr. H. Müther (Th)
Dr. A. Neskakis (E1)
Dr. W. Oelert (E1)
Dr. M. Ogawa (E2)
Dr. F. Osterfeld (Th)
Dr. M. Ploszajczak (Th)
DP H.J. Probst (Rp)
DP D. Protic (Dt)
DP J. Reich (Cy)
Dr. G. Riepe (Dt)
Dr. G. Rinker (Th)
Dr. M. Rogge (E1)
Dr. G. Sadler (E2)
Dr. J. Sanchez-Dehesa (Th)
Dr. K.W. Schmid (Th)
Prof. Dr. O. Schult (E2)
Dr. K. Shimizu (Th)
DP H.A. Selic(E2)
Dr. H. Seyfarth (E2)
DP J. Siefert (Da)
Dr. K. Sistemich (E2)
Dr. J. Speth (Th)
(Professor at the
University of Bonn)
Dr. H.J. Stein (E2)
Dr. H. Toki (Th)
Dr. P. Turek (E1)
Dr. M. Wakai (Th)
DP J. Wambach (Th)
Dr. S. Wiktor (E1)
Dr. P. Wucherer (Cy)
DP N. Wüst (E2)
Dr. H.L. Yadav (Th)

## Research visitors:

Dr. M. Betigeri (E1)
Dr. J. Blomqvist (E2)
Prof. Dr. V. Brown (Th)
Prof. Dr. Ch. Chen (Th)
M. da Graca Zilhao Cruz (E2)
Dr. M. Ekpo (E2)
Dr. M. Faber (Th)
Dr. M. Fenzl (E2)
Dr. B. Kardon (E2)
Prof. Dr. H.O. Lutz (E1)
Dr. M. Maier (E2)
Prof. Dr. H. Mavromatis (Th)
Prof. Dr. E. Nadjakov (Th)
Dr. G. Paic (E1)
Dr. M. Piiparinen (E2)
Dr. P.-G. Reinhard (Th)
S.M. Sahakundu (E1)
Dr. M. Shaanan (E2)
Prof. Dr. R.V. Sheline (E2)
Dr. B. Sinha (Th)
Dr. A. Stefanini (E2)
Prof. Dr. O.I. Sumbaev (E2)

## Staff:

K. Barth (Ec)
H. Beckers Frl. (Ad)
H.G. Böge (Cy)
W. Borgs (E2)
H. Borsch (Cy)
W. Briell (Cd)
R. Brings (Cy)
G. Brittner (Ec)
E. Brökel (Th)
J. But (Ws)
A. Dahmen (Ec)
H. Diesburg (Ec)
A. Dohmen Fr. (Ad)
N. Dolfus (Ec)
F. Drees (Cy)
C. Ehlers Frl. (Da)
K. Ehrhardt (Ms)
R. Enge (Ws)
P. Engels (Cy)
W.R. Ermer (E2)
W. Ernst (Ec)
R. Fiedler (Cy)
N. Gad (Cy)
J. Geremeck (Cd)
A. Germeroth (Ms)
G. Göbbels (Ws)
A. Golik (Ws)
D. Groß (Cd)
H. Hadamek (Ws)
A. Hamacher (Dt)
M. Heese Frl. (Ad)
H. Heinrichs (Cy)
A. Hillers (Ec)
H. Hintzen (Rp)
W. Hoffmeister (Cy)
K. Hütten (Ws)
H.M. Jäger (E1)
I. Jannakos (Cy)
H.J. Jansen (Ws)
M. Jansen Frl. (Da)
A. Jeglorz (E2)
K.H. Junglas (Ws)
M. Karnadi (Da)
M. Keuter (Ws)
J. Klaes (Da)
H. Klapperich (Ws)
K. Kraft (Rp)
K.P. Kruck (Ec)
D. Krüger Fr. (Th)
T. Künster (Dt)
E. Lawin Fr. (Dt)
J. Lemmens (Cy)
H. Lengerke Fr. (Ad)
H. Lippianowski (Ws)
G. Lürken (Ec)
H. Meuser (Ws)
A. Müller (Cy)
R. Nellen (Ec)
K. Nicoll (Dt)
J. Pfeiffer (Dt)
U. Pennartz Frl. (Ad)
M. Pier Frl. (Ad)
H.W. Pohl (E1)
K.H. Ramacher (Cd)
A. Retz (Cd)
U. Rindfleisch (Ws)
T. Sagefka (Ms)
H. Sauer (Ad)
G. Schlienkamp (Cy)
B. Schmid Fr. (Da)
P. Schmidt (E2)
Jos. Schmitz (Ws)
Jürg. Schmitz (Cy)
U. Schneider (Da)
F. Schultheiß (Ws)
H. Schwan (Ws)
R. Seidemann (E2)
W. Settels (Cy)

H. Sieling Fr. (Ad)
H. Spanier Fr. (Dt)
J. Strehl (Ws)

W. Weber (Ws)
K.P. Wieder (E2)
W. Wilms (Cy)

K. Winkler (Ec)
J. Wolanski (Ws)
H. Wolf (Ec)

(E1) Institute for Experimental Nuclear Physics I
(E2) Institute for Experimental Nuclear Physics II
(Th) Institute for Theoretical Nuclear Physics

(Ad) Administration
(Cd) Construction and Design
(Cy) Cyclotron Laboratory
(Da) Data Acquisition Group
(Dt) Detector and Target Laboratory
(Ec) Electronics
(Ms) Magnetic Spectrograph 'Big Karl'
(Rp) Radiation Protection
(Ws) Mechanical Workshop

# VII. Index to Authors

# VIII. Publications

IKP-100177
ALDEA,L. BECVAR,F.* HONZATKO,J.* POSPISIL,S.* TELEZHNIKOV,S.A.*
EVIDENCE FOR WIDTH CORRELATION IN THE YB-173(N,GAMMA) TB-174 REACTION.
CZECH. J. PHYS. B27(1977),1002-8
20.700

IKP-100277
ALDEA,L. KAROON,B. SCHULT,O.W.B. SEYFARTH,H. WUEST,N.
THE STUDY OF THE (N,ALPHA) AND (N,GAMMA ALPHA) REACTIONS ON ND 143.
Z. PHYS., A 283(1977),391-5
20.700

IKP-100377
ALEXEEV,V.L.* EMELIANOV,B.A.* EPOROV,A.I.* KABIU,L.P.* KAMINKER,D.M.* KHAZOV,YU.L.* KONDURCV,I.A.* LENSHKIN,G.K.* LOGINOV,YU.G.* MARTYNOV,V.V.* RUMINANTSEV,V.L.* SAKHAROV,S.L.* SUSHKOV,P.A.* BOERNER,H.G. DAVIDSON,W.F.* PINSTON,J.A.* SCHRECKENBACH,K.*
THE LEVEL STRUCTURE OF SB-122.
NUCL. PHYS. (IM DRUCK)
20.700

IKP-100477
ALMEIDA,J.A.* BOERNER,H.G. DAVIDSON,W.F.* SCHRECKENBACH,K.* NAMENSON,A.I.* EGIDY,T. VON* VANASSCHE,P.H.M.*
VIBRATIONAL AND SINGLE-PARTICLE STATES IN U-235.
PROCEEDINGS OF THE INTERNATIONAL CONFERENCE ON NUCLEAR STRUCTURE. TOKYO, 5.-10.9.1977. VOL. 1, S. 463
20.700

IKP-100577
AMOS,K.* FAESSLER,A. MORRISON,I.* SMITH,R.* MUETHER,H.
INELASTIC SCATTERING AS A TEST OF NUCLEAR STRUCTURE; THE CASE OF FE-054.
NUCL. PHYS. (IM DRUCK)
20.800

IKP-100677
ANASTASIC,M.R. FAESSLER,A. MUETHER,H. HOLINDE,K.* MACHLEIDT,R.*
MESONIC AND ISOBAR DEGREES OF FREEDOM IN THE GROUND STATE OF THE NUCLEAR MANY-BODY SYSTEM.
PHYS. REV. C (IM DRUCK)
20.800

IKP-100777
ANTROPOV,A.E.* GUSEV,V.P.* ZARUBIN,P.P.* IOANNU,P.D.* KORBEZKIJ,E.V.* ORLOV,B.N.* HEFTER,E.F.
ANALIS RASSEYANIYA PROTONOV S ENERGIYE 6 MEV NA YADRACH NI-058,060,062,064.
IZV. AKAD. NAUK SSSR, SER. FIS. (IM DRUCK)
20.800

IKP-100877
AYOUT,N.Y.* MAVROMATIS,H.A.
SUM RULES INVOLVING COEFFICIENTS OF FRACTIONAL PARENTAGE.
NUCL. PHYS., A 282(1977),153-8
20.800

IKP-100977
BAUR,G.
ON THE DIRECT CAPTURE TO UNBOUND STATES.
NUCL. PHYS., A 283(1977),521-5
20.800

IKP-101077
BAUR,G. LENSKE,H.
ON THE LINE SHAPE IN INELASTIC SCATTERING LEADING TO RESONANT STATES.
NUCL. PHYS., A 282(1977),201-20
20.800

IKP-101177
BAUR,G. MADSEN,V.A. OSTERFELD,F.
MICROSCOPIC THEORY OF THE IMAGINARY INELASTIC TRANSITION FORM FACTOR.
PHYS. REV. C (IM DRUCK)
20.800

IKP-101277
BAUR,G. ROESEL,F.* TRAUTMANN,D.*
EFFECTS OF THE POLARIZABILITY IN ELASTIC SCATTERING BELOW THE COULOMB BARRIER.
NUCL. PHYS., A 288(1977),113-31
20.800

IKP-101377
BAUR,G. ROESEL,F.* TRAUTMANN,D.*
ON THE THEORY OF DIRECT REACTIONS WITH 3 PARTICLE FINAL AND INTERMEDIATE STATES.
PROCEEDINGS OF THE INTERNATIONAL SYMPOSIUM "REACTION MODELS '77". BALATONFUERED, 27.6.-1.7.1977 (IM DRUCK)
20.800

IKP-101477
BAUR,G. ROESEL,F.* TRAUTMANN,D.*
CHARGED PARTICLE TRANSFER REACTIONS INTO THE CONTINUUM: THE LINE SHAPE OF (D,N) AND (HE-003,D) SPECTRA.
J. OF PHYSICS, G (IM DRUCK)
20.800

IKP-101577
BAZ,A.I.* GLADBERG,V.Z.* GRIDNEV,K.A.* SEMJONOV,V.M.* HEFTER,E.F.
A POTENTIAL FOR THE DESCRIPTION OF ALPHA-ALPHA INTERACTIONS.
Z. PHYS., A 280(1977),171-6
20.800

IKP-101677
BAZ,A.I.* GOLDBERG,V.Z.* DARWISCH,N.Z.* GRIDNEV,K.A.* SEMJONOV,V.M.* HEFTER,E.F.
A POTENTIAL FOR ALPHA-PARTICLE-NUCLEUS SCATTERING.
LETT. NUOVO CIM. 18(1977),7,227-32
20.800

IKP-101777
BENSON,D.* KLEINHEINZ,P. SHELINE,R.K.* SHERA,E.B.*
NUCLEAR LEVELS AND SPECTROSCOPY OF OS-191.
Z. PHYS., A 281(1977),145-57

IKP-101877
BENSON,D.* KLEINHEINZ,P. SHELINE,R.K.* SHERA,E.B.*
NUCLEAR LEVELS IN OS-193.
Z. PHYS.(IM DRUCK)
20.100

IKP-101977
BERNSTEIN,A.M.* BROWN,V.R.* MADSEN,V.A.
EXPLANATION OF THE NEAR EQUALITY OF ISOSCALAR ELECTROMAGNETIC TRANSITION RATES IN NEUTRON-EXCESS NUCLEI: COMPARISON WITH DATA.
PHYS. LETT., B 71(1977),48-52
20.800

IKP-102077
BEUSCHER,H. GONO,Y. LIEDER,R.M. MUELLER-VEGGIAN,M. NESKAKIS,A. MAYER-BOERICKE,C.
EXPERIMENTAL STUDY OF HIGH-SPIN STATES IN HEAVY NUCLEI NEAR LEAD.
PROCEEDINGS OF THE 15. WINTER-SCHOOL, ZAKOPANE, 6.-19.2.1977, S. 251. (POLEN, REPORT NO. 963/PL)
20.100

IKP-102177
BOERNER,H.G. KOCH,H.R. SEYFARTH,H. SCHULT,O.W.B. HECK,D.* MAMPE,W.* SCHRECKENBACH,K.* PINSTON,J.A.* JEUCH,P.*
COLLECTIVE STATES IN U-239.
PROCEEDINGS OF THE INTERNATIONAL CONFERENCE ON NUCLEAR STRUCTURE. TOKYO, 5.-10.9.1977. VOL. 1, S. 464
20.700

IKP-102277
BORCHERT,G.L. HANSEN,P.G.* JONSON,B.* RAVN,H.L.* SCHULT,O.W.B. TIDEMAND-PETERSSON,P.*
SHIFTS IN XENON K X-RAY ENERGIES FOLLOWING ELECTRON-CAPTURE BETA DECAY AND THE ROLE OF NUCLEAR HYPERFINE STRUCTURE.
PHYS. LETT. 63A(1977),15
20.100

IKP-102377
BREUER,H.* KNOEPFLE,K.T.* PAUL,P.* WAGNER,G.J.* MAYER-BOERICKE,C. ROGGE,M. TUREK,P.
PARTICLE DECAY OF THE ISOSCALAR GIANT QUADRUPOLE RESONANCE IN O-016.
PROCEEDINGS OF THE INTERNATIONAL CONFERENCE ON NUCLEAR STRUCTURE. TOKYO, 5.-10.9.1977. VOL. 1, S. 179
20.060

IKP-102477
BROWN,B.A.* CHUNG,W. WILDENTHAL,B.H.*
GAMOW-TELLER BETA DECAY IN SD-SHELL NUCLEI.
PROCEEDINGS OF THE INTERNATIONAL CONFERENCE ON NUCLEAR STRUCTURE. TOKYO, 5.-10.9.1977. VOL. 1, S. 182
20.060

IKP-102577
BROWN,V.R.* MADSEN,V.A.
CORE POLARIZATION IN INELASTIC SCATTERING AND CHARGE EXCHANGE REACTIONS.
PHYS. REV. (IM DRUCK)
20.800

IKP-102677
BROWN,V.R.* MADSEN,V.A.
CORE POLARIZATION IN INELASTIC SCATTERING AND CHARGE EXCHANGE REACTIONS.
PROCEEDINGS OF THE INTERNATIONAL SYMPOSIUM "REACTION MODELS '77". BALATONFUERED, 27.6.-1.7.1977 (IM DRUCK)
20.800

IKP-102777
CARTER,J.* CLARKSON,R.* HNIZDO,V.* OSTERFELD,F. RICHTER,A.* SELLSCHOP,J.P.F.* TOEPFFER,C.*
EXCITATION OF NON-COLLECTIVE STATES AND SCALING PROPERTIES IN HEAVY ION SCATTERING.
PROCEEDINGS OF THE INTERNATIONAL WORKSHOP ON GROSS PROPERTIES OF NUCLEI AND NUCLEAR EXCITATIONS 5. HIRSCHEGG, 17.-22.1.1977. AED-CONF 77-017-001 - AED-CONF 77-017-043 (1977) S. 131-4
20.800

IKP-102877
CARTER,J.* CLARKSON,R.C.* HNIZDO,V.* OSTERFELD,F. RICHTER,A.* SELLSCHOP,J.P.F.
EXCITATION OF THE LOWEST 1MINUS STATE IN O-018 BY SCATTERING FROM O-016.
PROCEEDINGS OF THE INTERNATIONAL CONFERENCE ON NUCLEAR STRUCTURE. TOKYO, 5.-10.9.1977. VOL. 1, S. 188
20.800

IKP-102977
CARTER,J.* CLARKSON,R.G.* HNIZDO,V.* OSTERFELD,F. RICHTER,A.* SELLSCHOP,J.P.F.*
EXCITATION OF THE LOWEST 1MINUS STATE IN O-018 BY SCATTERING FROM O-016.
PHYS. REV. (IM DRUCK)
20.800

IKP-103077
CASTEL,B.* GOEKE,K.
NUCLEAR ISOTOPIC SHIFTS AND LINEARIZED HARTREE-FOCK.
PHYS. REV. C (IM DRUCK)
20.800

IKP-103177
CASTEN,R.F.* WARNER,D.D.* DAVIDSON,W.F.* BOERNER,H.G. NAMENSON,A.I.*
AVERAGE SHAPE OF THE OS-194 NUCLEUS FROM STUDY OF GAMMA-RAYS FOLLOWING TWOFOLD NEUTRON CAPTURE.
PROCEEDINGS OF THE INTERNATIONAL CONFERENCE ON NUCLEAR STRUCTURE. TOKYO, 5.-10.9.1977. VOL. 1, S. 440
20.700

IKP-103277
CHEN,H.T.* MUETHER,H. FAESSLER,A.
PAIRING VIBRATIONAL AND ISOSPIN ROTATIONAL STATES IN A PARTICLE NUMBER AND ISOSPIN PROJECTED GENERATOR COORDINATE METHOD.
NUCL. PHYS. (IM DRUCK)
20.800

IKP-103377
CHENG,C.M.* MAHER,J.V.* OELERT,W. SNYDER,F.D.
OPTICAL POTENTIAL FOR C-012+SI-028 SCATTERING.
PHYS. LETT.(IM DRUCK)
20.060

IKP-103477
CIZEWSKI,J.A.* CASTEN,R.F.* SMITH,G.J.* STELTS,M.L.* KANE,W.R.* BOERNER,H.G. DAVIDSON,W.F.*
EVIDENCE FOR A NEW SYMMETRY IN NUCLEI. THE STRUCTURE OF PT-196 AND THE O(6) LIMIT.
PHYS. REV. LETT. (IN DRUCK)
20.700

IKP-103577
DAEHNICK,W.W.* SPISAK,M.J.* DELVECCHIO,R.M. OELERT,W.
DIRECT POPULATION OF JP+JN EQUAL TO JMAX TWO-PARTICLE STATES IN BI-206,208,210.
PHYS. REV., C 15(1977),594
20.060

IKP-103677
DALY,P.J. DORS,C.L.* HELPPI,H.* PIIPARINEN,M.* SAHA,S. K.* KHOO,T.L.* BERNTHAL,F.M.*
HIGH-SPIN LEVEL STRUCTURE OF PT-188.
PROCEEDINGS OF THE INTERNATIONAL SYMPOSIUM ON HIGH-SPIN STATES AND NUCLEAR STRUCTURE. DRESDEN, 19.-24.9. 1977. ZFK-366 (1977) S. 50
20.100

IKP-103777
DARWISCH,N.Z.* GRIONEV,K.A.* HEFTER,E.F. SEMJONOV,V.M. *
A GLOBAL POTENTIAL FOR THE INTERACTION OF ALPHA-PARTICLES WITH LIGHT NUCLEI?
IL NUOVO CIMENTO (IM DRUCK)
20.800

IKP-103877
DAURIA,J.M.* GRUETER,J.W. HAGBERG,E.* HANSEN,P.G.* HARDY,J.C.* HORNSHOJ,P.* JONSON,B.* MATTSON,S.* RAVN,H. L.* TIDEMANN-PETERSSON,P.*
PROPERTIES OF THE LIGHTEST KNOWN CAESIUM ISOTOPES: CS-114-118.
NUCL. PHYS.(IM DRUCK)
20.600

IKP-103977
DEHESA,J.S.
FRAGMENTATION OF GIANT MULTIPOLE STRENGTH IN CLOSED-SHELL NUCLEI.
PROCEEDINGS OF THE 18TH SCOTTISH UNIVERSITIES SUMMER SCHOOL IN PHYSICS. ST. ANDREWS, 31.7.-20.8.1977 (IM DRUCK)
20.800

IKP-104077
DEHESA,J.S.
THE ASYMPTOTICAL SPECTRUM OF JACOBI MATRICES.
J. OF COMPUT. AND APPL. MATHEM. 3(1977),167-71
20.800

IKP-104177
DEHESA,J.S.
ZEROS OF ORTHOGONAL POLYNOMIALS IN BIRTH-DEATH PROCESSES.
Z. ANGEW. MATH. UND MECHANIK (IM DRUCK)
20.800

IKP-104277
DEHESA,J.S.
ASYMPTOTICAL AVERAGE PROPERTIES OF THE ZEROS OF ORTHOGONAL POLYNOMIALS AND OF THE EIGENVALUES OF JACOBI MATRICES.
UNIV. OF ZARAGOZA, DISS., OKT. 1977
20.800

IKP-104377
DEHESA,J.S.
DIRECT AND INVERSE EIGENVALUE PROBLEMS IN PHYSICS AND BIOLOGY.
PROCEEDINGS OF THE 1ST WORLD CONFERENCE OF MATHEMATICS. BARCELONA, JULI 1977 (IM DRUCK)
20.800

IKP-104477
DEHESA,J.S. KREWALD,S. SPETH,J. FAESSLER,A.
SPREADING WIDTHS OF GIANT RESONANCES IN C-012 AND O-016.
PHYS. REV., C 15(1977),5,1858-65
20.800

IKP-104577
DEHESA,J.S. SPETH,J. FAESSLER,A.
FINE STRUCTURE OF THE MAGNETIC DIPOLE STATES IN PB-208.
PHYS. REV. LETT. 38(1977),5,208-11
20.800

IKP-104677
DEHESA,J.S. SPETH,J. FAESSLER,A.
FRAGMENTATION OF THE ELECTRIC MULTIPOLE STRENGTH IN PB-208.
PROCEEDINGS OF THE INTERNATIONAL CONFERENCE ON NUCLEAR STRUCTURE. TOKYO, 5.-10.9.1977. VOL. 1, S. 453
20.800

IKP-104777
DEHESA,J.S. SPETH,J. FAESSLER,A.
FINE STRUCTURE OF THE MAGNETIC DIPOLE STATES IN PB-208.
PROCEEDINGS OF THE INTERNATIONAL CONFERENCE ON NUCLEAR STRUCTURE. TOKYO, 5.-10.9.1977. VOL. 1, S. 452
20.800

IKP-104877
DEHESA,J.S. SPETH,J. KREWALD,S. FAESSLER,A.
SPREADING WIDTH OF THE GIANT QUADRUPOLE RESONANCE IN LIGHT NUCLEI.
INTERNATIONAL SYMPOSIUM ON HIGH-SPIN STATES AND NUCLEAR STRUCTURE. DRESDEN, 19.-24.9.1977. S. 110
20.800

IKP-104977
DELION,D.S.* GRIONEV,K.A.* HEFTER,E.F. SEMJONOV,V.M.*
THE NON-LINEAR SCHROEDINGER EQUATION AND ANOMALOUS BACKWARD SCATTERING.
J. PHYS., G (IM DRUCK)
20.800

IKP-105077
DJALOEIS,A. DIDELEZ,J.P. GALONSKY,A. OELERT,W.
ELASTIC SCATTERING OF 130 MEV HE-003.
PROCEEDINGS OF THE INTERNATIONAL CONFERENCE ON NUCLEAR STRUCTURE. TOKYO, 5.-10.9.1977. VOL. 1, S. 867
20.060

IKP-105177
DJALOEIS,A. DIDELEZ,J.P. GALONSKY,A. OELERT,W.
EXCITATION OF GIANT RESONANCES BY 130 MEV HE-003.
PROCEEDINGS OF THE INTERNATIONAL CONFERENCE ON NUCLEAR STRUCTURE. TOKYO, 5.-10.9.1977. VOL. 1, S. 857
20.060

IKP-105277
DO HUU PHUOC* CHERY,R.* BOERNER,H.G. DAVIDSON,W.F.* PINSTON,J.A.* ROUSSILLE,R.* SCHRECKENBACH,K.* KOCH,H.R. SEYFARTH,H. HECK,D.*
STUDY OF THE LEVEL STRUCTURE OF BR-080 AND BR-082 USING THE THERMAL NEUTRON CAPTURE REACTION.
Z. PHYS. (IN DRUCK)
20.700

IKP-105377
DO HUU PHUOC* CHERY,R.* CHARVET,A.* DUFFAIT,R.* BOERNER,H.G. DAVIDSON,W.F.* PINSTON,J.A.* ROUSSILLE,R. * SCHRECKENBACH,K.* KOCH,H.R. SEYFARTH,H. HECK,D.*
LEVELS IN BR-080 AND BR-082 OBSERVED IN (N, GAMMA) AND (P,N) REACTIONS.
PROCEEDINGS OF THE INTERNATIONAL CONFERENCE ON NUCLEAR STRUCTURE. TOKYO, 5.-10.9.1977. VOL. 1, S. 298
20.700

IKP-105477
EBERT,K.* MEYER-TERVEHN,J.
RADIATIVE PION AND MUON CAPTURE ON PB-208.
PHYS. LETT. (IM DRUCK)
20.800

IKP-105577
EBERT,K.* MEYER-TERVEHN,J. SPETH,J. WAMBACH,J.
CALCULATIONS OF RADIATIVE PION CAPTURE ON PB-208.
PROCEEDINGS OF THE INTERNATIONAL CONFERENCE ON NUCLEAR STRUCTURE. TOKYO, 5.-10.9.1977. VOL. 1, S. 807
20.800

IKP-105677
EHRHARDT,K.
MESSUNGEN AN EINEM MODELLMAGNETEN ZUR REPRODUZIERBARKEIT VON FELDERN, FELDHOEHEN UND MATERIALUNTERSUCHUNGEN IM HINBLICK AUF IHRE MAGNETISIERBARKEIT.
JUEL-1427

IKP-105777
ELKAZZAZ,S.* LIEN,J.R.* LOVHOIDEN,G.* KLEINHEINZ,P. ELLEGAARD,C.* BJERREGAARD,J.* KNUDSEN,P.*
A STUDY OF LEVELS IN ND-141 WITH THE (D,T) AND (HE-003,ALPHA) REACTIONS.
NUCL. PHYS., A 280(1977),1-12
20.100

IKP-105877
ELMASRI,Y.* VERVIER,J.* FAESSLER,A.
THE NATURE OF THE SUPERBAND IN BACKBENDING FOR THE NUCLEUS DY-156.
NUCL. PHYS., A 279 (1977),223-36
20.800

IKP-105977
ERNST,J.* BISPLINGHOFF,J.* MAYER-KUCKUK,T.* PAMPUS,J.* RAMA-RAO,J.* BAUR,G. LENSKE,H. ROESEL,F.* TRAUTMANN,D. *
INTERPRETATION OF DEUTERON BREAK-UP AND INELASTIC SCATTERING BY PREEQUILIBRIUM AND DWBA METHODS.
PROCEEDINGS OF THE CONFERENCE ON NUCLEAR REACTION MECHANISMS. VARENNA, 13.-17.6.1977 (IN DRUCK)
20.800

IKP-106077
FABER,M.* FAESSLER,A. MUETHER,H.
CAN THE RENORMALIZATION OF THE INTERACTION DESCRIBE THE EFFECTS OF (A+2) PARTICLES 2 HOLES EXCITATIONS?
Z. PHYSIK (IM DRUCK)
20.800

IKP-106177
FABER,M.* FAESSLER,A. PLOSZAJCZAK,M. TOKI,H.
THE FISSION BARRIER OF ACTINIDE NUCLEI AT VERY HIGH ANGULAR MOMENTUM.
PHYS. LETT. 70B(1977),399-400
20.800

IKP-106277
FAESSLER,A.
THE STRANGE BEHAVIOUR OF TRANSITIONAL NUCLEI.
PRE-CONFERENCE MEETING IN THE INSTITUTE OF NUCLEAR STUDIES IN TOKIO, 3.9.1977 (IN DRUCK)
20.800

IKP-106377
FAESSLER,A.
SPINS, HIGH SPINS, VERY HIGH SPINS.
PROCEEDINGS OF THE INTERNATIONAL WORKSHOP ON GROSS PROPERTIES OF NUCLEI AND NUCLEAR EXCITATIONS 5. HIRSCHEGG, 17.-22.1.1977. AED-CONF 77-017-001 - AED-CONF 77-017-043 (1977) S. 4-7
20.800

IKP-106477
FAESSLER,A. DICKHOFF,W.H. POLANE,J.M.* RENNER,T.R.
SPINS, HIGH SPINS, VERY HIGH SPINS.
LECTURE NOTES. THE NETHERLANDS' PHYSICAL SOCIETY 1977 INTERNATIONAL SUMMER SCHOOL ON NUCLEAR SPECTROSCOPY. BREUKELEN, 159-26.8.1977. S. 1-38
20.800

IKP-106577
FAESSLER,A. KUO,T.T.S.* MUETHER,H.
VARIATIONAL DEFINITION OF THE SELFCONSISTENT POTENTIAL.
NUCL. PHYS. (IN DRUCK)
20.800

IKP-106677
FAESSLER,A. PLOSZAJCZAK,M.
DESCRIPTION OF YRAST TRAPS IN HF-176.
PHYS. REV., C 16(1977),5,2032-8
20.800

IKP-106777
FAESSLER,A. PLOSZAJCZAK,M.
ANOMALY OF THE MOMENT OF INERTIA IN ER-158 ABOVE THE BACKBENDING REGION.
PHYS. LETT. (IN DRUCK)
20.800

IKP-106877
FAESSLER,A. PLOSZAJCZAK,M. SANDHYA-DEVI,K.R.*
DO WE REALLY UNDERSTAND THE CAUSES FOR BACKBENDING?
INTERNATIONAL SYMPOSIUM ON HIGH-SPIN STATES AND NUCLEAR STRUCTURE. DRESDEN, 19.-24.9.1977. S. 68-9
20.800

IKP-106977
FAESSLER,A. PLOSZAJCZAK,M. SANDHYA-DEVI,K.R.*
CAUSE OF BACKBENDING IN THE OS REGION.
NUCL. PHYS. (IN DRUCK)
20.800

IKP-107077
*FAESSLER,A. PLOSZAJCZAK,M. SANDHYA-DEVI,R.K.* WAKAI,M.*
SPINS, HIGH SPINS, VERY HIGH SPINS.
PROCEEDINGS OF THE INTERNATIONAL CONFERENCE ON NUCLEAR STRUCTURE. TOKYO, 5.-10.9.1977. VOL. 2 (IN DRUCK)
20.800

IKP-107177
FAESSLER,A. PLOSZAJCZAK,M. TOKI,H. WAKAI,M.
SPINS, HIGH SPINS, VERY HIGH SPINS.
PROCEEDINGS OF THE INTERNATIONAL CONFERENCE ON NUCLEAR STRUCTURE. TOKYO, 5.-10.9.1977. VOL. 1, S. 109
20.800

IKP-107277
FAESSLER,A. SANDHYA-DEVI,K.R.* BARROSO,A.*
INFLUENCE OF PROTONS ON BACKBENDING.
NUCL. PHYS., A 286(1977),101-4
20.800

IKP-107377
*FAESSLER,A. WAKAI,M.*
INFLUENCE OF QUADRUPOLE PAIRING ON BACKBENDING.
INTERNATIONAL SYMPOSIUM ON HIGH-SPIN STATES AND NUCLEAR STRUCTURE. DRESDEN, 19.-24.9.1977. S. 70-1
20.800

IKP-107477
GALONSKY,A. DIDELEZ,J.P. DJALOEIS,A. OELERT,W.
OBSERVATION OF THE GIANT GAMOW-TELLER RESONANCE IN THE (HE-003,T) REACTION AT 130 MEV.
PROCEEDINGS OF THE INTERNATIONAL CONFERENCE ON NUCLEAR STRUCTURE. TOKYO, 5.-10.9.1977. VOL. 1, S. 317
20.060

IKP-107577
GELLETLY,W.* DAVIDSON,W.F.* SIMIC,J.* BOERNER,H.G.
DIGGORY,A.F.* MAMPE,W.* SCHRECKENBACH,K.* WARNER,D.*
INTRABAND TRANSITION RATES IN THE GAMMA VIBRATIONAL BANDS OF DY-162 AND GR-168.
J. PHYS., G (IN DRUCK)
20.700

IKP-107677
GELLETLY,W.* DAVIDSON,W.F.* SIMIC,J.* BOERNER,H.G.
SCHRECKENBACH,K.* WARNER,D.D.* DIGGORY,A.F.* MAMPE,W.*
GAMMA BAND INTRABAND TRANSITIONS IN ER-168 AND DY-162.
PROCEEDINGS OF THE INTERNATIONAL CONFERENCE ON NUCLEAR STRUCTURE. TOKYO, 5.-10.9.1977. VOL. 1, S. 405
20.700

IKP-107777
GIZON,J.* GIZON,A.* MEYER-TERVEHN,J.
TRIAXIAL SHAPE AND ONSET OF HIGH-SPIN BANDS IN BA-129.
NUCL. PHYS., A 277(1977),464 76
20.800

IKP-107877
GOEKE,K.
COLLECTIVE MASSES BY TIME-DEPENDENT HARTREE-FOCK: APPLICATION TO MONOPOLE VIBRATIONS.
*PHYS. REV. LETT.* 38(1977),5,212-5
20.800

IKP-107977
GOEKE,K.
THE ADIABATIC TIME DEPENDENT HARTREE-FOCK THEORY.
PROCEEDINGS OF THE INTERNATIONAL SYMPOSIUM ON NUCLEAR COLLISIONS AND THEIR MICROSCOPIC DESCRIPTION. BLED, 26. 9.-1.10.1977. FIZIKA 9, SUPPL. 1 (1977) (IN DRUCK)
20.800

IKP-108077
GOEKE,K.
ON THE RELATION BETWEEN ATDHF AND GCM.
PROCEEDINGS OF THE INTERNATIONAL SYMPOSIUM ON NUCLEAR COLLISIONS AND THEIR MICROSCOPIC DESCRIPTION. BLED, 26. 9.-1.10.1977. FIZIKA 9, SUPP. 1 (1977) (IN DRUCK)
20.800

IKP-108177
GOEKE,K.
DETERMINATION OF THE COLLECTIVE PATH IN THE ADIABATIC TIME DEPENDENT HARTREE-FOCK THEORY.
PROCEEDINGS OF THE INTERNATIONAL SYMPOSIUM ON NUCLEAR COLLISIONS AND THEIR MICROSCOPIC DESCRIPTION. BLED, 26. 9.-1.10.1977. FIZIKA 9, SUPPL. 2(1977),S. 41
20.800

IKP-108277
GOEKE,K.
THE UNIQUE QUANTIZATION OF CLASSICAL HAMILTONIANS IN THE ATDHF-THEORY.
PROCEEDINGS OF THE INTERNATIONAL SYMPOSIUM ON NUCLEAR COLLISIONS AND THEIR MICROSCOPIC DESCRIPTION. BLED, 26. 9.-1.10.1977. FIZIKA 9, SUPPL. 2 (1977) S. 44
20.800

IKP-108377
GOEKE,K.
DIE ZEITABHAENGIGE HARTREE-FOCK-THEORIE FUER KOLLEKTIVE KERNBEWEGUNGEN.
JUEL-1361
20.800

IKP-108477
GOEKE,K. CASTEL,B.*
GIANT MONOPOLE RESONANCE PARAMETERS IN THE ATDHF FORMALISM.
PHYS. REV. (IN DRUCK)
20.800

IKP-108577
GOEKE,K. LANE,A.M.* MARTORELL,J.*
EXPOSURE OF RELATIONS BETWEEN COLLECTIVE THEORIES THROUGH THEIR ENERGY-WEIGHTED MOMENTS.
NUCL. PHYS. (IN DRUCK)
20.800

IKP-108677
GOEKE,K. LANE,A.M.* MARTORELL,J.*
*A UNIFYING VIEW OF COLLECTIVE THEORIES.*
PROCEEDINGS OF THE INTERNATIONAL CONFERENCE ON NUCLEAR STRUCTURE. TOKYO, 5.-10.9.1977. VOL. 1, S. 118
20.800

IKP-108777
GOEKE,K. REINHARD,P.G.*
A CONSISTENT MICROSCOPIC THEORY OF COLLECTIVE MOTION IN THE FRAMEWORK OF AN ATDHF APPROACH.
ANN. PHYS. (IN DRUCK)
20.800

IKP-108877
GOEKE,K. REINHARD,P.G.*
THE COLLECTIVE PATH IN THE ADIABATIC TIME DEPENDENT HF THEORY.
PROCEEDINGS OF THE INTERNATIONAL CONFERENCE ON NUCLEAR STRUCTURE. TOKYO, 5.-10.9.1977. VOL. 1, S. 116
20.800

*IKP-108977*
GONO,Y. HAENNI,D.R. BEUSCHER,H. LIEDER,R.M. MUELLER-VEGGIAN,M. MAYER-BOERICKE,C.
SIDE BANDS IN HF-172.
PROCEEDINGS OF THE INTERNATIONAL CONFERENCE ON NUCLEAR STRUCTURE. CONTRIBUTED PAPERS. TOKYO, 5.-10.9.1977, S. 866
20.100

IKP-109077
GONO,Y. LIEDER,R.M. MUELLER-VEGGIAN,M. NESKAKIS,A. MAYER-BOERICKE,C.
PARTICLE-HOLE SYMMETRY OBSERVED IN THE ANGULAR DISTRIBUTIONS OF GAMMA-RAYS IN AU-189,191,193.
PHYS. LETT., B 70(1977),2,159-62
20.100

IKP-109177
GONO,Y. LIEDER,R.M. MUELLER-VEGGIAN,M. NESKAKIS,A. BEUSCHER,H. MAYER-BOERICKE,C.
*HIGH SPIN STATES OF ODD-MASS AU, HG AND TL NUCLEI.*
PROCEEDINGS OF THE INTERNATIONAL WORKSHOP ON GROSS PROPERTIES OF NUCLEI AND NUCLEAR EXCITATIONS 5. HIRSCHEGG, 17.-22.1.1977. AED-CONF 77-017-001 - AED-CONF 77-017-043 (1977),S. 8-10
20.100

IKP-109277
GREENWOOD,R.C.* REICH,C.W.* BAADER,H.A.* KOCH,H.R. BRETTIG,D.* SCHULT,O.W.B. FOGELBERG,B.* BAECKLIN,A.* MAMPE,W.* EGIDY,T. VON* SCHRECKENBACH,K.*
COLLECTIVE AND TWO-QUASIPARTICLE STATES IN GD-158 OBSERVED THROUGH STUDY OF RADIATIVE NEUTRON CAPTURE IN GD-157.
NUCL. PHYS., A (IN DRUCK)
20.700

IKP-109377
GRIDNEV,K.A.* DARWISCH,N.Z.* SEMJONOV,B.M.* HEFTER,E.F.
O POTENZIALJE VZAIMODEYSTVIYA ALPHA-TSCHASTIZ S *LOCHKAMI YADRAMI.*
IZV. AKAD. NAUK SSSR, SER. FIS. (IN DRUCK)
20.800

IKP-109477
GRIDNEV,K.A.* DORU,D.* SEMJONOV,V.M.* HEFTER,E.F.
NELINEJNOE URAVNENIE SCHROEDINGERA N.ANOMAL'NOE RAEUYANIE NAS'AD.
IZV. AKAD. NAUK SSSR, SER. FIS. (IN DRUCK)
20.800

IKP-109577
GRIDNEV,K.A.* SEMJONOV,V.M.* HEFTER,E.F.
ANALIS REKZII SRIVA (D,P).
IZV. AKAD. NAUK SSSR, SER. FIS. (IN DRUCK)
20.800

IKP-109677
HAENNI,D.R. GONO,Y. ZOLNOWSKI,D.R.* SUGIHARA,T.T.*
SIDE BANDS IN HF-172.
PROCEEDINGS OF THE INTERNATIONAL CONFERENCE ON NUCLEAR STRUCTURE. TOKYO, 5.-10.9.1977. VOL. 1, S. 413
20.100

IKP-109777
HAENNI,D.R. SUGIHARA,T.T.*
VIBRATIONAL LEVELS IN THE 86-NEUTRON NUCLEUS GD-150.
PHYS. REV., C 16(1977),1129
20.100

IKP-109877
HAENNI,D.R. SUGIHARA,T.T.*
NEGATIVE-PARITY YRAST STATES IN GD-150.
PHYS. REV., C 16(1977),120
20.100

IKP-109977
HAGMANN,S.* ARMBRUSTER,P.* FOLKMANN,F.* KRAFT,G.*
MOKLER,P.* STEIN,H.J.
MEASUREMENT OF THE AVERAGE L IONIZATION PROBABILITY OF GOLD IN 25 MEV IODINEGOLD COLLISIONS.
PHYS. LETT. 61A(1977),451-3
20.600

IKP-110077
HANSEN,P.G.* BORCHERT,G.L. JONSON,B.* RAVN,H.L.*
TIDEMAND PETERSSON,P.* SCHULT,O.W.B.
HYPERFINE SHIFTS OF XE K X-RAY ENERGIES FOLLOWING ELECTRON CAPTURE.
PROCEEDINGS OF THE INTERNATIONAL CONFERENCE ON NUCLEAR STRUCTURE. VOL. 1. TOKYO, 5.-10.9.1977. S. 858
20.100

IKP-110177
HARDT,A. BISPLINGHOFF,J.* ERNST,J.* LOHR,R.* MACHNER,H.
MAYER-KUCKUK,T.*
ON-LINE APPARATUS BANDIT FOR HALF-LIFE DETERMINATION OF SHORT LIVED NEUTRON DEFICIENT ISOTOPES.
NUCL. INSTRUM. METHODS 143(1977),519
20.060

IKP-110277
HEFTER,E.F.
DIREKTE UND MEHRSTUFENPROZESSE IN UNELASTISCHER PROTONENSTREUUNG.
JUEL-1395
20.800

*IKP-110377*
HEFTER,E.F. BOSCHITZ,E.T.* HEIDT,V.* WEDDIGEN,C.*
THE CONVENTIONAL DWBA AND THE IMPULSE APPROXIMATION FOR N-014(D,P0)N-015 AT ED EQUAL TO 52 MEV.
NUCL. PHYS., A 275(1977),212-28
20.800

IKP-110477
HEFTER,E.F. GERAMB,H.V.* OSTERFELD,F. UDAGAWA,T.
TWO-STEP PROCESSES IN INELASTIC PROTON SCATTERING.
Z. PHYSIK (IM DRUCK)
20.800

IKP-110577
HEYDE,K.* SAU,J.* CHERY,R.* SCHUSSLER,F.* BLACHOT,J.*
BOCQUET,J.P.* MONNAND,E.* SISTEMICH,K.
HEAVY ODD-MASS SB-127-133 ISOTOPES.
PHYS. REV., C 16(1977),6,2437-41
20.650

IKP-110677
HOFF,R.W.* DAVIDSON,W.F.* WARNER,D.D.* SCHRECKENBACH,K.
* BOERNER,H. DIGGORY,A.F.* EGIDY,T. VON*
EXCITED LEVELS IN CM-249 FROM NEUTRON CAPTURE GAMMA-RAY MEASUREMENTS.
PROCEEDINGS OF THE INTERNATIONAL CONFERENCE ON NUCLEAR STRUCTURE. TOKYO, 5.-10.9.1977. VOL. 1, S. 465
20.700

IKP-110777
HOLINDE,K.* MACHLEIDT,R.* FAESSLER,A. MUETHER,H.
INFLUENCE OF THE DELTA RESONANCE ON GROUND-STATE PROPERTIES OF NUCLEI.
PHYS. REV., C 15(1977),4,1432-9
20.800

IKP-110877
IWASAKI,M.* SANO,M.* WAKAI,M.
MOMENTS OF INERTIA OF ROTATIONAL STATES IN THE GROUND AND BETAVIBRATIONAL BANDS.
PROCEEDINGS OF THE INTERNATIONAL CONFERENCE ON NUCLEAR STRUCTURE. TOKYO, 5.-10.9.1977. VOL. 1, S. 105
20.800

IKP-110977
KEMNITZ,P.* ODENAU,F.* FUNKE,L.* STRUSNY,H.* VENOS,D.*
WILL,E.* WINTER,G.* MEYER-TERVEHN,J.
INVESTIGATION OF THE I13/2 EXCITATION IN HG-197.
PROCEEDINGS OF THE INTERNATIONAL SYMPOSIUM ON HIGH-SPIN STATES AND NUCLEAR STRUCTURE. DRESDEN, 19.-24.9.1977. ZFK-336 (1977). S. 56-7
20.800

IKP-111077
KHAN,T.A.
LIFETIME OF THE LOWEST LYING 0+ STATE IN ZR-100.
BULL. AM. PHYS. SOC.(IM DRUCK)
20.650

IKP-111177
KHAN,T.A.
NUCLEAR STRUCTURE STUDIES AT JOSEF.
PROCEEDINGS OF THE AMES-BNL-WORKSHOP ON ISOL-SYSTEMS. UPTON, N.Y., 31.10.-1.11.1977(IM DRUCK)
20.650

IKP-111277
KHAN,T.A. LAUPPE,W.D. SISTEMICH,K. LAWIN,H. SELIC,H.A.
LIFETIME OF THE 331.3 KEV 02+ STATE IN ZR-100.
Z. PHYS., A 284(1978),313-7
20.650

IKP-111377
KHAN,T.A. LAUPPE,W.D. SISTEMICH,K. LAWIN,H. SADLER,G.*
SELIC,H.A.
THE BETA-DECAY OF Y-100: DISCOVERY OF A VERY LOW LYING 0+ STATE IN ZR-100.
Z. PHYS., A 283(1977),105-20
20.650

IKP-111477
KLEINHEINZ,P. LUNARDI,S. OGAWA,M. MAIER,M.R.*
THE 3- STATE IN THE DOUBLY CLOSED SHELL NUCLEUS GD-146.
Z. PHYS.(IM DRUCK)
20.100

IKP-111577
KLEINHEINZ,P. LUNARDI,S. OGAWA,M. MAIER,M.R.*
THE 3- STATE IN THE DOUBLY CLOSED SHELL NUCLEUS GD-146.
PROCEEDINGS OF THE INTERNATIONAL CONFERENCE ON NUCLEAR STRUCTURE. CONTRIBUTED PAPERS. VOL. 1. TOKYO, 5.-10.9.1977. S. 864
20.100

IKP-111677
KLEINHEINZ,P. LUNARDI,S. OGAWA,S. MAIER,M.R.*
THE 3- STATE IN THE DOUBLY CLOSED SHELL NUCLEUS GD-146.
PROCEEDINGS OF THE INTERNATIONAL SYMPOSIUM ON HIGH-SPIN STATES AND NUCLEAR STRUCTURE. DRESDEN, 19.-24.9.1977. ZFK-336 (1977), S. 25
20.100

IKP-111777
KLEINHEINZ,P. MAIER,M.R.* LUNARDI,S. OGAWA,M. BRODA,R.
ISOMERS IN THE N EQUAL TO 83 NUCLEUS GD-147.
PROCEEDINGS OF THE INTERNATIONAL CONFERENCE ON NUCLEAR STRUCTURE. CONTRIBUTED PAPERS. TOKYO, 5.-10.9.1977. VOL. 1, S. 865
20.100

IKP-111877
KLEINHEINZ,P. MAIER,M.R.* LUNARDI,S. OGAWA,M. BRODA,R.
ISOMERS IN THE N EQUAL TO 83 NUCLEUS GD-147.
PROCEEDINGS OF THE INTERNATIONAL SYMPOSIUM ON HIGH-SPIN STATES AND NUCLEAR STRUCTURE. DRESDEN, 19.-24.9.1977. ZFK-336 (1977), S. 26
20.100

IKP-111977
KLEINHEINZ,P. OGAWA,M. BRODA,R. DALY,P.J. HAENNI,D.
BEUSCHER,H. KLEINRAHM,A.*
PROPERTIES OF THE 3- FIRST EXCITED STATE IN THE DOUBLY CLOSED SHELL NUCLEUS GD-146.
*PHYS. LETT., B(IM DRUCK)*
20.100

IKP-112077
KLEINHEINZ,P. STEFANINI,A.M.* MAIER,M.R.* SHELINE,R.K.
* DIAMOND,R.M.* STEPHENS,F.S.*
DIFFERENT STRUCTURE COLLECTIVE BANDS IN THE N EQUAL TO 87 NUCLEI SM-149, GD-151 AND DY-153.
NUCL. PHYS., A 283(1977),189-22
20.100

IKP-112177
KLEMT,V. KREWALD,S. SPETH,J. WAMBACH,J.
HIGH-LYING GIANT M1 RESONANCES.
PROCEEDINGS OF THE INTERNATIONAL CONFERENCE ON NUCLEAR STRUCTURE. TOKYO, 5.-10.9.1977. VOL. 1, S. 457
20.800

IKP-112277
KREWALD,S. KLEMT,V. SPETH,J. FAESSLER,A.
ON THE USE OF SKYRME FORCES IN SELF-CONSISTENT RPA CALCULATIONS.
NUCL. PHYS., A 281 (1977),166-206
20.800

IKP-112377
LAUPPE,W.D. KHAN,T.A. SADLER,G.* SELIC,H.A.
SISTEMICH,K. TENTEN,W.*
STUDIES OF NEUTRON-RICH NUCLEI USING SPECIAL FEATURES OF THE GASFILLED SEPARATOR JOSEF.
PROCEEDINGS OF THE 5TH INTERNATIONAL WORKSHOP ON GROSS PROPERTIES OF NUCLEI AND NUCLEAR EXCITATIONS. HIRSCHEGG, 17.-22.1.1977. AED-CONF 77-017-001. S. 226-30
20.650

IKP-112477
LAUPPE,W.D. SISTEMICH,K. KHAN,T.A. LAWIN,H. SADLER,G.*
SELIC,H.A. SCHULT,O.W.B.
THE LEVEL SCHEME OF THE DOUBLY MAGIC NUCLEUS SN-132.
PROCEEDINGS OF THE INTERNATIONAL CONFERENCE ON NUCLEAR STRUCTURE. INVITED PAPERS. TOKYO, 5.-10.9.1977(IM DRUCK)
20.650

IKP-112577
LIEDER,R.M. GONO,Y. MUELLER-VEGGIAN,M. NESKAKIS,A.
BEUSCHER,H. MAYER-BOERICKE,C.
HIGH-SPIN STATES IN HEAVY TRANSITIONAL NUCLEI AROUND HG.
INTERNATIONAL SYMPOSIUM ON HIGH-SPIN STATES AND NUCLEAR STRUCTURE. DRESDEN, 19.-24.9.1977. S. 54-5
20.100

IKP-112677
LIEDER,R.M. NESKAKIS,A. MUELLER-VEGGIAN,M. GONO,Y.
MAYER-BOERICKE,C. BESHAI,S.* FRANSSON,K.* LINDEN,C.G.*
LINDBLAD,T.*
ROTATIONAL BANDS IN TL-195,197.
EINGEREICHT ZUR VEROEFFENTLICHUNG BEI NUCLEAR PHYSICS
20.100

IKP-112777
LIEDER,R.M. NESKAKIS,A. MUELLER-VEGGIAN,M. GONO,Y.
MAYER-BOERICKE,C. BESHAI,S.* FRANSSON,K. LINDEN,C.G.*
LINDBLAD,T.*
POSITIVE-PARITY BANDS IN TL-195,197.
PROCEEDINGS OF THE INTERNATIONAL CONFERENCE ON NUCLEAR STRUCTURE. CONTRIBUTED PAPERS. TOKYO, 5.-10.9.1977, S. 441
20.100

IKP-112877
LOVAS,I.* ROGGE,M. SCHWINN,U.* TUREK,P. INGHAM,D.*
MAYER-BOERICKE,C.
GIANT RESONANCE EFFECTS IN THE ANGULAR DISTRIBUTIONS OF INELASTIC PROTON SCATTERING ON MG-024.
NUCL. PHYS., A 286(1977),12-30
20.060

IKP-112977
LUNARDI,S. OGAWA,M. MAIER,M.R.* KLEINHEINZ,P.
HIGH-SPIN STATES AND THE 17 NS ISOMER IN THE N EQUAL TO 84 NUCLEUS GD-148.
INTERNATIONAL SYMPOSIUM ON HIGH-SPIN STATES AND NUCLEAR STRUCTURE. DRESDEN, 19.-24.9.1977. S. 27
20.100

IKP-113077
LUNARDI,S. OGAWA,M. MAIER,M.R.* KLEINHEINZ,P.
HIGH-SPIN STATES IN THE N EQUAL TO 84 NUCLEUS DY-150.
INTERNATIONAL SYMPOSIUM ON HIGH-SPIN STATES AND NUCLEAR STRUCTURE. DRESDEN, 19.-24.9.1977. S. 28
20.100

IKP-113177
MADSEN,V.A. BAUR,G. OSTERFELD,F.
THE IMAGINARY PART OF THE INELASTIC SCATTERING INTERACTION.
PROCEEDINGS OF THE CONFERENCE ON NUCLEAR REACTION MECHANISMS. VARENNA, 13.-17.6.1977 (IM DRUCK)
20.800

IKP-113277
MADSEN,V.A. OSTERFELD,F. BAUR,G.
MICROSCOPIC THEORY OF THE IMAGINARY INELASTIC SCATTERING FACTOR.
PROCEEDINGS OF THE INTERNATIONAL SYMPOSIUM "REACTION MODELS '77". BALATONFUERED, 27.6.-1.7.1977 (IM DRUCK)
20.800

IKP-113377
MARISCOTTI,M.A.M.* BEUSCHER,H. DAVIDSON,W.F. GONO,Y. JAEGER,H.M. LIEDER,R.M. MUELLER-VEGGIAN,M. NESKAKIS,A. ZOLNOWSKI,D.R.*
IN BEAM STUDY OF GD-144.
PROCEEDINGS OF THE INTERNATIONAL CONFERENCE ON NUCLEAR STRUCTURE. TOKYO, 5.-10.9.1977. VOL. 1, S. 863
20.100

IKP-113477
MAVROMATIS,H.A.
A STUDY OF THE GROUND STATE ENERGY OF CA-040.
NUCL. PHYS. (IM DRUCK)
20.800

IKP-113577
MAVROMATIS,H.A. MUETHER,H. FAESSLER,A.
RENORMALIZED SHELL MODEL MATRIX ELEMENTS DERIVED FROM NUCLEON-NUCLEON PHASE SHIFTS.
Z. PHYS., A 284(1978),195-202
20.800

IKP-113677
MAVROMATIS,H.A. SKOURAS,L.D.* DEDES,C.*
EFFECTIVE THREE-BODY INTERACTION IN TC-093, MO-093, AND RU-094.
PHYS. REV., C 16(1977),895-8
20.800

IKP-113777
MAYER-BOERICKE,C.
EXPERIMENTAL INVESTIGATIONS OF GIANT RESONANCES IN LIGHT NUCLEI.
JUEL-1436
20.060

IKP-113877
MAYER-BOERICKE,C.
EVIDENCE FOR NEW HIGHER MULTIPOLE GIANT RESONANCES IN LIGHT NUCLEI.
PROCEEDINGS OF THE RCNP SYMPOSIUM ON HIGHLY EXCITED STATES AND POLARIZATION PHENOMENA. OSAKA, 14.-16.9.1977. S. 38
20.060

IKP-113977
MAYER-BOERICKE,C.
EXPERIMENTAL INVESTIGATIONS OF GIANT RESONANCES MAINLY BY ALPHA-SCATTERING: MACROSCOPIC AND MICROSCOPIC ASPECTS.
PROCEEDINGS OF THE INTERNATIONAL SYMPOSIUM "REACTION MODELS '77". BALATONFUERED, 27.6.-1.7.1977 (IM DRUCK)
20.060

IKP-114077
MAYER-BOERICKE,C.
MULTIPOLE GIANT RESONANCES IN LIGHT NUCLEI.
PROCEEDINGS OF THE 10TH SUMMER SCHOOL ON NUCLEAR PHYSICS "STUDY OF NUCLEAR STRUCTURE BY MEANS OF NUCLEAR REACTIONS". MIKOLAJKI, 30.8.-11.9.1977.
NUKLEONIKA 1977
20.060

IKP-114177
MAYER-BOERICKE,C.
INVESTIGATION OF NEW MULTIPOLE GIANT RESONANCES IN LIGHT NUCLEI BY INELASTIC HADRONIC SCATTERING AND COMPARISON WITH CAPTURE REACTION RESULTS.
PROCEEDINGS OF THE CONFERENCE ON ELECTRO AND PHOTOEXCITATION. SENDAI, 12.-13.9.1977; SUPPL. OF THE RESEARCH REPORT OF THE LABORATORY OF NUCLEAR SCIENCE, TOHOKU UNIV. 1977
20.060

IKP-114277
MAYER-BOERICKE,C. OELERT,W. KISS,A. ROGGE,M. TUREK,P. WIKTOR,S.
OCTUPOLE-STRENGTH CONCENTRATION OBSERVED IN ALPHA-SCATTERING ON AL-027.
NUCL. PHYS., A (IM DRUCK)
20.060

IKP-114377
MAYER-BOERICKE,C. OELERT,W. KISS,A. ROGGE,M. TUREK,P. WIKTOR,S.
OCTUPOLE-STRENGTH CONCENTRATION OBSERVED IN ALPHA-SCATTERING ON AL-027.
PROCEEDINGS OF THE INTERNATIONAL CONFERENCE ON NUCLEAR STRUCTURE. TOKYO, 5.-10.9.1977. VOL. 1, S. 211
20.060

IKP-114477
MAYER-BOERICKE,C. REICH,J.
JULIC GROSSES ISOCHRONZYKLOTRON AM INSTITUT FUER KERNPHYSIK.
KFA INTERN (1977),1,4
20.300

IKP-114577
MEYER-TERVEHN,J.
NO PION CONDENSATION IN NORMAL NUCLEI.
PROCEEDINGS OF THE 7TH INTERNATIONAL CONFERENCE ON HIGH ENERGY PHYSICS AND NUCLEAR STRUCTURE. ZUERICH, 29.8.-2.9.1977. ABSTRACT VOL., S. 173
20.800

IKP-114677
MEYER-TERVEHN,J.
TRANSITIONAL NUCLEI AND TRIAXIAL SHAPES.
J. PHYS. (IM DRUCK)
20.800

IKP-114777
MEYER-TERVEHN,J.
ON PION CONDENSATION IN FINITE NUCLEI.
Z. PHYS. (IM DRUCK)
20.800

IKP-114877
MEYER-TERVEHN,J.
ON PION CONDENSATION IN FINITE NUCLEI.
PROCEEDINGS OF THE INTERNATIONAL WORKSHOP ON GROSS PROPERTIES OF NUCLEI AND NUCLEAR EXCITATIONS 5. HIRSCHEGG, 17.-22.1.1977. AED-CONF 77-017-001 - AED-CONF 77-017-043 (1977) S. 77-82
20.800

IKP-114977
MORSCH,H.P.
MICROSCOPIC STUDY OF INELASTIC HEAVY ION SCATTERING.
PROCEEDINGS OF THE INTERNATIONAL WORKSHOP ON GROSS PROPERTIES OF NUCLEI AND NUCLEAR EXCITATIONS 5. HIRSCHEGG, 17.-22.1.1977. AED-CONF 77-017-001 - AED-CONF 77-017-043 (1977), S. 135-9
20.060

IKP-115077
MUELLER-VEGGIAN,M. BEUSCHER,H. GONO,Y. HAENNI,D. LIEDER,R.M. NESKAKIS,A. MAYER-BOERICKE,C.
HIGH-SPIN STATES AND ISOMERS IN LIGHT TRANSITIONAL NUCLEI AROUND N EQUAL TO 80.
INTERNATIONAL SYMPOSIUM ON HIGH-SPIN STATES AND NUCLEAR STRUCTURE. DRESDEN, 19.-24.9.1977. S. 19-20
20.100

IKP-115177
MUELLER-VEGGIAN,M. BEUSCHER,H. GONO,Y. HAENNI,D. LIEDER,R.M. NESKAKIS,A. MAYER-BOERICKE,C.
ISOMERIC 10+ STATES IN NUCLEI WITH N EQUAL TO 78.
PROCEEDINGS OF THE INTERNATIONAL CONFERENCE ON NUCLEAR STRUCTURE. TOKYO, 5.-10.9.1977. VOL. 1, S. 861
20.100

IKP-115277
MUELLER-VEGGIAN,M. GONO,Y. LIEDER,R.M. NESKAKIS,A. MAYER-BOERICKE,C.
LEVEL STRUCTURE IN THE LIGHT TRANSITIONAL NUCLEI CE-136,137,138.
PROCEEDINGS OF THE INTERNATIONAL CONFERENCE ON NUCLEAR STRUCTURE. TOKYO, 5.-10.9.1977. VOL. 1, S. 862
20.100

IKP-115377
MUETHER,H. GOEKE,K. ALLAART,K.* FAESSLER,A.
SINGLE-PARTICLE DEGREES OF FREEDOM AND THE GENERATOR-COORDINATE METHOD.
PHYS. REV., C 15(1977),15,1467-76
20.800

IKP-115477
MUETHER,H. WAGHMARE,Y.R.* FAESSLER,A.
BRUECKNER RANDOM PHASE APPROXIMATION, A MICROSCOPIC DESCRIPTION OF PARTICLE-HOLE STATES.
NUCL. PHYS. (IM DRUCK)
20.800

IKP-115577
NEERGARD,K.* TOKI,H. PLOSZAJCZAK,M. FAESSLER,A.
VERY HIGH SPIN STRUTINSKY CALCULATIONS WITH A WOODS-SAXON POTENTIAL.
NUCL. PHYS., A 287(1977),48-76
20.800

IKP-115677
NEERGARD,K.* TOKI,H. PLOSZAJCZAK,M. FAESSLER,A.
NOTE ON VERY HIGH SPIN STRUTINSKY CALCULATIONS.
PROCEEDINGS OF THE 15. WINTER SCHOOL ON NUCLEAR PHYSICS "SELECTED TOPICS IN NUCLEAR STRUCTURE". ZAKOPANE, 6.-19.2.1977. S. 197
20.800

IKP-115777
OELERT,W. OJALOEIS,A. MAYER-BOERICKE,C. TUREK,P. WIKTOR,S.
INVESTIGATION OF THE (D,LI-006) REACTION ON O-016 AT ED EQUAL TO 80 MEV.
ZUR VEROEFFENTLICHUNG EINGEREICHT.
20.060

IKP-115877
OELERT,W. DJALOEIS,A. MAYER-BOERICKE,C. TUREK,P. WIKTOR,S.
O-016(D,LI-006)C-012 INVESTIGATION AT ED EQUAL TO 80 MEV.
PROCEEDINGS OF THE INTERNATIONAL CONFERENCE ON NUCLEAR STRUCTURE. CONTRIBUTED PAPERS. TOKYO, 5.-10.9.1977. S. 868
20.060

IKP-115977
OELERT,W. MAYER-BOERICKE,C. DJALOEIS,A. KISS,A. ROGGE,M. TUREK,P. WIKTOR,S.
STRENGTH CONCENTRATION OBSERVED IN (ALPHA,ALPHA') AND (D,LI-006) REACTIONS AT EX CIRCA 32/A 1/3 MEV.
PROCEEDINGS OF THE 4. E.P.S. NUCLEAR PHYSICS DIVISIONAL CONFERENCE "PHYSICS OF MEDIUM-LIGHT NUCLEI" TOPICAL CONFERENCE. CONTRIBUTIONS. FLORENCE, 7.-10.6. 1977. S. 75
20.060

IKP-116077
OGAWA,M. ARAI,E.*
RECOIL-DISTANCE LIFETIME MEASUREMENTS IN NE-022, NA-022 AND AL-027.
J. PHYS. SOC. JAP. 42(1977),2,376-81
20.100

IKP-116177
OGAWA,M. KLEINHEINZ,P. LUNARDI,S. FENZL,M.* SCHULT,O.W.B.
MULTIPLICITY MEASUREMENTS IN THE PRE-COMPOUND REGION.
PROCEEDINGS OF THE RCNP SYMPOSIUM ON HIGHLY EXCITED STATES AND POLARIZATION PHENOMENA. OSAKA, 14.-16.9. 1977. S. 29
20.100

IKP-116277
OGAWA,M. KLEINHEINZ,P. LUNARDI,S. SCHULT,O.W.B. FENZL,M.*
GAMMA-RAY MULTIPLICITIES IN ALPHA-INDUCED COMPOUND AND PRECOMPOUND REACTIONS.
Z. PHYS.(IM DRUCK)
20.100

IKP-116377
OGAWA,M. LUNARDI,S. MAIER,M.R.* KLEINHEINZ,P.
ENERGY LEVELS IN TB-149 POPULATED IN THE (ALPHA, 6N) REACTION.
INTERNATIONAL SYMPOSIUM ON HIGH-SPIN STATES AND NUCLEAR STRUCTURE. DRESDEN, 19.-24.9.1977. S. 31
20.100

IKP-116477
OSTERFELD,F. HNIZDO,V.* TOEPFFER,C.*
IS THE DIFFERENCE BETWEEN C-012-NE-020 AND O-016-O-016 SCATTERING DUE TO ENTRANCE CHANNEL EFFECTS?
PHYS. LETT., B 68(1977),319-22
20.800

IKP-116577
OSTERFELD,F. HNIZDO,V.* TOEPFFER,C.*
IS THE DIFFERENCE BETWEEN C-012-NE-020 AND O-016-O-016 SCATTERING DUE TO ENTRANCE CHANNEL EFFECTS?
PROCEEDINGS OF THE INTERNATIONAL SYMPOSIUM "REACTION MODELS '77", BALATONFUERED, 27.6.-1.7.1977 (IM DRUCK)
20.800

IKP-116677
OSTERFELD,F. UDAGAWA,T.* WOLTER,H.H.*
EFFECTS OF NONORTHOGONALITY CORRECTIONS IN TWO-STEP PROCESSES IN (TAU,T) REACTIONS.
NUCL. PHYS., A 278(1977),1-15
20.800

IKP-116777
PAAR,V.* MATHEWS,G.* DICKHOFF,W.
VIBRATION COUPLING.
LECTURE NOTES. THE NETHERLANDS' PHYSICAL SOCIETY 1977 INTERNATIONAL SUMMER SCHOOL ON NUCLEAR SPECTROSCOPY. BREUKELEN, 15.-26.8.1977. S. 138-49
20.800

IKP-116877
PAMPUS,J.* ERNST,J.* MAYER-KUCKUK,T.* RAMA-RAO,J.* BAUR,G. ROESEL,F.* TRAUTMANN,D.*
EXCLUSIVE AND INCLUSIVE CONTRIBUTIONS TO DEUTERON BREAK UP.
PROCEEDINGS OF THE INTERNATIONAL CONFERENCE ON NUCLEAR STRUCTURE. TOKYO, 5.-10.9.1977. VOL. 1, S. 517
20.800

IKP-116977
PERRIN,G.* LEBRUN,D.* CHAUVIN,J.* MARTIN,P.* DESANTIGNON,P.* EPPEL,D.* GERAMB,H.V.* YADAV,H.L. MADSEN,V.A.
THE OCTUPOLE GIANT RESONANCE STRENGTH IN O-016.
PHYS. LETT., B 68(1977),55-7
20.800

IKP-117077
PLOSZAJCZAK,M.
HOHE UND HOECHSTE DREHIMPULSE IN KERNEN.
JUEL-1429
20.800

IKP-117177
PLOSZAJCZAK,M. FAESSLER,A.
DESCRIPTION OF NEGATIVE PARITY YRAST STATES IN ER-156.
Z. PHYS., A 283(1977),349-56
20.800

IKP-117277
PLOSZAJCZAK,M. FAESSLER,A.
BACKBENDING IN THE NEGATIVE PARITY ROTATIONAL BANDS IN ER-156.
INTERNATIONAL SYMPOSIUM ON HIGH-SPIN STATES AND NUCLEAR STRUCTURE. DRESDEN, 19.-24.9.1977. S. 72-3
20.800

IKP-117377
PLOSZAJCZAK,M. FAESSLER,A. LEANDER,G.* NILSSON,S.G.*
UNIFIED DESCRIPTION OF THE YRAST TRAPS AT VERY HIGH ANGULAR MOMENTA.
NUCL. PHYS. (IM DRUCK)
20.800

IKP-117477
PLOSZAJCZAK,M. SANDHYA-DEVI,K.R.* FAESSLER,A.
MICROSCOPIC DETERMINATION OF ENERGY SURFACES AT VERY HIGH SPIN STATES.
Z. PHYS., A 282(1977),267-76
20.800

IKP-117577
PLOSZAJCZAK,M. TOKI,H. FAESSLER,A.
DEFORMATION ENERGY SURFACES AT VERY HIGH SPIN STATES.
INTERNATIONAL SYMPOSIUM ON HIGH-SPIN STATES AND NUCLEAR STRUCTURE. DRESDEN, 19.-24.9.1977. S. 93-4
20.800

IKP-117677
PLOSZAJCZAK,M. TOKI,H. FAESSLER,A.
VERY HIGH SPIN STATES IN SPHERICAL AND TRANSURANIC NUCLEI.
J. PHYS. G (IM DRUCK)
20.800

IKP-117777
PLOSZAJCZAK,M. TOKI,H. FAESSLER,A.
ROTATION OF NUCLEI AROUND A PROLATE SYMMETRY AXIS AT VERY HIGH SPIN STATES.
NUCL. PHYS. (IM DRUCK)
20.800

IKP-117877
PROKOFJEV,P.T.* BALODIS,M.K.* KRUMINA,A.J.* KRAMER,N.D.* PLATE,M.N.* SIMONOVA,L.I.* SCHRECKENBACH,K.* DAVIDSON,W.F.* PINSTON,J.A.* WARNER,D.D.* BOERNER,H.G. VANASSCHE,P.H.M.*
LOW-ENERGY STATES OF EU-155 OBSERVED IN THERMAL NEUTRON CAPTURE.
PROCEEDINGS OF THE INTERNATIONAL CONFERENCE ON NUCLEAR STRUCTURE. TOKYO, 5.-10.9.1977. VOL. 1, S. 394
20.700

IKP-117977
PROKOFJEV,P.T.* BALODIS,M.K.* KRUMINA,A.J.* KRAMER,N.D.* PLATE,M.N.* SIMONOVA,L.I.* SCHRECKENBACH,K.* DAVIDSON,W.F.* PINSTON,J.A.* WARNER,D.D.* BOERNER,H.G. VANASSCHE,P.H.M.*
LOW-K ROTATIONAL BANDS IN EU-154.
PROCEEDINGS OF THE INTERNATIONAL CONFERENCE ON NUCLEAR STRUCTURE. TOKYO, 5.-10.9.1977. VOL. 1, S. 390
20.700

IKP-118077
RAMA-RAO,J.* MACHNER,H. ERNST,J.* MAYER-KUCKUK,T.*
MECHANISM OF THE REACTION TH-232(D,2N)PA-232.
PHYS. REV., C 15(1977),2255
20.060

IKP-118177
REINHARD,P.G.* GOEKE,K.
ON REALITY CONDITIONS OF CLASSICAL MOTION ALONG COLLECTIVE PATHS.
PHYS. REV. C (IM DRUCK)
20.800

IKP-118277
REINHARD,P.G.* GOEKE,K.
THE TWO PARAMETER GENERATOR-COORDINATE METHOD AND ITS RELATION TO THE ADIABATIC TIME-DEPENDENT HARTREE-FOCK THEORY.
PHYS. LETT. B (IM DRUCK)
20.800

IKP-118377
REINHARD,P.G.* GOEKE,K.
THE CONCEPT OF A COLLECTIVE PATH AND ITS RANGE OF VALIDITY.
Z. PHYSIK (IN DRUCK)
20.800

IKP-118477
REINHARD,P.G.* GOEKE,K.
THE UNIQUE QUANTIZATION OF CLASSICAL HAMILTONIANS IN THE ADIABATIC TIME DEPENDENT HF-THEORY.
PROCEEDINGS OF THE INTERNATIONAL CONFERENCE ON NUCLEAR STRUCTURE, TOKYO, 5.-10.9.1977. VOL. 1, S. 117
20.800

IKP-118577
REINHARD,P.G.* GOEKE,K.
CONDITIONS FOR THE VALIDITY OF ATDHF AND THE LOCAL HARMONIC APPROACH.
PHYS. LETT., B 69(1977),1,17-9
20.800

IKP-118677
RINKER,G.A. SPETH,J.
A RESOLUTION OF THE NUCLEAR POLARIZATION ANOMALIES IN PB-208.
PHYS. LETT. (IM DRUCK)
20.800

IKP-118777
SANCHEZ-DEHESA,J.
MICROSCOPIC DESCRIPTION OF GIANT ELECTRIC AND MAGNETIC MULTIPOLE RESONANCES IN CLOSED-SHELL NUCLEI.
JUEL-1425
20.800

IKP-118877
SANO,M.* TAKEMASA,T.* WAKAI,M.
E2-TRANSITON RATES OF THE GROUND-STATE ROTATIONAL MEMBER.
PROGRESS OF THEOR. PHYS. (IM DRUCK)
20.800

IKP-118977
SANO,M.* TAKEMASA,T.* WAKAI,M.
E2-TRANSITION RATES OF THE GROUND-STATE ROTATIONAL MEMBER.
PROCEEDINGS OF THE INTERNATIONAL CONFERENCE ON NUCLEAR STRUCTURE. TOKYO, 5.-10.9.1977. VOL. 1, S. 402
20.800

IKP-119077
SANO,M.* TANAKA,M.* WAKAI,M.
DWBA ANALYSIS OF MAGNETIC SUBSTATE POPULATIONS OF RESIDUAL NUCLEUS IN THE B-011(D,P)B-012 REACTIONS.
PROGRESS OF THEOR. PHYS. (IM DRUCK)
20.800

IKP-119177
SANO,M.* TANAKA,M.* WAKAI,M.
DWBA ANALYSIS OF MAGNETIC SUBSTATE POPULATIONS OF RESIDUAL NUCLEUS IN THE B-011(D,P)B-012 REACTION.
PROCEEDINGS OF THE INTERNATIONAL CONFERENCE ON NUCLEAR STRUCTURE. TOKYO, 5.-10.9.1977. VOL. 1, S. 537
20.800

IKP-119277
SANO,M.* WAKAI,M.
ANGULAR MOMENTUM DEPENDENCE OF THE COLLECTIVE GYROMAGNETIC RATIO.
PROGRESS OF THEOR. PHYS. (IM DRUCK)
20.800

IKP-119377
SCHMID,K.W. DO DANG,G.*
A MICROSCOPIC APPROACH TO THE GIANT MULTIPOLE RESONANCES IN NE-020.
PHYS. LETT. 66B(1977),5-8
20.800

IKP-119477
SCHMID,K.W. DO DANG,G.*
MICROSCOPIC STUDY OF THE GIANT MULTIPOLE RESONANCES IN LIGHT DEFORMED NUCLEI VIA RADIATIVE CAPTURE REACTIONS.
PHYS. REV., C 15(1977),4,1515-29
20.800

IKP-119577
SCHMID,K.W. MUETHER,H.
INFLUENCE OF 2HQUEROMEGA EXCITATIONS ON THE LOW ENERGY SPECTRA OF NUCLEI.
PHYS. REV., C 16(1977),2050-8
20.800

IKP-119677
SCHRECKENBACH,K.* BOERNER,H.G. DESCLAUX,J.P.*
HIGH PRECISION MEASUREMENTS AND CALCULATION OF THE HYPERSATELLITE K ALPHA 1H X-RAY ENERGY FOR Z EQUAL TO 80.
PHYS. LETT. 63A(1977),330-2
20.700

IKP-119777
SCHULT,O.W.B.
IN BEAM GAMMA-RAY SPECTROSCOPY AT TANDEM VAN DE GRAAFF-ACCELERATORS.
NUCL. INSTRUM. METHODS 146(1977),161-70
20.100

IKP-119877
SCHULT,O.W.B.
APPLIED NUCLEAR PHYSICS FOR LIFE SCIENCES.
NUCL. INSTRUM. METHODS 146(1977),301-6
20.600

IKP-119977
SCHULTHEIS,H.* SCHULTHEIS,R.* WILDERMUTH,K.* FAESSLER,A. GRUEMMER,F.
ALPHA PARTICLE MODEL CALCULATION FOR S-032.
PROCEEDINGS OF THE 15. INTERNATIONAL WINTER MEETING ON NUCLEAR PHYSICS. BORMIO, 17.-22.1.1977. S. 71-7
20.800

IKP-120077
SCHULTHEIS,H.* SCHULTHEIS,R.* WILDERMUTH,K.* FAESSLER,A. GRUEMMER,F.
STUDY OF MANY-NUCLEON CORRELATIONS IN S-032 AS A MODEL FOR FRAGMENT SHELL EFFECTS IN FISSION.
Z. PHYSIK (IM DRUCK)
20.800

IKP-120177
SCHUSSLER,F.* BOCQUET,J.P.* MONNAND,E.* SISTEMICH,K. GRUETER,J.W.
DEPENDANCE OF THE ISOMERIC YIELDS IN SN-131 WITH THE KINETIC ENERGY OF THE FISSION PRODUCTS.
PROCEEDINGS OF THE INTERNATIONAL CONFERENCE ON NUCLEAR STRUCTURE. CONTRIBUTED PAPERS. TOKYO, 5.-10.9.1977. S. 749
20.650,20.600

IKP-120277
SELIC,H.A.
UNTERSUCHUNGEN ZUR KERNSTRUKTUR DER SPALTPRODUKTE SR-097, Y-097, ZR-097, Y-099, ZR-099 UND NB-099.
JUEL-1431
20.650

IKP-120377
SEYFARTH,H. WUEST,N. SCHULT,O.W.B.
ON THE INTENSITIES OF K X-RAYS FOLLOWING THERMAL NEUTRON CAPTURE.
Z. PHYS., A 280(1977),239-42
20.700

IKP-120477
SHIMIZU,K. FAESSLER,A.
RESCATTERING EFFECT IN BOUND 2P-PION ABSORPTION.
PHYS. REV. LETT. (IM DRUCK)
20.800

IKP-120577
SHURPIN,J.* MUETHER,H. KUO,T.T.S.* FAESSLER,A.
THE INFLUENCE OF A SELF-CONSISTENT MODEL SPACE ON THE FOLDED DIAGRAM EXPANSION OF NUCLEAR EFFECTIVE INTERACTIONS.
NUCL. PHYS. (IM DRUCK)
20.800

IKP-120677
SISTEMICH,K. LAUPPE,W.D. KHAN,T.A. GRUETER,J.W. LAWIN,H. SELIC,H.A. BOCQUET,J.P.* SELLAM,R.* MONNAND,E.* SCHUSSLER,F.*
THE LEVEL SCHEME OF SB-133.
PROCEEDINGS OF THE INTERNATIONAL CONFERENCE ON NUCLEAR STRUCTURE. CONTRIBUTED PAPERS. VOL. 1. TOKYO, 5.-10.9.1977. S. 860
20.650

IKP-120777
SISTEMICH,K. LAUPPE,W.D. KHAN,T.A. LAWIN,H. SELIC,H.A.
STUDIES OF SN-132 AND SB-133.
INTERNATIONAL SYMPOSIUM ON HIGH-SPIN STATES AND NUCLEAR STRUCTURE. DRESDEN, 19.-24.9.1977. S. 21-2
20.650

IKP-120877
SISTEMICH,K. LAUPPE,W.D. KHAN,T.A. LAWIN,H. SELIC,H.A. BOCQUET,J.P.* MONNAND,E.* SCHUSSLER,F.*
THE LEVEL SCHEME OF SB-133.
Z. PHYS.(IM DRUCK)
20.650

IKP-120977
SISTEMICH,K. LAWIN,H.
JOSEF - EIN SEPARATOR FUER SPALTPRODUKTE.
KERNFORSCHUNGSANLAGE JUELICH. JAHRESBERICHT. 1976/77. S. 47-56
20.650

IKP-121077
SISTEMICH,K. SADLER,G.* KHAN,T.A. LAWIN,H. LAUPPE,W.D. SELIC,H.A. SCHUSSLER,F.* BLACHOT,J.* MONNAND,E.* BOCQUET,J.P.* PFEIFFER,B.*
THE BETA-DECAY OF Y-098 AND THE LEVEL SCHEME OF ZR-098.
Z. PHYS., A 281(1977),169-81
20.650

IKP-121177
SMITHER,R.K.* SCHRECKENBACH,K.* NAMENSON,A.I.* DAVIDSON,W.F.* BOERNER,H.G. PINSTON,J.A.* WARNER,D.D.* EGIDY,T. VON*
ENERGY LEVELS IN SM-155.
PROCEEDINGS OF THE INTERNATIONAL CONFERENCE ON NUCLEAR STRUCTURE. TOKYO, 5.-10.9.1977. VOL. 1, S. 393
20.700

IKP-121277
SPETH,J.
STRUCTURE OF THE NEW GIANT RESONANCES.
PROCEEDINGS OF THE 15. INTERNATIONAL WINTER MEETING ON NUCLEAR PHYSICS. BORMIO, 17.-22.1.1977. S. 1-25
20.800

IKP-121377
SPETH,J.
THE NEW GIANT RESONANCES.
PROCEEDINGS OF THE 18TH SCOTTISH UNIVERSITIES SUMMER SCHOOL IN PHYSICS. ST. ANDREWS, 31.7.-20.8.1977 (IM DRUCK)
20.800

IKP-121477
SPETH,J.
MICROSCOPIC CALCULATIONS OF THE GIANT MULTIPOLE RESONANCES.
PROCEEDINGS OF THE CONFERENCE ON NUCLEAR REACTION MECHANISMS. VARENNA, 13.-17.6.1977 (IM DRUCK)
20.800

IKP-121577
SPETH,J.
STRUCTURE OF THE NEW GIANT RESONANCES.
PROCEEDINGS OF THE SENDAI CONFERENCE ON ELECTRO- AND PHOTOEXCITATIONS. SENDAI, 12.-13.9.1977. S. 65-76
20.800

IKP-121677
SPETH,J.
HIGHLY EXCITED COLLECTIVE STATES.
PROCEEDINGS OF THE RCNP SYMPOSIUM ON HIGHLY EXCITED STATES AND POLARIZATION PHENOMENA. OSAKA, 14.-16.9.1977. S. 44-5
20.800

IKP-121777
SPETH,J. DEHESA,J.S. FAESSLER,A. MADSEN,V.A. RINKER,G.A. WAMBACH,J.
FRAGMENTATION OF THE ELECTRIC MULTIPOLE STRENGTH IN PB-208.
PROCEEDINGS OF THE INTERNATIONAL CONFERENCE ON NUCLEAR STRUCTURE. TOKIO, 5.-10.9.1977. VOL. 2 (IM DRUCK)
20.800

IKP-121877
SPETH,J. HENNING,W.* KIENLE,P.* MEYER,J.
ISOMER SHIFTS AND NUCLEAR MODELS.
IN: MOESSBAUER ISOMER SHIFTS. AMSTERDAM, NORTH-HOLLAND PUBL. 1977
20.800

IKP-121977
SPETH,J. WERNER,E.* WILD,W.*
THEORY OF FINITE FERMI SYSTEMS AND APPLICATIONS TO THE LEAD REGION.
PHYS. REP. 33C(1977),127-208
20.800

IKP-122077
STEIN,H.J.
NATIONALE UND INTERNATIONALE MESSPROGRAMME.
SONNENENERGIE. 2. S. 155-63
20.600

# IX. Conference Contributions, Patents, Applications for a Patent



IKP-122177
STEPHENS,F.S.* YADAV,H.L. ZALM,P.C.*
HIGH-SPIN STATES.
LECTURE NOTES. THE NETHERLANDS' PHYSICAL SOCIETY 1977 INTERNATIONAL SUMMER SCHOOL ON NUCLEAR SPECTROSCOPY. BREUKELEN, 15.-26.8.1977. S. 39-63
20.800

IKP-122277
TOKI,H.
STRONG DECOUPLING STRUCTURES IN TRANSITIONAL NUCLEI.
PROCEEDINGS OF THE 15. WINTER SCHOOL ON NUCLEAR PHYSICS "SELECTED TOPICS IN NUCLEAR STRUCTURE". ZAKOPANE, 6.-19.2.1977. S. 203
20.800

IKP-122377
TOKI,H.
GAMMA-DEFORMATION IN TRANSITIONAL NUCLEI.
PROCEEDINGS OF THE RCNP SYMPOSIUM ON HIGHLY EXCITED STATES AND POLARIZATION PHENOMENA. OSAKA, 14.-16.9. 1977. S. 24-5
20.800

IKP-122477
TOKI,H. FAESSLER,A.
COMPETITION BETWEEN STRONG AND DECOUPLING STRUCTURES IN TRANSITIONAL NUCLEI.
PROCEEDINGS OF THE INTERNATIONAL WORKSHOP ON GROSS PROPERTIES OF NUCLEI AND NUCLEAR EXCITATIONS 5. HIRSCHEGG, 17.-22.1.1977. AED-CONF 77-017-001 - AED-CONF 77-017-043 (1977) S. 11-4
20.800

IKP-122577
TOKI,H. FAESSLER,A. YADAV,H.L.
DECOUPLING AND STRONG COUPLING IN TRANSITIONAL NUCLEI.
PROCEEDINGS OF THE INTERNATIONAL CONFERENCE ON NUCLEAR STRUCTURE. TOKYO, 5.-10.9.1977. VOL. 1, S. 436
20.800

IKP-122677
TOKI,H. NEERGARD,K. VOGEL,P. FAESSLER,A.
NON-AXIAL DEFORMATIONS AND THE ODD PARITY STATES IN THE EVEN PT AND HG ISOTOPES.
NUCL. PHYS., A 279 (1977),1-28
20.800

IKP-122777
TOKI,H. YADAV,H.L. FAESSLER,A.
STRONG AND DECOUPLING STRUCTURE IN TRANSITIONAL ODD-ODD MASS NUCLEI.
PHYS. LETT., B 66(1977),4,310-4
20.800

IKP-122877
TOKI,H. YADAV,H.L. FAESSLER,A.
DECOUPLED AND STRONGLY COUPLED PARTICLES SYSTEM IN ODD-ODD MASS NUCLEI.
PHYS. LETT. 71B(1977),1-4
20.800

IKP-122977
TRAUTMANN,D.* BAUR,G.
ON THE THEORY OF DIRECT REACTIONS WITH MANY PARTICLE FINAL STATES.
NUKLEONIKA 22(1977),485-528
20.800

IKP-123077
TUREK,P.
INVESTIGATION OF GIANT QUADRUPOLE RESONANCES IN LIGHT NUCLEI BY INELASTIC ALPHA SCATTERING.
PROCEEDINGS OF 15. INTERNATIONAL WINTER MEETING ON NUCLEAR PHYSICS. BORMIO, JAN. 1977
20.060

IKP-123177
HAKAI,M. FAESSLER,A.
INFLUENCE OF QUADRUPOLE PAIRING ON BACKBENDING.
NUCL. PHYS. (IM DRUCK)
20.800

IKP-123277
HANBACH,J. HADSEN,V.A. RINKER,G.A. SPETH,J.
HAS THE BREATHING MODE BEEN KNOWN FOR MANY YEARS?
PHYS. REV. LETT. 39(1977),1443-7
20.800

IKP-123377
YADAV,H.L. TOKI,H. FAESSLER,A.
ANOMALIES IN THE YRAST BAND OF PT AND HG ISOTOPES.
PROCEEDINGS OF THE INTERNATIONAL SYMPOSIUM ON HIGH-SPIN STATES AND NUCLEAR STRUCTURE. DRESDEN, 19.-24.9. 1977. ZFK-336 (1977). S. 51-2
20.800

IKP-123477
YADAV,H.L. TOKI,H. FAESSLER,A.
POSITIVE PARITY STATES IN PT AND HG ISOTOPES AND THE CORIOLIS ANTIPAIRING EFFECT IN THE DEFORMED ROTOR MODEL.
PHYS. REV. LETT. 39(1977),1128-30
20.800

IKP-123577
ZAWISCHA,D.* SPETH,J.
GIANT MULTIPOLE RESONANCES IN DEFORMED RARE EARTH NUCLEI.
PROCEEDINGS OF THE INTERNATIONAL CONFERENCE ON NUCLEAR STRUCTURE. TOKYO, 5.-10.9.1977. VOL. 1, S. 392
20.800

IKP-200177
ALDERLIESTEN,C. BOUSSHID,O. DJALOEIS,A. JAHN,P. MACHNER,H. MAYER-BOERICKE,C.
UNTERSUCHUNG DES REINEN KONTINUUMS IN DER INELASTISCHEN PROTONENSTREUUNG.
FRUEHJAHRSTAGUNG DER DPG, FACHGRUPPE KERNPHYSIK. KONSTANZ, 21.-25.3.1977. VERHANDL. DPG (VI), 12(1977), S. 1016-7
20.060

IKP-200277
ALDERLIESTEN,C. BOUSSHID,O. JAHN,P. PROBST,H.J. MAYER-BOERICKE,C.
MEASUREMENT AND HYBRID-MODEL ANALYSIS OF AU-197(HE-003,XNYP) EXCITATION FUNCTIONS.
CONFERENCE ON NUCLEAR REACTION MECHANISMS. VARENNA, 13. -17.6.1977
20.060

IKP-200377
ALDERLIESTEN,C. BOUSSHID,O. JAHN,P. PROBST,H.J. MAYER-BOERICKE,C.
MESSUNG UND HYBRID-MODELL-ANALYSE VON AU-197 (HE-003,XNYP)-ANREGUNGSFUNKTIONEN.
FRUEHJAHRSTAGUNG DER DPG, FACHGRUPPE KERNPHYSIK. KONSTANZ, 21.-25.3.1977. VERHANDL. DPG (VI), 12(1977), S. 1018
20.060

IKP-200477
ANTROPOV,A.E.* GUSEV,V.P.* ZARUBIN,P.P.* IOANNU,P.D.* KROBEZKIJ,E.V.* ORLOV,B.N.* HEFTER,E.F.
ANALYSE DER STREUUNG VON PROTONEN MIT EP GLEICH 6 MEV AN DEN KERNEN NI-058,060,062,064.
27. KONFERENZ FUER KERNSPEKTROSKOPIE UND STRUKTUR DER ATOMKERNE. TASCHKENT, 22.-25.3.1977. MATERIALIEN ZUR 27. KONFERENZ FUER KERNSPEKTROSKOPIE UND STRUKTUR DER ATOMKERNE. S. 132
20.800

IKP-200577
BAUR,G.
ON THE THEORY OF DIRECT REACTIONS WITH THREE PARTICLE FINAL AND INTERMEDIATE STATES.
INTERNATIONAL SYMPOSIUM "REACTION MODELS '77". BALATONFUERED, 27.6.-1.7.1977
20.800

IKP-200677
BAUR,G.
DEUTERONAUFBRUCH UND KONTINUUMSTRIPPING.
KOLLOQUIUM AM PHYSIKALISCHEN INSTITUT DER UNIV. HAMBURG. 24.10.1977
20.800

IKP-200777
BAUR,G. LENSKE,H.
LINIENFORMEN BEI INELASTISCHER STREUUNG ZU RESONANZZUSTAENDEN.
FRUEHJAHRSTAGUNG DER DPG, FACHGRUPPE KERNPHYSIK. KONSTANZ, 21.-25.3.1977. VERHANDL. DPG (VI), 12(1977), S. 911
20.800

IKP-200877
BAUR,G. ROESEL,F.* TRAUTMANN,D.*
KERNREAKTIONEN MIT DREITEILCHENENDZUSTAENDEN.
FRUEHJAHRSTAGUNG DER DPG, FACHGRUPPE KERNPHYSIK. KONSTANZ, 21.-25.3.1977. VERHANDL. DPG (VI), 12(1977), S. 835
20.800

IKP-200977
BAUR,G. WOLTER,H.H.*
SIMULTANEOUS AND SEQUENTIAL TWO-NUCLEON TRANSFER IN ELASTIC TRANSFER REACTIONS.
FRUEHJAHRSTAGUNG DER DPG, FACHGRUPPE KERNPHYSIK. KONSTANZ, 21.-25.3.1977. VERHANDL. DPG (VI), 12(1977), S. 884
20.800

IKP-201077
BAZ,A.I.* GOLDBERG,V.Z.* DARWISCH,N.Z.* GRIDNEV,K.A.* SEMJONOV,V.M.* HEFTER,E.F.
EIN PHAENOMENOLOGISCHES POTENTIAL FUER (ALPHA,ALPHA) STREUUNG AN LEICHTEN KERNEN.
FRUEHJAHRSTAGUNG DER DPG, FACHGRUPPE KERNPHYSIK. KONSTANZ, 21.-25.3.1977. VERHANDL. DPG (VI), 12(1977), S. 837
20.800

IKP-201177
BENSON,D.* SHELINE,R.K.* KLEINHEINZ,P. SHERA,E.B.*
SINGLE PARTICLE EXCITATIONS IN THE ISOTOPES OS-189, OS-191, OS-193.
FRUEHJAHRSTAGUNG DER DPG, FACHGRUPPEN KERNPHYSIK. KONSTANZ, 21.-25.3.1977. VERHANDL. DPG (VI), 12(1977), S. 942
20.100

IKP-201277
BEUSCHER,H.
EXPERIMENTAL STUDY OF HIGH SPIN STATES IN HEAVY NUCLEI NEAR LEAD.
15. WINTER SCHOOL. ZAKOPANE, 6.-19.2.1977
20.100

IKP-201377
BEUSCHER,H. GONO,Y. LIEDER,R.M. MUELLER-VEGGIAN,M. NESKAKIS,A. MAYER-BOERICKE,C.
PARTICLE AND COLLECTIVE PROPERTIES OF HIGH-SPIN STATES IN HEAVY NUCLEI NEAR Z EQUAL TO 82.
FRUEHJAHRSTAGUNG DER DPG, FACHGRUPPE KERNPHYSIK. KONSTANZ, 21.-25.3.1977. VERHANDL. DPG (VI), 12(1977), S. 985-6
20.100

IKP-201477
BEUSCHER,H. GOND,Y. LIEDER,R.M. MUELLER-VEGGIAN,M. MAYER-BOERICKE,C. NESKAKIS,A.
SYSTEMATIC FEATURES OF ISOMERIC STATES IN CE, ND, SM NUCLEI.
FRUEHJAHRSTAGUNG DER DPG, FACHGRUPPE KERNPHYSIK. KONSTANZ, 21.-25.3.1977. VERHANDL. DPG (VI), 12(1977), S. 892
20.100

IKP-201577
BEUSCHER,H. GOND,Y. LIEDER,R.M. MUELLER-VEGGIAN,M. MAYER-BOERICKE,C. NESKAKIS,A. HAENNI,D.R. ZOLNOWSKI,D. R.* SUGIHARA,T.T.*
SIDE BANDS IN HF-172.
FRUEHJAHRSTAGUNG DER DPG, FACHGRUPPE KERNPHYSIK. KONSTANZ, 21.-25.3.1977. VERHANDL. DPG (VI), 12(1977), S. 940
20.100

IKP-201677
BOERNER,H.G. KOCH,H.R. SEYFARTH,H. SCHULT,O.W.B. HECK,D.* MAMPE,W.* SCHRECKENBACH,K.* PINSTON,J.A.*
EXCITED LEVELS IN U-239 FROM NEUTRON CAPTURE GAMMA-RAY MEASUREMENTS.
FRUEHJAHRSTAGUNG DER DPG, FACHGRUPPEN KERNPHYSIK. KONSTANZ, 21.-25.3.1977. VERHANDL. DPG (VI), 12(1977), S. 991
20.700

IKP-201777
BOJOWALD,J. MAYER-BOERICKE,C. ROGGE,M. TUREK,P.
ELASTISCHE DEUTERONENSTREUUNG BEI 85 MEV.
FRUEHJAHRSTAGUNG DER DPG, FACHGRUPPE KERNPHYSIK. KONSTANZ, 21.-25.3.1977. VERHANDL. DPG (VI), 12(1977), S. 866
20.060

IKP-201877
BORCHERT,G.L. SCHULT,O.W.B. HANSEN,P.G.* JONSON,B.* RAVN,H.L.*
ROENTGENENERGIEVERSCHIEBUNGEN IN NEUTRONENARMEN XE-ISOTOPEN.
FRUEHJAHRSTAGUNG DER DPG, FACHGRUPPEN KERNPHYSIK. KONSTANZ, 21.-25.3.1977. VERHANDL. DPG (VI), 12(1977), S. 854
20.100

IKP-201977
BRAEUTIGAM,W. WUCHERER,P.
IMPROVEMENT OF EXTRACTION ELEMENTS AT JULIC.
*14. EUROPEAN CYCLOTRON PROGRESS MEETING. UPPSALA*, 1.-3.6.1977.
20.300

IKP-202077
BREUER,H.* KNOEPFLE,K.T.* PAUL,P.* WAGNER,G.J.* MAYER-BOERICKE,C. ROGGE,M. TUREK,P.
DECAY PROPERTIES OF THE NEW GIANT RESONANCES IN O-016.
FRUEHJAHRSTAGUNG DER DPG, FACHGRUPPE KERNPHYSIK. KONSTANZ, 21.-25.3.1977. VERHANDL. DPG (VI), 12(1977), S. 983-4
20.060

IKP-202177
BRODA,R.
GAMMA-MULTIPLICITY IN LOW ENERGY ALPHA INDUCED REACTIONS.
SEMINARVORTRAG, INSTITUTE OF PHYSICS, UNIVERSITY OSLO. BLINDERN, 19.8.1977
20.100

IKP-202277
CASTEN,R.F.* MACPHAIL,M.R.* KANE,W.R.* CIZEWSKI,J.A.* BOERNER,H. PINSTON,J.A.* DAVIDSON,W.F.*
LEVEL SCHEME OF 191-OS FROM THE (N,GAMMA) REACTION.
FRUEHJAHRSTAGUNG DER DPG, FACHGRUPPEN KERNPHYSIK. KONSTANZ, 21.-25.3.1977. VERHANDL. DPG (VI), 12(1977), S. 942
20.700

IKP-202377
DALY,P.J.
YRAST SPECTROSCOPY IN PT AND HG EVEN AND ODD A NUCLEI.
SEMINARVORTRAG AM INSTITUT FUER KERNPHYSIK DER TH DARMSTADT. SEP. 1977
20.100

IKP-202477
DALY,P.J. DORS,C.L.* HELPPI,H.* PIIPARINEN,M.* SAHA,S. K.* KHOO,T.L.* BERNTHAL,F.M.*
*HIGH SPIN LEVEL STRUCTURE OF PT-188.*
INTERNATIONAL SYMPOSIUM ON HIGH-SPIN STATES AND NUCLEAR STRUCTURE. DRESDEN, 19.-24.9.1977
20.100

IKP-202577
DAVID,P.* GERAMB,K.A.* GRIDNEV,K.A.* SEMJONOV,V.M.* HEFTER,E.F. ESSEN,H.*
STUDIUM DER DEFORMATIONSPARAMETER DER KERNE PB-208, TH-232, U-234,236,238.
27. KONFERENZ FUER KERNSPEKTROSKOPIE UND STRUKTUR DER ATOMKERNE. TASCHKENT, 22.-25.3.1977. MATERIALIEN ZUR 27. KONFERENZ FUER KERNSPEKTROSKOPIE UND STRUKTUR DER ATOMKERNE. S. 182
20.800

IKP-202677
DEBOER,J.* DO HUU PHUOC* MYINT THEIN* KOCH,H.R. SCHULT,O.W.B. SEYFARTH,H. WUEST,N.
KERNSPEKTROSKOPISCHE UNTERSUCHUNGEN MITTELS THERMISCHEN NEUTRONENEINFANGS.
FRUEHJAHRSTAGUNG DER DPG, FACHGRUPPEN KERNPHYSIK. KONSTANZ, 21.-25.3.1977. VERHANDL. DPG (VI), 12(1977), S. 844
20.700

IKP-202777
DEHESA,J.S.
ZEROS OF POLYNOMIALS RELATED TO BIRTH-DEATH PROCESSES.
ANNUAL CONGRESS OF THE GERMAN APPLIED MATHEMATICS SOCIETY AND THE DANISH CENTER ON APPLIED MATHEMATICS. KOPENHAGEN, JUNI 1977
20.800

IKP-202877
DEHESA,J.S.
NEW PROBLEMS IN THE THEORY OF ORTHOGONAL POLYNOMIALS.
SEMINAR DER UNIV. BONN. JUNI 1977
20.800

IKP-202977
DEHESA,J.S. FAESSLER,A. KREWALD,S. KLEMT,V. SPETH,J. WAMBACH,J.
THEORETISCHE UNTERSUCHUNGEN DER MULTIPOLRIESENRESONANZEN.
FRUEHJAHRSTAGUNG DER DPG, FACHGRUPPE KERNPHYSIK. KONSTANZ, 21.-25.3.1977. VERHANDL. DPG (VI), 12(1977), S. 984-5
20.800

IKP-203077
DELION,D.S.* GRIDNEV,K.A.* HEFTER,E.F.
EINE NICHTLINEARE SCHROEDINGER-GLEICHUNG ZUR BESCHREIBUNG ELASTISCHER STREUUNG VON SCHWERIONEN.
FRUEHJAHRSTAGUNG DER DPG, FACHGRUPPE KERNPHYSIK. KONSTANZ, 21.-25.3.1977. VERHANDL. DPG (VI), 12(1977), S. 837
20.800

IKP-203177
DEMEIJER,R.J.* KAMERMANS,R.* MORSCH,H.P. GIRISCH,R.* PROJECTILE EXCITATION IN ALPHA-SCATTERING ON MG-024.
FRUEHJAHRSTAGUNG DER DPG, FACHGRUPPE KERNPHYSIK. KONSTANZ, 21.-25.3.1977. VERHANDL. DPG (VI), 12(1977), S. 912
20.060

IKP-203277
DIDELEZ,J.P. DJALOEIS,A. GALONSKY,A. OELERT,W.
NEUTRON-HOLE STATES OBSERVED IN THE (HE-003,ALPHA) REACTION.
FRUEHJAHRSTAGUNG DER DPG, FACHGRUPPE KERNPHYSIK. KONSTANZ, 21.-25.3.1977. VERHANDL. DPG (VI), 12(1977), S. 962-3
20.060

IKP-203377
*DIDELEZ,J.P. MAYER-BOERICKE,C. ROGGE,M. TUREK,P.*
WIKTOR,S.
INVESTIGATION OF THE GIANT QUADRUPOLE RESONANCE IN AR-040 BY (ALPHA,ALPHA') SCATTERING.
FRUEHJAHRSTAGUNG DER DPG, FACHGRUPPE KERNPHYSIK. KONSTANZ, 21.-25.3.1977. VERHANDL. DPG (VI), 12(1977), S. 1011
20.060

IKP-203477
DJALOEIS,A. DIDELEZ,J.P. GALONSKY,A. OELERT,W.
EXCITATION OF GIANT RESONANCES BY 130 MEV HE-003.
FRUEHJAHRSTAGUNG DER DPG, FACHGRUPPE KERNPHYSIK. KONSTANZ, 21.-25.3.1977. VERHANDL. DPG (VI), 12(1977), S. 1011-2
20.060

IKP-203577
DO,H.P.* CHERY,R.* BOERNER,H. DAVIDSON,W.F.* PINSTON,J. A.* ROUSSILLE,R.* SCHRECKENBACH,K.* KOCH,H.R. SEYFARTH,H. HECK,D.*
LEVEL STRUCTURE OF BR-080 AND BR-082 FROM THERMAL NEUTRON CAPTURE REACTIONS.
FRUEHJAHRSTAGUNG DER DPG, FACHGRUPPEN KERNPHYSIK. KONSTANZ, 21.-25.3.1977. VERHANDL. DPG (VI), 12(1977), S. 846
20.700

IKP-203677
EBERT,K.* MEYER-TERVEHN,J.
RADIATIVER PI-EINFANG AN PB-208.
FRUEHJAHRSTAGUNG DER DPG, FACHGRUPPE KERNPHYSIK. KONSTANZ, 21.-25.3.1977. VERHANDL. DPG (VI), 12(1977), S. 830
20.800

IKP-203777
FABER,M.* FAESSLER,A. TOKI,H.
DIE DEFORMATIONSENERGIEOBERFLAECHE SPALTENDER KERNE MIT HOHEN UND SEHR HOHEN DREHIMPULSEN.
*FRUEHJAHRSTAGUNG DER DPG, FACHGRUPPE KERNPHYSIK.*
KONSTANZ, 21.-25.3.1977. VERHANDL. DPG (VI), 12(1977), S. 1025
20.800

IKP-203877
FAESSLER,A.
DESCRIPTION OF DECOUPLING IN TRANSITIONAL NUCLEI.
SEMINAR OF THE UNISOR-GROUP. OAK RIDGE NATIONAL LABORATORY, TENN., 13.4.1977
20.800

IKP-203977
FAESSLER,A.
DO WE REALLY UNDERSTAND THE CAUSES FOR BACKBENDING?
INTERNATIONAL SYMPOSIUM ON HIGH-SPIN STATES AND NUCLEAR STRUCTURE. DRESDEN, 20.9.1977
20.800

IKP-204077
FAESSLER,A.
DO WE REALLY UNDERSTAND THE TRANSITIONAL NUCLEI?
MEETING KOELN-AMSTERDAM IN BAD HONNEF, 10.12.1977
20.800

IKP-204177
FAESSLER,A.
DAS SELTSAME VERHALTEN DER KERNE IN HOHEN DREHIMPULSZUSTAENDEN.
PHYSIKALISCHES KOLLOQUIUM DER UNIV. MAINZ, 13.12.1977
20.800

IKP-204277
FAESSLER,A.
DESCRIPTION OF GIANT MULTIPOLE RESONANCES.
NUCLEAR PHYSICS SEMINAR. UNIVERSITY OF MELBOURNE, 21.11.1977
20.800

IKP-204377
FAESSLER,A.
THE STRANGE BEHAVIOUR OF NUCLEI AT HIGH SPINS.
NUCLEAR PHYSICS SEMINAR. NATIONAL UNIV. OF AUSTRALIA, CANBERRA, 14.11.1977
20.800

IKP-204477
FAESSLER,A.
BOUND PION ABSORPTION IN NUCLEI.
THEORETICAL SEMINAR, SCHOOL OF PHYSICS, UNIV. OF MELBOURNE, 10.11.1977
20.800

IKP-204577
FAESSLER,A.
A PHASE TRANSITION IN NUCLEI?
PHYSIKALISCHES KOLLOQUIUM. UNIV. OF MELBOURNE, 10.11.1977
20.800

IKP-204677
FAESSLER,A.
THE STRANGE BEHAVIOUR OF NUCLEI AT HIGH SPINS.
PHYSIKALISCHES KOLLOQUIUM. FLINDERS UNIV., ADELAIDE, 7.11.1977
20.800

IKP-204777
FAESSLER,A.
SPINS, HIGH SPINS, VERY HIGH SPINS.
CONFERENCE ON NUCLEAR STRUCTURE. TOKYO, 7.9.1977
20.800

IKP-204877
FAESSLER,A.
THE STRANGE BEHAVIOUR OF NUCLEI AT HIGH SPINS.
SEMINAR DES INSTITUTE OF NUCLEAR STUDIES IN A PRE-CONFERENCE ON COLLECTIVE MOTION OF NUCLEI. TOKYO, 4.9.1977
20.800

IKP-204977
FAESSLER,A.
COLLECTIVE MOTION IN NUCLEI.
VORTRAGSREIHE AN DER INTERNATIONAL SUMMER SCHOOL ON NUCLEAR SPECTROSCOPY. NIJENRODE, 16.-26.8.1977
20.800

IKP-205077
FAESSLER,A.
THE BEHAVIOUR OF NUCLEI IN VERY STRONG CORIOLIS AND CENTRIFUGAL FIELDS.
SEMINAR IN THE THEORETICAL NUCLEAR PHYSICS GROUP. LOS ALAMOS, N.MEX., 14.7.1977
20.800

IKP-205177
FAESSLER,A.
DESCRIPTION OF GIANT MULTIPOLE RESONANCES.
KOLLOQUIUM DER THEORETICAL NUCLEAR PHYSICS GROUP. NATIONAL LABORATORY, LOS ALAMOS, N.MEX., 21.7.1977
20.800

IKP-205277
FAESSLER,A.
SELFCONSISTENT BRUECKNER RANDOM PHASE CALCULATIONS AND THE LANDAU RECIPE FOR THE PARTICLE-HOLE FORCE.
SEMINAR IN THE THEORETICAL NUCLEAR PHYSICS GROUP. UCLA, LOS ANGELES, CAL., 7.7.1977
20.800

IKP-205377
FAESSLER,A.
THE STRANGE BEHAVIOUR OF NUCLEI AT HIGH SPIN STATES.
NUCLEAR PHYSICS SEMINAR. CALIFORNIA INSTITUTE OF TECHNOLOGY, PASADENA, CAL., 6.7.1977
20.800

IKP-205477
FAESSLER,A.
SPINS, HIGH SPINS, VERY HIGH SPINS.
SEMINAR IN THE THEORETICAL NUCLEAR PHYSICS GROUP. UCLA, LOS ANGELES, CAL., 5.7.1977
20.800

IKP-205577
FAESSLER,A.
SPINS, HIGH SPINS, VERY HIGH SPINS.
KOLLOQUIUM DER STANFORD UNIV., CAL., 1.7.1977
20.800

IKP-205677
FAESSLER,A.
THE BEHAVIOUR OF NUCLEI IN STRONG CORIOLIS AND CENTRIFUGAL FIELDS.
KOLLOQUIUM DES LAWRENCE RADIATION LABORATORY. LIVERMORE, CAL., 30.6.1977
20.800

IKP-205777
FAESSLER,A.
DO WE REALLY UNDERSTAND THE TRANSITIONAL NUCLEI?
LUNCHEON SEMINAR. LAWRENCE RADIATION LABORATORY, LIVERMORE, CAL., 30.6.1977
20.800

IKP-205877
FAESSLER,A.
SPINS, HIGH SPINS, VERY HIGH SPINS.
SEMINAR AM LAWRENCE RADIATION LABORATORY, BERKELEY, CAL., 29.6.1977
20.800

IKP-205977
FAESSLER,A.
SPINS, HIGH SPINS, VERY HIGH SPINS.
KERNPHYSIKALISCHES KOLLOQUIUM. NATIONAL LABORATORY IN BROOKHAVEN, N.Y., 24.5.1977
20.800

IKP-206077
FAESSLER,A.
TEACHING AND RESEARCH IN GERMANY.
ANTRITTSVORLESUNG, PHYSICS DEPARTMENT, UNIV. OF NEW YORK, STONY BROOK, N.Y., 22.5.1977
20.800

IKP-206177
FAESSLER,A.
DESCRIPTION OF TRANSITIONAL NUCLEI.
PHYSIKALISCHES KOLLOQUIUM. RUTGERS UNIV., NEW BRUNSWICK, N.J., 2.5.1977
20.800

IKP-206277
FAESSLER,A.
GIANT MULTIPOLE RESONANCES.
PHYSIKALISCHES KOLLOQUIUM. UNIV. OF FLORIDA, GAINESVILLE, FLA., 21.4.1977
20.800

IKP-206377
FAESSLER,A.
THE STRANGE BEHAVIOUR OF NUCLEI AT HIGH SPIN STATES.
PHYSIKALISCHES KOLLOQUIUM. VANDERBILT UNIV., NASHVILLE, TENN., 11.4.1977
20.800

IKP-206477
FAESSLER,A.
SPINS, HIGH SPINS, VERY HIGH SPINS.
KOLLOQUIUM DES PHYSICS DEPARTMENT, UNIV. OF KENTUCKY, LEXINGTON, KY., 8.4.1977
20.800

IKP-206577
FAESSLER,A.
STRANGE BEHAVIOUR OF NUCLEI AT HIGH SPIN STATES.
PHYSICS COLLOQUIUM, UNIV. OF NEW YORK, STONY BROOK, N.Y., 30.3.1977
20.800

IKP-206677
FAESSLER,A.
DO WE UNDERSTAND THE TRANSITIONAL NUCLEI?
NUCLEAR SEMINAR. UNIV. OF NEW YORK, STONY BROOK, N.Y., 22.3.1977
20.800

IKP-206777
FAESSLER,A.
SELFCONSISTENT DESCRIPTION OF MULTIPOLE RESONANCES.
SEMINAR OF THEORETICAL NUCLEAR PHYSICS. UNIV. OF NEW YORK, STONY BROOK, N.Y., 3.3.1977
20.800

IKP-206877
FAESSLER,A.
DO WE REALLY UNDERSTAND THE TRANSITIONAL NUCLEI?
WINTER SYMPOSIUM ON NUCLEAR STRUCTURE. GEILO, 10.2.1977
20.800

IKP-206977
FAESSLER,A.
BEHAVIOUR OF NUCLEI IN STRONG CORIOLIS AND CENTRIFUGAL FIELDS.
WINTER SYMPOSIUM ON NUCLEAR STRUCTURE. GEILO, 8.2.1977
20.800

IKP-207077
FAESSLER,A.
SPINS, HIGH SPINS, VERY HIGH SPINS.
PHYSIKALISCHES KOLLOQUIUM DER UNIV. DE PARIS. ORSAY, 27.1.1977
20.800

IKP-207177
FAESSLER,A.
THE STRANGE BEHAVIOUR OF NUCLEI AT HIGH AND VERY HIGH SPIN STATES.
WORKSHOP ON GROSS PROPERTIES OF NUCLEI AND NUCLEAR EXCITATIONS 5. HIRSCHEGG, 17.1.1977
20.800

IKP-207277
FAESSLER,A.
THE SELFCONSISTENT DESCRIPTION OF GIANT MULTIPLE RESONANCES.
THEORETICAL NUCLEAR PHYSICS SEMINAR. OAK RIDGE NATIONAL LABORATORY, TENN., 13.4.1977
20.800

IKP-207377
FAESSLER,A.
SPINS, HIGH SPINS, VERY HIGH SPINS.
KERNPHYSIKALISCHES KOLLOQUIUM. OAK RIDGE NATIONAL LABORATORY, TENN., 13.4.1977
20.800

IKP-207477
FAESSLER,A. WAKAI,M.
EFFECT OF QUADRUPOLE PAIRING ON BACKBENDING.
FRUEHJAHRSTAGUNG DER DPG, FACHGRUPPE KERNPHYSIK. KONSTANZ, 21.-25.3.1977. VERHANDL. DPG (VI), 12(1977), S. 1023-4
20.800

IKP-207577
FRASCARIA,N.* DIDELEZ,J.P. CHANT,N.S.* CHANG,C.C.* WU,J.*
HIGH SPIN STATES IN TL-202,204,206 OBSERVED IN (D,ALPHA) REACTIONS AT 80 MEV.
FRUEHJAHRSTAGUNG DER DPG, FACHGRUPPE KERNPHYSIK. KONSTANZ, 21.-25.3.1977. VERHANDL. DPG (VI), 12(1977), S. 989
20.060

IKP-207677
GOEKE,K.
THE ADIABATIC TIME-DEPENDENT HARTREE-FOCK THEORY.
INTERNATIONAL SYMPOSIUM ON NUCLEAR COLLISIONS AND THEIR MICROSCOPIC DESCRIPTION. BLED, 26.9.-1.10.1977
20.800

IKP-207777
GOEKE,K.
PHYSIKALISCHE METHODEN BEI FRUEHGESCHICHTLICHEN AUSGRABUNGEN.
ANTRITTSVORLESUNG IN DER MATHEMATISCH-NATURWISS. FAKULTAET DER UNIV. BONN, 9.12.1977
20.800

IKP-207877
GOEKE,K.
*THEORIES OF LARGE AMPLITUDE COLLECTIVE MOTION.*
SERIE VON NEUN VORLESUNGEN AM PHYSIKALISCHEN INSTITUT DER UNIV. COIMBRA IM JULI UND AUG. 1977.
20.800

IKP-207977
GOEKE,K.
EFFEKTIVE MASSEN FUER KOLLEKTIVE KERNBEWEGUNGEN.
KOLLOQUIUM FUER PHYSIK DER UNIV. KOELN, 20.1.1977
20.800

IKP-208077
GOEKE,K.
A CONSISTENT MICROSCOPIC THEORY OF COLLECTIVE MOTION IN THE FRAMEWORK OF AN ATDHF APPROACH.
KOLLOQUIUM IM INSTITUT FUER THEORETISCHE PHYSIK DER UNIV. HEIDELBERG. 3.5.1977
20.800

IKP-208177
GOEKE,K.
ZEITABHAENGIGE HARTREE-FOCK-THEORIE: EIN REVIEW.
KERNPHYSIKALISCHES KOLLOQUIUM DER UNIV. HAMBURG. 23.5.1977
*20.800*

IKP-208277
GOEKE,K.
THEORIE KOLLEKTIVER BEWEGUNGEN GROSSER AMPLITUDEN.
PHYSIKALISCHES KOLLOQUIUM DER UNIV. REGENSBURG. 29.6.1977
20.800

IKP-208377
GOEKE,K.
STRUKTUR VON ATOMKERNEN BEI HOHEN DREHIMPULSEN.
HABILITATIONSKOLLOQUIUM, UNIV. BONN, 27.6.1977
20.800

IKP-208477
GONO,Y.
HIGH SPIN STATES OF ODD-MASS AU, HG AND TL NUCLEI.
INTERNATIONAL WORKSHOP ON GROSS PROPERTIES OF NUCLEI AND NUCLEAR EXCITATIONS 5. HIRSCHEGG, 17.1.1977
20.100

IKP-208577
GRIDNEV,K.A.* DARWISCH,N.Z.* SEMJONOV,V.M.* HEFTER,E.F.
PHAENOMENOLOGISCHE ANALYSE ELASTISCHER RESONANZSTREUUNG VON ALPHA-TEILCHEN AN KOHLENSTOFF.
27. KONFERENZ FUER KERNSPEKTROSKOPIE UND STRUKTUR DER ATOMKERNE. TASCHKENT, 22.-25.3.1977. MATERIALIEN ZUR 27. KONFERENZ FUER KERNSPEKTROSKOPIE UND STRUKTUR DER ATOMKERNE. S. 268
20.800

IKP-208677
GRIDNEV,K.A.* DARWISCH,N.Z.* SEMJONOV,V.M.* HEFTER,E.F.
UEBER DAS WECHSELWIRKUNGSPOTENTIAL VON ALPHA-TEILCHEN MIT LEICHTEN KERNEN.
27. KONFERENZ FUER KERNSPEKTROSKOPIE UND STRUKTUR DER ATOMKERNE. TASCHKENT, 22.-25.3.1977. MATERIALIEN ZUR 27. KONFERENZ FUER KERNSPEKTROSKOPIE UND STRUKTUR DER ATOMKERNE. S. 267
20.800

IKP-208777
GRIDNEV,K.A.* DORU,D.* SEMJONOV,V.M.* HEFTER,E.F.
DIE NICHTLINEARE SCHROEDINGER-GLEICHUNG UND ANOMALE RUECKWAERTSSTREUUNG.
27. KONFERENZ FUER KERNSPEKTROSKOPIE UND STRUKTUR DER ATOMKERNE. TASCHKENT, 22.-25.3.1977. MATERIALIEN ZUR 27. KONFERENZ FUER KERNSPEKTROSKOPIE UND STRUKTUR DER ATOMKERNE. S. 360
20.800

IKP-208877
GRIDNEV,K.A.* SEMJONOV,V.M.* HEFTER,E.F.
ANALYSE VON (D,P) REAKTIONEN.
27. KONFERENZ FUER KERNSPEKTROSKOPIE UND STRUKTUR DER ATOMKERNE. TASCHKENT, 22.-25.3.1977. MATERIALIEN ZUR 27. KONFERENZ FUER KERNSPEKTROSKOPIE UND STRUKTUR DER ATOMKERNE. S. 162
20.800

IKP-208977
HAFNER,H.* BHATIA,T.S.* DUHM,H.H.* HEINECKE,H.* MASCHUN,R.*OSTERFELD,F. WIEDNER,C.A.*
UNTERSUCHUNG DER CA-048(LI-006,HE-006) SC-048-REAKTION BEI 48 MEV.
FRUEHJAHRSTAGUNG DER DPG, FACHGRUPPE KERNPHYSIK. KONSTANZ, 21.-25.3.1977. VERHANDL. DPG (VI), 12(1977), S. 950
20.800

IKP-209077
HARAKEH,M.N.* VANDERBORG,K.* MORSCH,H.P. VANDERWOUDE,A.* BERTRAND,F.E.* ISHIHATSU,T.*
STUDY OF GIANT RESONANCES BY INELASTIC ALPHA SCATTERING.
FRUEHJAHRSTAGUNG DER DPG, FACHGRUPPE KERNPHYSIK. KONSTANZ, 21.-25.3.1977. VERHANDL. DPG (VI), 12(1977), S. 982-3
20.060

IKP-209177
HEFTER,E.F. GERAMB,H.V.* OSTERFELD,F. UDAGAWA,T.*
DIE ROLLE INTERMEDIAERER DEUTERONEN IN UNELASTISCHER NUKLEONENSTREUUNG.
FRUEHJAHRSTAGUNG DER DPG, FACHGRUPPE KERNPHYSIK. KONSTANZ, 21.-25.3.1977. VERHANDL. DPG (VI), 12(1977), S. 880
20.800

IKP-209277
HOFF,R.W.* DAVIDSON,W.F.* WARNER,D.D.* SCHRECKENBACH,K.* BOERNER,H. DIGGORY,A.F.* EGIDY,T. VON*
EXCITED LEVELS IN CM-249 FROM NEUTRON CAPTURE GAMMA-RAY MEASUREMENTS.
FRUEHJAHRSTAGUNG DER DPG, FACHGRUPPEN KERNPHYSIK. KONSTANZ, 21.-25.3.1977. VERHANDL. DPG (VI), 12(1977), S. 992
*20.700*

IKP-209377
JAHN,P.
MEASUREMENT AND HYBRID-MODEL ANALYSIS OF AU-197(HE-003,XNYP) EXCITATION FUNCTIONS.
CONFERENCE ON NUCLEAR REACTION MECHANISMS. VARENNA, 15.6.1977
20.060

IKP-209477
JAHN,P.
ENERGIEABHAENGIGKEIT DER LADUNGSVERTEILUNG VON SPALTPRODUKTEN BEI DER HOCHENERGIESPALTUNG AU-197(ALPHA,FISSION).
KERNPHYSIKALISCHES SEMINAR IM RAUM BONN-JUELICH-KOELN, ISKP, UNIV. BONN, 28.1.1977
20.060

IKP-209577
JAHN,P. PROBST,H.J. ALDERLIESTEN,C. MAYER-BOERICKE,C.
ZUR LADUNGSVERTEILUNG DER SPALTPRODUKTE BEI AU-197(ALPHA,SPALTUNG).
FRUEHJAHRSTAGUNG DER DPG, FACHGRUPPE KERNPHYSIK. *KONSTANZ, 21.-25.3.1977. VERHANDL. DPG (VI),* 12(1977), S. 974
20.060

IKP-209677
KENNEPOHL,K. BRAEUTIGAM,W. HERSCHBACH,M. REICH,J.
BEAM PHASE DETECTION USING HETERODYNE PRINCIPLE AT JULIC.
14. EUROPEAN CYCLOTRON PROGRESS MEETING. UPPSALA, 1.-3.6.1977
20.300

IKP-209777
KHAN,T.A.
NUCLEAR STRUCTURE STUDIES AT JOSEF.
BNL-WORKSHOP ON ISOL-SYSTEMS. UPTON, N.Y., 31.10.1977
20.650

IKP-209877
KHAN,T.A.
RESEARCH AT THE GASFILLED SEPARATOR JOSEF.
KOLLOQUIUM DES DEPARTMENT OF PHYSICS, UNIVERSITAET TORONTO. 24.10.1977
20.650

IKP-209977
KHAN,T.A. LAUPPE,W.D. LAWIN,H. SADLER,G.* SELIC,H.A. SISTEMICH,K. TENTEN,W.*
EIN MIKROSEKUNDEN-ISOMER IM DOPPELTMAGISCHEN KERN SN-132.
FRUEHJAHRSTAGUNG DER DPG, FACHGRUPPEN KERNPHYSIK. KONSTANZ, 21.-25.3.1977. VERHANDL. DPG (V), 12(1977), S. 887
20.650

IKP-210077
KHAN,T.A. LAUPPE,W.D. LAWIN,H. SADLER,G.* SELIC,H.A. SISTEMICH,K. TENTEN,W.*
DISCOVERY OF A VERY LOW LYING 02+ STATE IN ZR-100.
FRUEHJAHRSTAGUNG DER DPG, FACHGRUPPEN KERNPHYSIK. KONSTANZ, 21.-25.3.1977. VERHANDL. DPG (V), 12(1977), S. 806
20.650

IKP-210177
KLEINHEINZ,P.
ISOMERIC STATES AND YRAST SPECTROSCOPY IN THE A EQUAL TO 150 REGION.
WINTER SCHOOL OF NUCLEAR SPECTROSCOPY. ZAKOPANE, 7.-18.2.1977
20.100

IKP-210277
KLEINHEINZ,P.
SPECTROSCOPY WITH (ALPHA,XN GAMMA) REACTIONS.
NUCLEAR STRUCTURE GORDON CONFERENCE. TILTON, N.H., 11.-15.7.1977
20.100

IKP-210377
KLEINHEINZ,P.
GAMMA-RAY STUDIES OF ODD-A TRANSITIONAL NUCLEI FOLLOWING HIGH SPIN COMPOUND REACTIONS.
SCANDINAVIAN WINTER SYMPOSIUM ON NUCLEAR STRUCTURE. GEILO, 7.-11.2.1977
20.100

IKP-210477
KLEINHEINZ,P.
RECENT PROGRESS IN UNDERSTANDING COLLECTIVE YRAST FEATURES OF ODD-A RARE EARTH NUCLEI AND APPLICATIONS TO NUCLEI WITH 83 LESS THAN EQUAL TO N LESS THAN EQUAL TO 89.
SEMINARVORTRAG, UNIVERSITAET PADUA. 14.3.1977
20.100

IKP-210577
KLEINHEINZ,P.
GAMMA RAY MULTIPLICITY STUDIES AT HIGH BOMBARDING ENERGIES.
EXPERTENTREFFEN, SCHLECHING, MAERZ 1977
20.100

IKP-210677
KLEINHEINZ,P.
IN BEAM GAMMA-RAY STUDIES OF HIGH SPIN SHELL MODEL STATES.
IN BEAM GAMMA-SPECTROSCOPY MEETING AMSTERDAM/KOELN. BAD HONNEF, 9.-10.12.1977
20.100

IKP-210777
KLEINHEINZ,P.
SPHERICAL AND DEFORMED HIGH-SPIN CONFIGURATIONS IN THE A CA 150 REGION.
INTERNATIONAL SYMPOSIUM ON HIGH-SPIN STATES AND NUCLEAR STRUCTURE. DRESDEN, 19.-24.9.1977
20.100

IKP-210877
KLENT,V. SPETH,J. WAMBACH,J.
DER EINFLUSS HOCHLIEGENDER CORE-VIBRATIONEN AUF LADUNGS- UND STROMDICHTEN IN U-G KERNEN.
FRUEHJAHRSTAGUNG DER DPG, FACHGRUPPE KERNPHYSIK. KONSTANZ, 21.-25.3.1977. VERHANDL. DPG (VI), 12(1977), S. 1019
20.800

IKP-210977
KNOEPFLE,K.T.* RIEDESEL,R.* WAGNER,G.J.* MAYER-BOERICKE,C. OELERT,W. ROGGE,M.
INFLUENCE OF VALENCE PARTICLES OR HOLES ON THE ISOSCALAR GIANT RESONANCES IN THE OXYGEN REGION.
BULL. AM. PHYS. SOC. 22(1977),541
20.060

IKP-211077
KNOEPFLE,K.T.* RIEDESEL,R.* WAGNER,G.J.* MAYER-BOERICKE,C. OELERT,W. ROGGE,M.
INFLUENCE OF VALENCE PARTICLES OR HOLES ON THE ISOSCALAR GIANT RESONANCES IN THE OXYGEN REGION.
FRUEHJAHRSTAGUNG DER DPG, FACHGRUPPE KERNPHYSIK. KONSTANZ, 21.-25.3.1977. VERHANDL. DPG (VI), 12(1977) ,S. 1009
20.060

IKP-211177
KREINER,A.J.* FENZL,M.* LUNARDI,S. MARISCOTTI,M.A.J.* ROTATIONSSTRUKTUREN IN U-U TL-198.
FRUEHJAHRSTAGUNG DER DPG, FACHGRUPPEN KERNPHYSIK. KONSTANZ, 21.-25.3.1977. VERHANDL. DPG (VI), 12(1977), S. 989
20.100

IKP-211277
LIEDER,R.M.
BLOCKING AND VECTOR COUPLING IN TRANSITIONAL NUCLEI NEAR HG.
KERNPHYSIKALISCHES SEMINAR, ILL GRENOBLE. GRENOBLE, 27.4.1977
20.100

IKP-211377
LIEDER,R.M.
DREITEILCHENZUSTAENDE IN TL-195,197.
KERNPHYSIKALISCHES SEMINAR BONN-JUELICH-KOELN. BONN, 11.11.1977
20.100

IKP-211477
LIEDER,R.M.
BANDENSTRUKTUR IN UEBERGANGSKERNEN.
EXPERTENTREFFEN FUER KERNPHYSIK. SCHLECHING, 9.3.1977
20.100

IKP-211577
LIEDER,R.M.
HIGH-SPIN STATES IN HEAVY TRANSITIONAL NUCLEI AROUND HG.
INTERNATIONAL SYMPOSIUM ON HIGH-SPIN STATES AND NUCLEAR STRUCTURE. DRESDEN, 21.9.1977
20.100

IKP-211677
LUNARDI,S. OGAWA,M. KLEINHEINZ,P. MAIER,M.R.*
HIGH SPIN STATES IN THE N EQUAL TO 84 NUCLEI GD-148 AND DY-150.
FRUEHJAHRSTAGUNG DER DPG, FACHGRUPPEN KERNPHYSIK. KONSTANZ, 21.-25.3.1977. VERHANDL. DPG (VI), 12(1977), S. 893
20.100

IKP-211777
MADSEN,V.A.
GIANT RESONANCES IN NUCLEI.
KOLLOQUIUM, PHYSICS DEPARTMENT, OREGON STATE UNIV. CORVALLIS, OREG., 17.10.1977
20.800

IKP-211877
MADSEN,V.A.
THE IMAGINARY INELASTIC FORM FACTOR.
EXPERIMENTAL PHYSICS DIVISION SEMINAR. LAWRENCE LIVERMORE LABORATORY, LIVERMORE, CAL., 13.9.1977
20.800

IKP-211977
MADSEN,V.A.
THE IMAGINARY PART OF THE INELASTIC SCATTERING INTERACTION.
CONFERENCE ON NUCLEAR REACTION MECHANISMS. VARENNA, 13.-17.6.1977
20.800

IKP-212077
MADSEN,V.A.
IMAGINARY INELASTIC FORM FACTOR.
SEMINAR IN RAUM KOELN-BONN-JUELICH. UNIV. BONN, MAI 1977
20.800

IKP-212177
MADSEN,V.A.
CORE POLARIZATION IN INELASTIC SCATTERING AND CHARGE EXCHANGE.
KERNPHYSIKALISCHES KOLLOQUIUM DES CEN. SACLAY, 17.2.1977
20.800

IKP-212277
MAYER-BOERICKE,C.
EVIDENCE FOR NEW HIGHER MULTIPOLE GIANT RESONANCES IN LIGHT NUCLEI.
RCNP SYMPOSIUM ON HIGHLY EXCITED STATES AND POLARIZATION PHENOMENA. RESEARCH CENTRE FOR NUCL. PHYS. , OSAKA UNIV., SUITA, 14.-16.9.1977. INVIITED TALK
20.060

IKP-212377
MAYER-BOERICKE,C.
INVESTIGATION OF NEW MULTIPOLE GIANT RESONANCES IN LIGHT NUCLEI BY INELASTIC HADRONIC SCATTERING AND COMPARISON WITH CAPTURE REACTION RESULTS.
CONFERENCE ON ELECTRO AND PHOTOEXCITATION. SENDAI, 12.-13.9.1977. INVITED TALK
20.060

IKP-212477
MAYER-BOERICKE,C.
EXPERIMENTAL INVESTIGATIONS OF GIANT RESONANCES IN LIGHT NUCLEI: MACROSCOPIC AND MICROSCOPIC ASPECTS.
INTERNATIONAL SYMPOSIUM ON NUCLEAR REACTION MODELS 1977. BALATONFUERED, 27.6.-1.7.1977. INVITED TALK
20.060

IKP-212577
MAYER-BOERICKE,C.
MULTIPOLE GIANT RESONANCES IN LIGHT NUCLEI. 2
10TH SUMMER SCHOOL ON NUCLEAR PHYSICS "STUDY OF NUCLEAR STRUCTURE BY MEANS OF NUCLEAR REACTIONS". MIKOLAJKI, 30.8.-11.9.1977. INVITED TALK
20.060

IKP-212677
MAYER-BOERICKE,C.
MULTIPOLE GIANT RESONANCES IN LIGHT NUCLEI. 1
10TH SUMMER SCHOOL ON NUCLEAR PHYSICS "STUDY OF NUCLEAR STRUCTURE BY MEANS OF NUCLEAR REACTIONS". MIKOLAJKI, 30.8.-11.9.1977. INVITED TALK
20.060

IKP-212777
MAYER-BOERICKE,C.
EXPERIMENTAL INVESTIGATIONS OF GIANT RESONANCES IN LIGHT NUCLEI: MACROSCOPIC AND MICROSCOPIC ASPECTS
INTERNATIONAL SYMPOSIUM ON NUCLEAR REACTION MODELS 1977. BALATONFUERED, 27.6.-1.7.1977. INVITED TALK
20.060

IKP-212877
MAYER-BOERICKE,C. OELERT,W. KISS,A. ROGGE,M. TUREK,P. WIKTOR,S.
MOEGLICHE OKTUPOL-ANREGUNG IN AL-027(ALPHA,ALPHA') BEI HOHER E EXC.
FRUEHJAHRSTAGUNG DER DPG, FACHGRUPPE KERNPHYSIK. KONSTANZ, 21.-25.3.1977. VERHANDL. DPG (VI), 12(1977), S. 1010-1
*20.060*

IKP-212977
MEYER-TERVEHN,J.
DREIACHSIG-DEFORMIERTE ATOMKERNE.
SEMINAR AN DER UNIV. BONN. 28.10.1977
20.800

IKP-213077
MEYER-TERVEHN,J.
EMPIRICAL LIMITS ON PION CONDENSATION.
SEMINAR AM SCHWEIZER INSTITUT FUER NUKLEARFORSCHUNG. VILLIGEN, 5.8.1977
20.800

IKP-213177
MEYER-TERVEHN,J.
EMPIRICAL LIMITS ON PION CONDENSATION.
SEMINAR DER UNIV. REGENSBURG. 22.7.1977
20.800

IKP-213277
MEYER-TERVEHN,J.
TRANSITIONAL NUCLEI AND TRIAXIAL NUCLEAR SHAPES.
ANNUAL MEETING OF THE FRENCH PHYSICAL SOCIETY. 28.6.1977
20.800

IKP-213377
MEYER-TERVEHN,J.
ON PION CONDENSATION IN FINITE NUCLEI.
SEMINAR DES LAWRENCE BERKELEY LABORATORY. BERKELEY, CAL., 9.6.1977
20.800

IKP-213477
MEYER-TERVEHN,J.
DREIACHSIG-DEFORMIERTE ATOMKERNE.
SEMINAR AN DER UNIV. ZUERICH. 27.4.1977
20.800

IKP-213577
MEYER-TERVEHN,J.
SPINS, SHAPES AND SINGLE PARTICLES.
SEMINAR AM INSTITUT FUER THEORETISCHE PHYSIK DER UNIV. HEIDELBERG. 18.4.1977
20.800

IKP-213677
MEYER-TERVEHN,J.
PION CONDENSATION IN FINITE NUCLEAR SYSTEMS.
KERNPHYSIK-SEMINAR DER UNIV. FRANKFURT. 5.4.1977
20.800

IKP-213777
MEYER-TERVEHN,J.
HIGH AND VERY HIGH SPIN STATES IN NUCLEI.
VORLESUNGSREIHE, EXPERTENTREFFEN FUER KERNPHYSIK IN SCHLECHING, 2.-11.3.1977
20.800

IKP-213877
MEYER-TERVEHN,J.
ON PION CONDENSATION IN FINITE NUCLEAR SYSTEMS.
INTERNATIONAL WORKSHOP ON GROSS PROPERTIES OF NUCLEI AND NUCLEAR EXCITATIONS 5. HIRSCHEGG, 18.1.1977
20.800

IKP-213977
MEYER-TERVEHN,J.
PION-KONDENSATION IN ENDLICHEN SYSTEMEN.
FRUEHJAHRSTAGUNG DER DPG, FACHGRUPPE KERNPHYSIK.
KONSTANZ, 21.-25.3.1977. VERHANDL. DPG (VI), 12(1977), S. 876
20.800

IKP-214077
*MEYER-TERVEHN,J. DIAMOND,R.M.* STEPHENS,F.S.**
DREIACHSIGE KERNDEFORMATIONEN.
FRUEHJAHRSTAGUNG DER DPG, FACHGRUPPE KERNPHYSIK.
KONSTANZ, 21.-25.3.1977. VERHANDL. DPG (VI), 12(1977), S. 890
20.800

IKP-214177
MOERIKE,M.* ROHWER,T.* SCHOLL,K.* SCHILLING,B.* STAUDT,G.* WENG,F.* OESCHLER,H.* TUREK,P.
DER GERADE-UNGERADE-EFFEKT BEI (N,ALPHA)- UND (P,ALPHA)-REAKTIONEN AN LEICHTEN KERNEN.
FRUEHJAHRSTAGUNG DER DPG, FACHGRUPPE KERNPHYSIK.
KONSTANZ, 21.-25.3.1977. VERHANDL. DPG (VI), 12(1977), S. 913-4
20.060

IKP-214277
MORSCH,H.P.
MICROSCOPIC STUDY OF INELASTIC HEAVY ION SCATTERING.
INTERNATIONAL WORKSHOP ON GROSS PROPERTIES OF NUCLEI AND NUCLEAR EXCITATIONS 5. HIRSCHEGG, 19.1.1977
20.060

IKP-214377
MORSCH,H.P. DEHNHARD,D.* LI,T.K.* DECOWSKI,D.* BENENSON,W.* WILDENTHAL,B.H.*
MONOPOL-KERNANREGUNGEN.
FRUEHJAHRSTAGUNG DER DPG, FACHGRUPPE KERNPHYSIK.
KONSTANZ, 21.-25.3.1977. VERHANDL. DPG (VI), 12(1977), S. 911-2
20.060

IKP-214477
MORSCH,H.P. LEWIS,D.A.* PETERSEN,J.F.*
MIKROSKOPISCHE UNTERSUCHUNG VON INELASTISCHER O-016 UND O-018-STREUUNG.
FRUEHJAHRSTAGUNG DER DPG, FACHGRUPPE KERNPHYSIK.
KONSTANZ, 21.-25.3.1977. VERHANDL. DPG (VI), 12(1977), S. 948
20.060

IKP-214577
MUELLER-VEGGIAN,M.
HIGH-SPIN STATES AND ISOMERS IN LIGHT TRANSITIONAL NUCLEI AROUND N EQUAL TO 80.
INTERNATIONAL SYMPOSIUM ON HIGH-SPIN STATES AND NUCLEAR STRUCTURE. DRESDEN, 21.9.1977
20.100

IKP-214677
MUETHER,H.
STRANGE BEHAVIOUR OF NUCLEI DESCRIBED WITH AN EXTENDED GENERATOR COORDINATE METHOD.
KOLLOQUIUM AM INSTITUTO DE FISICA, UNIV. DE SAO PAULO. 12.1.1977
20.800

IKP-214777
MUETHER,H.
COLLECTIVE AND QUASIPARTICLE EXCITATIONS IN NUCLEI.
KOLLOQUIUM DES DEPARTMENT OF PHYSICS, SUNY. STONY BROOK, N.Y., 5.5.1977
20.800

IKP-214877
MUETHER,H.
THE DENSITY DEPENDENCE OF THE NUCLEON-NUCLEON INTERACTION.
KOLLOQUIUM DES DEPARTMENT OF PHYSICS, RUTGERS UNIV. NEW BRUNSWICK, N.J., 2.5.1977
20.800

IKP-214977
MUETHER,H.
MICROSCOPIC DESCRIPTION OF COLLECTIVE AND SINGLE PARTICLE DEGREES OF FREEDOM OF NUCLEI.
KOLLOQUIUM AM INSTITUTO DE FISICA, UNIV. FEDERAL DO RIO DE JANEIRO. 2.2.1977
20.800

IKP-215077
OELERT,W. DJALOEIS,A. MAYER-BOERICKE,C. TUREK,P. WIKTOR,S.
RESONANCE-LIKE PHENOMENA IN FEW-NUCLEON TRANSFER REACTIONS.
INTERNATIONAL CONFERENCE ON THE RESONANCES IN HEAVY ION REACTIONS. HVAR, 30.5.-3.6.1977
20.060

IKP-215177
OELERT,W. DJALOEIS,A. MAYER-BOERICKE,C. TUREK,P. WIKTOR,S.
FEW-NUCLEON PICKUP REAKTIONEN AN O-012, MG-024,025,026 UND CA-040.
FRUEHJAHRSTAGUNG DER DPG, FACHGRUPPE KERNPHYSIK.
KONSTANZ, 21.-25.3.1977. VERHANDL. DPG (VI), 12(1977), S. 916
20.060

IKP-215277
OELERT,W. MAYER-BOERICKE,C. DJALOEIS,A. KISS,A. ROGGE,M. TUREK,P. WIKTOR,S.
STRENGTH CONCENTRATION OBSERVED IN (ALPHA,ALPHA') AND (D,LI-006) REACTIONS AT EX CIRCA 32/A 1/3 MEV.
4. E.P.S. NUCLEAR PHYSICS DIVISIONAL CONFERENCE PHYSICS OF MEDIUM-LIGHT NUCLEI. TOPICAL CONFERENCE. FLORENCE, 7.-10.6.1977
20.060

IKP-215377
OGAWA,M. LUNARDI,S. KLEINHEINZ,P. MAIER,M.R.*
THE YRAST LEVELS IN TB-149.
FRUEHJAHRSTAGUNG DER DPG, FACHGRUPPEN KERNPHYSIK.
KONSTANZ, 21.-25.3.1977. VERHANDL. DPG (VI), 12(1977), S. 893
20.100

IKP-215477
OSTERFELD,F.
MICROSCOPIC THEORY OF THE IMAGINARY INELASTIC SCATTERING FORM FACTOR.
INTERNATIONAL SYMPOSIUM "REACTION MODELS '77".
BALATONFUERED, 27.6.-1.7.1977
20.800

IKP-215577
OSTERFELD,F.
COUPLING TO DIRECT CHANNELS IN C-012-NE-020 AND O-016-O-016 SCATTERING.
INTERNATIONAL SYMPOSIUM "REACTION MODELS '77".
BALTONFUERED, 27.6.-1.7.1977
20.800

IKP-215677
OSTERFELD,F.
EXCITATION OF NON-COLLECTIVE STATES AND SCALING PROPERTIES IN HEAVY ION SCATTERING.
INTERNATIONAL WORKSHOP ON GROSS PROPERTIES OF NUCLEI AND NUCLEAR EXCITATIONS 5. HIRSCHEGG, 17.-22.1.1977
20.800

IKP-215777
OSTERFELD,F. KNIZDO,V.* TOEPFFER,C.*
KOPPLUNG AN DIREKTE KANAELE IN C-012-NE-020 UND O-016-O-016 STREUUNG.
FRUEHJAHRSTAGUNG DER DPG, FACHGRUPPE KERNPHYSIK.
KONSTANZ, 21.-25.3.1977. VERHANDL. DPG (VI), 12(1977), S. 1000-1
20.800

IKP-215877
PFEIFFER,B.* BLACHOT,J.* BOCQUET,J.P.* MONNAND,E.* SCHUSSLER,F.* LAWIN,H. SISTEMICH,K.
EXCITED STATES IN PR-145, CE-145, LA-145.
FRUEHJAHRSTAGUNG DER DPG, FACHGRUPPEN KERNPHYSIK.
KONSTANZ, 21.-25.3.1977. VERHANDL. DPG (VI), 12(1977), S. 892
20.650

IKP-215977
PLOSZAJCZAK,M.
K-ISOMERIC STATES AND YRAST TRAPS IN HF-176.
SEMINAR DES INSTITUTE OF NUCLEAR PHYSICS, UNIV. KRAKAU. NOV. 1977
20.800

IKP-216077
PLOSZAJCZAK,M.
DESCRIPTION OF YRAST TRAPS.
KERNPHYSIKALISCHES KOLLOQUIUM DES C.R.N.S. STRASBOURG, DEZ. 1977
20.800

IKP-216177
PLOSZAJCZAK,M.
SPINS, HIGH SPINS, VERY HIGH SPINS IN NUCLEI.
SEMINAR DES INSTITUTE OF NUCLEAR PHYSICS. KRAKAU, OKT. 1977
20.800

IKP-216277
PLOSZAJCZAK,M.
DESCRIPTION OF YRAST TRAPS.
INTERNATIONAL SYMPOSIUM ON HIGH-SPIN STATES AND NUCLEAR STRUCTURE. DRESDEN, 19.-24.9.1977
20.800

IKP-216377
PLOSZAJCZAK,M.
SPINS, HOHE SPINS UND SEHR HOHE SPINS IN KERNEN.
EXPERTENTREFFEN FUER KERNPHYSIK. SCHLECHING, 2.-11.3.1977
20.800

IKP-216477
PLOSZAJCZAK,M.
DESCRIPTION OF YRAST TRAPS.
KERNPHYSIKALISCHES SEMINAR DES TECHNICAL DEPARTMENT OF MATHEMATICAL PHYSICS, UNIV. OF LUND. MAERZ 1977
20.800

IKP-216577
PLOSZAJCZAK,M.
K ISOMERIC STATES AND YRAST TRAPS IN HF-176.
KERNPHYSIKALISCHES SEMINAR DES A.F.J. STOCKHOLM, FEB. 1977
20.800

IKP-216677
REICH,J. BRAEUTIGAM,W. LINZ,J. MAYER-BOERICKE,C. WUCHERER,P.
JULIC: STATUS UND WEITERENTWICKLUNGEN.
FRUEHJAHRSTAGUNG DER DPG, FACHGRUPPE KERNPHYSIK. KONSTANZ, 21.-25.3.1977. VERHANDL. DPG (VI), 12(1977), S. 857
20.300

IKP-216777
RIEPE,G. PROTIC,D.
TEILCHENDETEKTOREN AUS HOCHREINEM GERMANIUM.
KERNPHYSIKALISCHES SEMINAR BONN-JUELICH-KOELN.
INSTITUT FUER KERNPHYSIK DER UNIV. KOELN, 7.1.1977
20.200

IKP-216877
ROGGE,M.
GIANT QUADRUPOLE RESONANCE IN C-012, MG-024, AL-027.
MICHIGAN STATE UNIV., EAST LANSING, MICH.
20.060

IKP-216977
ROGGE,M. KISS,A. MAYER-BOERICKE,C. TUREK,P. WIKTOR,S.
ANREGUNG VON QUADRUPOL-RIESENRESONANZEN IN AL-027 UND MG-024,025,026 MIT ALPHA-TEILCHEN.
FRUEHJAHRSTAGUNG DER DPG, FACHGRUPPE KERNPHYSIK. KONSTANZ, 21.-25.3.1977. VERHANDL. DPG (VI), 12(1977), S. 1011
20.060

IKP-217077
SCHMID,K.W.
MICROSCOPIC DESCRIPTION OF GIANT RESONANCES IN LIGHT DEFORMED NUCLEI.
SEMINAR IM RAUM KOELN-BONN-JUELICH. UNIV. KOELN, 24.6. 1977
20.800

IKP-217177
SCHMID,K.W.
RIESENRESONANZEN IN LEICHTEN DEFORMIERTEN KERNEN.
KERNTHEORETISCHES KOLLOQUIUM DER UNIV. HAMBURG. 10.5. 1977
20.800

IKP-217277
SCHMID,K.W.
GIANT MULTIPOLE RESONANCES IN LIGHT DEFORMED NUCLEI.
15. INT. WINTER MEETING ON NUCLEAR PHYSICS. BORMIO, 17. -22.1.1977
20.800

IKP-217377
SCHMID,K.W. DO DANG,G.*
A MICROSCOPIC APPROACH TO THE MULTIPOLE RESONANCES IN NE-020
FRUEHJAHRSTAGUNG DER DPG, FACHGRUPPE KERNPHYSIK. KONSTANZ, 21.-25.3.1977. VERHANDL. DPG (VI), 12(1977), S. 1010
20.800

IKP-217477
SCHULT,O.W.B.
THE LEVEL SCHEME OF THE DOUBLY MAGIC NUCLEUS SN-132.
INTERNATIONAL CONFERENCE ON NUCLEAR STRUCTURE. TOKYO, 6.9.1977
20.650

IKP-217577
SCHULT,O.W.B.
MULTIPLICITY MEASUREMENTS IN THE PRE-COMPOUND REGION.
SYMPOSIUM ON HIGHLY EXCITED STATES AND POLARIZATION PHENOMENA. OSAKA, 19.9.1977
20.100

IKP-217677
SCHULT,O.W.B.
DO WE UNDERSTAND THE K X-RAY ENERGIES?
KOLLOQUIUM, DEPARTMENT OF PHYSICS, FACULTY OF SCIENCE, HIROSHIMA UNIVERSITY. HIROSHIMA, 13.9.1977
20.100

IKP-217777
SCHULT,O.W.B.
UNTERSUCHUNGEN ZU KERNREAKTIONEN UND STRUKTUREN DURCH GAMMA-MULTIPLIZITAETSMESSUNGEN.
EXPERTENTREFFEN, SCHLECHING, 2.-11.3.1977
20.100

IKP-217877
SCHULT,O.W.B.
RECENT WORK AT THE JUELICH ON LINE RECOIL SEPARATOR FOR FISSION PRODUCTS.
SYMPOSIUM ON ON-LINE ISOTOPE SEPARATORS. TOKYO, 4.9. 1977
20.650

IKP-217977
SCHULT,O.W.B. SEYFARTH,H. WUEST,N.
UNTERSUCHUNG DER K-ROENTGENEMISSION NACH THERMISCHEM NEUTRONENEINFANG.
FRUEHJAHRSTAGUNG DER DPG, FACHGRUPPEN KERNPHYSIK. KONSTANZ, 21.-25.3.1977. VERHANDL. DPG (V), 12(1977), S. 1007-8
20.700

IKP-218077
SCHULTHEIS,H.* SCHULTHEIS,R.* WILDERMUTH,K.* FAESSLER,A. GRUEMMER,F.
ALPHA-ARTIGE UNTERSTRUKTUREN IN S-032.
FRUEHJAHRSTAGUNG DER DPG, FACHGRUPPE KERNPHYSIK. KONSTANZ, 21.-25.3.1977. VERHANDL. DPG (VI), 12(1977), S. 976
20.800

IKP-218177
SELIC,H.A. BORGS,J.W. KHAN,T.A. LAUPPE,W.D. LAWIN,H. SADLER,G.* SISTEMICH,K.
WINKELKORRELATIONSMESSUNGEN AN NEUTRONENREICHEN KERNEN DER MASSE A CA 100.
FRUEHJAHRSTAGUNG DER DPG, FACHGRUPPEN KERNPHYSIK, KONSTANZ, 21.-25.3.1977. VERHANDL. DPG (V), 12(1977), S. 804
20.650

IKP-218277
SEYFARTH,H.
NUCLEAR STRUCTURE STUDIES AT THE JUELICH FRJ-2 RESEARCH REACTOR.
SEMINAR DES UNIVERSITY OF LONDON REACTOR CENTRE. ASCOT, 18.2.1977
20.700

IKP-218377
SEYFARTH,H.
NUCLEAR STRUCTURE STUDIES IN THE A CA 100 REGION.
KOLLOQUIUM DES ENERGIEONDERZOEK CENTRUM NEDERLAND, PETTEN, 21.1.1977
20.700

IKP-218477
SISTEMICH,K.
THE DOUBLY MAGIC NUCLEUS SN-132 AND ITS NEIGHBOUR SN-133.
KOLLOQUIUM DES AMES LABORATORY ERDA. 7.7.1977
20.650

IKP-218577
SISTEMICH,K.
KERNENERGIE - NOTWENDIGKEIT UND RISIKEN.
DIE BEGEGNUNG, VEREIN FUER BILDUNG UND KULTUR. HERZOGENRATH, 2.2.1977
20.650

IKP-218677
SMITHER,R.K.* NAMENSON,A.I.* DAVIDSON,W.F.* BOERNER,H. G. PINSTON,J.A.* WARNER,D.D.* SCHRECKENBACH,K.* EGIDY,T. VON* STOEFFL,W.*
THE LEVEL SCHEME OF SM-155 BASED ON (N,GAMMA) AND (N,E) EXPERIMENTS.
FRUEHJAHRSTAGUNG DER DPG, FACHGRUPPEN KERNPHYSIK. KONSTANZ, 21.-25.3.1977. VERHANDL. DPG (VI), 12(1977), S. 937-8
20.700

IKP-218777
SPETH,J.
FRAGMENTATION OF THE ELECTRIC MULTIPOLE STRENGTH IN PB-208.
INTERNATIONAL CONFERENCE ON NUCLEAR STRUCTURE. TOKYO, 5.-10.9.1977
20.800

IKP-218877
SPETH,J.
DIE STRUKTUR DER NEUEN RIESENRESONANZEN.
KERNPHYSIKALISCHES KOLLOQUIUM DER UNIV. GIESSEN, 12.5. 1977
20.800

IKP-218977
SPETH,J.
THEORETICAL ASPECTS OF THE GIANT MULTIPOLE RESONANCES.
GIANT RESONANCES MEETING. GRONINGEN, 16.12.1977
20.800

IKP-219077
SPETH,J.
HIGHLY EXCITED COLLECTIVE STATES.
RCNP SYMPOSIUM ON HIGHLY EXCITED STATES AND POLARIZATION PHENOMENA. OSAKA, 14.-16.9.1977
20.800

IKP-219177
SPETH,J.
DIE NEUEN RIESENRESONANZEN IN KERN.
PHYSIKALISCHES KOLLOQUIUM DER UNIV. MUENSTER. 6.7.1977
20.800

IKP-219277
SPETH,J.
STRUCTURE OF THE NEW GIANT RESONANCES.
SENDAI CONFERENCE ON ELECTRO- AND PHOTOEXCITATION. SENDAI, 12.-13.9.1977
20.800

IKP-219377
SPETH,J.
MICROSCOPIC CALCULATIONS OF THE GIANT MULTIPOLE RESONANCES.
CONFERENCE ON NUCLEAR REACTION MECHANISMS. VARENNA, 13. -17.6.1977
20.800

IKP-219477
SPETH,J.
STRUCTURE OF THE NEW GIANT RESONANCES
15. INT. WINTER MEETING ON NUCLEAR PHYSICS. BORMIO, 17. -22.1.1977
20.800

IKP-219577
SPETH,J.
THE NEW GIANT RESONANCES.
18TH SCOTTISH UNIVERSITIES SUMMER SCHOOL IN PHYSICS. ST. ANDREWS, 31.7.-20.8.1977
20.800

IKP-219677
STEIN,H.J.
NATIONALE UND INTERNATIONALE MESSPROGRAMME.
2. STATUSSEMINAR SONNENENERGIE. BONN, 20.-21.9.1977
20.600

IKP-219777
TOKI,H.
COMPETITION BETWEEN STRONG AND DECOUPLING STRUCTURES IN TRANSITIONAL NUCLEI.
INTERNATIONAL WORKSHOP ON GROSS PROPERTIES OF NUCLEI AND NUCLEAR EXCITATIONS 5. HIRSCHEGG, 17.1.1977
20.800

IKP-219877
TOKI,H.
DECOUPLING AND STRONG COUPLING.
KERNPHYSIKALISCHES SEMINAR DER TECHNISCHEN HOCHSCHULE DARMSTADT. DEZ. 1977
20.800

IKP-219977
TOKI,H.
STATUS OF THE NUCLEAR PHYSICS IN JUELICH AND DECOUPLING AND STRONG COUPLING.
SEMINAR DES DEPARTMENT OF PHYSICS, UNIV. OF OSAKA. SEP. 1977
20.800

IKP-220077
TOKI,H.
DECOUPLING AND STRONG COUPLING STRUCTURE IN TRANSITIONAL ODD-ODD MASS NUCLEI.
KERNPHYSIKALISCHES KOLLOQUIUM, DEPARTMENT OF PHYSICS. KYOTO, SEP. 1977
20.800

IKP-220177
TOKI,H.
DECOUPLING AND STRONG COUPLING.
KERNPHYSIKALISCHES KOLLOQUIUM DES RCFS. KYOTO, SEP. 1977
20.800

IKP-220277
TOKI,H.
GAMMA-DEFORMATION IN TRANSITIONAL NUCLEI.
KERNPHYSIKALISCHES SEMINAR AM RCNS. OSAKA, SEP. 1977
20.800

IKP-220377
TOKI,H.
DECOUPLING AND STRONG COUPLING.
KERNPHYSIKALISCHES SEMINAR AM ISN. GRENOBLE, JUNI 1977
20.800

IKP-220477
TOKI,H.
DECOUPLING AND STRONG COUPLING.
KOLLOQUIUM DES PHYSIK-DEPARTMENT, UNIV. REGENSBURG. JUNI 1977
20.800

IKP-220577
TOKI,H.
NOTE ON VERY HIGH SPIN STRUTINSKY CALCULATIONS.
15. WINTER SCHOOL ON NUCLEAR PHYSICS "SELECTED TOPICS IN NUCLEAR STRUCTURE". ZAKOPANE, 6.-19.2.1977
20.800

IKP-220677
TOKI,H.
STRONG AND DECOUPLING STRUCTURES IN TRANSITIONAL NUCLEI.
15. WINTER SCHOOL IN NUCLEAR PHYSICS "SELECTED TOPICS IN NUCLEAR STRUCTURE". ZAKOPANE, 6.-19.2.1977
20.800

IKP-220777
TOKI,H. YADAV,H.L. FAESSLER,A.
STRONG AND DECOUPLING STRUCTURE IN TRANSITIONAL ODD-ODD MASS NUCLEI.
FRUEHJAHRSTAGUNG DER DPG, FACHGRUPPE KERNPHYSIK. KONSTANZ, 21.-25.3.1977. VERHANDL. DPG (VI), 12(1977), S. 1024
20.800

IKP-220877
TUREK,P.
INVESTIGATION OF GIANT QUADRUPOLE RESONANCES IN LIGHT NUCLEI BY INELASTIC ALPHA SCATTERING.
15. INTERNATIONAL WINTER MEETING ON NUCLEAR PHYSICS. BORMIO, JAN. 1977
20.060

IKP-220977
TUREK,P. KISS,A. MAYER-BOERICKE,C. ROGGE,M. WIKTOR,S.
STAERKEVERTEILUNG IM E2-RIESENRESONANZBEREICH VON C-012.
FRUEHJAHRSTAGUNG DER DPG, FACHGRUPPE KERNPHYSIK. KONSTANZ, 21.-25.3.1977. VERHANDL. DPG (VI), 12(1977), S. 1008-9
20.060

IKP-221077
WIKTOR,S. KISS,A. MAYER-BOERICKE,C. ROGGE,M. TUREK,P.
STUDIES OF UNIQUENESS OF THE OPTICAL POTENTIAL IN HIGH-ENERGY ALPHA-SCATTERING.
FRUEHJAHRSTAGUNG DER DPG, FACHGRUPPE KERNPHYSIK. KONSTANZ, 21.-25.3.1977. VERHANDL. DPG (VI), 12(1977), S. 865
20.060

IKP-221177
WUCHERER,P. BRINGS,R. FIEDLER,R. LINZ,J. REICH,J.
HARMONIC COILS IMBEDDED IN NEW ISOCHRONOUS TRIM COILS AT JULIC.
14. EUROPEAN CYCLOTRON PROGRESS MEETING. UPPSALA, 1.-3.6.1977
20.300

IKP-221277
YADAV,H.L.
STUDIES IN TRANSITIONAL NUCLEI.
SEMINAR DES INDIAN INSTITUTE OF TECHNOLOGY, KHARAGPUR, DEZ. 1977
20.800

IKP-221377
YADAV,H.L.
GAMMA-BAND IN TRANSITIONAL NUCLEI.
INTERNATIONAL SUMMER SCHOOL ON NUCLEAR SPECTROSCOPY. NIJENRODE, 15.-26.8.1977
20.800

PATENTE

IKP-300177
LABUS,H.
ABDICHTUNGSVORRICHTUNG FUER EINE DREHKOLBENMASCHINE IN TROCHOIDENBAUART.
DE:24 56 252 (31.10.1977) US:4,028,023 (7.6.1977)